

FINAL REPORT

CONCEPTS AND
PRACTICES FOR
CONSIDERING GA AIRPORT
PAVEMENT PERFORMANCE
AND LONGEVITY
Project IA-A1, FY 92

Prepared by
T. J. Van Dam, M. R. Thompson,
E. J. Barenberg and B. J. Dempsey
Department of Civil Engineering
University of Illinois at Urbana-Champaign

December 1994

Illinois Transportation Research Center
Illinois Department of Transportation

ILLINOIS TRANSPORTATION RESEARCH CENTER

This research project was sponsored by the State of Illinois, acting by and through its Department of Transportation, according to the terms of the Memorandum of Understanding established with the Illinois Transportation Research Center. The Illinois Transportation Research Center is a joint Public-Private-University cooperative transportation research unit underwritten by the Illinois Department of Transportation. The purpose of the Center is the conduct of research in all modes of transportation to provide the knowledge and technology base to improve the capacity to meet the present and future mobility needs of individuals, industry and commerce of the State of Illinois.

Research reports are published throughout the year as research projects are completed. The contents of these reports reflect the views of the authors who are responsible for the facts and the accuracy of the data presented herein. The contents do not necessarily reflect the official views or policies of the Illinois Transportation Research Center or the Illinois Department of Transportation. This report does not constitute a standard, specification, or regulation.

Neither the United States Government nor the State of Illinois endorses products or manufacturers. Trade or manufacturers' names appear in the reports solely because they are considered essential to the object of the reports.

Illinois Transportation Research Center Members

Bradley University
DePaul University
Eastern Illinois University
Illinois Department of Transportation
Illinois Institute of Technology
Lewis University
Northern Illinois University
Northwestern University
Southern Illinois University at Carbondale
Southern Illinois University at Edwardsville
University of Illinois at Chicago
University of Illinois at Urbana-Champaign
Western Illinois University

Reports may be obtained by writing to the administrative offices of the Illinois Transportation Research Center at 200 University Park, Edwardsville, IL 62026-1806 [telephone (618) 692-2972], or you may contact the Engineer of Physical Research, Illinois Department of Transportation, at (217) 782-6732.

1. Report No. IA-A1, FY 92	2. Government Accession No.	3. Recipient's Catalog No.	
4. Title and Subtitle CONCEPTS AND PRACTICES FOR CONSIDERING GA AIRPORT PAVEMENT PERFORMANCE AND LONGEVITY		5. Report Date December, 1994	
		6. Performing Organization Code	
7. Author(s) T. VanDam - M. Thompson - E. Barenberg - B. Dempsey		8. Performing Organization Report No.	
9. Performing Organization Name and Address Department of Civil Engineering University of Illinois @ Urbana-Champaign		10. Work Unit (TRAIS)	
		11. Contract or Grant No.	
12. Sponsoring Agency Name and Address Illinois Transportation Research Center Illinois Department of Transportation 200 University Park Edwardsville, IL 62026-1806		13. Type of Report and Period Covered Final Report	
		14. Sponsoring Agency Code	
15. Supplementary Notes			
<p>16. Abstract This study examines Illinois Department of Transportation - Division of Aeronautics (IDOT-DOA) General Aviation (GA) airport pavement performance and the impact that load, climate, and materials/construction factors have on the formation and propagation of pavement distress and evaluates the adequacy and efficacy of current GA airport pavement design and construction practices. The research approach incorporated the review of construction specifications and records, an analysis of statewide climatic factors and their influence on pavement material behavior, state-of-the-art structural and materials modeling and testing, and the analysis of pavement performance and distress data collected during the IDOT-DOA biennial pavement distress inspections. IDOT-DOA pavement inventory and distress data were used to establish a relational pavement performance data base containing 195 non-rehabilitated pavement sections.</p> <p>The most significant findings are:</p> <ul style="list-style-type: none"> • Load (as evaluated by the relative amount of Beechcraft King Air B200 traffic) was not a major distress formation/propagation factor. • Asphalt Concrete Pavements (ACP): * Longitudinal and transverse cracking and paving lane cracking are the two most prevalent distress types. * Illinois GA ACP sections are generally structurally adequate for typical GA loading. • Portland Cement Concrete Pavements (PCCP): * Commonly occurring PCCP distresses include corner breaking, corner and joint spalling, D-cracking, joint seal damage, and longitudinal, transverse, and diagonal cracking. * The most important factor influencing PCCP distress formation and propagation is slab size. * Larger slabs have considerably higher distress occurrences and severities than smaller slabs. * For normal GA loading conditions, both 6-in and 5-in thick PCCP are structurally adequate. The structural adequacy of a 4-in thick PCCP is questionable. <p>The following specific recommendations are offered:</p> <ul style="list-style-type: none"> • The effects of the recently modified AC specifications (P-201 and P-401), pertaining to the construction of paving lane joints, should be monitored. • Current AC mixture design practices should be evaluated. The AC mixtures have "checked" in numerous GA projects. The use of SHRP asphalt cement binder specifications and Level 1 mix design procedures, featuring the use of the SHRP gyratory compactor, should be thoroughly evaluated for potential use. • The advantages/disadvantages of various PCCP slab sizes up to 15 ft in should be further investigated. • A DESIGN CATALOG approach should be considered to standardize Illinois GA ACP and PCCP design procedures. Mechanistic-empirical design approaches can be utilized to design pavement structures for Illinois climatic conditions and commonly used materials. The catalog can be arranged according to climatic zone, traffic loading, and subgrade strength/stiffness properties. A number of alternative pavement designs would be presented for a given set of design conditions. 			
17. Key Words Airport Pavements Paving Materials Pavement Design Pavement Performance		18. Distribution Statement No restrictions. This document is available to the public through the National Technical Information Service, Springfield, Virginia 22161	
19. Security Classif. (of this report) Unclassified	20. Security Classif. (of this page) Unclassified	21. No. of Pages 332	22. Price



TABLE OF CONTENTS

EXECUTIVE SUMMARY	1
Introduction	1
Observations	1
Recommendations	4
I. INTRODUCTION	5
I.1. Problem Statement	5
I.2. Objectives	6
I.3. Scope	7
II. DESIGN AND CONSTRUCTION PRACTICES	8
II.1. Historical Perspective	8
II.2. Current Pavement Thickness Design Methodologies	11
<u>II.2.1. AC Pavement Thickness Design</u>	11
<i>FAA Methodology for the Design of AC Pavements</i>	11
<i>Asphalt Institute Methodology for the Design of AC Pavements</i>	14
<i>Summary</i>	15
<u>II.2.2. PCC Pavement Thickness Design</u>	16
<i>FAA Methodology for the Design of PCC Pavements</i>	16
<i>ACPA Methodology for the Design of PCC Pavements</i>	18
<i>Summary</i>	19
II.3. Material and Construction Specifications	20
<u>II.3.1. AC Material and Construction Specifications</u>	20
<i>Aggregate Type and Gradation</i>	20
<i>Job Mix Formula</i>	21
<i>Construction Practices</i>	23
<i>Acceptance Testing</i>	25
<i>Summary</i>	26
<u>II.3.2. PCC Material and Construction Specifications</u>	26
<i>Aggregate Type and Gradation</i>	27

TABLE OF CONTENTS (Continued)

<i>Cementitious Materials and Admixtures</i>	27
<i>Proportions</i>	28
<i>Acceptance Testing</i>	29
<i>Summary</i>	29
II.3.3. <u>Granular Materials</u>	29
<i>Summary</i>	31
III. PAVEMENT DISTRESS AND THE PAVEMENT CONDITION INDEX	32
III.1. Types of Pavement Distress	32
III.1.1. <u>Distress Types Affecting AC Pavements</u>	33
<i>Distress No. 1: Alligator or Fatigue Cracking</i>	33
<i>Distress No. 2: Bleeding</i>	34
<i>Distress No. 3: Block Cracking</i>	34
<i>Distress No. 4: Corrugations</i>	35
<i>Distress No. 5: Depressions</i>	35
<i>Distress No. 6: Jet Blast Erosion</i>	36
<i>Distress No. 7: Joint Reflection Cracking from PCC</i>	36
<i>Distress No. 8: Longitudinal and Transverse Cracking</i>	36
<i>Distress No. 9: Oil Spillage</i>	37
<i>Distress No. 10: Patching and Utility Cut Patch</i>	37
<i>Distress No. 11: Polished Aggregate</i>	37
<i>Distress No. 12: Raveling and Weathering</i>	37
<i>Distress No. 13: Rutting</i>	38
<i>Distress No. 14: Shoving of Asphalt Pavement by PCC Slabs</i>	38
<i>Distress No. 15: Slippage Cracking</i>	38
<i>Distress No. 16: Swell</i>	39
<i>Distress No. 17: Paving Lane Cracking (IDOT-DOA only)</i>	39
<i>Summary</i>	39

TABLE OF CONTENTS (Continued)

III.1.2.	<u>Distress Types Affecting PCC Pavements</u>	40
	<i>Distress No. 1: Blowup</i>	40
	<i>Distress No. 2: Corner Break</i>	40
	<i>Distress No. 3: Longitudinal, Transverse, and Diagonal Cracking</i>	41
	<i>Distress No. 4: Durability (D-) Cracking</i>	41
	<i>Distress No. 5: Joint Seal Damage</i>	41
	<i>Distress No. 6: Small Patch</i>	42
	<i>Distress No. 7: Large Patch</i>	42
	<i>Distress No. 8: Popouts</i>	42
	<i>Distress No. 9: Pumping</i>	43
	<i>Distress No. 10: Scaling, Map Cracking, and Cracking</i>	43
	<i>Distress No. 11: Settlements and Faulting</i>	43
	<i>Distress No. 12: Shattered Slab/Intersecting Cracks</i>	44
	<i>Distress No. 13: Shrinkage Cracking</i>	44
	<i>Distress No. 14: Transverse and Longitudinal Joint Spalling</i>	44
	<i>Distress No. 15: Corner Spalling</i>	45
	<i>Summary</i>	45
III.2.	The Pavement Condition Index Procedure	45
III.3.	IDOT-DOA Inspection Procedures	48
III.4.	Summary	49
IV.	FACTORS AFFECTING DISTRESS FORMATION AND PROPAGATION	50
IV.1.	Climate Related Factors	50
IV.1.1.	<u>Climatic Considerations</u>	50
	<i>Climatic Considerations for AC Pavements</i>	51
	<i>Climatic Considerations for PCC Pavements</i>	53
	<i>Summary</i>	54
IV.1.2.	<u>Climatic Models</u>	54

TABLE OF CONTENTS (Continued)

<u>IV.1.3.</u>	<u>Project Approach</u>	58
<u>IV.1.4.</u>	<u>Summary</u>	59
IV.2.	Load Related Factors	59
<u>IV.2.1.</u>	<u>Structural Considerations</u>	59
	<i>Structural Considerations for AC Pavements</i>	60
	<i>Structural Considerations for PCC Pavements</i>	60
<u>IV.2.2.</u>	<u>Loading Conditions</u>	61
<u>IV.2.3.</u>	<u>Structural Models</u>	62
	<i>AC Structural Models</i>	63
	<i>PCC Structural Models</i>	63
	<i>Summary</i>	64
<u>IV.2.4.</u>	<u>Project Approach</u>	64
	<i>Project Approach to Loading</i>	65
	<i>Project Approach to AC Structural Analysis</i>	66
	<i>Project Approach to PCC Structural Analysis</i>	70
IV.3.	Material/Construction Related Factors	76
<u>IV.3.1.</u>	<u>Material/Construction Considerations in AC Pavements</u>	77
<u>IV.3.2.</u>	<u>Material/Construction Considerations in PCC Pavements</u>	82
<u>IV.3.3.</u>	<u>Project Approach to Material/Construction Factors</u>	83
	<i>Classification of Pavement Type</i>	83
	<i>Summary</i>	84
V.	DESCRIPTION OF DATA BASE	85
V.1.	The ACCESS® Data Base	85
V.2.	Distribution of Pavement Sections	87
VI.	PAVEMENT PERFORMANCE AND LONGEVITY TRENDS	89
VI.1.	Pavement Performance Trends of Non-Rehabilitated Pavement Sections	90
<u>VI.1.1.</u>	<u>Initial Analysis of PCI Versus Age Performance Trends</u>	91

TABLE OF CONTENTS (Continued)

<u>VI.1.2</u>	<u>Development of Performance Trends Based on Deterioration Rate</u>	94
	<i>AC Pavement Performance Trends</i>	97
	<i>PCC Pavement Performance Trends</i>	98
<u>VI.1.3.</u>	<u>Summary</u>	99
VI.2.	Analysis of Rehabilitated Sections	100
VII.	PAVEMENT DISTRESS FORMATION AND PROPAGATION TRENDS	102
VII.1.	Deterioration Trends for AC Surfaced Pavements	102
<u>VII.1.1.</u>	<u>Alligator Cracking</u>	104
<u>VII.1.2.</u>	<u>Depressions</u>	108
<u>VII.1.3.</u>	<u>Longitudinal and Transverse Cracking</u>	108
<u>VII.1.4.</u>	<u>Oil Spillage</u>	109
<u>VII.1.5.</u>	<u>Paving Lane Cracking</u>	110
<u>VII.1.6.</u>	<u>Summary</u>	111
VII.2.	Deterioration Trends for PCC Pavements	111
<u>VII.2.1.</u>	<u>Corner Breaking</u>	113
<u>VII.2.2.</u>	<u>Corner and Joint Spalling</u>	114
<u>VII.2.3.</u>	<u>D-Cracking</u>	115
<u>VII.2.4.</u>	<u>Joint Seal Damage</u>	116
<u>VII.2.5.</u>	<u>Longitudinal, Transverse, and Diagonal Cracking</u>	117
<u>VII.2.6.</u>	<u>Summary</u>	119
VIII.	OBSERVATIONS AND RECOMMENDATIONS	120
VIII.1.	Observations	120
VIII.2.	Recommendations	126
IX.	REFERENCES	129
	TABLES	138
	FIGURES	163

TABLE OF CONTENTS (Continued)

APPENDIX A: Development of ILLI-PAVE-Based Algorithms for Conventional and FULL-DEPTH Asphalt Concrete GA Pavements	A-1
APPENDIX B: FWD Testing Procedures and Analysis at Pontiac and Morris Airports	B-1
APPENDIX C: AC Laboratory Testing Program	C-1
APPENDIX D: IDOT-DOA AC Mixture Properties	D-1
APPENDIX E: Summary of ILLI-SLAB Results	E-1
APPENDIX F: ACCESS® Data Base	F-1

EXECUTIVE SUMMARY

Introduction

There are 74 publicly owned airports in Illinois. The majority serve only general aviation (GA) aircraft having gross maximum weights less than 30,000 lbs. The Illinois Department of Transportation — Division of Aeronautics (IDOT-DOA) maintains general overall administrative responsibility for these airport pavements. This study, entitled Concepts and Practices for Considering GA Airport Pavement Performance and Longevity, was initiated by IDOT-DOA through the Illinois Transportation Research Center to examine GA pavement performance and the impact that load, climate, and materials/construction factors have on the formation and propagation of distress in GA pavements.

This project has evaluated the adequacy and efficacy of current GA airport pavement design and construction practices. The research approach incorporated the review of construction specifications and records, an analysis of statewide climatic factors and their influence on pavement material behavior, state-of-the-art structural and materials modeling and testing, and the analysis of pavement performance and distress data collected during the IDOT-DOA biennial pavement distress inspections. As a result, a better understanding of the distress mechanisms afflicting GA pavements has been obtained, potentially leading to improved material selection, design, and construction of GA pavements.

Observations

Based on the results of this study, the following general observations are made:

- IDOT-DOA distress data collection procedures are based on those recommended by the Federal Aviation Administration (FAA), with some notable modifications. It is difficult to directly compare Pavement Condition Index (PCI) values obtained by IDOT-DOA to those obtained in strict accordance with FAA procedures.

- The most recent IDOT-DOA specifications feature an increased reliance on IDOT-DOH (Division of Highways) specifications.
- Climatic variations can be considered by dividing the State into three climatic zones that correspond to existing IDOT-DOA administrative regions. Pavement temperature is the most relative climatic factor.
- Illinois GA airports carry a wide assortment of aircraft. The heaviest aircraft cited at the majority of airports included in this study is the Beechcraft King Air B200. In this study, load was not a major distress formation/propagation factor.
- IDOT-DOA pavement distress and inventory data were used to establish a relational data base containing 195 non-rehabilitated pavement sections. The data base contains loading, climatic, construction/material, and pavement condition information for each section. Specific pavement condition factors included section PCI values, sample unit PCI values, and distress types, severities, and quantities for each sample unit. A Deterioration Rate (DR) concept was developed to describe pavement performance and longevity trends. The DR is defined as the PCI loss per year.

Based on the results of this study, the following major observations are made concerning asphalt concrete (AC) pavements:

- IDOT-DOA accepts both the FAA and Asphalt Institute (AI) AC design procedures. Typical sections were designed using the FAA and the AI design procedures. An ILLI-PAVE-based mechanistic-empirical design approach indicates that the sections are structurally adequate for typical GA loading.
- Longitudinal and transverse cracking and paving lane cracking are the two most prevalent distress types. Both distresses had a high number of occurrences within the first five years of service, and continued to develop with time until almost all sample units are eventually affected. Significant amounts of alligator cracking were also recorded. It is believed that alligator cracking has been confounded with other distress types (i.e. block cracking, checking), and is likely considerably less prevalent than currently recorded.

- IDOT-DOA uses a PCI “trigger value” of 70 in programming a pavement section for future rehabilitation. AC pavement performance trends indicate that a PCI of 70 is observed prior to 20 years of service. Distinct differences in AC pavement performance between climatic zones could not be differentiated. Differences in short-term pavement performance (within the first 10-years of service) between pavements constructed with thin (≤ 5 inches) and thick (> 5 inches) AC layers were not observed. There are indications that long-term performance of pavements constructed with thick AC layers is better than that of pavements constructed with thin AC layers.

Based on the results of this study, the following major observations are made concerning portland cement concrete pavements (PCCP):

- IDOT-DOA accepts both FAA and the American Concrete Paving Association (ACPA) design methods for PCCP. Typical PCCP sections were designed using FAA and ACPA design methods. An ILLI-SLAB-based mechanistic-empirical design approach indicates that for normal GA loading conditions, both 6-in and 5-in thick PCCP are structurally adequate. Under some conditions, a 4-in thick PCCP is allowable using the ACPA design procedure. The structural adequacy of a 4-in thick PCCP is questionable.
- Commonly occurring PCCP distresses include corner breaking, corner and joint spalling, D-cracking, joint seal damage, and longitudinal, transverse, and diagonal cracking. The most important factor influencing PCCP distress formation and propagation is slab size, as characterized by the ratio of the slab length divided by the radius of relative stiffness (L/ℓ). Larger slabs have considerably higher distress occurrences and severities than smaller slabs.
- For 6-in thick PCCP slabs, slab lengths of 15 ft or less perform significantly better than longer slabs. At a PCI of 70, small slabs have projected service lives at or in excess of 20 years in two of the three climatic zones.

Recommendations

The observations from this study support the following major recommendations:

- Recent IDOT-DOA specification modifications (dated April, 1994) provide improved construction quality control. This effort should be continued. The effects of the AC specifications (P-201 and P-401), pertaining to the construction of paving lane joints, should be monitored.
- Current AC mixture design practices should be evaluated. The low VMA/low air content mixtures have "checked" in numerous GA projects. The use of SHRP asphalt cement binder specifications and Level 1 mix design procedures, featuring the use of the SHRP gyratory compactor, should be thoroughly evaluated for potential use.
- The most important PCCP design parameter is slab size. This study has shown that, in general, small slabs have lower Deterioration Rates (DRs) than medium or large slabs. Short joint spacing results in increased construction costs and more joint related distress (such as D-cracking and spalling). Higher joint re-sealing costs are also incurred with shorter joint spacing. The advantages/disadvantages of various slab sizes up to 15 ft in should be further investigated. L/l should be used to select appropriate PCC slab lengths.
- A DESIGN CATALOG approach should be considered to standardize Illinois GA pavement design procedures. Mechanistic-empirical design approaches can be utilized to design pavement structures for Illinois climatic conditions and commonly used materials. The catalog can be arranged according to climatic zone, traffic loading, and subgrade strength/stiffness properties. A number of alternative pavement designs would be presented for a given set of design conditions.

I. INTRODUCTION

I.1. Problem Statement

In the State of Illinois, there are 74 publicly owned airports, the majority of which serve only general aviation (GA) aircraft having gross maximum weights less than 30,000 lbs. Although less visible than the larger air carrier, reliever, and commercial airports found near metropolitan centers, the smaller GA airports provide a valuable service to many communities. The GA airport pavement network within the State represents a considerable public investment, with initial construction and major rehabilitation costs heavily subsidized by both Federal and State funding. The Illinois Department of Transportation — Division of Aeronautics (IDOT-DOA) maintains general overall administrative responsibility for these airport pavements. This study, entitled Concepts and Practices for Considering GA Airport Pavement Performance and Longevity, was initiated by IDOT-DOA through the Illinois Transportation Research Center to examine GA pavement performance and the impact that load, climate, and materials/construction factors have on the formation and propagation of distress in GA pavements.

It appears that both IDOT-DOA personnel and many local governments assume a 20-year pavement life although a 20-year design period is not explicitly stated in the Federal Aviation Administration (FAA) design procedure [FAA, 1978]. This assumption is based on the observation that GA pavement construction is typically funded through bond issues maturing in 20 years. IDOT-DOA has noted that in some cases pavement life is not meeting design expectation. Although major rehabilitation costs are substantially subsidized by the State and Federal governments, routine maintenance activities, including crack and joint sealing, patching, and the application of surface treatments are currently the sole responsibility of the local governing agency. As a result, in many instances, maintenance work is delayed or simply not conducted, contributing to continued pavement deterioration.

This project examines the adequacy and efficacy of current GA airport pavement design and construction practices in light of the data collected during the IDOT-DOA biennial pavement

distress inspections. The research approach is based on the analysis of the pavement distress data, review of the construction records, an analysis of statewide climatic factors and their influence on pavement material behavior, and limited structural and materials modeling and testing. A better understanding of the distress mechanisms affecting GA pavements has been obtained, potentially leading to improved material selection, design, and construction of GA pavements in the State of Illinois.

I.2. Objectives

The objective of this research study is to establish performance trends for GA airport pavements subjected to the diverse climatic conditions and material characteristics found throughout the State. This objective was addressed through examination of the influence loading, climate, and materials has had on the formation of pavement distress and the resulting impact on pavement performance and life . Specific objectives include:

- Use historical pavement distress data, collected in accordance with the pavement condition index (PCI) procedure, and state-of-the-art soils, materials, climatic, and pavement analysis and design technology, to quantify the combined damaging effects of load, climatic, and materials/construction factors on typical GA airport pavements.
- Identify/separate and quantify, to the extent possible, the relative contribution of load, climatic, and material/construction factors to the observed pavement performance.
- Consider, from the perspective of this study, the adequacy and efficacy of the FAA procedures presented in FAA Advisory Circular 150/5320-6C for the design of Illinois GA airport pavements.
- Develop suggested modifications and improved/refined procedures and techniques for achieving more cost effective, better performing, and increased longevity GA airport pavements.

I.3. Scope

This study focuses exclusively on the pavement performance trends of Illinois GA pavements and the scope is limited to the following:

- Only Illinois GA airport air-side pavements are investigated, including runways, taxiways, and aircraft parking aprons. Access roads, service roads, and land-side vehicle parking areas are not considered.
- Pavement types investigated are thin asphalt concrete (AC) (2 to 5 in of AC on one or more granular layers), thick AC (greater than 5 in of AC with or without a granular layer) and portland cement concrete (PCC).
- Distress data collected only on non-overlaid pavement sections are used. This limits the application of the results of this study to newly constructed pavement sections only.
- GA pavement sections are defined as those subjected to typical aircraft loading of 30,000 pounds or less. This primarily restricts this investigation to GA airports only. Some larger airports maintain facilities for the exclusive use of GA aircraft, and some of these sections have been incorporated into the study.

The distress data used in this study were collected by IDOT-DOA over the last 14 years. The pavement distress, performance, and expected life trends developed will reflect actual manifestation of pavement distress observed in the field and also the inherent variability connected to the PCI procedure as utilized by IDOT-DOA engineers and technicians.

II. DESIGN AND CONSTRUCTION PRACTICES

In the design and construction of new GA airport pavements, IDOT-DOA provides guidance and review, but does not design pavements or provide project level construction inspection services. This limits IDOT-DOA's ability to influence the design and construction process. In extreme/rare instances, approval of a design may be withheld. IDOT-DOA provides oversight, but is not involved in the daily inspection of the construction. During construction, inspections are conducted by the airport's consultant, who then prepares and submits a final engineering report to meet State and Federal funding requirements. Thus, the types of designs submitted and the quality of construction inspection is highly dependent on the local consultant, not IDOT-DOA.

Pavement design schemes accepted by IDOT-DOA include those described in the FAA AC 150/5320-6C, Airport Pavement Design and Evaluation [FAA, 1978], and also those available from the Asphalt Institute (AI) [AI, 1987] and the American Concrete Paving Association (ACPA)[ACPA, 1993]. Material and construction specifications are provided in an IDOT-DOA document entitled, Standard Specifications for Construction of Airports [IDOT-DOA, 1985], which has been modified periodically.

A brief historical review of the Illinois GA design and construction process begins this discussion. It is followed by a detailed review of the current design procedures and material/construction specifications.

II.1. Historical Perspective

The earliest "all-weather" surfaced GA airport pavements constructed in Illinois were built in the mid to late 1930's near metropolitan areas. These pavements, which replaced turf facilities, typically consisted of bituminous surface treatments over granular base to facilitate use during wet weather. During and immediately after World War II, the federal government participated in the construction of a number of airports throughout the country including several

in Illinois. These airports all shared similar layouts and pavement designs, consisting of three PCC runways and a supporting network of taxiways and aprons. In Central Illinois, Champaign, Decatur, Springfield, Peoria, and Quincy are examples of airports built at this time. Although most of the original pavement sections have long since been rehabilitated or abandoned, a few remain in service, including sections at Champaign and Quincy. It was also during this time that the Illinois Department of Aeronautics was formed to oversee the development of the State's airport network.

Large-scale development of Illinois' GA airports continued in the 1950's. Although both PCC and conventional AC pavements were built during this decade, the historical record shows that the most common pavement section consisted of a 6-in thick granular layer covered with a bituminous surface treatment. This design was based on federally issued specifications that were quite simple in both scope and flexibility. When conventional flexible pavements were constructed, they typically had AC thickness of 2 in or less. PCC pavements continued to be built, including some 6-in thick runway sections. By the end of the 1950's, the Department of Aeronautics had issued their own specifications book for the construction of GA pavements.

Considerable GA pavement construction was performed in the 1960's. In the early part of the decade, a 2-in thick AC surface on a granular base/subbase became the most common type of pavement, replacing bituminous surface treatments of the 1950's. The first FULL-DEPTH AC pavements were constructed by the end of the 1960's. PCC sections continued to be built, most often restricted to apron areas at some of the busier GA airports. It was during this decade that federal influence increased, and the Department of Aeronautics rescinded their own specifications and adopted those issued by the Federal Aviation Administration.

In the early 1970's, the Department of Aeronautics was incorporated into the Department of Transportation and was renamed the Division of Aeronautics. Standardization of the design procedures and construction specifications was established in the 1970's with the issuance of FAA AC 150/5370-10, Standards for Specifying Construction of Airports [FAA, 1974] and FAA AC 150/5320-6C, Airport Pavement Design and Evaluation [FAA, 1978]. Both these documents

were used by IDOT-DOA and the consultants who designed and constructed GA airport pavements. The trend toward thicker AC layers continued during this decade, with continued construction of FULL-DEPTH AC pavement sections at a number of airports. The use of lime-treatment for subgrades became more common, a practice which continues today. Conventional AC designs featuring the use of granular base and/or subbase typically employed thicker AC layers (commonly 3 to 5 in) than in the 1960's. PCC pavements continued to be built at about the same rate as before, primarily restricted to more heavily trafficked facilities and to apron areas, although more PCC taxiways and runways were constructed. PCC Joint spacing was commonly 20 ft.

Significant changes to IDOT-DOA pavement design and construction policy occurred during the 1980's. IDOT-DOA published their own construction specifications in 1985 in a document entitled Standard Specifications for Construction of Airports [IDOT-DOA, 1985]. These were based on FAA specifications, with modifications made to address issues that were specific to the State of Illinois (e.g. the use of IDOT standardized aggregate gradations) and those that dealt with the unique aspects of GA pavement performance under the State's climatic conditions (e.g. AC mix designs were modified to reduce air voids and increase asphalt cement content in an attempt to address asphalt aging problems inherent in many older pavements). Changes to pavement design were also implemented, with shorter joint spacing and innovative jointing practices becoming more common for PCC. A minimum 3-in AC layer thickness was established by IDOT-DOA based on inadequate performance of previously constructed 2-in thick AC surface courses.

Toward the end of the 1980's and into the early 1990's, there were major modifications to the FAA and IDOT-DOA materials specifications. Most significant were changes implemented in the quality assurance/quality control (QA/QC) elements of the specifications, which were modified to employ more sophisticated statistical procedures. Other changes were added to address some specific construction defects and durability problems observed in existing pavements.

The general trend in IDOT-DOA AC pavement design in the 1990's has been to move away from FULL-DEPTH AC pavement sections through the insertion of a granular subbase layer above the subgrade to facilitate drainage. New pavement sections are rarely FULL-DEPTH AC, but include either thick or thin AC layers on granular base/subbase. The thickness design schemes have not been significantly modified since the late 1970's, however material selection and construction specifications have been changed to reflect recent industry innovations.

II.2. Current Pavement Thickness Design Methodologies

Most Illinois GA pavement designs are based on the guidelines provided in Chapter 5 of FAA 150/5320-6C [FAA, 1978]. These procedures are not calibrated for specific climatic or geographical regions, but are meant to serve the country as a whole. No design period is explicitly stated for GA pavements.

IDOT-DOA also accepts the AC thickness design procedures advocated by the AI in their publication entitled, Thickness Design—Asphalt Pavements for General Aviation [AI, 1987] and the PCC design procedures described by the ACPA in their document entitled, Concrete Pavements for General-Aviation Airports [ACPA, 1993]. Although not commonly used, each of these design procedures will be reviewed along with the FAA procedures.

II.2.1. AC Pavement Thickness Design

FAA Methodology for the Design of AC Pavements

In the procedures presented in FAA AC 150/5320-6C [FAA, 1978], the required AC pavement thickness is a function of two factors: the gross weight of the aircraft and soil strength. The interaction of these two factors is shown in Figure 1, which is used to determine the pavement thickness given the California Bearing Ratio (CBR) of the subgrade soil and the maximum aircraft gross weight. Neither the number of aircraft coverages nor gear configuration is a design input. It is apparently assumed that for GA airport traffic, an AC pavement designed

for the heaviest aircraft loading will be structurally sufficient to accommodate the entire expected traffic volume and aircraft mix over the design period. The key to extending design life is thus based on addressing climatic and material/construction deterioration factors through material/construction specifications.

The thickness design process is conducted as follows. First, the subgrade soil CBR is entered into the chart along the upper horizontal axis. A vertical line is projected downward from the selected CBR value to a curve representing the maximum gross weight of the heaviest aircraft expected to use the pavement. A horizontal line is then extended from that intersection to the diagonal pivot line, at which point a vertical projection is made downward to read the required total pavement thickness from the lower horizontal axis. In the example illustrated in Figure 1 (a CBR of 7.5 and maximum gross aircraft weight of 24,000 lbs), the required total pavement thickness is 12.25 in.

This initial thickness determination produces the required total pavement thickness. The same design chart is then used in a second iteration to determine the subbase thickness. A CBR of 20 is assumed and the same process is followed as previously described. The difference between this thickness, which represents the required thickness of the surfacing and base and the total pavement thickness, is the required thickness of the subbase. The design procedure further indicates that the required range in subbase thickness is 0-14 in and the range in base thickness is from 3 to 6 in. In the previous example, a CBR of 20 would yield a required thickness of 6.75 in, thus the subbase thickness is $12.25 \text{ in} - 6.75 \text{ in} = 5.5 \text{ in}$. If a 2-in AC surface is used, a 4.75-in thick base is required to provide the full pavement thickness.

Although FAA AC 150/5320-6C allows for AC surfacing as thin as 2 in, IDOT-DOA recommends a minimum AC thickness of 3-in for GA airport pavements. According to IDOT-DOA personnel, this recommendation, although not a written policy statement, reflects years of experience that indicates thinner AC layers do not provide desired performance levels.

A typical conventional AC pavement design consists of a thin AC layer on one or more granular layers. Alternatively, one or both granular layers can be replaced with a stabilized material using the equivalency factors provided in Chapter 3 of FAA AC 150/5320-6C. These equivalency factors are shown in Tables 1 and 2. If the base and/or subbase layers are replaced with AC, the pavement section would approach what is commonly referred to as a FULL-DEPTH AC pavement

FULL-DEPTH AC design is addressed very briefly in paragraph 85 of FAA AC 150/5320-6C. This paragraph defers to paragraph 37 in the same Advisory Circular, which states that the equivalency factors can be used to design a FULL-DEPTH AC pavement section. It also permits the methodology described in Asphalt Institute Manual Series No. 11 to be used if approved by the FAA. A 1992 draft of the revised Advisory Circular designated FAA AC 150/5320-6D proposes modifications to the GA pavement design that are relevant to this study, particularly concerning FULL-DEPTH AC pavement sections. It states that the guidance provided in Asphalt Institute Information Series No.154, "Thickness Design—Asphalt Pavements for General Aviation," [AI, 1987] can be used to design FULL-DEPTH AC pavements on a case-by-case basis.

To conduct a FULL-DEPTH AC design using equivalency factors, a conventional design is executed, then each layer thickness is subsequently converted to an "equivalent" AC thickness. For the example describe previously, the section is converted to FULL-DEPTH thickness using mid-range equivalency factors as described below:

- 2-in thick AC surface.
- Convert 4.75-in base to AC using an equivalency factor of 1.4, yielding an additional 3.4-in thick AC layer.
- Convert 5.5-in subbase into AC using and equivalency factor of 2.0, yielding an additional 2.75-in thick AC layer.
- The total FULL-DEPTH AC thickness would thus be 8.15 in.

The conventional AC pavement thickness is reduced from 12.25 in to a 8.15 in FULL-DEPTH AC section. Depending on the choice of equivalency factors within the recommended range, the FULL-DEPTH AC section can have thickness from 7.4 in to 9.2 in.

The FAA procedure provides a description of soil stabilization techniques available to the engineer in FAA AC 150/5320-6C, Chapter 5, Paragraph 82 and Chapter 2, Paragraph 13. In Chapter 5, Paragraph 82 (3b), it is stated that lime-treated subgrade can be used as a subbase course, but no specific guidance is provided to assign a structural value to the improved soil.

The procedures presented in FAA AC 150/5320-6C permit the use of bituminous surface treatments in-place of the AC surface, using an equivalency of 1.2 to 1.6 to replace the AC surfacing with granular base material. This practice, although used by IDOT-DOA in the past, was discontinued in the mid-1960's due to the short service life observed for surface treatment pavements. According to IDOT-DOA personnel, the short service life was significantly less than the maturation time for the construction bonds.

Asphalt Institute Methodology for the Design of AC Pavements

The AI flexible GA pavement design methodology is provided in their document entitled, Thickness Design—Asphalt Pavements for General Aviation. [AI, 1987]. This design scheme considers three factors that influence the required thickness of the flexible pavement: aircraft gross weight, subgrade support, and properties of the pavement materials. The procedure used a mechanistic-empirical approach, employing an elastic-layered program and empirically derived transfer functions to estimate allowable aircraft loading. The results of the analysis were used to develop design charts to determine thicknesses for three pavement types.

The AI FULL-DEPTH AC pavement design is conducted using the chart reproduced in Figure 2. The gross weight of the aircraft is entered on the horizontal axis, and a vertical projection is made to the diagonal line representing the subgrade soil support value. A horizontal projection is then made from this intersection to determine the required thickness of AC read

from the vertical axis. For the example described in the previous section, a subgrade CBR of 7.5 and a gross maximum aircraft weight of 24,000 lbs would result in a required FULL-DEPTH pavement thickness of 8 in. This compares favorably with the 8.15-in thickness recommended using the mid-range FAA equivalency factors.

Figures 3 and 4 show the AI design charts for emulsified asphalt base and untreated base, respectively. These design charts are used in a fashion similar to that for FULL-DEPTH pavement, except that Figure 3 is used to determine the thickness of the emulsified base given an AC surface thickness of 2 in. When using Figure 4, the AC thickness is determined assuming that a 6-in thick P-208 granular base is used. The recommended minimum AC thickness is 4 in. For the previously described example, the conventional flexible pavement design approach requires a 6-in thick AC layer on a 6-in granular base. When compared to the FULL-DEPTH AC section, a 2 in reduction in AC thickness results from the use of the 6-in thick granular base.

Soil-lime treatment is only superficially addressed in the AI pavement design method, referring to the use of "improved subgrade" in a footnote. No provision is made to incorporate the use of soil-lime layers into the pavement design.

Summary

The two AC pavement design schemes used for GA airport pavements are based solely on the support value of the subgrade (i.e. CBR or resilient modulus) and the maximum gross weight of the aircraft. Climatic conditions and number of load repetitions are not considered. The designer has some flexibility in material selection, most notably by thickening the AC surface to reduce or eliminate the need for the granular base, and possibly the subbase. Greater flexibility exists with the FAA procedure, which allows for a variety of materials and thicknesses.

II.2.2. PCC Pavement Thickness Design

Design of PCC (rigid) pavements is discussed both in FAA and ACPA publications. A review of both methodologies is presented below.

FAA Methodology for the Design of PCC Pavements

Chapter 5 of FAA AC 150/5320-6C provides guidance for the design of PCC pavements. The thickness design method is a "standard structure" procedure. If the gross maximum aircraft weight is 12,500 lbs or less, a 5-in thick PCC slab should be used. If the gross maximum aircraft weight is between 12,500 and 30,000 lbs, a 6-in thick PCC slab is required. Subgrade strength, number of aircraft load repetitions, and climatic conditions are not considered. If the pavement is to serve aircraft between 12,500 lbs and 30,000 lbs, a minimum 4-in thick granular subbase is required. A subbase is not required for aircraft weighing less than 12,500 lb, unless the subgrade is classified as OL, MH, CH, or OH.

Recommended jointing design practices are also presented. FAA AC 150/5320-6C recommends that longitudinal joint spacing should be 12.5 ft and transverse joint spacing should be 15 ft. IDOT-DOA has allowed the use of 20 ft transverse joint spacing in the past, but currently follows the FAA recommendations.

Typical PCC joints are shown in Figure 5. Specific jointing requirements are as follows:

- Keyed joints are restricted to pavement thicker than 9 in.
- Thickened edges are not required when design is based on aircraft weighing 12,500 lbs or less.
- The last three transverse joints on a runway or taxiway should be doweled (Type D) joints.
- The outer lanes of all features should be tied to the inner lane with Type C hinged joints.
- Odd shaped slabs should be reinforced with 0.05% steel in both directions.

Engineering Brief No. 27, published by the FAA in 1981, addresses the jointing of PCC pavements for GA airports in much greater detail [FAA, 1981]. Although the Engineering Brief recommendations were never fully adopted by the FAA or IDOT-DOA, they have been largely embraced by the ACPA and are included in the draft version of the latest FAA Advisory Circular [FAA, 1992]. The author of the Engineering Brief states that the modifications will "result in cost savings and should provide adequate performance" as compared to recommendations made in FAA AC 150/5320-6C.

The concept espoused in Engineering Brief No. 27 is the creation of a "tension ring" to hold interior joints tightly closed. The following major modifications to AC 150/5320-6C are listed in the Engineering Brief [FAA, 1981]:

- Dowels are required for transverse construction joints only.
- A half round keyway is used for load transfer in longitudinal construction joints.
- The last three contraction joints and longitudinal construction joints at the free edge of the pavement are tied with #4 deformed bars, 20-in long, spaced 36-in center to center. Although a risk of cracking exists, it is the stated belief of the authors that the risk is worth the benefit resulting from keeping interior joints tight. All other joints are dummy groove untied (Type E).
- A thickened edge (Type B) should be located in trafficked areas, having a 3 ft taper to 1.5 times the slab thickness.
- The slab size in feet should not exceed twice the slab thickness in inches (i.e. 6-in) slabs should not exceed 12 ft in length.

Figures 6 and 7 are reproduced from the Engineering Brief, showing the recommended joint layout for a 50 ft and 60 ft wide pavement section, respectively.

The influence of Engineering Brief No. 27 is readily evident in the draft copy of FAA AC 150/5320-6D [FAA, 1992]. The tension ring concept is fully described, including recommended jointing patterns for 50 ft and 60 ft wide features that include tying together exterior joints as

described above. Also allowed is the use of the half round keyed longitudinal joint. The thickened edge requirement was reduced from 1.25 to 1.5 times the slab thickness.

One notable change from Engineering Brief No. 27 is the recommendation that the maximum allowable joint spacings be 12.5 ft for longitudinal and 15 ft for transverse, which is consistent with the past Advisory Circular. If the last three contraction joints at the end of a feature are tied as recommended, 37.5 ft of pavement would be tied together if the joint spacing is 12.5 ft. Allowing 15 ft joint spacing would extend this length to 45 ft.

ACPA Methodology for the Design of PCC Pavements

The American Concrete Paving Association recommendations are presented in their Concrete Information Series entitled, Concrete Pavements for General-Aviation Airport [ACPA, 1993]. The ACPA recommendations are:

- A subbase is not needed under most applications, recommended only if there are over 100 daily operations of the heaviest aircraft and/or uniform subgrade support cannot be achieved. If a subbase is to be used, it should be a 4-in thick non-plastic granular material with less than 15% passing the No. 200 sieve.
- Simplified and detailed thickness designs are provided. The simplified procedure is based solely on heaviest aircraft loading as tabulated in Table 3. The detailed thickness design method uses the 90-day PCC flexural strength (third point loading), the subgrade k-value, and the magnitude, number, and gear configuration of the design aircraft loading as reproduced in Figures 8 and 9. The design flexural stress is obtained by dividing the flexural strength by a safety factor (ranges from 1.4 to 2.0) that depends on the number of aircraft operations.
- If it is anticipated that the pavement will carry heavy service vehicles or fuel trucks, the recommendations made in Table 3 can be used to design the pavement thickness. Using this criteria, the recommendation for an 18 kip dual tandem axle load service vehicle would be a 5-in thick PCC pavement.

- Joint spacing should "not greatly exceed" 25 times the slab thickness, with maximum recommended joint spacing of 10 ft for a 5-in thick slab and 12.5 ft for a 6-in thick slab.
- Trapezoidal keyways are allowed.
- It is recommended that all longitudinal joints be tied for runways and taxiways having widths of 60 ft or less. In wider sections, tied joints are recommended within 30 ft of the pavement edge.
- Transverse joints should be dowelled if a "large number" of design aircraft loadings are expected. In these situations, dowels should be used in the last six joints back from the pavement end.

The simplified ACPA procedure recommends a 5.5-in thick slab for a 24,000 lb dual wheel aircraft. If the more detailed analysis is used (assuming a k-value of 100 pci, 30,000 total operations, and a 90-day PCC flexural strength of 650 psi), a design thickness of 4.8 in for a dual-wheel landing gear is obtained. Compared to the FAA design (a 6-in thick slab), the ACPA methodology results in a significant reduction in pavement thickness.

Little mention of climatic effects is addressed in either of the design procedures examined. An exception is that joint spacing was linked to regional experience in the ACPA procedure. Only the detailed ACPA method considered material properties, subgrade support, and traffic type and volumes.

Summary

For PCC pavement design, the FAA recommends a standard section structure of 6 in if the maximum gross aircraft weight is in excess of 12,500 lbs. For lighter aircraft, a 5-in thick PCC slab is acceptable. There is no input for subgrade support or number of aircraft repetitions. Maximum recommended joint spacing is 12.5 ft and 15 ft for longitudinal and transverse joints, respectively.

The ACPA has two design methodologies. In the more rigorous approach, subgrade support, PCC strength, aircraft gear configuration, and number of repetitions are included as design inputs. The minimum PCC thickness can be as low as 4-in. Recommendations for joint spacing are related to slab thickness, and are typically shorter than that recommended by the FAA.

II.3. Material and Construction Specifications

IDOT-DOA and the FAA use similar paving material codes. Material codes of particular interest to this project are defined in Table 4. The following discussion will focus on the IDOT-DOA and FAA specifications addressing AC, PCC, and granular base/subbase layers.

II.3.1. AC Material and Construction Specifications

FAA AC 150/5370-10 classifies all hot-mix AC as Item P-401, "Bituminous Surface Course." To eliminate confusion in specifying a surface course and a base/binder course, IDOT-DOA uses Item P-401 to specify bituminous surface courses and Item P-201 for bituminous base/binder courses. Both the FAA and IDOT-DOA specifications have been modified since originally issued, and this discussion will use the most current specification unless otherwise noted. The current FAA specification is dated January 25, 1994 [FAA, 1994A], while the most recent IDOT specifications are dated April 1, 1994 [IDOT-DOA, 1994B]. IDOT-DOA specifications are further separated according to the size of the project. Method I is for projects having less than 2,500 tons/pay item/location and Method II covers larger projects. Only Method II will be examined.

Aggregate Type and Gradations

Allowable aggregate types and gradations specified for Item P-401 in the IDOT-DOA specifications differ slightly from the FAA. In the IDOT-DOA specifications, it is stated that "aggregates shall consist of crushed stone or crushed gravel, blended with crushed or natural

sand(s) and/or mineral filler." The use of slag is not allowed in the IDOT-DOA specifications, although it is permitted in the FAA specifications.

In comparing coarse aggregate quality tests, the FAA allows an LA abrasion percentage wear of 40% and 50% for surface and base layers, respectively, compared to 40% and 45% for IDOT-DOA mixes. The sodium sulfate loss, as measured by ASTM C 88, is less restrictive for IDOT-DOA mixes at 15% and 20% for surface and base layers, respectively. The FAA maintains a requirement of 10% regardless of the layer. IDOT-DOA also include requirements related to the presence of deleterious materials, including the maximum percent allowable shales (2.0%), clay lumps (0.5%), soft and unsound fragments (6.0%), and other deleterious materials (2.0%), for a total maximum allowable deleterious material content of 6.0%.

Both specifications allow for the use of natural sand to obtain a desired aggregate blend or to improve workability. The FAA restricts the amount added to 20%, but no restriction is applied by IDOT-DOA. The FAA maintains limits on the plasticity index and liquid limit values for fine aggregate, at 6 and 25, respectively. Instead of maintaining plasticity limits, IDOT-DOA specifications limit the percent minus No. 200 material allowable (6.0%) and the maximum percent clay allowable (3.0%). IDOT-DOA has requirements on the type and amount of deleterious material allowed, with a total maximum allowance of 5.0%. This is in contrast to the FAA specification which states that the fine aggregate must be "free from coatings of clay, silt, or other objectional matter and shall contain no clay balls."

The FAA, IDOT-DOA, and the AI have different recommendations for aggregate gradations, as shown in Table 5. In the most recent IDOT-DOA specifications, 3/4 in and 1 in maximum aggregate size gradations are used for P-401 and P-201, respectively.

Job Mix Formula

This discussion considers comparison of mix designs for pavements serving aircraft having a gross maximum weight of less than 60,000 lbs. FAA and IDOT-DOA mix design is

based on the Marshall Method described in the current version of Asphalt Institute MS-2, Mix Design Methods for Asphalt Concrete [AI, 1993].

For GA mixes, a 50 blow mix design is specified. IDOT-DOA requires a 1500 lb minimum stability, 8 to 18 (in units of 1/100 in) flow, and 2 to 3 percent air voids compared to the FAA requirements of 1350 lb stability, 10-18 flow, and 2.8 to 4.2 percent air voids. The latest version of the FAA specifications includes requirements for stability, flow, and air voids and allowable maximum standard deviations for each. The standard deviation provision takes mixture variability into account, resulting in higher stabilities than those normally required, as well as the use of mid-range values for flow and air voids.

IDOT-DOA specifications require an AC-10 asphalt cement. The FAA allows a wide-range of asphalt cement grades (AC-2.5, AC-5, AC-10, AC-20, AC-30, and AC-40). A major difference between the two specifications is the approach to voids in the mineral aggregate (VMA). Current FAA and previous IDOT-DOA specifications set a minimum VMA percentage based on the maximum aggregate size of the mix. In the most recent IDOT-DOA specifications, a range of 75% to 90% voids filled with asphalt (VFA) is used. The VFA approach eliminates the need to link VMA to maximum aggregate size. It is noted that the use of VFA in lieu of VMA by itself does not ensure that AC mixtures that are less susceptible to age hardening will be specified. In the modified IDOT-DOA specifications, a possible VMA range from 7% to 30% can be obtained within the VFA and air content ranges. Because specified mixture properties are broad, the specification does not ensure that AC mixtures that are less susceptible to age hardening will be produced.

The IDOT-DOA specifications for central plant hot-mix base course is designated Item P-201. The major difference in this specification is that it provides an additional gradation for a maximum aggregate size of 1.25-in. At the discretion of the Resident Engineer, 25% of recycled asphalt pavement (RAP) may be added to the mix. RAP is also allowed under the most recent FAA specifications, which require that design procedures contained in Asphalt Institute MS-20, Asphalt Hot-Mix Recycling [AI, 1981], be used in the design of the mix.

The FAA stipulates that for gross maximum aircraft weights less than 12,500 lbs, high-quality state highway department hot-mixes with a proven record of good performance may be used. A similar provision is provided in the AI recommendations, but not in IDOT-DOA specifications.

Construction Practices

The FAA and IDOT-DOA specifications require a test section be constructed to establish an acceptable rolling pattern. The most recent revisions to the IDOT-DOA specification changed the test section procedure. A two step approach is specified. The first step establishes a growth curve for a specified vibratory roller to determine the maximum "compactability" of the mix. The Contractor then establishes a rolling pattern for the equipment he plans to use. The Contractor proposed construction equipment must meet the compaction efficiency of the IDOT-DOA specified vibratory roller. The minimum density of the completed test section is 94% (6% air voids) of the maximum theoretical specific gravity of the mix as measured by ASTM D 2041. This is determined from core samples.

A unique feature of the IDOT-DOA test section is that the Contractor must provide a nuclear density gauge for construction quality control. This nuclear density gauge shall be calibrated during test section construction and used "to maintain quality control of density" as specified. The nuclear gauge density data are not for acceptance testing. Acceptance testing is based on cores obtained after mat compaction is completed. The test section is constructed in a single lane, and thus joint densities are not examined.

In contrast, the FAA specifications require that two paving lanes be constructed in the test section, with a cold longitudinal joint formed between them. A specified number of cores and un-compacted plant samples are taken to evaluate stability, flow, mat density, air voids, joint density, gradation, asphalt cement content, and VMA. FAA specifications do not require the use a nuclear density gauge for quality control.

IDOT-DOA specifications permit the use of bituminous mixing plants approved by the IDOT Division of Highways for the production of Class I bituminous mixtures [IDOT, 1994]. If the plant is not approved for Class I mix production, it must meet a very specific list of IDOT-DOA requirements.

IDOT-DOA P-201 and P-401 specifications permit a maximum lift thickness of 2 in, with 3-in lifts allowable if authorized by the Resident Engineer. IDOT-DOA personnel indicated that this specification was established to address poor compaction of thicker AC lifts. If the ability to construct thicker lifts of acceptable densities can be demonstrated, a Contractor would be allowed to exceed the 3-in maximum lift requirement.

Current IDOT-DOA specifications require a minimum 10 ft paver width and a minimum 1 ft offset between the joints in successive lifts. The uppermost longitudinal joint is located at the centerline of the pavement. This is similar to the FAA requirement, except that the FAA stipulates that "the Engineer should specify the widest paving lane practicable in an effort to hold the number of longitudinal joints to a minimum." [FAA, 1994A].

When compacting adjoining lanes, IDOT-DOA requires that the first pass be along the common longitudinal joint, with the vibratory roller overlapping the previously compacted lane by 6 to 8 in. If a static roller is being used, the overlap should be such that 6 to 8 in is on the fresh mix, with the remaining width of the roller on the cold lane. Specifically, it is required that all joints have the same texture, density, and smoothness as other sections of the AC course.

In the most recent specifications, IDOT-DOA has addressed joint compaction with the insertion of the following paragraph:

All longitudinal joints constructed are to be compacted in such a manner that they are "pinched" to provide adequate density at the joint. The method of "pinching" shall be as defined in the most recent issue of the N.A.P.A. (*sic*) Superintendent's Manual on Compaction of Asphalt Pavements [IDOT-DOA, 1994A and 1994B].

By including this paragraph, IDOT-DOA is attempting to benefit from the most recent developments in joint compaction, realizing that research is continuing in this area. The FAA specifications are based on meeting the same density requirements as for the mat, with the only requirements being that the joints are continuously bonded and have the same texture as other sections of the course, meeting smoothness and grade requirements.

Another recent addition to the IDOT-DOA compaction requirement is that a self-propelled pneumatic-tired roller be used during construction of the top lift of the surface course mixture (P-401).

Acceptance Testing

~~Significant recent changes have been made in acceptance testing procedures. This brief discussion will only introduce the criteria being used by IDOT-DOA and the FAA, but will not provide a detailed description of the procedures.~~

IDOT-DOA accepts the constructed pavement on the basis of percent air voids in the final compacted mat. Each P-201 and P-401 course shall be compacted to a minimum density of 93% (7% air voids) of the maximum theoretical specific gravity (ASTM D 2041). A statistical sampling procedure is used based on two cores from each 500 ton subplot. Four sublots compose a lot, which is the basic payment unit. Each core is evaluated using Marshall, extraction, maximum specific gravity, and air void test procedures. The payment schedule is based solely on the air void content of the mix, with 100% payment made if the percent within limits (PWL) lies between 90% and 100%. Penalties are assessed when the PWL lies between 65% and 90%, and a lot that has a PWL below 65% must be removed and replaced at the Contractor's expense. There is no provision for incentive payments in the IDOT-DOA specifications.

The comprehensive FAA acceptance criteria uses stability, flow, air voids, mat density, joint density, thickness, smoothness, and grade to determine payment. Only one core is obtained

from each subplot in addition to a sufficient quantity of un-compacted plant mix to conduct all necessary tests. The FAA and IDOT-DOA price adjustment schedules are the same for mat density and air voids. If the stability, flow, and joint density PWL requirements fall between 80% and 90%, the Contractor must take corrective action. If the PWL falls below 80%, the plant must be shut down until adjustments are made. Pavement thickness must meet the requirement shown on the plans. Pavement smoothness is measured with a 12-ft straight-edge and the maximum allowable tolerance depends on whether the lift is a base or surface course. The finished pavement surface grade must be within 0.5 in of that shown on the plans to be accepted. If more than 15% of the smoothness or grade measurements fall outside the tolerances within a 2000 yd² lot, the deficient area must be corrected by the Contractor.

Summary

Modifications to the AC material specification address some of the deficiencies noted in previous construction. The most recent longitudinal joint compaction requirements and pneumatic-tired rolling of the surface course are designed to address defects in past construction that have lead to paving lane cracking and surface checking.

IDOT-DOA has attempted to address age hardening of the asphalt cement through the use of low air voids and low VMA mixes. The VFA approach eliminates the need to link VMA to maximum aggregate size. It is noted that the use of VFA in lieu of VMA, by itself, does not ensure that less age hardening susceptible AC mixtures will be specified. In the modified IDOT-DOA specifications, a possible VMA range from 7% to 30% can be obtained within the VFA and air content ranges. Because specified mixture properties are broad, the specification does not ensure that less age hardening susceptible AC mixtures will be produce in all cases.

II.3.2. PCC Material and Construction Specifications

Specifications for portland cement concrete are presented under Item P-501 of the FAA and IDOT-DOA standards. The P-501 specifications have been recently updated. IDOT-DOA's

most recent release is dated April 1, 1994 [IDOT-DOA, 1994C] and the FAA's current specification is dated May 20, 1994 [FAA, 1994B]. For this discussion, only the specifications relevant to aircraft loadings typical of GA airports will be reviewed. Also, the IDOT-DOA Method II specification for placements over 1,500 yd³, will be examined.

Aggregate Type and Gradations

IDOT-DOA specifies the use of an FA-1 fine aggregate, and CA-11 for 1-1/2 in to #4, or CA-7 for a 1 in to #4 coarse aggregate gradations [IDOT, 1994]. These gradations are slightly different from those recommended by the FAA, as shown in Table 6. IDOT-DOA provides a detailed description of fine and coarse aggregate, as well as the quality and deleterious material test requirements for aggregate approval. In the FAA specification, ASTM C 33 is the basis for accepting aggregate sources. The FAA has also added a section to address the problems of alkali reactivity. A similar provision has not been added to the IDOT-DOA specification (alkali reactivity has not been identified as a problem in Illinois).

The most recent IDOT-DOA specification added a requirement that coarse aggregate be non D-cracking susceptible, as determined by the Illinois Department of Transportation. The FAA uses a similar approach by requiring that all coarse aggregate sources be approved by the local department of transportation. If the aggregate source has not been approved, the Contractor must produce certification that the aggregate source passed ASTM C 666, Resistance of Concrete to Rapid Freezing and Thawing.

Cementitious Materials and Admixtures

IDOT-DOA requires the use of Type I cement. The FAA allows a wide variety of cements. Both IDOT-DOA and FAA specifications allow the use of flyash, as long as the quality of the flyash meets the requirements of ASTM C 618. IDOT-DOA further requires that the flyash be approved by the Illinois Department of Transportation, meeting the conditions outlined

by Policy Memorandum No. 88-1, Quality Control Requirements for Fly Ash for Use in Portland Cement Concrete [IDOT, 1988].

Admixtures, including air entraining and water reducing agents, must be approved by the Resident Engineer. IDOT-DOA specifications require that air entraining and water reducing admixtures be approved by the Illinois Department of Transportation.

Proportions

IDOT-DOA and the FAA allow compressive strength testing to be used in lieu of flexural strength testing for GA pavements. IDOT-DOA requires that the mixture be designed for a 28-day field compressive strength of 4,000 psi. The Engineer will provide a mix design based on the IDOT computer generated mix design system having a compressive strength of at least 800 psi over the specified field strength. This results in an actual specified minimum 28-day design compressive strength of 4,800 psi. A test batch is then prepared to verify that the PCC 28-day compressive strength is at least 800 psi greater than the specified field strength. A Contractor prepared mix is also acceptable if approved by the Engineer.

In the FAA specifications, a maximum of 20% of the 28-day compressive strengths can fall below the design compressive strength of 4,400 psi. This will result in a mix design average strength that is considerably higher than the minimum. The amount of over-design necessary to meet the specification is dependent on the producer's standard deviation for the compressive strength test results.

IDOT-DOA specifies a slump between 2 in and 3 in for side-form paving, and between 0.75 in and 1.5 in for slip form paving operations. The Contractor is required to provide all quality control personnel, who will follow the guidelines presented in IDOT-DOA's Policy Memorandum No. 87-3, Mix Design, Test Batch, Quality Control, and Acceptance Testing of PCC Mixture [IDOT, 1987]. These recommendations differ slightly from the FAA slumps of 1 in to 2 in and 0.5 in to 1.5 in for side-form and slip form paving, respectively.

FAA and ACPA air content requirements are based on the maximum aggregate size and the climatic exposure level anticipated. For a severe climate and a 1-in maximum aggregate size, the FAA and ACPA recommend $6.0\% \pm 1\%$ air content. IDOT-DOA specifies an air content of $6.5\% \pm 1.5\%$ for all mixes.

Acceptance Testing

Acceptance testing is based on the lot. Each lot includes four to six sublots of 300 yd³. The acceptance criteria are PCC compressive strength and slab thickness. PWL procedures are used as previously described. IDOT-DOA and the FAA both use only the two criteria listed above for determining the payment schedule. The FAA acceptance criteria also consider smoothness, grade, edge slump, and dowel bar alignment.

Summary

The most recent IDOT-DOA and FAA P-501 specifications have added requirements to address some of the PCC durability related concerns. The use of standardized IDOT Division of Highways classifications and standards should be beneficial, adding uniformity and consistency to airport work that was not previously available. The recent emphasis on Contractor quality control and a statistical basis for payment should yield improved construction.

II.3.3. Granular Material Specifications

IDOT-DOA and FAA specifications include two non-stabilized granular base courses (Item P-208 Aggregate Base Course and the Item P-209 Crushed Aggregate Base Course) for GA airport pavement construction. The FAA specifications also have a provision for Item P-154 subbase.

Item P-154 is a granular material constructed on a prepared subgrade. The gradation requirements cover a wide band as shown in Table 7. The specification states that the material

be free of "vegetable matter, lumps of excessive amounts of clay, and other objectionable or foreign substances. Pit-run materials may be used, provided the material meets the requirements specified." [FAA, 1974]. The material passing the No. 40 sieve should not have a liquid limit greater than 25 or a plasticity index greater than 6. In frost susceptible areas, the percent material finer than 0.02 mm shall be less than 3%. According to FAA AC 150/5320-6C, the assumed design CBR value for a subbase is 20 [FAA, 1978].

IDOT-DOA specifications do not include P-154. Prior to 1985, P-154 was used both in AC and PCC GA construction in Illinois. Current construction commonly uses P-208 in lieu of P-154.

The two available granular base course materials, Item P-208 and Item P-209, differ primarily in the amount of crushed material present. P-208 material is crushed or partially crushed aggregate (FAA also allows all uncrushed) and P-209 is all crushed material. The FAA and IDOT-DOA gradations for Items P-208 and P-209 are presented in Tables 7 and 8, respectively. In each specification, there are three available gradations: Gradation A has a 2-in maximum aggregate size, Gradation B has a 1.5-in maximum aggregate size, and Gradation C has a 1-in maximum aggregate size.

The FAA P-208 gradation specification allows 5% to 15% passing the No. 200 sieve. The higher quality P-209 base course gradation allows 3% to 10% passing the No. 200 sieve. In FAA AC 150/5320-6C, the P-209 is used as a base course for pavements serving all aircraft design loads. It is assumed to have a CBR value of 80 [FAA, 1978]. The P-208 material is not permitted as base material if aircraft design loads exceed 30,000 lbs, but is acceptable for use as a subbase. P-208 base course is allowable for pavements servicing aircraft with design loads below 30,000 lbs.

In the IDOT-DOA specifications, the same gradation is used for the P-208 and P-209. Both are based on the same IDOT Modified CA-4, Modified CA-6, and CA-10 specifications [IDOT, 1994]. The parent material for the P-208 can be gravel or stone mixed with sand, stone

dust, or other suitable fillers. The P-209 material is entirely crushed stone and crushed stone screenings. Gravel is not acceptable under the IDOT-DOA P-209 specification.

Summary

The FAA has three commonly used granular base and subbase specifications. P-154 subbase is of lowest quality, with an assigned CBR of 20. The highest quality granular base is P-209, which is a 100% crushed material assigned a CBR of 80%. P-208 is a base course for use on pavements serving aircraft with design loads less than 30,000 lbs. The IDOT-DOA specifications do not include P-154. The same gradations are used for P-208 and P-209. The primary difference between the two materials is that P-209 is wholly crushed stone, but P-208 can contain crushed or uncrushed gravel.

III. PAVEMENT DISTRESS AND THE PAVEMENT CONDITION INDEX

Several indicators are used to measure/estimate pavement condition and performance. This study uses observed pavement distress, collected in accordance with the pavement condition index (PCI) procedures outlined in FAA AC 150/5380-6 [FAA, 1982]. The following discussion presents a description of the various observable pavement distresses, how they are utilized in the PCI procedure, and how IDOT-DOA has modified the standard procedure to suit their specific needs.

III.1. Types of Pavement Distress

Pavement distress is typically identified as cracking, distortion, disintegration, and/or poor skid resistance observed visually on the pavement surface. In most cases, distress is a result of deterioration that occurs as the pavement ages and is subjected to loading and climatic processes. Well written and enforced specifications limit construction defects and new pavements are generally considered distress free. This is not always the case as some defects may be constructed into a pavement.

Accurate identification of pavement distress is critical in associating pavement deterioration with its probable cause or imperfection. Generally, distresses are classified as being load related, climate related, or materials/construction related. Many distresses result from a combination of more than one factor. When a distress is identified as load related, load is considered the primary distress formation factor with the understanding that both climate and materials/construction factors may have contributed.

In addition to identifying the type of distress observed, it is also important to determine the extent and severity of that distress. The basic questions of "How much distress?" and "How bad is it?" are as relevant as "What is it?". In combination, the three criteria of "What?", "How much?", and "How bad?" can be used to estimate the condition of the pavement feature.

The most rigorous method commonly used to evaluate airport pavement distress is the pavement condition index procedures described in FAA AC 150/5380-6, Guidelines and Procedures for Maintenance of Airport Pavements [FAA, 1982]. Distress types are identified for AC and PCC pavements and descriptions and photographs are provided to identify distress type, severity, and extent. The following discussion of pavement distress is based on the FAA document, which is the basis for the inspection procedures used by IDOT-DOA. An ASTM standard (ASTM D 5340-93) has recently been released on the PCI procedure, implementing some minor changes to the methodology. The ASTM method has not been used by IDOT-DOA.

III.1.1.1. Distress Types Affecting AC Pavements

The FAA has identified 16 different distress types that commonly occur in AC- surfaced airport pavements. IDOT-DOA has added an additional distress by separating paving lane cracking from longitudinal and transverse cracking. These distresses are listed in Table 9. Reflection cracking and shoving are only found on AC overlays of PCC pavements, and are not considered in this study. Jet blast erosion is not commonly observed on smaller GA airports.

The following text provides a brief description of relevant distresses, including their appearance, likely cause, other associated distresses, and means of measurement as summarized from FAA AC 150/3380-6 [FAA, 1982]. For detailed inspection procedures, refer to FAA AC 150/5380-6.

Distress No. 1: Alligator or Fatigue Cracking

Alligator cracking is a series of interconnected cracks that form a pattern resembling that of an alligator's skin. This distress is primarily load related and is isolated to areas subjected to repeated traffic loadings. The distress initiates at the bottom of the AC (or stabilized) layer as a result of load induced tensile stresses and strains, propagating upward until it becomes visible on the pavement surface. Alligator cracking can occur in poorly constructed areas and/or where inadequate pavement thickness exists to support the applied load. It is usually associated with

high surface deflections. Saturation of the base and/or "weak" subgrades are usually contributing factors.

In its initial manifestation, it appears as a series of fine, hairline cracks running parallel to the direction of traffic. These cracks eventually are connected by transverse cracks, forming individual pieces that are less than 2 ft on the longest side. Rutting may be observed along with alligator cracking. Both distresses are counted separately. Alligator cracking is measured in square feet of surface area.

Distress No. 2: Bleeding

Bleeding is a surface film of asphalt cement that has migrated upward from the underlying mat. It causes a reduction in skid resistance. Bleeding is primarily a material/construction related distress, and is associated with excessive amounts of asphalt cement binder in the mix and/or low air void content. During hot weather, the asphalt cement fills the available void space and then expands out onto the pavement surface.

Bleeding is counted as a distress if it is in sufficient quantity that it causes a reduction in skid resistance. If bleeding is counted as a distress, the PCI procedure requires that polished aggregate not be counted in the same area. Bleeding is measured in square feet of surface area.

Distress No. 3: Block Cracking

Block cracking is characterized by a series of cracks that divide the pavement into roughly rectangular pieces. They may be as small as 1 ft by 1 ft, but are more typically larger, with a maximum size of 10 ft by 10 ft. Block cracking is primarily climate related, although it has a strong material/construction component. The properties of the asphalt cement binder and particular mix properties play a large role in determining a pavement's susceptibility to block cracking. Block cracking results as the AC shrinks under temperature cycling and loss of volatiles from the asphalt cement. It is indicative of AC hardening and is more common in non-

trafficked locations, where the kneading action and post-construction compactive efforts of traffic are not experienced.

Block cracking and alligator cracking are commonly confused, but can easily be differentiated by determining the failure mode. Alligator cracking does not form in low traffic areas where block cracking is most prevalent, but is usually isolated to wheel paths. Alligator cracking typically forms smaller, irregularly shaped, pieces having sharp angles unlike block cracking which forms rectangles.

Block cracking usually progresses from longitudinal and transverse cracking. When the cracking pattern becomes dense and it is difficult to make individual measurements of crack lengths, the area is declared to be block cracked. This transition occurs when each side of the block falls at or below 10 ft in length. When block cracking is recorded, no longitudinal or transverse cracking should be recorded for that area. Block cracking is measured in square feet of surface area.

Distress No. 4: Corrugation

Corrugations are a series of closely spaced ridges and valleys (ripples) that form perpendicular to the flow of traffic. The interval between ridges is usually quite close (less than 5 ft). This distress is primarily load related with a strong material/construction component. It is caused by the action of traffic combined with an unstable pavement surface or base, and/or poor bonding between pavement layers. Corrugation is recorded in square feet of surface area.

Distress No. 5: Depression

Localized areas where the pavement surface has an elevation slightly lower than the surrounding surface are called depressions. Depressions are most easily identified after a rain as water ponding in the depression forms a "bird bath". Depressions can pose a hydroplaning hazard if located in a high-speed aircraft movement area.

Depressions are generally considered a materials/construction related defect. They are associated with settlement of the pavement layers beneath the surface or are constructed into the pavement through poor grade control. Loading can contribute, although it is not considered a major factor. Depressions are measured in square feet of surface area.

Distress No. 6: Jet Blast Erosion

Jet blast erosion is the burning of the asphalt cement binder by the hot jet engine exhaust. It is very rare on GA airports. It is measured in square feet of surface area.

Distress No. 7: Joint Reflection Cracking from PCC

This distress type only occurs on AC overlays of PCC. It therefore is not considered in this study.

Distress No. 8: Longitudinal and Transverse Cracking

Longitudinal cracking occurs parallel to the lay down direction (typically in the direction of the taxiway or runway centerline). Transverse cracking runs perpendicular to the lay down direction. The most frequent causes of these two types of cracking are shrinkage of the AC surface due to extremely low temperatures, temperature cycling, and/or AC age hardening. Reflection cracking from underlying stabilized layers are also counted as longitudinal and transverse cracking. A major cause of longitudinal cracking is poorly performing longitudinal construction joints, a distress mode which IDOT-DOA defines separately as paving lane cracking.

Longitudinal and transverse (L & T) cracking is almost entirely climate and materials/construction related, with load playing a very minor role. As the pavement continues to age, the asphalt binder becomes progressively harder and crack spacing decreases. If crack

spacing is close enough, it is classified as block cracking. Longitudinal and transverse cracking is measured in linear feet.

Distress No. 9: Oil Spillage

Oil spillage is caused by fuel, oil, or other solvents spilling onto the AC pavement and softening the asphalt cement binder. The pitting of the surface and the freeing of aggregate particles is most prevalent on apron areas where aircraft are fueled and maintained. This distress is related to the asphalt cement binder, and is considered primarily a material/construction related phenomena. It is measured in square feet of surface area.

Distress No. 10: Patching and Utility Cut Patch

Any patch, regardless of how well it is performing, is considered to be a defect. All distress within the patch boundary is counted as part of the patch and is not counted separately in the survey. Patching is measured in square feet of surface area.

Distress No. 11: Polished Aggregate

Polished aggregate is the loss of skid resistance from repeated traffic applications. It is both load and material/construction related. Sound, non-polishing susceptible aggregate will not suffer this distress. This distress is measured in square feet of surface area.

Distress No. 12: Raveling and Weathering

Raveling and weathering is the wearing away of the AC surface, exposing/dislodging aggregate particles. It may be an indication that significant hardening of the asphalt binder has occurred and is considered both a climate and material/construction related defect. At high severity levels, the loose aggregate poses a significant foreign object potential threat to aircraft and personnel. Raveling and weathering is measured in square feet of surface area.

Distress No. 13: Rutting

A rut is similar to a depression, except it runs along the wheel path, indicative of the load related nature of the distress. In many instances, rutting is only noticeable after rain, as the water in the ruts makes them visible. Permanent deformation in any of the paving layers contributes to surface rutting. It is caused by repeated load applications, but climatic and materials/construction factors contribute to the rutting potential of the pavement structure. AC rutting may be due to an unstable mix. Rutting in underlying layers is caused by permanent deformation that may be attributable to poor construction and weakening of the granular base/subbase and/or subgrade due to climatic effects.

Rutting can occur in conjunction with alligator cracking, in which case each distress is counted separately. The mean rut depth is used to determine severity and rutting quantity is recorded in square feet of surface area.

Distress No. 14: Shoving of Asphalt Pavement by PCC Slabs

This distress only occurs in AC overlays of PCC pavements, and is therefore not considered in this study.

Distress No. 15: Slippage Cracking

Slippage cracking is characterized by crescent- or half-moon-shaped cracks having the two ends pointing away from the direction of traffic. They are produced under braking or turning action which generates a shear failure in the AC surface. Slippage cracking is most commonly associated with poor bonding characteristics between the paving layers. A low strength AC surface can also suffer this problem. This distress is considered both a load and material/construction related distress.

Slippage cracking is generally an isolated problem. It occurs where aircraft are braking or turning, such as on runways in the vicinity of high-speed exits or near the end of a parallel taxiway where it turns to enter the runway. Slippage cracking is measured in square feet of surface area.

Distress No. 16: Swell

Swell is an upward bulge in the pavement surface that may occur sharply over a very short area or gradually over longer distances. Surface cracking may be associated with swell. Frost action or swelling soils contribute to swell formation. Swell is climate and materials/construction related. Swell severity is based on the functional use of the feature (i.e. runway, taxiway, or apron). Less swell is tolerated in areas subjected to higher aircraft speeds. Swell is recorded in square feet of surface area.

Distress No. 17: Paving Lane Cracking (IDOT-DOA only)

Paving lane cracking is longitudinal cracking that occurs at the cold paving lane joint between two adjacent lanes. It is believed to be caused by insufficient densification of the longitudinal joint during construction, and is exacerbated by climatic conditions and AC material properties that lead to shrinkage of the AC as it ages. It is measured in linear feet.

Summary

Table 9 provides a summary of the AC distresses recorded as part of the PCI inspection process and includes an indication of the primary and secondary factors that contribute to distress formation. The factors leading to pavement distress are complex. Although many of the mechanisms are well understood, there are always instances that deviate from the norm. Classification of a distress as load, climate, or material/construction related is useful in gaining better insight into pavement deterioration.

III.1.2. Distress Types Affecting PCC Pavements

The FAA and IDOT-DOA have identified the 15 PCC distress types listed in Table 10. All of these distresses could be observed on typical GA airport pavements.

The following text provides a brief description of each distress, including its appearance, likely cause, and other associated distresses. In PCC pavement inspection, distress quantities are not individually measured, but instead, only the number of affected slabs are recorded. This discussion is based on the information provided in FAA AC 150/5380-6. For detailed inspection procedures, refer to FAA AC 150/5380-6.

Distress No. 1: Blowup

Blowups occur during hot weather at transverse joints that are unable to accommodate temperature induced pavement expansion. The slab edges in the vicinity of the joint buckle upwards and usually shatter. Blowups can result when the joint is infiltrated by incompressible material due to poorly performing joint sealant. Alkali-silica reactivity, which produces an expansive reaction in the concrete, can also lead to joint closing and blowups.

Blowups are a severe distress, demanding immediate attention when they occur. If the blowup occurs at a mid-panel crack, it is counted as one slab. If it occurs at a joint, two slabs are counted.

Distress No. 2: Corner Break

Corner breaks are identified as cracks intersecting the joints at a slab corner a distance less than or equal to one-half of the slabs length on both sides. They are distinguished from corner spalls in that the crack projects vertically through the entire depth of the slab. A number of load and climatic factors contribute to corner breaking, but they are primarily caused by load repetitions at unsupported slab corners. Poor load transfer, loss of support attributed to subbase

erosion, and slab curling under temperature differentials all contribute to the formation of corner breaks.

Distress No. 3: Longitudinal, Transverse, and Diagonal Cracking

Longitudinal, transverse, and diagonal (L, T, & D) cracking divides the slab into two or three pieces. If the slab is further divided into four or more pieces, it is considered a shattered or divided slab. Causes of L, T, & D cracking are numerous. A combination of repeated loading, curling, and shrinkage stresses are commonly recognized as the primary deterioration factors. For the same thickness and support conditions, these stresses are more acute in larger slabs which develop higher curling and shrinkage stresses than shorter slabs. In some instances, poor construction practices may be a major factor. Construction induced cracking can result if joints are not sawed deep enough or on-time, or if joint lock-up occurs due to misalignment of load transfer devices. This distress is considered a major indicator of PCC pavement performance.

Distress No. 4: Durability (D-) Cracking

D-cracking is readily identified by the distinct pattern of fine cracks aligned parallel to the joints or cracks in PCC. The problem is climate and materials related. As the distress progresses, concrete spalling occurs and complete disintegration is observed in severe cases. D-cracking is related to the size and pore structure characteristics of the coarse aggregate particles in a PCC. In D-cracking susceptible aggregates, internal pressures created during freezing can not be adequately relieved and fracturing of the particle results. Both coarse aggregate type and size contribute. Larger sized aggregates are more susceptible. If a distressed area is counted as D-cracking, spalling is not counted separately.

Distress No. 5: Joint Seal Damage

Joint sealant minimizes the infiltration of water and incompressible material into the joint. This leads to improved pavement performance through a reduction in moisture related

deterioration (pumping and faulting, for example), spalling, and blowups. The joint sealant should be pliable and firmly attached to the joint sidewall. Joint sealant is considered to be a distress when it is debonded from the sidewall, is extruded from the joint, has hardened, is suffering weed growth, or is missing. Joint sealant damage is not counted on a slab by slab basis, but the condition of all the slabs within the sample unit are combined into a single severity rating.

Distress No. 6: Small Patch

A small patch has a surface area less than 5 ft². These patches are typically partial depth patches used to repair crack or joint spalling or surface scaling. The patch severity is rated according to the amount of deterioration present, but in almost all circumstances, the presence of the patch is considered a distress. The only exception is if a narrow patch (4 in to 10 in) was used to repair a crack, in which case only the crack is counted. If the original distress that was repaired is still present and is more severe than the patch itself, then that distress should be recorded, and not the patch.

Distress No. 7: Large Patch

Large patches have a surface area greater than 5 ft². Most FULL-DEPTH repairs fall into this category, including those used to repair corner breaks, D-cracking, blowups, and cracked slabs. Utility cut patches are counted as a large patch. Large patches are always counted as a distress, even if performing adequately. If the original distress that was being repaired is still present and is more severe than the patch itself, that distress should be recorded, and not the patch.

Distress No. 8: Popouts

Popouts are related to climatic and material factors. Popouts are identified as a series of pock marks on the pavement surface. Coarse aggregate particles that expand and fracture under

the influence of moisture and freeze-thaw cycling are the leading cause of popouts. Popouts usually have a diameter of 1 in to 4 in and a depth of 0.5 in to 2 in. To be counted, there must be an average popout density of at least three popouts per square yard of pavement surface. No severity level is assigned.

Distress No. 9: Pumping

Pumping is the ejection of water and material from beneath the slab under applied repeated loading. It is identified by the presence of staining and/or ejected material on the pavement surface and is usually associated with faulting, poor joint sealant, and loss of support beneath the slab. This distress is considered a major contributor to the formation of corner breaks. The primary distress formation factor is loading, but water (a climatic factor) must be available. Pumping is recorded on a slab by slab basis.

Distress No. 10: Scaling, Map Cracking, and Crazeing

Map cracking and crazing is a network of fine, hairline cracks that barely extend into the concrete surface. These cracks tend to intersect at approximately 120°, and are usually caused by over-finishing or poor curing practices during construction. Other causes include freeze-thaw damage as a result of an inadequate air void system, deicing salts, and alkali-silica or alkali-carbonate reactions. Map cracking and crazing is only counted if scaling is likely to develop in the future. Scaling is characterized by loss of surface material to a depth of 0.25 in to 0.5 in. Scaling is primarily a materials/construction related distress, although climate can play a role. It is measured on a slab by slab basis.

Distress No. 11: Settlement or Faulting

Faulting is a difference in elevation across a joint or crack. It is commonly associated with pumping and is caused by repeated load applications that predominantly occur in a single direction. Climatic factors contribute through the presence of moisture and the reduction of joint

load transfer that occurs during cool weather. This distress results in a decrease in ride quality as it becomes more severe. Severity levels are related to the functional classification (i.e. runway, taxiway, or apron) of the pavement. In counting settlement, faulting between two slabs is counted as one slab.

Distress No. 12: Shattered Slab/Intersecting Cracks

Cracking that divides a slab into four or more pieces is identified as shattered slab/intersecting cracks. It is usually caused by excessive loading or loss of support. Poor design (i.e. long joint spacing for a given thickness) is another potential cause. If all the pieces are contained within a corner break, the distress is labeled as a severe corner break. The severity level is related to the number of pieces in the broken slab and the severity of the cracks. If the severity is medium or high, no other distress is recorded for that slab.

Distress No. 13: Shrinkage Cracking

Shrinkage cracks are partial depth hairline cracks that do not extend across the entire slab. They are caused by improper curing of the concrete during construction and are construction related. There is no degree of severity assigned to shrinkage cracking.

Distress No. 14: Transverse and Longitudinal Joint Spalling

Joint spalling is the breakdown of the joint edge within 2 ft of the joint. Joint spalls do not normally pass vertically through the slab, but instead intersect the joint at an angle. Spalling can result when incompressible material infiltrates the joint, leading to excessively high stresses at the joint interface when the slab expands. Weak concrete and traffic can also contribute to joint spalling. If the joint spall is small enough that it can be filled with joint sealant, it is not recorded. Joint spalling is counted only once per slab, with the highest severity observed being recorded.

Distress No. 15: Corner Spalling

Corner spalling differs from joint spalling in location, occurring within 2 ft of the corner. It is sometimes confused with corner breaking, but is differentiated in that a corner spall angles toward the joint, intersecting it before reaching the bottom of the slab. If the corner spall can be filled with joint sealant, it is not recorded. Corner spalling is counted only once per slab, with the highest severity observed being recorded.

Summary

Table 10 provides a summary of the PCC distresses recorded as part of the PCI inspection process. Include is an indication of the primary and secondary factors that contribute to distress formation. PCC distress formation factors are complex, and can not easily be assigned a single deterioration factor. Classifying a distress as load, climate, or material/construction related is useful in gaining better insight into pavement deterioration.

III.2. The Pavement Condition Index Procedure

IDOT-DOA has collected pavement condition data on all publicly owned GA airports since 1980. Inspections are generally conducted on a two year cycle. The data are collected in accordance with FAA AC 150/5380-6, Guidelines and Procedures for the Maintenance of Airport Pavements [FAA, 1982], which describes the procedures used to determine the pavement condition index (PCI). Recent revisions to this procedure have been standardized in ASTM D 5340-93, Standard Test Methods for Airport Pavement Condition Index Surveys. The methods described in ASTM D 5340-93 are very similar to the FAA methods, except some enhancements have been made to address minor discrepancies in the original system. To-date, all IDOT-DOA inspections have been conducted under the FAA procedure.

The first step in conducting a PCI survey is to divide the airport pavement network into a series of unique features according to pavement design, construction history, and traffic.

Typically, runways, taxiways, and aprons are separated. Differences in construction, rehabilitation history, and traffic are then used to further divide the network. A final division can be made if a preliminary survey finds significantly different conditions present over a pre-selected feature.

Each feature is then divided into small inspection units called sample units. The procedure states that each sample unit should be marked and numbered in such a way that it "can be relocated for additional inspections to verify distress data or for comparison with future inspections" [FAA, 1982]. A sample unit on an AC surfaced pavement has a surface area of approximately 5000 ft², while a PCC sample unit consists of approximately 20 slabs. The sample units are randomly pre-selected for inspection based on a statistical approach. The total number of sample units is selected according to the desired confidence level (normally set at 95%) and the variability of distress within the feature. Figure 10 shows the chart commonly used to estimate this number. Higher desired confidence levels and greater variability requires an increased inspection rate. If during the inspection process, an atypical area of distress is observed that is not within a sample unit to be inspected, this sample unit should be added as an "additional sample unit."

The distress types, severities, and densities measured in each sample unit are used to determine deduct values from the appropriate curves provided in the Advisory Circular. A total deduct value (TDV) for each sample unit is determined by adding the individual distress deduct values together. The TDV is then modified to a corrected deduct value (CDV) for the sample unit according to Figure 11 for AC surfaced pavements or Figure 12 for jointed PCC pavements. The PCI of the sample unit is determined by subtracting the CDV from 100. A PCI rating of 100 corresponds to a pavement that is free of visible distress, and is usually reserved only for newly constructed pavement sections. A PCI rating of 0 (zero) is assigned to a pavement in extremely poor condition.

If the CDV of the sample unit is less than the highest individual distress deduct value, the highest value should be used to calculate PCI. It is not uncommon for the CDV to be less than

the highest individual distress deduct. For example, if a sample unit had only low severity weathering and raveling over its entire surface, it would have a TDV and CDV of 27, resulting in a PCI of 73. If this same sample unit also had low severity L & T cracking at a density of 0.1, it would have a TDV of 32, but a CDV of 20, resulting in a PCI of 80. Thus, it appears that the sample unit with cracking is in better condition than the one without unless the TDV is used in lieu of the CDV. In the above example, no reduction in condition is incurred through the addition of the cracking. In other cases, it is possible that an increase in sample unit PCI can be obtained when numerous distresses are recorded. The most recent revision of the PCI procedure, described in ASTM D 5340-93, addresses this discrepancy.

The PCI for the pavement feature is calculated as the average PCI for all the sample units inspected. Figure 13 presents an excellent schematic of the entire procedure, and Figures 14 and 15 show examples of completed inspection sheets for AC and PCC, respectively. Typically, computer programs are used to calculate PCI given the distress data. IDOT-DOA maintains its own software for this purpose.

The PCI of an in-service pavement section usually lies between 50 and 100. Fifty is commonly considered an un-acceptable condition. According to IDOT-DOA personnel, a pavement with a PCI below 70 is in need of major rehabilitation in the form of an overlay to restore it. Occasionally, a pavement is so seriously deteriorated that an overlay will not cost effectively restore it to useful life; at this time reconstruction is considered.

PCI procedures are well documented and repeatable if carefully conducted. Pavement condition and deterioration rate can be effectively monitored year after year. These data can be used to program rehabilitation and monitor the effectiveness of various pavement design, material selection, construction, and maintenance techniques.

III.3. IDOT-DOA Inspection Procedures

IDOT-DOA follows the basic inspection procedures described in FAA AC 150/5380-6, with some notable exceptions. In accordance with the FAA Advisory Circular, IDOT-DOA pre-selects features and sample units to be inspected, but no effort is made to re-inspect the same sample units year after year. IDOT-DOA inspectors have stated that it might be better to purposefully inspect different sample units during each cycle as it provides a more random measure of pavement condition. This is not necessarily in conflict with the Advisory Circular, although it makes it impossible to monitor the deterioration of specific sample units.

The IDOT-DOA methodology is less rigorous than that advocated in the Advisory Circular. Instead of meticulously measuring each crack width and length, IDOT-DOA inspectors estimate the quantity and severity of each distress as they walk briskly over each sample unit. This process is not as critical on PCC pavements, where little measurement is required; but it may be very important on AC surfaced pavements, where each crack length or distressed area is recorded.

A typical runway sample unit is inspected by two or three individuals, with one acting as recorder. The sample unit is walked over once. The types, quantities, and severities of the various distresses are mentally tallied by each inspector and the data conveyed to the recorder at the end of the sample unit. If considerable distress is present, distress information may be relayed to the recorder more frequently. Although the IDOT-DOA procedure is not as accurate/precise as the FAA procedure, IDOT-DOA personnel feel that the PCI data are adequate for their primary purposes of programming future capital improvement projects. In this study, it was observed that certain distress types are sometimes misidentified. This issue will be discussed in later chapters of this report. Overall, the inspections appear to be conducted in a consistent and timely fashion.

A significant IDOT-DOA modification to the standard PCI procedure is the addition of AC paving lane cracking as a separate distress. In the FAA procedure, paving lane cracking is

counted as longitudinal and transverse cracking. Recording it as a separate distress is quite useful, providing insight related to distress formation and propagation that is not available if the distresses are combined. Difficulties arise in the calculation of the PCI, because the inclusion of an additional distress can change the resultant PCI even if the overall distress quantity does not change.

This is true even though IDOT-DOA uses the same deduct curve for both distresses. For example, assume that in a 5000 ft² sample unit that there is 300 ft of low severity paving lane cracking and 200 ft of low severity transverse cracking. If there are no other distresses recorded, and the two are counted as one distress, the TDV and CDV equal 24, and the sample unit PCI is 76. If these two distresses are counted separately, the TDV would equal 28 and the CDV is 18, resulting in a PCI of 82. The significance of this difference is debatable, but it must be acknowledged. Because of this modification, IDOT-DOA PCI values are not directly comparable to those calculated in strict accordance with FAA procedures.

III.4. Summary

The systematic identification of pavement distress provides an excellent method for estimating current pavement condition and tracking pavement performance over time. It also provides significant insights into the mechanisms leading to pavement deterioration. The PCI procedure described in FAA AC 150/5380-6 is a widely accepted method of airport pavement inspection. IDOT-DOA's modifications to the FAA methodology simplify the procedure and substantially reduce inspection times. The IDOT-DOA recorded distress quantities are less precise/accurate. The overall effect on PCI is unknown. The separation of paving lane cracking into an additional distress by IDOT-DOA offers better insights into the distress mechanisms leading to pavement deterioration, but makes it difficult to compare the IDOT-DOA PCI to one calculated using the FAA format.

IV. FACTORS AFFECTING DISTRESS FORMATION AND PROPAGATION

Many factors contribute to the formation and propagation of pavement distress. These factors can act alone or in combination, further complicating the process of identifying the cause of an observed distress. To assist in identifying the primary cause of distress, distress formation and propagation factors are commonly separated into climate related, load related, and material/construction related factors.

IV.1. Climate Related Factors

IV.1.1. Climatic Considerations

The State of Illinois has a north-south orientation, stretching over 400 miles from the northern border to the southern tip. This orientation results in significant climatic differences from one end of the State to the other, with the northern portion receiving more severe winter weather while the south has hotter summer conditions. This observation is noted by AASHTO, which roughly divides the State in half; the northern portion falls in the wet, hard-freeze, spring thaw region and the southern portion in the wet, freeze-thaw cycling region [AASHTO, 1993]. There are also east to west differences, although these are less pronounced.

Climatic factors are complex. Their influence on pavement performance is indisputably strong. The two most important climatic factors are temperature and moisture [Thompson, 1992B]. According to Dempsey, "Although there are differences of opinion concerning the relative importance of the various factors, it is generally agreed that the temperature variation in a pavement system at any location is caused by the climate of that area, and that the response of the pavement system and its subgrade to the climate is controlled by the thermal properties of the materials." [Dempsey, 1985B]. Moisture content also effects subgrade soil and granular base and subbase strength/modulus characteristics, playing a major role in many material durability problems.

Climatic Considerations for AC Pavements

Asphalt concrete is a thermoplastic material experiencing significant changes in stiffness as temperature varies. During hot weather, the reduction in stiffness can lead to distortions, such as rutting and corrugations. The pavement will also deflect more under loading, potentially resulting in structural distress. As pavement temperature drops, the AC stiffens. At extremely cold temperatures, the stiff AC material may no longer be able to accommodate contraction without fracturing and low-temperature cracking occurs. Thermal fatigue cracking of AC pavements is also common, resulting from daily temperature cycling rather than large seasonal changes.

Both low-temperature and thermal fatigue cracking are exacerbated by aging/hardening of the asphalt cement binder. Long-term hardening of asphalt cement is related to temperature, as well as other climatic and material factors. The mechanisms leading to asphalt cement aging, or hardening, are complex and are still under investigation. The general consensus of the research community is that oxidation and the formation of molecular structures are the two primary mechanisms contributing to long-term aging of AC mixes at ambient pavement temperatures. A companion report developed in this study, [Aging Phenomenon in Asphalt Concrete Pavements - A Literature Review](#), provides a series of abstracts prepared from the most recent literature on this topic. Also included are descriptions of a number of proposed laboratory test methods that might be useful in identifying the asphalt cement aging characteristics. (NOTE: The companion report is available from the Illinois Transportation Research Center.)

Strategic Highway Research Program (SHRP) research extensively examined the relationship between climate and the aging/hardening of the asphalt cement binder, and subsequent low-temperature cracking [Jung, 1994][Bell, 1994A][Bell, 1994B][Anderson, 1994]. As a result, new asphalt cement binder specifications are proposed to account for the physical/chemical properties of the binder and the field service temperatures [Anderson, 1994].

Moisture effects in AC pavements affect both the material durability and pavement structural response. The most common durability problem is AC stripping. Stripping is the removal of the asphalt cement film from the coarse aggregate particle in the presence of water. Usually traffic is a contributing factor. Stripping is strongly influenced by aggregate and asphalt cement properties, but moisture plays a significant role in its development and propagation.

Moisture affects pavement structural response through its impact on paving material strength/stiffness. At higher saturation levels, there is a significant reduction in the strength and resilient modulus for fine-grained soil and some granular materials. There is also a corresponding increase in permanent deformation and rutting potential under repeated load applications [Thompson, 1992B].

The combined effect of temperature and moisture is most evident under freeze-thaw conditions. A frozen pavement structure is considered to be quite strong as the frozen subgrade and granular base have greater stiffness than in the unfrozen state. When this structure thaws, the effects of freezing and saturation may significantly reduce the subgrade and granular base/subbase strength/stiffness characteristics [Thompson, 1992B]. It is during this time that "Spring Breakup" occurs, as many pavements suffer extensive structural deterioration due to reduced support.

Potential heaving problems arise if the water table is close to the surface, and the subgrade is "frost-susceptible". The most frost susceptible subgrades are silts. Silts have a combination of small particle size and sufficient permeability that facilitates the rapid movement of moisture upward as it is drawn to a growing ice lens.

Significant loss of strength in high strength stabilized bases (HSSB) can result from the damaging effects of freezing and thawing. This is a consideration when cold temperatures slow or stop the pozzolanic or cement hydration reactions prior to full strength gain or damages the structural integrity of the material. This may pose long-term structural concerns if not addressed in the design process.

Climatic Considerations for PCC Pavements

Temperature and moisture effects are the two primary climatic concerns related to PCC pavement performance. Temperature induced expansion/contraction and slab curling have major impacts on the formation and propagation of many PCC pavement distresses. Improperly sealed joints may fill with incompressible material during cold temperatures as the slabs contract. The slabs expand as the temperature rises. Stress concentrations may form, leading to spalling or blow-ups. When joints open during cooler weather, aggregate interlock decreases and increased load induced tensile stresses result.

A temperature differential commonly exists between the surface and bottom of a PCC slab. This temperature gradient produces curling stresses, which can lead to significantly higher tensile stress for longer, thinner slabs. The cyclic nature of load and curling induced tensile stresses can ultimately fatigue a PCC slab, leading to slab cracking. Corner breaks are also partially attributed to temperature curling, which alternately pushes the corners down into the supporting layer and lifts them off their support as the slab temperature gradient changes through its daily cycle. In combination with load, significant tensile stresses can be generated both at the top and bottom of the slab corner. When the corner is curled upward, higher deflections are incurred under loading. In the presence of moisture, increased corner deflections can lead to pumping and void formation, perhaps leading to faulting and corner breaks.

PCC pavements are influenced by freezing and thawing. Non-stabilized supporting layers lose stiffness as they thaw and become saturated. Heaving can also be a problem under certain moisture and subgrade soil conditions. One of the most severe problems affecting PCC pavements in the State of Illinois is freeze-thaw induced D-cracking. Freezing and thawing can also lead to scaling of the PCC if an inadequate air void system exists

Summary

Climatic conditions have a profound effect on AC and PCC pavement performance. In combination with load and/or material/construction factors, climate becomes a major consideration. An understanding of climatic conditions is essential to evaluate of Illinois GA pavement performance data.

IV.1.2. Climatic Models

Climatic effects on Illinois pavement performance have been extensively studied. Climatic effects contribute to weathering/raveling, longitudinal, transverse, and block cracking in AC pavements and slab cracking, spalling, and D-cracking in PCC pavements. The NCHRP 1-26 study [Thompson, 1992A][Thompson, 1992B] provides an extensive review of the two most advanced climatic models available for pavement analysis: the Climatic-Materials-Structural (C-M-S) Model and the Integrated Model (IM). NCHRP 1-26 found that the IM was more comprehensive and sophisticated, but is difficult to use due to the number and complexity of the inputs required. It was thus recommended that the C-M-S model be the primary climatic model for pavement applications in which detailed site specific information is not available [Thompson, 1992B].

The C-M-S Model has been described in a number of published reports [Dempsey, 1985B][Dempsey, 1986]. Heat transfer and moisture models calculate pavement temperature and moisture profiles as a function of time. Climatic inputs include maximum and minimum daily air temperatures, wind speed, and solar radiation data. Material inputs, in addition to the pavement structure, include thermal properties of the soil and pavement materials, liquid and plastic limits of the soil, soil type, saturated water content, depth to the water table, and unit weights of all materials. A schematic of the C-M-S Model is provided in Figure 16 [Dempsey, 1986].

The C-M-S Model was used to prepare an Illinois climatic database for characterization of temperature effects on pavement analysis and design [Thompson, 1987]. It was demonstrated that the Illinois Climatic Data Base for Pavements could be successfully used to predict the temperature profiles in both AC and PCC pavements. Table 11 presents typical 12-in full depth AC pavement temperature profile data for Rockford, Urbana, and Cairo. The temperatures differ significantly from one end of the State to the other, with warmer air and pavement temperatures recorded in southern locations.

AC temperature algorithms were developed from a C-M-S data base for Rockford, Urbana, and Cairo [Thompson, 1987]. These algorithms relate the average monthly AC pavement temperature to mean monthly air temperature (MMAT). The results of these algorithms compared favorably to those used by Shell Oil [Shell, 1978] and those developed by Witczak for the Asphalt Institute [Witczak, 1972] [AI, 1982]. The main emphasis is to accurately estimate average monthly maximum and minimum AC temperatures for use in characterizing AC mixes for structural design. More recent NCHRP 1-26 research used the C-M-S Model to develop pavement temperature (PT) and mean monthly pavement temperature (MMPT) algorithms for various locations around the country [Thompson, 1992B].

A practical use of AC temperature data is reflected in the current Illinois Department of Transportation's highway design schemes for conventional and full depth AC pavements [Thompson, 1986][Thompson, 1988], as well as in the Asphalt Institute's [AI, 1991] and Shell Oil's [Shell, 1978] design methods. The Design Time concept is used in the Illinois design procedures. The AC fatigue damage incurred throughout the year under various temperature conditions is reduced to a single equivalent Design Time. AC mix temperatures are calculated for this Design Time. The AC mix temperature is then related to the stiffness of a standard IDOT Class I mix, depending on the type of binder (i.e. AC-10 or AC-20) used. In the two IDOT design procedures, maps of the State are used to select the appropriate AC mix temperature for the project location.

The effect of daily maximum and minimum temperatures on pavement performance are not considered in any of the current AC design schemes. The maximum and minimum daily pavement temperatures are far more extreme than those averaged over longer time periods. The data in the Illinois Climatic Data Base for Pavements were calculated on a weekly basis, although the diurnal effect of temperature cycling was recognized [Thompson, 1987]. The implications of asphalt cement hardening and its corresponding effect on thermal cracking is not directly considered in the current design schemes.

SHRP research addresses some of these issues, leading to the formation of a climatic database entitled, Weather Database for the SUPERPAVE™ Mix Design System [Solaimanian, 1993][Huber, 1994]. This database provides the maximum average daytime air temperature during the hottest consecutive 7-day period and the minimum air temperature recorded in an average year. A series of algorithms are provided to convert the maximum average 7-day air temperature into a pavement temperature using the latitude of the pavement location as an input. In the initial approach, minimum pavement temperature is assumed to be equal to minimum air temperature, although the validity of this assumption has been questioned by a number of researchers. Work is continuing to develop an improved algorithms to predict minimum pavement temperature.

Under the SHRP procedure, the minimum and maximum air temperatures are used to specify an asphalt cement binder best suited for the field temperature conditions. This binder selection process includes tests to simulate both short- and long-term aging of the binder, thus addressing some of the limitations that exist in current design schemes.

A current University of Illinois study (Project IHR 424 entitled, SHRP Asphalt Testing for Performance Specification) is evaluating the SHRP methodology. Maximum and minimum pavement temperatures provided in the SHRP data base are being compared to those measured/calculated within the State. Asphalt cements commonly used within the State will be graded according to the SHRP performance grading system [Petersen, 1994]. Anticipated completion date is in 1996.

PCC pavement temperatures are essential in considering slab curling. In curling stress analyses, it is not the extreme maximum and minimum pavement temperatures that are of primary concern, but instead the magnitude of the temperature gradient (i.e. the difference in temperature from the top of the slab to the bottom) through the slab. These effects are primarily diurnal, but seasonal variations can also influence the temperature curling of PCC [Thompson, 1987].

Curling stresses were first calculated by Westergaard [Westergaard, 1926] using superposition to find total stresses induced by a wheel load and a linear temperature gradient. Finite element programs allow for more complex solutions, accounting for different slab dimensions, wheel loadings, subgrade models, and most recently, non-linear temperature gradients. A number of closed-form solutions have recently been developed that model the finite element solution, providing a simplified means for conducting what has previously been a complex analysis [Salsilli, 1993] [Lee, 1993].

Investigations of the maximum positive temperature gradients typically encountered in Illinois were conducted as part of the NCHRP 1-26 study [Thompson, 1992B][Salsilli, 1993]. The gradient data have been incorporated into the computer program ILLICON. Table 12 shows calculated 6-in slab temperature differentials for Rockford, Urbana, and Cairo. Temperature gradients calculated for various locations within the State do not reveal a marked difference even though the maximum and minimum air temperatures vary considerably. Thus, PCC slab curling can be calculated using a single temperature gradient for the entire State.

Although the C-M-S Model is capable of generating moisture profiles for given material and climatic characteristics, the complexity of the problem prevents the creation of simple algorithms similar to those developed to estimate temperature effects. It is also difficult to significantly alter a moisture profile under field conditions in typical pavement applications. Calculated moisture profiles are rarely a direct pavement design input. Instead, potential moisture problems are addressed in pavement design through application of preventative techniques, including the use of less moisture sensitive materials or removal of water through

drainage. Material specifications are written to minimize the deleterious affects of moisture, including tests for stripping susceptibility of AC mixtures (ASTM D 4867) and D-cracking in PCC pavements (ASTM-C 666).

IV.1.3. Project Approach

Climatic has a significant effect on pavement performance. The climatic modeling tools currently available, including the IM and C-M-S Model, are powerful, but are limited by the extensive inputs required. In the context of this project, the data required to utilize these sophisticated model are not available. Therefore, the direct application of either the C-M-S Model or the IM is not considered feasible.

The climatic algorithms discussed previously show promise. Those determined using the Illinois Climatic Data Base for Pavements are most applicable to the State, but address only weekly or monthly average temperature effects. This approach is adequate for structural thickness design, but does not provide the accuracy required in examining low-temperature cracking. The SHRP algorithms are formulated specifically to addressed both fatigue and thermal cracking problems, yet require verification for applicability to Illinois conditions. The asphalt cement binder and AC mix properties are not available on the pavement sections included in the project data base. It was decided that a less specific approach be utilized to examine the influence of climate on GA pavement performance within the State.

There are quantifiable differences along the north-south orientation of the State. The State was divided into three climatic regions, using the two major east-west Interstate highways (I-80 to the north and I-70 to the south) as major dividing lines. As shown in Figure 17, IDOT-DOA's administrative division of the State roughly approximates these boundaries. It was concluded that the most efficient and meaningful method for incorporating climatic considerations into this study was to work within the existing IDOT-DOA Administrative Regions. Thus, the Northern Climatic Zone contains Administrative Regions 1 and 2, the

Central Climatic Zone consists of Administrative Region 3, and the Southern Climatic Zone includes Administrative Regions 4 and 5.

Specific climatic considerations related to structural performance and asphalt aging are addressed subsequently under structural and material/construction considerations.

IV.1.4. Summary

Climatic factors have a large impact on pavement performance. Sophisticated heat transfer and moisture models are available for estimating pavement temperature and moisture profiles. The number and complexity of the inputs limits their practical use. Simplified algorithms for calculating pavement temperatures have been developed for the State of Illinois for the selection of binder and estimating AC mixture properties (particularly modulus). Recent SHRP asphalt research shows promise, and a current University of Illinois project is evaluating the SHRP approach.

Specific concerns related to the structural performance and aging of asphalt cement is addressed in subsequent chapters. In considering the pavement condition data, it was determined that the most effective approach is to use the existing IDOT-DOA Administrative Regions, dividing the State into northern, central, and southern climatic regions.

IV.2. Load Related Factors

IV.2.1. Structural Considerations

Pavement responses (stress, strain, and deflection) to applied loading are analyzed to characterize structural behavior and predict probable pavement performance. Factors that influence structural response include loading, pavement design, paving layer properties, subgrade characteristics, construction control, and climatic influences on material properties. There are excellent models available for the structural analysis of pavement systems. In this study, the

ILLI-PAVE and ILLI-SLAB finite element models were used to analyze AC and PCC pavements, respectively.

Structural Considerations for AC Pavements

The two major AC pavement structural distresses are alligator (or fatigue cracking) and permanent deformation (surface rutting). Alligator cracking appears on the pavement surface as repeated load applications propagate cracks upward from the bottom of the AC (or stabilized base) layer. The cracking initiates as the AC material fatigues under repeated tensile stress/strain applications. Empirical relationships have linked fatigue cracking to load induced AC tensile strain. AC tensile strain is therefore a primary indicator of potential structural performance.

Permanent deformation can occur in any or all of the pavement layers or subgrade. It is critical if it leads to substantial surface rutting. Typically, rutting in the AC layer and granular base material is controlled through proper mix design, material selection criteria, and construction specifications. Surface rutting in well constructed pavements is thus closely linked to subgrade rutting. There are a number of empirical relationships that relate subgrade vertical strain to rutting. IDOT highway pavement design practices relate rutting potential to the subgrade stress ratio (SSR). SSR is defined as the load induced deviator stress divided by the unconfined compressive strength of the soil [Thompson, 1986][Thompson, 1988].

Climatic and material factors have a large impact on structural performance. Through adequate pavement design and material specifications, the impact is minimized, but never eliminated. The previously described Design Time concept incorporates climatic effects into flexible pavement structural design. Other well known design schemes also address the climatic issue through the seasonal adjustment of material properties [AI, 1991][AASHTO, 1993][Shell, 1978].

Structural Considerations for PCC Pavements

The primary structural failure mechanism in PCC pavements is slab fatigue cracking caused by load induced tensile stresses at the bottom of the slab. Empirically derived transfer functions are normally used to relate a "percentage of slabs cracked" to the ratio of induced tensile stress divided by the modulus of rupture of the PCC (σ/M_R). The factors that influence the magnitude of the induced stress include the loading conditions, slab size and thickness, PCC modulus, PCC Poisson's ratio, and the modulus of subgrade reaction (k). The problem is further complicated when temperature curling and load transfer efficiency at joints and cracks are considered.

Slab cracking is only one structural problem observed in PCC pavements. Another common structural defect is corner breaking. Corner breaking is highly influenced by climatic factors. Under a fully supported slab with even moderate load transfer efficiency, the critical location for tensile stress is almost invariably at the mid-point of the longest joint (NOTE: load configuration and orientation can change this critical location). In situations where high vertical corner deflections occur due to poor load transfer, temperature curling, and/or loss of support, corner loading can become critical. In these instances, corner breaking can result.

Other distresses, including joint and corner spalling, have a structural component, but are primarily a result of other factors.

IV.2.2. Loading Conditions

An important consideration in pavement structural analysis is to identify the loading conditions. A total of 27 GA airport managers throughout the State were contacted and interviewed to determine the largest aircraft using their facility on a daily, infrequent, and one-time basis. Information on the type of fueling and snow removal equipment employed was also sought. The Illinois Airport Inventory Report - 1993 was consulted to determine annual

operations and the number and type of based aircraft reported at each airport under investigation [IDOT-DOA, 1993].

The vast majority of aircraft using GA facilities are single engine or light twins (gross weight < 8,000 lbs). The heaviest aircraft typically observed on a monthly basis is the Beechcraft King Air B200 (maximum gross weight of approximately 12,500 lbs). Considerably less common are small corporate jets such as a Citation or Lear (maximum gross weights of less than 20,000 lbs). The heavier King Air and small corporate jets use dual wheel main landing gears. There are loading differences between GA airports. Those located near metropolitan areas generally have more frequent applications of the heavier aircraft. Large corporate aircraft based at an airport can also lead to higher than normal traffic.

Most Illinois GA airports use fueling pumps instead of fuel trucks. When trucks are used, the single axle load is always less than normal highway levels of 18,000 lbs. Typically, a 2500 gallon, single dual rear axle fuel truck is used. Heavier 5000 gal trucks were reported, but these featured twin dual rear axles. The heavier fuel trucks were generally located at larger airports. Some airports use a modified pickup truck with a 300 gal tank mounted in the bed.

Snow plowing is typically conducted by the local governing agency using street snow removal equipment. Pickup and dump trucks were the most common pieces of equipment employed, although road graders and farm tractors were also reported. At some of the larger airports, specialized snow removal equipment was used, such as Oshkosh snow blowers.

IV.2.3. Structural Models

A number of structural models are available for the analysis of pavement systems. These include both elastic-layer programs and finite element models. Because of the differing load carrying characteristics of AC and PCC pavements, separate models are used for each.

AC Structural Models

AC pavement analysis has traditionally been conducted using elastic-layer analysis methods. It is assumed that all the layers are homogenous, isotropic, linear elastic, infinite in extent with a finite depth, except for the bottom layer which is considered to be infinite in depth. Each layer is assigned a modulus and Poisson's ratio, and the interface between the layers is set to be fully-, partially-, or un-bonded. The most recent FAA design developments currently undergoing evaluation are based on the elastic-layer model.

The University of Illinois has developed a widely used finite element program (called ILLI-PAVE) for the analysis of flexible pavements. ILLI-PAVE accommodates the stress dependent behavior of granular base materials (stress-hardening) and the subgrade soil (stress-softening). ILLI-PAVE only accommodates a single wheel load. ILLI-PAVE has been used to create extensive pavement structural response data bases and pavement structural response algorithms have been derived for conventional and FULL-DEPTH AC highway pavements [Thompson, 1985][Gomez-Achecar, 1986].

PCC Structural Models

The earliest PCC structural analysis models stems from Westergaard's work. He developed a series of equations to estimate PCC slab stress and deflections using closed-form solutions [Westergaard, 1927]. This work has undergone modifications since its initial publication, but continues to be an important tool in the analysis and design of PCC pavements.

The finite element solution has gained popularity as the availability of computing power increased. The most popular finite element model utilized for PCC pavement analysis is ILLI-SLAB. The development of this two-dimensional finite element model continues, with enhanced features allowing more and more complex analysis of the PCC pavement system.

Even though computers and PC versions of ILLI-SLAB are readily available, the complexity of the finite element solution restricts its use primarily to the research community. Considerable efforts have led to the development of pavement response algorithms to approximate the ILLI-SLAB response to various loading configurations, temperature curling conditions, and load transfer efficiencies. Salsilli significantly advanced the accuracy and usability of these pavement response algorithms in his work conducted for NCHRP 1-26 [Salsilli, 1993]. His work was incorporated into a highway design computer program called ILLICON. Lee continued to develop pavement response algorithms, using advanced statistical techniques as well as deriving a dimensionless parameter for use in the calculation of curling stresses [Lee, 1993].

Summary

There are several structural models for the analysis and design of pavements. Computer-based elastic-layer and finite element programs are readily available. The ILLI-PAVE and ILLI-SLAB finite element models contain advanced analytical features and widespread acceptability, and have been used extensively within the State of Illinois for the design and analysis of highway pavements. Finite element models are complex, requiring in-depth knowledge and a large number of inputs to be run effectively. To address this short-coming, pavement response algorithms derived from finite element data bases are frequently used for routine pavement analysis and design. These algorithms provide a rapid means to calculate pavement response(s) without sacrificing the efficacy of the finite element method.

IV.2.4. Project Approach

In considering structural factors that contribute to GA pavement deterioration, typical loading conditions were first identified. Sophisticated structural models and state-of-the-art distress transfer functions were then used to estimate structural life as a function of design aircraft passes. The specific project approach for AC and PCC pavements is discussed below.

Project Approach to Loading

GA airport loading was considered in two ways. In the structural analysis of current design procedures, a design aircraft was selected. Surveys of airport managers and review of the Illinois Airport Inventory—1993 [IDOT-DOA, 1993] indicated that the Beech King Air B200 (or aircraft of similar weight and configuration) was the heaviest aircraft serviced by many of the GA airports on a monthly basis. For many airports, it was the heaviest aircraft to use their facility at any time. The King Air B200 is also the heaviest aircraft used by IDOT-DOA. It was therefore selected as the design aircraft for this study.

The Beechcraft Super King Air B200 has a maximum takeoff and landing weight of 12,500 lbs. The main gear carries approximately 11,250 lbs (assuming approximately 90% of the gross maximum weight). This main gear consists of two dual wheel combinations, resulting in each of the four tires carrying approximately 2,800 lbs. The tire pressure is 105 psi, with each dual tire being spaced 11 in center-to-center. The spacing between the dual tire assemblies is 14 ft 11.5 in center-to-center.

GA airport service vehicle weights are generally at or below that typically encountered in highway applications. Load applications are less frequent and less channelized than normally observed on streets and highways. As these loading conditions were not considered critical, the structural analyses conducted in this study are restricted to the King Air B200 aircraft loading.

A "Loading Code" was also assigned to each pavement section included in the project data base. This Loading Code was useful in examining the occurrence of load related distress. Airport specific factors that contributed to the Load Code were the number of annual operations, the number and length of the runways, the number of based aircraft, and the number of based aircraft that were multi-engine prop or jets. Each pavement section was examined to determine the type and frequency of traffic that it would normally service. The Loading Code is designated as either low, medium, or high. A medium Load Code was assigned to pavements subjected to infrequent (approximately once a month) King Air B200 aircraft operations. A low Load Code

was set for pavement sections that would not be expected to receive any King Air B200 loading. The high Load Code is for pavements expected to service numerous King Air B200 and/or corporate jet aircraft.

For example, at a larger airport, taxiway sections leading to small T-hangers that can not accommodate large aircraft would be assigned a low Loading Code. A primary taxiway at the same airport may receive a Medium or High rating, depending on annual operations, runway length, and based aircraft. In this way, a basis for identifying load related distress modes was implemented.

Project Approach to AC Structural Analysis

The impact of GA loading on the structural response/performance of AC pavements was quantified through development of a GA pavement response data base using the ILLI-PAVE finite element program. Pavement response algorithms were derived from the data base using the same model forms previously developed for highway loading [Thompson, 1985] [Gomez-Achecar, 1986]. The design aircraft was the Beechcraft King Air B200. The material properties used in the ILLI-PAVE analysis are presented in Table 13.

For conventional AC sections, AC thicknesses of 3, 4, and 6 in and granular base thicknesses of 6, 9, and 12 in were investigated. FULL-DEPTH AC sections included thicknesses of 4, 6, 8, and 10 in. The Systat® statistical analysis program was used to develop the pavement response algorithms for conventional and FULL-DEPTH pavements presented in Tables 14 and 15, respectively. The critical pavement response parameters and the procedure used to derive the algorithms for the two pavement types are presented in Appendix A of this report.

Limited field and laboratory testing were conducted as part of this study to develop some typical AC pavement structural response and material properties for GA airports. This effort provided useful AC modulus information for typical P-201/P-401 mixtures.

Falling weight deflectometer (FWD) testing was conducted on newly constructed pavement sections at Pontiac (3-in AC over 8-in granular) and Morris (9.5-in AC over 4-in granular). A description of this investigation is presented in Appendix B of this report. Tables 16 and 17 summarize the results of this analysis for Pontiac and Morris, respectively. Backcalculations of E_{AC} and E_{RI} were accomplished using 9-kip pavement response algorithms developed for IDOT highway applications. Backcalculated E_{AC} values from Pontiac are not considered, as it is generally acknowledged that this procedure is unreliable for thin AC sections. Only the Morris data were used to backcalculate E_{AC} .

Compared to a typical IDOT Class I AC-10 mixture, the backcalculated E_{AC} values from Morris are slightly lower than would be expected over a similar temperature range. This finding suggests that although both the IDOT-DOA P-201/P-401 and the IDOT Class I mixes are high quality, the emphasis on addressing climatic effects through lower air voids and high asphalt content in the IDOT-DOA mixes may have reduced the AC stiffness.

A laboratory investigation was conducted on 74 AC thickness core samples (90 total specimens produced after sawing) obtained from three recently constructed projects at Pontiac, Morris, and Mt. Sterling. The core samples included both surface mixes (P-401) and binder mixes (P-201). Bulk specific gravity, resilient modulus (@ 70° F and 90° F), and split tensile testing was conducted to determine selected AC material properties. The results of this laboratory investigation are presented in Appendix C of this report. Table 18 summarizes the laboratory results for each airport.

Relatively low E_{AC} values were obtained for the Pontiac cores. Some of the cores suffered inexplicable creep at 90° F and two of 13 cores "fell apart" prior to testing. In one core, the rubber band used to attach the label cut deeply into the core and severely deformed it. Mt. Sterling and Morris cores showed stiffness behavior slightly lower than expected for a IDOT Class I mixture [IDOT, 1994].

Because the resilient behavior of the Morris and Mt. Sterling AC materials were only slightly lower than that expected for an IDOT Class I mixture, it was considered appropriate (for the purpose of this study) to use Class I AC properties in the structural analysis.

Typical GA pavements (typical conventional flexible and FULL-DEPTH) were designed using the FAA and AI procedures for the King Air B200. Soil CBR values of 3, 5, and 7 (roughly equivalent to subgrade resilient modulus, E_{R1} , values of 3.0, 7.7, and 12.3 ksi) were used. E_{R1} is defined as the break-point resilient modulus, which occurs approximately at a repeated deviator stress of 6 psi. The FAA and AI pavement design thicknesses are presented in Table 19.

The ILLI-PAVE pavement response algorithms derived in the course of this study were used to estimate AC strain and subgrade stress ratios for the FAA and AI design sections. Climatic effects on AC mixture temperature were incorporated according to the procedures used by IDOT for highway design [Thompson, 1986][Thompson, 1988]. The resulting AC mix temperature and corresponding estimated AC moduli (For IDOT Class I AC-10 mixture) are presented in Table 20.

A discussion of IDOT-DOA AC mixture stiffness and fatigue properties is presented in Appendix D of this report. As a result, it was considered acceptable, for the purpose of this study, to estimate pavement fatigue life in allowable passes using the IDOT Class I fatigue relationship presented below [Thompson, 1986]:

$$N = 5 \times 10^{-6} \left(\frac{1}{\epsilon_{AC}} \right)^{3.0}$$

Where: N is the allowable load repetitions (coverages)
 ϵ_{AC} is the AC tensile strain (in/in)

Allowable coverages are converted to allowable passes using a pass-to-coverage (P/C) ratio that reflects the lateral distribution of the aircraft. For dual wheeled aircraft, the P/C ratio for channelized flow is 3.48 [FAA, 1978].

The estimated allowable passes for the conventional and FULL-DEPTH sections are shown in Figures 18 and 19, respectively. In all cases, the allowable passes for conventional pavements is in excess of 100,000. The AI provides a more conservative design. The number of allowable passes are based on a fully loaded King Air B200. This aircraft operates at most airports considered in this study about once a month. The FAA and AI designs show the effect of reduced AC mixture stiffness for the warmer southern climates, with fewer allowable passes. Even though, it is emphasized that southern pavement sections would be considered structurally adequate. The FAA design is insensitive to subgrade stiffness, but the AI designs show decreasing structural life (allowable passes) for stiffer subgrades, suggesting that pavement thickness was reduced disproportionately for stronger subgrades.

The analysis of FULL-DEPTH sections reveal even greater structural capacity, with estimated allowable passes in excess of 1,000,000. The same climatic trends exists as for the conventional AC designs, with reduced structural life estimated for southern sections. The FAA design was most conservative. The factors used to "convert" granular base and subbase to AC control the AC thickness. It is noted that the validity of the conversion factor approach is questionable. The FAA and AI designs are more conservative at lower subgrade stiffness values.

Subgrade stress ratios (SSR) were also calculated for the various designs. In no case did the SSR exceed 0.44 for the conventional pavement sections, and then only in the case of the weakest subgrade conditions. For the two stronger subgrade conditions, the SSR was less than 0.30. The SSR was always below 0.20 for the FULL-DEPTH AC designs. Rutting is typically not a concern in pavement sections where the SSR is less than 0.5. Thus, it is expected that GA airport subgrade rutting would not be a problem for the designs considered.

It is concluded that load related distress factors should not contribute significantly to GA flexible pavement deterioration. It is emphasized that the structural analysis was conducted using IDOT Class I mixture properties and fatigue relationships. To develop an AC structural design methodology for State GA airport pavements, specific mix properties and fatigue relationships need to be established for IDOT-DOA P-201 and P-401 mixes.

Project Approach to PCC Structural Analysis

For PCC pavement analysis, the ILLI-SLAB model was used. Slab thickness was set at 6 in, corresponding to IDOT-DOA practices to-date on all air-side PCC pavements. Three slab sizes (12.5 ft by 12.5 ft, 12.5 ft by 15 ft, and 12.5 ft by 20 ft) were evaluated on support values (modulus of subgrade reaction, k) ranging from 50 to 500 pci. Free edge loading for the Beechcraft King Air B200 was placed at the critical longitudinal and transverse edge locations. The initial experimental matrix consisted of 108 ILLI-SLAB runs conducted without a temperature gradient. This analysis found that the longitudinal joint loading condition was critical in all instances. Relevant ILLI-SLAB pavement response parameters as well as a more detailed description of the PCC structural analysis are presented in Appendix E of this report.

The climatic effect of slab curling was considered by including a 2.5° F/in temperature gradient (15° F from top to bottom of the slab). In Illinois, a 2.5° F/in temperature gradient is considered critical as it is typically exceeded only 10% of the time over the course of a year (see Table 12). A positive temperature gradient (the top of the slab is warmer than the bottom) is most critical as the curl stress is additive to the load stress. An additional 54 ILLI-SLAB runs were conducted with a temperature gradient, with the load positioned on the longitudinal joint.

ILLI-SLAB results are shown in Figures 20, 21, and 22 for PCC modulus of elasticity (E_{PCC}) values of 3, 4, and 5 million psi, respectively. These critical stresses are based on free edge conditions and are not representative of field conditions, but the trends are significant. For any given slab length, curling stresses contribute to significantly higher critical stress levels. This effect is most pronounced as slab size increases from 12.5 ft to 15 ft, indicating that under

identical conditions, the same loading will induce higher stresses in the 15 ft slab than in a 12.5 ft slab with a positive temperature gradient.

To better reflect actual field conditions, the free edge stresses were reduced by 25% to reflect the load transfer efficiency of the joints as recommended by the FAA [FAA, 1978]. It is noted this stress load transfer efficiency translates to a deflection load transfer efficiency of approximately 85%. Figure 23 shows the plot of the reduced critical stress conditions for E_{PCC} of 4,000,000 psi, illustrating the influence of curling stresses and of slab length.

PCC fatigue cracking is commonly related to the stress ratio (SR) which is equal to the stress over PCC modulus of rupture (σ/M_R). The following relationship was developed by Foxworthy to estimate the PCC modulus of rupture given the E_{PCC} [Foxworthy, 1985]:

$$M_R = 43.5 \left(\frac{E_{PCC}}{10^6} \right) + 488.5$$

Where: M_R is the PCC modulus of rupture (psi).
 E_{PCC} is the PCC modulus of elasticity (psi).

The equivalent M_R for E_{PCC} of 3, 4, and 5 million psi are 619, 662, and 706 psi, respectively. The minimum quality that would typically be built under a P-501 specification would have a 28-day M_R of 650 psi. The remaining discussion is based only on an E_{PCC} of 4,000,000 psi.

A number of PCC fatigue/slab cracking transfer functions are represented in the published literature. Two have been selected for examination in this study. The Zero-Maintenance Design equation (ZM) was derived from a 140 laboratory beam tests collected under three previous studies [Darter, 1977]. The least squares regression curve has the following form [Darter, 1977]:

$$\text{Log } N = 17.61 - 17.61SR$$

Where: N is equal to the number of stress applications to failure.
SR is the stress ratio (σ/M_R).

This design equation was developed for a failure probability of 50%.

Typically, laboratory testing does not directly relate to field performance, as the variability inherent in field conditions (i.e. loading variability, support conditions, construction variability, climatic conditions, etc.) is not accounted for. To address these concerns, it is necessary to calibrate laboratory observation to field performance. An example of such a field calibrated mechanistic design model (MD) is presented below [Salsilli, 1993]:

$$\text{Log } N = \left[\frac{-SR^{-5.367} \text{Log}(1-P)}{0.0032} \right]^{0.2276}$$

Where: N is equal to the number of stress applications to failure.
P is equal to the failure probability level

In this analysis, both PCC fatigue transfer functions were used to estimate the allowable coverages to slab cracking. The M_R was set at 662 psi (for $E_{PCC} = 4,000,000$ psi), and the critical tensile stresses were reduced 25% for load transfer. A pass-to-coverage ratio (P/C) of 3.48 was applied per FAA recommendations [FAA, 1978]. A percent probability of failure of 50% was used.

Figure 24 presents the estimated allowable passes to 50% slab cracking for each fatigue model for no curl or curl conditions. Slab thickness was set at 6 in. The general trends show with increasing modulus of subgrade reaction, there is an increase in estimated passes to failure. This trend is most pronounced when curl is not considered. The Zero-Maintenance (ZM) model predicts higher allowable passes than the Calibrated Mechanistic Design (MD) model under the same conditions.

Both fatigue models predict allowable passes in excess of 10,000,000 if only load related stresses are used in the analysis. When curling stress is added to loading stress, however, the resulting reduction in passes is several orders of magnitude. With the MD model, the estimated number of allowable passes to failure drops into the hundreds of thousands.

The severe curling condition assumed is quite rare, with the pavement being exposed to such conditions approximately 10% of the time. In typical GA airport applications, King Air B200 loading is infrequent. Under such circumstances, a 6-in thick PCC slab appears to be structurally adequate. It is possible, under heavier and more frequent traffic volumes, that the combined effects of load and temperature curl may coincide and lead to structural fatigue failures in 6-in PCC slabs.

Edge curling stresses in PCC pavements can be calculated using a procedure developed by Westergaard [Westergaard, 1926]. His approach was simplified by Bradbury, appearing in the equation below [Bradbury, 1938]:

$$\sigma_e = \frac{CE_{PCC}\alpha_T\Delta T}{2}$$

Where:

- σ_e is the edge curling stress (psi).
- C is a coefficient determined from Figure 29.
- ΔT is the temperature differential between the top and bottom of the slab ($^{\circ}$ F).
- E_{PCC} is the PCC modulus of elasticity (psi).
- α_T is the PCC coefficient of thermal expansion ($^{\circ}$ F).

In Figure 25, the ratio B/ℓ is critical in determining the coefficient C. B is defined as the free edge length or width of the slab in inches. Generally, the length of the slab is most critical, so the B is replaced with an L. The radius of relative stiffness, ℓ , is calculated from the following equation [Westergaard, 1926]:

$$\ell = \left[\frac{E_{PCC} h^3}{12(1 - \mu^2)k} \right]^{0.25}$$

Where: ℓ is the radius of relative stiffness (in).
 h is the thickness of the slab (in).
 μ is the PCC Poisson's ratio.
 k is the modulus of subgrade reaction (pci).

Using these two equations, it is observed that curling stresses increase progressively as slab size increases, until an L/ℓ of approximately 8.5 is reached. Studies have shown that slab cracking increases as L/ℓ increases [Smith, 1990].

Figure 26 is a plot of estimated number of passes to failure against slab length for two subgrade support values. If curling is not considered, slab length has little effect on the estimate passes to failure, with an excess of 100,000,000 passes predicted in all cases. When curling and load related stresses are combined, a slab effect is evident, especially for the lower subgrade support conditions (i.e. $k = 100$ pci). Under these conditions, the longer slabs have fewer estimated passes to failure. It is also noted that the drop in estimated passes to failure is higher for stiffer support values (i.e. $k = 500$ pci) when curling stresses are added. This observation suggests that stiffer support beneath a slab has a reduced structural effect when curling stresses are considered.

Because of the complexity of conducting finite element runs, the use of pavement response algorithms is very appealing. Algorithms derived by Salsilli [Salsilli, 1993] and Lee [Lee, 1993] were compared to the results obtained from the ILLI-SLAB model. In Figure 27 the maximum flexural stresses due to loading for each pavement response algorithms as compared to ILLI-SLAB. The predictions are quite good. There is a tendency to under-predict the stress by a few psi, but this is inconsequential when considering the overall pavement variability.

When curling and load stresses are combined and compared (see Figure 28), the correspondence between the various methods is not as close, but is still good. The model incorporated in ILLICON and Lee's model were plotted. Lee, by using advanced statistical techniques and deriving a new dimensionless parameter, was able to develop a more rigorous solution [Lee, 1993]. The major drawback of Lee's solution is increased complexity, although the algorithm is available in spreadsheet format. The ILLI-CON model is simpler, but may lack accuracy in computing curling stresses under extraordinary conditions. The verification of his model reduces the reliance on the ILLI-SLAB finite element model in future investigations of the curling phenomena.

The FAA and ACPA allow for 5-in thick PCC slabs for aircraft having gross maximum weights of 12,500 lbs or less. The ACPA, in their detailed design procedure, permit the use of 4-in thick PCC for a dual wheeled aircraft weighing 12,500 lbs [ACPA, 1993]. Lee's closed form solution and the calibrated mechanistic model were used to examine allowable passes using the procedures and inputs previously described. The slab sizes were designed as recommended by ACPA, with 8 ft and 10 ft joint spacing used for the 4-in and 5-in thick pavements, respectively.

Results of this analysis are presented graphically in Figure 29. In considering loading effects only, the 5-in thick slab is estimated to carry over 1,000,000 passes if the modulus of subgrade reaction is greater than 100 pci. Under severe curling conditions, the allowable passes are reduced to just over 100,000. For lightly trafficked GA pavements that service King Air B200 aircraft, a 5-in thickness appears to be adequate. It is emphasized that this conclusion is based on the use of 10 ft joint spacing and does not consider service vehicles. Longer joint spacing, heavier and more frequent aircraft volume, and/or heavy service vehicles would be expected to have an impact.

Examination of the 4-in thick slab is not as promising. Although the MD fatigue algorithm calculates allowable passes in the tens of thousands, it is likely outside the range for which it was developed. The stress ratio under some loading conditions approaches 92%, a situation that would lead to rapid pavement failure. A beam model, such as the ZM equation, is

more appropriate. The ZM equation predicts under 100 estimated passes of the King Air B200 aircraft to failure (assuming a reliability of 50%) for a modulus of subgrade reaction value of 50 pci. It does not seem likely that a 4-in thick pavement can provide adequate structural performance. This analysis was conducted assuming 8.5 ft joint spacing and service vehicles were not considered. Longer joint spacing, heavier and/or more frequent aircraft loading, or the use of any service vehicles approaching highway loading conditions would likely lead to early structural failure of a 4-in thick PCC pavement.

In summary, analysis of the structural capacity of 6-in thick PCC pavements indicates that under loading typically encountered on GA pavements, a long structural life can be anticipated. It also appears that a 5-in thick pavement, with 10 ft joint spacing, should support the design aircraft, although concerns related to service vehicles use must be addressed. Structural response considerations indicate that 4-in thick PCC pavement do not possess adequate thickness to address GA airport loading conditions. The use of pavement response algorithms, particularly that developed by Lee [Lee, 1993], offer excellent flexibility with little sacrifice to accuracy.

IV.3. Material/Construction Related Factors

In most instances, structural factors are not the primary contributors to GA pavement failure. More importantly are material/construction factors. In AC pavements, weathering/raveling, paving lane cracking, longitudinal and transverse cracking, block cracking, and stripping are influenced by material/construction factors. Structural defects, such as rutting, corrugations, and alligator cracking, can also be strongly linked to material properties and construction practices. Similar concerns exist for PCC pavements. Durability problems, such as D-cracking, are linked directly to material selection. Poor construction practices can contribute to the development of slab cracking, crazing, and scaling through inadequate PCC thickness, low PCC strength, poorly timed or inadequate depth for joint sawing, or inadequate air void distribution. For these reasons, a thorough consideration of material/construction factors must be made.

IV.3.1. Material/Construction Considerations in AC Pavements

From the previous analysis, it appears that typical Illinois GA AC pavements have adequate structural capacity. The two factors that most significantly influence the long-term performance of GA pavements are the quality of the initial construction and the influence of climatic factors on material performance. Through addressing these two factors, longer lasting, better performing GA pavements can be built.

Material and construction specifications should be written to ensure that the constructed product is of high and lasting quality. Material specifications in particular have been continually revised, incorporating the results of recent experiences to improve long-term performance. This is evident in recent revisions to the FAA and IDOT-DOA hot-mix specifications, which feature numerous changes reflecting industry's current state-of-the-practice.

Section II of this report provides a comprehensive summary of these specifications. Of particular interest to this discussion are three observed construction factors that lead directly to the formation/propagation of AC pavement distress: depressions, roller checking, and the construction of the longitudinal paving lane joint.

Depressions are localized areas where the pavement surface that is lower in elevation than the surrounding surface. PCI data and visual surveys conducted during this study indicate depressions are observed at many GA airports. In many instances, depressions constructed into the pavement as a result of poor grade or compaction control in the supporting layers. Although these defects do not typically worsen with time, they do provide a potential serviceability hazard in wet weather. The pooling of water on the pavement surface also allows increased infiltration into the pavement structure, potentially increasing moisture related damage.

AC surface checking under roller compaction is another commonly encountered construction problem. Checking is a series of fine, transverse cracks that do not penetrate the full depth of the mat. The cracks are spaced 1 to 3 in apart, having lengths of 1 to 4 in. Checking is

caused either by excessive deflection of the pavement structure or a deficiency in the AC mix design that leads to tenderness under the rollers [Corps of Engineers, 1991]. The Corps of Engineers Handbook further states that the second cause is most prevalent. AC mixes with too much liquid (i.e. binder or moisture), a non-uniform sand gradation, or low voids in the mineral aggregate (VMA) are most susceptible to checking.

Evidently, IDOT-DOA is addressing asphalt cement binder aging by using low VMA/low air content AC mixtures. In this study, five separate mix designs prepared for projects at Pontiac, Morris, and Mt. Sterling were examined for mix properties. All the mixtures had VMA values below the level specified in IDOT-DOA's Standard Specifications for Construction of Airports [IDOT-DOA, 1985]. Air contents were set at 2%. The voids filled with asphalt (VFA) ranged from 82% to 85.5%. If these mix designs are typical, it helps to explain why checking is a widespread problem.

The current IDOT-DOA P-401 specification requires the use of pneumatic-tired rollers on the top lift of the surface course to address checking problems [IDOT-DOA, 1994B]. The specification also features a modified job mix formula, specifying a range for VFA versus VMA. Although this removes the requirement for different minimum VMA values based on the maximum aggregate size, the specified range of percent voids filled with asphalt (VFA) of 75% to 90% is relatively large.

Many pavement engineers believe that checking is only an aesthetic deficiency. Others believe that it is harmful to the long-term performance of the pavement, and may lead to premature aging and fatigue cracking [Abd El Halim, 1993]. Checking looks very similar to alligator cracking, and in many cases, checking has probably been classified as alligator cracking during the IDOT-DOA biennial inspections. Thus, some pavement sections with reported alligator cracking and a correspondingly low PCI are in reality showing checking distress.

The third construction related distress commonly observed on AC pavements is paving lane cracking. It is recognized that longitudinal joints have reduced density compared to the

interior portion of the paving mat [Burati, 1985]. The reduced density is believed to contribute to the occurrence of paving lane joint cracking. Research recently conducted by the National Center for Asphalt Technology examined the effect of different longitudinal joint compaction techniques on the joint density and performance [Kandhal, 1994]. Although the results are still preliminary, they suggest that construction technique has a profound impact on joint density and the resulting performance.

Paving lane cracking typically occurs within a few years of construction. Climatic and material factors that lead to age hardening of the AC also contribute to the formation and propagation of paving lane joint cracking. Paving lane cracking will probably form along with L & D cracking regardless of the joint density, but inadequate joint compaction is strongly implicated in the early formation of this distress. Poorly compacted joints act as a plane of weakness within the AC mat, and cracking results soon after construction. Through improved joint densities, the occurrence of paving lane cracking can be delayed.

In the most recent releases of the IDOT-DOA P-201 and P-401 specifications, longitudinal joint compaction is addressed in the following paragraph [IDOT-DOA, 1994A and 1994B]:

All longitudinal joints constructed are to be compacted in such a manner that they are "pinched" to provide adequate density at the joint. The method of "pinching" shall be as defined in the most recent issue of the N.A.P.A. (*sic*) Superintendent's Manual on Compaction of Asphalt Pavements.

The lack of commitment to a specific longitudinal construction technique reflects the current industry emphasis on new techniques that are emerging to improving joint compaction [Kandhal, 1994]. As research and development findings emerge, IDOT-DOA should consider being more specific in the manner in which joint densification is specified.

IDOT-DOA and the FAA specifications also require that joints in successive lifts be offset a minimum of 1 ft. This prevents the rapid propagation of a surficial paving lane joint to the bottom of the mat, avoiding large crack openings and the associated infiltration of water.

Once the AC pavement is constructed, climatic and material factors interact to age the asphalt cement binder. This aging leads to progressively stiffer AC over time. Age hardening phenomena results in numerous distresses including weathering/raveling, block cracking, longitudinal and transverse cracking, and paving lane joint cracking. A companion document provided with this report, Aging Phenomenon in Asphalt Concrete Pavements - A Literature Review, provides the results of a extensive literature review of recently conducted research on this topic. The literature suggests that asphalt cement binders undergo both short-term and long-term aging, with potentially different mechanisms contributing to each.

Short-term asphalt binder aging occurs during the construction process. High mixing and lay down temperatures lead to the loss of volatile components and oxidation. In-service pavements suffer progressive long-term age hardening of the binder primarily as a result of continued oxidation, although other factors, such as the thixotropic formation of internal structure, can contribute.

Efforts to duplicate short-term aging in the laboratory have been reasonably successful, as the main aging factors are heat and air. The rolling thin film oven test (RTFOT) has been used for many years to evaluate short-term binder aging characteristics, and its continued use is recommended by SHRP. SHRP Superpave also has specifications for short-term AC mixture aging. In this test, loose AC mixture is placed in a forced draft oven for four hours at 275° F, prior to compaction [Cominsky, 1994].

Less success has been achieved in developing laboratory tests to predict long-term asphalt cement aging characteristics. As long-term aging is primarily responsible for the distress formation and propagation trends previously identified, considerable efforts have been directed towards developing an effective test method to characterize this behavior. These methods have

included long-term oven heating, exposure to ultraviolet and infrared light, and the use of a pressure aging vessel (PAV). The PAV has gained acceptance in the SHRP binder characterization procedures [Petersen, 1994]. This testing protocol requires that after the binder passes through the RTFOT, it is heated in a PAV for 20 hours at a temperature between 190° F to 230° F under 305 ± 15 psi pressure. The induced physical and chemical changes are thought to simulate those that occur "in asphalt binders as a result of long-term, in-service oxidative aging in the field." [Petersen, 1994]. Petersen further notes that this is a binder test, and that mix properties will have an impact on actual field performance.

An optional long-term mix aging procedure is provided in the SHRP Superpave mix design. In this test, compacted specimens prepared from the loose AC mixtures exposed to the "short-term" aging procedure are placed in a forced draft oven at 185° F. The samples remain in the oven for varying periods depending on the expected length of pavement service life. Two days are considered equivalent to 10 years in service. Current University of Illinois research is evaluating the applicability of the SHRP methods to the State of Illinois.

IDOT-DOA is addressing asphalt binder aging by increasing the thickness of the asphalt film covering the coarse aggregate particles while simultaneously reducing the air void content of the mix. This approach produces mixtures with low air void content and relatively high asphalt content. Although thicker asphalt cement films reduce the aging effect, the drawback of this approach is reduced mixture stiffness and the propensity toward checking during construction. It is suggested that mix design specifications be evaluated, examining gradation changes that may allow for increased asphalt film thickness without sacrificing stability of the mixture during construction. The SHRP gyratory compactor can be used to evaluate the compactability of the mix during the mix design process.

Most AC material/construction considerations are addressed through the use of material and construction specifications. The most recent specification address some of the most relevant issues, including stripping, checking, and longitudinal joint densification. Recent SHRP research has investigated promising techniques for characterizing asphalt cement age hardening behavior,

and the University of Illinois is currently validating these procedures. Designing AC mixes with thicker asphalt cement films is one technique currently used to address asphalt age hardening. It is recommended that the current IDOT-DOA material selection and mix design practices be evaluated (modified as needed) to minimize asphalt cement aging and maintain mix stability under construction and traffic.

IV.3.2. Material/Construction Considerations in PCC Pavements

PCC pavements material and construction considerations are addressed through application of the appropriate specifications. The FAA and IDOT-DOA P-501 specifications have both been recently revised, reflecting the current trends in the industry. Structural performance is closely tied to the PCC thickness and concrete strength. Significant deviation of either parameter significantly impacts pavement life. Aggregate selection is extremely important to limit D-cracking. Air void content is another parameter that must be closely controlled, otherwise freeze-thaw damage may be incurred. Concrete density is also important, as poor consolidation can lead to poor strength and durability characteristics.

D-cracking is the most influential PCC material/construction factor encountered in this study. The new specifications stipulate that only non-D-cracking susceptible aggregate sources, as certified by IDOT, can be used in the construction of GA pavements. An alternative is to test an unapproved source using ASTM C 666. Through improved aggregate selection, D-cracking should be greatly reduced. Note that the use of shorter slabs will increase the number of joint and will exacerbate the D-cracking problem if susceptible aggregate are used.

Aggregate selection can also have a large impact on curling stresses. One important parameter in the calculation of curling stresses is the PCC coefficient of thermal expansion, α_T , which is typically assumed to be equal to $5.5 \times 10^{-6}/^{\circ}\text{F}$. This coefficient can vary greatly and is highly dependent on the aggregate type, with the coarse aggregate having the greatest influence [Mindess, 1981]. A concrete made with siliceous sand and quartz gravel would have a

coefficient of thermal expansion of approximately $6 \times 10^{-6}/^{\circ}\text{F}$; a typical concrete made wholly of limestone would have a coefficient of thermal expansion of approximately $3.5 \times 10^{-6}/^{\circ}\text{F}$.

Figure 30 shows the effect of different coefficient of thermal expansions on PCC slab curling stresses. A significant differences is observed in PCC made with limestone aggregate as compared to quartz gravel. Joint spacing and subgrade support also contribute. The most dramatic increase in curling stresses is observed when the modulus of subgrade support is increased from 50 to 100 pci. This analysis suggests that the PCC coefficient of thermal expansion, which is largely dependent on the coarse aggregate selected, has a large impact on the induced curling stresses. This factor should be considered in selecting joint spacing for GA airports.

IV.3.3. Project Approach to Material/Construction Factors

Classification of Pavement Type

The airport pavements in this study are classified as thin asphalt concrete (TNAC), thick asphalt concrete (TKAC), or PCC. TNAC pavements have a hot-mix AC surface between 2 and 5 in, supported by one or more granular layers of varying thicknesses. TKAC pavements have AC thickness greater than 5-in, supported by a granular layer or placed directly on the prepared subgrade. Subgrade lime treatment or stabilization is commonly used with TNAC and TKAC pavements to provide additional support and/or expedite construction. Under these classifications, most conventional pavements are considered TNAC and most FULL-DEPTH pavements are classified as TKAC. Illinois GA PCC airport pavements have a 6 to 8-in thick PCC surface (typically 6-in is used). A thin granular subbase is sometimes used. The three pavement types are illustrated in Figure 31.

PCC pavements were also separated on the basis of their L/l ratio. Actual slab length and thickness values were used in the calculation, but values for modulus of subgrade reaction ($k = 100$ pci.), PCC elastic modulus ($E_{\text{PCC}} = 4$ million psi), and Poisson's ratio ($\mu = 0.15$) were

assumed as indicated. This additional separation provided valuable insight into the performance characteristics of the various PCC sections

Summary

Material and construction factors are considered through specifications. The most recent releases of the IDOT-DOA specifications address many important issues relating to distress formation, including AC stripping, D-cracking, AC checking, and AC paving lane cracking. In the P-201 and P-401 specifications, an evaluation of the job mix formula should be conducted to examine gradation and mix design parameters to minimize the effects of asphalt cement aging. Tender AC mixes are probably due to low air voids and low VMA. Pontiac is a case in point, where low mix stiffness was measured in the laboratory along with the observation of unacceptable creep behavior in some of the samples. Research is currently being conducted at the University of Illinois into the SHRP asphalt binder test procedures and specifications and Gyrotory Compactor AC mixture design methods. These studies may provide improved AC mixture design and achieve better AC pavement performance. Studies should be conducted to better characterize IDOT-DOA AC mixture stiffness and fatigue properties.

V. DESCRIPTION OF DATA BASE

IDOT-DOA has collected PCI data on its GA airport network since 1980. This biennial inspection data represents a wealth of information on Illinois GA pavement performance and distress formation and propagation trends.

The importance of this data goes well beyond the planning and programming function that it currently serves. In conjunction with pavement inventory data, careful PCI data evaluation can discern performance trends for the various pavement types. Factors (loading, climatic, and materials/construction) contributing directly to distress formation and propagation can also be considered. To facilitate data manipulation, a relational data base called Microsoft Access® was selected.

Access® provides complete flexibility in extracting data. It allows custom designed queries to be performed with ease and almost any criteria can be used to extract selected pieces of information. For example, a query can be formulated to display all PCC pavement sections constructed in the Northern Climatic Zone from 1970 to 1979 that have current PCI values greater than 70. Data can also be imported directly into a Microsoft Excel® spreadsheet and/or the Systat® statistical analysis package for further analysis.

V.1. The ACCESS® Data Base

Relevant pavement inventory and inspection information were entered into Access®. The data base was divided into nine nested tables as illustrated schematically in Figure 32.

The first table, called APSITE, contains site specific airport information. There are four data columns included in this table. They are the airport name, the airport identification number (AID), the climatic code (indicating whether the airport is located in the Northern, Central, or Southern Climatic Zone), and a comment field. There is one primary key: the AID number.

Forty two airports are listed in this table (13 in the Northern Climatic Zone, 14 in the Central Climatic Zone, and 15 in the Southern Climatic Zone).

There are four tables in the level below APSITE: APLOAD, APSEC, APINV, and APCLIM. APLOAD contains 21 data columns. Stored information includes the airport name, AID number, the types and numbers of based aircraft, annual operations, and the number and length of each runway. Information provided by airport manager concerning aircraft and service vehicle loading is also included. A number of subjectively derived codes created to assist in the quantifying load related effects are also listed. The primary key is the AID number. A related table, SecLOAD, contains the Load Code for each pavement section.

APCLIM contains site specific climatic data in 17 data columns. The airport name, AID number, climatic zone, airport longitude, latitude, and elevation are tabulated. The SHRP average low and high air and pavement temperatures for each site and the recommended SHRP asphalt cement performance grade for 50% and 98% reliability are also provided. The primary key is the airport AID number.

The APSEC and APINVT tables are closely linked. APSEC contains five data columns related to specific pavement sections, including section number, feature (i.e. runway, taxiway, or apron), and the type of construction (i.e. TNAC, TKAC, or PCC). A total of 195 pavement sections are included in this table. This table has two primary keys: the AID number and section number.

Table 21 shows the distribution of pavement sections according to Climatic Zone, pavement type, and feature (i.e. RW, TW, or AP) contained in APSEC. Table 22 lists all the airport sections examined in this study, including the airport name, AID number, climatic zone, section number, type of feature, and pavement code. Pavement section inventory and PCI inspection information are presented in Appendix F of this report.

The APINVT table includes 17 data columns containing construction information for each section. This table includes the construction date, section area, number and size of slabs for PCC sections, and the various layer thicknesses and materials the FAA/IDOT-DOA material codes. The primary keys are the AID number and the section number.

The third level in the data base contains the APINSP table. This table has nine data columns containing data specifically related to the inspection of each section including inspection dates, section PCI values for each date, and the percent deducts as calculated by the IDOT-DOA PCI program. The primary keys in this table are the AID and section number. There are 893 entries in this table.

APSAMP lies below APINSP. It includes six data columns containing data relevant to sample units inspected within each section. The data includes sample unit numbers, sample unit area, and sample unit PCI. The primary keys are AID number, section number, inspection date, and sample unit number. There are 3,906 entries in this table.

The bottom table in the data base is APDIST. This table has seven data columns containing specific distress data, including the type, severity, and quantity recorded in each sample unit. The primary keys for this table are the AID number, section number, inspection date, and sample unit number. APDIST currently contains 8,275 rows of data.

V.2. Distribution of Pavement Sections

In addition to the 195 sections included in the data base, another 134 sections were included in a rehabilitated sections study to be discussed later. In total, the 329 individual pavement sections represent a large portion of the total GA airport network within the State. The examination and evaluation of pavement performance and distress trends is facilitated by considering when the pavement sections were constructed. In this way, a better understanding of the evolution of IDOT-DOA pavement design can be obtained.

Figures 33 through 38 show the observed construction trends for the TNAC, TKAC, and PCC sections. Figure 33 shows TNAC trends. The earliest sections were constructed prior to 1946 and all nine have been overlaid. Few TNAC pavements were constructed during from the mid-1940's to the mid-1950's, reflecting the dominance of surface treatments during this time. From the mid-1950's through the 1960's, many TNAC sections were built. It is not until the mid-1960's to mid 1970's that non-overlaid TNAC sections appear in the data base. The two oldest TNAC sections in the data base were built in 1967; one at Peoria Mt. Hawley (TW B/8) and the other at Jacksonville (AP EE/3). There was a steady decline in the number of TNAC pavements built after peaking in the early to mid-1960's, reflecting the trend to use thicker AC sections.

Figure 34 shows the year of construction for overlaid and nonoverlaid TKAC sections. The first TKAC pavements were constructed between 1966 and 1975. The oldest sections were built in 1968 at Dixon Springs and at Freeport (TW A/04). Over half of these pavements remained in service through 1993. Between 1976 and 1985, 43 TKAC sections were constructed that appear in the data base or have since been overlaid. Since 1986, TKAC continues to be the most popular pavement type.

Figure 35 presents the construction dates for PCC sections. PCC has a long history in Illinois GA airport construction, although it has never been the dominant pavement type. Eight sections in this study were constructed from the mid-1940's to the mid-1950's and three are still in service. All PCC sections constructed since 1966 are still in service. Figure 36 shows a further breakdown of non-overlaid PCC sections according to slab length. Joint spacing decreases over time and the most recent designs feature 12.5 ft to 15 ft joint spacing.

Figure 37 shows the construction date distribution for all 329 sections. Fewer TNAC sections are being built, although the total number built since 1986 is greater than the number of PCC sections constructed. There appears to have been a gradual increase in the number of PCC sections being built. TKAC is by far the dominant pavement type. These trends are also evident in Figure 38, which shows only the distribution of non-overlaid sections. The inclusion of such a widespread distribution of pavement types and construction dates provides an excellent

opportunity for a broad based examination of GA pavement performance and deterioration trends.

VI. PAVEMENT PERFORMANCE AND LONGEVITY TRENDS

"Pavement performance" can be measured in many different ways. Some transportation agencies use such characteristics as roughness and skid resistance to define pavement performance. In this study, pavement performance is defined using the PCI values calculated from observed pavement distress data. Distress data provide a measure of condition at the time of inspection. To define pavement performance, distress data collected over numerous inspection periods are combined and changes in condition as the pavement sustains traffic and ages are examined.

In contrast to pavement management, which uses performance data to estimate future maintenance and rehabilitation needs, this study focuses on identifying performance trends with the goal of improving material selection, pavement design and construction practices. Although the difference is subtle, it is of major importance in the manner in which the data are treated.

For example, in pavement management applications, condition data from existing pavement sections are monitored and combined to make projections of future maintenance and rehabilitation needs. Combining various pavement sections into "families" is a method used to provide data for the prediction process. As more data are collected, pavement families are further divided into smaller sub-families. Ideally, enough data are collected to monitor the performance of very unique sub-families, possibly containing data from only a few individual sections located within the same geographical region. This type of monitoring is useful for planning and programming purposes.

The continued refinement of the network into smaller and smaller groups of pavements is not particularly beneficial for future design applications. Each refined/improved pavement performance curve becomes more exclusively oriented to a unique pavement section subjected to

specific climatic, loading, and materials/construction factors. This does not necessarily improve the design of a new pavement section which will be subjected to different climatic, loading, and materials/construction factors. The refinement and exclusivity that makes pavement management models useful planning tools limits their applicability in the study of materials, pavement design, and construction factors. To be of practical significance, a study of materials, design, and construction factors must strive to be more inclusive through the examination of a wide spectra of data.

In this study, pavement sections were grouped into gross classifications based on pavement type (i.e. TNAC, TKAC, or PCC). An additional separation according to climatic zone was necessary to address the previously described Illinois climatic variability. Some modifications to these initial groupings were made to address specific issues as the data analysis progressed.

Two different stages were included in the examination of pavement performance and longevity trends. One featured the analysis of the data base which contained only pavement sections that had not been rehabilitated at the time this project was started. The second examined the age at first overlay (or rehabilitation) for many rehabilitated sections contained in the Illinois GA network. In combination, these two analyses provide a comprehensive and improved perspective of Illinois GA pavement performance trends.

VI.1. Pavement Performance Trends of Non-Rehabilitated Pavement Sections

Estimation of pavement performance (as measured by the PCI change over time) is of great importance to IDOT-DOA. Bond issues are commonly used to fund GA pavement construction and it is desirable to have maturation dates consistent with actual pavement life. Maintenance and rehabilitation costs are closely linked to pavement performance. Anticipated life information is helpful in accounting for the timing and magnitude of future maintenance and rehabilitation costs. From a design perspective, a thorough understanding of pavement

performance trends assists in identifying material selection and construction practices that extend initial pavement life and reduce future maintenance and rehabilitation needs.

PCI data were analyzed using an iterative process. Analysis procedures/techniques were modified to extract the most meaningful relationships from the data. The following discussion describes the major steps taken in establishing the pavement performance and longevity trends.

VI.1.1. Initial Analysis of PCI Versus Age Performance Trends

Figures 39, 40, and 41 are plots of sample unit PCI values versus age for TNAC, TKAC, and PCC pavements, respectively. The data are widely scattered. Linear regression estimates of the performance trends (PCI-Age relationships) are shown. The y-axis intercept was fixed at 100 (i.e. PCI equals 100 when age equals 0) to accommodate the assumption that no distress is present in newly constructed pavements. The correlations are not impressive (low R^2), reflecting a high degree of variability. The linear regression equations, corresponding correlation coefficients, and standard error of estimates for this initial analysis are present in Table 23. The equation coefficient defines the deterioration rate, representing the PCI loss/year. Non-linear regression models were also fitted to the data, but the correlations were not improved.

A variety of tools are commonly used to develop performance curves for pavement management applications. Typically, "expert knowledge" is used to assign a terminal PCI value at a given date. Thus, the initial PCI is fixed at 100 and the terminal ordinate is also set at an estimated age and PCI value. Another common practice is to fit pre-determined, higher-order models to the data to produce a pre-conceived performance curve shape. Correlations to the raw data are in many instances not improved, and may be worse than simple linear model correlations. These techniques have been used with success in pavement management applications, but their use is not considered appropriate for this study. Artificially imposing restraints on the observed data may obscure some of the trends that are important from material selection, pavement design, and construction perspectives.

Pavement performance trends for section PCI data were plotted and linear regression models established as shown in Figures 42, 43, and 44. The PCI was set at 100 at age 0 (zero). The linear models, correlation coefficients, and standard errors of estimate are presented in Table 23. The section data analysis reduced the "noise" observed in the sample unit data, but the correlations are not significantly improved. Although climatic effects (between Northern, Central, Southern Climatic Zones) are discernible, the high degree of variability makes it difficult to discern differences in the performance trends between TNAC and TKAC. TKAC sections appear to show lower deterioration rates (as represented by the slope of the linear regression equation) than TNAC sections. PCC sections constructed in the Central Climatic Zone have the lowest deterioration rate of all pavement type. Note that these PCC sections have a correlation coefficient (R^2) of 0.000 and a standard error of estimate in excess of 14 PCI points.

The overall poor correlation highlights one of the major limitations in this type of approach. When inspection data collected for specific sections are combined and plotted as a series of points, the performance trend for any given section is lost. For example, in the TKAC sections shown in Figure 43, there is one section inspection point in the southern climatic zone with a PCI value below 40 at 12 years of age while other sections in the same climatic zone have PCI values above 90 in years 11 and 13. Nothing about the past or future condition of the section is known; or whether the point is an anomaly or consistent with the overall section performance trend. All that is known is that inspection points observed over adjacent ages are very different. The linear model simply minimizes error between the points, contributing to poor correlation and poor model predictive capability. To improve upon this, the unique performance characteristics of individual sections should be incorporated.

A second problem is of greater concern. As a pavement section ages, its deterioration rate is influenced by its unique loading, climatic, and materials/construction factors. Local airport maintenance practices also impact the PCI deterioration rate. For example, in the PCI procedure a medium severity crack in an AC pavement would be re-classified as a low severity crack once it is filled, raising the PCI of the section. IDOT-DOA uses a PCI of 70 threshold value for programming pavement rehabilitation. Pavement section deterioration rates greater

than 3 PCI points per year would require programmed rehabilitation within 10 years. After rehabilitation, poorly performing pavement sections are removed from the data base while pavement sections that are either performing well and/or are being maintained would remain.

As time progresses, the sections remaining in the data base have deterioration rates that are less than the norm. Pavement sections with service lives of 20 years or more represent only a small number of the initial sections included in the data base. Yet, the "long-lived" sections strongly impact derived pavement longevity models by "pulling" the linear regression models upward. The models thus predict longer pavement lives than actually occur on average. The PCC sections shown in Figure 44 are an obvious example. A series of data points (age 34 years and greater) for three Quincy pavement sections unduly influence the Central Climatic Zone PCC regression model. The model predicts average PCC PCI values of 70 after 84.5 years of service. The removal of the Quincy data more than doubles the deterioration rate to 0.9 PCI points per year, reducing expected life to 33 years. The sensitivity of the model to a set of "long-lived" data points and the poor correlations severely reduce the usefulness of the prediction.

In this initial analysis, it was noted that PCC section variability was great. This was particularly true in the first 10 years of service. Some PCC sections show no distress while others had PCI values below 40. To determine if slab length was a factor, PCI section values for different slab sizes were plotted for each climatic zone. The analysis showed that slab length had a major impact. This observation is shown in Figure 45 where the average of all sample unit PCI values for PCC sections having slab lengths of 12.5 ft or less, 15 ft, 20 ft, and 25 ft are compared.

It is clear that joint spacing is a significant factor. The best performance is observed in 12.5 ft slabs. Pavements constructed with 25 ft joint spacing had the worst performance. In Figure 45, an inconsistency is observed, as the next best performing slab length is 20 ft, not 15 ft as would be expected. This occurrence is highly influenced by the 40+ year old pavement sections at Quincy, which have performed extremely well even though the joint spacing is 20 ft joint. Although the predominate PCC thickness in the data base is 6-in, the Quincy PCC sections are 8.5 in thick. Other PCC thicknesses in the data base range up to 9.5 in. To compare slabs of

various thickness and lengths, the L/ℓ ratio described in Section IV.3.2 was calculated for each PCC section. This "normalization" of PCC thickness and slab length was successfully used in all future analyses to develop PCC performance and longevity trends.

Initially all PCI data collected since the inception of the inspection program in 1980 were considered. The preliminary analyses discussed above indicated that inconsistencies in the 1980 and 1981 data existed. Discussions with IDOT-DOA revealed that these data were collected by summer interns, and its accuracy was suspect. The practice of using summer interns to collect pavement condition data was ended by IDOT-DOA prior to the 1982 inspection season. As a result, the 1980 and 1981 inspection data are not included in the detailed analyses described below.

VI.1.2. Development of Performance Trends Based on Deterioration Rate

In the initial analysis, severe limitations were observed in using PCI-Age plots to identify and compare pavement performance trends. An alternative approach was devised to address the limitations. This approach is based on the most important concept used in the study of pavement longevity: the deterioration rate (DR). Deterioration rate is defined as the PCI loss per year, or the slope of the linear PCI-Age model. An improved understanding of pavement performance can be obtained by using the DR concept.

DR calculation is straight forward. PCI data are analyzed on a section by section basis by determining the PCI loss between subsequent inspections, and dividing the loss by the number of years between the two PCI surveys. In this study, it was assumed that the first inspection for a new pavement was the date of construction and the initial PCI was set at 100.

As long as the section performance curve is monotonic, having a DR equal to or less than zero, the calculations proceed without difficulty. A problem is encountered when there is a PCI "improvement" between subsequent inspections. This difficulty is illustrated by the Effingham data shown in Figure 46. Three of the seven sections demonstrate "expected behavior" with each

inspection showing either no change or a PCI reduction. The remaining four sections show that on at least one occasion, a subsequent inspection resulted in a PCI increase. For example, the performance of sections RW 01/091 and RW 01/092 show an expected decreasing trend until age 11. In the next inspection, conducted at age 13, the PCI has increased from below 60 to above 70. Sections RW 11/11 and TW C/11 show similar trends.

There are two possible explanations for these observations. The first is that maintenance activities (such as crack sealing, patching, or seal coating) improved the pavement condition. For example, if cracks were sealed on Effingham's RW 09/27 between the surveys conducted in years 11 and 13, this may explain the improvement noted.

The other explanation is the variability in inspection and/or PCI calculation procedures. Many factors influence the accuracy of the inspection procedure. The time of year, the angle of sunlight, and the dampness of the pavement surface at the time of inspection are a few. The methods employed by IDOT-DOA personnel in conducting a survey could also contribute to differing results. For example, if checking was observed and labeled as alligator cracking in one inspection but in the next was recognized as checking, a shift in PCI may be incurred. By not inspecting the same sample units in each inspection cycle, IDOT-DOA introduces another source of variability. A third source of variability is the IDOT-DOA practice to estimate (rather than measure) distress quantities.

To address the inconsistency in the PCI data, an iterative method was used. Deterioration Rates for each section were calculated. Positive DRs (indicating an improvement in pavement condition) were individually examined to determine if a singular data point is due to an obvious error. Obvious errors were deleted. The analysis continued by eliminating the segment of the deterioration trend having a positive DR. If the next segment also had a positive DR, the data point was removed and the DRs for the remaining segments re-calculated. Thus, the deterioration trend for a single section was represented by a series of line segments having only negative DRs. In the vast majority of cases, only a single segment was eliminated.

This approach is justified on the basis that improvement resulting from maintenance activities should not be allowed to bias the study of pavement longevity trends. It is assumed that the pavement will continue to deteriorate after the maintenance activity, thus later inspections will again establish the DR that was temporarily interrupted by the maintenance activity. Error introduced due to inspection variability are beyond the control of this study. In either case, this method provides a standardized approach to address non-monotonic performance curve behavior.

One strength of this approach is that although some inspection data were lost, no sections were dropped from the study. The results thus reflect performance of all the sections initially included in the study, not just sections that gravitate toward "normal" behavior. This approach also deals effectively with the influence of maintenance and inherent inspection error. The most important feature of this approach is that the pavement trends are not unduly influenced by long-lived pavement sections that make up only a small percentage of the data base.

Data for each section were plotted using line segments to represent the deterioration rates. An example TKAC plot for the Northern Climatic Zone is shown in Figure 47. The variability in performance for various sections is readily observed and a performance trend is noted.

A preliminary statistical analysis indicated a performance period of five years was appropriate. Annual DR estimates were made by interpolating between inspection points for each section. Five year DR averages were then calculated for each pavement type and climatic region. The trendline was established through significance testing ($\alpha = 0.05$) conducted to compare the average DRs for adjacent performance periods. For example, the average DR for 1-5 years was compared to that for 6-10 years. If these were found to be significantly different, the 6-10 year average was compared to the 11-15 average. In cases where significant differences were not observed, the data from adjacent performance periods were combined and then compared to the next performance periods.

AC Pavement Performance Trends

AC surfaced pavement deterioration trends (based on DR) are shown in Table 24. Figures 48 and 49 present the pavement performance trends for TNAC and TKAC, respectively. Figure 50 shows the calculated trend-line for the section data in Figure 47.

Significance testing was conducted ($\alpha = 0.05$) for each pavement type to assess the overall effects of climate on DR. For TNAC sections, significant DR differences were observed between the Central Climatic Zone and the Southern and Northern Climatic Zones. There is not a significant difference between the Northern and Southern Zones. In TKAC sections, the Central and Southern Climatic Zones were found to have significant DR difference. There was not a significant difference between the DR for the Northern Climatic Zone as compared to either the Central or Southern Climatic Zones.

DR comparisons were also made between TNAC and TKAC sections constructed in the same climatic zone. The only overall significant DR difference ($\alpha = 0.05$) was in the Central Climatic Zone, where TKAC had lower overall DRs than TNAC. When DR differences were analyzed within specific age ranges, TKAC had lower DRs than TNAC in the 1-10 years age range in the Central Climatic Zone, the 11-20 year age range in the Northern Climatic Zone, and the 6-15 year age range in the Southern Climatic Zone. TNAC had lower DRs than TKAC in the 6-10 year age range in the Northern Climatic Zone.

In 1985, IDOT-DOA established their GA airport material and construction specifications [IDOT-DOA, 1985]. The impact of these specifications was considered for AC pavements. Deterioration trends for TNAC and TKAC pavements were established for pavement sections constructed before and after 1985. No significant DR differences in performance were found. The time frame is short (only nine years of data for sections constructed under the IDOT-DOA specifications) and it was not until the late 1980's that significant AC mix design modifications were implemented. It is concluded that more time is required before the impact of IDOT-DOA AC mix design modifications can be adequately assessed.

PCC Pavement Performance Trends

The same analysis procedures were employed in establishing PCC pavement deterioration trends. The PCC pavement sections were subdivided according to the estimated L/ℓ as described in Section IV.3.2 of this report. Slab sizes were classified as Small, Medium, or Large according to the two divisions of L/ℓ shown in Table 25. Division 1 was initially selected based on previously developed criteria. Division 2 was subsequently added to represent a breakdown consistent with joint spacing of 12.5 ft, 15 ft, and 20 ft (given 6-in thick PCC slab, $E_{PCC} = 4,000,000$ psi, $k = 100$ pci, and $\mu = 0.15$). Figure 51 shows the relationships between slab size, k-value, and L/ℓ given an E_{PCC} of 4,000,000 psi and a thickness of 6 in.

Deterioration rates were calculated for Division 1 and Division 2 slab sizes for each climatic zone. Deterioration trends were established for each slab size within a climatic zone using significance testing to compare DRs over successive age ranges. If the DR in one range could not be statistically differentiated from that in the adjacent age range, the two were combined. This process was continued until the final deterioration trends were established as shown in Figures 52, 53, and 54 (for Division 1 slab sizes in the Northern, Central, and Southern Climatic Zones, respectively). Table 26 summarizes this analysis.

Slab size significantly affects the deterioration trends. Small slabs always perform better than medium slabs and medium slabs perform better than large slabs. For large slabs, there were significant differences in performance in the Northern and Southern Climatic Zones, both of which performed better than large slabs in the Central Climatic Zone. For medium slabs, those in the Central Climatic Zone had significantly better performance than Southern Climatic Zone, which in turn performed better than those in the Northern Climatic Zone. There was no demonstrable difference in the performance of small slabs in the Northern and Southern Climatic Zones, although small slabs in the Central Climatic Zone out-performed those to the north and south.

Large PCC slab DRs were significantly higher than those recorded for TNAC and TKAC, regardless of the climatic zone. In contrast, small PCC slabs had lower DRs than the TNAC and

TKAC in the same climatic zone. In the Central and Southern Climatic Zones, the medium PCC slab size pavements had significantly lower DRs than TNAC or TKAC. In the northern climatic zone no significant difference was observed in comparing medium PCC slab sizes to either TNAC or TKAC.

Division 2 slab sizes were established to approximate 12.5 ft, 15 ft, and 20 ft slab lengths (6-in PCC slab, $E_{PCC} = 4,000,000$ psi, $k = 100$ pci, and $\mu = 0.15$). The data set is not as complete, as there are no "small" slabs found in the Central Climatic Zone and only 10 years of data exists for large slabs in the Northern Climatic Zone and medium slabs in the Southern Climatic Zone. Data shown in Figures 55, 56, and 57, and tabulated in Table 27, indicate a slab size effect on DR. In all cases, smaller slabs have the lowest DRs within a climatic zone. However, the differences between small and medium are not as great as before, and when the data sets are compared, there is no significant difference in DR between the two. In comparing the DRs for Division 1 and Division 2 small slabs, no difference could be shown. Although the established deterioration trends suggests that 12.5 ft slabs are performing better than 15 ft slabs, this analysis can not statistically separate the two. The gaps in the data set make long-term comparisons impossible in all but the Central Climatic Zone, where only medium and large slabs are found.

VI.1.3. Summary

Pavement performance and longevity trends established through regressing scatter plots of PCI versus age data are limited in their usefulness. The limitations include poor correlations, the inability to address pavement improvement resulting from maintenance activities or errors in the condition assessment, and the tendency for long-lived pavement sections to unduly influence the performance model regression.

A deterioration rate (DR) approach is used in this study to address the limitations of the traditional approach. Pavement performance and longevity trends were established for the various pavement types for the three climatic zones. PCC pavement sections were further

divided using the L/l ratio to account for marked differences in pavement performance incurred due to slab size effects. Small slab PCC pavements had the best overall performance. Differences in performance between TNAC and TKAC were not easily discerned, but it appears that TKAC may offer improved long-term performance, with lower DRs after 10 years of service. The results present an improved estimation of Illinois GA airport pavement deterioration rates and performance trends.

VI.2. Analysis of Rehabilitated Sections

IDOT-DOA construction data were reviewed to further investigate performance and longevity trends. The review established when various pavement sections were rehabilitated, looking specifically at sections with construction types (i.e. TNAC, TKAC, or PCC) within the scope of this study. It was attempted to include only sections that were rehabilitated due to distress. Sections overlaid as part of staged construction or as a transition from an adjacent project were not included. The distribution of the 134 sections included in this analysis is shown in Table 28.

There is a predominance of TNAC pavements in this study. Many of the flexible pavements constructed in the late 1950's and early 1960's consisted of granular base layers surfaced with 2 in of AC. It was not until the early 1970's that the first FULL-DEPTH AC pavements began to appear.

This analysis provides a good indication of expected life, as GA pavements are only rehabilitated when conditions require it. The analysis is limited because the cause of deterioration and that the condition at the time of repair are not known for most of the sections. Table 29 shows the results of this analysis, including the mean, standard deviation, coefficient of variation, and number of sections for each pavement type within each climatic region.

ANOVA and t-test analyses were run ($\alpha = 0.05$) to determine which, if any, means were statistically different than the others. In the Central Climatic Zone, all three means were

different, with PCC sections having the highest age and TNAC sections the lowest age at the time of rehabilitation. In the Northern Climatic Zone, the mean age for the PCC was higher than for the TKAC, but could not be statistically differentiated from TNAC, nor could the TNAC and TKAC be statistically differentiated. In the Southern Climatic Zone, the mean age at rehabilitation for the PCC pavement was significantly different than the TKAC or TNAC. No difference in the mean age at rehabilitation could be observed between the TNAC and TKAC. The results of this "age at rehabilitation" analysis are consistent with the results obtained in the DR study. The PCC pavements had the highest age at the time of rehabilitation while differences between TNAC and TKAC were difficult to show.

Estimates of pavement life made from the pavement performance trends established in the previous section of this report are shown in Table 30. Terminal PCI was considered to be 70. Comparisons between the two analyses indicate that pavements are typically rehabilitated later than would be predicted. IDOT-DOA normally considers a PCI of 70 as a trigger for programming pavement rehabilitation. The actual construction would likely occur one to two years later, thus the terminal PCI would be lower than 70. Also, many of these pavement sections probably should have been overlaid sooner, but prior to biennial inspections, there was not a standardized method of determining the overall condition of the pavement network. It is likely that rehabilitations are conducted in a more timely fashion under the current IDOT-DOA system.

VII. PAVEMENT DISTRESS FORMATION AND PROPAGATION TRENDS

The pavement performance and longevity trends were established using the section PCI values collected during the IDOT-DOA biennial inspections. PCI values are calculated from observed distress data, providing standardized measurements of the distress type, quantity, and severity observed in each sample unit. The usefulness of the PCI data extends beyond the development of longevity trends. Specific distress data can be examined to discern the leading causes of deterioration for Illinois GA airport pavements.

AC and PCC pavements are discussed separately in this section of the study. The most common distress types are first identified. Then, the occurrence of each distress type is evaluated over time (through multiple distress surveys) to examine distress formation and propagation trends.

VII.1. Deterioration Trends for AC Surfaced Pavements

Figures 58, 59, and 60 show the percent TNAC sample units affected by each distress type in the Northern, Central, and Southern Climatic Zones, respectively. The distribution of sample units used in this analysis are provided in Table 31. The distress data are divided according to distress severity. The percent sample units affected measures whether a distress of a given severity is recorded in a given sample unit or not. It is readily evident that alligator cracking, depressions, longitudinal and transverse (L & T) cracking, oil spillage, and paving lane cracking are the most prevalent distress types.

In the Northern Climatic Zone, approximately 38% of the TNAC sample units are affected by low severity paving lane cracking. It is the most commonly recorded distress. Low severity L & T cracking is the second most commonly observed distress, occurring in approximately 33% of the sample units surveyed. Medium severity alligator cracking is the third most common distress observed (approximately 20% of the sample units) and there are also significant amounts of low and high severity alligator cracking.

In the Central Climatic Zone, the most commonly recorded distress type is L & T cracking, with low and medium severities affecting approximately 65% and 40% of the sample units, respectively. Low and medium severity paving lane cracking are observed in about 35% of the sample units. This high incidence of L & T and paving lane cracking dominates the deterioration trends in this climatic zone. A significant number of sample units are affected by alligator cracking (approximately 15% low severity and 10% medium severity).

Similar trends exist for the Southern Climatic Zone where approximately 70% of the sample units are affected by low severity L & T cracking and approximately 58% are affected by low severity paving lane cracking. Medium severity L & T and paving lane cracking were observed in approximately 40% of the sample units. Approximately 10% of the sample units were affected by low severity alligator cracking.

The same distress types also dominate TKAC pavement deterioration as shown in Figures 61, 62, and 63 for the Northern, Central, and Southern Climatic Zones, respectively. In all three climatic zones, the most prevalent distress is the low severity L & T cracking, observed in approximately 55% to 65% of the sample units. The next most prevalent distress, low severity paving lane cracking, affects 40% to 50% of the inspected sample units. Significant quantities of medium severity L & T and paving lane cracking are also observed. Alligator cracking has occurred in fewer sample units and in reduced severity than for the TNAC pavements, but is present in 7% to 12% of the sample units.

Each of the five most prevalent AC distresses (in alphabetical order: alligator cracking, depressions, L & T cracking, oil spillage, and paving lane cracking) was analyzed to discern distress formation and propagation trends. The distress data were evaluated in consecutive 5 year periods, corresponding to the age ranges utilized in establishing the longevity trends.

VII.1.1. Alligator Cracking

Alligator cracking is a fatigue related distress, resulting from repeated load applications. Thus, by definition, it is restricted to areas subjected to repeated traffic loadings. In Section IV.2.4 of this report, a mechanistic-empirical design check of typical pavement sections designed using the FAA and AI design schemes indicated that structural distress should not be widespread on pavements subjected to GA aircraft loading. The relatively high incidence of alligator cracking observed in the data base is not consistent with this finding.

Figures 64 (TNAC) and 65 (TKAC) show the percent sample units affected by alligator cracking in each five year period for the three climatic zones. In the first 5 years of service TNAC and TKAC sample units show alligator cracking in all climatic regions, although the percent affected is below 10%. Although the incidence rate is low, it is surprising that any is recorded in the first 5 years of service, especially in TKAC sections.

In the age range of 6-10 years, an increasing amount of alligator cracking is reported. In the TNAC sections, 10% to 20% of the sample units had alligator cracking and the TKAC sample units showed slightly more at 15% to 25%. In the first 10 years of life, roughly one fifth of the sample units showed fatigue related distress. This finding was disturbing in light of the relatively light GA traffic conditions.

Field evaluations of GA airports conducted in the course of this study provided some perspective. During two separate IDOT-DOA inspections, it was observed that alligator cracking was not properly identified. In one instance, an area of checking located at the edge of a taxiway was recorded as alligator cracking. Although checking is similar to alligator cracking in appearance, its presence in a non-trafficked edge area immediately rules out structural fatigue as the cause.

A second instance of improper identification occurred on a runway. IDOT-DOA inspectors debated whether the observed cracking pattern was block or alligator cracking,

deciding that it had become spaced closely enough to be classified as alligator cracking. The deterioration modes for the two distress types are not directly related, and confusion between block cracking and alligator cracking should be resolved through analysis of the distress location with respect to traffic patterns. In this instance, it was in the middle section of the runway where traffic is non-channelized and moving rapidly. In addition, the cracking was widely distributed across the width of the runway, even near the runway edge. This observation suggests that the distress was most likely block cracking.

Confusion between block cracking and alligator cracking was also observed at Dixon. Sections RW-08/09 and TW-A/09 were constructed in 1983 using FULL-DEPTH construction (2 in P-401 on 6 in P-201). Transverse joints were sawed and sealed at estimated 100 ft intervals with the intent of "controlling" thermal cracking. The first inspection following construction (1984) identified no distress in either section, but by the next inspection (1986), the section PCI for the RW and TW had decreased to 61 and 60, respectively. In some instances, 20% to 30% of the sample unit surface was recorded as having low severity alligator cracking. By the 1992 inspection, the section PCI values had dropped to 53 for the runway and 40 for the taxiway. Although L & T cracking and paving lane cracking were reported, the primarily distress observed was low and medium severity alligator cracking, with over 50% of the sample unit area affected in one instance.

The extremely poor performance of these two sections drew the attention of the project researchers, and the site was visited in September, 1993. The cracking pattern on the pavement surface was observed and photographed. It was concluded that the distress was not load related as it was as prevalent in non-trafficked and in trafficked areas. Although it does not appear to be typical block cracking, it is evidently a result of climate and/or material/construction factors due to its widespread distribution over the pavement surface. Additional evidence supporting this belief is the abnormal widening (to approximately 3 in) of the sawed transverse joints. Apparently, the AC material is very susceptible to shrinkage as it ages. The classification of the distress as alligator cracking severely depresses the PCI of the sections and inappropriately attributes the distress to structural failure instead of climate and material/construction factors.

The belief that alligator and block cracking have been confounded is further supported by the observation that little block cracking is recorded in the data base. Only a small percentage of total sample units have been affected by block cracking as shown in Figures 66 and 67 for TNAC and TKAC sample units, respectively. In TNAC sample units that range in age from 16 to 25 years, block cracking is observed in appreciable quantities only in the Central Climatic Zone. The Southern Climatic Zone has no recorded block cracking while the Northern Climatic Zone has under 10% in the older pavement sections. In contrast, 100% of the TNAC sample units in the Northern Climatic Zone greater than 15 years of age are affected by alligator cracking.

In the same age range of 16 to 25 years, 35% to 50% of the TKAC sample units in the Northern Climatic Zone are affected by block cracking. Of the 118 sample units between the ages of 16 and 20 yrs in the Central Climatic Zone, there is not one instance of block cracking recorded. In the Southern Climatic Zone, less than 16% block cracking is noted for pavements older than 10 years. This apparent lack of block cracking, accompanied by the high recorded instances of alligator cracking suggests that confounding between the two distress types has occurred.

To further examine the relationship between loading and load related distress, the Load Code for each section was correlated to the sample unit distress data. Table 32 shows the number of TNAC, TKAC, and PCC sample units distributed with respect to low, medium, and high Load Code. Note that very few TNAC and TKAC sample units (less than 3%) lie in high Load Code sections, with the majority in low Load Code conditions. The PCC sample units are most likely to be in high Load Code applications (approximately 19%).

Load Codes were correlated to instances of alligator cracking for TNAC and TKAC as shown in Table 33. It would be expected that sample units with medium to high Load Codes would suffer more structural distress and of higher severity than those sections with low Load Codes. In low Load Code TKAC sections, 10.54% of the sample units are affected by low severity, 1.53% by medium severity, and 0.12% by high severity alligator cracking. In contrast, sample units having medium and high Load Codes have less recorded instances of low severity

alligator cracking, with 7.99% and 6.82%, respectively. None of the sample units having high Load Codes suffered medium or high severity alligator cracking. In TNAC sample units, there was no alligator cracking recorded in sample units having high Load Codes. Most of the alligator cracking recorded in TNAC sample units was observed in sections with a medium Load Code but low Load Code sample units still had a significant amount of alligator cracking, with 7.87% suffering low severity and 3.55% suffering medium severity alligator cracking. The results of this analysis suggest that for the TKAC pavements, Load Code and alligator cracking cannot be related. In TNAC sections, the results were inconclusive.

Figure 68 shows the percent sample unit area affected by alligator cracking for all TNAC and TKAC sample units. Alligator cracking is typically isolated to a relatively small areas of the pavement surface, as it occurs only where channelized traffic flow is common. In Figure 68, a significant number of sample units have greater than 10% of their surface area affected. This observation is most common in older TNAC sample units, but is also observed in TKAC sample units as young as three years (Dixon). This high percentage of area affected again suggests that load is not the primary cause of the observed distress, as load related distress is typically isolated to small areas that receive frequent load applications (i.e. wheel paths). This further supports the belief that alligator cracking was inappropriately assigned in some of these sample units.

It is concluded that the relatively extensive occurrence of alligator cracking in the AC surfaced pavements is primarily the result of misidentification of the distress and not widespread structural failure. Alligator cracking is present in the Illinois GA airport pavement network, but it has been confounded in some cases with other distress types (block cracking, checking). Thus, it is difficult to utilize the inspection data to accurately assess the contribution of load to pavement deterioration. It is generally believed as a result of limited visual inspections and the structural analysis conducted during this study that load is not a primary pavement deterioration factor for Illinois GA airport pavements.

VII.1.2. Depressions

Depressions are frequently observed in both TNAC and TKAC pavements. Primarily considered a construction related distress, they are not normally expected to increase in number or severity with age.

Figures 69 and 70 show the percent TNAC and TKAC sample units affected by depressions, respectively. Many depressions are recorded in the first five years of service, supporting the belief that construction contributes to their presence. The number of occurrences fluctuates with time, but does not show a distinguishable trend toward increasing occurrences. Nor are depressions observed more often in TNAC or TKAC. There does appear to be a general trend toward fewer recorded occurrences of depressions in the first five years of service, although this trend may reflect recent improvements in construction practices.

VII.1.3. Longitudinal and Transverse Cracking

L & T cracking is a frequently observed distress type in AC surfaced pavements. Figures 71 and 72 show the percent TNAC and TKAC sample units affected, respectively. L & T cracking appears soon after construction in many TNAC and TKAC pavements. Approximately 20% to 53% of the TNAC and 20% to 40% in the TKAC sample units are affected within the first five years of service. Within the age range of 6 to 10 years, 59% to 86% of the TKAC sample units are affected. Slightly more TNAC sample units are affected (65% to 92%) over the same time period.

For pavement ages beyond 10 years, the percent TKAC sample units affected remains high. In the TNAC, there appears to be a decrease in occurrences after 15 years. This decrease coincides with the high amounts of alligator cracking recorded, particularly in the Northern Climatic Zone. In examining the data in detail, L & T cracking was not counted in the inspection of AP-NW/09 at Dupage in the more recent surveys. Instead, high amounts of alligator cracking was recorded as shown in Figure 64 (Northern Climatic Zone: age in excess of 16 years). Under

the guidelines in FAA AC 150/5380-6, both alligator cracking and L & T cracking should be recorded if both are present. Thus, L & T cracking should have been counted in the most recent Dupage AP-NW/09 inspections. If block cracking is observed, L & T cracking is not counted. In older pavement sections suffering block cracking, a decrease in the amount of L & T cracking would thus be expected.

Figure 73 shows the average density (ft of cracking/ft² area of sample unit) of L & T cracking for TNAC and TKAC sample units. The points are average values for all affected sample units of the same age and do not show the variability within each pavement type. They also represent a compilation of all three severities. The general trend indicates that in affected sample units, TKAC has lower cracking densities than TNAC. This trend is most pronounced in sample units older than 10 years.

Figures 74 and 75 are examples of cracking severity trends for the Northern Climatic Zone for TNAC and TKAC, respectively. The trendlines are best linear fits through the data (density set to zero at age zero). The trendlines for low and high severity cracking are similar, but the trendline for medium severity cracking is steeper for TNAC.

Overall, the analysis suggests that L & T cracking is a frequently occurring distress. It is manifest early in pavement life, and it is progressive both in quantity and severity with time. The climate/material related nature of this distress type indicates that improved material selection leading to a reduction in L & T cracking would have immediate and long-term benefits to AC pavement performance.

VII.1.4. Oil Spillage

Oil spillage is a common problem on aircraft parking aprons, where fuel, oil, and hydraulic fluid are spilled during fueling and maintenance activities. In total, 83% of the sample units affected by oil spillage are located in apron sections. Figures 76 and 77 show the percent

sample units affected for TNAC and TKAC, respectively. Oil spillage occurs with similar frequency regardless of pavement type or climatic zone.

VII.1.5. Paving Lane Cracking

Paving lane cracking is a frequently observed distress on AC surfaced pavements. Figures 78 and 79 show the percent sample units affected by this distress for TNAC and TKAC, respectively. Within the first five years of service, the distress has occurred in 30% to 48% of the TNAC sample units and 24% to 42% of the TKAC. This rapid onset makes it one of the leading cause of early deterioration in AC surfaced pavements.

As the pavement ages, increasing occurrences of this distress are noted in TKAC pavements through the entire age range, with 90% to 100% affected in the age range of 21-25 years. In TNAC pavements, there appears to be a decrease in the number of sample units affected past 15 years. This is likely due to the presence of increased amounts of alligator and block cracking previously discussed under L & T cracking.

Figure 80 shows the average paving lane cracking density (ft paving lane cracking/ft² area of sample unit) for sample units in which the distress occurred. This figure represents the average combined cracking of all severities in all climatic zones. There are no clear differences between the average cracking density for TNAC and TKAC sample units, with each having similar amounts of cracking at each age. It is noted that the density of paving lane cracking remains fairly constant with age, suggesting that once the distress is manifest, the crack lengths do not increase with time. This observation is consistent with this distress type, as there are only a limited number of longitudinal joints within a given sample unit that can crack. The distress density cannot increase past the point where all the paving lane joints are affected.

Figures 81 and 82 further illustrate this point for TNAC and TKAC sample units in the Central Climatic Zone. It was necessary to fit non-linear trendlines to the data because of the very early manifestation and the apparent subsequent "leveling off" of the distress density. These

trendlines show that once the paving lane joints cracks, the density within a sample unit remains relatively constant. Changes after initial cracking do not lead to increased crack length, but instead increased crack severity, with higher severity levels occurring over time. This is observed in Figure 81. Low severity paving lane cracking decreases slightly over time, as medium and high severity cracking increases.

In summary, paving lane cracking is a frequently observed distress, appearing soon after construction. Over time, low severity cracking deteriorates into medium and high severity cracking, but the overall density does not increase past the point where all paving lane joints are affected. The early manifestation of this distress makes it one of the leading causes of premature deterioration in AC surfaced pavements. Construction techniques that would address the formation and subsequent propagation of this distress would have an immediate and long-term positive effect on AC pavement performance.

VII.1.6. Summary

The most prevalent and damaging distress types observed in the AC data are L & T and paving lane cracking. Both types of cracking are observed in significant quantities within the first five years of service, and eventually affect the majority of sample units within 10 years. Alligator cracking is also commonly observed in the data. It is believed that it is not as widespread as the data suggests, but that alligator cracking has been confounded with other distress types (block cracking and checking). The most dramatic improvement in short- and long-term AC pavement performance can be obtained through material selection and construction practices that lead to a significant reduction in L & T and paving lane cracking.

VII.2. Deterioration Trends for PCC Pavements

Figures 83 through 91 show the percent PCC sample units affected by distress for the various Division 1 slab sizes and climatic regions. Table 34 shows the distribution of sample units used in this analysis. Large slab data are shown in Figures 83, 84, and 85 for the Northern,

Central, and Southern Climatic Zones, respectively. Low and medium severity longitudinal, transverse, and diagonal cracking (L, T, & D cracking) are quite common, with the majority of sample units affected. Shattered slabs were frequently recorded in the Northern and Southern Climatic Zones. Other distress types observed in over 20% of the sample units include corner breaking, corner spalling, D-cracking (in the Central Climatic Zone), faulting (in the Central Climatic Zone), joint seal damage, and joint spalling.

Figures 86, 87, and 88 show the percent sample units affected by distress for medium slabs in the Northern, Central, and Southern Climatic Zones, respectively. In general, the percent sample units affected and the distress severities are less than for the large slabs. In particular, shattered slabs are significantly reduced. Faulting is another distress that is not commonly observed in medium sized slabs. Corner spalling, D-cracking, joint seal damage, joint spalling, and L, T, & D cracking occur in 20% or more of the sample units.

Compared to medium and large slabs, a significant reduction in distress occurrences and severities is observed in the small slabs. This is shown in Figures 89, 90, and 91 for the Northern, Central, and Southern Climatic Zones, respectively. In all cases, the percent sample units affected by distress is less than 40%. In the Northern, Central, and Southern Climatic Zones, L, T, & D cracking is observed in approximately 5%, 14%, and 23% of the sample units. Corner breaking is below 5% and shattered slabs are almost non-existent. Other frequently occurring small slab distress types include corner spalling, D-cracking, joint seal damage, and joint spalling.

Further examination of distress formation trends for PCC pavements is presented below. The occurrence of distress over time for the three slab sizes in the three climatic zones will be examined for corner breaking, corner spalling, D-cracking, joint seal damage, joint spalling, L, T, & D cracking, and shattered slabs (listed in alphabetical order).

VII.2.1. Corner Breaking

Figures 92, 93, and 94 show the percent sample units affected by corner breaking in the Northern, Central, and Southern Climatic Zones, respectively. Each plot includes the effect of slab size and age. In the Northern and Central Climatic Zones, corner breaking is least for small slabs. This is not the case in the Southern Climatic Zone where small and medium slabs have similar performance. Corner breaking in small slabs appears to be progressive in nature; the percentage increases for each successive age range. A similar trend is observed for medium slabs in the Southern Climatic Zone, but is not observed in the other two climatic zones. For large slabs, age does not appear to be correlated with the number of sample units affected by corner breaking.

The Load Code was used to examine the effect of loading on corner breaking. Table 35 presents the sample unit distribution for various slab sizes and Load Codes. Medium slabs are most common under high Load Code conditions. Small slabs are most common under low and medium Load Code conditions.

Table 36 shows the percent sample units affected by the various distress types and severities for each Load Code and slab size. In comparing the incidence of corner breaking to Load Code, it is important to examine the effect of slab size. Small slabs have less occurrences of corner breaking and lower severity in each Load Code category. Large slabs have the highest occurrences of corner breaking. Corner breaking is also more severe in large slabs. Comparing slab sizes across the three Load Codes shows no influence of loading on the occurrences or severity of corner breaking. The greatest number of occurrences of corner breaking is found in large slabs located in low Load Code sections and the occurrences in small slabs are very similar for high and low Load Codes. These observations suggest that corner breaking is not strongly related to load in GA airport applications.

In summary, corner breaking is most closely related to slab size. Smaller slabs have less corner breaking than large slabs. This finding implicates climatic effects as the most important

factor in the formation of this distress in GA pavement applications. A direct relationship between loading condition and corner breaking could not be established.

VII.2.2. Corner and Joint Spalling

Corner and joint spalling are combined in this discussion as the formation factors for these distresses are similar. Figures 95, 96, and 97 show the deterioration trends for corner spalling and Figures 98, 99, 100 show the deterioration trends for joint spalling. These figures present the percent sample units affected by each distress over five year time periods for large, medium, and small slab sizes.

In the Northern Climatic Zone, all of the large slab sample units show joint spalling and 75% experienced corner spalling within the first five years of service. High levels of both joint and corner spalling in large slabs were observed in other climatic regions and age ranges as well. The fairly rapid appearance of spalling in large slabs suggests that slab size plays a significant role in the early formation of this distress.

In early age ranges that have all three slab sizes represented, spalling generally appears more often in large slabs than in small or medium slabs. But the difference between the occurrence of spalling for different slab sizes decreases with time. After an age of 15 to 20 years, the number of sample units affected by spalling in older pavements cannot easily be related to slab size.

Corner spalling in small slabs appears to be progressive. In the first five years, corner spalling occurs in 0% to 10% of the sample units. In the 6-10 year age range, corner spalling ranges from 0 to 45%, with the highest occurrence in the Northern Climatic Zone. In the 16-20 year range, 39% to 62% of the sample units are affected, with the highest number recorded in the Northern Climatic Zone. Joint spalling follows similar trends, with the highest occurrences in small slabs observed in the Northern Climatic Zone. In the 16-20 year range, joint spalling occurring in 38% to 75% of the sample units.

Table 36 presents the relationships between Load Code and corner and joint spalling. Medium and high Load Code sections have higher amounts of corner spalling for each slab size than low Load Code sections. Joint spalling has the opposite trend, with the highest occurrences in low Load Code sections for medium and large slabs. The severity of the large slab spalling is also higher in the low Load Code sections than in the High Load Code sections. For medium slabs, higher Load Codes produce higher severity joint spalling, although the percent sample units affected is not very sensitive to load level. These findings suggest that loading may contribute to the formation and propagation of corner spalling. Joint spalling occurs in significant amounts under all loading conditions, but its severity is highest under higher loading conditions. Slab size effects are most pronounced, with small slabs always having less spalling than medium or large slabs under similar loading conditions. This slab size effect decreases with age, as climatic and load related factors appear to progressively increase spalling in the smaller slab sizes.

In summary, slab size effect appears to be related to corner and joint spalling, particularly in the early service life of the pavement. Although not as pronounced as slab size, higher loading appears to contribute to greater amounts and higher severities of corner spalling under similar conditions. Occurrences of joint spalling can not be related to loading level, although the severity of spalling increases at higher load levels. This same analysis found that the largest effects are not load related, as even lightly trafficked sections suffer significant amounts of corner and joint spalling.

VII.2.3. D-Cracking

Figures 101, 102, and 103 show the D-cracking trends in the Northern, Central, and Southern Climatic Zones, respectively. D-cracking is more widely distributed in the Northern Climatic Zone, but occurs in all climatic zones within the State. D-cracking is directly related to the coarse aggregate source. It is generally found throughout a section and is not isolated to a single sample unit within a section.

Slab size effects play no discernible role in the occurrence or propagation of the distress. D-cracking was not observed in the Central and Southern Climatic Zone in the first five years of service. The percent sample units affected generally increase with age. It is noted that PCC constructed with non-D-cracking susceptible aggregate will not develop this distress over time and therefore will not be affected regardless of their age. This point is illustrated in the long-lived PCC sections constructed at Quincy that were evidently constructed with non-susceptible aggregate. No evidence of D-cracking has been observed in these sections even after 40+ years of service.

D-cracking can be addressed through proper aggregate selection. The use of non-D-cracking susceptible aggregate is essential if this distress is to be controlled. D-cracking is normally situated near joints or cracks in the PCC. If D-cracking susceptible aggregate is inadvertently used, more of the pavement area would be affected if shorter joint spacing had been used.

VII.2.4. Joint Seal Damage

Joint seal damage may influence the development of other distress types. If a routine joint re-sealing program is maintained by the airport, joint seal damage will not occur. Figures 104, 105, and 106 show the percent sample units affected by joint seal damage in the Northern, Central, and Southern Climatic Zones, respectively.

There does not appear to be a slab size effect. The distress does not usually occur in the first five years of service, but becomes more common in subsequent age ranges. The maintenance practices of individual airports have the greatest impact on this distress, and therefore it is not possible to generate clear distress formation and propagation trends. Different sealant materials also have different expected lives. The sealant used in the initial construction will contribute directly to when this distress is first observed. It is interesting to note that 60% of the 40+ year old PCC sections at Quincy are suffering joint sealant damage, most of which is low

severity. The relatively low occurrence of joint seal damage after so many years of service may have contributed to the excellent performance of these sections.

VII.2.5. Longitudinal, Transverse, and Diagonal Cracking

L, T, & D cracking is a major structural indicator for PCC pavements. Figures 107, 108, and 109 show the percent sample units affected by L, T, and D cracking in the Northern, Central, and Southern Climatic Zones, respectively. A related distress, shattered or divided slabs, develops when a slab breaks into three or more pieces. Shattered slabs and L, T, & D cracking will be discussed concurrently. Figures 110, 111, and 112 show the percent sample units affected by shattered slabs in the Northern, Central, and Southern Climatic Zones, respectively.

An immediate observation is that large slabs are suffering extensive L, T, & D cracking. Near 100% occurrence rates occur in the first five years of service. This suggests that the distress forms early in the pavement life, leading to rapid decreases in PCI. Many large slabs are also affected by shattered slabs. Unlike L, T, & D cracking, the occurrence of shattered slabs appears to increase over time in some cases (Northern Climatic Zone). These findings strongly implicate slab size as a primary distress formation factor for large slabs.

Slab size effects on the occurrence of L, T, & D cracking are also readily observed in medium slabs. In age ranges where medium slabs are represented, over 50% are affected. Medium slabs are also prone to shattering, although at far less occurrence rates than large slabs.

Small slabs are less likely to incur slab cracking than the two larger slab sizes. With the exception of the 1-5 year age range in the Southern Climatic Zone (possibly construction related), the small slab cracking is at or below 20% in all climatic zones for the first 20 years of service. Only small slabs over 36 years of age had any record of shattered slabs, and those occurred in less than 2% of the sample units inspected. Although the occurrence of L, T, & D cracking remains relatively flat in the Southern Climatic Zone, it appears to grow progressively

in the other two climatic zones. In all cases, slab cracking is less for small slabs than medium or large slabs within an age range.

It is observed in Figures 82 through 91 that L, T, & D cracking of small slabs have lower severity levels. This suggests that even when cracking occurs, it remains at a lower severity level than cracking in medium and large slabs, resulting in better performance for small slabs.

Table 36 shows the relationship between Load Code and the occurrence and severity of L, T, & D cracking and Shattered Slabs. For large slab sizes, the effect of loading is overshadowed by the slab size effect, with equally high amounts of L, T, & D cracking occurring under all three loading conditions. The severity of the cracking increases at higher Load Codes, suggesting that loading contributes more to the propagation of cracking of large slabs than crack formation. Load may contribute to the formation and severity of shattered slabs in large slabs, as roughly twice the occurrences are observed in high Load Code sections compared to low Load Code sections. It is noted that even in low Load Code sections, nearly 30% and 15% of the large slab sample units have low and medium severity shattered slabs, respectively. This suggests that slab size is the most important factor in the formation of this distress, with high loading conditions playing a secondary role.

In medium slab sections, loading conditions may contribute slightly, as the occurrence and severity of L, T, & D cracking is greater in high Load Code sections than in medium Load Code sections. Only 11 sample units are contained in the low Load Code-medium slab size category, none of which suffer L, T, & D cracking. About twice as many shattered slabs occur for medium slabs under high Load Code conditions than medium Load Code conditions, again implicating load as a contributing factor. It is emphasized that considerable slab cracking is present for medium slabs under both high and medium loading conditions.

Small slabs suffer the least amount of cracking under all loading conditions. There is no trend linking higher load levels to increased L, T, & D cracking in small slabs; on the contrary, there is more slab cracking in low Load Code sections than high Load Code sections for small

slabs. Very few small slabs shatter, and those that did are in medium Load Code sections after many years of service. For small slabs, loading can not be implicated in slab cracking.

The primary factor governing the formation and propagation of L, T, & D cracking and shattered slabs is the slab size effect, with load playing a secondary role. Large slabs show high incidence of L, T, & D cracking within the first five years of service. Load effects appear to play a secondary role in the formation of L, T, & D cracking and shattered slabs in medium slabs. Small slabs incur less cracking under all circumstances, although the cracking appears to be progressive, with more occurrences observed as the pavement ages. Load could not be implicated as a factor in small slab cracking.

VII.2.6. Summary

The most important PCC deterioration factor is slab size. Shorter slabs (as measured by the estimated L/ℓ ratio) had less corner breaking, L, T, & D cracking, and shattered slabs. Corner and joint spalling were also reduced initially, but over time, the distress increases until similar occurrences are observed in all slab sizes (age ranges greater than 15 years). Load related factors were a secondary influence, most obvious in high Load Code sections where large slab size led to accelerated L, T, & D cracking and shattered slabs. Through better selection of slab joint spacing and improved material selection (non D-cracking susceptible aggregate), improved PCC performance can be obtained. The initial selection of longer lasting joint sealant and improved joint re-sealing scheduling and practices can reduce joint seal damage as well as the expected long-term reduction of other distress types such as joint and corner spalling.

VIII. OBSERVATIONS, CONCLUSIONS AND RECOMMENDATIONS

This study has focused on the performance and deterioration of Illinois GA airport pavements. It has entailed a review of current GA pavement design and construction specifications, an examination of the PCI procedure as applied by IDOT-DOA, an analysis of pavement performance and deterioration factors for both AC and PCC pavements, the determination of pavement performance trends, and an investigation of specific GA pavement distress formation and propagation trends. The first section of this chapter provides observations and conclusions obtained in the course of this study. The second sections lists potential areas of future research that can further develop some of these findings.

VIII.1. Observations and Conclusions

In the design and construction of AC pavements, the following major observations and conclusions were made as a result of this study:

- The FAA AC thickness design procedure (Chapter 5 of FAA AC 150/5320-6C) is most often used in the design of Illinois GA airport pavements. The Asphalt Institute (AI) procedure is also acceptable to IDOT-DOA.
- The FAA AC thickness design procedure uses the CBR method for conventional AC design. Conversion of the conventional design into an alternative design (i.e. FULL-DEPTH AC, cement treated base, etc.) is accomplished by using material equivalency factors. A minimum 2-in thick AC layer is required. Climatic effects are not directly considered.
- The AI AC thickness design method is mechanistically-empirically based. Design charts are presented for FULL-DEPTH, AC treated base, and conventional AC designs. In the conventional AC thickness design, the granular base thickness is set at 6-in and a minimum AC thickness of 4-in is required.

- IDOT-DOA requires a minimum AC thickness of 3-in. Current practice is to use a granular base course in all AC pavement construction. Surface treatments are not used in new construction of GA pavements.
- IDOT-DOA follows the material codes presented in FAA AC 150/5370-10, with the addition of Item P-201 (bituminous base course). The most recent IDOT-DOA AC specifications specifically address checking (requiring the use of pneumatic tired roller on surface courses) and paving lane cracking (requiring the use of the most recent NAPA joint compaction guidelines). There is an emphasis on the use of standardized IDOT-DOH gradation specifications.
- Recent modifications to the IDOT-DOA AC mix design specifications have replaced voids in the mineral aggregate requirements (VMA) with voids filled with asphalt (VFA). The VFA approach eliminates the need to link VMA to maximum aggregate size. It is noted that the use of VFA in lieu of VMA by itself does not ensure that AC mixtures with reduced age hardening characteristics will be specified. In the modified IDOT-DOA specifications, a possible VMA range from 7% to 30% can be obtained within the specified VFA and air content ranges.

In the design and construction of PCC pavements, the following major observations and conclusions were made as a result of this study:

- The FAA PCC thickness design procedure (Chapter 5 of FAA AC 150/5320-6C) is most often used in the design of Illinois GA airport pavements. The American Concrete Paving Association (ACPA) methodology is also acceptable to IDOT-DOA.
- The FAA PCC thickness design procedures requires a 6-in thick slab and a 4-in thick subbase for pavement servicing aircraft with gross weights in excess of 12,500 lbs. For pavements servicing lighter aircraft, a 5-in thick slab and no subbase is required. The maximum recommended joint spacing is 15 ft.

- The ACPA thickness design approach contains both a simplified and rigorous methodology. A wider range of acceptable thickness are presented than in the FAA method, with a minimum PCC thickness of 4-in. A 4-in thick subbase is required when constructing a PCC pavement on certain subgrades. ACPA recommends a joint spacing of 25 times the slab thickness. This results in a maximum joint spacing of just over 8 ft for a 4-in thick slab and 12.5 ft for a 6-in thick slab.
- IDOT-DOA air-side PCC pavements have been constructed with a 6-in minimum thickness. Current IDOT-DOA jointing practices follow FAA recommendations with an allowable maximum joint spacing of 15 ft.
- The most recent IDOT-DOA PCC specifications feature an increased reliance on IDOT-DOH specifications. Aggregate durability requirements are addressed through IDOT-DOH aggregate source certification.

The following major observations and conclusions were made related to GA pavement distress data collection, performance and deterioration trends, and distress formation and propagation trends:

- IDOT-DOA pavement distress data collection procedures are based on those described in FAA AC 150/5380-6. IDOT-DOA has modified the rigorous FAA data collection procedures through estimating distress quantities in lieu of measuring. IDOT-DOA has also added paving lane cracking to the FAA identified AC distresses. It is difficult to directly compare FAA and IDOT-DOA PCI values.
- Climatic considerations should be included in evaluating pavement performance data. There is a north-south orientation in Illinois. In this study, the State was divided into Northern, Central, and Southern Climatic Zones. Pavement temperature considerations are the most relevant climatic consideration found in this study. For AC pavements,

temperature has a pronounced effect on AC mixture stiffness. In PCC pavements, the slab temperature gradient produces curling stresses in the slab.

- Illinois GA airport pavements carry a wide assortment of aircraft and service vehicles. The most frequently cited maximum aircraft loading was applied by the Beechcraft King Air B200 (maximum gross weight of approximately 12,500 lbs). This aircraft was selected as the design aircraft for pavement structural analysis. For the airports in this study, the vast majority of service vehicles were at or below typical highway loads.
- ILLI-PAVE pavement response algorithms were developed for the King Air B200 aircraft loading. Structural analyses of typical AC sections (designed using FAA and AI procedures) were conducted using ILLI-PAVE and IDOT-DOH Class I AC material properties. These analyses suggest that structural failures (i.e. rutting and alligator cracking) of conventional and FULL-DEPTH AC pavements should not be a major concern under normal GA operating conditions. Estimated AC fatigue lives were considerably larger than expected traffic for most of the sections considered in this study.
- ILLI-SLAB was used to analyze 6-in thick PCC pavements subjected to King Air B200 loading and to verify previously derived pavement response algorithms. Typical GA PCC sections (designed using FAA and ACPA procedures) were structurally evaluated using a calibrated mechanistic design model. The analyses indicate that 5-in and 6-in thick pavements are structurally adequate under normal GA operating conditions. High stress ratios in 4-in thick PCC slabs suggest that they might be structurally inadequate. The combined effects of load and curl stresses significantly decreases predicted allowable aircraft passes to failure. Larger slabs are more affected by curling than smaller slabs making joint spacing an important PCC design factor.
- Pavement distress and inventory data provided by IDOT-DOA were used to establish a relational data base. In total, 195 non-rehabilitated pavement sections were included. The data base contains extensive loading, climatic, construction/material, and pavement

condition information for each section. Specific pavement condition factors include section PCI values, sample unit PCI values, and distress types, severities, and quantities for each sample unit inspected.

- A Deterioration Rate (DR) concept was developed to describe pavement performance and longevity trends. The DR is defined as the PCI loss per year. DRs for five year periods were estimated and statistically tested for significance for each pavement type and climatic zone. Deterioration trends for each pavement type and climatic zone were established by joining the DRs for successive five year period.
- The AC surfaced pavements had similar deterioration trends in the Southern and Northern Climatic Zone. TKAC had an overall lower DR than TNAC in the Central Climatic Zone. The results of this analysis suggested that in the first 10 years of service, there was little difference in TNAC and TKAC performance. After 10 years, pavements constructed with thicker AC layers appeared to have a reduced rate of deterioration.
- PCC pavement sections were separated to account for slab size effects. The ratio of the slab length divided by the slab radius of relative stiffness (L/ℓ) was used to divide slabs into "small", "medium", and "large" classifications. Markedly different performance trends were observed for each slab size. Small slabs had the lowest DRs and large slabs had the highest DRs in each climatic zone. Slab size was the most important indicator of PCC pavement performance.
- An analysis of rehabilitated sections identified the age when various pavement types were overlaid. The results of this analysis were consistent with the deterioration trends previously identified in that PCC pavements had overall better performance than AC pavements. Differences in performance between TKAC and TNAC were not readily observed.

- Efforts to differentiate the deterioration trends for 12.5 ft slabs from 15 ft slabs (assuming 6-in thickness) were not successful. There was no statistical difference between the DR rates of the two slab sizes, although the smaller slabs had a lower DR. Slabs having greater lengths than 15 ft performed significantly worse than smaller slabs.
- Longitudinal and transverse cracking (L & T cracking) and paving lane cracking were the two most commonly occurring distress types in AC surfaced pavements. Both distresses had a high number of occurrences within the first five years of service, and continued to develop with time until almost all sample units were eventually affected. Other distress types commonly observed are alligator cracking, oil spillage and depressions.
- Higher than expected amounts of alligator cracking were recorded for AC sections. After a thorough examination, it has been concluded that the identification of alligator cracking has been confounded with other distress types (i.e. block cracking, checking). This makes it impossible to determine the extent of load related distress within the GA pavement network from these data. It is believed that alligator cracking is considerably less prevalent than currently recorded.
- Commonly occurring PCC distresses are corner breaking, corner and joint spalling, D-cracking, joint seal damage, and longitudinal, transverse, and diagonal slab cracking (L, T, & D). PCC distress formation and propagation are highly dependent on the slab size. Large slabs have considerably higher distress occurrences and severities than small slabs. Load could not be strongly related to distress formation or propagation except in the case of corner spalling. Load appears to play a small role in the propagation of joint spalling and L, T, & D cracking. Overall, the most important factor leading to PCC distress is slab size.

VIII.2. Recommendations for Further Research

The observations and conclusions from this study support the following recommendations for further research:

- Recent IDOT-DOA specification modifications (dated April, 1994) provide improved construction quality control. This effort should be continued. The effects of the AC specifications (P-201 and P-401), pertaining to the construction of paving lane joints, should be monitored for effectiveness. As successful techniques are identified (leading to a reduction in the early formation of paving lane cracking), these should be specifically identified in the specification.
- It is recommended that current AC mixture design practices be evaluated. The low VMA/low air content mixtures have "checked" in numerous GA projects. Aggregate gradations should be examined to see if reduced age hardening characteristics of the asphalt cement can be obtained without sacrificing mix compactability. SHRP Level 1 mix design procedures, featuring the use of the SHRP gyratory compactor, should be thoroughly evaluated for potential application to GA mixture design. This method allows the AC mixture compactability to be assessed during the mix design process.
- The SHRP performance grading system offers the potential for selecting asphalt cement binders that can better resist L & T cracking problems. Before adopting these specifications, a number of concerns first must be addressed. The first is the methodology used to calculate minimum pavement temperatures. Many have voiced concerns that the current method is not accurate. Secondly, the proposed models should be evaluated to determine if the specifications will truly result in less thermal cracking.
- The most important PCC design parameter is slab size. This study has shown that, in general, shorter slabs have lower Deterioration Rates (DRs) than larger slabs. This is true even though a statistical difference ($\alpha = 0.05$) in DR could not be shown between 12.5 ft

and 15 ft slabs. Short joint spacing results in increased construction costs and more joint related distress (such as D-cracking and spalling). Higher joint re-sealing costs are also incurred with shorter joint spacing. An effort should be undertaken to determine the specific advantages and disadvantages of various slab sizes up to 15 ft in length (for 6-in thick slabs). L/ℓ should be used to select appropriate PCC slab lengths. Typical coarse aggregate sources should be examined to determine their effect on the PCC coefficient of thermal expansion.

- The PCI data collection procedures used by IDOT-DOA were not as rigorous as those recommended by the FAA. Although the inspections can be conducted in a more timely manner, there is some concern that accuracy has been sacrificed. A study could be implemented to examine the costs and benefits involved with inspections conducted with varying degrees of precision. Through this effort, a more optimal inspection technique may be identified, improving accuracy without significantly increasing inspection time.
- This study observed that the performance of TNAC and TKAC pavements was similar in the early service life, but that TKAC pavements appeared to have lower DRs after 10 years of service. It is hypothesized that this translates into improved maintainability for pavements constructed with thicker AC layers. A study that investigates the effects of maintenance on AC pavements would be able to address this issue. This is important when considering life cycle costing, as the use of thicker AC pavements may provide a more cost effective alternative even with higher initial costs.
- As a mechanistically based design procedure is considered for GA airports, materials properties must be more accurately assessed. In particular, the specific temperature-stiffness relationships must be developed for the P-201/P-401 materials. Preliminary analysis conducted as part of this study found that typical IDOT-DOA P-201/P-401 AC mixtures are slightly less stiff than comparable IDOT-DOH Class I mixtures. Fatigue relationships for these mixtures must also be established.

- The use of distress transfer functions developed for highway applications might not be appropriate for the analysis of GA airport pavements. In particular, highway stress applications are relatively small and frequent, and the vehicle path is channelized. In contrast, stresses induced in airport pavements are typically high and infrequent, and the traffic is less channelized. In this project, one difficulty encountered in applying highway distress transfer functions occurred when using the calibrated mechanistic design model for PCC fatigue analysis. For the 4-in thick PCC, even when the tensile stress over modulus of rupture ratio approached 1.0, the allowable passes still exceeded 5,000. Research should be conducted to examine high stress/strain, low repetition transfer functions for GA airport applications.
- A DESIGN CATALOG should be considered to standardize Illinois GA pavement design procedures. A mechanistic-empirical approach can be utilized to design pavement structures for Illinois climatic conditions and commonly used materials. The catalog can be arranged according to climatic zone, traffic loading, and subgrade strength/stiffness properties. A number of alternative pavement designs would be presented for a given set of design conditions.

IX. REFERENCES

Abd El Halim, A.O., W.A. Phang, and R.C. Haas [El Halim, 1993], "Unwanted Legacy of Asphalt Pavement Compaction," Journal of Transportation Engineering, Vol. 119, No. 6, November/December, pp. 914-932.

American Association of State Highway and Transportation Officials [AASHTO, 1993], AASHTO Guide for the Design of Pavement Structures, Washington, D.C.

American Concrete Paving Association [ACPA, 1993], Concrete Pavements for General-Aviation Airports, IS202.01P, Skokie, IL.

American Society for Testing and Materials [ASTM, 1993], Standard Test Method for Airport Pavement Condition Index Surveys, ASTM Designation: D 5340-93, Philadelphia, PA.

Asphalt Institute [AI, 1981], Asphalt Hot-Mix Recycling, Manual Series No. 20 (MS-20), College Park, MD.

Asphalt Institute [AI, 1982], Research and Development of the Asphalt Institute's Thickness Design Manual (MS-1) Ninth Addition, Research Report 82-2, , College Park, MD.

Asphalt Institute [AI, 1987], Thickness Design—Asphalt Pavements for General Aviation, Information Series No. 154 (IS-154), Third Addition, College Park, MD.

Asphalt Institute [AI, 1991], Thickness Design—Asphalt Pavements for Highways and Streets, Manual Series No. 1 (MS-1), Lexington, KY.

Asphalt Institute [AI, 1993], Mix Design Methods for Asphalt Concrete and Other Hot-Mix Types, Manual Series No. 2 (MS-2), Sixth Addition, Lexington, KY.

Barenberg, E.J. [Barenberg, 1994], Calibrated Mechanistic Structural Analysis Procedure for Jointed Concrete Pavements, ILLI-CON Software, Department of Civil Engineering, University of Illinois, August 1.

Bradbury, R.D. [Bradbury, 1938], Reinforced Concrete Pavements, Wire Reinforcement Institute, Washington, D.C.

Burati, James L., and George B. Elzoghbi [Burati, 1985], Study of Acceptance Criteria for Joint Densities in Bituminous Airport Pavements, U.S. Department of Transportation, Federal Aviation Administration, DOT/FAA/PM-85/5, Washington, D.C.

U.S. Army Corps of Engineers [COE, 1991], Hot-Mix Asphalt Paving—Handbook, UN-13 (CEMP-ET), July.

Cominsky, R.J., G.A. Huber, T.W. Kennedy, and M. Anderson [Cominsky, 1994], The Superpave Mix Design Manual for New Construction and Overlays, SHRP-A-407, Strategic Highway Research Program, Washington, D.C.

Darter, M.I., and E.J. Barenberg [Darter, 1977], Design of Zero-Maintenance Plain Jointed Concrete Pavements, Volume 1—Developments of Design Procedures, FHWA-RD-77-111, Federal Highway Administration, Washington, D.C.

Dempsey, B.J., W.A. Herlache, and A.J. Patel [Dempsey, 1985A], The Climatic-Materials-Structural Pavement Analysis Program: User's Manual, Final Report, Contract No. DTFH 61-80-C-00013, U.S. Department of Transportation, Federal Highway Administration, Washington, D.C., February.

Dempsey, B.J., W.A. Herlache, and A.J. Patel [Dempsey, 1985B], Climatic-Materials-Structural Pavement Analysis Program: Volume 3: Environmental Effects on

Pavements—Theory Manual, Final Report, Contract No. DTFH 61-80-C-00013, U.S. Department of Transportation, Federal Highway Administration, Washington, D.C., February.

Dempsey, B.J., W.A. Herlache, and A.J. Patel [Dempsey, 1986], Climatic-Materials-Structural Pavement Analysis Program, TRB Record 1095, Transportation Research Board, National Research Council, Washington, D.C.

Elliot, R.L., and M.R. Thompson [Elliot, 1985], Mechanistic Design Concepts for Conventional Flexible Pavements, Civil Engineering Studies, Transportation Engineering Series No. 42, University of Illinois, Urbana, February.

Federal Aviation Administration [FAA, 1974], Standards for Specifying Construction of Airports, FAA AC 150/5370-10, Department of Transportation, Washington, D.C.

Federal Aviation Administration [FAA, 1978], Airport Pavement Design and Evaluation, FAA AC 150/5320-6C, Department of Transportation, Washington, D.C.

Federal Aviation Administration [FAA, 1981], Joint Design for Light Duty Rigid Pavements, Engineering Brief No. 27, Department of Transportation, Washington, D.C.

Federal Aviation Administration [FAA, 1982], Guidelines and Procedures for Maintenance of Airport Pavements, FAA AC 150/5380-6, Department of Transportation, Washington, D.C.

Federal Aviation Administration [FAA, 1992], Airport Pavement Design and Evaluation, Draft, FAA AC 150/5320-6D, Department of Transportation, Washington, D.C.

Federal Aviation Administration [FAA, 1994A], Addendum: Item P-401 Plant Mix Bituminous Pavements, FAA AC 150/5370-10A CHG 6, Department of Transportation, Washington, D.C., January 25.

Federal Aviation Administration [FAA, 1994B], Addendum: Item P-501 Portland Cement Concrete Pavement, FAA AC 150/5370-10A CHG 7, Department of Transportation, Washington, D.C., May 20.

Federal Aviation Administration [FAA, 1994C], Draft User's Manual for LEDFAA, Federal Aviation Administration Technical Center, Department of Transportation, Atlantic City, NJ, September 20.

Figuroa, J.L. [Figuroa, 1979], Resilient Based Flexible Pavement Design Procedure for Secondary Roads, Ph.D. Dissertation, University of Illinois, Urbana.

Gomez-Achecar, M., and M.R. Thompson [Gomez-Achecar, 1984], Mechanistic Design Concepts for Full-Depth Asphalt Concrete Flexible Pavements, Civil Engineering Studies, Transportation Engineering Series No. 41, University of Illinois, Urbana, August.

Gomez-Achecar, M., and M.R. Thompson [Gomez-Achecar, 1986], "ILLI-PAVE-Based Response Algorithms for Full-Depth Asphalt Concrete Flexible Pavements," Transportation Research Record 1095, Transportation Research Board, National Research Council, Washington, D.C.

Hoffman, M.S., and M.R. Thompson [Hoffman, 1981], Mechanistic Interpretation of Nondestructive Pavement Testing Deflections, Civil Engineering Studies, Transportation Engineering Studies, Transportation Engineering Series No. 32, University of Illinois, Urbana, June.

Huber, G.A. [Huber, 1994], Weather Database for the SUPERPAVE™ Mix Design System, SHRP-A-648A, The Strategic Highway Research Program, National Research Council, Washington, D.C.]

Illinois Department of Transportation [IDOT, 1987], Mix Design, Test Batch, Quality Control, and Acceptance Testing of PCC Mixture, Policy Memorandum No. 87-3, Springfield, IL.

Illinois Department of Transportation—Bureau of Materials and Physical Research [IDOT, 1988], Quality Control Requirements for Fly Ash for Use in Portland Cement Concrete, Policy Memorandum No. 88-1, Springfield, IL, January 1.

Illinois Department of Transportation [IDOT, 1994], Standard Specifications for Road and Bridge Construction, Springfield, IL, July 1.

Illinois Department of Transportation—Division of Aeronautics [IDOT-DOA, 1985], Standard Specifications for Construction of Airports, Policy IDA-2, Springfield, Illinois, January.

Illinois Department of Transportation—Division of Aeronautics [IDOT-DOA, 1993], Illinois Airport Inventory Report—1993, Springfield, Illinois, January.

Illinois Department of Transportation—Division of Aeronautics [IDOT-DOA, 1994A], Addendum: Item P-201 Bituminous Base Course, Springfield, Illinois, April 1.

Illinois Department of Transportation—Division of Aeronautics [IDOT-DOA, 1994B], Addendum: Item P-401 Bituminous Surface Course, Springfield, Illinois, April 1.

Illinois Department of Transportation—Division of Aeronautics [IDOT-DOA, 1994C], Addendum: Item P-501 Portland Cement Concrete Pavement, Springfield, Illinois, April 1.

Ioannides, A.M., M.R. Thompson, and E.J. Barenberg [Ioannides, 1985], "Finite Element Analysis of Slabs-On-Grade Using a Variety of Support Models," Proceedings: Third

International Conference on Concrete Pavement Design and Rehabilitation, Purdue University, April.

Kandhal, Prithvi S., and Shridhar S. Roa [Kandhal, 1994], Evaluation of Longitudinal Joint Compaction Techniques for Asphalt Pavements, Preprint No. 94-0436, Transportation Research Board, Washington, D.C.

Lee, Ying-Haur, M.I. Darter [Lee, 1993], "Mechanistic Design Models of Loading and Curling in Concrete Pavements," Airport Pavement Innovations Theory to Practice, Proceedings of the Conference, Airfield Pavement Committee, Air Transport Division, American Society of Civil Engineers, Vicksburg, Mississippi.

Maupin, G.W., and J.R. Freeman [Maupin, 1976], Simple Procedure for Fatigue Characterization of Bituminous Concrete, Report No. FHWA-RD-76-102, Federal Highway Administration, Office of Research and Development, McLean, VA.

Mindess, S., J.F. Young [Mindess, 1981], Concrete, Prentice-Hall, Inc., Englewood Cliffs, New Jersey.

Petersen, J.C., R.E. Robertson, J.F. Branthaver, P.M. Harnsberger, J.J. Duvall, S.S. Kim, D.A. Anderson, D.W. Christiansen, H.U. Bahia, R. Dongre, C.E. Antle, M.G. Sharma, J.W. Button, and C.J. Glover [Petersen, 1994], Binder Characterization and Evaluation—Volume 4: Test Methods, SHRP-A-370, Strategic Highway Research Program, National Research Council, Washington, D.C.

Raad, L., and J.L. Figueroa [Raad, 1980], "Load Response of Transportation Support Systems," Transportation Engineering Journal of ASCE, Vol. 106, No. TE1, January.

Rada, G., and M.W. Witczak [Rada, 1981], "Comprehensive Evaluation of Laboratory Resilient Moduli Results for Granular Material," TRR Record No. 766, Transportation Research Board, National Research Council, Washington, D.C.

Rauhut, J.B., R.L. Lytton, and M.I. Darter [Rauhut, 1984], Pavement Damage Functions for Cost Allocation, Vol. 2: Descriptions of Detailed Studies, Report No. FHWA-RD-84-019, Federal Highway Administration, McLean, VA, June.

Salsilli, R.A., E.J. Barenberg, and M.I. Darter [Salsilli, 1993], "Calibrated Mechanistic Design Procedure to Prevent Transverse Cracking of Jointed Plain Concrete Pavements," Proceedings: Fifth International Conference on Concrete Pavement Design and Rehabilitation, Volume 2, Purdue University, West Lafayette, IN.

Shell International Petroleum Company, Ltd. [Shell, 1978], Shell Pavement Design Manual, London, England.

Smith, K.D., D.G. Peshkin, M.I. Darter, A.L. Mueller, and S.H. Carpenter [Smith, 1990], Performance of Jointed Concrete Pavements. Volume I—Evaluation of Concrete Pavement Performance and Design Features, FHWA-RD-89-136, Federal Highway Administration, Washington, D.C.

Solaimanian, M., T.W. Kennedy [Solaimanian, 1993], "Predicting Maximum Pavement Surface Temperature Using Maximum Air Temperature and Hourly Solar Radiation," TRR No. 1417, Transportation Research Board, National Research Council, Washington, D.C.

Tabatabaie, A.M., and E.J. Barenberg [Tabatabaie, 1980], "Structural Analysis of Concrete Pavement Systems," Transportation Engineering Journal, ASCE, Vol. 106, No. TE5.

Transportation Facilities Group [TFG, 1990], ILLI-PAVE PC Version-User's Manual, Submitted to the National Cooperative Highway Research Program as a Deliverable from NCHRP 1-26, Department of Civil Engineering, University of Illinois, Urbana, April.

Thompson, M.R., and Q.L. Robnett [Thompson, 1979], "Resilient Properties of Subgrade Soils," Transportation Engineering Journal of ASCE, Vol. 105, No. TE1, January.

Thompson, M.R., and R.P. Elliot [Thompson, 1985], "ILLI-PAVE-Based Response Algorithms for Design of Conventional Flexible Pavements," Transportation Research Record 1043, Transportation Research Board, National Research Council, Washington, D.C.

Thompson, M.R., and K. Cation [Thompson, 1986], A Proposed Full-Depth Asphalt Concrete Thickness Design Procedure, Civil Engineering Studies, Transportation Engineering Series No. 45, Illinois Cooperative Highway and Transportation Series No. 213, University of Illinois.

Thompson, M.R., B.J. Dempsey, H. Hill, and J. Vogel [Thompson, 1987], "Characterizing Temperature Effects for Pavement Analysis and Design," TRR 1121, Transportation Research Board, Washington, D.C.

Thompson, M.R., and T.G. LaGrow [Thompson, 1988], A Proposed Conventional Flexible Pavement Thickness Design Procedure, Civil Engineering Studies, Transportation Engineering Series No. 55, Illinois Cooperative Highway and Transportation Series No. 223, University of Illinois.

Thompson, M.R. [Thompson, 1989], "ILLI-PAVE Based NDT Analysis Procedures," Nondestructive Testing of Pavements and Backcalculation of Moduli, ASTM STP 1026, American Society for Testing and Materials, Philadelphia, Pennsylvania.

Thompson, M.R., E.J. Barenberg, S.H. Carpenter, M.I. Darter, B.J. Dempsey, A.M. Ioannides, Robert Packard, Richard May, C. Beckemeyer, J. Naughton, R. Salsilli-Mura, and N. Heil [Thompson, 1992A], NCHRP 1-26: Calibrated Mechanistic Structural Analysis Procedures For Pavements Phase 2, Volume I - Final Report, Prepared for the National Cooperative Highway Research Program, Transportation Research Board, National Research Council, Washington, D.C.

Thompson, M.R., E.J. Barenberg, S.H. Carpenter, M.I. Darter, B.J. Dempsey, A.M. Ioannides, Robert Packard, Richard May, C. Beckemeyer, J. Naughton, R. Salsilli-Mura, and N. Heil, NCHRP 1-26: Calibrated Mechanistic Structural Analysis Procedures For Pavements Phase 2, Volume II - Appendices [Thompson, 1992B], Prepared for the National Cooperative Highway Research Program, Transportation Research Board, National Research Council, Washington, D.C.

Westergaard, H.M. [Westergaard, 1926], "Analysis of Stresses in Concrete Pavements Computed by Theoretical Analysis," Public Roads, Vol. 7, No. 2, pp. 25-35.

Witczak, M.W., "Design of Full Depth Asphalt Airfield Pavements [Witczak, 1972], "Proceedings: Third International Conference on the Structural Design of Asphalt Pavements, London, England.

Table 1. Recommended Equivalency Factor Range for Stabilized Subbase [FAA, 1978].

Item Code	Material	Equivalency Factor Range
P-401	Bituminous Surface Course	1.7 to 2.3
P-201	Bituminous Base Course	1.7 to 2.3
P-215	Cold Laid Bituminous Base Course	1.5 to 1.7
P-216	Mixed In-Place Base Course	1.5 to 1.7
P-304	Cement Treated Base Course	1.6 to 2.3
P-301	Soil Cement Base Course	1.5 to 2.0
P-209	Crushed Aggregate Base Course	1.4 to 2.0
P-154	Subbase Course	1.0

Table 2. Recommended Equivalency Factor Range for Stabilized Base [FAA, 1978].

Item Code	Material	Equivalency Factor Range
P-401	Bituminous Surface Course	1.2 to 1.6
P-201	Bituminous Base Course	1.2 to 1.6
P-215	Cold Laid Bituminous Base Course	1.0 to 1.2
P-216	Mixed In-Place Base Course	1.0 to 1.2
P-304	Cement Treated Base Course	1.2 to 1.6
P-301	Soil Cement Base Course	N/A
P-209	Crushed Aggregate Base Course	1.0
P-154	Subbase Course	N/A

Table 3. Simplified ACPA PCC design scheme [ACPA, 1993].

Pavement Thickness		Allowable Gross Aircraft Weight			
inches	mm	Single-Wheel Gear		Dual-Wheel Gear	
		lbs	kg	lbs	kg
5.0	127	15,000	6,800	21,000	9,500
5.5	140	18,000	8,100	26,000	11,800
6.0	152	21,000	9,500	31,000	14,100
6.5	165	25,000	11,300	36,000	16,300
7.0	178	29,000	13,200	41,000	18,600
7.5	190	-	-	47,000	21,300
8.0	203	-	-	53,000	24,000
8.5	216	-	-	60,000	27,200

Table 4. Relevant material codes used by IDOT-DOA and the FAA.

Item	Description	Item	Description
P-152	Excavation and Embankment	P-209	Crushed Aggregate Base Course
P-154 ¹	Subbase Course	P-216 ¹	Mixed In-Place Base Course
P-155	Lime Treated Subgrade	P-304	Cement Treated Base Course
P-201 ²	Bituminous Base Course	P-401	Bituminous Surface Course
P-208	Aggregate Base Course	P-501	Portland Cement Concrete Pavement

¹ This item is not currently part of the IDOT-DOA specifications.

² This item is not currently part of the FAA specifications.

Table 5. Recommended AC aggregate gradations.

Sieve Size	Percentage by Weight Passing Sieves								
	1 inch Maximum			3/4 inch Maximum			1/2 inch Maximum		
	IDOT	FAA	AI	IDOT ¹	FAA	AI	IDOT ²	FAA	AI
1"	100	100	90-100	100	100	100	100	100	100
3/4"	84-100	76-98	-	100	100	90-100	100	100	100
1/2"	64-86	66-86	-	81-100	79-99	-	100	100	90-100
3/8"	55-78	57-77	56-80	70-100	68-88	56-80	79-99	79-99	-
No. 4	40-62	40-60	35-65	47-73	48-68	35-65	56-76	58-78	44-74
No. 8	28-50	26-46	23-49	30-60	33-53	23-49	40-60	39-59	28-58
No. 16	22-43	17-37	-	22-47	20-40	-	28-46	26-46	-
No. 30	17-32	11-27	-	17-34	14-30	-	20-36	19-35	-
No. 50	-	7-19	5-17	-	9-21	5-19	-	12-24	5-21
No. 100	6-16	6-16	-	6-16	6-16	-	7-17	7-17	-
No. 200	3-8	3-6	2-8	3-8	3-6	2-8	3-8	3-6	2-10
AC %	4.5-7.0	4.5-7.0		5.0-7.0	5.0-7.5		5.0-7.0	5.5-8.0	

¹ This is the recommended gradation for IDOT-DOA surface mixes.

² This gradation is for leveling courses only

Table 6. Recommended PCC coarse aggregate gradations.

Sieve Size	Percentage by Weight Passing Sieves							
	Fine Aggregate		From 1-1/2" to No. 4				From 1" to No. 4	
	IDOT (FA-1)	FAA	1-1/2" to 3/4"		3/4" to No. 4		IDOT (CA-07)	FAA
			IDOT	FAA	IDOT (CA-11)	FAA		
2"	-	-	-	100	-	-	-	-
1-1/2"	-	-	-	90-100	-	-	100	100
1"	-	-	-	20-55	100	100	90-100	95-100
3/4"	-	-	-	0-15	84-100	90-100	-	-
1/2"	-	-	-	-	30-60	-	30-60	25-60
3/8"	100	100	-	0-5	-	20-55	-	-
No. 4	94-100	95-100	-	-	0-12	0-10	0-10	0-10
No. 8	-	80-100	-	-	-	0-5	-	0-5
No. 16	45-85	50-85	-	-	-	-	-	-
No. 30	-	25-60	-	-	-	-	-	-
No. 50	3-29	10-30	-	-	-	-	-	-
No. 100	0-10	2-10	-	-	-	-	-	-

Table 7. FAA gradation requirements for granular subbase and base materials [FAA, 1974].

Sieve Designation	Percentage by Weight Passing Sieves						
	Item P-154	Item P-208			Item P-209		
		A 2-in max	B 1.5-in max	C 1-in max	A 2-in max	B 1.5-in max	C 1-in max
3-inch	100	-	-	-	-	-	-
2-inch	-	100	-	-	100	-	-
1.5-inch	-	-	100	-	-	100	-
1-inch	-	55-85	70-95	100	55-85	70-95	100
0.75-inch	-	50-80	55-85	70-100	50-80	55-85	70-100
No. 4	-	30-60	30-60	35-65	30-60	30-60	35-65
No. 10	20-100	-	-	-	-	-	-
No. 40	5-60	10-30	10-30	15-30	10-25	10-25	15-25
No. 200	0-15	5-15	5-15	5-15	3-10	3-10	3-10

Table 8. IDOT-DOA gradation requirements for granular subbase and base materials [IDOT, 1985].

Sieve Designation	Item P-208			Item P-209		
	A 2-in max	B 1.5-in max	C 1-in max	A 2-in max	B 1.5-in max	C 1-in max
2-inch	100	-	-	100	-	-
1.5-inch	90-100	100	-	90-100	100	-
1-inch	70-95	80-100	100	70-95	80-100	100
0.5-inch	45-75	55-80	65-95	45-75	55-80	65-95
No. 4	30-50	30-56	40-60	30-50	30-56	40-60
No. 16	15-35	10-40	15-45	15-35	10-40	15-45
No. 200	4-12	4-12	5-14	4-12	4-12	5-14
IDOT Grad.	Mod. CA-4	Mod. CA-6	CA-10	Mod. CA-4	Mod. CA-6	CA-10

Table 9. AC distress types identified in the PCI procedure.

Distress Number	Distress Type	Factors Leading to Distress Formation ¹		
		Load	Climate	Materials/ Construction
1	Alligator or Fatigue Cracking	P	S	S
2	Bleeding	NF	S	P
3	Block Cracking	NF	P	P
4	Corrugation	P	M	P
5	Depression	M	M	P
6	Jet Blast Erosion	NF	NF	P
7	Joint Reflection Cracking ²			
8	Longitudinal and Transverse Cracking	NF	P	P
9	Oil Spillage	NF	NF	P
10	Patching and Utility Cut Patching	S	M	S
11	Polished Aggregate	P	NF	P
12	Raveling and Weathering	NF	P	P
13	Rutting	P	S	P
14	Shoving By PCC Slab ²			
15	Slippage Cracking	P	M	P
16	Swell	NF	P	P
17	Paving Lane Cracking ³	NF	S	P

¹ P = Primary Factor, S = Secondary Factor, M = Minor Factor, NF = Not a Factor.

² This distress is not considered in this study.

³ This distress is unique to IDOT-DOA.

Table 10. PCC distress types identified in the PCI procedure.

Distress Number	Distress Type	Factors Leading to Distress Formation ¹		
		Load	Climate	Materials/Construction
1	Blow Up	NF	P	P
2	Corner Break	P	S	NF
3	Longitudinal, Transverse, and Diagonal Cracking	S	P	S
4	Durability (D-) Cracking	NF	S	P
5	Joint Seal Damage	NF	P	P
6	Patching, Small	S	S	P
7	Patching, Large	S	S	P
8	Popouts	NF	S	P
9	Pumping	P	S	NF
10	Scaling, Map Cracking, and Cracking	NF	S	P
11	Settlement or Faulting	P	S	NF
12	Shattered Slab/Intersecting Cracks	P	P	NF
13	Shrinkage Cracks	NF	S	P
14	Joint Spalling	S	P	S
15	Corner Spalling	S	P	S

¹ P = Primary Factor, S = Secondary Factor, M = Minor Factor, NF = Not a Factor.

Table 11. Pavement temperature and MMAT¹ estimated for a 12-in full depth AC pavement using the C-M-S Model (F°) [Thompson, 1987].

Rockford												
	Jan.	Feb.	March	April	May	June	July	Aug.	Sept.	Oct.	Nov.	Dec
MMAT	21.0	24.6	35.6	48.5	59.4	69.1	74.0	71.9	64.2	52.3	38.4	26.0
@ 1.5 in	25.1	29.2	41.5	56.7	69.5	80.3	85.5	82.3	72.1	57.5	42.3	29.5
@6.0 in	27.8	29.9	40.5	54.8	67.2	77.8	83.3	81.1	72.3	58.7	44.4	32.0
@10.5 in	30.3	30.7	39.7	53.1	65.0	75.3	81.2	79.9	72.3	59.8	46.4	34.3
Urbana												
	Jan.	Feb.	March	April	May	June	July	Aug.	Sept.	Oct.	Nov.	Dec
MMAT	26.1	28.8	39.5	51.4	61.8	71.3	75.2	73.2	66.7	55.0	41.2	30.1
@ 1.5 in	29.7	33.5	45.7	59.7	71.9	81.9	85.8	82.8	74.9	61.1	45.7	33.5
@6.0 in	31.4	33.9	44.7	57.8	69.6	79.4	83.8	81.6	74.8	62.1	47.6	35.7
@10.5 in	33.1	34.4	43.9	56.1	67.4	77.0	81.7	80.6	72.3	63.0	49.5	37.7
Cairo												
	Jan.	Feb.	March	April	May	June	July	Aug.	Sept.	Oct.	Nov.	Dec
MMAT	35.9	39.2	48.4	59.4	68.3	77.0	80.5	78.6	72.2	61.2	48.7	38.9
@ 1.5 in	39.3	43.9	54.7	68.0	81.7	88.4	92.2	89.5	80.9	67.4	53.2	42.4
@6.0 in	40.1	43.8	53.4	65.9	76.6	85.7	89.9	88.0	80.5	68.1	54.7	44.1
@10.5 in	40.9	43.7	52.2	63.8	74.2	83.1	87.6	86.5	80.0	68.7	56.1	45.6

¹ MMAT is the mean monthly air temperature.

Table 12. Temperature differentials calculated for a 6-in thick PCC slab in three Illinois locations using the C-M-S Model [ILLICON, 1994].

Temperature Differential (F°)	Percent Time Slab Experiences Gradient During Typical Year (%)		
	Rockford	Urbana	Cairo
-18	0	0	0
-16	0	0	0
-14	0	0	0
-12	0	0	0
-10	1	0	0
-8	13	13	11
-6	17	17	19
-4	13	15	18
-2	8	8	7
0	6	6	3
2	6	5	4
4	5	5	4
6	5	5	4
8	4	5	6
10	4	4	5
12	4	5	5
14	4	4	4
16	5	5	5
18	4	4	5
20	0	0	1
22	0	0	0
24	0	0	0
26	0	0	0
28	0	0	0
30	0	0	0

Table 13. Summary of material properties employed in the ILLI-PAVE solutions.

Parameter	Asphalt Concrete			Crushed Stone	Subgrade			
	40° F	70° F	100° F		Stiff	Medium	Soft	Very Soft
Unit Weight (pcf)	145	145	145	135	125	120	115	110
Lateral Pressure Coefficient at Rest	0.37	0.67	0.85	0.60	0.82	0.82	0.82	0.82
Poisson's Ratio	0.27	0.40	0.46	0.38	0.45	0.45	0.45	0.45
Unconfined Compressive Strength (psi)	-	-	-	-	32.80	22.85	12.90	6.21
Deviator Stress Upper Limit (psi)	-	-	-	-	32.80	22.85	12.90	6.21
Deviator Stress Lower Limit (psi)	-	-	-	-	2.00	2.00	2.00	2.00
K1(ksi/psi)	-	-	-	-	-1.11	-1.11	-1.11	-1.11
K2 (ksi/psi)	-	-	-	-	-0.178	-0.178	-0.178	-0.178
Deviator Stress @ "Breakpoint" (psi)	-	-	-	-	6.20	6.20	6.20	6.20
E _r (ksi)	-	-	-	-	12.34	7.68	3.02	1.00
E _{-failure} (ksi)	-	-	-	4.00	7.605	4.716	1.827	1.00
E-Const. Mod. (ksi)	1400	500	100	-	-	-	-	-
E _r -Model (psi)	-	-	-	5000 ^{0.5}	-	-	-	-
Frict. Angle (deg)	-	-	-	40	0	0	0	0
Cohesion (psi)	-	-	-	-	16.4	11.425	6.45	3.105

Table 14. ILLI-PAVE conventional pavement response algorithms for the Beechcraft King Air B200.

Response Algorithm	R ²	SEE
$\text{Log } \epsilon_{AC} = 2.941 + 0.190T_{AC} - 0.097(\text{Log}T_{BSE})/T_{AC} - 0.114(\text{Log}E_{AC})T_{AC} - 0.043(\text{Log}E_{RI})$	0.981	0.045
$\text{Log } SD = 1.632 - 0.088T_{AC} - 0.017T_{BSE} - 0.277(\text{Log}E_{AC}) + 0.024E_{RI}$	0.862	0.084
$\text{Log } SSR = 0.103 + 0.084T_{AC} - 0.017\text{Log}T_{BSE} - 0.066(\text{Log}E_{AC})T_{AC} - 0.396(\text{Log}E_{RI})$	0.939	0.063
$\text{Log } D_0 = 1.671 + 0.099T_{AC} - 0.118(\text{Log}T_{BSE})/T_{AC} - 0.068(\text{Log}E_{AC})T_{AC} - 0.199(\text{Log}E_{RI})$	0.978	0.029
$\text{Log } D_s = 2.088 - 0.003T_{AC} - 1.308(\text{Log}T_{BSE})/T_{AC} - 0.052(\text{Log}E_{AC})T_{AC} - 0.302(\text{Log}E_{RI})$	0.950	0.045
$\text{Log } \epsilon_{AC} = 0.841 + 1.334\text{Log}D_0$	0.839	0.114
$\text{Log } SSR = -2.080 + 1.189\text{Log}D_0$	0.804	0.114

ϵ_{AC} = Strain in the AC (microstrain)

T_{AC} = Thickness AC (inches)

T_{BSE} = Thickness of granular base (inches)

E_{AC} = Resilient modulus of AC (ksi)

E_{RI} = Breakpoint resilient modulus of subgrade (ksi)

SD = Subgrade deviator stress (psi)

SSR = Subgrade stress ratio (SD/unconfined compressive strength)

D_0 = Surface deflection at center of load (mils)

D_s = Deflection at top of subgrade at center of load (mils)

Table 15. ILLI-PAVE FULL-DEPTH pavement response algorithms for the Beechcraft King Air B200.

Response Algorithm	R ²	SEE
$\text{Log } \epsilon_{AC} = 5.518 - 1.563\text{Log}T_{AC} - 0.751\text{Log}E_{AC} - 0.083\text{Log}E_{Ri}$	0.994	0.034
$\text{Log } SD = 2.323 - 1.125\text{Log}T_{AC} - 0.439\text{Log}E_{AC} + 0.375\text{Log}E_{Ri}$	0.936	0.084
$\text{Log } D_0 = 3.003 - 0.852\text{Log}T_{AC} - 0.418\text{Log}E_{AC} - 0.259\text{Log}E_{Ri}$	0.987	0.031
$\text{Log } D_s = 2.957 - 0.996\text{Log}T_{AC} - 0.365\text{Log}E_{AC} - 0.285\text{Log}E_{Ri}$	0.985	0.034
$\text{Log } SSR = 1.530 - 1.125\text{Log}T_{AC} - 0.439\text{Log}E_{AC} - 0.279\text{Log}E_{Ri}$	0.929	0.084
$\text{Log } \epsilon_{AC} = 0.614 + 1.525\text{Log}D_0$	0.863	0.161
$\text{Log } SSR = -1.863 + 1.092\text{Log}D_0$	0.884	0.105

- ϵ_{AC} = Strain in the AC (microstrain)
 T_{AC} = Thickness AC (inches)
 E_{AC} = Resilient modulus of AC (ksi)
 E_{Ri} = Breakpoint resilient modulus of subgrade (ksi)
 SD = Subgrade deviator stress (psi)
 SSR = Subgrade stress ratio (SD/unconfined compressive strength)
 D_0 = Surface deflection at center of load (mils)
 D_s = Deflection at top of subgrade at center of load (mils)

Table 16. Summary of data and analysis for Pontiac (for 9,000 lb normalized load).

Feature	Max. Deflection (mils)			E_{Ri} (ksi)		
	Mean	Std. Dev.	COV	Mean	Std. Dev.	COV
Runway	23.6	3.24	14%	8.0	2.50	31%
Taxiway	15.1	3.52	23%	10.6	2.27	21%
Apron	23.7	4.00	17%	9.26	2.75	30%

Table 17. Summary of data and analysis for Morris (for 9,000 lb normalized load).

Feature	Max. Deflection (mils)			E _{RI} (ksi)			E _{AC} (ksi)		
	Mean	Std. Dev.	COV	Mean	Std. Dev.	COV	Mean	Std. Dev.	COV
Runway	9.9	1.65	17%	8.5	2.59	30%	394	106.0	27%
Taxiway	10.6	2.00	19%	8.9	2.28	26%	314	56.4	18%

Table 18. Summary of results from laboratory testing.

Airport	Course	Average Bulk Specific Gravity	Mean AC Resilient Modulus		Mean Split Tensile Strength @ 72°F	Mean Slope ¹
			70°F	90°F		
Morris	Surface	2.319	404 ksi	106 ksi	125 psi	-0.029
	Composite	2.355	576 ksi	164 ksi	133 psi	-0.027
	Binder	2.377	679 ksi	205 ksi	150 psi	-0.026
Mount Sterling	Surface	2.277	550 ksi	151 ksi	116 psi	-0.028
	Binder	2.328	308 ksi	61 ksi	134 psi	-0.035
Pontiac	Surface	2.335	176 ksi	49 ksi	106 psi	-0.027

¹ Log(E_{AC}) = A - Slope*Temperature

Table 19. Summary of AC pavement thickness designs for King Air B200.

CBR	FAA Design			Asphalt Institute Design		
	Conventional		FULL-DEPTH	Conventional		FULL-DEPTH
	AC (in)	Base (in)	AC (in)	AC (in)	Base (in)	AC (in)
3	3	13	9.75	5.25	6	7.5
5	3	9	7.75	4.25	6	6.25
7	3	6.5	6.5	4	6	5.5

Table 20. Estimated AC mix design temperatures and mix stiffnesses.

Location	Conventional [Thompson, 1988]		FULL-DEPTH [Thompson, 1986]	
	Design Temp.	Mix Stiffness	Design Temp.	Mix Stiffness
Rockford	72° F	650 ksi	77° F	540 ksi
Urbana	76° F	550 ksi	80° F	470 ksi
Cairo	84° F	380 ksi	86° F	350 ksi

Table 21. Summary of section information in Access® database.

Feature	Climatic Region									Total
	Central			Northern			Southern			
	PCC	TKAC	TNAC	PCC	TKAC	TNAC	PCC	TKAC	TNAC	
AP	3	7	7	9	6	8	5	6	3	54
RW	2	6	2	6	8	2	3	9	4	42
TW	4	9	6	5	36	19	5	10	5	99
Total	9	22	15	20	50	29	13	25	12	195

Table 22. Summary of airport information contained in data base.

Airport	AID	ClimaticZone	Section	Feature	Code
Beardstown	K06	C	K06-AP-NN/2	AP	TNAC
Canton	CTK	C	CTK-RW-09/03	RW	TKAC
Canton	CTK	C	CTK-TW-A/1-03	TW	TKAC
Carbondale	MDH	S	MDH-AP-SS/19	AP	PCC
Carbondale	MDH	S	MDH-AP-SS/20	AP	PCC
Carmi	CUL	S	CUL-AP-EE/1	AP	PCC
Carmi	CUL	S	CUL-TW-B/1	TW	TKAC
Casey	1H8	C	1H8-TW-B/1-5	TW	TNAC
Casey	1H8	C	1H8-TW-B/2-5	TW	PCC
Casey	1H8	C	1H8-TW-B/5	TW	TNAC
Casey	1H8	C	1H8-TW-C/5	TW	TNAC
Centralia	ENL	S	ENL-AP-VVV/06	AP	PCC
Centralia	ENL	S	ENL-AP-VVV/09	AP	TKAC
Centralia	ENL	S	ENL-RW-18/13	RW	TNAC
Centralia	ENL	S	ENL-TW-A/13	TW	TNAC
Dekalb	DKB	N	DKB-AP-EE/01	AP	TKAC
Dekalb	DKB	N	DKB-AP-EE/02	AP	PCC
Dekalb	DKB	N	DKB-RW-09/02	RW	TKAC
Dekalb	DKB	N	DKB-TW-B/03	TW	TKAC
Dekalb	DKB	N	DKB-TW-B/1-03	TW	TKAC
Dekalb	DKB	N	DKB-TW-B/2-03	TW	TKAC
Dekalb	DKB	N	DKB-TW-B/3-03	TW	TKAC
Dekalb	DKB	N	DKB-TW-B/4-03	TW	TKAC
Dekalb	DKB	N	DKB-TW-B/4-04	TW	TKAC
Dekalb	DKB	N	DKB-TW-D/01	TW	TKAC
Dekalb	DKB	N	DKB-TW-D/1-01	TW	TKAC
Dixon	C73	N	C73-RW-08/09	RW	TKAC
Dixon	C73	N	C73-TW-A/09	TW	TKAC
Dixon Sprgs	Y51	S	Y51-AP-EE/01	AP	TKAC
Dixon Sprgs	Y51	S	Y51-RW-15/01	RW	TKAC
Dixon Sprgs	Y51	S	Y51-TW-A/01	TW	TKAC
Dupage	DPA	N	DPA-AP-EE/1	AP	PCC
Dupage	DPA	N	DPA-AP-EE/2	AP	TNAC
Dupage	DPA	N	DPA-AP-NE/10	AP	PCC
Dupage	DPA	N	DPA-AP-NW/24	AP	PCC
Dupage	DPA	N	DPA-AP-NW/9	AP	TNAC
Dupage	DPA	N	DPA-RW-1-R/1	RW	PCC
Dupage	DPA	N	DPA-TW-T/1	TW	TKAC
Dupage	DPA	N	DPA-TW-T/1-1	TW	TKAC
Dupage	DPA	N	DPA-TW-T/2	TW	TKAC
Dupage	DPA	N	DPA-TW-T/2-1	TW	TKAC
Dupage	DPA	N	DPA-TW-T/3-1	TW	TKAC
Dupage	DPA	N	DPA-TW-T/4-1	TW	TKAC
Dupage	DPA	N	DPA-TW-T/5-1	TW	TKAC
Dupage	DPA	N	DPA-TW-X/1	TW	PCC
Dupage	DPA	N	DPA-TW-X/2-1	TW	PCC
Dupage	DPA	N	DPA-TW-X/4-1	TW	PCC
Dupage	DPA	N	DPA-TW-X/6-1	TW	PCC
Effingham	1H2	S	1H2-AP-NN/01	AP	TKAC

Table 22. Summary of airport information contained in data base.

Airport	AID	ClimaticZone	Section	Feature	Code
Effingham	1H2	S	1H2-AP-NN/03	AP	PCC
Effingham	1H2	S	1H2-RW-01/091	RW	TKAC
Effingham	1H2	S	1H2-RW-01/092	RW	TKAC
Effingham	1H2	S	1H2-RW-09/08	RW	TNAC
Effingham	1H2	S	1H2-RW-11/11	RW	PCC
Effingham	1H2	S	1H2-TW-C/11	TW	PCC
Fairfield	2H3	S	2H3-RW-09/03	RW	TKAC
Fairfield	2H3	S	2H3-TW-A/01	TW	TKAC
Fairfield	2H3	S	2H3-TW-A/1-01	TW	TKAC
Flora	H84	S	H84-AP-VVV/4	AP	TKAC
Flora	H84	S	H84-RW-3/2	RW	TKAC
Flora	H84	S	H84-TW-C/6	TW	TKAC
Freeport	FEP	N	FEP-AP-NN/01	AP	TNAC
Freeport	FEP	N	FEP-RW-06/02	RW	TNAC
Freeport	FEP	N	FEP-TW-A/04	TW	TKAC
Freeport	FEP	N	FEP-TW-A/2-01	TW	TNAC
Freeport	FEP	N	FEP-TW-B/06	TW	TKAC
Freeport	FEP	N	FEP-TW-C/06	TW	TKAC
Freeport	FEP	N	FEP-TW-C/1-06	TW	TKAC
Freeport	FEP	N	FEP-TW-D/01	TW	TNAC
Freeport	FEP	N	FEP-TW-D/02	TW	TNAC
Freeport	FEP	N	FEP-TW-D/1-01	TW	TNAC
Freeport	FEP	N	FEP-TW-D/2-01	TW	TNAC
Freeport	FEP	N	FEP-TW-D/3-01	TW	TNAC
Galesburg	GBG	C	GBG-AP-NN/14	AP	TKAC
Galesburg	GBG	C	GBG-AP-NN/8	AP	TKAC
Greenville	GRE	S	GRE-AP-EE/4	AP	TNAC
Grtr. Kankakee	IKK	N	IKK-AP-SS/10	AP	TNAC
Grtr. Kankakee	IKK	N	IKK-RW-04/20	RW	TKAC
Grtr. Kankakee	IKK	N	IKK-RW-16/01	RW	TKAC
Grtr. Kankakee	IKK	N	IKK-TW-A/20	TW	TKAC
Grtr. Kankakee	IKK	N	IKK-TW-A/3-22	TW	TNAC
Grtr. Kankakee	IKK	N	IKK-TW-D/22	TW	TNAC
Grtr. Kankakee	IKK	N	IKK-TW-D/23	TW	TKAC
Jacksonville	IJX	C	IJX-AP-SS/9	AP	PCC
Jacksonville	IJX	C	IJX-TW-B/8	TW	TNAC
Joliet PD	JOT	N	JOT-AP-NW/2	AP	TKAC
Joliet PD	JOT	N	JOT-AP-NW/4	AP	PCC
Joliet PD	JOT	N	JOT-TW-B/1	TW	TNAC
Joliet PD	JOT	N	JOT-TW-B/1-1	TW	TNAC
Joliet PD	JOT	N	JOT-TW-B/2-1	TW	TNAC
Joliet PD	JOT	N	JOT-TW-B/3-1	TW	TNAC
Joliet PD	JOT	N	JOT-TW-C-1/2-2	TW	TKAC
Joliet PD	JOT	N	JOT-TW-C/2	TW	TKAC
Joliet PD	JOT	N	JOT-TW-C/2-2	TW	TKAC
Joliet PD	JOT	N	JOT-TW-C/5	TW	TKAC
Joliet PD	JOT	N	JOT-TW-D/1-1	TW	TKAC
Joliet PD	JOT	N	JOT-TW-D/1-6	TW	TKAC
Joliet PD	JOT	N	JOT-TW-D/2-1	TW	TKAC

Table 22. Summary of airport information contained in data base.

Airport	AID	ClimaticZone	Section	Feature	Code
Joliet PD	JOT	N	JOT-TW-D/2-6	TW	TKAC
Joliet PD	JOT	N	JOT-TW-D/3-6	TW	TKAC
Joliet PD	JOT	N	JOT-TW-D/6	TW	TKAC
Kewanee	C07	N	C07-AP-SE/04	AP	TKAC
Kewanee	C07	N	C07-AP-SE/06	AP	TKAC
Kewanee	C07	N	C07-RW-09/01	RW	TKAC
Kewanee	C07	N	C07-TW-A/05	TW	TKAC
Lacon	C75	C	C75-AP-WW/03	AP	TKAC
Lacon	C75	C	C75-RW-13/01	RW	TKAC
Lacon	C75	C	C75-TW-C/01	TW	TKAC
Lansing	3HA	N	3HA-AP-NN/01	AP	PCC
Lansing	3HA	N	3HA-AP-NN/03	AP	PCC
Lansing	3HA	N	3HA-AP-NN/04	AP	PCC
Lansing	3HA	N	3HA-AP-WW/02	AP	TNAC
Lansing	3HA	N	3HA-RW-09/02	RW	TNAC
Lansing	3HA	N	3HA-TW-A/01	TW	TNAC
Lansing	3HA	N	3HA-TW-B/01	TW	TNAC
Lansing	3HA	N	3HA-TW-B/1-01	TW	TNAC
Lansing	3HA	N	3HA-TW-B/2-01	TW	TNAC
Lansing	3HA	N	3HA-TW-B/3-01	TW	TNAC
Litchfield	3LF	C	3LF-AP-EE/1	AP	PCC
Litchfield	3LF	C	3LF-AP-EE/7	AP	TKAC
MaComb	MQB	C	MQB-RW-08/03	RW	TKAC
Marion	MWA	S	MWA-RW-11/3	RW	PCC
Marion	MWA	S	MWA-TW-D/1	TW	PCC
Marion	MWA	S	MWA-TW-D/1-1	TW	PCC
Metropolis	M30	S	M30-RW-18/04	RW	TKAC
Metropolis	M30	S	M30-RW-18/05	RW	TKAC
Mt. Carmel	I02	S	I02-AP-NN/01	AP	TNAC
Mt. Carmel	I02	S	I02-RW-12/01	RW	TKAC
Mt. Carmel	I02	S	I02-TW-A/06	TW	TKAC
Mt. Carmel	I02	S	I02-TW-A/1-02	TW	TKAC
Mt. Carmel	I02	S	I02-TW-B/01	TW	TNAC
Paris	PRG	C	PRG-AP-SS/01	AP	TKAC
Paris	PRG	C	PRG-RW-09/01	RW	TKAC
Paris	PRG	C	PRG-TW-A/01	TW	TKAC
Paris	PRG	C	PRG-TW-B/01	TW	TKAC
Pekin	C15	C	C15-AP-EE/07	AP	TNAC
Pekin	C15	C	C15-RW-09/03	RW	TNAC
Peoria	3MY	C	3MY-AP-EE/3	AP	TNAC
Peoria	3MY	C	3MY-AP-EE/5	AP	PCC
Peoria	3MY	C	3MY-AP-EE/6	AP	TKAC
Peoria	3MY	C	3MY-AP-EE/8	AP	TNAC
Peoria	3MY	C	3MY-RW-17/2	RW	TNAC
Peoria	3MY	C	3MY-TW-A/3	TW	TNAC
Peoria	3MY	C	3MY-TW-A/3-1	TW	TNAC
Peru	VYS	N	VYS-AP-EE/01	AP	TNAC
Peru	VYS	N	VYS-AP-EE/02	AP	PCC
Peru	VYS	N	VYS-AP-EE/04	AP	PCC

Table 22. Summary of airport information contained in data base.

Airport	AID	ClimaticZone	Section	Feature	Code
Peru	VYS	N	VYS-AP-EE/05	AP	TKAC
Peru	VYS	N	VYS-RW-18/01	RW	TKAC
Peru	VYS	N	VYS-RW-18/02	RW	TKAC
Peru	VYS	N	VYS-TW-A/01	TW	TKAC
Pickneyville	K16	S	K16-AP-WW/01	AP	TNAC
Pickneyville	K16	S	K16-AP-WW/02	AP	TKAC
Pickneyville	K16	S	K16-RW-18/01	RW	TKAC
Pickneyville	K16	S	K16-RW-18/02	RW	TNAC
Pickneyville	K16	S	K16-TW-A/02	TW	TKAC
Quincy	UIN	C	UIN-RW-04/06	RW	PCC
Quincy	UIN	C	UIN-RW-18/011	RW	PCC
Quincy	UIN	C	UIN-TW-A/06	TW	PCC
Quincy	UIN	C	UIN-TW-B/01	TW	PCC
Quincy	UIN	C	UIN-TW-B/1-01	TW	PCC
Rochelle	12C	N	12C-RW-07/03	RW	TKAC
Rochelle	12C	N	12C-TW-C/01	TW	TNAC
Savanna	SFY	N	SFY-AP-NW/01	AP	TNAC
Savanna	SFY	N	SFY-AP-WW/01	AP	TNAC
Savanna	SFY	N	SFY-TW-B/01	TW	TNAC
Shelbyville	2H0	C	2H0-AP-EE/6	AP	TKAC
Shelbyville	2H0	C	2H0-AP-EE/7	AP	TNAC
Shelbyville	2H0	C	2H0-RW-18/9	RW	TKAC
Sparta	SAR	S	SAR-AP-WW/03	AP	TKAC
Sparta	SAR	S	SAR-RW-18/03	RW	TNAC
Sparta	SAR	S	SAR-TW-B/03	TW	TKAC
St. Louis DT	CPS	S	CPS-RW-12L/24	RW	PCC
St. Louis DT	CPS	S	CPS-TW-B/1-24	TW	PCC
St. Louis DT	CPS	S	CPS-TW-B/2-24	TW	PCC
St. Louis DT	CPS	S	CPS-TW-C/10	TW	TKAC
Sterling	SQI	N	SQI-AP-WW/01	AP	TKAC
Sterling	SQI	N	SQI-AP-WW/10	AP	TKAC
Taylorville	3TV	C	3TV-AP-EE/04	AP	TNAC
Taylorville	3TV	C	3TV-AP-EE/07	AP	TNAC
Taylorville	3TV	C	3TV-RW-18/08	RW	TKAC
Taylorville	3TV	C	3TV-TW-A/1-08	TW	TKAC
Taylorville	3TV	C	3TV-TW-A/2-08	TW	TKAC
Taylorville	3TV	C	3TV-TW-A/3-08	TW	TKAC
Taylorville	3TV	C	3TV-TW-A/4-08	TW	TKAC
Taylorville	3TV	C	3TV-TW-A/5-02	TW	TKAC
Vandalia	VLA	S	VLA-TW-B/7	TW	TNAC
Vandalia	VLA	S	VLA-TW-D/1-7	TW	TNAC
Vandalia	VLA	S	VLA-TW-D/7	TW	TNAC
Waukegan	UGN	N	UGN-RW-14/08	RW	PCC
Waukegan	UGN	N	UGN-RW-14/09	RW	PCC
Waukegan	UGN	N	UGN-RW-14/111	RW	PCC
Waukegan	UGN	N	UGN-RW-14/112	RW	PCC
Waukegan	UGN	N	UGN-RW-14/14	RW	PCC
Waukegan	UGN	N	UGN-TW-C/07	TW	TKAC

Table 23. Linear regression of sample unit and section PCI data.

Region	Pavement Type	Based on SUs			Based on Sections		
		Model	R ²	SEE	Model	R ²	SEE
Northern	TNAC	Y = 100 - 4.072x	0.761	15.79	Y = 100 - 3.314x	0.711	12.02
	TKAC	Y = 100 - 1.775x	0.304	12.13	Y = 100 - 1.668x	0.362	10.23
	PCC	Y = 100 - 1.906x	0.435	17.16	Y = 100 - 1.906x	0.435	14.62
Central	TNAC	Y = 100 - 2.506x	0.610	13.46	Y = 100 - 2.825x	0.439	17.67
	TKAC	Y = 100 - 1.776x	0.461	10.37	Y = 100 - 1.916x	0.543	7.66
	PCC	Y = 100 - 0.355x	0.000	12.89	Y = 100 - 0.355x	0.000	14.04
Southern	TNAC	Y = 100 - 2.008x	0.454	9.70	Y = 100 - 1.984x	0.467	9.52
	TKAC	Y = 100 - 1.979x	0.484	12.89	Y = 100 - 1.743x	0.592	11.43
	PCC	Y = 100 - 1.469x	0.367	10.98	Y = 100 - 1.469x	0.367	9.88

Table 24. Summary of deterioration rates established for AC surface sections.

TNAC Section			TKAC Sections		
Region	Age Range (yrs)	Deterioration Rate (PCI/Yr)	Region	Age Range (yrs)	Deterioration Rate (PCI/Yr)
Central	1-10	-5.36	Central	1-25	-2.71
	11-25	-3.41	Northern	1-5	-2.59
Northern	1-5	-2.23		6-10	-4.47
	6-10	-3.57		11-25	-2.02
	11-20	-6.77	Southern	1-5	-2.83
Southern	1-10	-2.89		6-15	-3.59
	11-20	-5.50		16-25	-4.86

Table 25. Division of PCC sections using L/l.

Division1		Division2	
Size Designation	L/l	Size Designation	L/l
Small	< 6.5	Small	< 5.5
Medium	Between 6.5 and 8.5	Medium	Between 5.5 and 6.5
Large	> 8.5	Large	> 6.5

Table 26. Summary of deterioration rates established for Division 1 PCC pavements.

Region	Small Slab (L/l < 6.5)		Medium Slab (6.5 < L/l < 8.5)		Large Slab (L/l > 8.5)	
	Age Range (yrs)	Deterioration Rate (PCI/Yr)	Age Range (yrs)	Deterioration Rate (PCI/Yr)	Age Range (yrs)	Deterioration Rate (PCI/Yr)
Northern	1-10	-1.18	1-10	-2.67	1-5	-10.8
	11-20	-4.25	11-20	-3.54	6-20	-3.33
			21-25	-7.38		
Central	1-10	-0.56	1-15	-0.625	1-5	-7.83
	11-15	-1.20	16-25	-2.58	6-15	-15.61
	16-40	-0.44				
	41-45	-2.15				
Southern	1-5	-0.76	1-5	-2.25	1-10	-6.22
	6-15	-1.74	6-20	-1.67	11-20	-2.0

Table 27. Summary of deterioration rates established for Division 2 PCC pavements.

Region	Small Slab ($L/l < 5.5$)		Medium Slab ($5.5 < L/l < 6.5$)		Large Slab ($L/l > 6.5$)	
	Age Range (yrs)	Deterioration Rate (PCI/Yr)	Age Range (yrs)	Deterioration Rate (PCI/Yr)	Age Range (yrs)	Deterioration Rate (PCI/Yr)
Northern	1-5	-0.97	1-10	-2.67	1-5	-4.40
	6-20	-2.96	11-20	-3.54	6-10	-2.80
			21-25	-7.38	11-25	-3.83
Central	No Data		1-10	-0.56	1-25	-3.74
			11-15	-1.20		
			16-40	-0.44		
			41-45	-2.15		
Southern	1-5	-0.55	1-5	-0.97	1-10	-3.34
	6-15	-1.26	6-10	-3.66	11-20	-1.65

Table 28. Summary of section information included in rehabilitated section study.

Feature	Climatic Region									Total
	Central			Northern			Southern			
	PCC	TKAC	TNAC	PCC	TKAC	TNAC	PCC	TKAC	TNAC	
AP	1	4	8	0	1	7	2	1	9	33
RW	1	4	11	2	2	13	2	1	21	57
TW	0	5	11	1	3	7	1	1	15	44
Total	2	13	30	3	6	27	5	3	45	134

Table 29. Summary of pavement age in years at time of rehabilitation.

Pavement Type	Central Climatic Region			Northern Climatic Region			Southern Climatic Region		
	Mean	STDEV	COV	Mean	STDEV	COV	Mean	STDEV	COV
PCC	39.0	1.41	3.6%	23.0 ¹	0.00	0.0%	36.8	11.10	30.2
TKAC	21.0	3.37	16.0%	14.5	3.02	20.8%	14.7	2.08	14.2
TNAC	15.2	6.20	40.9%	16.5	5.85	35.4%	17.2	9.5	55.6

¹ Note: This mean is based on the average of three sections at Dupage, two of which were built and overlaid at the same time.

Table 30. Summary of pavement life predictions assuming terminal PCI of 70.

Climatic Zone	TNAC	TKAC	PCC Sections		
			Small Slab	Medium Slab	Large Slab
Northern	10 yrs	8 yrs	14 yrs	11 yrs	3 yrs
Central	6 yrs	12 yrs	40+ yrs	23 yrs	4 yrs
Southern	10 yrs	9 yrs	20 yrs	16 yrs	5 yrs

Table 31. Summary of AC sample units inspections used in analysis.

Age (yrs)	TNAC				TKAC			
	Central	Northern	Southern	Total	Central	Northern	Southern	Total
1-5	116	243	57	416	50	138	72	260
6-10	75	185	58	318	38	74	74	186
11-15	113	25	78	216	26	1843	60	129
16-20	118	8	56	182	12	1718	19	49
21-25	0	12	31	43	14	17	0	31
26-30	0	0	0	0	4	0	0	4
Total	422	473	280	1175	144	290	225	659

Table 32. Load Code distribution according to pavement type.

Pavement Type	Load Code (Number of Sample Units)			
	Low	Medium	High	Total
TNAC	339	231	13	583
TKAC	703	513	35	1251
PCC	201	554	176	931
Total	1243	1298	224	2765

Table 33. Percent sample units affected by alligator cracking for different Load Codes.

Distress Severity	Percent Sample Units Affected for Each Load Code					
	TNAC			TKAC		
	Low	Medium	High	Low	Medium	High
Low	7.87%	15.07%	0.00%	10.54%	7.99%	6.82%
Medium	3.55%	3.55%	0.00%	1.52%	2.24%	0.00%
High	0.76%	0.76%	0.00%	0.12%	0.00%	0.00%

Table 34. Summary of PCC sample units inspections used in analysis.

Age (yrs)	PCC			
	Central	Northern	Southern	Total
1-5	5	94	87	186
6-10	10	42	101	153
11-15	44	46	38	128
16-20	60	47	53	160
21-25	60	50	0	110
26-30	5	24	0	29
36-40	89	0	0	89
41-45	76	0	0	76
Total	349	303	279	931

Table 35. Number of Division 1 sample units according to slab size and Load Code.

Load Code	Division 1 Slab Size			Total
	Small	Medium	Large	
Low	176	11	14	201
Medium	404	150	0	554
Large	17	129	30	176
Total	597	290	44	931

Table 36. Percent PCC sample units affected by distress for different Load Codes.

Distress Type	Severity	Low Load Code				Medium Load Code			High Load Code			
		Large	Medium	Small	Total	Medium	Small	Total	Large	Medium	Small	Total
Corner Breaking	L	29%	18%	5%	7%	19%	2%	7%	7%	11%	6%	10%
	M	14%	0%	2%	2%	6%	0%	2%	10%	2%	0%	3%
	H	0%	0%	0%	0%	0%	0%	0%	7%	0%	0%	1%
Corner Spalling	L	21%	9%	19%	18%	35%	24%	27%	37%	26%	0%	26%
	M	7%	0%	8%	7%	33%	7%	14%	20%	9%	0%	10%
	H	0%	0%	1%	1%	9%	0%	3%	13%	0%	0%	2%
Faulting	L	36%	0%	3%	5%	3%	3%	3%	20%	5%	0%	7%
	M	7%	0%	1%	1%	2%	0%	1%	17%	1%	0%	3%
Joint Spalling	L	64%	55%	24%	28%	31%	29%	30%	37%	45%	6%	40%
	M	50%	0%	14%	15%	25%	13%	16%	17%	34%	0%	28%
	H	14%	0%	1%	2%	9%	1%	3%	10%	1%	0%	2%
L, T, & D Cracking	L	93%	0%	24%	28%	51%	11%	22%	60%	61%	0%	55%
	M	36%	0%	11%	12%	39%	7%	16%	70%	43%	12%	44%
	H	0%	0%	2%	2%	4%	1%	2%	0%	1%	0%	1%
Pumping	L	7%	0%	3%	3%	1%	2%	1%	0%	1%	0%	1%
Shattered Slab	L	29%	0%	0%	2%	7%	0%	2%	50%	14%	0%	19%
	M	14%	0%	0%	1%	6%	0%	2%	20%	2%	0%	5%
	H	0%	0%	0%	0%	1%	0%	1%	10%	1%	0%	2%

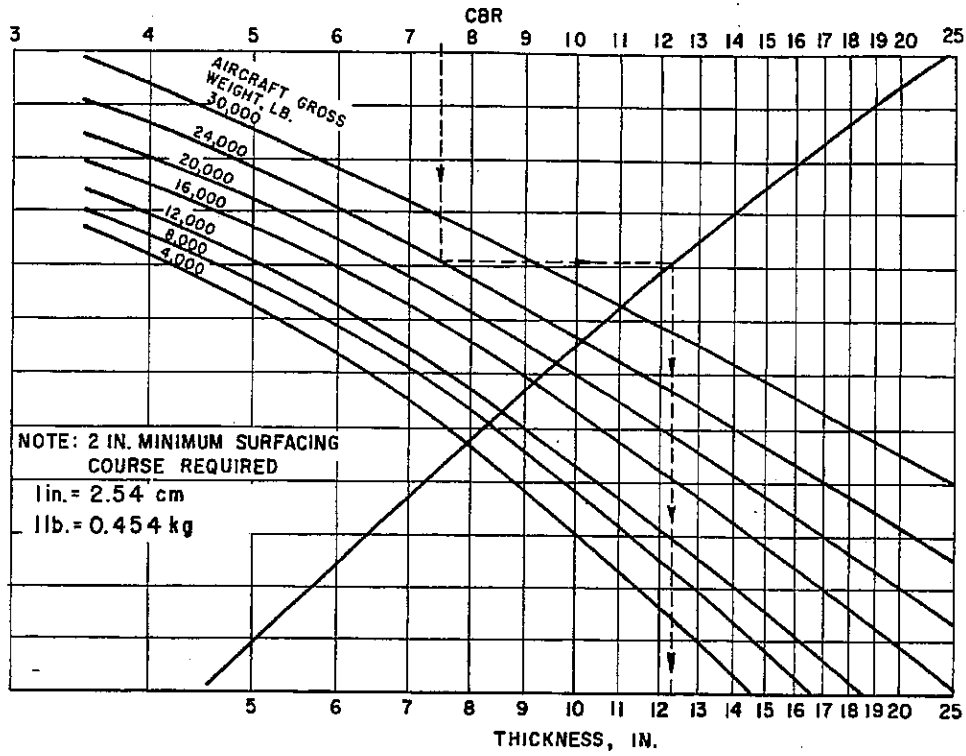


Figure 1. FAA Design curves for flexible pavements - light aircraft [FAA, 1978].

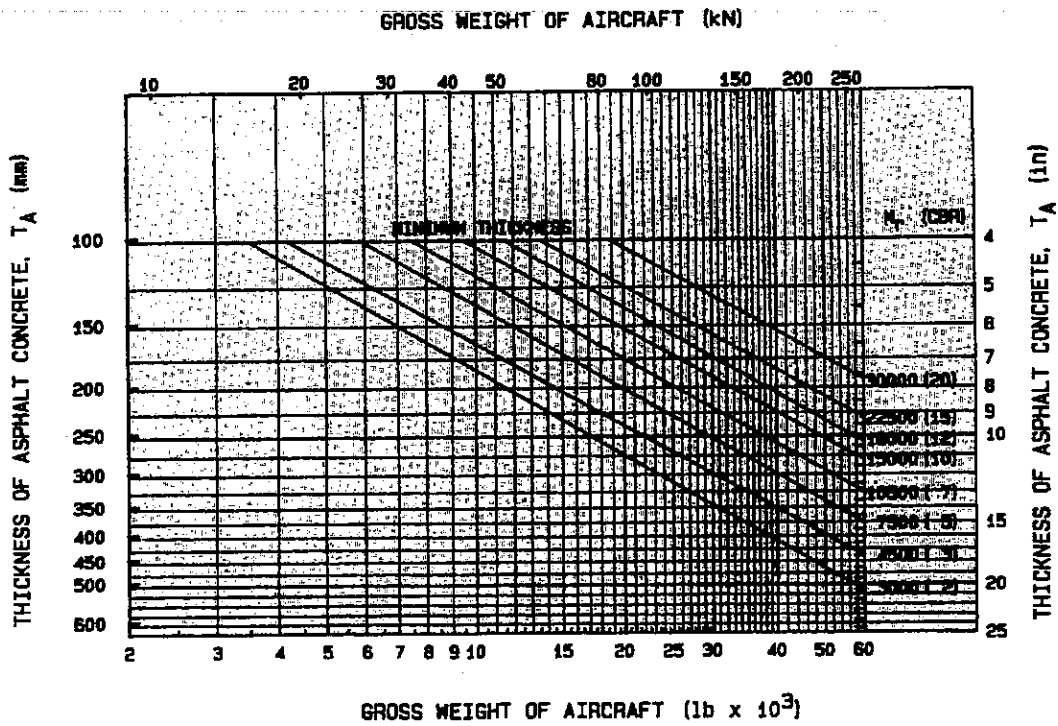


Figure 2. Asphalt Institute design chart for FULL-DEPTH pavement [AI, 1987].

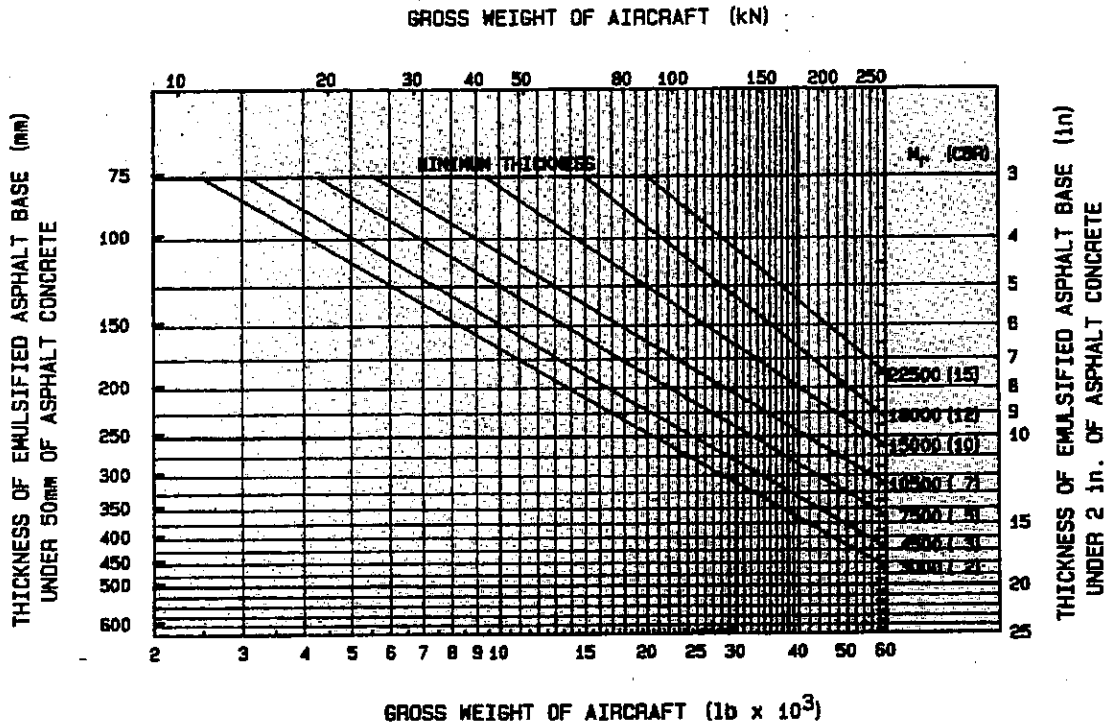


Figure 3. Asphalt Institute design chart for emulsified asphalt base [AI, 1987].

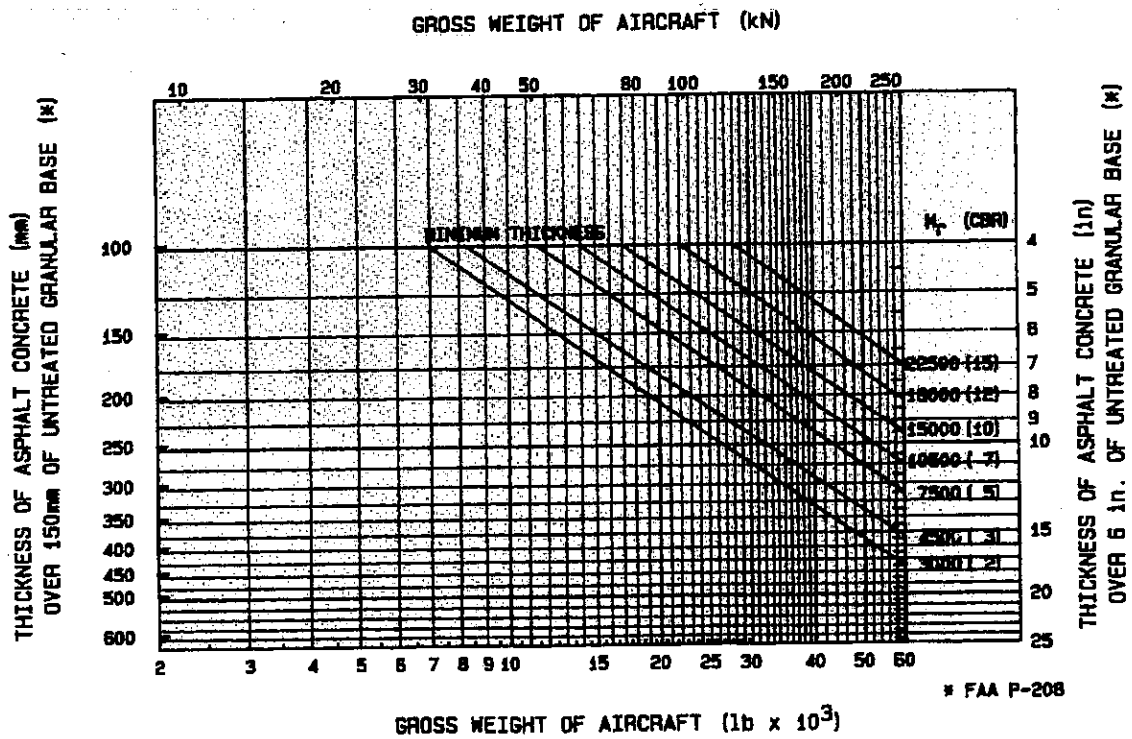


Figure 4. Asphalt Institute design chart for untreated base [AI, 1987].

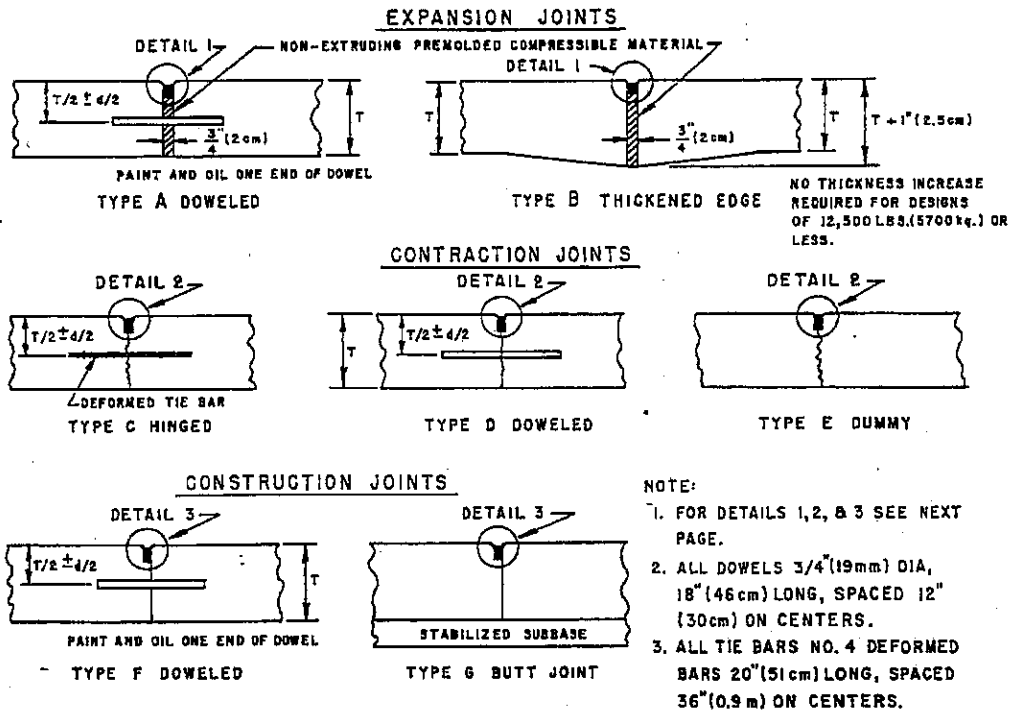


Figure 5. Jointing details provided in FAA AC 150/5320-6C [FAA, 1978].

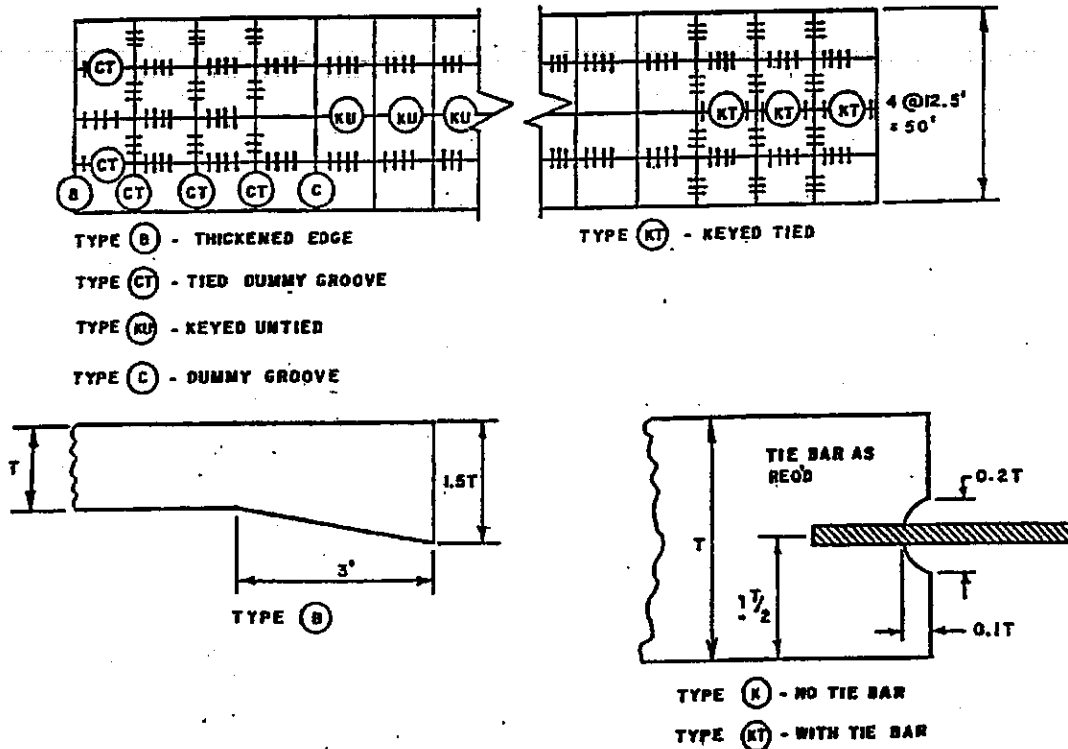


Figure 6. Jointing plans and details for 50' wide pavement provided in Engineering Brief No. 27 [FAA, 1981].

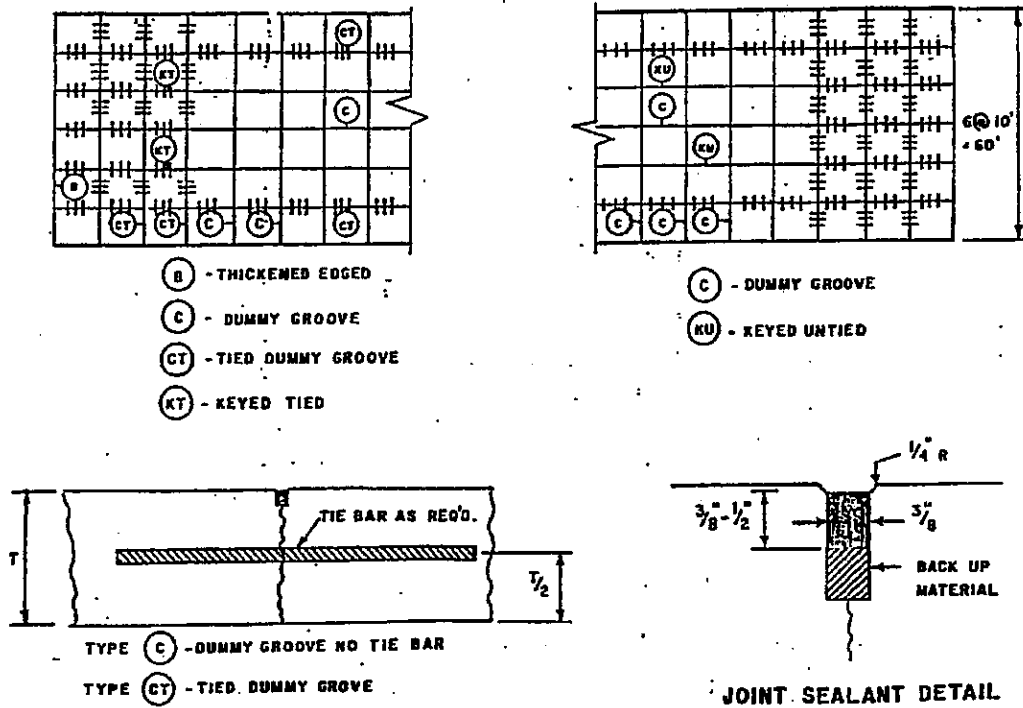


Figure 7. Jointing plans and details for 60' wide pavement provided in Engineering Brief No. 27 [FAA, 1981].

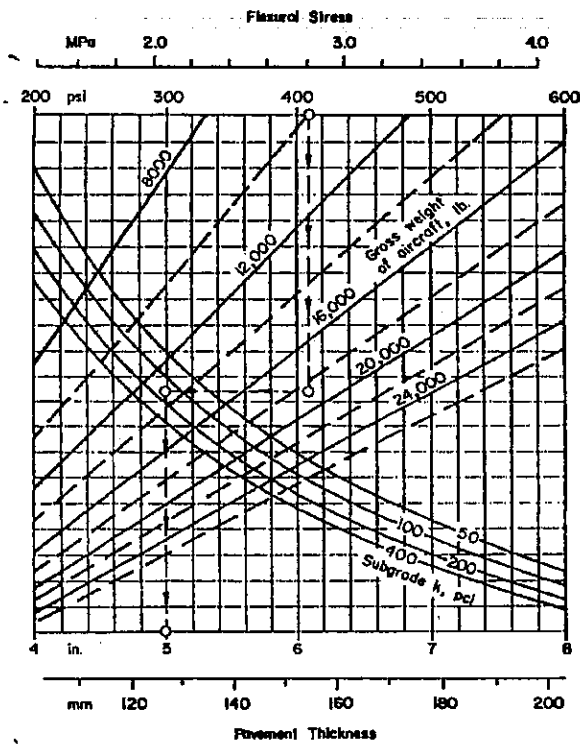


Figure 8. ACPA thickness design chart for single-wheel landing gear [ACPA,1993].

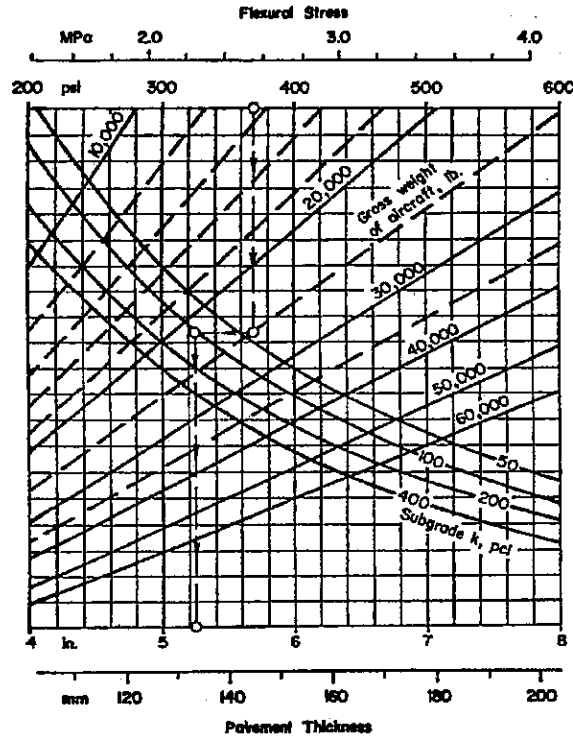


Figure 9. ACPA thickness design chart for dual-wheel landing gear [ACPA,1993].

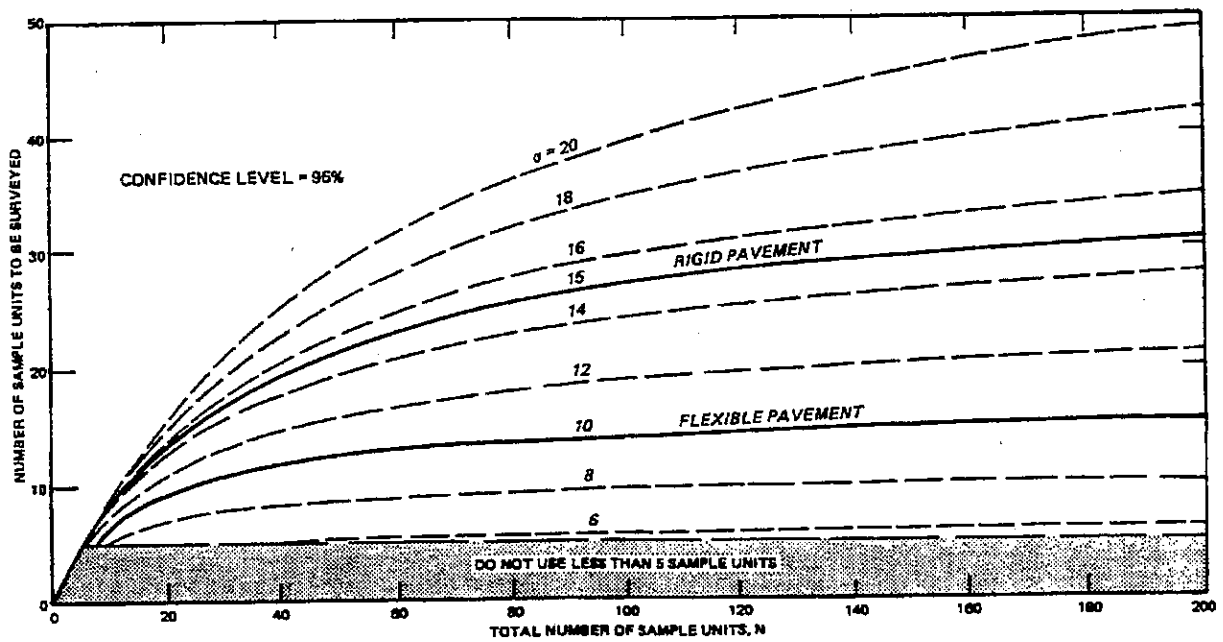


Figure 10. Selection of minimum number of sample units to be inspected [FAA, 1982].

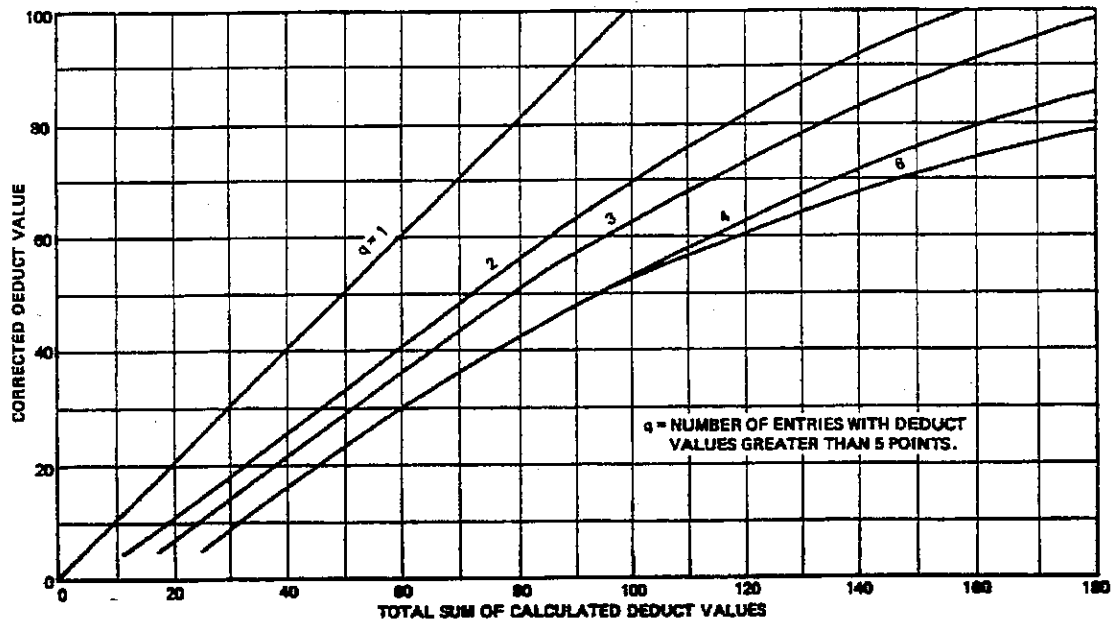


Figure 11. Corrected deduct values for AC surfaced pavements [FAA, 1982].

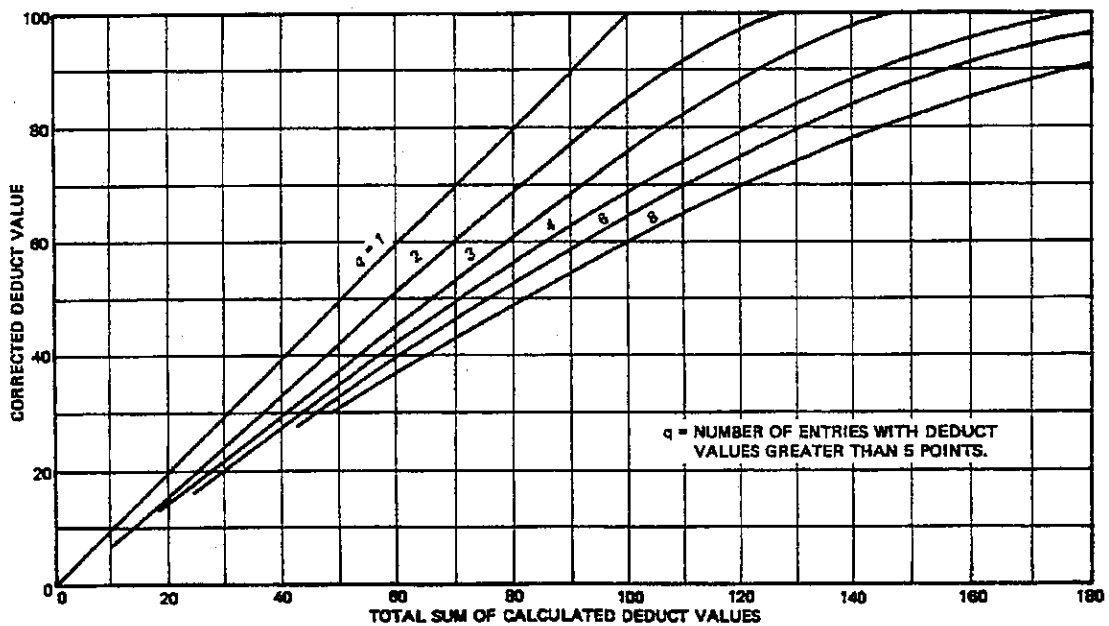
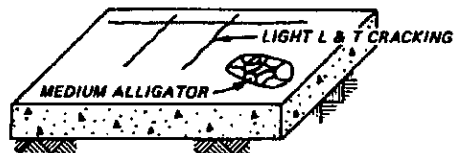


Figure 12. Corrected deduct values for jointed PCC pavements [FAA, 1982].

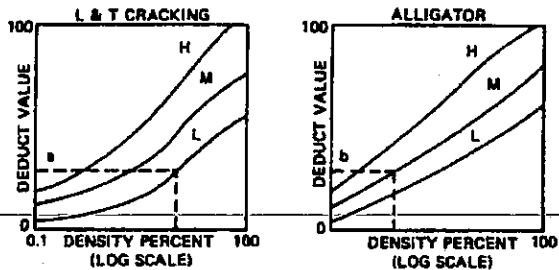
STEP 1. DIVIDE PAVEMENTS INTO FEATURES.

STEP 2. DIVIDE PAVEMENT FEATURE INTO SAMPLE UNITS.

STEP 3. INSPECT SAMPLE UNITS; DETERMINE DISTRESS TYPES AND SEVERITY LEVELS AND MEASURE DENSITY.

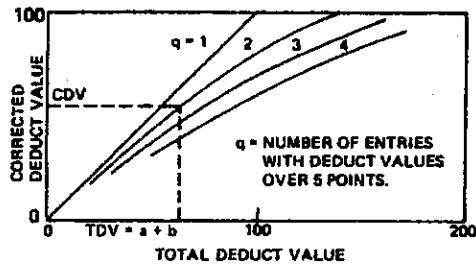


STEP 4. DETERMINE DEDUCT VALUES



STEP 5. COMPUTE TOTAL DEDUCT VALUE (TDV) $a + b$.

STEP 6. ADJUST TOTAL DEDUCT VALUE



STEP 7. COMPUTE PAVEMENT CONDITION INDEX
(PCI) = 100 - CDV FOR EACH SAMPLE
UNIT INSPECTED.

STEP 8. COMPUTE PCI OF ENTIRE FEATURE (AVERAGE PCI'S OF SAMPLE UNITS).

STEP 9. DETERMINE PAVEMENT
CONDITION RATING
OF FEATURE.

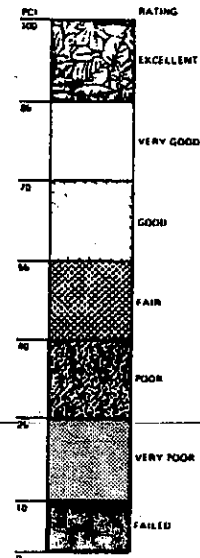


Figure 13. Steps for determining PCI of a pavement feature [FAA, 1982].

FLEXIBLE PAVEMENT CONDITION SURVEY DATA SHEET FOR SAMPLE UNIT																							
AIRPORT WORLD INTERNATIONAL					DATE 5/26/79																		
FACILITY TXE		FEATURE T-11		SAMPLE UNIT 4																			
SURVEYED BY JH/DE			AREA OF SAMPLE 6000 SQ FT																				
<p style="text-align: center;"><u>DISTRESS TYPES</u></p> <table style="width:100%; border: none;"> <tr> <td style="width: 50%;">1. ALLIGATOR CRACKING</td> <td style="width: 50%;">10. PATCHING</td> </tr> <tr> <td>2. BLEEDING</td> <td>11. POLISHED AGGREGATE</td> </tr> <tr> <td>3. BLOCK CRACKING</td> <td>12. RAVELING/WEATHERING</td> </tr> <tr> <td>4. CORRUGATION</td> <td>13. RUTTING</td> </tr> <tr> <td>5. DEPRESSION</td> <td>14. SHOVING FROM PCC</td> </tr> <tr> <td>6. JET BLAST</td> <td>15. SLIPPAGE CRACKING</td> </tr> <tr> <td>7. JT. REFLECTION (PCC)</td> <td>16. SWELL</td> </tr> <tr> <td>8. LONG. & TRANS. CRACKING</td> <td></td> </tr> <tr> <td>9. OIL SPILLAGE</td> <td></td> </tr> </table>			1. ALLIGATOR CRACKING	10. PATCHING	2. BLEEDING	11. POLISHED AGGREGATE	3. BLOCK CRACKING	12. RAVELING/WEATHERING	4. CORRUGATION	13. RUTTING	5. DEPRESSION	14. SHOVING FROM PCC	6. JET BLAST	15. SLIPPAGE CRACKING	7. JT. REFLECTION (PCC)	16. SWELL	8. LONG. & TRANS. CRACKING		9. OIL SPILLAGE		<p style="text-align: center;">SKETCH:</p>		
1. ALLIGATOR CRACKING	10. PATCHING																						
2. BLEEDING	11. POLISHED AGGREGATE																						
3. BLOCK CRACKING	12. RAVELING/WEATHERING																						
4. CORRUGATION	13. RUTTING																						
5. DEPRESSION	14. SHOVING FROM PCC																						
6. JET BLAST	15. SLIPPAGE CRACKING																						
7. JT. REFLECTION (PCC)	16. SWELL																						
8. LONG. & TRANS. CRACKING																							
9. OIL SPILLAGE																							
EXISTING DISTRESS TYPES																							
TOTAL SEVERITY	L M H	1	6	8	12																		
		4 X 4 M	8 X 4 L	10 L	3 X 10 M																		
		2 X 3 L		6 L																			
				15 L																			
				6 M																			
				10 L																			
				6 M																			
PCI CALCULATION																							
DISTRESS TYPE	SEVERITY	DENSITY %	DEDUCT VALUE	<p>PCI = 100 - CDV = <u>75</u></p> <p>RATING = <u>VERY GOOD</u></p>																			
1	L	0.22	7																				
1	M	0.32	19																				
6	L	0.48	2																				
8	L	0.80	6																				
8	M	0.20	6																				
12	M	0.60	7																				
DEDUCT TOTAL			45																				
CORRECTED DEDUCT VALUE (CDV)			25																				

Figure 14. Condition survey inspection form for AC surfaced pavements [FAA, 1982].

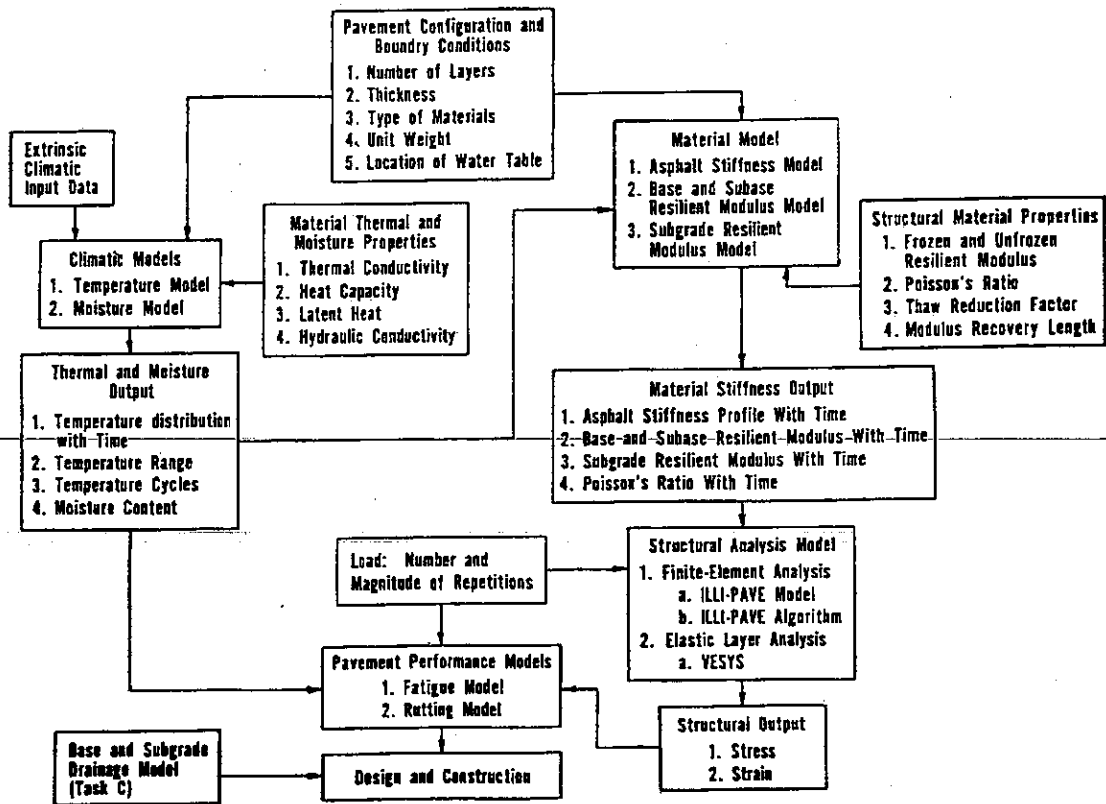


Figure 16. Schematic of C-M-S Model incorporated with structural analysis and pavement performance models [Dempsey, 1986].

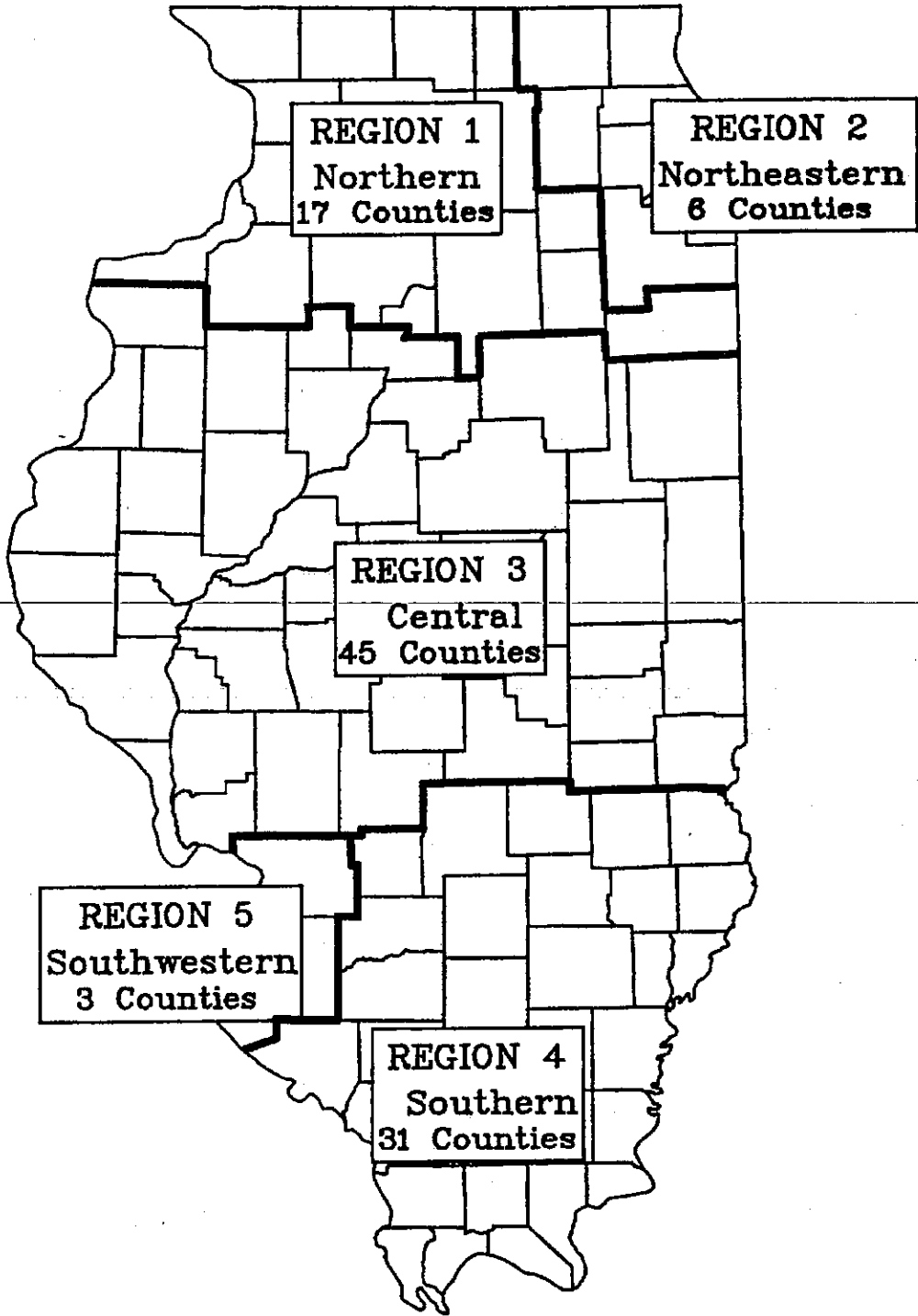


Figure 17. Illinois map showing the five administrative regions.

Allowable Passes Based on AC Fatigue for FAA and AI Conventional Designs

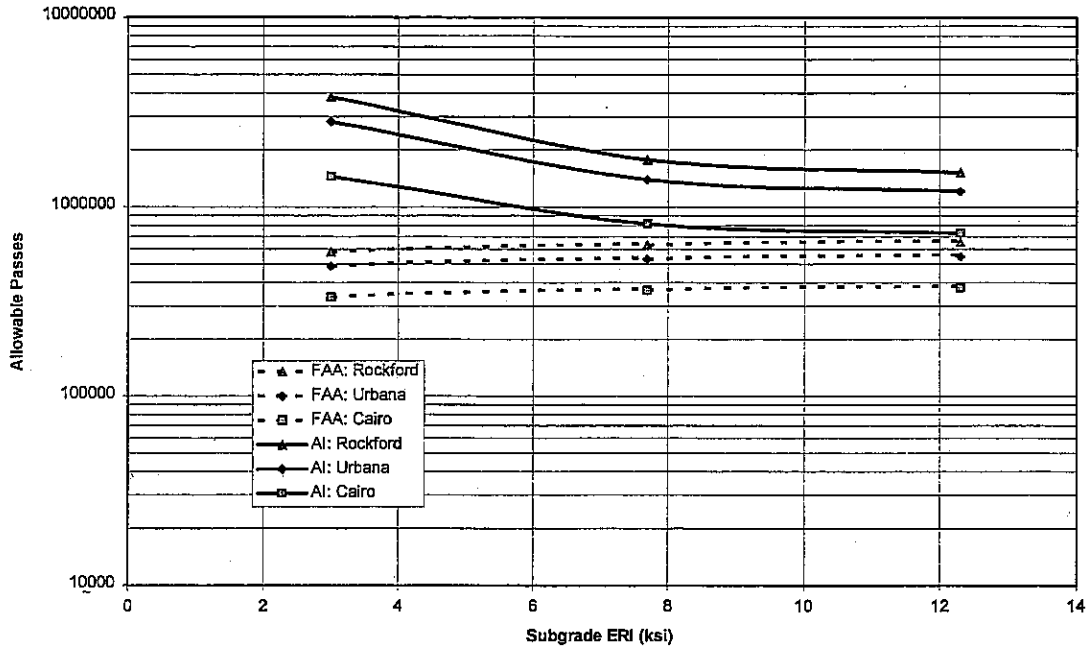


Figure 18. Estimated FAA and AI fatigue lives for conventional AC pavements.

Allowable Passes Based on AC Fatigue for FAA and AI Full-Depth Designs

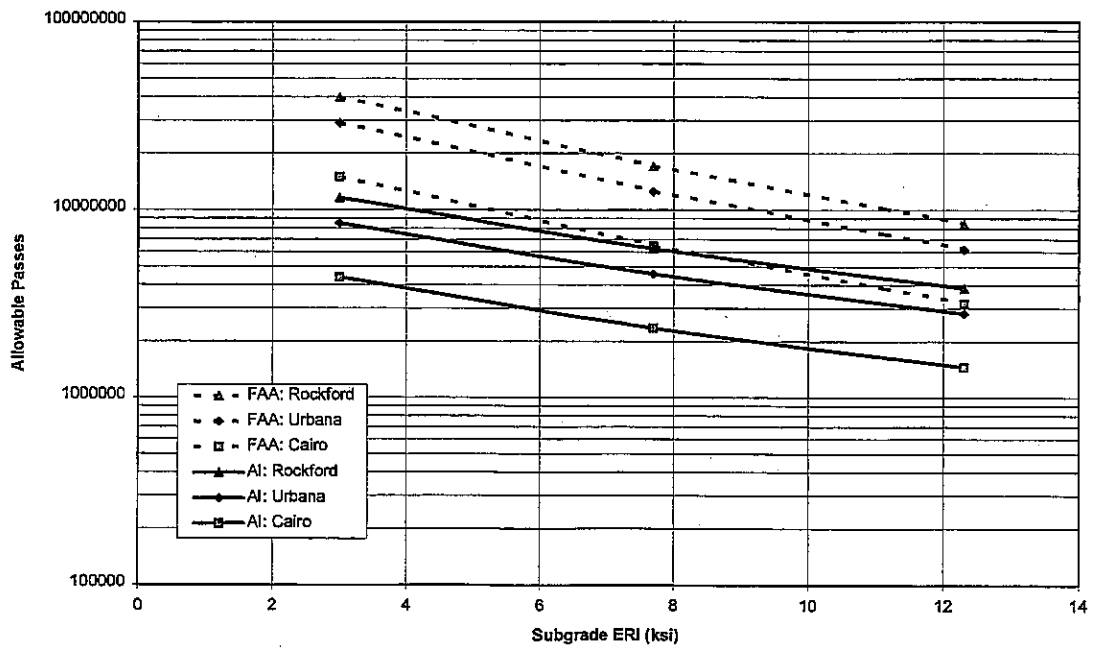


Figure 19. Estimated FAA and AI fatigue lives for FULL-DEPTH AC pavements.

Critical Flexural Stresses In PCC Based on ILLI-SLAB Analysis ($E_{pcc} = 3,000,000$ psi)

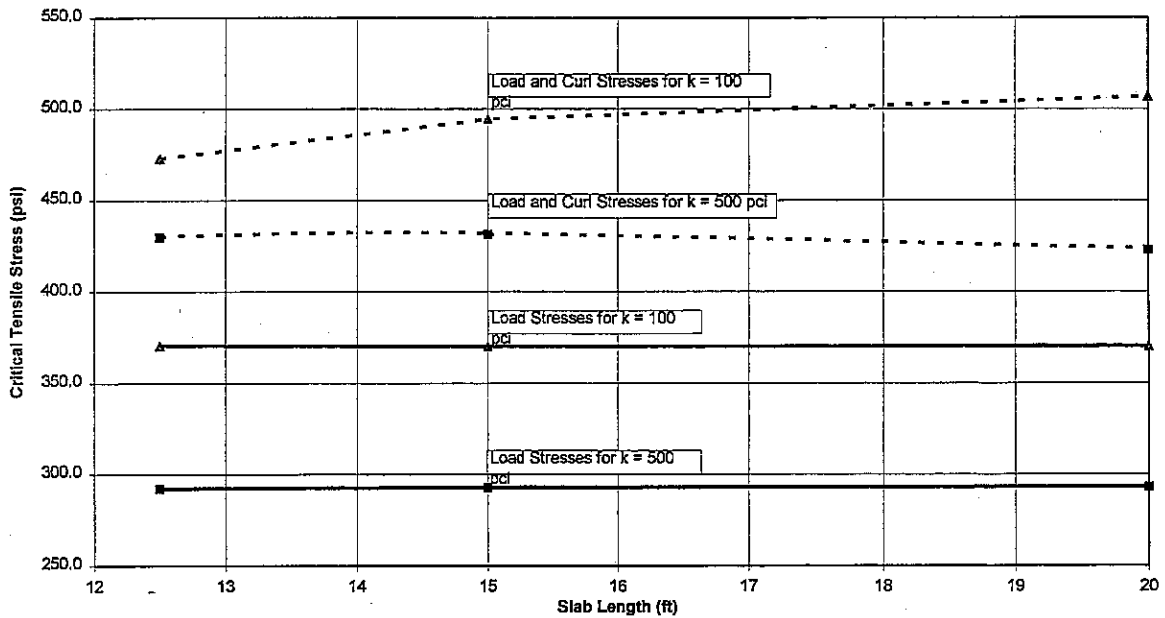


Figure 20. Calculated free edge tensile stresses from ILLI-SLAB for $E_{PCC} = 3,000,000$ psi.

Critical Flexural Stresses In PCC Based on ILLI-SLAB Analysis ($E_{pcc} = 4,000,000$ psi)

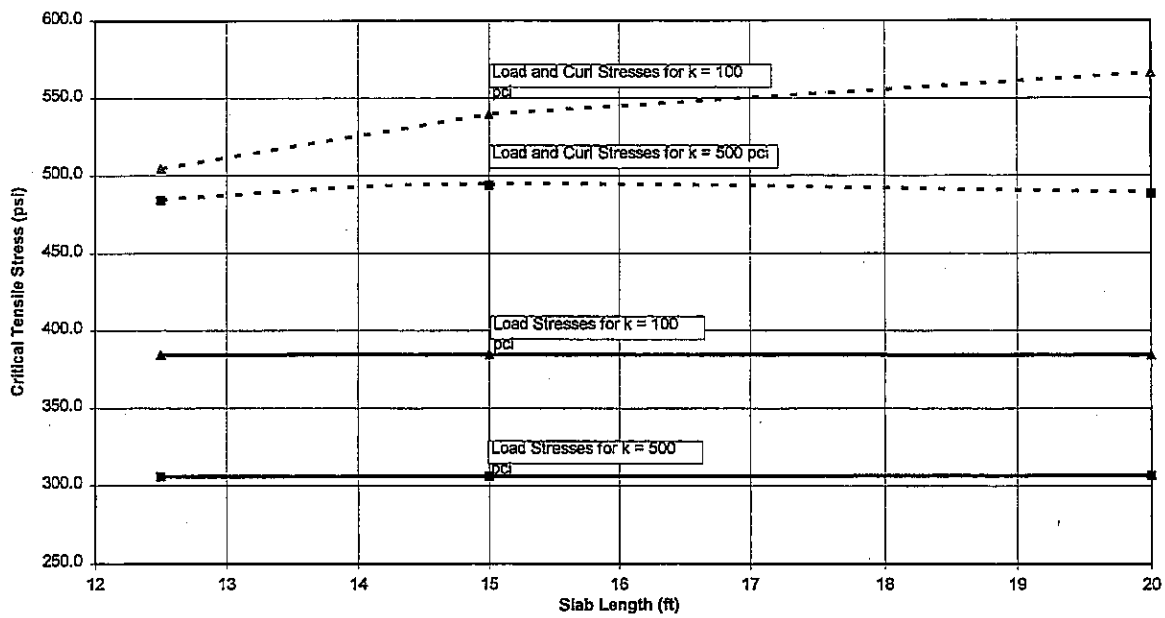


Figure 21. Calculated free edge tensile stresses from ILLI-SLAB for $E_{PCC} = 4,000,000$ psi.

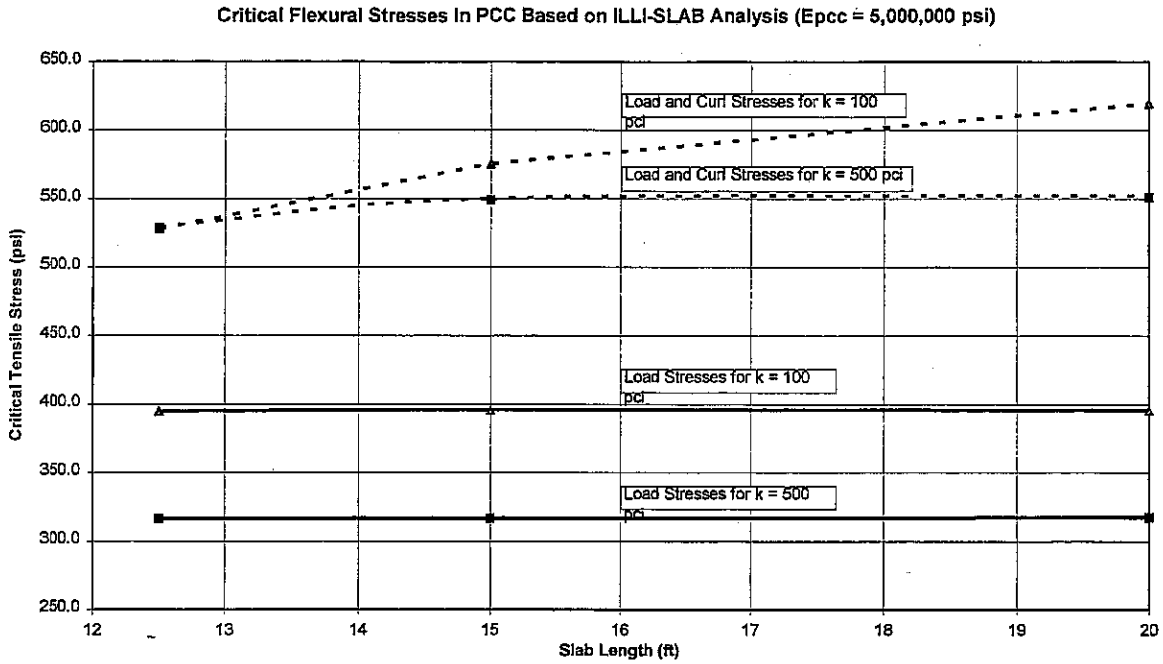


Figure 22. Calculated free edge tensile stresses from ILLI-SLAB for $E_{PCC} = 5,000,000$ psi.

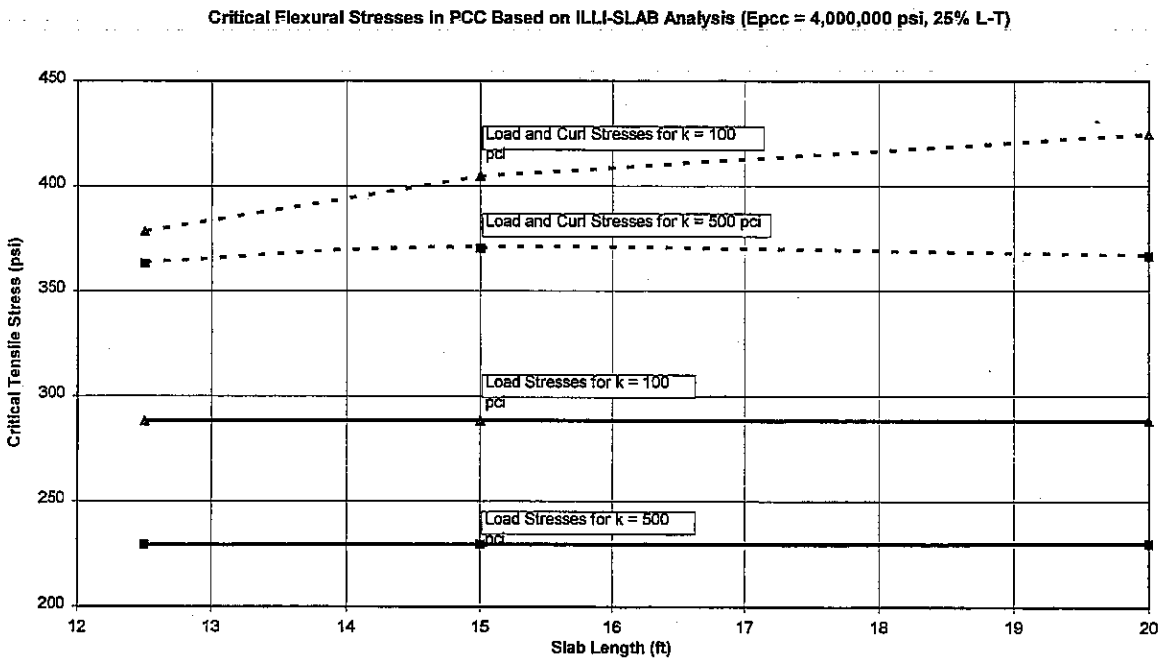


Figure 23. Calculated critical edge tensile stresses assuming a stress load transfer efficiency of 25% ($E_{PCC} = 4,000,000$ psi).

Passes to Failure Using Fatigue Relationships ($E_{pcc} = 4,000,000$ psi)

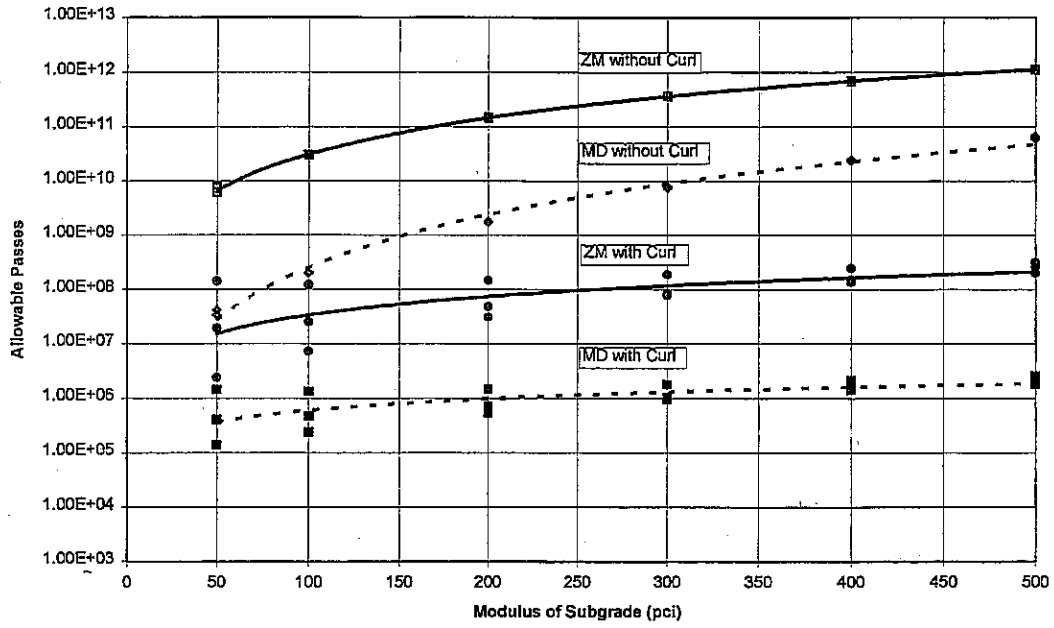


Figure 24. Estimated allowable passes for $E_{PCC} = 4,000,000$ psi.

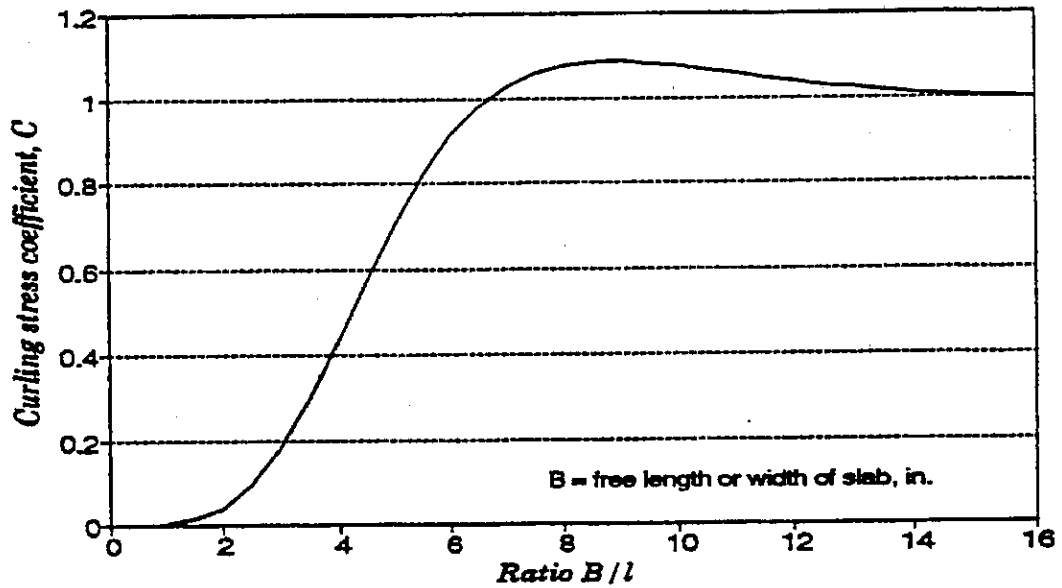


Figure 25. Curling stress coefficients [Bradbury, 1938].

Passes to Failure for Various Slab Length Using Calibrated Mechanistic Design Equation
($E_{pcc} = 4,000,000$ psi)

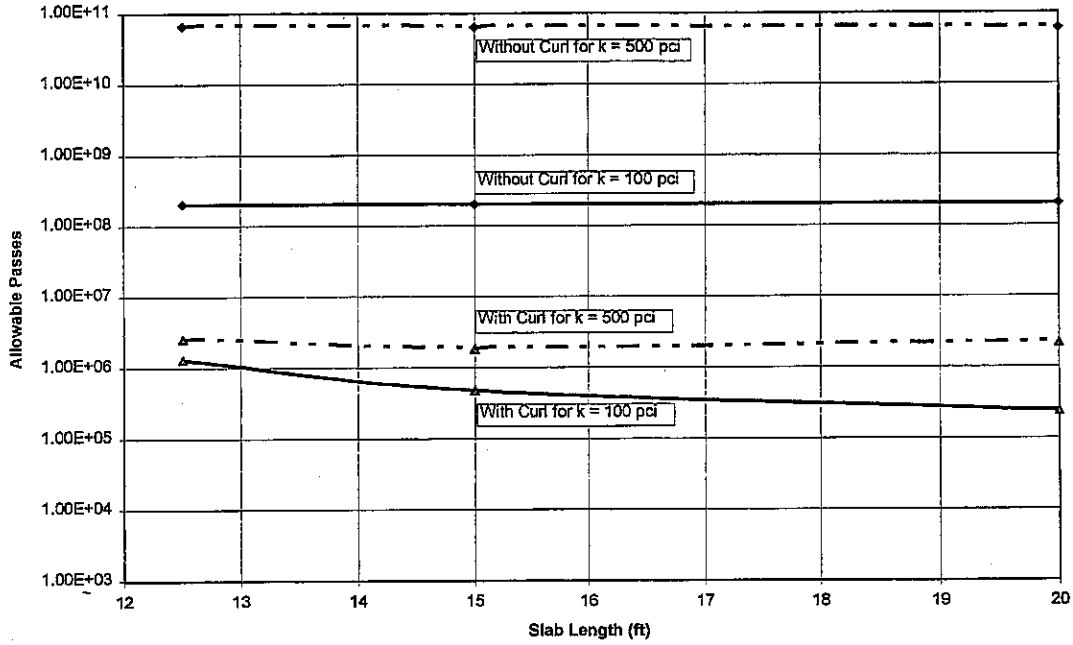


Figure 26. Slab length versus estimated allowable passes ($E_{pcc} = 4,000,000$ psi).

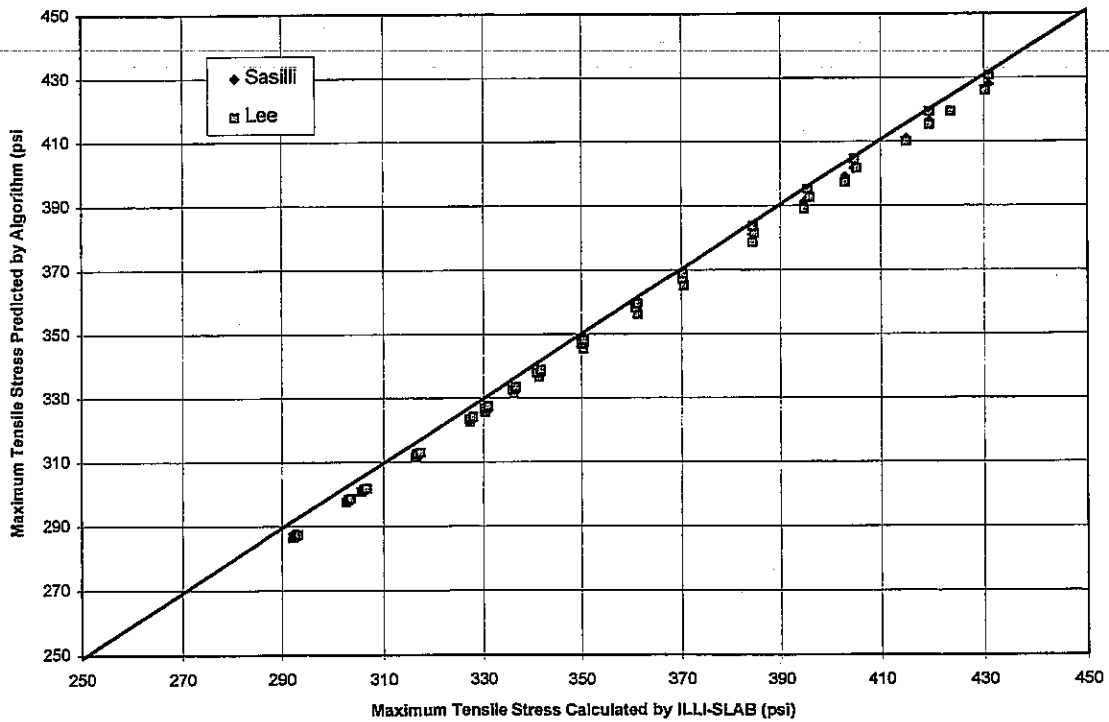


Figure 27. Comparison of ILLI-SLAB to regression model solutions for load induced stress.

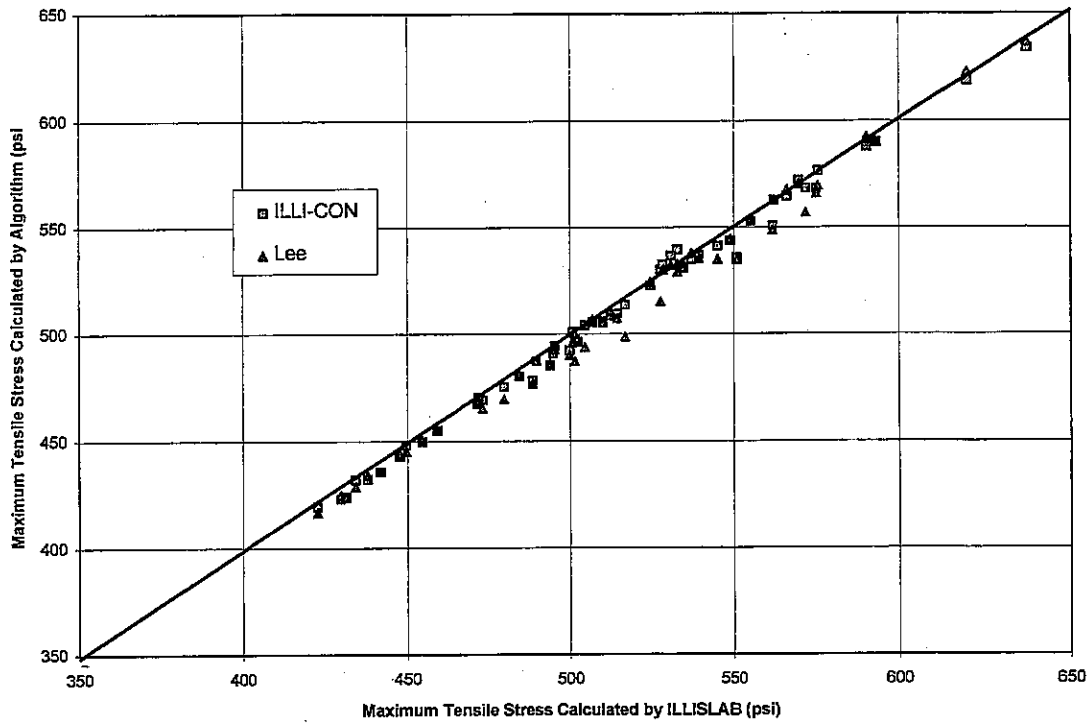


Figure 28. Comparison of ILLI-SLAB to regression model solutions for combined loading and curling stress.

Passes to Failure for 4-in and 5-in Thick PCC Slabs Using the Calibrated Mechanistic Model

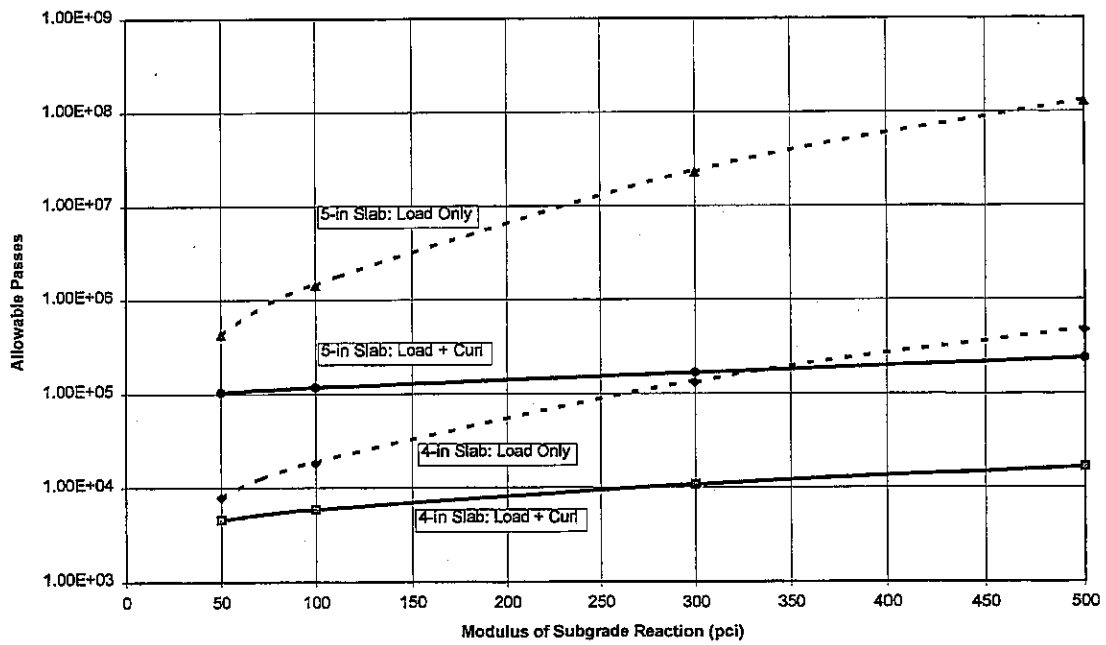


Figure 29. Estimated allowable passes for 4-in and 5-in thick PCC.

Comparison of Curling Stresses for Different Aggregate Types

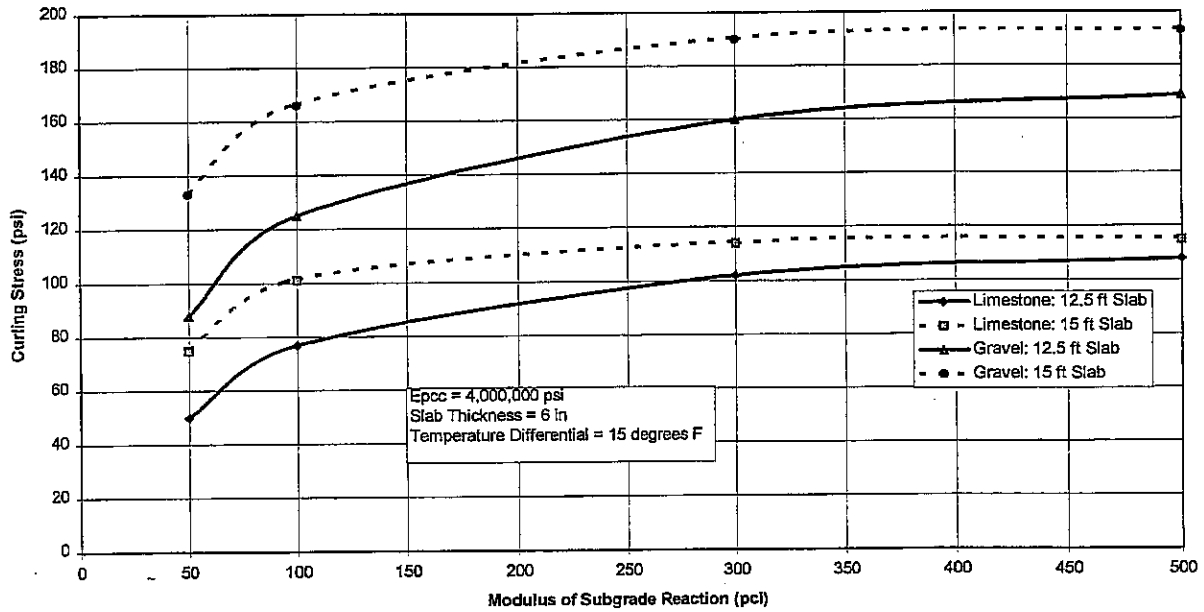


Figure 30. Comparison of curling stresses calculated for PCCs made from siliceous gravel and limestone.

Thin AC	Thick AC	PCC
2 to 5-in AC Surface	> 5-in AC Surface	5 to 8-in PCC
Granular Base	Granular Subbase (optional)	Granular Subbase (optional)
Granular Subbase	Subgrade(w/ or w/o Lime)	
Subgrade(w/ or w/o Lime)		

Figure 31. The three typical sections examined in this study.

Layout of Access Data Base

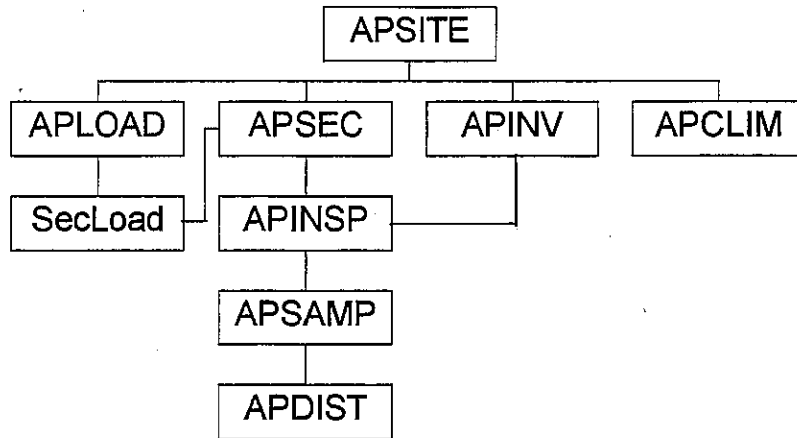


Figure 32. Layout of Access data base.

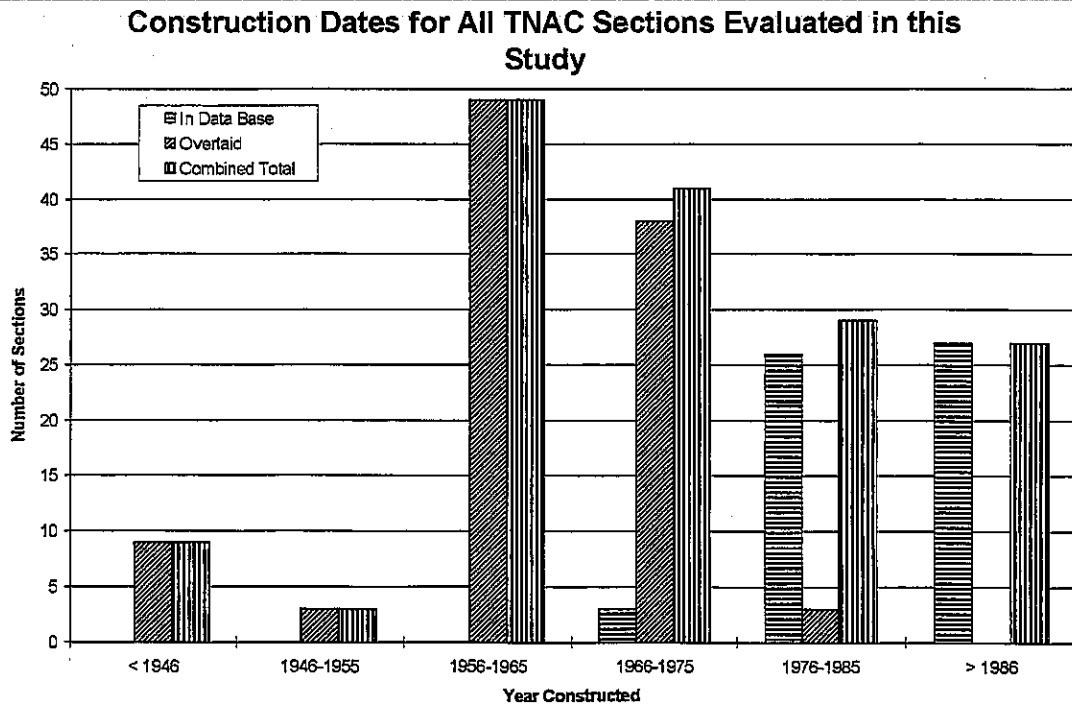


Figure 33. Distribution of construction dates for all TNAC sections evaluated.

Construction Dates for All TKAC Sections Evaluated in this Study

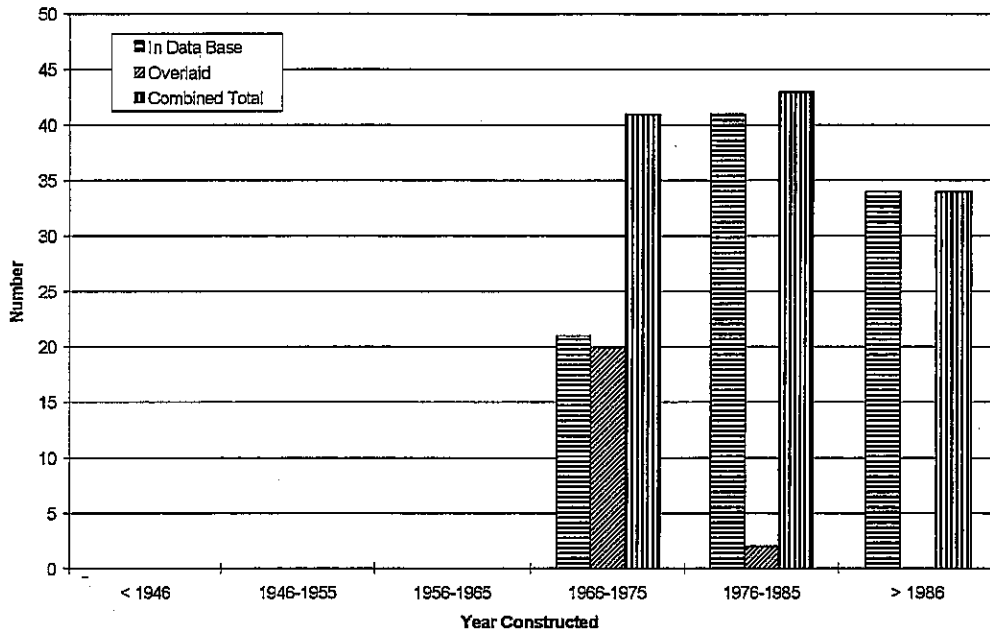


Figure 34. Distribution of construction dates for all TKAC sections evaluated.

Construction Dates for All PCC Sections Evaluated in this Study

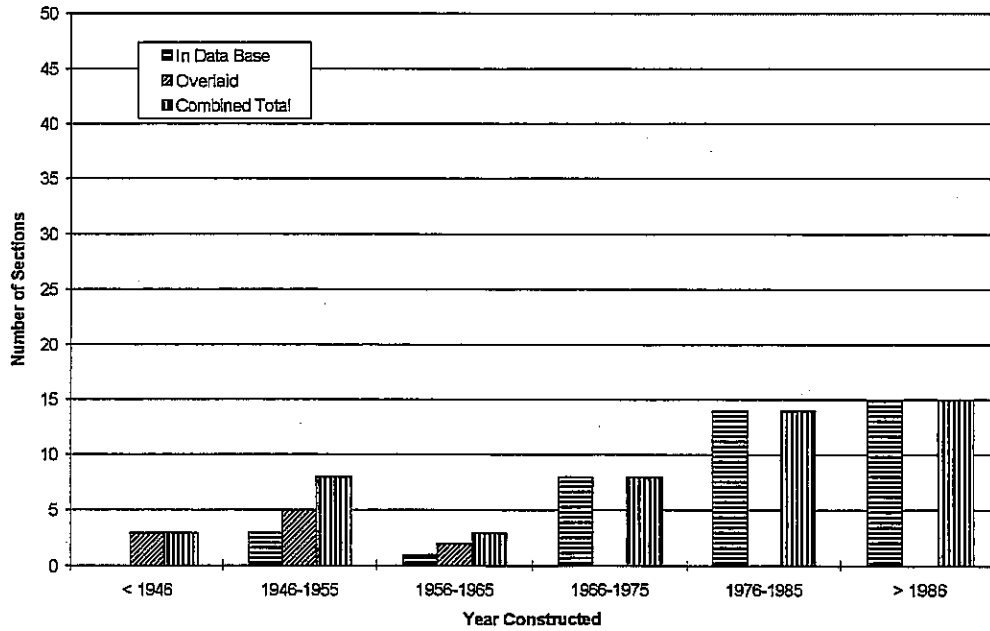


Figure 35. Distribution of construction dates for all PCC sections evaluated.

Construction Date of PCC Sample Units According to Slab Size

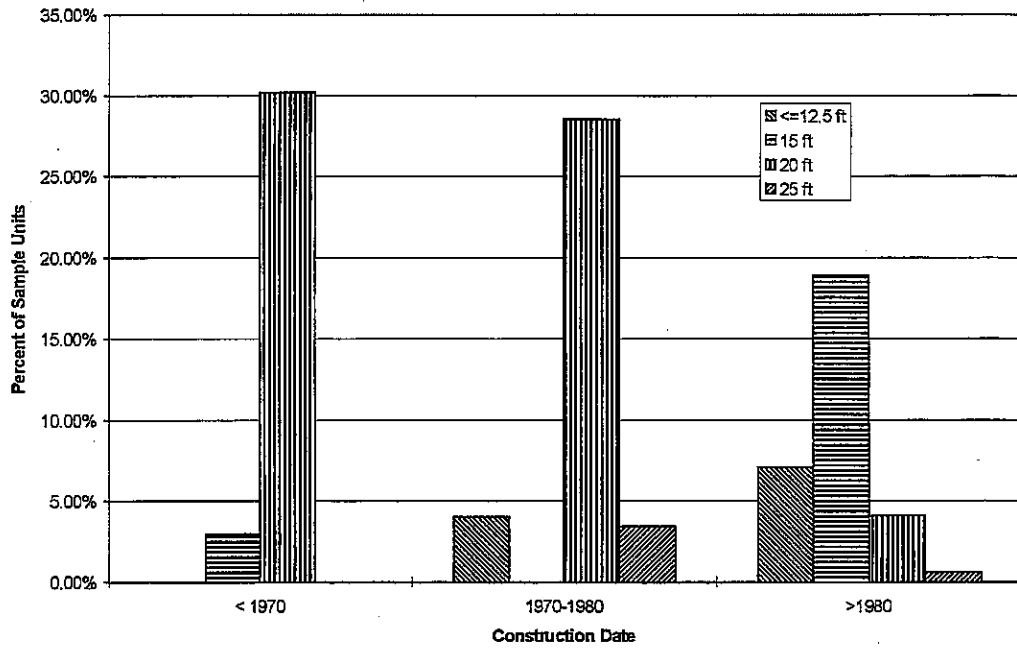


Figure 36. Construction date distribution for PCC sections in the data base according to slab size.

Age Distribution for all Sections Evaluated in the Study

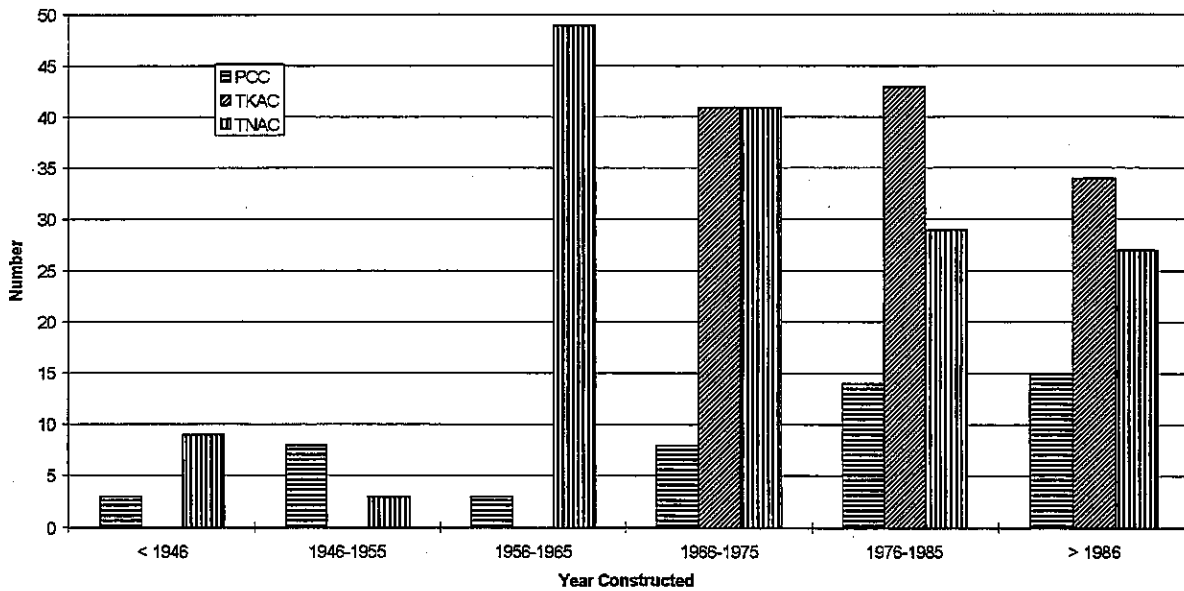


Figure 37. Distribution of construction dates for all TNAC, TKAC, and PCC sections evaluated.

Age Distribution of Sections in Data Base

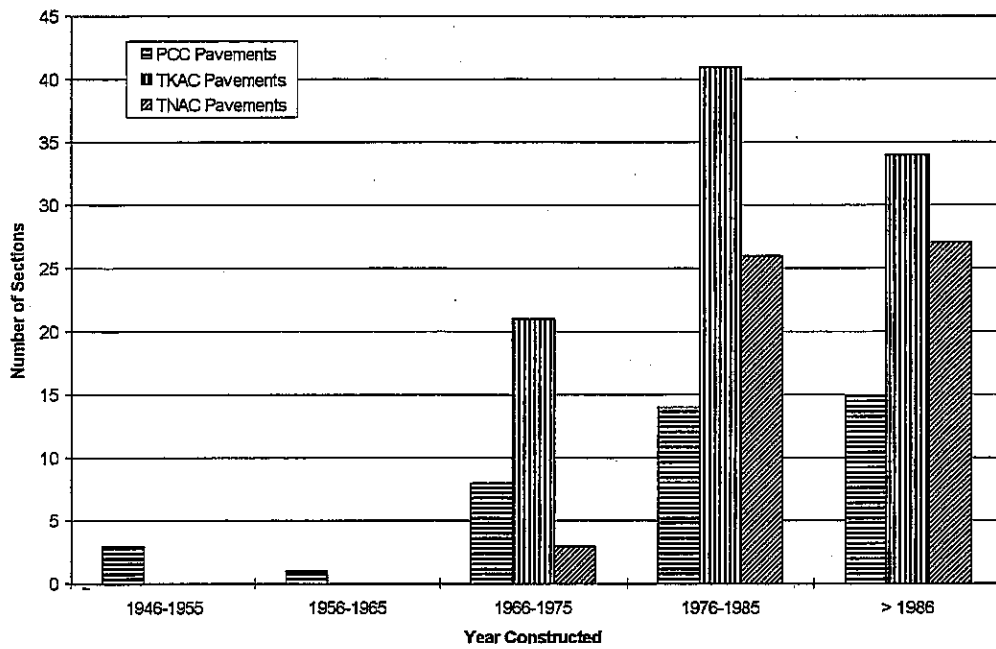


Figure 38. Distribution of construction dates for TNAC, TKAC, and PCC sections in data base.

TNAC: PCI vs Age Based On Sample Units (All Data)

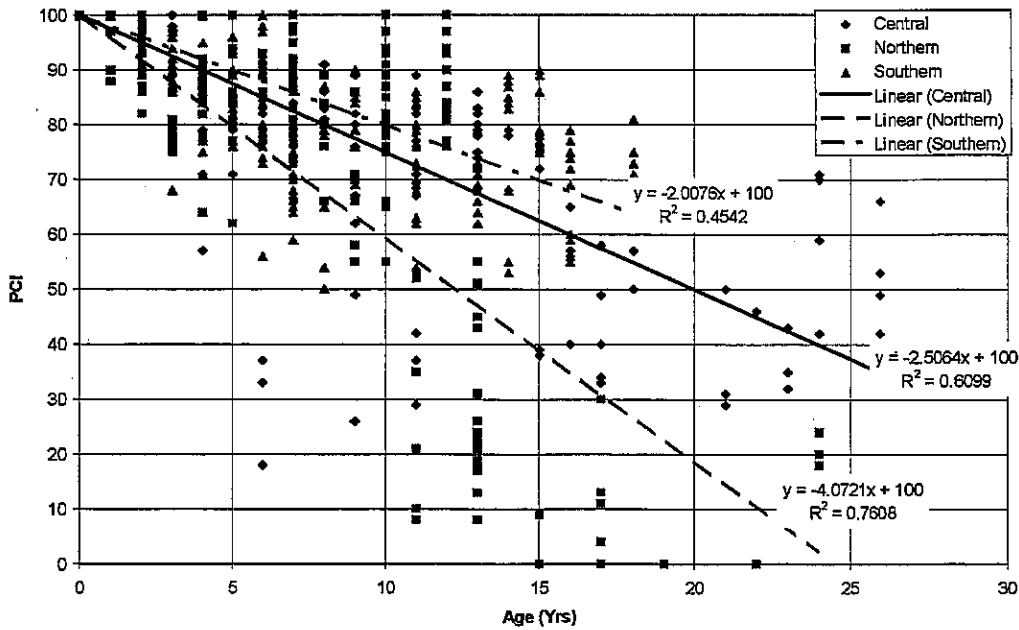


Figure 39. Sample unit PCI versus age for TNAC pavements.

TKAC: PCI vs Age Based On Sample Units (All Data)

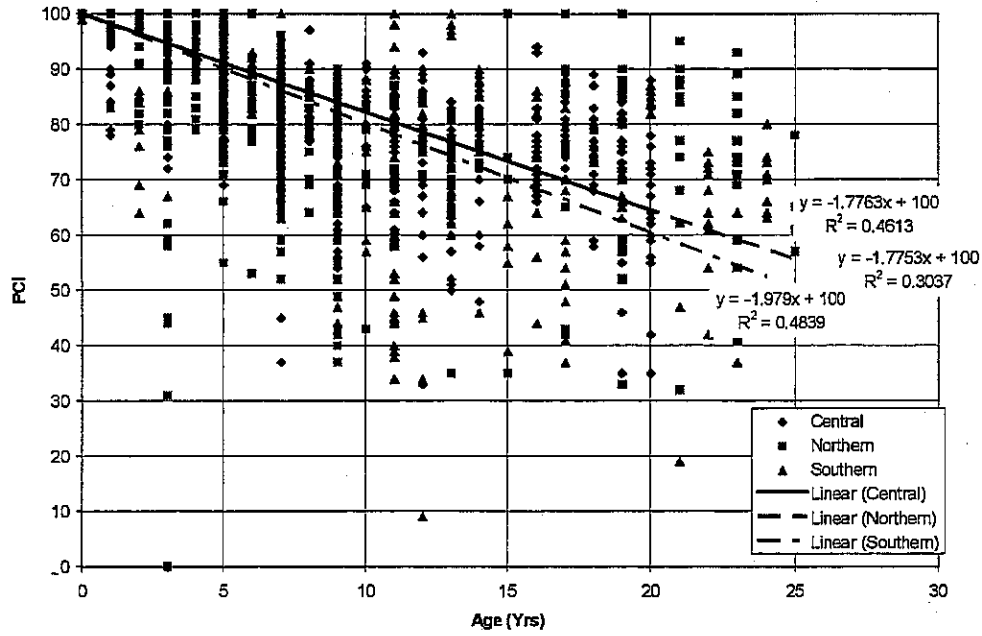


Figure 40. Sample unit PCI versus age for TKAC pavements.

PCC: PCI vs Age Based On Sample Units (All Data)

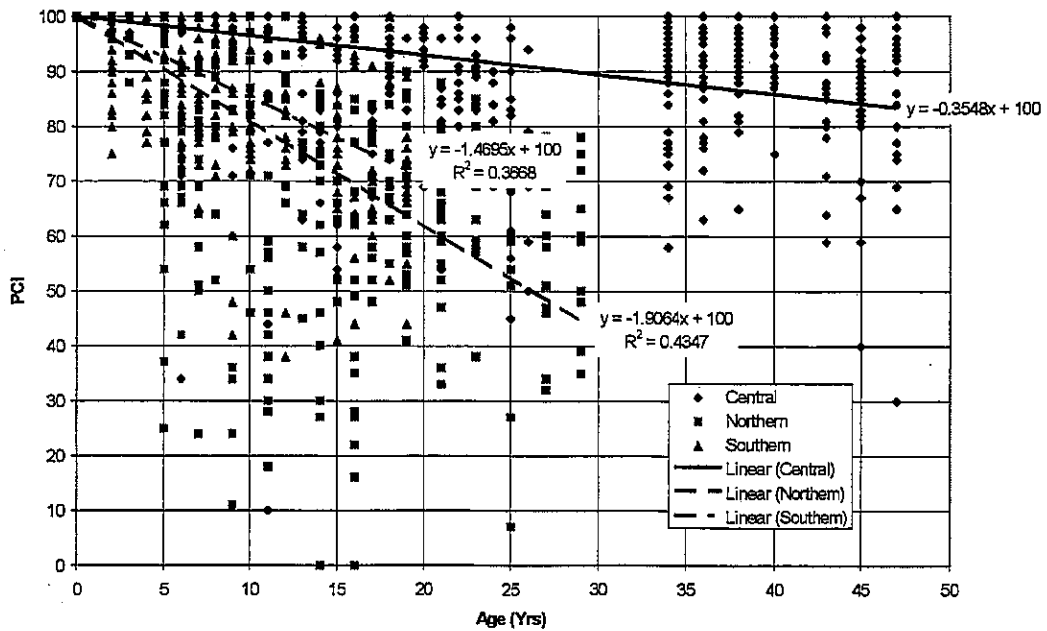


Figure 41. Sample unit PCI versus age for PCC pavement.

TNAC: PCI vs Age Based On Section Data

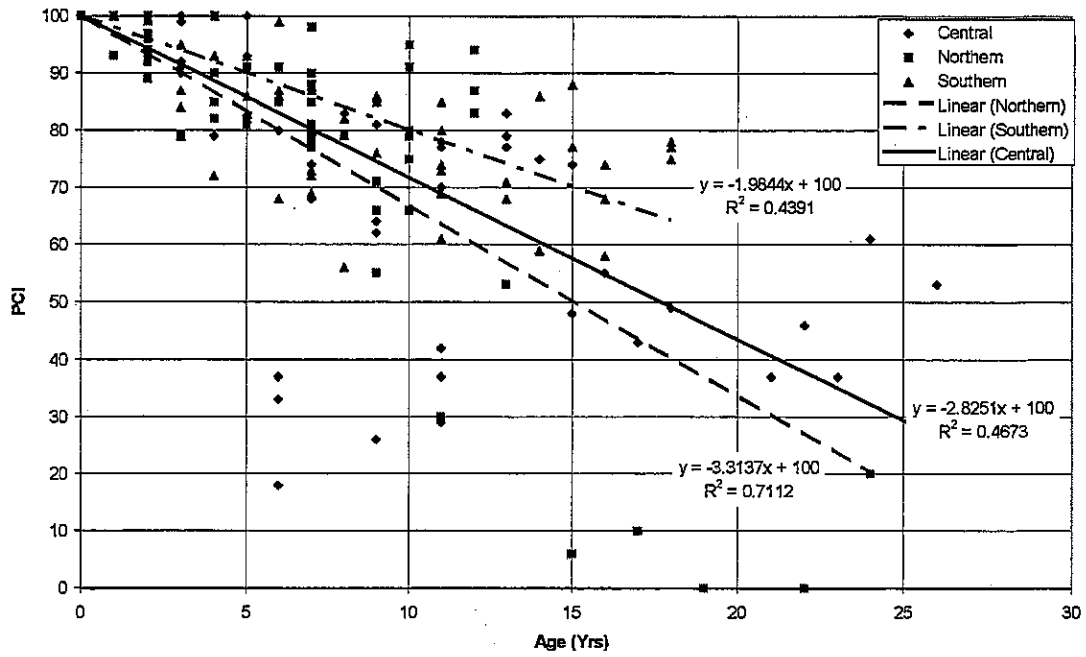


Figure 42. PCI versus age for TNAC sections.

TKAC: PCI vs Age Base On Section Data

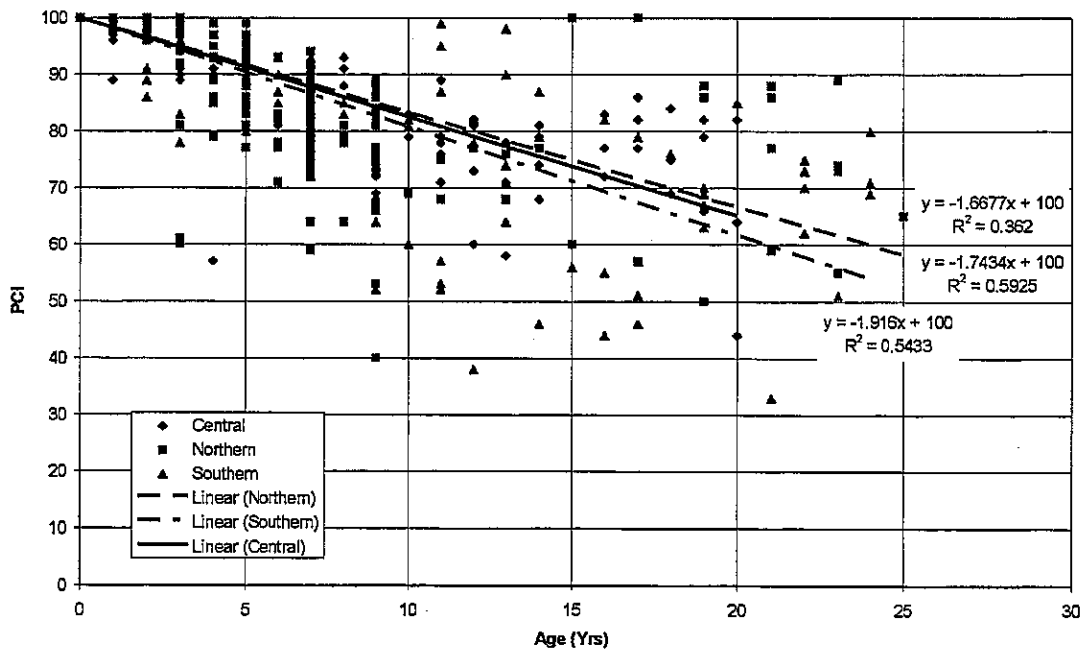


Figure 43. PCI versus age for TKAC sections.

PCC: PCI vs Age Based On Section Data

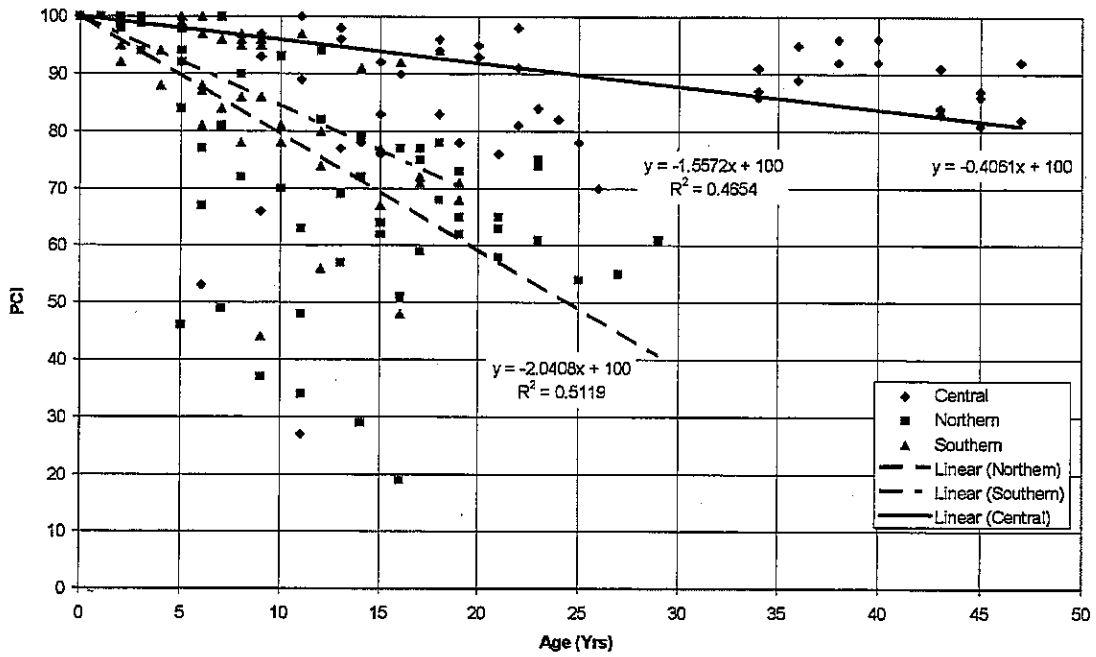


Figure 44. PCI versus age for PCC sections.

Average Sample Unit PCI vs Age for Different Slab Lengths

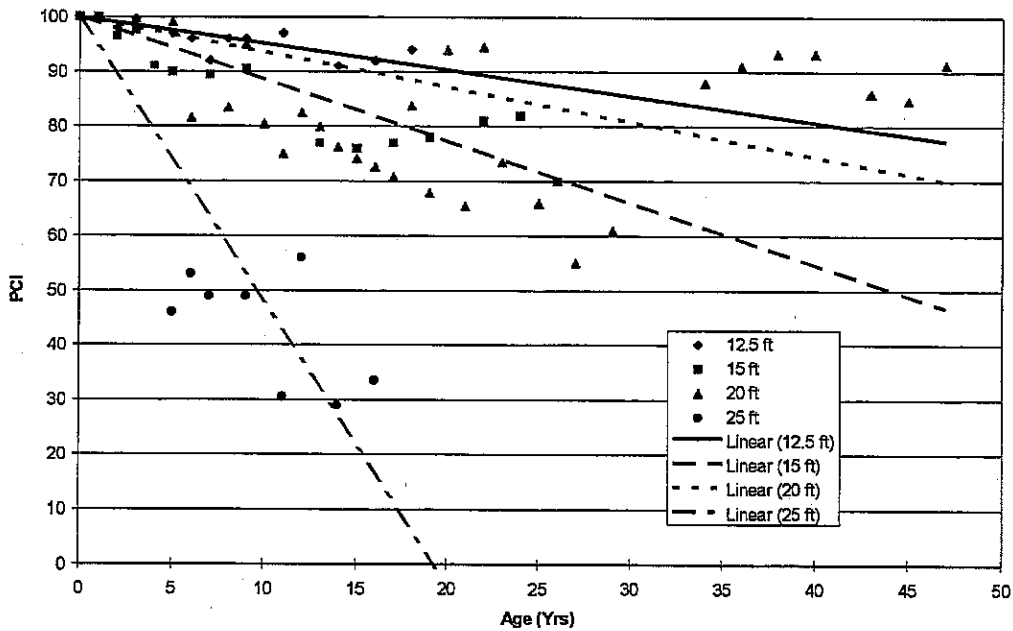


Figure 45. The effect of slab length on average sample unit PCI.

PCI versus Age for Pavement Sections at Effingham.

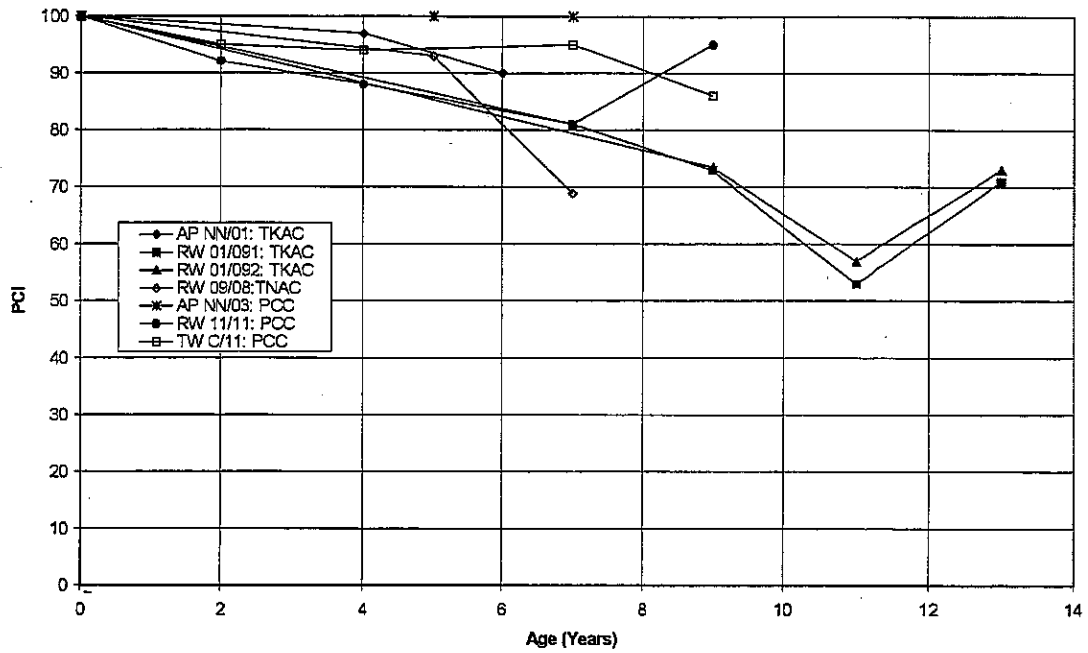


Figure 46. PCI versus age for sections at Effingham.

Deterioration Trends for Northern TKAC

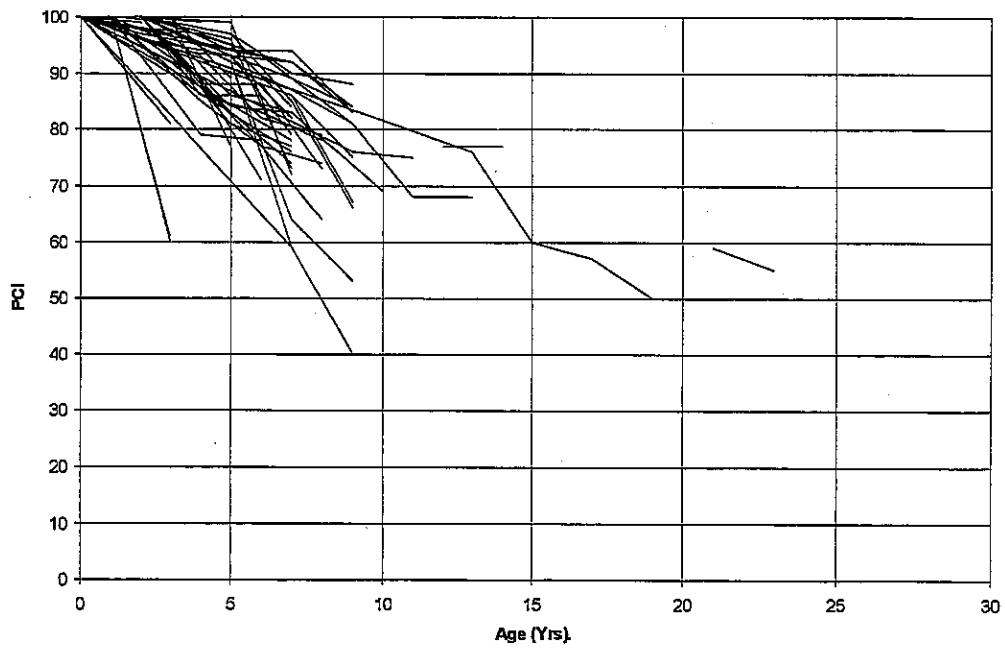


Figure 47. Section performance curves for TKAC in the northern climatic zone.

Pavement Performance Trends Established for TNAC

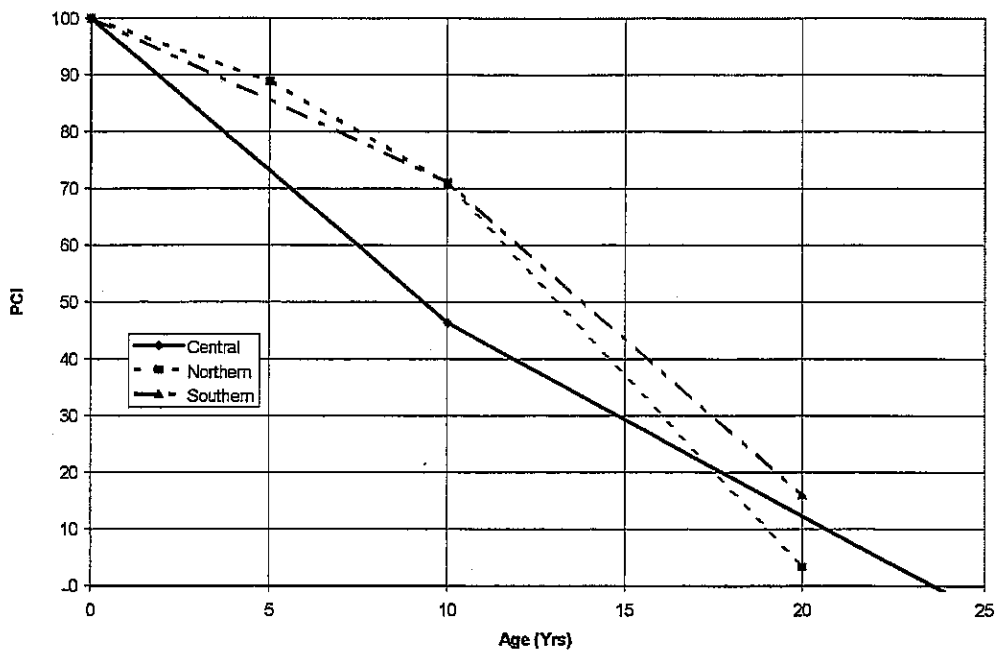


Figure 48. Pavement performance trends for TNAC.

Pavement Performance Trends Established for TKAC

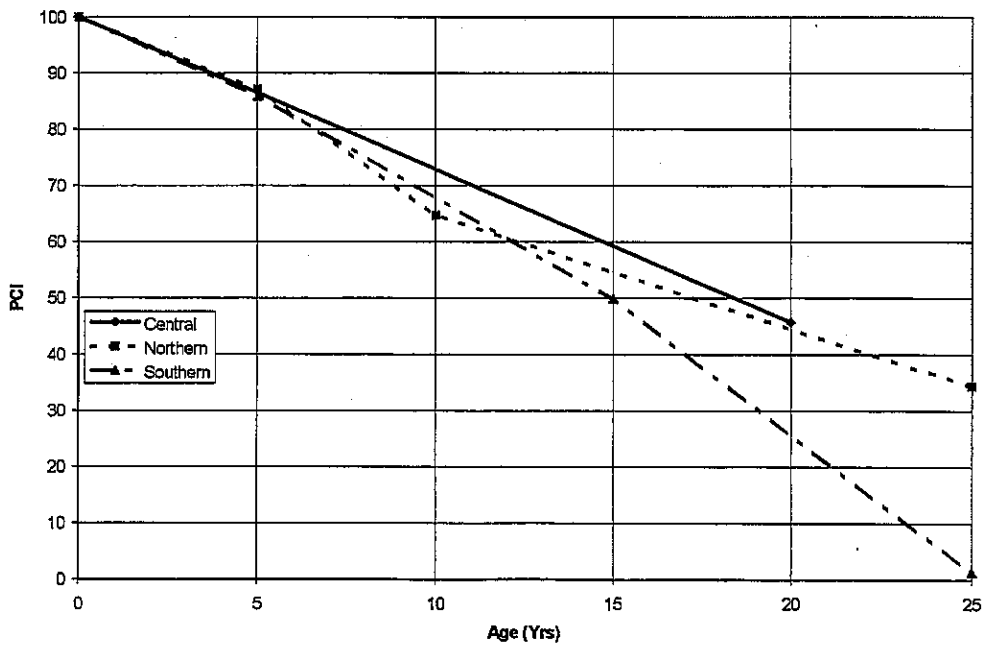


Figure 49. Pavement performance trends for TKAC.

Deterioration Trends for Northern TKAC

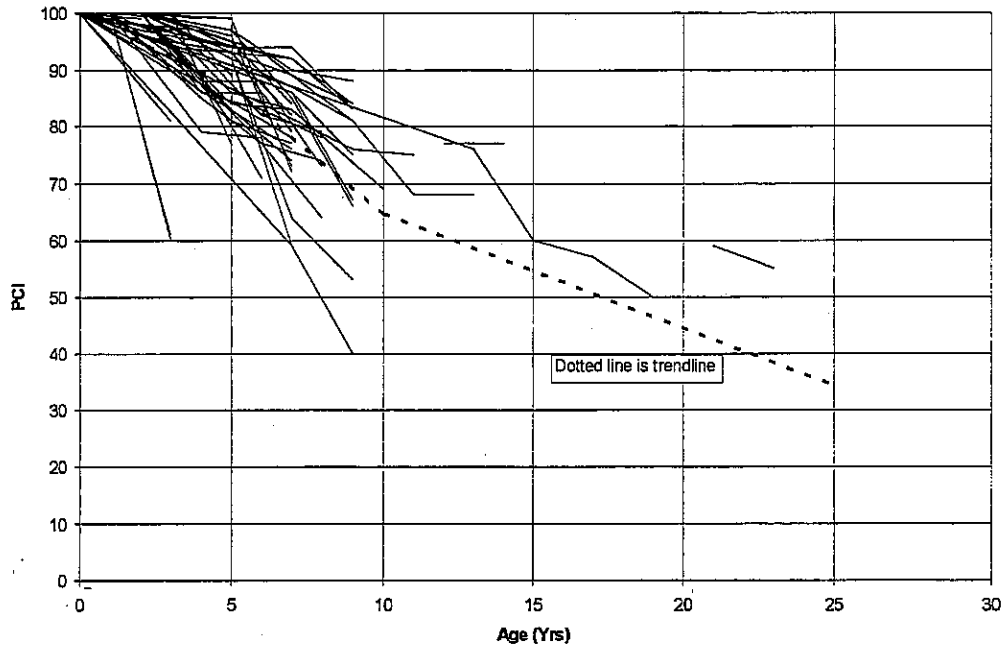


Figure 50. Section data and the pavement performance trends for TKAC in northern climatic zone.

L/I Versus Modulus of Subgrade Reaction for Different Slab Lengths

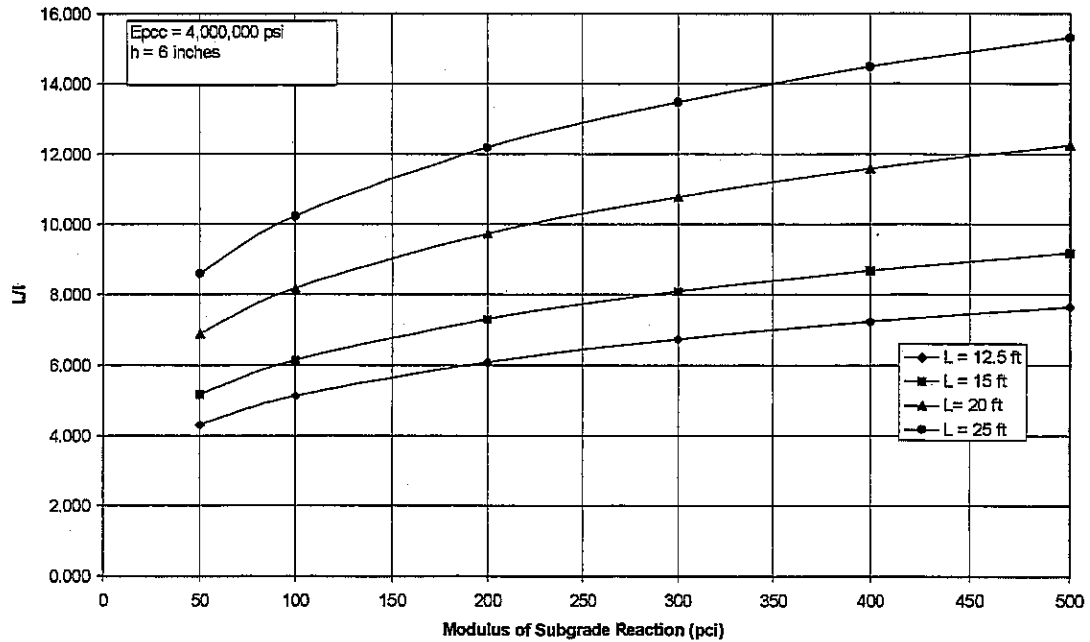


Figure 51. The relationship between L/I and the modulus of subgrade reaction for a 6-in thick PCC slab.

Deterioration Trends for PCC in Northern Climatic Zone

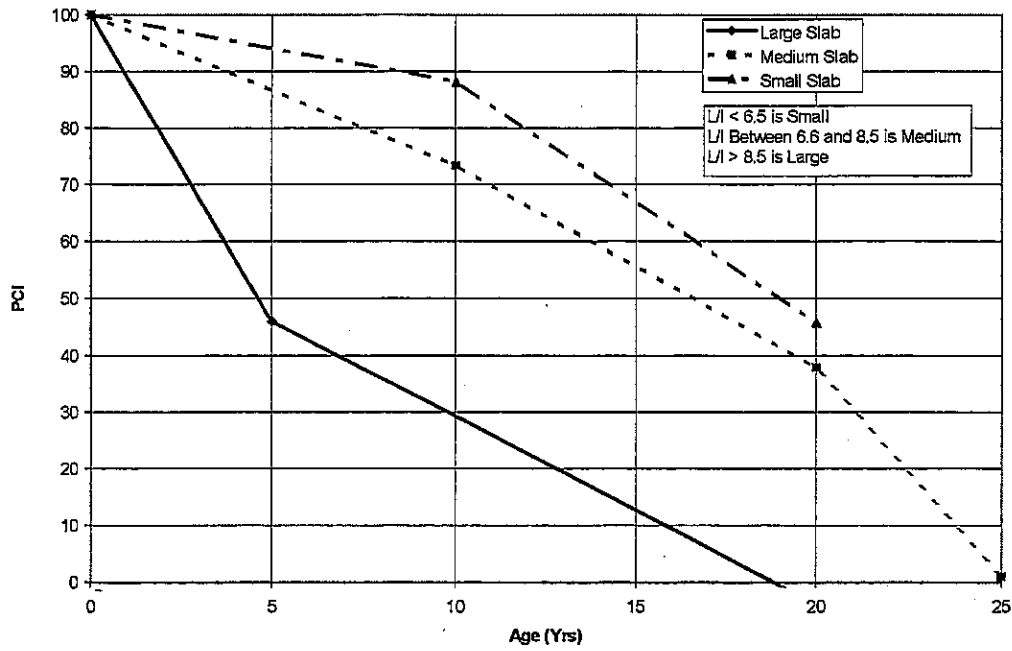


Figure 52. Deterioration trends for Division 1 slab size in the Northern Climatic Zone.

Deterioration Trends for PCC in Central Climatic Zone

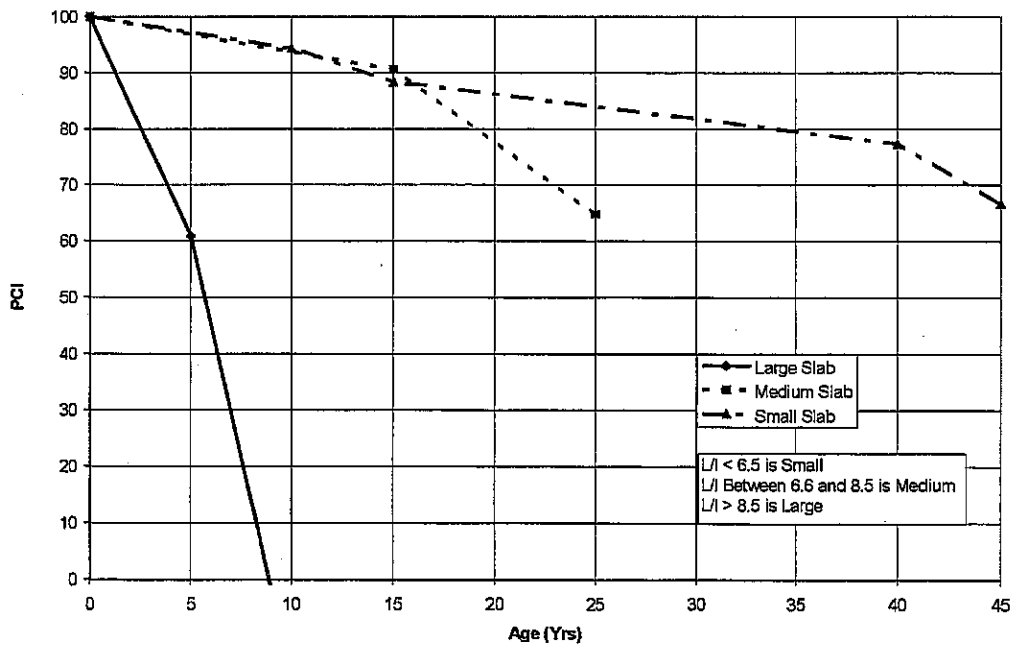


Figure 53. Deterioration trends for Division 1 slab size in the Central Climatic Zone.

Deterioration Trends for PCC in Southern Climatic Zone

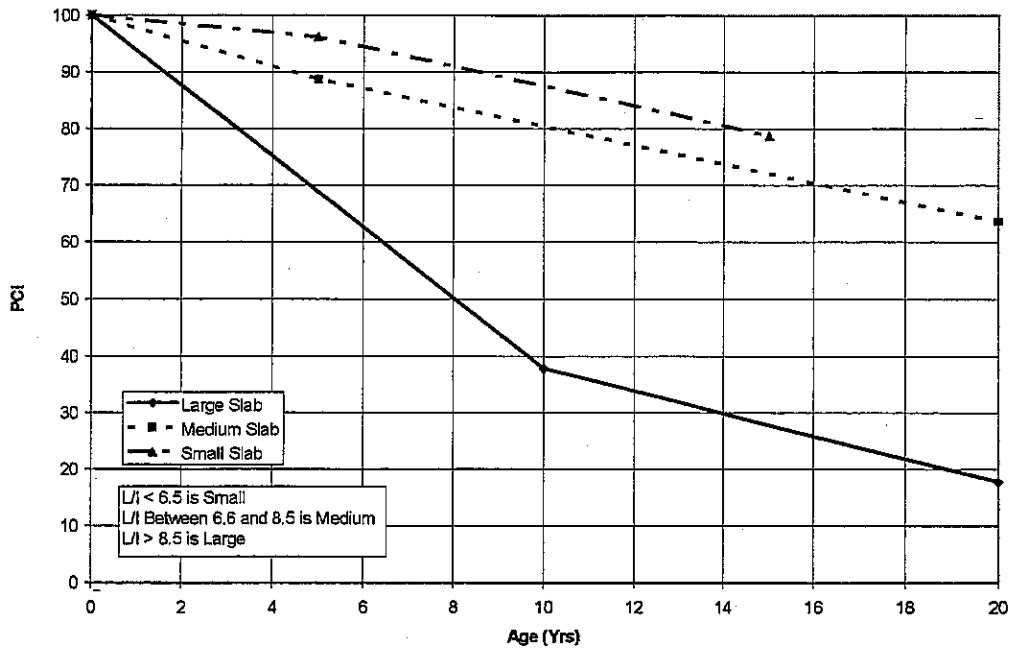


Figure 54. Deterioration trends for Division 1 slab size in the Southern Climatic Zone.

Division 2 Slab Deterioration Rate in the Northern Climatic Zone

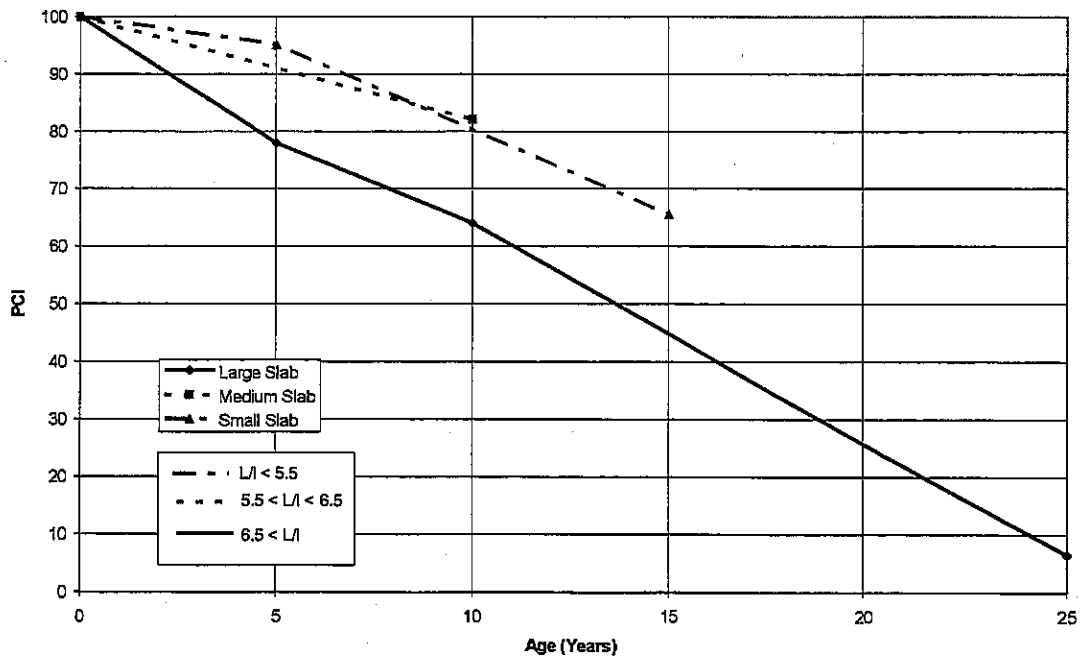


Figure 55. Deterioration trends for Division 2 slab size in the Northern Climatic Zone.

Division 2 Slab Deterioration Rate in the Central Climatic Zone

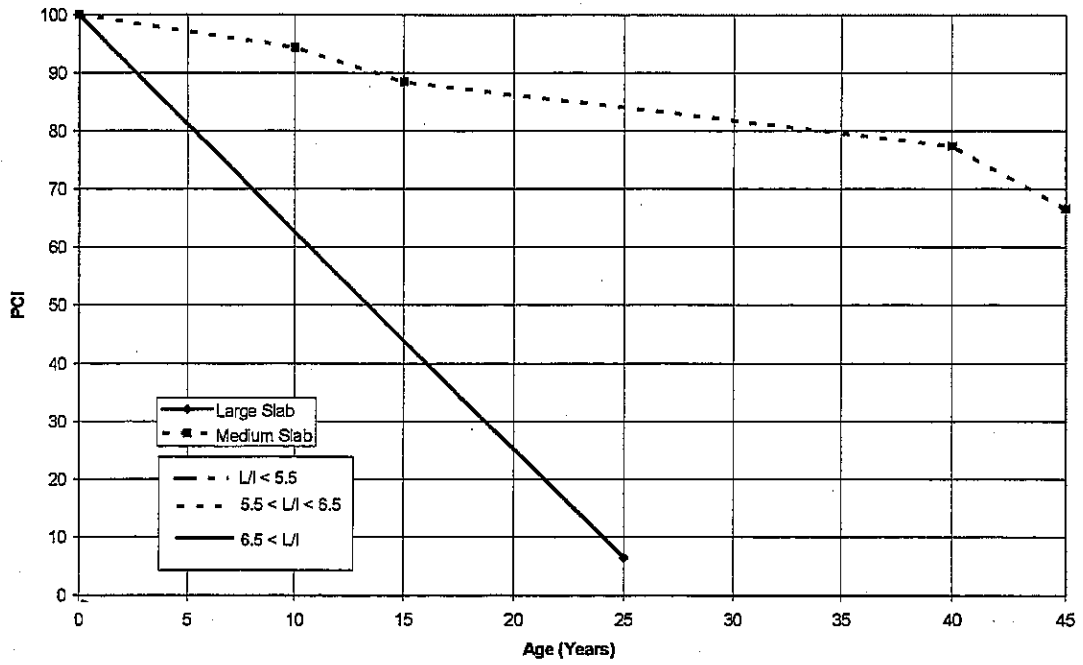


Figure 56. Deterioration trends for Division 2 slab size in the Central Climatic Zone.

Division 2 Slab Deterioration Rate in the Southern Climatic Zone

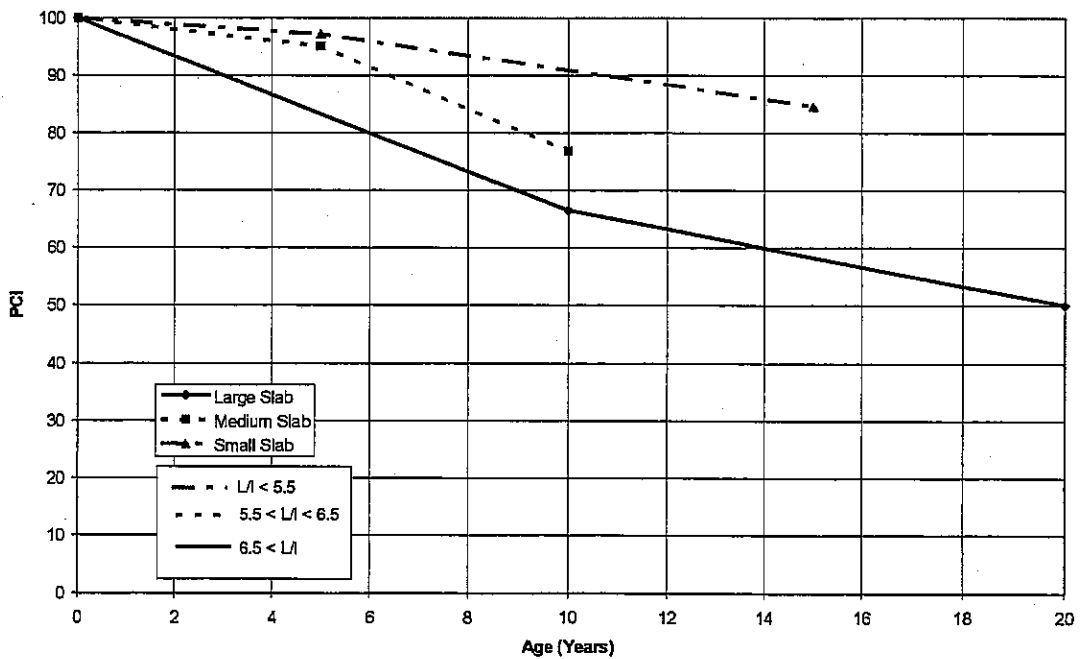


Figure 57. Deterioration trends for Division 2 slab size in the Southern Climatic Zone.

Northern TNAC: Percent Sample Units Affected by Distress

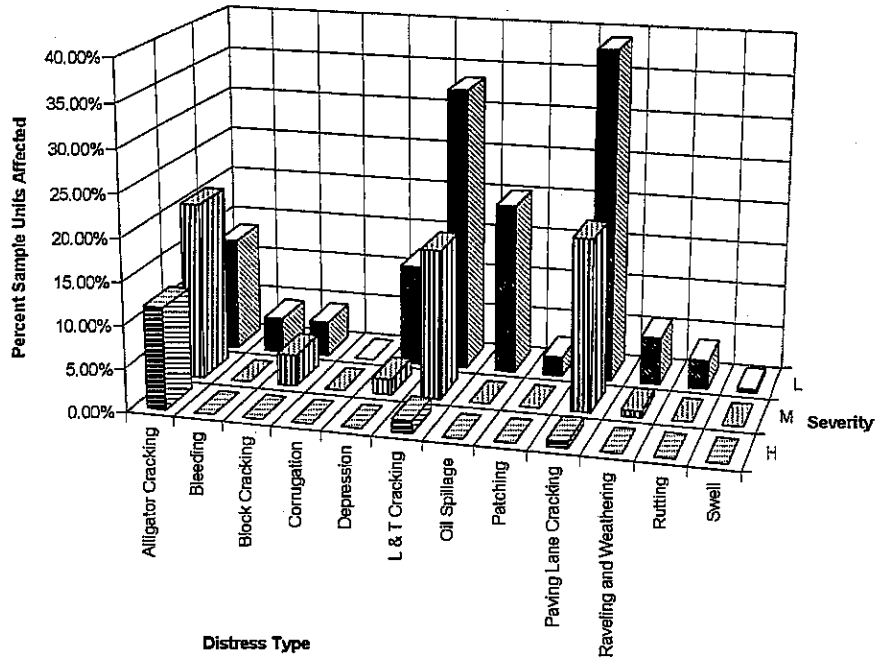


Figure 58. Percent TNAC sample units affected by distress in Northern Climatic Zone.

Central TNAC: Percent Sample Units Affected by Distress

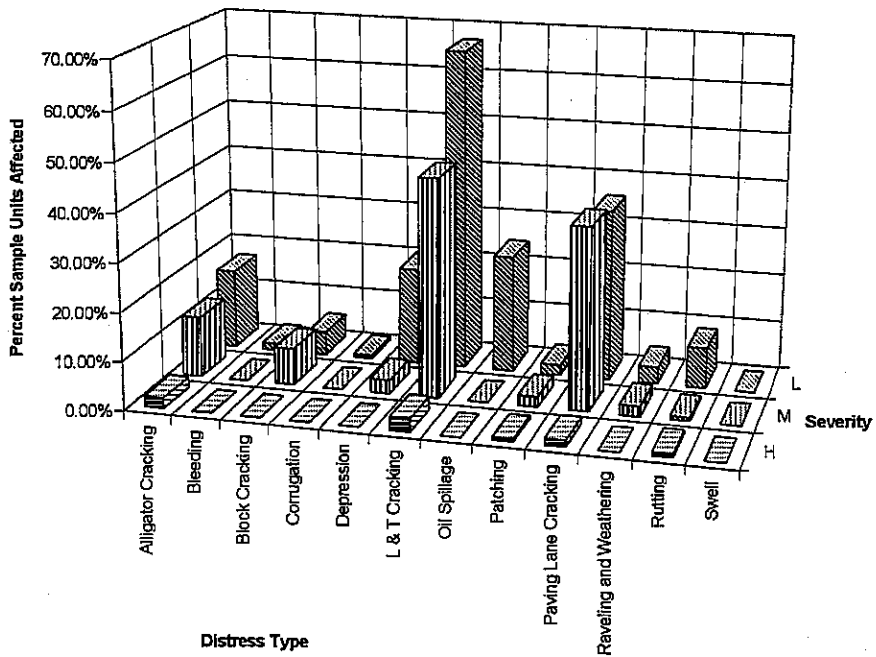


Figure 59. Percent TNAC sample units affected by distress in Central Climatic Zone.

Southern TNAC: Percent Sample Units Affected by Distress

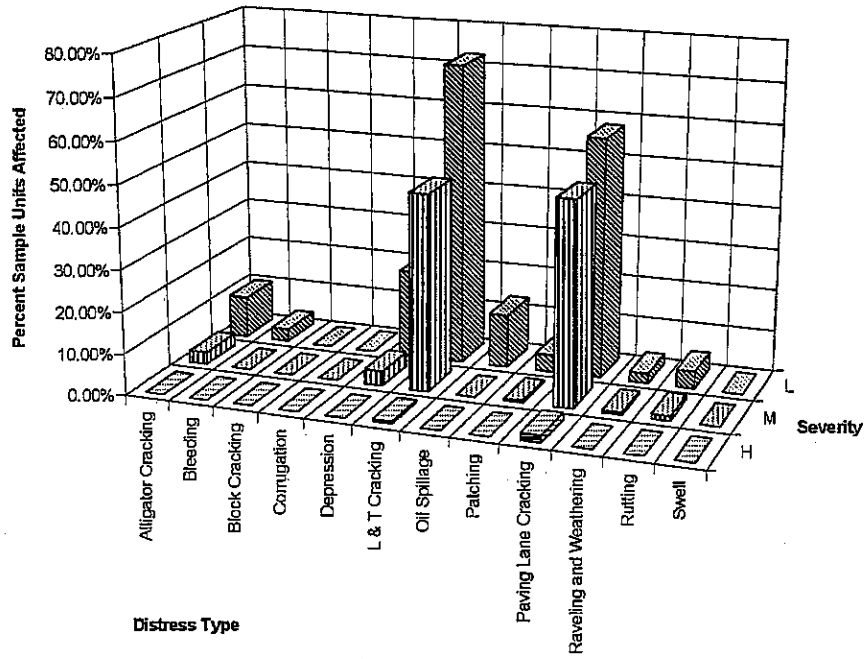


Figure 60. Percent TNAC sample units affected by distress in Southern Climatic Zone.

Northern TKAC: Percent Sample Units Affected by Distress

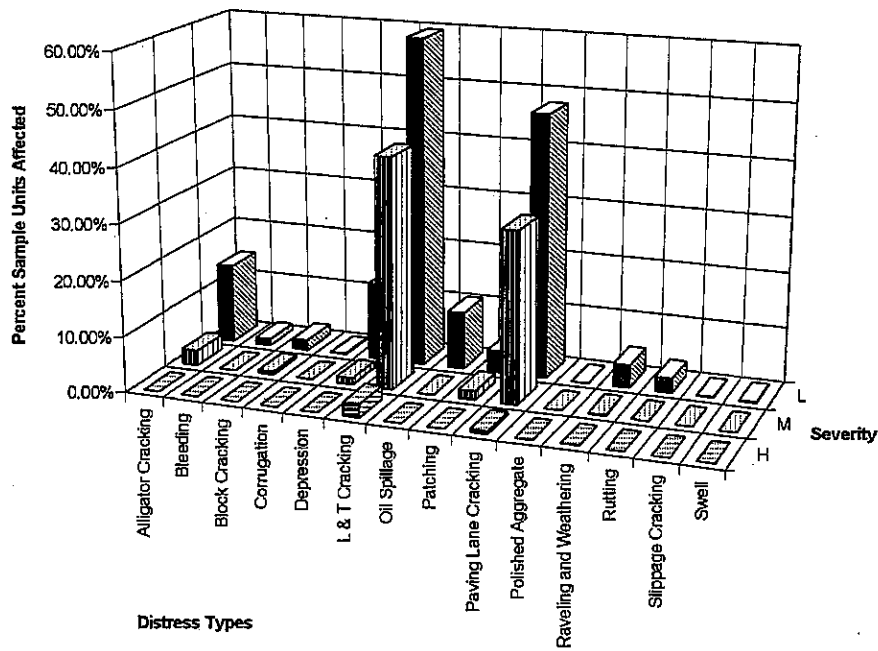


Figure 61. Percent TKAC sample units affected by distress in Northern Climatic Zone.

Central TKAC: Percent Sample Units Affected by Distress

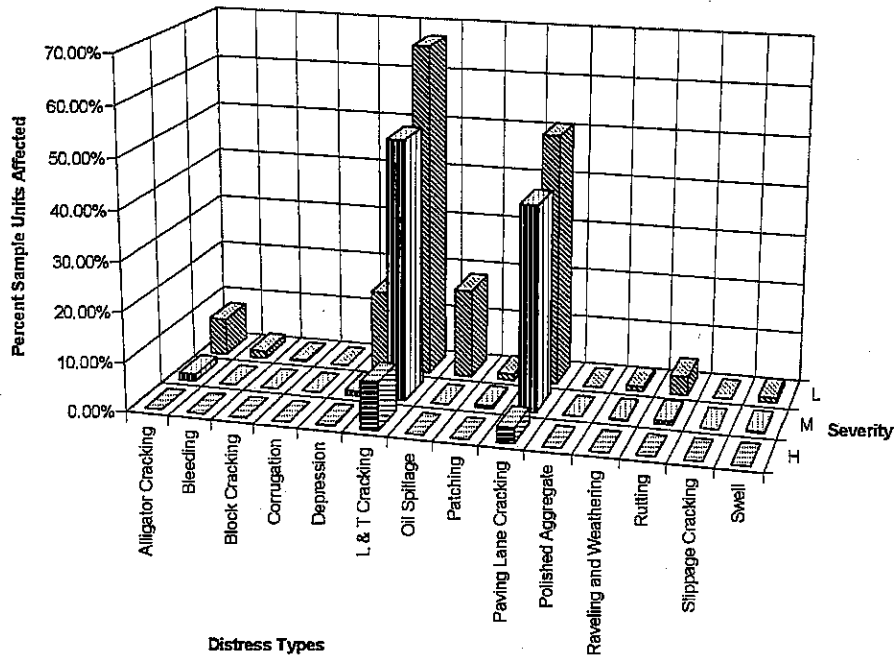


Figure 62. Percent TKAC sample units affected by distress in Central Climatic Zone.

Southern TKAC: Percent Sample Units Affected by Distress

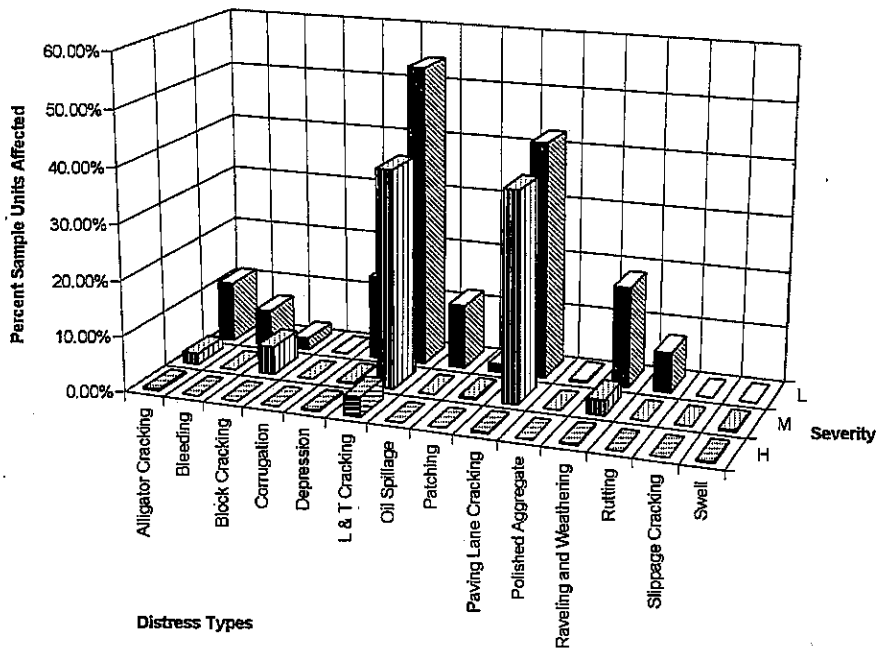


Figure 63. Percent TKAC sample units affected by distress in Southern Climatic Zone.

Alligator Cracking in TNAC Sample Units

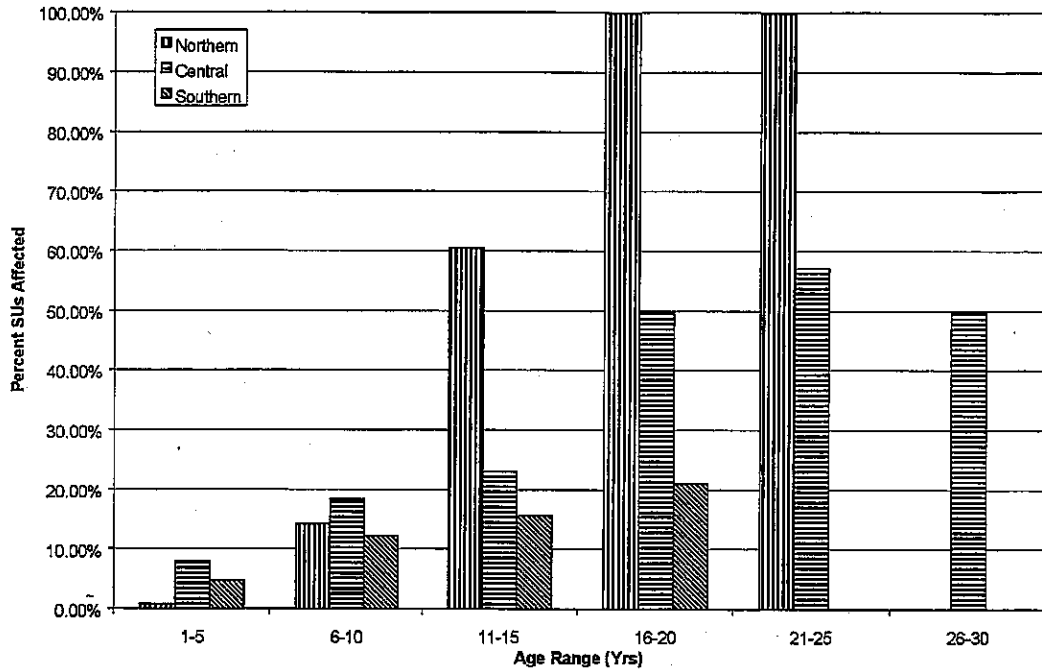


Figure 64. Percent TNAC sample units affected by alligator cracking.

Alligator Cracking in TKAC Sample Units

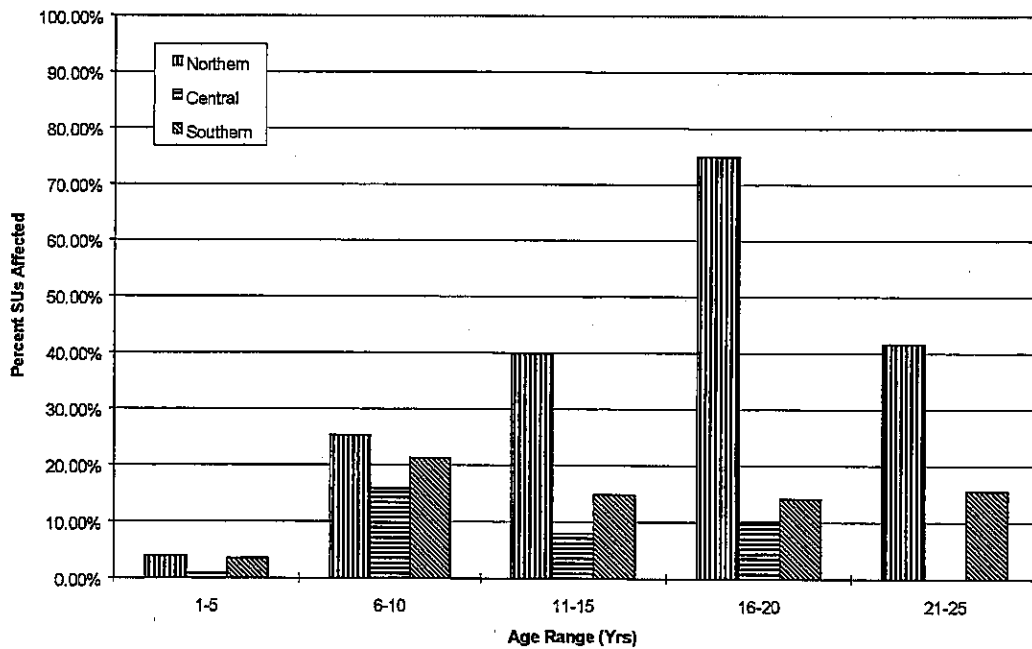


Figure 65. Percent TKAC sample units affected by alligator cracking.

Block Cracking in TNAC Sample Units

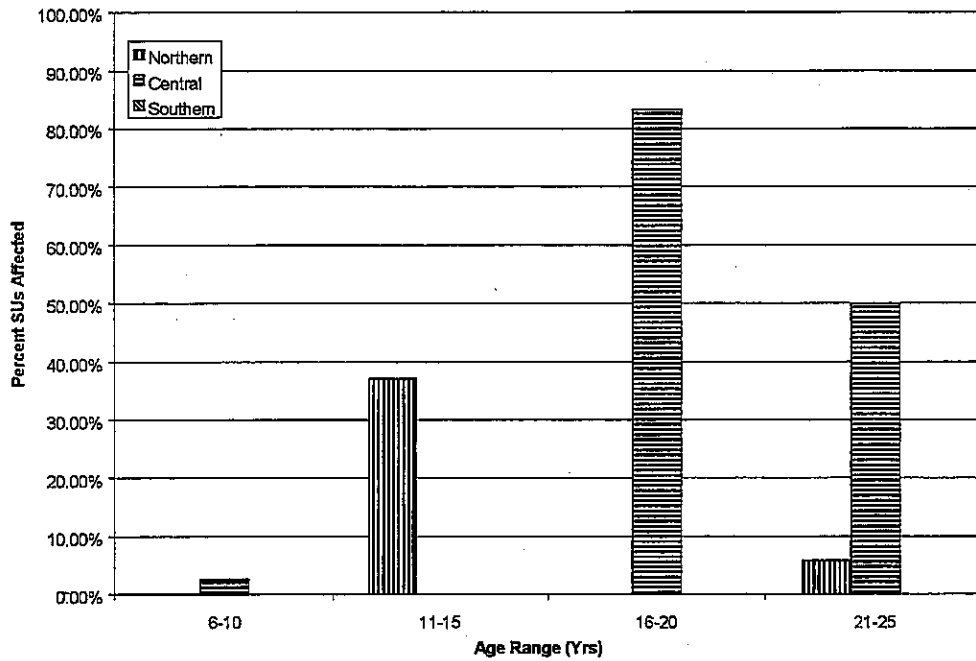


Figure 66. Percent TNAC sample units affected by block cracking.

Block Cracking in TKAC Sample Units

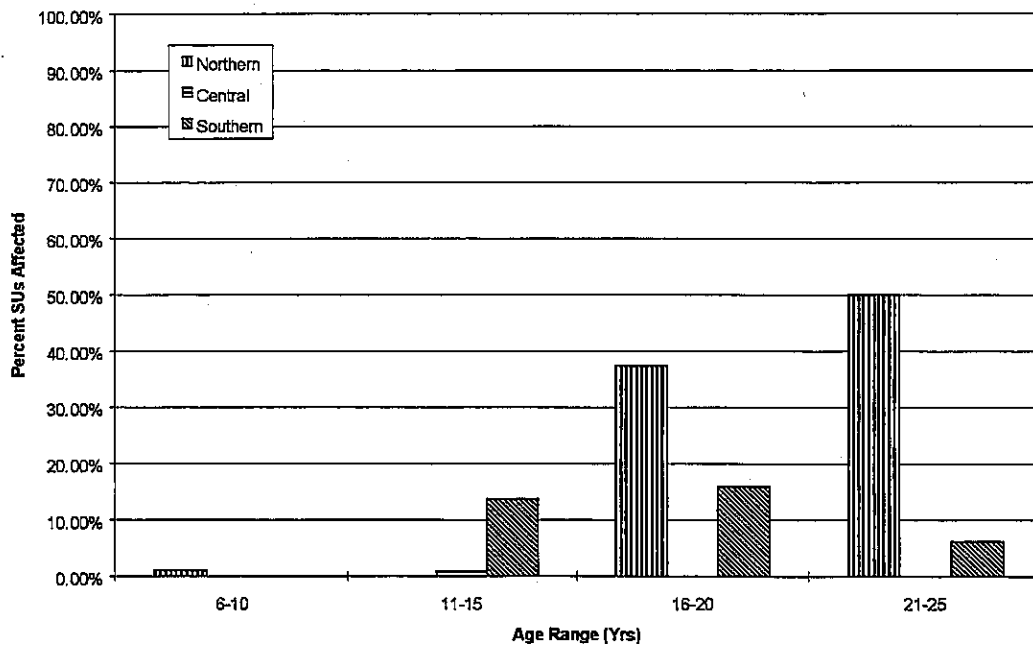


Figure 67. Percent TKAC sample units affected by block cracking.

All Regions: Percent of Sample Unit Area Affected by Alligator Cracking

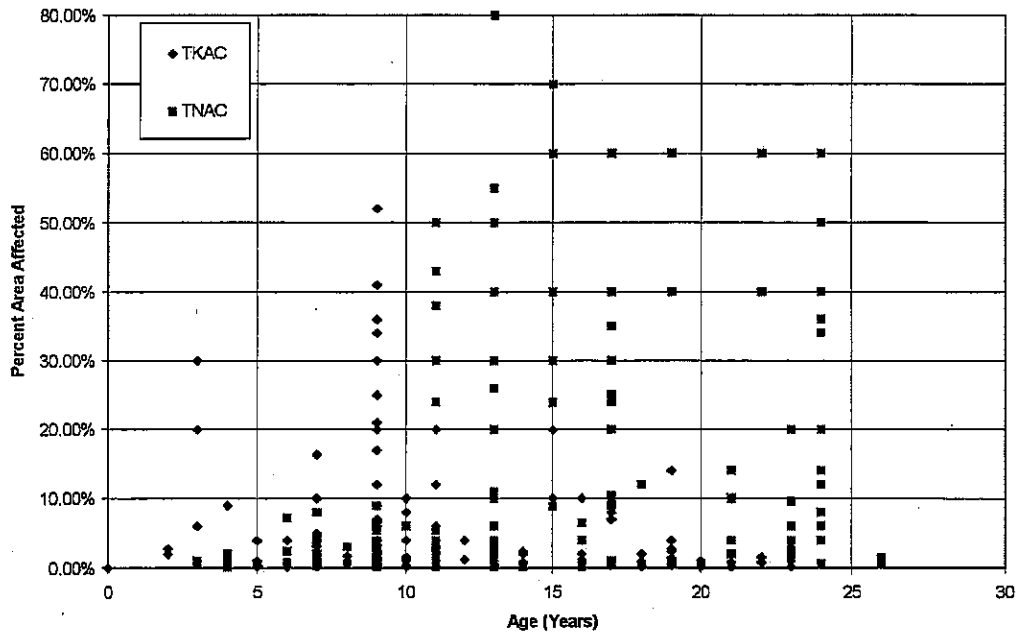


Figure 68. Percent of sample unit area affected by alligator cracking in all regions.

Depressions in TNAC Sample Units

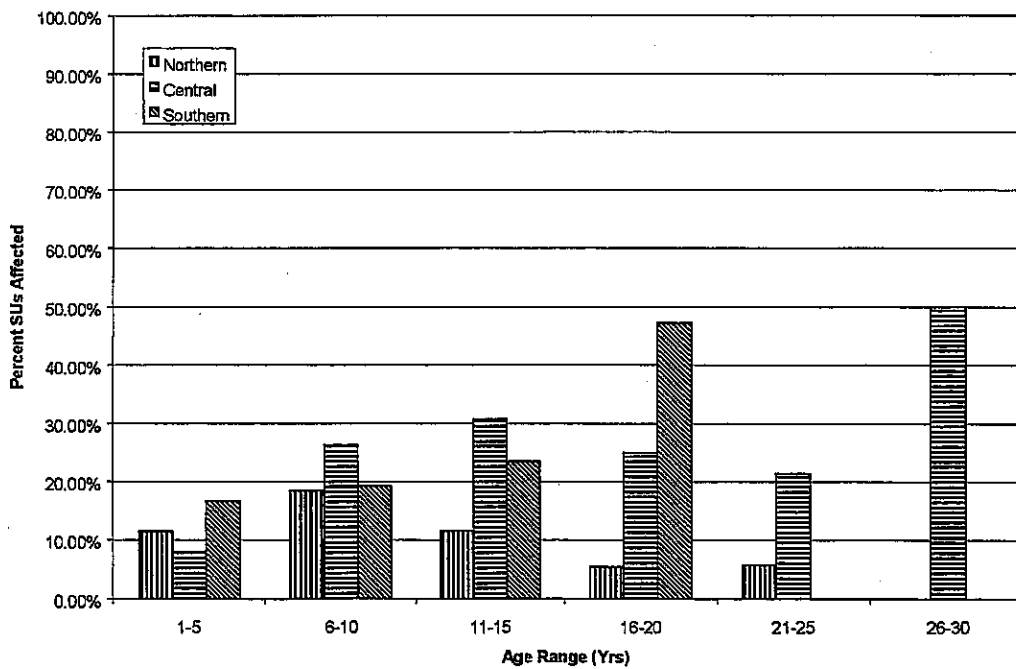


Figure 69. Percent TNAC sample units affected by depressions.

Depressions in TKAC Sample Units

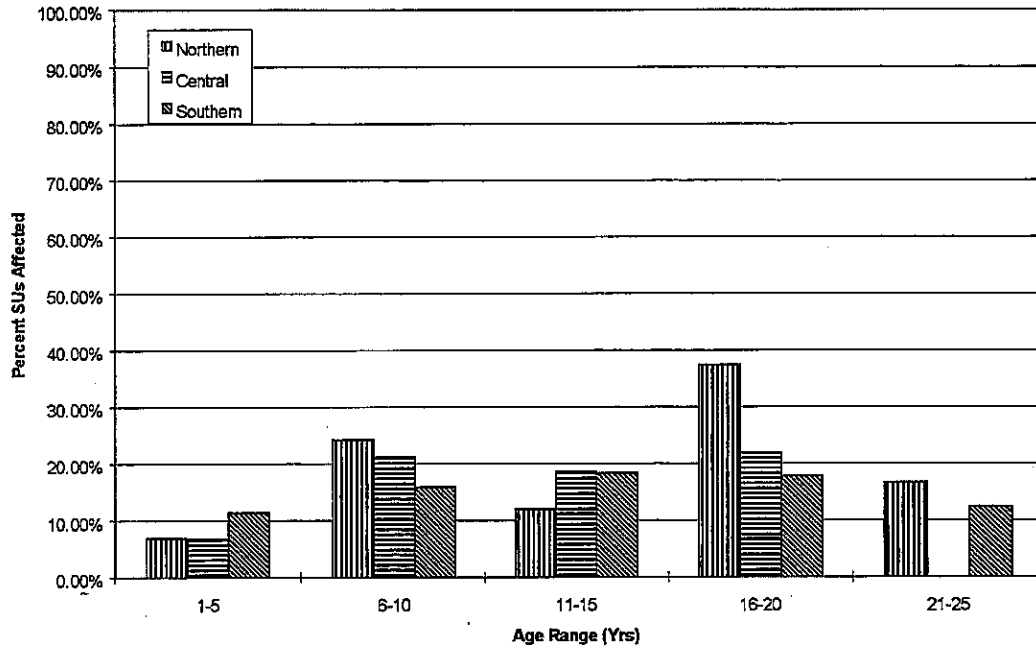


Figure 70. Percent TKAC sample units affected by depressions.

L & T Cracking in TNAC Sample Units

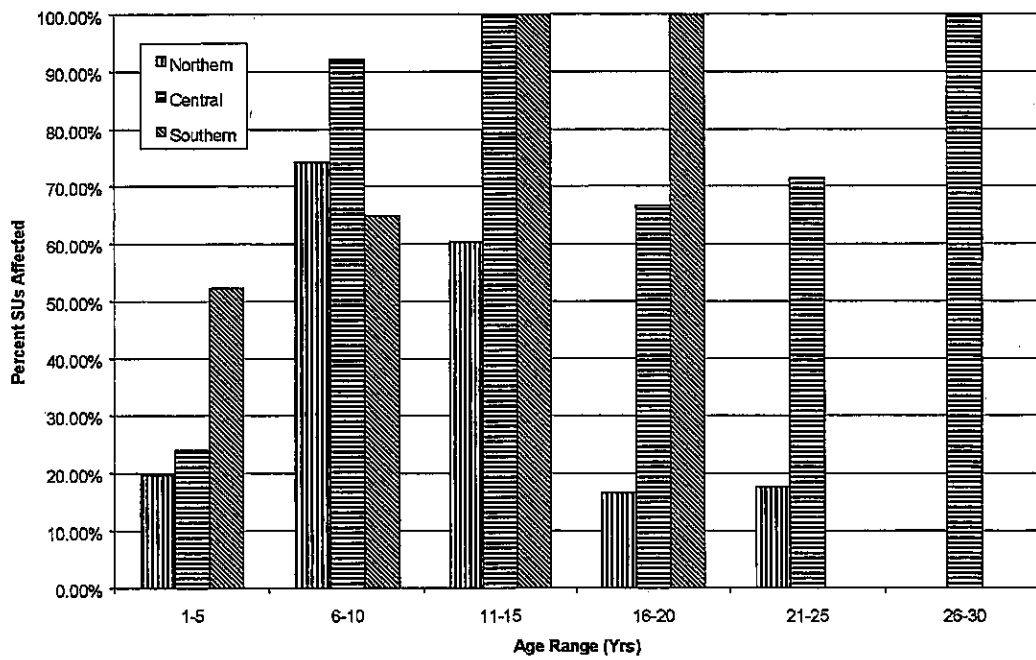


Figure 71. Percent TNAC sample units affected by L & T cracking.

L & T Cracking in TKAC Sample Units

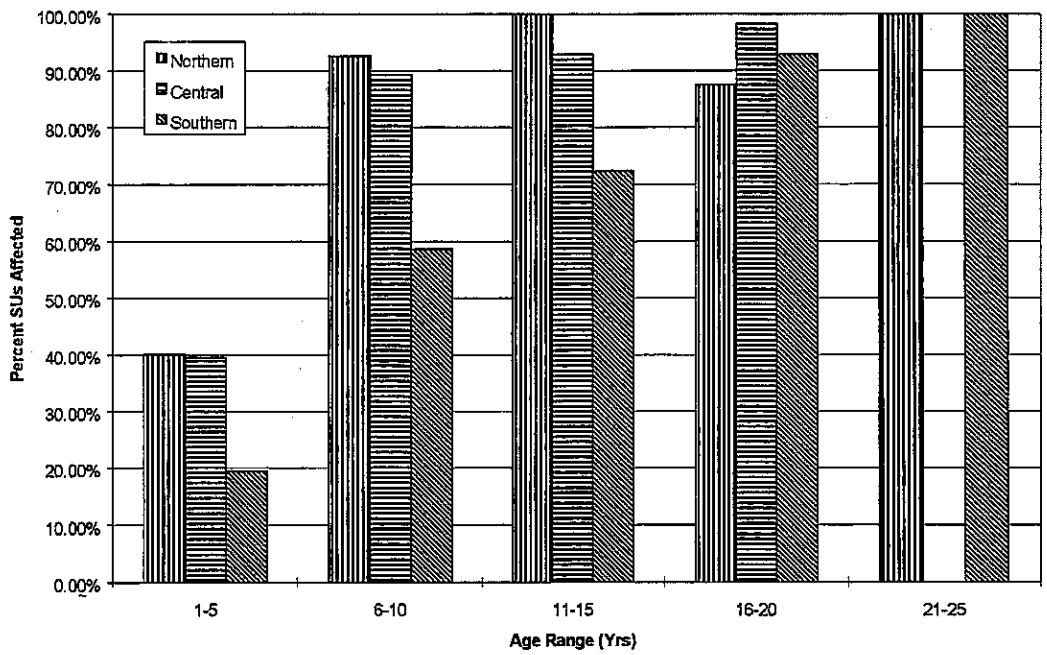


Figure 72. Percent TKAC sample units affected by L & T cracking.

L & T Cracking Distress Density vs. Age - All Severities

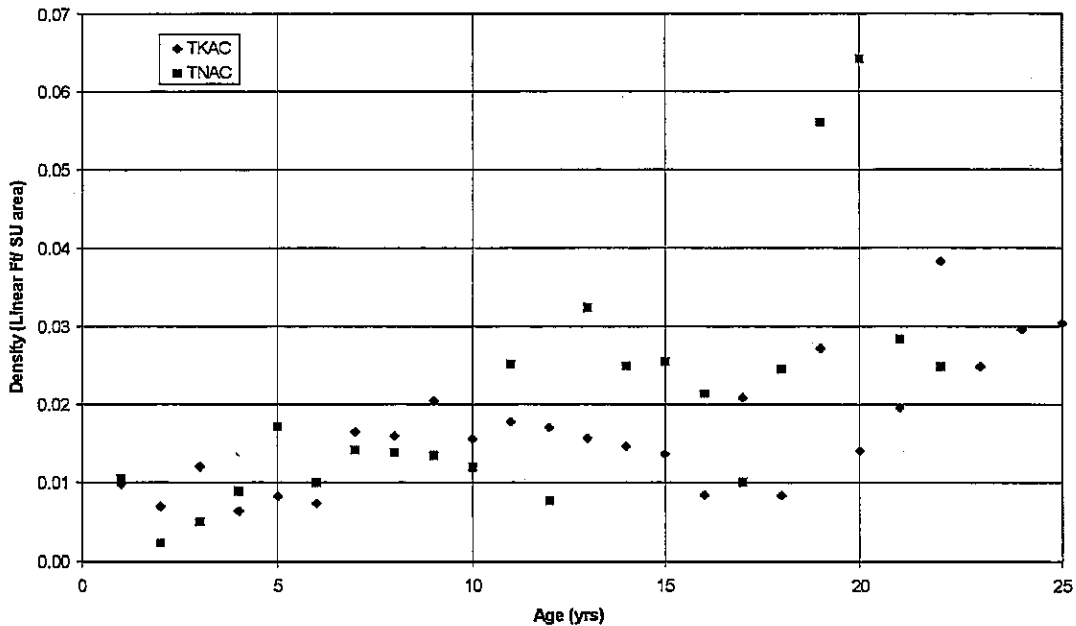


Figure 73. Average density of L & T cracking.

Northern: TNAC L & T Cracking Distress Density vs Age

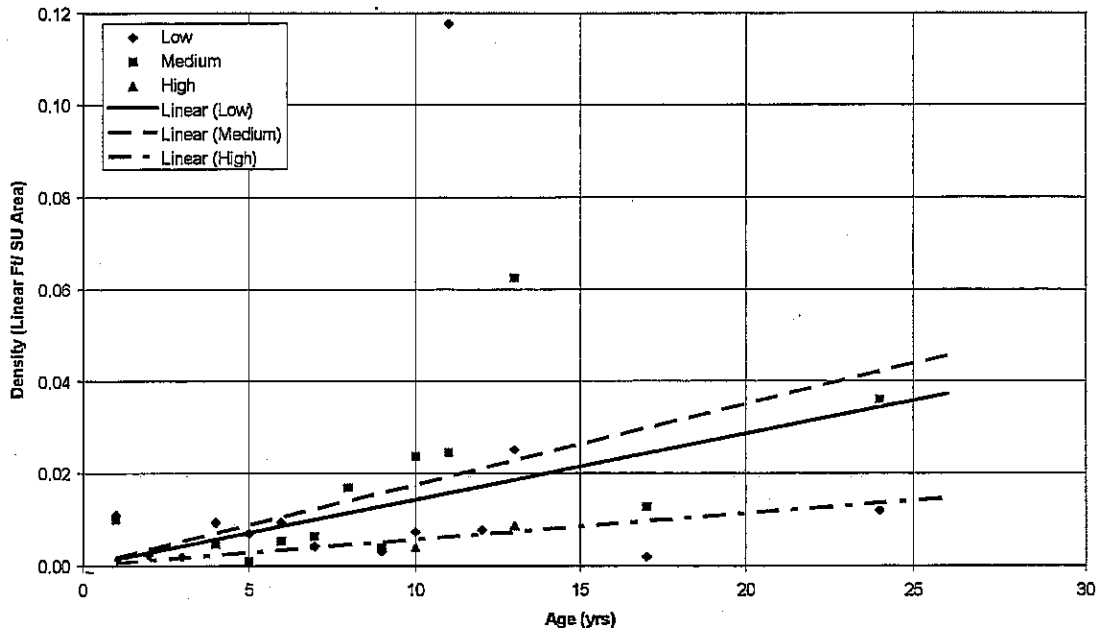


Figure 74. L & T cracking density for TNAC in the Northern Climatic Zone.

Northern: TKAC L & T Cracking Distress Density vs Age

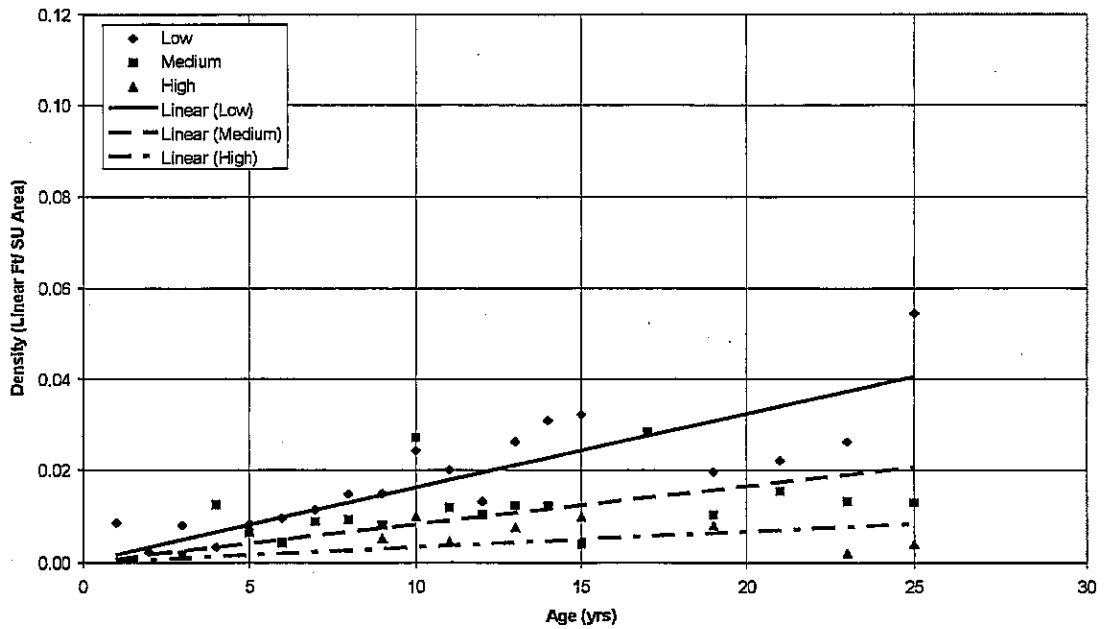


Figure 75. L & T cracking density for TKAC in the Northern Climatic Zone.

Oil Spillage in TNAC Sample Units

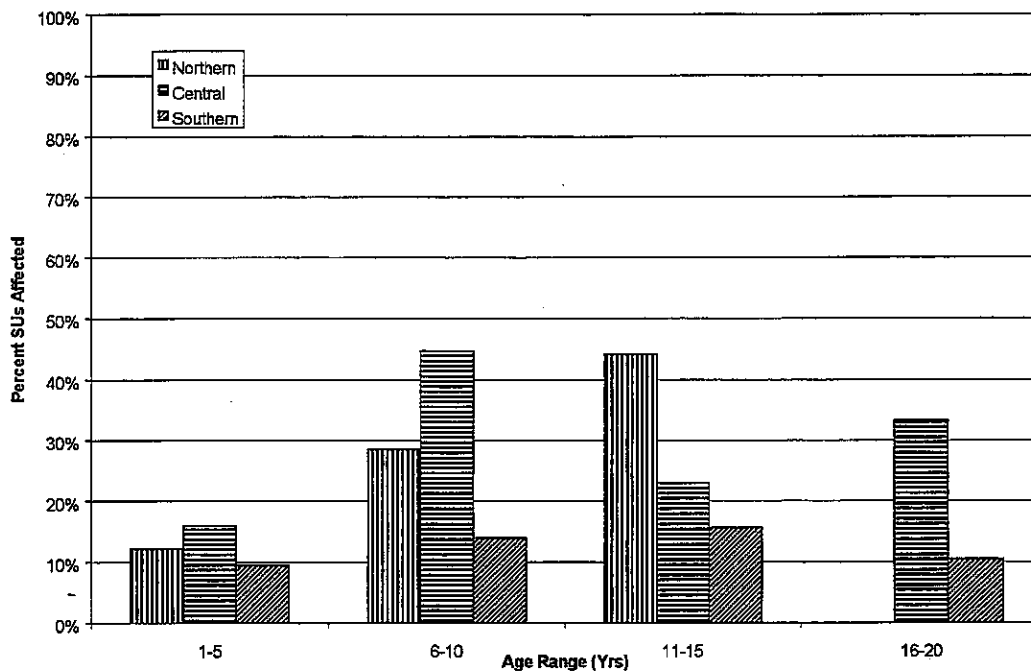


Figure 76. Percent TNAC sample units affected by oil spillage.

Oil Spillage in TKAC Sample Units

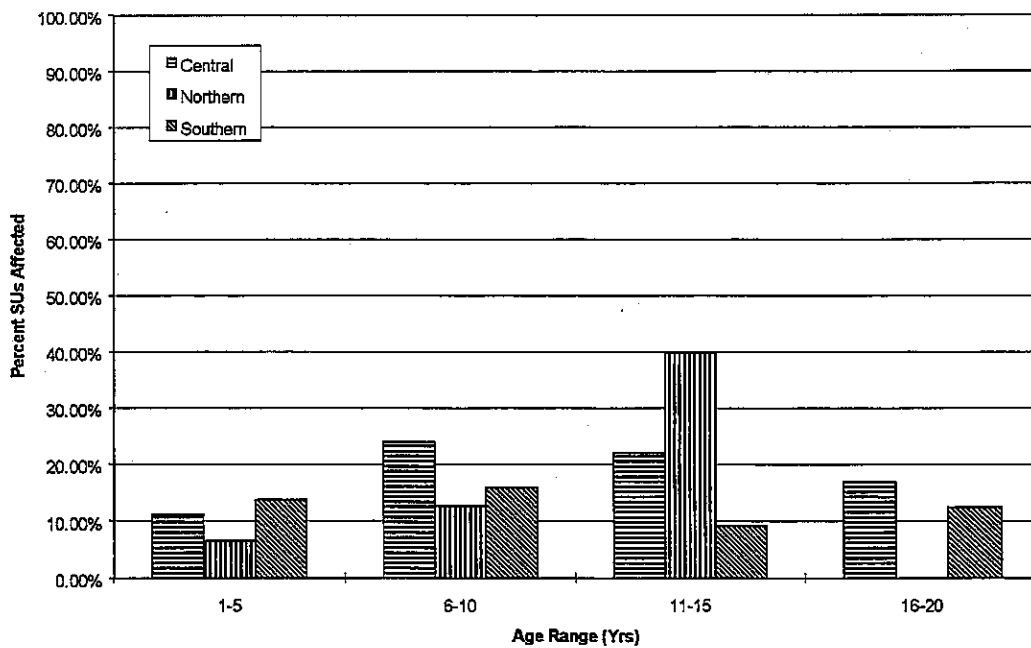


Figure 77. Percent TKAC sample units affected by oil spillage.

Paving Lane Cracking in TNAC Sample Units

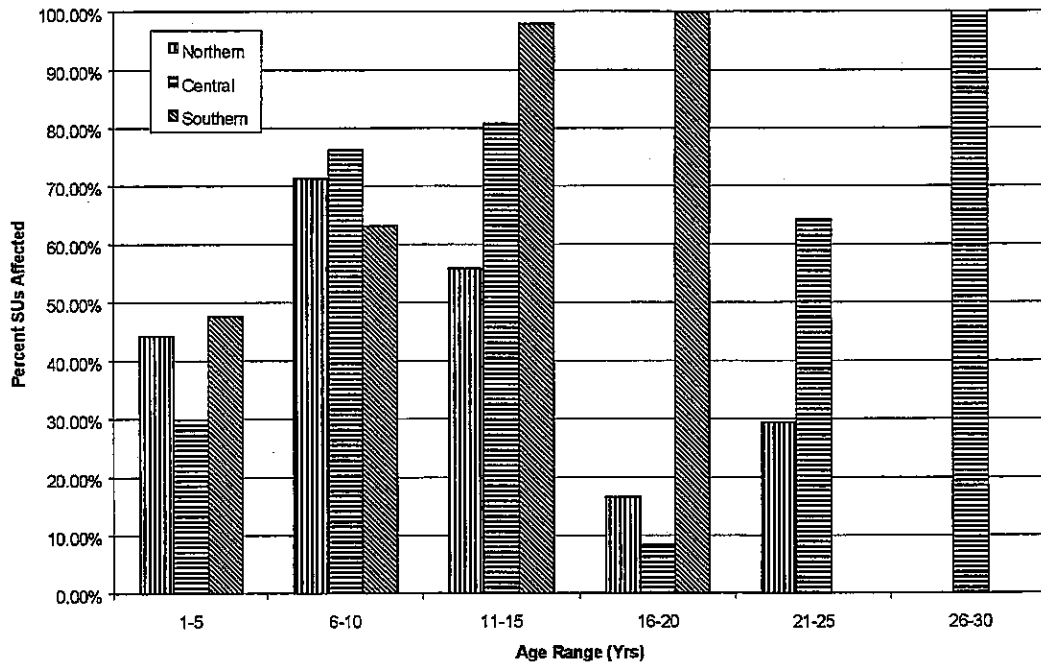


Figure 78. Percent TNAC sample units affected by paving lane cracking.

Paving Lane Cracking in TKAC Sample Units

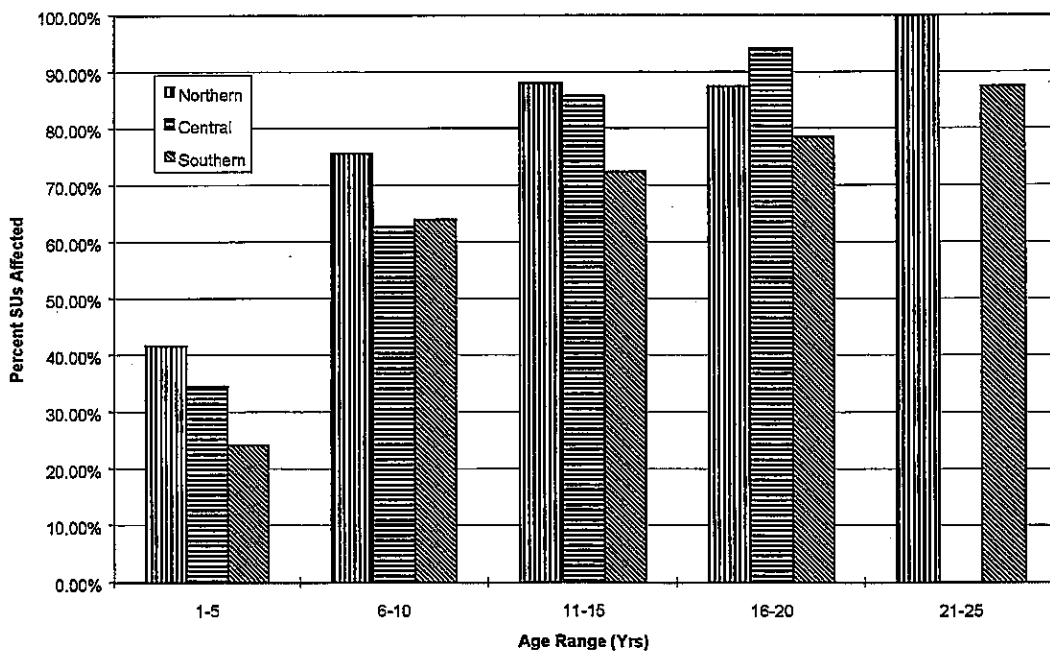


Figure 79. Percent TKAC sample units affected by paving lane cracking.

Average Density of Sample Unit Paving Lane Cracking

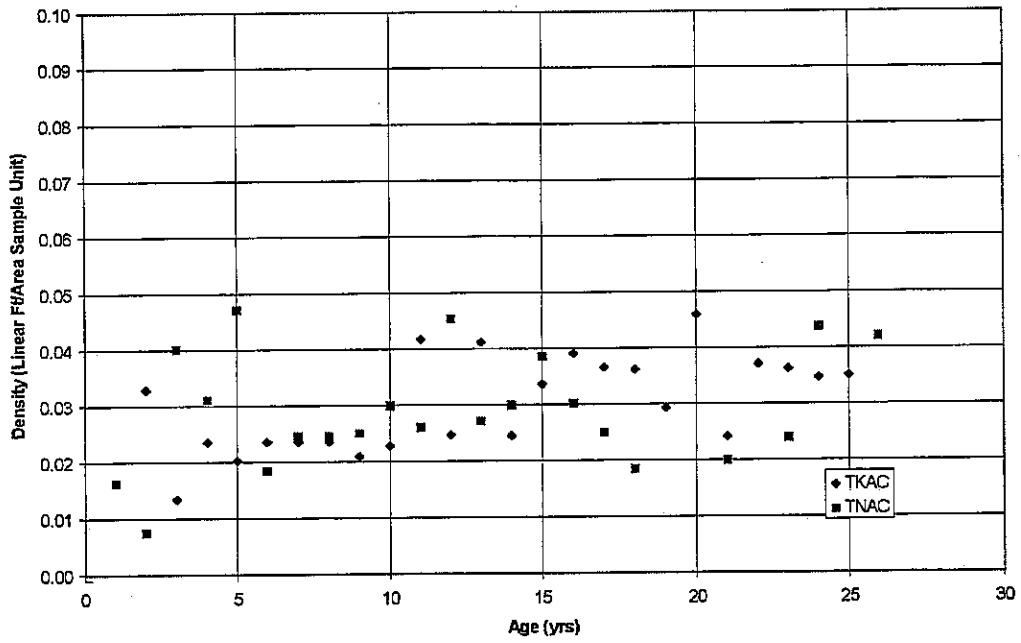


Figure 80. Average density of sample unit paving lane cracking.

TNAC: Average Density Paving Lane Cracking in Central Climatic Zone

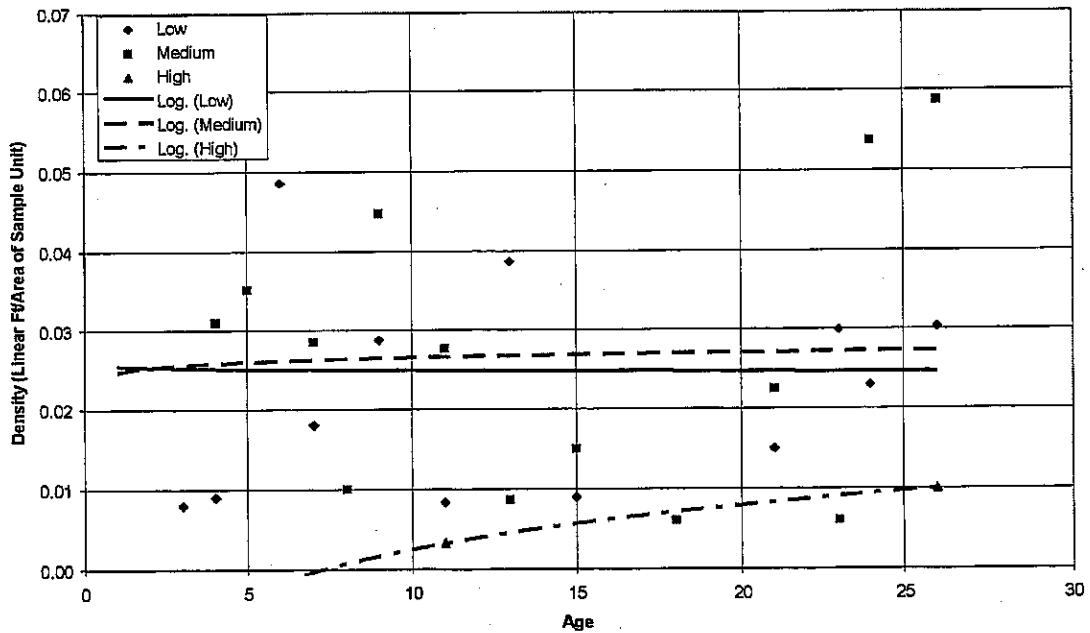


Figure 81. Average density of TNAC paving lane cracking in the Central Climatic Zone.

TKAC: Average Density Paving Lane Cracking in Central Climatic Zone

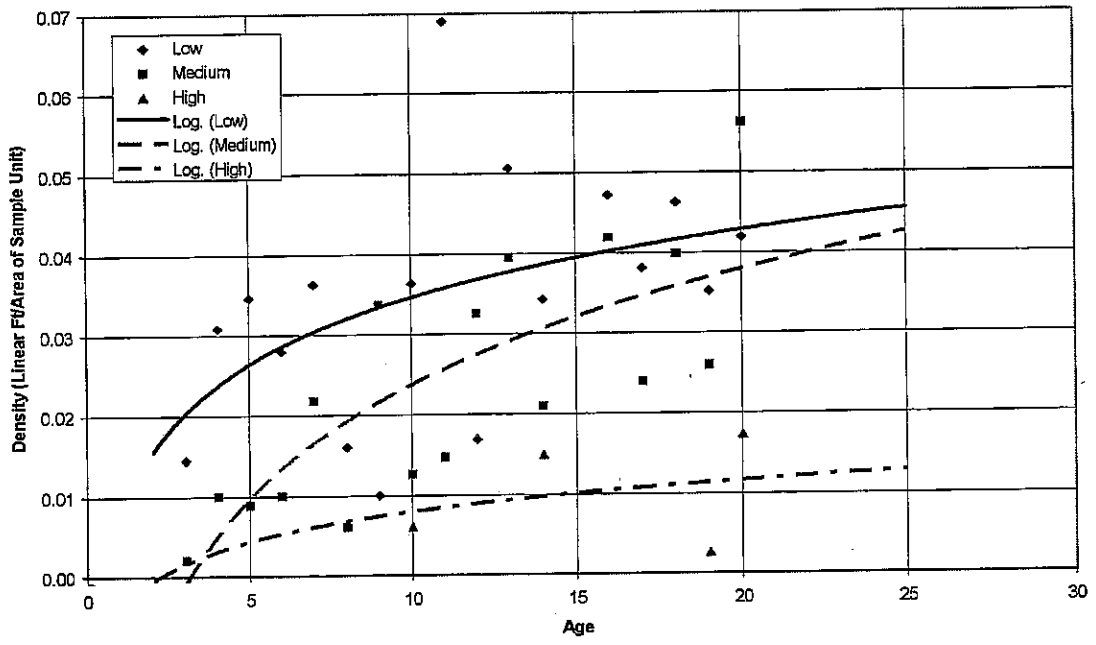


Figure 82. Average density of TKAC paving lane cracking in the Central Climatic Zone.

Large Slab: Percent Sample Units Affected by Distress in Northern Climatic Zone

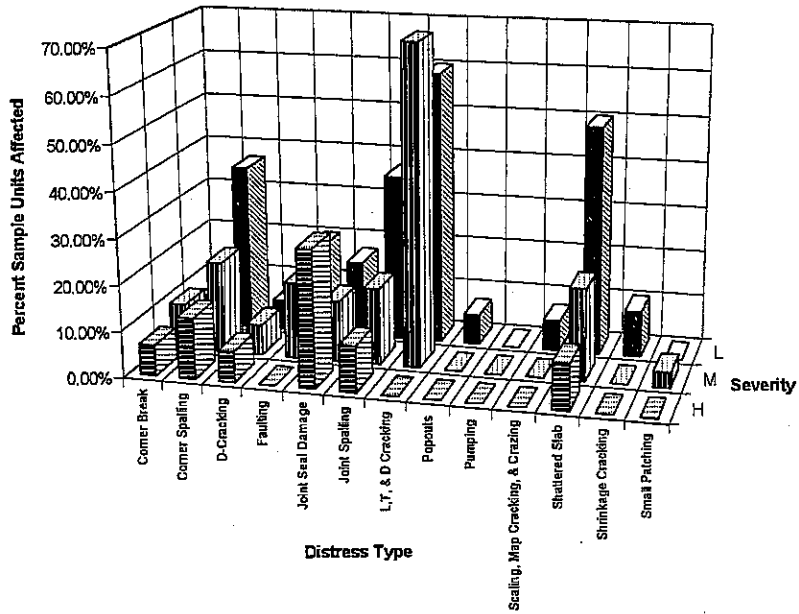


Figure 83. Percent large slab sample units affected by distress in Northern Climatic Zone.

Large Slab: Percent Sample Units Affected by Distress in Central Climatic Zone

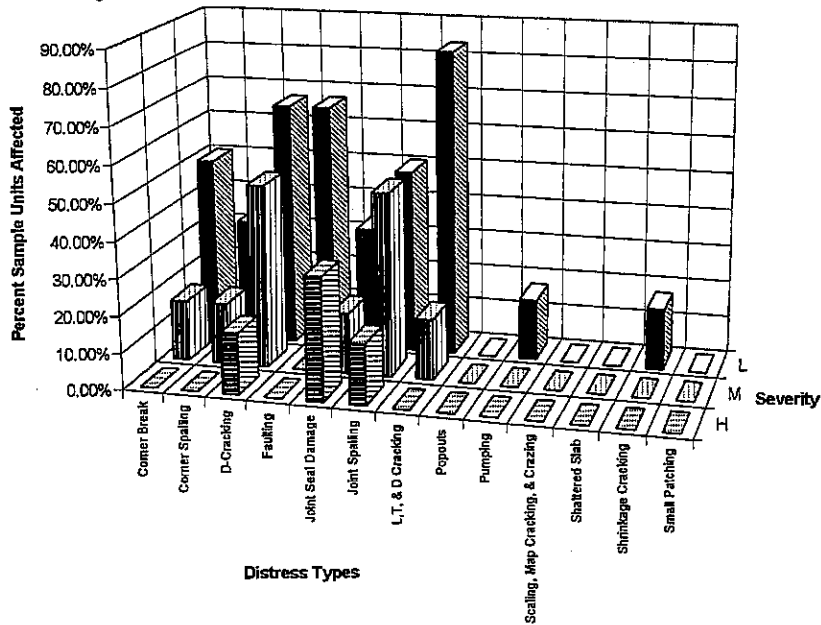


Figure 84. Percent large slab sample units affected by distress in Central Climatic Zone.

Large Slab: Percent Sample Units Affected by Distress in Southern Climatic Zone

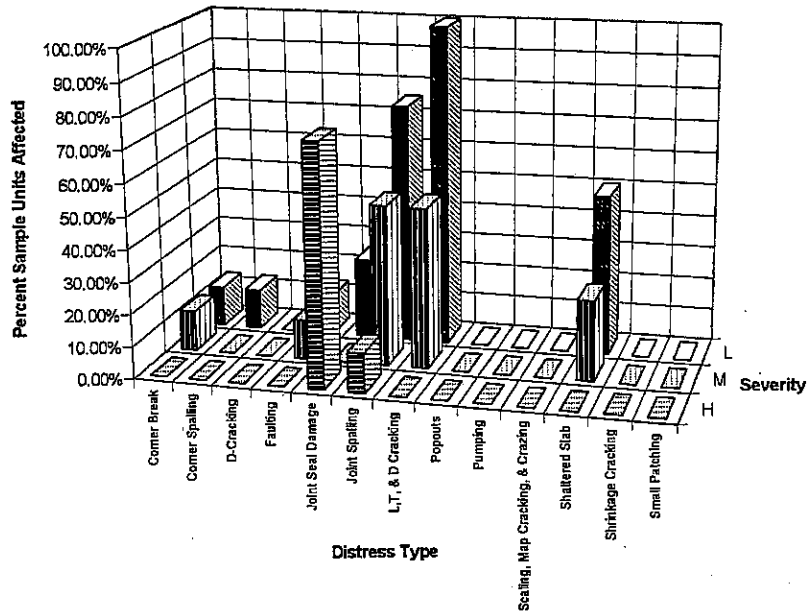


Figure 85. Percent large slab sample units affected by distress in Southern Climatic Zone.

Medium Slab: Percent Sample Units Affected by Distress in Northern Climatic Zone

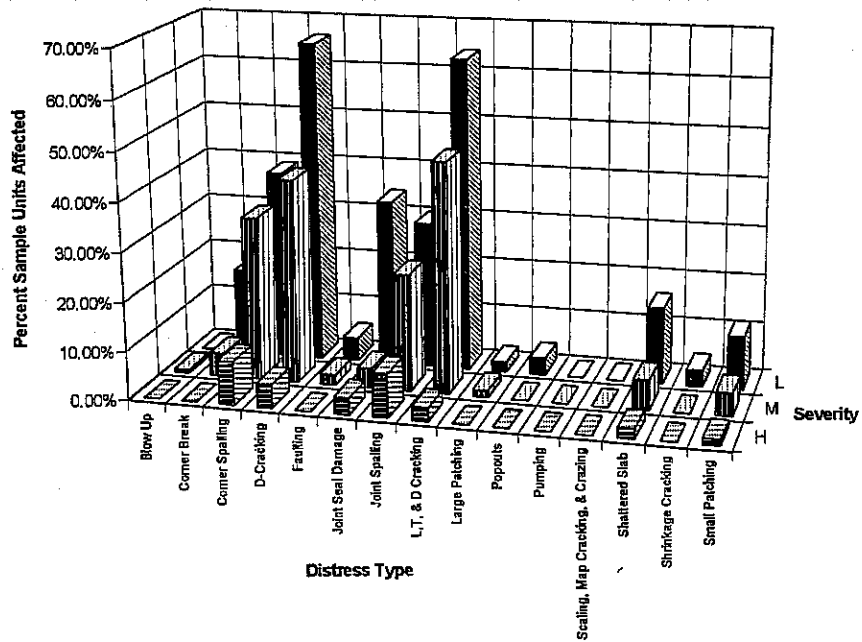


Figure 86. Percent medium slab sample units affected by distress in Northern Climatic Zone.

Medium Slab: Percent Sample Units Affected by Distress in Central Climatic Zone

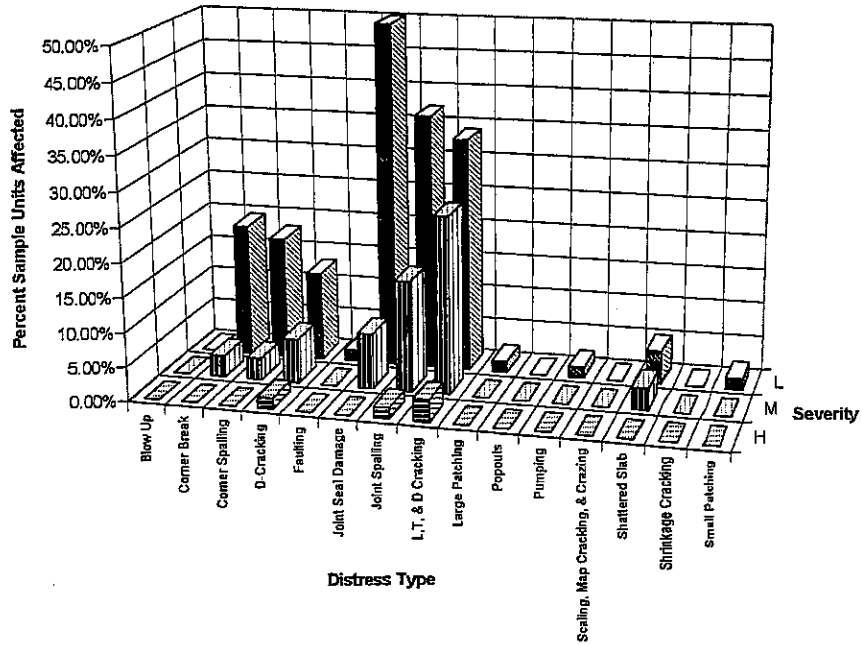


Figure 87. Percent medium slab sample units affected by distress in Central Climatic Zone.

Medium Slab: Percent Sample Units Affected by Distress in Southern Climatic Zone

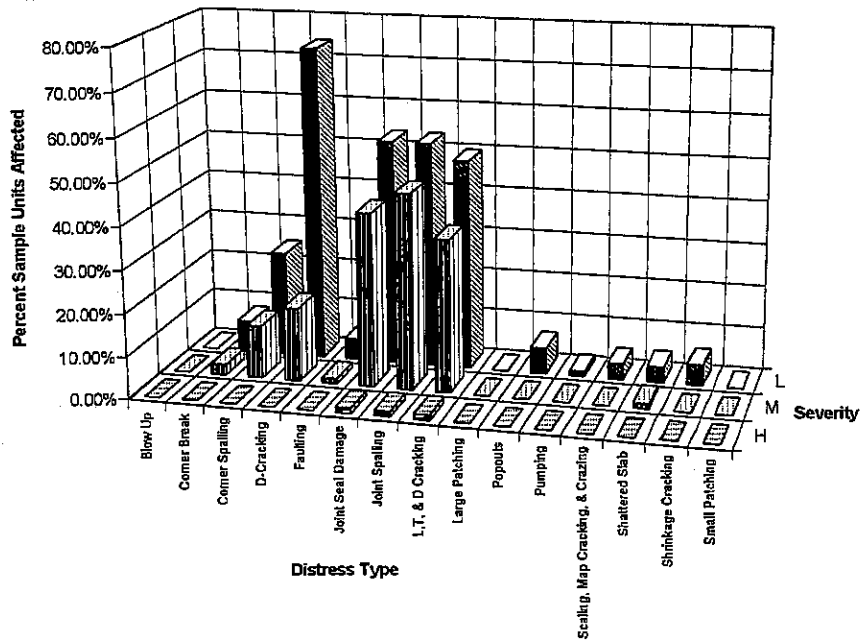


Figure 88. Percent medium slab sample units affected by distress in Southern Climatic Zone.

Small Slab: Percent Sample Units Affected by Distress in Northern Climatic Zone

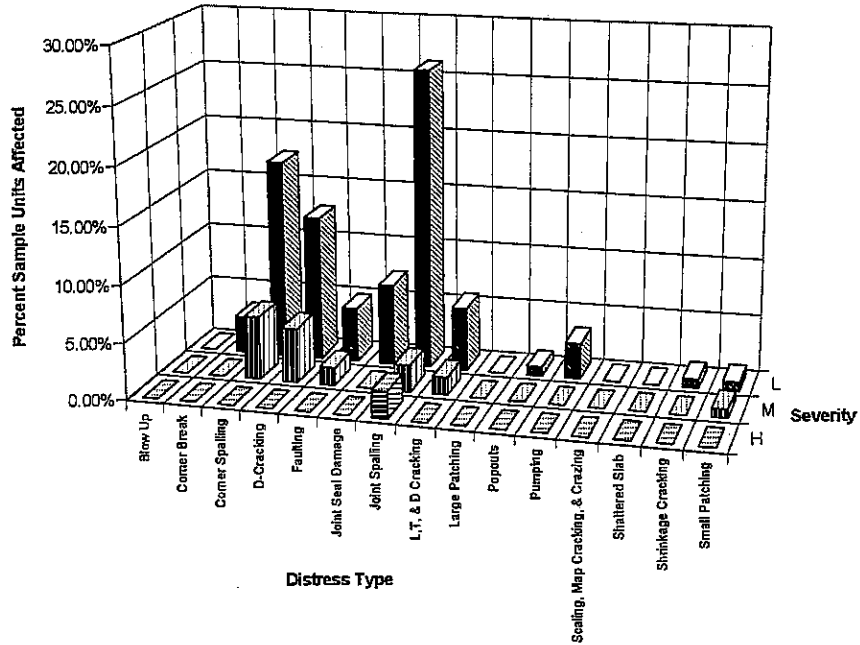


Figure 89. Percent small slab sample units affected by distress in Northern Climatic Zone.

Small Slab: Percent Sample Units Affected by Distress in Central Climatic Zone

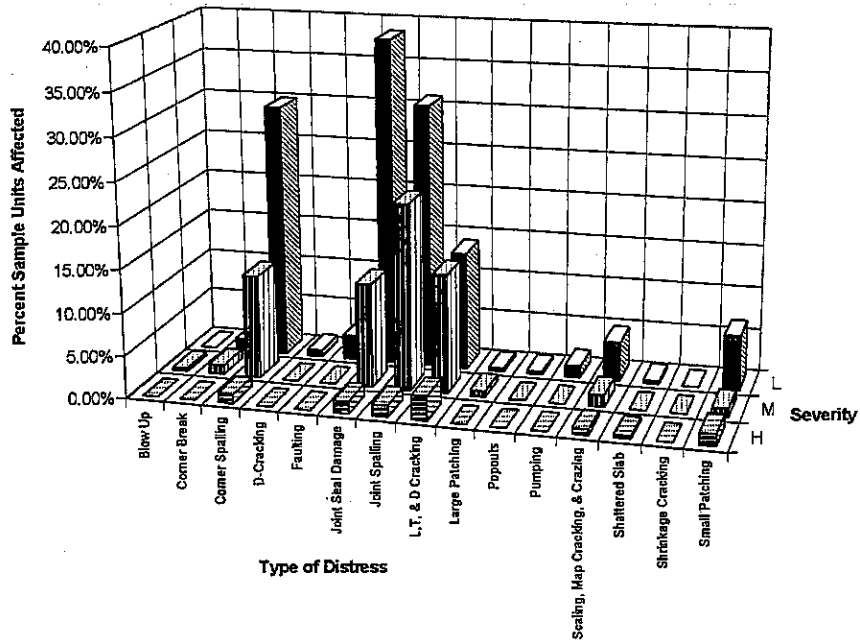


Figure 90. Percent small slab sample units affected by distress in Central Climatic Zone.

Small Slab: Percent Sample Units Affected by Distress in Southern Climatic Zone

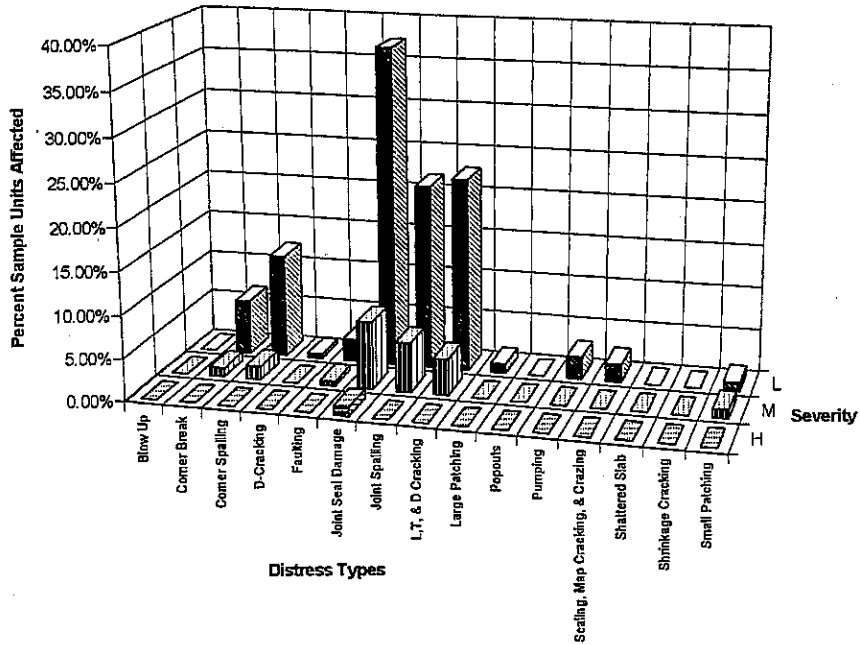


Figure 91. Percent small slab sample units affected by distress in Southern Climatic Zone.

Percent Sample Units Affected by Corner Breaks in the Northern Climatic Zone

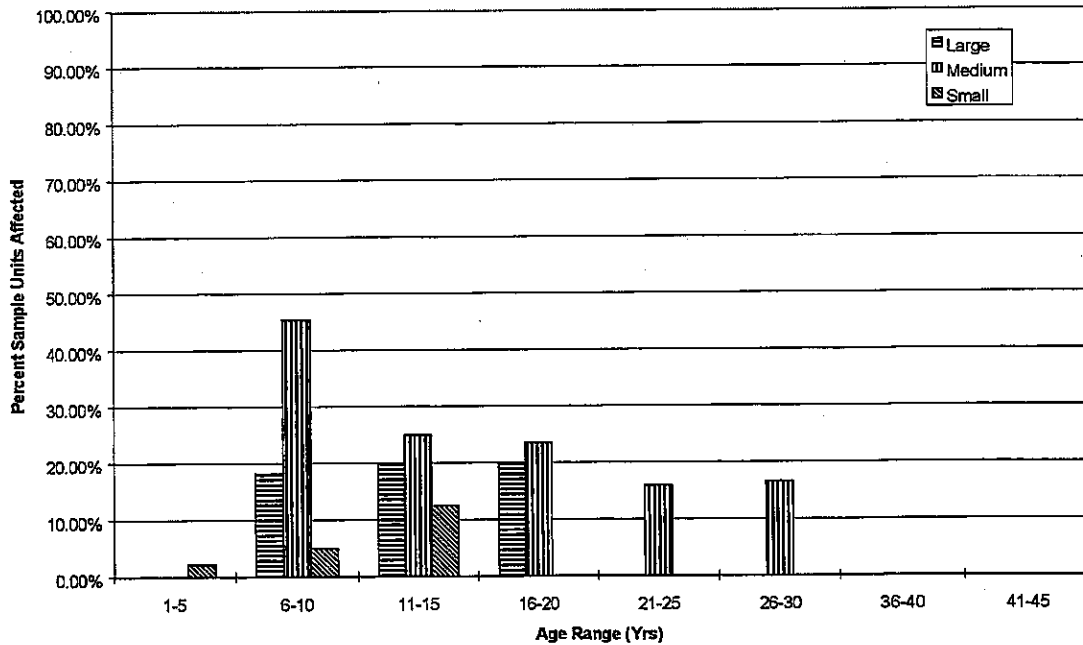


Figure 92. Percent sample units affected by corner breaks in the Northern Climatic Zone.

Percent Sample Units Affected by Corner Breaks in the Central Climatic Zone

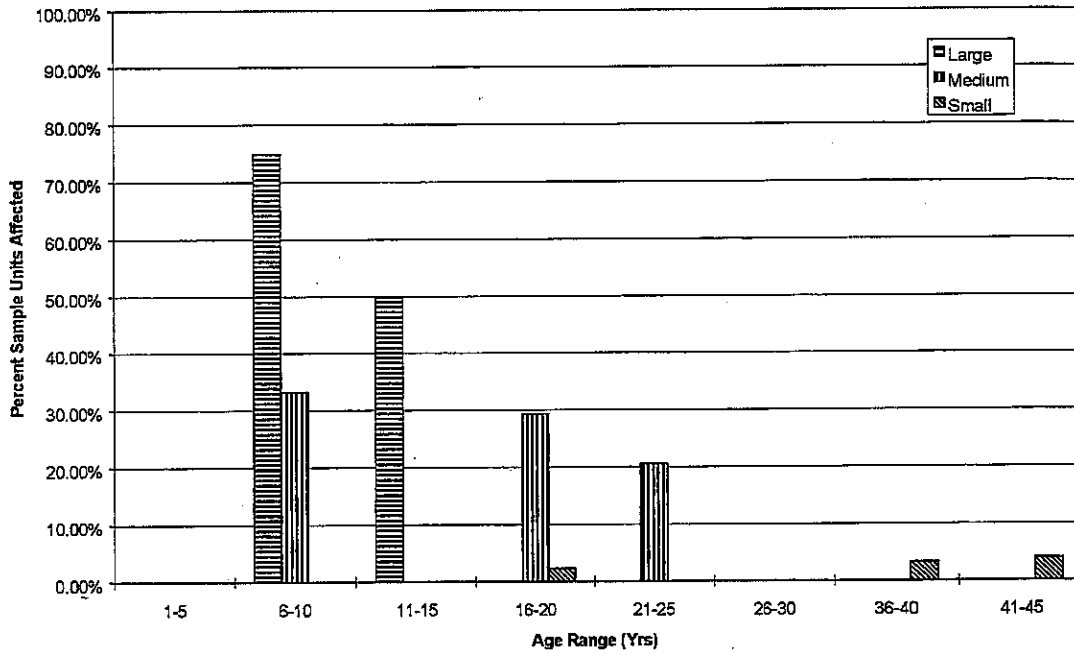


Figure 93. Percent sample units affected by corner breaks in the Central Climatic Zone.

Percent Sample Units Affected by Corner Breaks in the Southern Climatic Zone

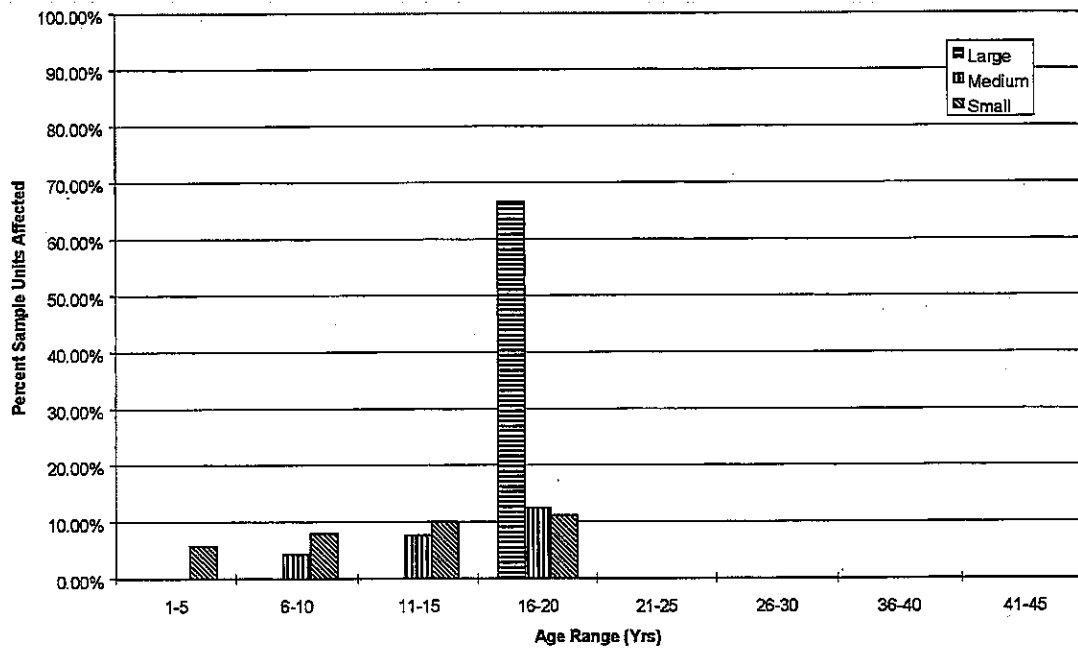


Figure 94. Percent sample units affected by corner breaks in the Southern Climatic Zone.

Percent Sample Units Affected by Corner Spalling in Northern Climatic Zone

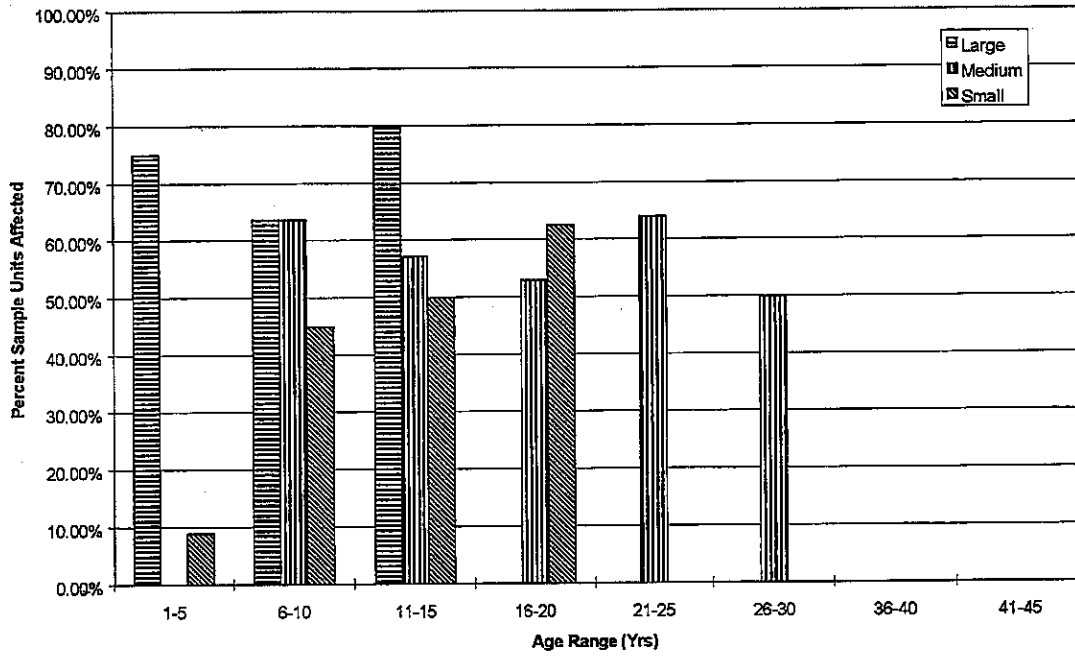


Figure 95. Percent sample units affected by corner spalling in the Northern Climatic Zone.

Percent Sample Units Affected by Corner Spalling in Central Climatic Zone

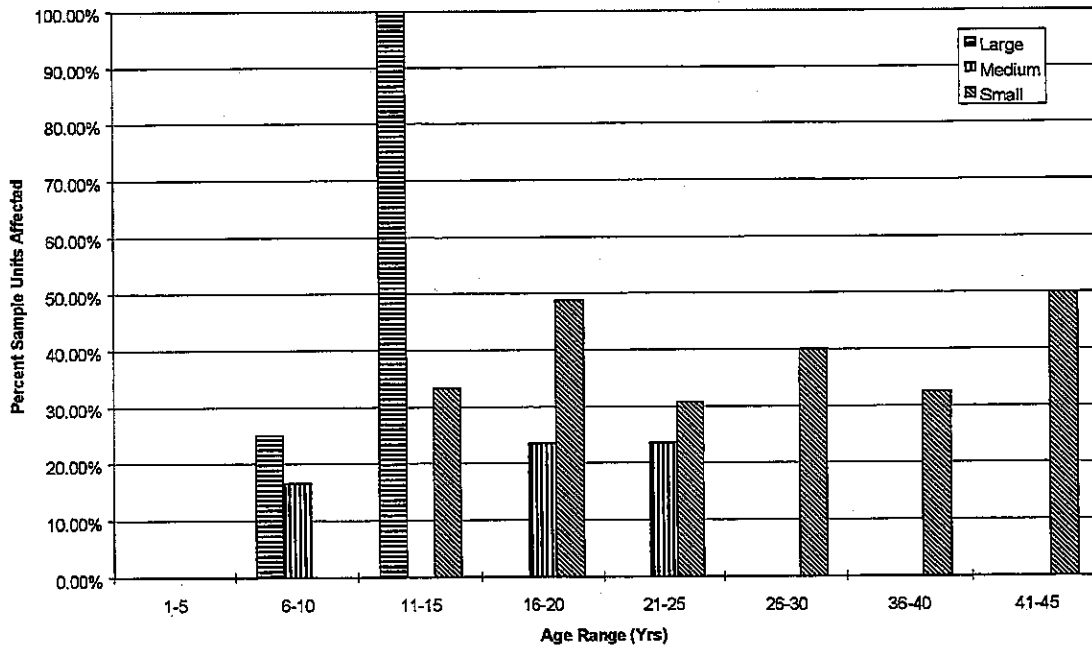


Figure 96. Percent sample units affected by corner spalling in the Central Climatic Zone.

Percent Sample Units Affected by Corner Spalling in Southern Climatic Zone

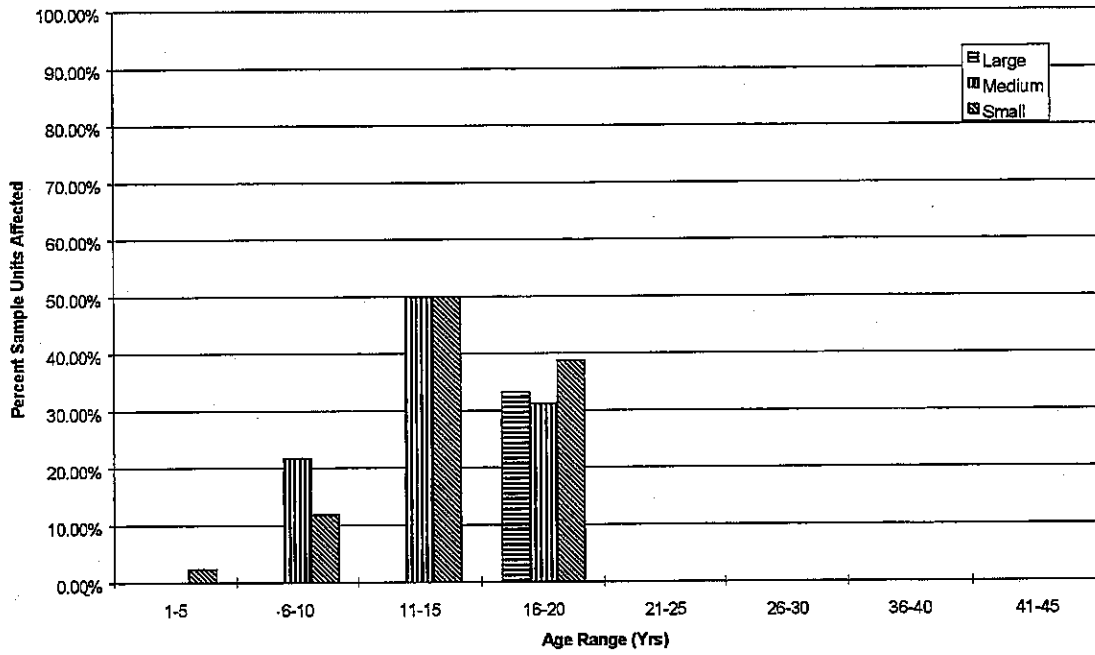


Figure 97. Percent sample unit affected by corner spalling in the Southern Climatic Zone.

Percent Sample Units Affected by Joint Spalling in Northern Climatic Zone

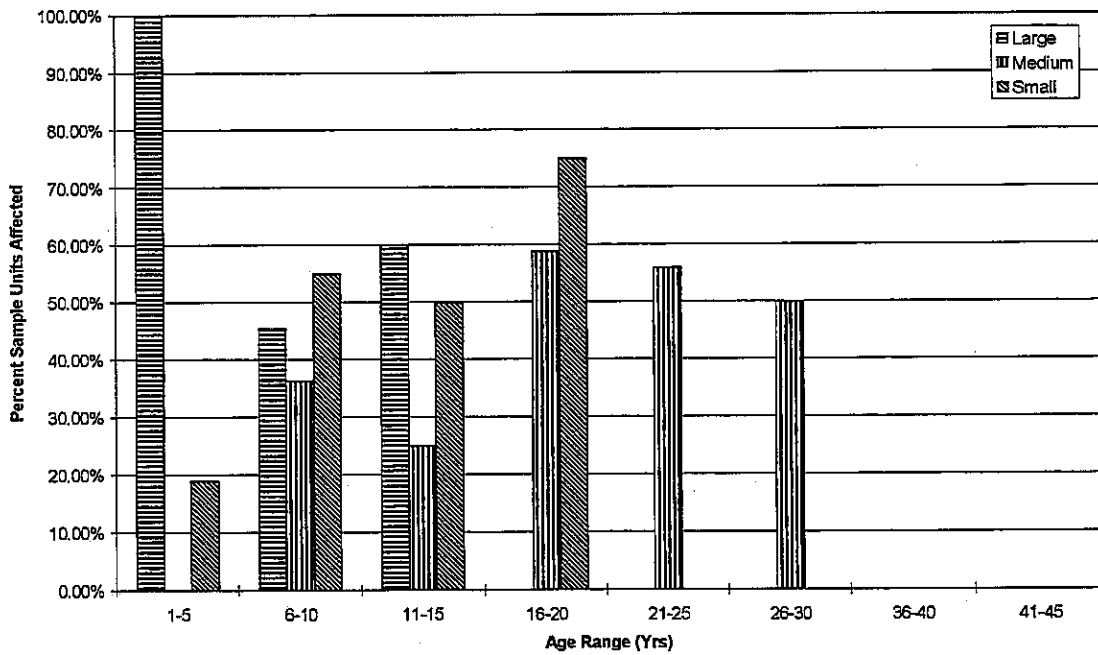


Figure 98. Percent sample units affected by joint spalling in Northern Climatic Zone.

Percent Sample Units Affected by Joint Spalling in Central Climatic Zone

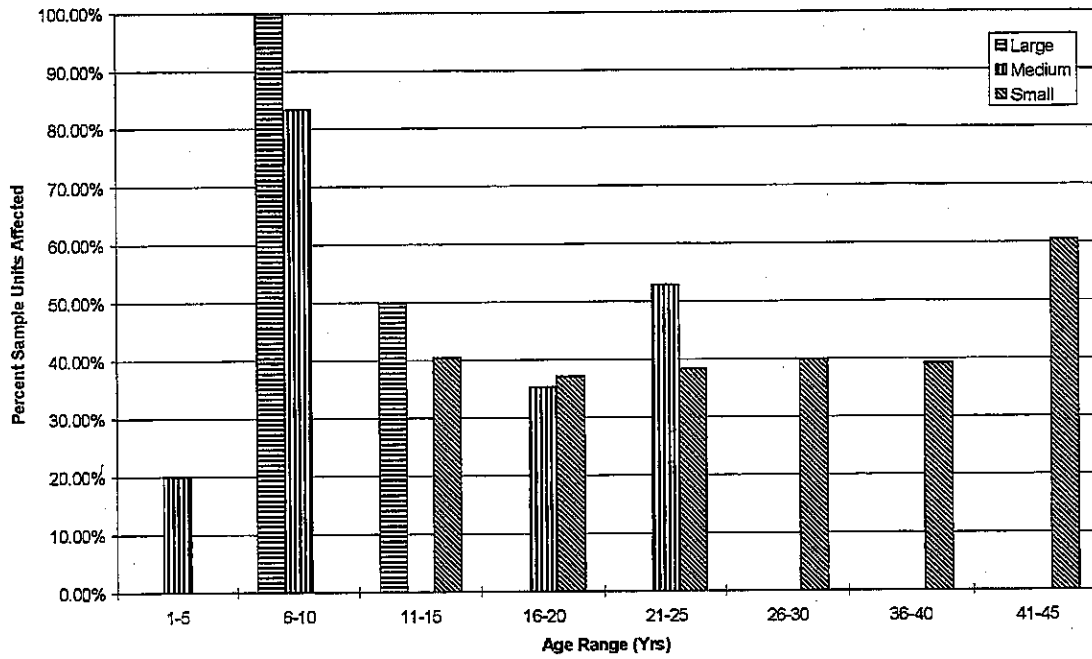


Figure 99. Percent sample units affected by joint spalling in Central Climatic Zone.

Percent Sample Units Affected by Joint Spalling in Southern Climatic Zone

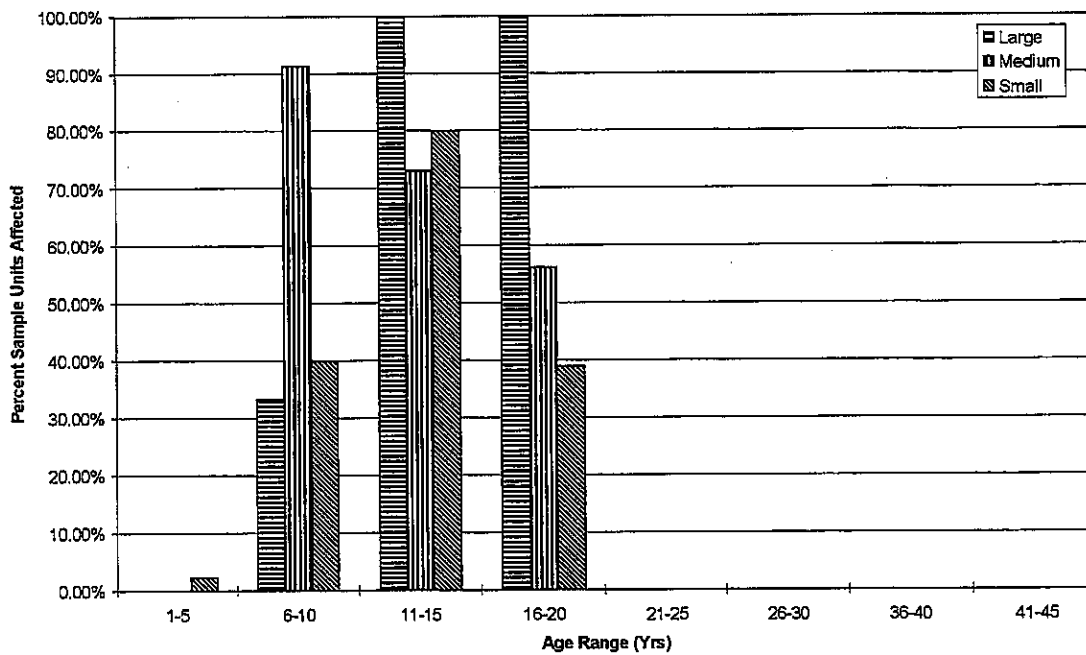


Figure 100. Percent sample units affected by joint spalling in Southern Climatic Zone.

Percent Sample Units Affected by D-Cracking in Northern Climatic Zone

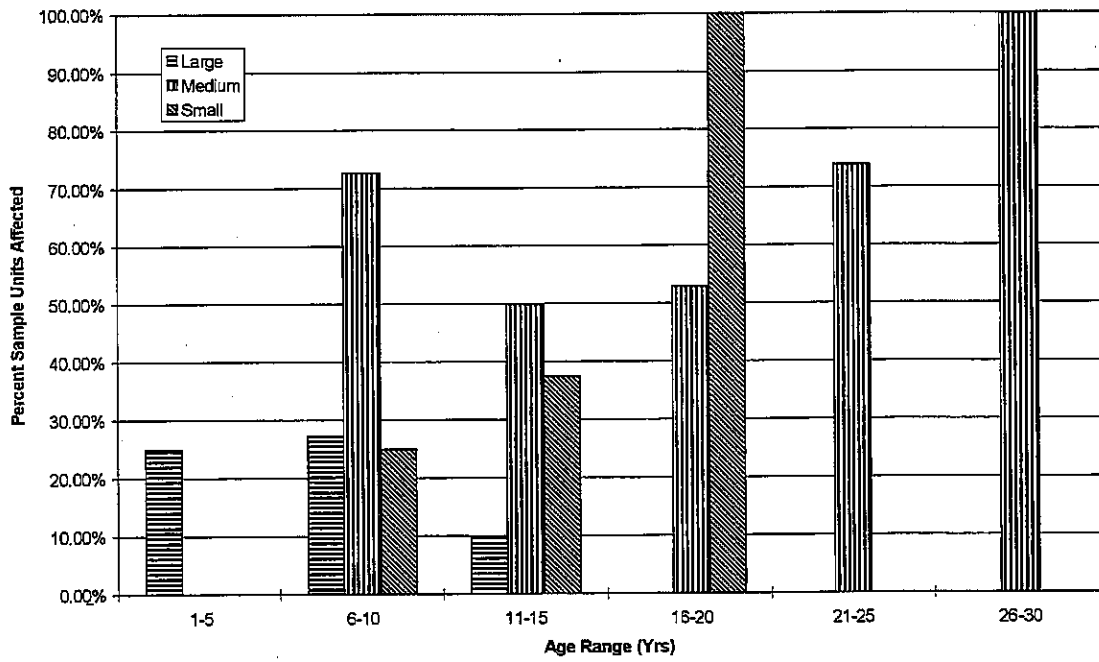


Figure 101. Percent sample units affected by D-cracking in Northern Climatic Zone.

Percent Sample Units Affected by D-Cracking in Central Climatic Zone

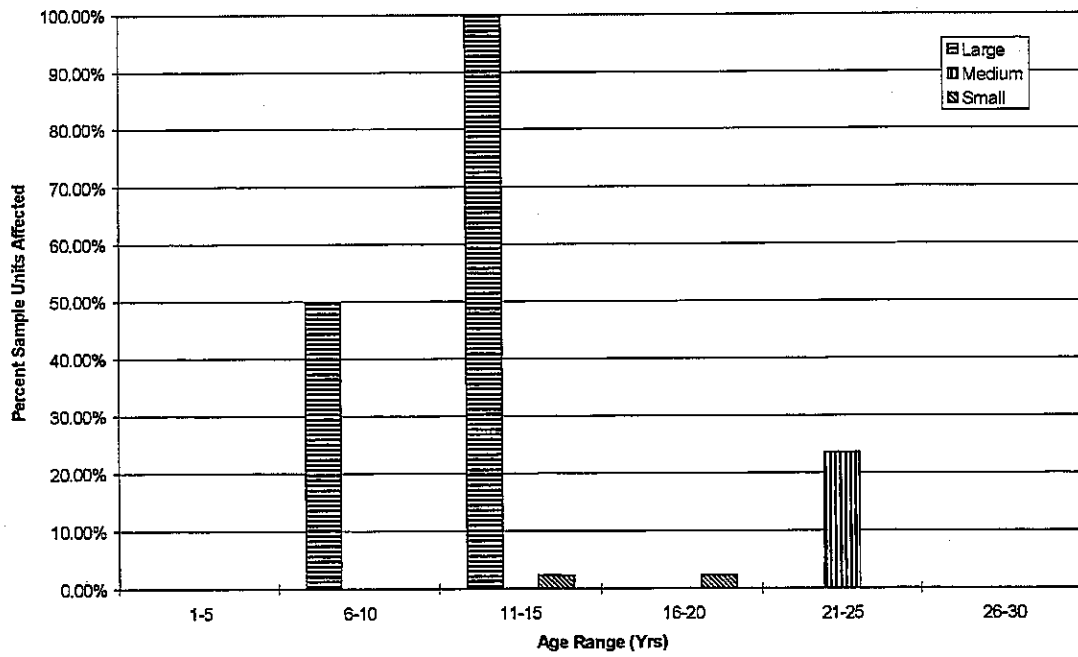


Figure 102. Percent sample units affected by D-cracking in Central Climatic Zone.

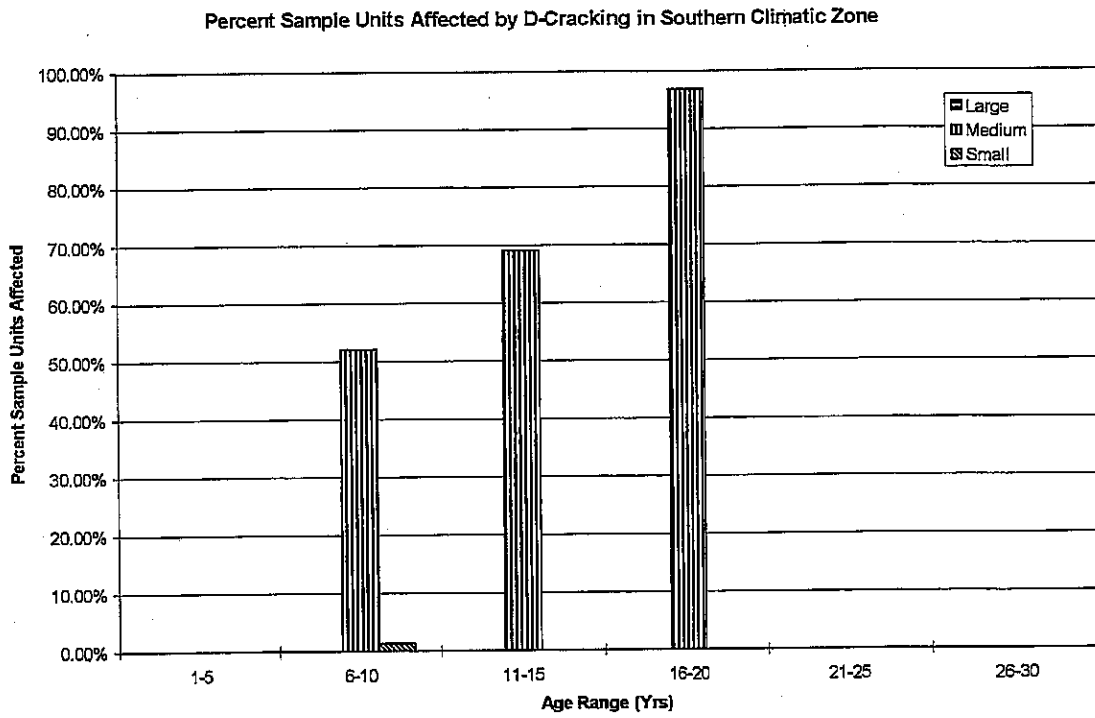


Figure 103. Percent sample units affected by D-cracking in Southern Climatic Zone.

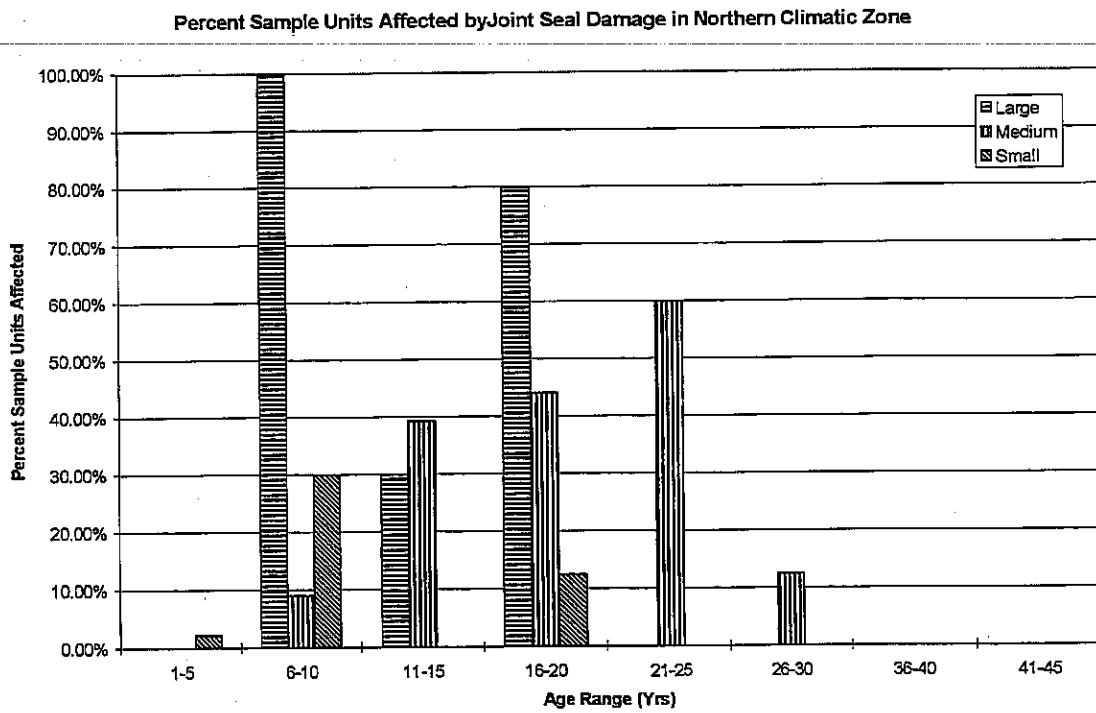


Figure 104. Percent sample units affected by joint seal damage in Northern Climatic Zone.

Percent Sample Units Affected by Joint Seal Damage in Central Climatic Zone

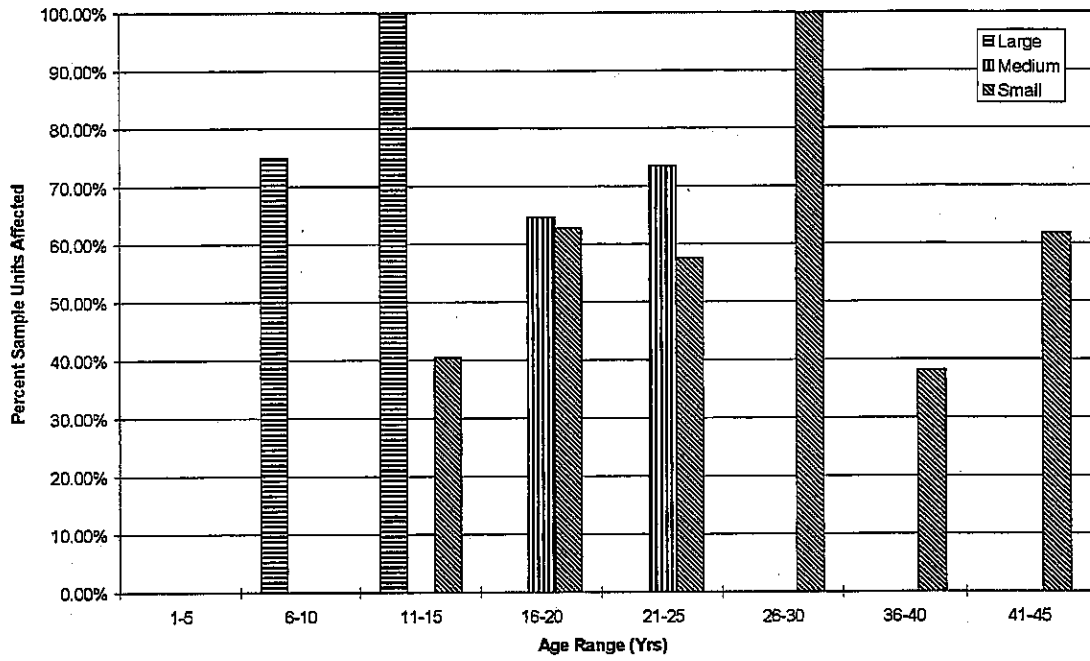


Figure 105. Percent sample units affected by joint seal damage in Central Climatic Zone.

Percent Sample Units Affected by Joint Seal Damage in Southern Climatic Zone

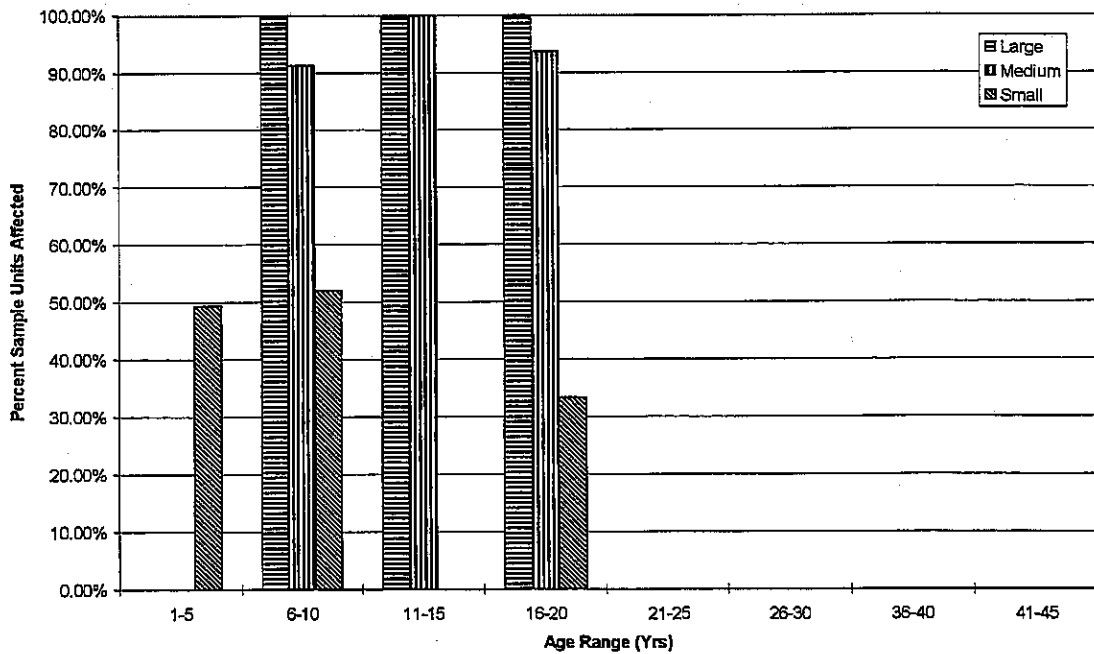


Figure 106. Percent sample units affected by joint seal damage in Southern Climatic Zone.

Percent Sample Units Affected by L, T, & D Cracking in Northern Climatic Zone

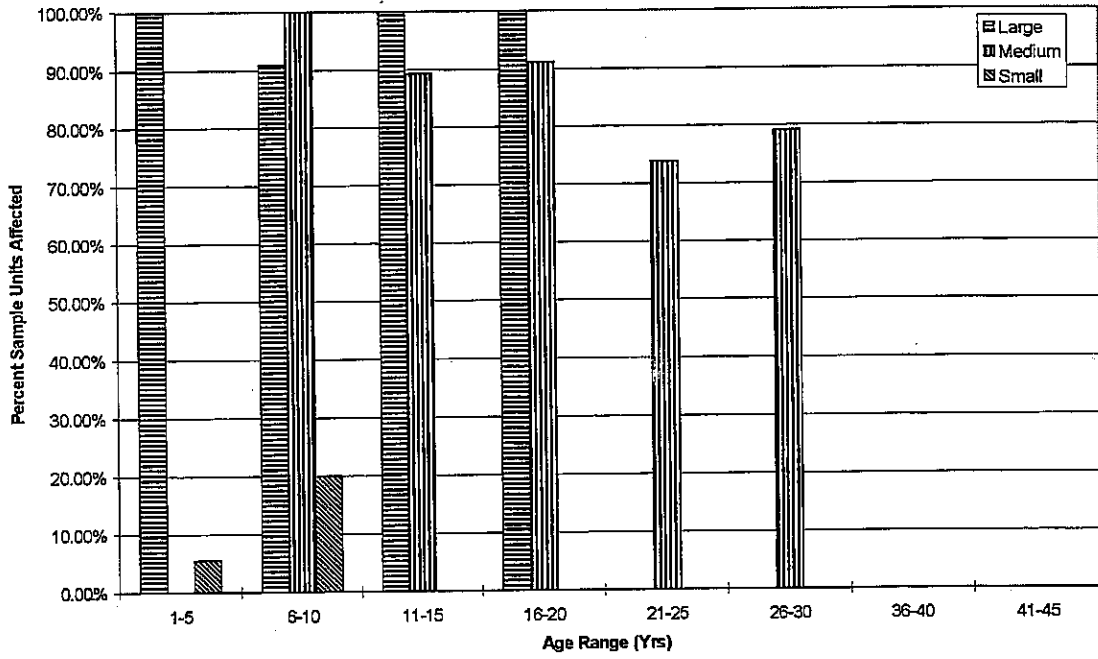


Figure 107. Percent sample units affected by L, T, & D cracking in Northern Climatic Zone.

Percent Sample Units Affected by L, T, & D Cracking in Central Climatic Zone

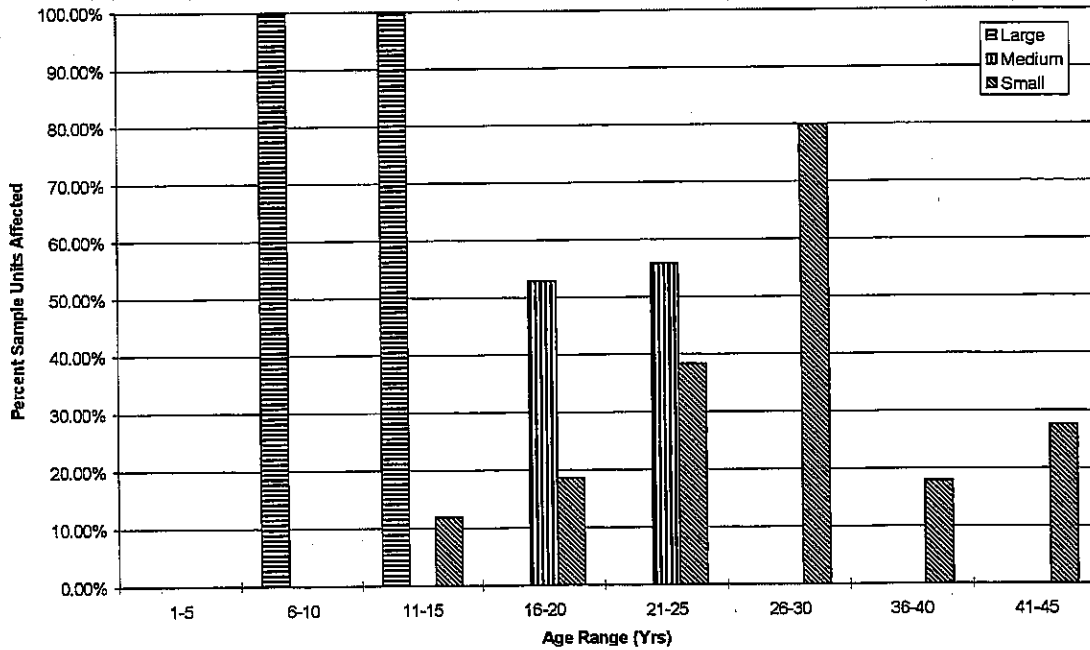


Figure 108. Percent sample units affected by L, T, & D cracking in Central Climatic Zone.

Percent Sample Units Affected by L, T, & D Cracking in Southern Climatic Zone

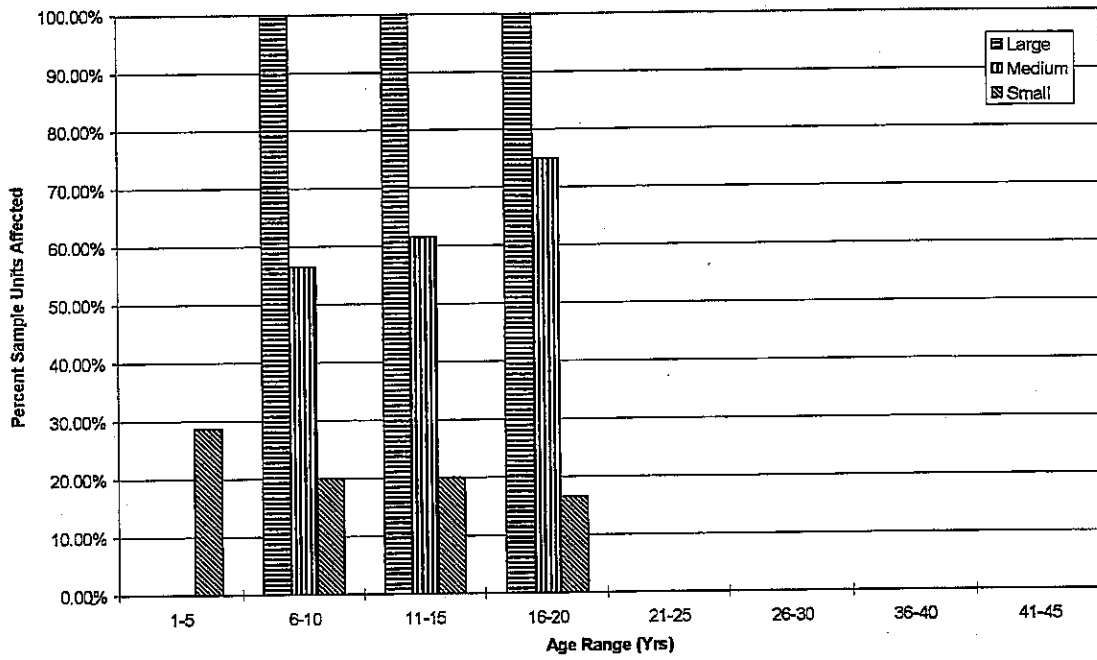


Figure 109. Percent sample units affected by L, T, & D cracking in Southern Climatic Zone.

Percent Sample Units Affected by Shattered Slabs in the Northern Climatic Zone

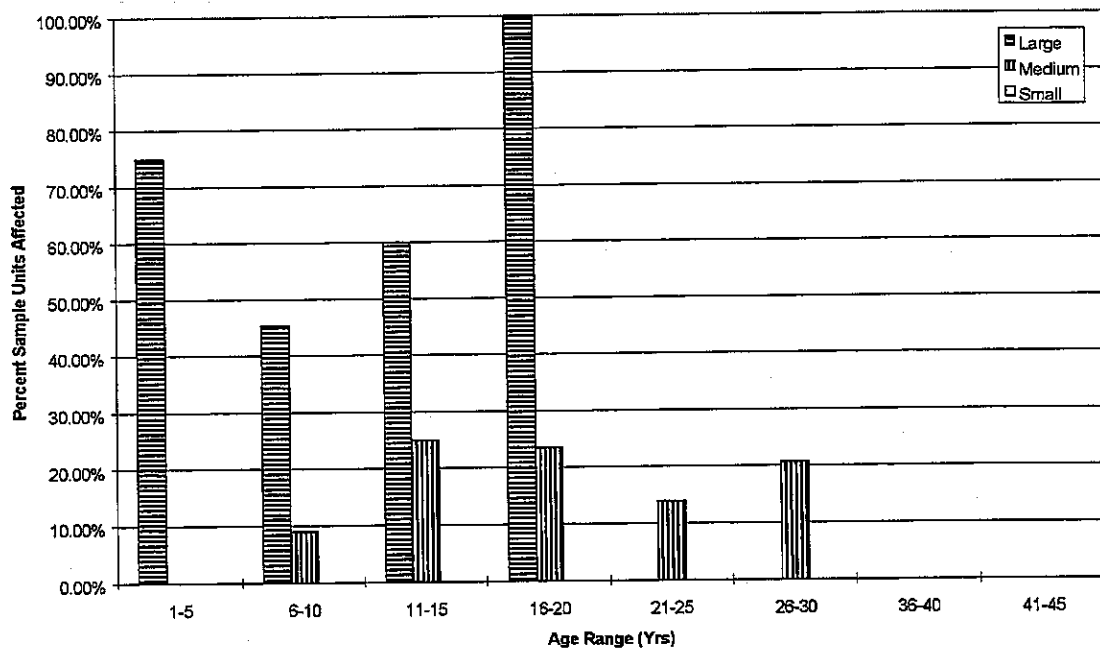


Figure 110. Percent sample units affected by shattered slabs in the Northern Climatic Zone.

Percent Sample Units Affected by Shattered Slabs in Central Climatic Zone

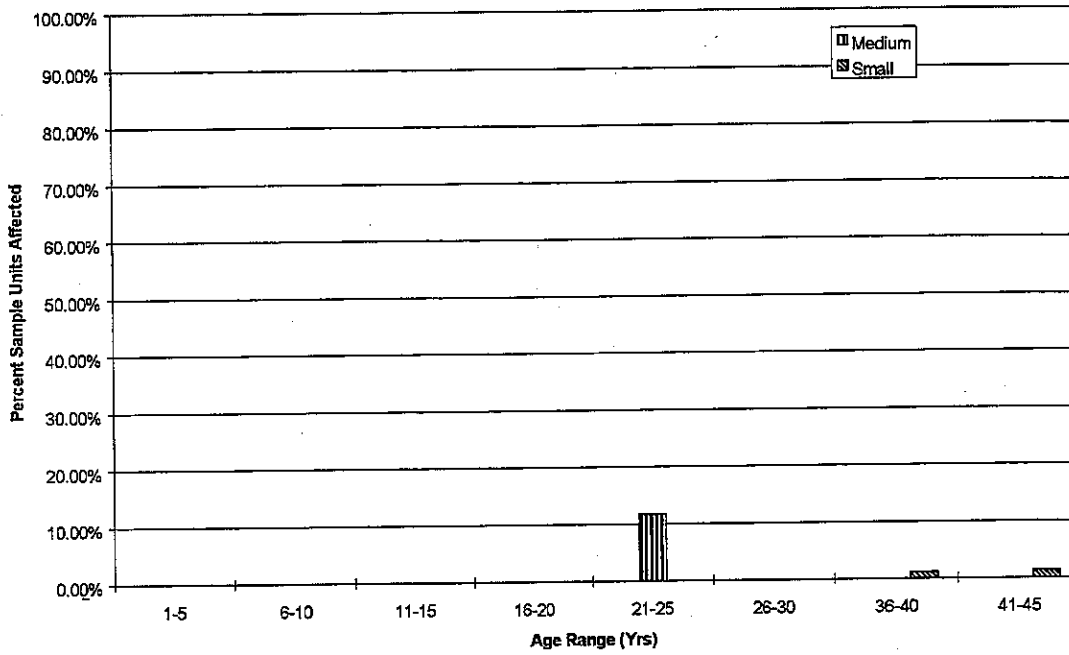


Figure 111. Percent sample units affected by shattered slabs in the Central Climatic Zone.

Percent Sample Units Affected by Shattered Slabs in the Southern Climatic Zone

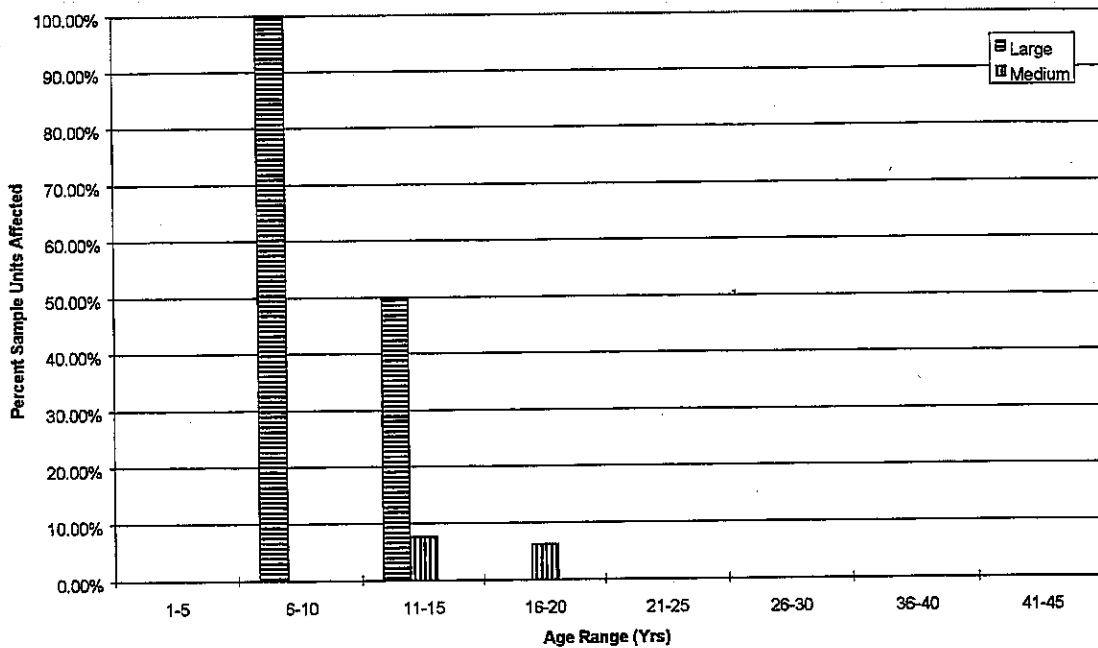


Figure 112. Percent sample units affected by shattered slabs in the Southern Climatic Zone.



APPENDIX A: DEVELOPMENT OF ILLI-PAVE-BASED ALGORITHMS FOR CONVENTIONAL AND FULL-DEPTH ASPHALT CONCRETE GA AIRPORT PAVEMENTS

This appendix describes the development of ILLI-PAVE-based pavement response algorithms for conventional and FULL-DEPTH AC pavements for GA airports. The response algorithms were derived from a pavement response data base created using the ILLI-PAVE finite element structural model. The methodology employed is similar to that used in the past to develop mechanistic pavement design schemes for roadway pavements [Elliot, 1985][Thompson, 1988][Gomez, 1984][Thompson, 1986].

ILLI-PAVE is a finite element structural model that considers the pavement to be an axisymmetric solid of revolution [Raad, 1980]. This is shown in Figure A.1. ILLI-PAVE considers nonlinear, stress-dependent resilient behavior models and failure criteria for granular materials and fine-grained soils [Raad, 1980][Figueroa, 1979][Hoffman, 1981]. In this study, the ILLI-PAVE PC Version was utilized [TFG, 1990].

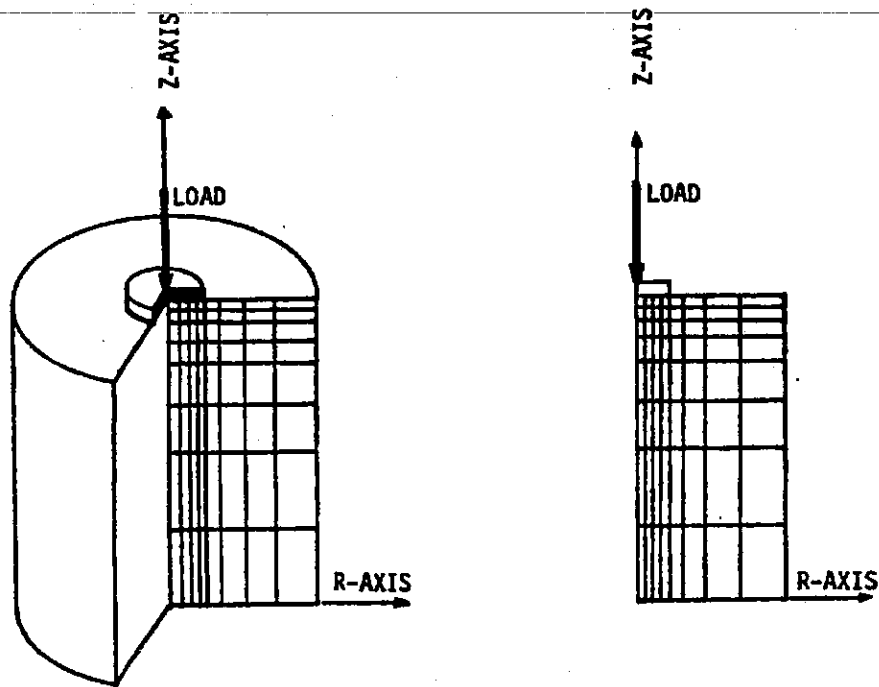


Figure A.1. ILLI-PAVE's cylindrical solid of revolution [Elliot, 1985].

To model the dual wheel gear configuration of the Beechcraft King Air B200, it was assumed that the total main gear load was approximately 10,600 lbs, placing 5,300 lbs on each dual wheel assembly. Assuming a tire pressure of 105 psi, the total contact area was calculated at 50.5 in². This results in an assumed single equivalent circular contact area (a) having a radius of 4.0 in.

The Standard Structure feature of ILLI-PAVE was used to compute a finite element mesh having the required accuracy. In this routine, the mesh has a width equal to 12 times the radius of the loaded area and a depth equal to 50 times this same radius [TFG, 1990]. This configuration ensures stress and strain resolution of acceptable accuracy at the top of the subgrade. The Standard Structure feature generates meshes that are satisfactory for most typical pavement systems, eliminating the need for mesh input by the user. An example of a standard section generated for a 6 in radius is shown in Figure A.2

The resilient behavior of granular and fine-grained materials must be considered in the structural analysis of flexible pavements. The most commonly used method to characterize resilient behavior is the resilient modulus as defined in Equation A.1.

$$E_R = \sigma_D / \epsilon_R \quad \text{Equation A.1}$$

Where: E_R = resilient modulus
 σ_D = repeated deviator stress
 ϵ_R = recoverable axial strain

Both granular and fine-grained materials show stress-dependent resilient behavior. Granular materials become stiffer under increasing stress. This is referred to as stress hardening. Figure A.3 shows an example of this behavior. Fine-grained subgrade soils show the opposite behavior, becoming less stiff under increasing stress levels. This is referred to as stress softening. Figure A.4 demonstrates a typical example of this behavior.

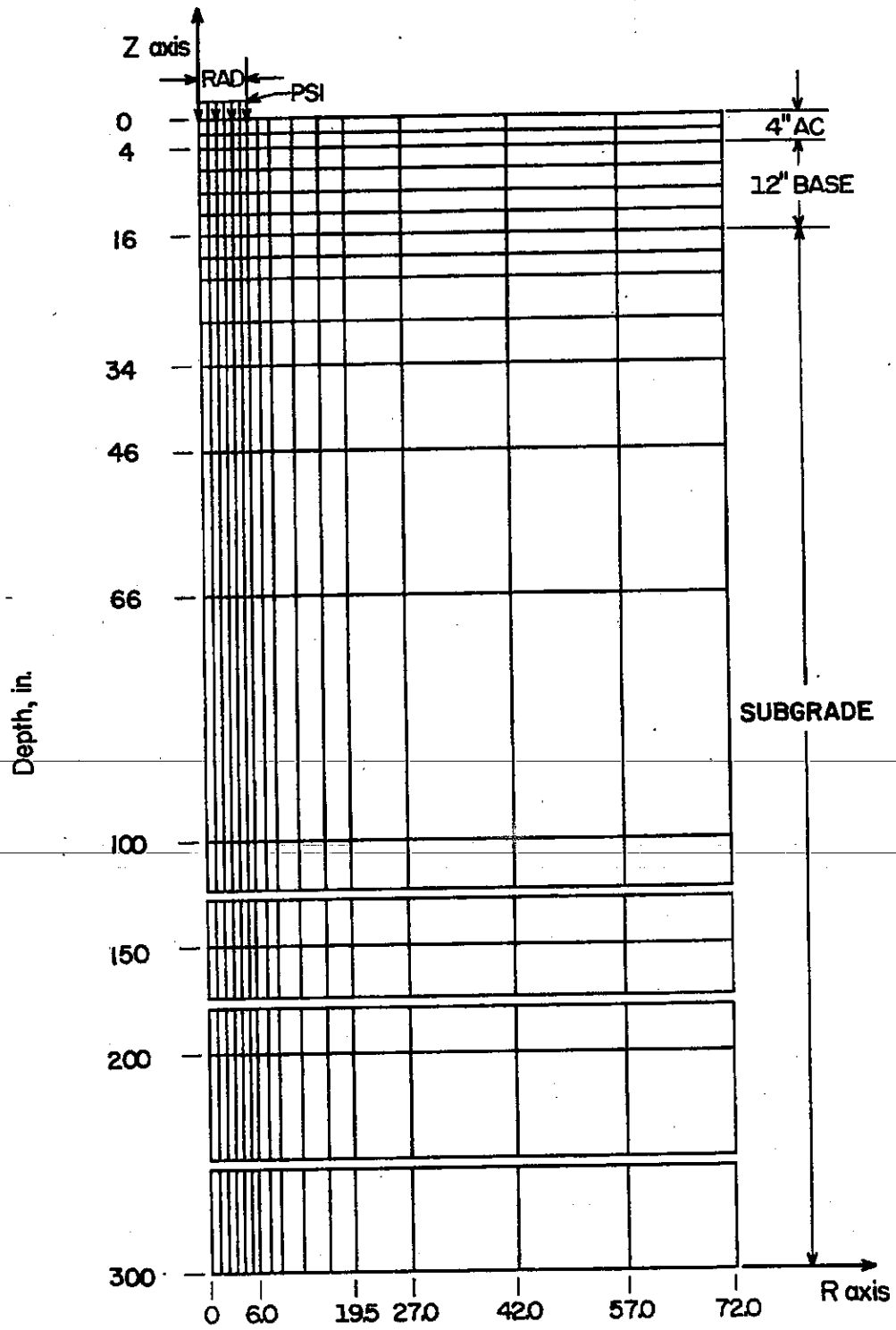


Figure A.2. ILLI-PAVE Standard Structure for a 6 in loading radius [Elliot, 1985].

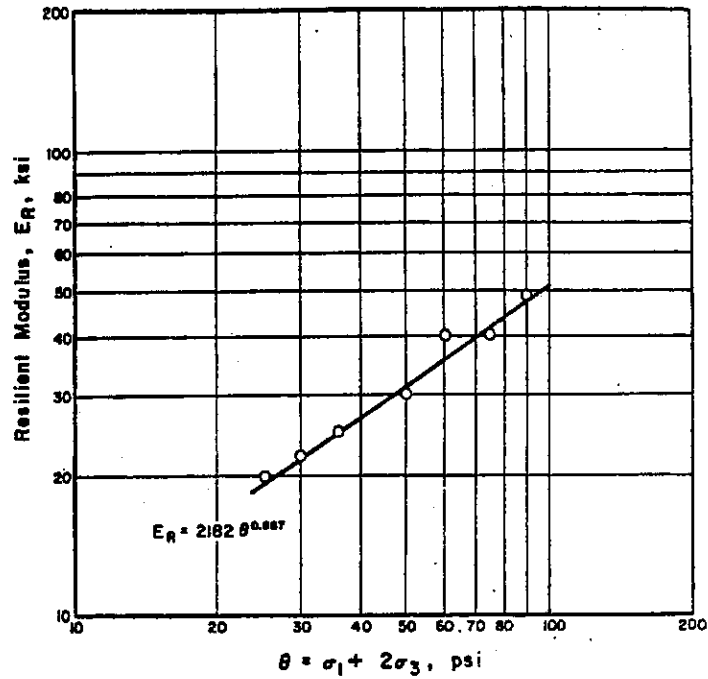


Figure A.3. Resilient modulus- θ relation for an AASHTO A-1-b(0) sandy gravel [Thompson, 1985].

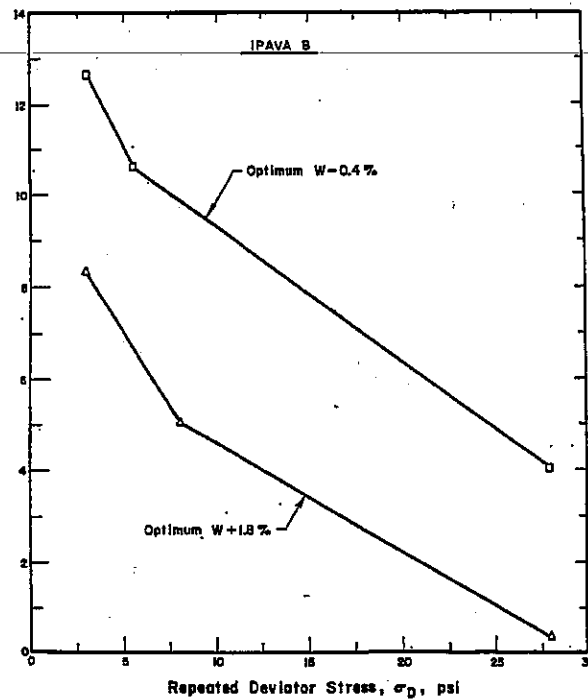


Figure A.4. Typical stress-dependent resilient behavior of fine-grained AASHTO A-7-6 (36) soil [Thompson, 1985].

ILLI-PAVE allows each type of stress dependent behavior to be modeled. For granular materials, the resilient modulus is considered a function of the applied stress state according to the relation shown in Equation A.2 .

$$E_R = K\theta^n \quad \text{Equation A.2}$$

Where: E_R is the resilient modulus
K and n are experimentally derived factors
 θ is the first stress invariant equal to $\sigma_1 + \sigma_2 + \sigma_3$

Rada and Witzak did a extensive statistical study of E_R - θ relationships for a wide range of granular materials [Rada, 1981]. Based on this study, the values of K and n were set at 5000 and 0.5 in this study. The granular material properties used in the ILLI-PAVE analysis are presented in Table 13 in the .

For fine-grained soils, the stress-dependent relationship used is the arithmetic model [Thompson, 1979]. An idealization of this model is shown in Figure A.5 [TFG, 1990]. In Figure A.5, KTWO corresponds to the "breakpoint" resilient modulus (E_{Ri}), which typically occurs at a KONE equal to 6 psi. The stress dependent behavior of a fine-grained soil is characterized through a the bilinear curve. In this study, four fine-grained subgrades were analyzed (very soft, soft, medium, and stiff). The properties used in the ILLI-SLAB analysis are presented in Table 13 of this report.

ILLI-PAVE also features a stress adjustment routine to account for the shear strength limitations present in granular and fine-grained materials [Elliot, 1985]. An iterative approach is applied that adjusts the predicted stress levels to prevent a violation of the Mohr-Coulomb failure envelope. In this way, a more realistic selection of resilient modulus values is selected.

The properties of the AC at three temperatures (40° F, 70° F, and 100° F) are present in Table 13 in the report. The AC layer is represented with a constant linear resilient

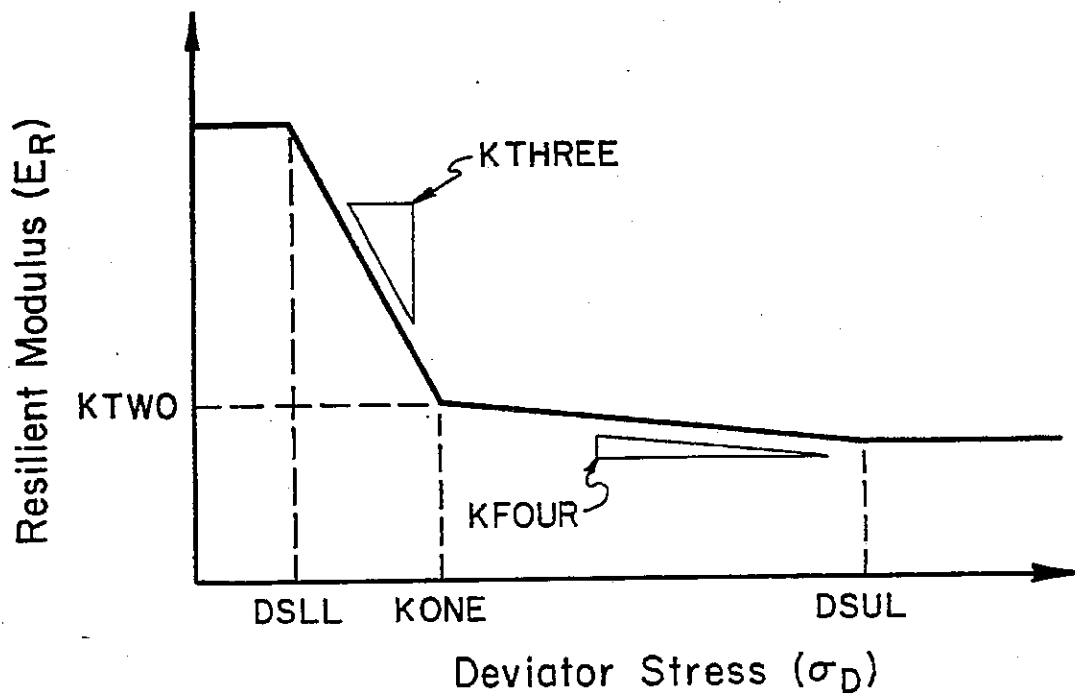


Figure A.5. Idealization of the arithmetic model of fine-grained soil resilient behavior used in the ILLI-PAVE model [TFG, 1990].

modulus. The AC material properties selected are considered consistent with the range of materials and temperatures expected in Illinois.

ILLI-PAVE was executed for conventional flexible sections having AC thicknesses of 2, 3, 4, and 6 in and granular base thicknesses of 6, 9, and 12 in. FULL-DEPTH AC sections of 4, 6, 8, and 10 in were also investigated. Relevant ILLI-PAVE response parameters calculated for conventional and FULL-DEPTH AC pavements subjected to King Air 200 loading are presented in Tables A.1 and A.2, respectively. The variables are defined as follows:

CODE Identification code: VSoft - Very Soft Subgrade
 Soft - Soft Subgrade
 Med - Medium Subgrade
 Stiff - Stiff Subgrade
 Conv - Conventional Pavement
 FD - Full Depth AC Pavement

THICKAC	Thickness of AC layer	inches
MODAC	Modulus of Elasticity of AC layer	ksi
THICKBS	Thickness of granular base	inches
ERI	Subgrade breakpoint resilient modulus	ksi
SURFDEF	Surface deflection at the center of load	mils
SGDEF	Deflection on top of subgrade directly beneath load	mils
ACSTRAIN	Maximum radial strain at bottom of AC layer	Microstrain
SIGMA1	Maximum subgrade vertical stress	psi
SIGMA3	Maximum subgrade confining stress	psi
DEVSTRSS	Maximum subgrade deviator stress	psi
SGUNCNFD	Subgrade unconfined compressive strength	psi
SSR	Subgrade stress ratio (DEVSTRSS/SGUNCNFD)	

Plots of the pavement response parameters make it immediately clear that the same “membrane” behavior observed in previous studies also effect the response of the thin conventional AC pavements under GA loading. This point is illustrated in Figure A.6, which shows the relationship between AC surface thickness and calculated AC tensile strain. As can be seen, there is a decrease in AC strain given a 2-in thick surface compared to a 3-in thick surface. Due to this behavior, and because IDOT-DOA uses a minimum AC thickness of 3 in, all 2-in thick AC sections were eliminated from this analysis.

Examples of typical pavement response plots are provided in Figures A.7 to A.11 for conventional AC pavements and A.12 to A.15 for full depth AC pavements. Figure A.7 shows the relationship between surface deflection and AC thickness for a conventional AC pavement on a soft subgrade with a 9-in thick granular base. The AC modulus was varied

Table A.1. ILLI-PAVE response parameters for conventional AC pavements.

CODE	THICKAC	MODAC	THICKBS	ERT	SURFDEF	SGDEF	ACSTRAIN	SIGMA1	SIGMA3	DEVSTRSS	SGUNCNFD	SSR
VSoft-Conv	2	100	6	1	48.89	40.62	315	6.76	3.46	3.3	6.21	0.531
VSoft-Conv	3	100	6	1	39.16	31.42	714	6.1	3.51	2.59	6.21	0.417
VSoft-Conv	4	100	6	1	33.21	25.89	552	5.72	3.51	2.21	6.21	0.356
VSoft-Conv	6	100	6	1	25.36	18.55	479	5.65	2.3	3.35	6.21	0.539
VSoft-Conv	2	500	6	1	36.96	30.12	614	5.84	3.37	2.47	6.21	0.398
VSoft-Conv	3	500	6	1	25.88	21.01	417	5.98	2.82	3.16	6.21	0.509
VSoft-Conv	4	500	6	1	20.41	16.43	322	5.32	2.18	3.14	6.21	0.506
VSoft-Conv	6	500	6	1	14.21	11.51	188	3.68	1.54	2.14	6.21	0.345
VSoft-Conv	2	1400	6	1	26.22	21.65	240	6.02	3.14	2.88	6.21	0.464
VSoft-Conv	3	1400	6	1	18.23	15.08	243	4.89	1.92	2.97	6.21	0.478
VSoft-Conv	4	1400	6	1	14.09	11.79	156	3.78	1.65	2.13	6.21	0.343
VSoft-Conv	6	1400	6	1	10.13	8.73	75.4	2.53	1.36	1.17	6.21	0.188
Soft-Conv	2	100	6	3.02	38.91	30.57	330	10.4	3.93	6.47	12.9	0.502
Soft-Conv	3	100	6	3.02	32.56	24.74	670	8.99	3.75	5.24	12.9	0.406
Soft-Conv	4	100	6	3.02	28.24	20.77	532	8.01	3.58	4.43	12.9	0.343
Soft-Conv	6	100	6	3.02	22.01	15.21	456	6.71	2.64	4.07	12.9	0.316
Soft-Conv	2	500	6	3.02	30.68	23.9	568	8.51	3.52	4.99	12.9	0.387
Soft-Conv	3	500	6	3.02	22.11	17.34	394	7.21	3.12	4.09	12.9	0.317
Soft-Conv	4	500	6	3.02	17.49	13.57	305	5.94	2.15	3.79	12.9	0.294
Soft-Conv	6	500	6	3.02	12.1	9.38	182	4.23	1.8	2.43	12.9	0.188
Soft-Conv	2	1400	6	3.02	22.49	17.99	234	7.3	3.2	4.1	12.9	0.318
Soft-Conv	3	1400	6	3.02	15.64	12.5	232	5.45	1.92	3.53	12.9	0.274
Soft-Conv	4	1400	6	3.02	11.97	9.65	151	4.47	2.01	2.46	12.9	0.191
Soft-Conv	6	1400	6	3.02	8.37	6.93	75	2.92	1.59	1.33	12.9	0.103
Med-Conv	2	100	6	7.68	28.91	20.69	387	15.3	3.89	11.41	22.85	0.499
Med-Conv	3	100	6	7.68	24.99	17.21	619	12.9	3.73	9.17	22.85	0.401
Med-Conv	4	100	6	7.68	22.21	14.73	513	11	3.22	7.78	22.85	0.340
Med-Conv	6	100	6	7.68	17.82	11.05	428	8.45	2.97	5.48	22.85	0.240
Med-Conv	2	500	6	7.68	23.36	16.81	490	12.5	3.66	8.84	22.85	0.387
Med-Conv	3	500	6	7.68	17.32	12.6	360	9.42	3.36	6.06	22.85	0.265
Med-Conv	4	500	6	7.68	13.85	9.91	282	7.54	2.69	4.85	22.85	0.212
Med-Conv	6	500	6	7.68	9.6	6.85	170	5.05	2.03	3.02	22.85	0.132
Med-Conv	2	1400	6	7.68	17.69	13.16	227	9.99	3.53	6.46	22.85	0.283
Med-Conv	3	1400	6	7.68	12.41	9.26	214	6.89	2.44	4.45	22.85	0.195
Med-Conv	4	1400	6	7.68	9.47	7.11	143	5.07	1.87	3.2	22.85	0.140
Med-Conv	6	1400	6	7.68	6.41	4.93	74.4	3.4	1.7	1.7	22.85	0.074
Stiff-Conv	2	100	6	12.34	24	15.9	369	18.4	3.98	14.42	32.8	0.440
Stiff-Conv	3	100	6	12.34	21.16	13.42	598	15.5	3.86	11.64	32.8	0.355
Stiff-Conv	4	100	6	12.34	19.07	11.58	494	13.2	3.55	9.65	32.8	0.294
Stiff-Conv	6	100	6	12.34	15.61	8.8	410	9.52	2.8	6.72	32.8	0.205
Stiff-Conv	2	500	6	12.34	19.61	13.2	456	15.1	3.96	11.14	32.8	0.340
Stiff-Conv	3	500	6	12.34	14.74	10.06	338	10.7	2.98	7.72	32.8	0.235
Stiff-Conv	4	500	6	12.34	11.88	8	269	8.53	2.78	5.75	32.8	0.175
Stiff-Conv	6	500	6	12.34	8.3	5.53	163	5.7	2.23	3.47	32.8	0.106
Stiff-Conv	2	1400	6	12.34	15.04	10.53	219	11.6	3.26	8.34	32.8	0.254
Stiff-Conv	3	1400	6	12.34	10.66	7.5	202	8.06	2.81	5.25	32.8	0.160
Stiff-Conv	4	1400	6	12.34	8.15	5.76	138	5.84	2.14	3.7	32.8	0.113
Stiff-Conv	6	1400	6	12.34	5.47	3.94	73	3.79	1.79	2	32.8	0.061
VSoft-Conv	2	100	9	1	40.06	29.7	338	6.01	3.53	2.48	6.21	0.399
VSoft-Conv	3	100	9	1	34.23	24.49	671	5.68	3.59	2.09	6.21	0.337
VSoft-Conv	4	100	9	1	30.09	20.63	519	6.35	2.99	3.36	6.21	0.541
VSoft-Conv	6	100	9	1	24.13	15.8	446	5.41	2.19	3.22	6.21	0.519
VSoft-Conv	2	500	9	1	32.54	23.84	537	5.57	3.56	2.01	6.21	0.324
VSoft-Conv	3	500	9	1	24.52	17.98	393	5.81	2.49	3.32	6.21	0.535
VSoft-Conv	4	500	9	1	19.78	14.5	311	4.87	2.01	2.86	6.21	0.461
VSoft-Conv	6	500	9	1	14.02	10.53	184	3.57	1.67	1.9	6.21	0.306
VSoft-Conv	2	1400	9	1	24.77	18.38	219	6.06	2.74	3.32	6.21	0.535
VSoft-Conv	3	1400	9	1	17.87	13.54	236	4.4	1.74	2.66	6.21	0.428
VSoft-Conv	4	1400	9	1	13.94	10.82	153	3.48	1.5	1.98	6.21	0.319
VSoft-Conv	6	1400	9	1	10.1	8.24	74.6	2.8	1.78	1.02	6.21	0.164
Soft-Conv	2	100	9	3.02	33.82	23.3	343	8.5	3.52	4.98	12.9	0.386
Soft-Conv	3	100	9	3.02	29.53	19.7	630	7.69	3.45	4.24	12.9	0.329
Soft-Conv	4	100	9	3.02	26.26	16.82	508	7.45	3.11	4.34	12.9	0.336
Soft-Conv	6	100	9	3.02	21.2	12.89	438	6.1	2.44	3.66	12.9	0.284

Table A.1. ILLI-PAVE response parameters for conventional AC pavements.

CODE	THICKAC	MODAC	THICKBS	ERI	SURFDEF	SGDEF	ACSTRAIN	SIGMA1	SIGMA3	DEVSTRSS	SGUNCNFD	SSR
Soft-Conv	2	500	9	3.02	28.01	19.29	512	7.49	3.37	4.12	12.9	0.319
Soft-Conv	3	500	9	3.02	21.23	14.81	375	6.49	2.37	4.12	12.9	0.319
Soft-Conv	4	500	9	3.02	17.11	11.89	299	5.44	2.08	3.36	12.9	0.260
Soft-Conv	6	500	9	3.02	12.01	8.48	180	4	1.85	2.15	12.9	0.167
Soft-Conv	2	1400	9	3.02	21.55	15.18	218	6.46	2.42	4.04	12.9	0.313
Soft-Conv	3	1400	9	3.02	15.45	11.1	226	5.04	1.94	3.1	12.9	0.240
Soft-Conv	4	1400	9	3.02	11.92	8.74	150	4.04	1.84	2.2	12.9	0.171
Soft-Conv	6	1400	9	3.02	8.38	6.49	74.9	2.96	1.75	1.21	12.9	0.094
Med-Conv	2	100	9	7.68	26.81	16.15	384	12.2	3.84	8.36	22.85	0.366
Med-Conv	3	100	9	7.68	23.84	13.87	603	10.5	3.55	6.95	22.85	0.304
Med-Conv	4	100	9	7.68	21.48	12.04	501	9.2	3.16	6.04	22.85	0.264
Med-Conv	6	100	9	7.68	17.6	9.29	423	7.15	2.37	4.78	22.85	0.209
Med-Conv	2	500	9	7.68	22.38	13.75	462	10.1	3.19	6.91	22.85	0.302
Med-Conv	3	500	9	7.68	17.12	10.71	350	8.04	2.83	5.21	22.85	0.228
Med-Conv	4	500	9	7.68	13.83	8.62	280	6.4	2.14	4.26	22.85	0.186
Med-Conv	6	500	9	7.68	9.67	6.07	171	4.55	1.92	2.63	22.85	0.115
Med-Conv	2	1400	9	7.68	17.42	11.12	217	8.34	2.84	5.5	22.85	0.241
Med-Conv	3	1400	9	7.68	12.5	8.1	213	6.01	2.2	3.81	22.85	0.167
Med-Conv	4	1400	9	7.68	9.56	6.31	143	4.58	1.84	2.74	22.85	0.120
Med-Conv	6	1400	9	7.68	6.49	4.52	74	3.36	1.86	1.5	22.85	0.066
Stiff-Conv	2	100	9	12.34	23.19	12.55	384	14	3.53	10.47	32.8	0.319
Stiff-Conv	3	100	9	12.34	20.85	10.89	596	12	3.18	8.82	32.8	0.269
Stiff-Conv	4	100	9	12.34	18.94	9.48	486	10.4	2.92	7.48	32.8	0.228
Stiff-Conv	6	100	9	12.34	15.69	7.34	412	8	2.55	5.45	32.8	0.166
Stiff-Conv	2	500	9	12.34	19.38	10.82	441	11.4	2.78	8.62	32.8	0.263
Stiff-Conv	3	500	9	12.34	14.9	8.52	336	8.96	2.73	6.23	32.8	0.190
Stiff-Conv	4	500	9	12.34	12.09	6.87	268	7.19	2.29	4.9	32.8	0.149
Stiff-Conv	6	500	9	12.34	8.47	4.85	165	5.18	2.2	2.98	32.8	0.091
Stiff-Conv	2	1400	9	12.34	15.17	8.85	214	9.56	3.07	6.49	32.8	0.198
Stiff-Conv	3	1400	9	12.34	10.92	8.37	204	6.93	2.51	4.42	32.8	0.135
Stiff-Conv	4	1400	9	12.34	8.35	5.06	139	5.25	2.15	3.1	32.8	0.095
Stiff-Conv	6	1400	9	12.34	5.58	3.55	73.7	3.7	2.02	1.68	32.8	0.051
VSoft-Conv	2	100	12	1	35.13	22.62	336	6.2	3.38	2.82	6.21	0.454
VSoft-Conv	3	100	12	1	31.3	19.52	623	6.41	2.73	3.68	6.21	0.593
VSoft-Conv	4	100	12	1	28.36	17.28	496	6.01	2.64	3.37	6.21	0.543
VSoft-Conv	6	100	12	1	23.32	13.78	447	4.98	2.11	2.87	6.21	0.462
VSoft-Conv	2	500	12	1	29.91	19.29	504	6.33	2.96	3.37	6.21	0.543
VSoft-Conv	3	500	12	1	23.42	15.51	374	5.29	2.14	3.15	6.21	0.507
VSoft-Conv	4	500	12	1	19.25	12.9	302	4.59	2.06	2.53	6.21	0.407
VSoft-Conv	6	500	12	1	13.84	9.69	182	3.5	1.84	1.66	6.21	0.267
VSoft-Conv	2	1400	12	1	23.65	15.81	208	5.38	2.26	3.12	6.21	0.502
VSoft-Conv	3	1400	12	1	17.49	12.13	231	4.09	1.68	2.41	6.21	0.388
VSoft-Conv	4	1400	12	1	13.79	9.96	151	3.5	1.81	1.69	6.21	0.272
VSoft-Conv	6	1400	12	1	10.06	7.84	74.2	2.8	1.8	1	6.21	0.161
Soft-Conv	2	100	12	3.02	30.84	18.22	340	7.78	3.63	4.15	12.9	0.322
Soft-Conv	3	100	12	3.02	27.64	15.87	615	7.19	2.91	4.28	12.9	0.332
Soft-Conv	4	100	12	3.02	25.12	14.06	498	6.53	2.53	4	12.9	0.310
Soft-Conv	6	100	12	3.02	20.71	11.15	432	5.43	2.14	3.29	12.9	0.255
Soft-Conv	2	500	12	3.02	26.24	15.74	476	7.1	2.99	4.11	12.9	0.319
Soft-Conv	3	500	12	3.02	20.52	12.65	362	5.82	2.13	3.69	12.9	0.286
Soft-Conv	4	500	12	3.02	16.82	10.47	292	5.05	2.13	2.92	12.9	0.226
Soft-Conv	6	500	12	3.02	11.93	7.73	177	3.8	1.88	1.92	12.9	0.149
Soft-Conv	2	1400	12	3.02	20.78	12.96	209	5.92	2.18	3.74	12.9	0.290
Soft-Conv	3	1400	12	3.02	15.22	9.81	223	4.8	2.14	2.66	12.9	0.206
Soft-Conv	4	1400	12	3.02	11.86	7.96	148	3.91	1.98	1.93	12.9	0.150
Soft-Conv	6	1400	12	3.02	8.39	6.11	74.6	2.97	1.84	1.13	12.9	0.088
Med-Conv	2	100	12	7.68	25.6	12.88	388	9.85	3.35	6.5	22.85	0.284
Med-Conv	3	100	12	7.68	23.09	11.31	589	8.74	3.11	5.63	22.85	0.246
Med-Conv	4	100	12	7.68	21.13	10.04	496	7.82	2.72	5.1	22.85	0.223
Med-Conv	6	100	12	7.68	17.55	7.97	418	6.35	2.32	4.03	22.85	0.176
Med-Conv	2	500	12	7.68	21.7	11.25	455	8.78	3.27	5.51	22.85	0.241
Med-Conv	3	500	12	7.68	16.92	9.07	344	7.02	2.51	4.51	22.85	0.197
Med-Conv	4	500	12	7.68	13.86	7.5	278	5.83	2.23	3.6	22.85	0.158
Med-Conv	6	500	12	7.68	9.74	5.46	170	4.34	2.04	2.3	22.85	0.101

Table A.1. ILLI-PAVE response parameters for conventional AC pavements.

CODE	THICKAC	MODAC	THICKBS	ERI	SURFDEF	SGDEF	ACSTRAIN	SIGMA1	SIGMA3	DEVSTRSS	SGUNCNFD	SSR
Med-Conv	2	1400	12	7.68	17.19	9.36	211	7.1	2.43	4.67	22.85	0.204
Med-Conv	3	1400	12	7.68	12.52	7.06	212	5.4	2.08	3.32	22.85	0.145
Med-Conv	4	1400	12	7.68	9.65	5.66	143	4.17	1.74	2.43	22.85	0.106
Med-Conv	6	1400	12	7.68	6.56	4.19	74.4	3.27	1.91	1.36	22.85	0.060
Stiff-Conv	2	100	12	12.34	22.8	10.06	373	11.2	3.13	8.07	32.8	0.246
Stiff-Conv	3	100	12	12.34	20.67	8.86	576	9.7	2.84	6.86	32.8	0.209
Stiff-Conv	4	100	12	12.34	19.03	7.9	497	8.55	2.56	5.99	32.8	0.183
Stiff-Conv	6	100	12	12.34	15.89	6.26	413	7.04	2.49	4.55	32.8	0.139
Stiff-Conv	2	500	12	12.34	19.27	8.87	440	9.82	3.12	6.7	32.8	0.204
Stiff-Conv	3	500	12	12.34	15.02	7.16	333	7.7	2.47	5.23	32.8	0.159
Stiff-Conv	4	500	12	12.34	12.31	5.93	270	6.41	2.29	4.12	32.8	0.126
Stiff-Conv	6	500	12	12.34	8.64	4.31	166	4.74	2.16	2.58	32.8	0.079
Stiff-Conv	2	1400	12	12.34	15.26	7.41	211	8.03	2.61	5.42	32.8	0.165
Stiff-Conv	3	1400	12	12.34	11.1	5.6	204	5.96	2.17	3.79	32.8	0.116
Stiff-Conv	4	1400	12	12.34	8.53	4.48	140	4.78	2.11	2.67	32.8	0.081
Stiff-Conv	6	1400	12	12.34	5.69	3.26	73.9	3.53	2.01	1.52	32.8	0.046

Table A.2. ILLI-PAVE response parameters for full-depth AC pavements.

CODE	THICKAC	MODAC	ERI	SURFDEF	SGDEF	ACSTRAIN	SIGMA1	SIGMA3	DEVSTRSS	SGUNCNFD	SSR
VSoft-FD	4	100	1.00	48.60	46.87	1198.4	7.20	3.77	3.43	6.21	0.552
VSoft-FD	6	100	1.00	30.02	27.57	672.0	5.13	3.09	2.04	6.21	0.329
VSoft-FD	8	100	1.00	22.84	19.62	443.5	5.52	2.85	2.67	6.21	0.430
VSoft-FD	10	100	1.00	18.91	15.15	285.7	4.99	2.04	2.95	6.21	0.475
VSoft-FD	4	500	1.00	21.85	21.46	345.6	6.64	3.09	3.55	6.21	0.572
VSoft-FD	6	500	1.00	14.51	13.96	189.7	4.41	1.93	2.48	6.21	0.399
VSoft-FD	8	500	1.00	11.41	10.71	120.3	3.21	1.49	1.72	6.21	0.277
VSoft-FD	10	500	1.00	9.80	8.99	76.5	2.65	1.45	1.20	6.21	0.193
VSoft-FD	4	1400	1.00	14.34	14.19	164.0	4.52	2.13	2.39	6.21	0.385
VSoft-FD	6	1400	1.00	10.19	9.97	84.8	2.74	1.42	1.32	6.21	0.213
VSoft-FD	8	1400	1.00	8.60	8.32	51.1	2.21	1.32	0.89	6.21	0.143
VSoft-FD	10	1400	1.00	7.83	7.51	32.1	2.05	1.38	0.67	6.21	0.108
Soft-FD	4	100	3.02	38.69	36.90	1060.8	12.50	5.63	6.87	12.9	0.533
Soft-FD	6	100	3.02	25.21	22.70	618.2	8.26	3.85	4.41	12.9	0.342
Soft-FD	8	100	3.02	19.63	16.39	415.4	6.72	3.07	3.65	12.9	0.283
Soft-FD	10	100	3.02	16.38	12.61	269.4	5.72	2.81	2.91	12.9	0.226
Soft-FD	4	500	3.02	18.47	18.08	327.5	7.68	3.59	4.09	12.9	0.317
Soft-FD	6	500	3.02	12.19	11.64	181.7	5.12	2.15	2.97	12.9	0.230
Soft-FD	8	500	3.02	9.47	8.77	116.4	3.72	1.58	2.14	12.9	0.166
Soft-FD	10	500	3.02	8.01	7.20	74.6	2.98	1.48	1.50	12.9	0.116
Soft-FD	4	1400	3.02	12.05	11.90	157.6	5.30	2.42	2.88	12.9	0.223
Soft-FD	6	1400	3.02	8.32	8.10	82.8	3.19	1.52	1.67	12.9	0.129
Soft-FD	8	1400	3.02	6.84	6.56	50.3	2.45	1.36	1.09	12.9	0.084
Soft-FD	10	1400	3.02	6.12	5.78	31.7	2.20	1.40	0.80	12.9	0.062
Med-FD	4	100	7.68	27.25	25.43	861.8	20.50	7.28	13.22	22.85	0.579
Med-FD	6	100	7.68	19.17	16.61	530.2	12.70	4.05	8.65	22.85	0.379
Med-FD	8	100	7.68	15.54	12.25	364.1	9.22	2.99	6.23	22.85	0.273
Med-FD	10	100	7.68	13.26	9.46	240.9	7.17	2.37	4.80	22.85	0.210
Med-FD	4	500	7.68	14.09	13.70	295.8	10.30	4.43	5.87	22.85	0.257
Med-FD	6	500	7.68	9.37	8.82	167.4	6.61	2.49	4.12	22.85	0.180
Med-FD	8	500	7.68	7.24	6.54	109.0	4.67	1.80	2.87	22.85	0.126
Med-FD	10	500	7.68	6.04	5.22	70.8	3.65	1.55	2.10	22.85	0.092
Med-FD	4	1400	7.68	9.26	9.10	146.2	6.91	2.99	3.92	22.85	0.172
Med-FD	6	1400	7.68	6.22	5.99	78.7	4.10	1.75	2.35	22.85	0.103
Med-FD	8	1400	7.68	4.94	4.66	48.6	2.98	1.51	1.47	22.85	0.064
Med-FD	10	1400	7.68	4.29	3.97	30.9	2.52	1.43	1.09	22.85	0.048
Stiff-FD	4	100	12.34	21.56	19.73	740.7	25.80	7.82	17.98	32.8	0.548
Stiff-FD	6	100	12.34	15.90	13.31	470.1	15.80	4.04	11.76	32.8	0.359
Stiff-FD	8	100	12.34	13.27	9.95	325.5	11.20	2.79	8.41	32.8	0.256
Stiff-FD	10	100	12.34	11.56	7.73	218.9	8.48	2.39	6.09	32.8	0.186
Stiff-FD	4	500	12.34	11.61	11.22	271.0	12.90	4.88	8.02	32.8	0.245
Stiff-FD	6	500	12.34	7.86	7.30	156.7	7.85	2.64	5.21	32.8	0.159
Stiff-FD	8	500	12.34	6.10	5.40	103.0	5.53	1.91	3.62	32.8	0.110
Stiff-FD	10	500	12.34	5.07	4.26	67.6	4.23	1.64	2.59	32.8	0.079
Stiff-FD	4	1400	12.34	7.75	7.59	137.4	8.29	3.40	4.89	32.8	0.149
Stiff-FD	6	1400	12.34	5.17	4.95	75.3	4.86	1.94	2.92	32.8	0.089
Stiff-FD	8	1400	12.34	4.04	3.76	47.0	3.47	1.51	1.96	32.8	0.060
Stiff-FD	10	1400	12.34	3.45	3.13	30.2	2.82	1.46	1.36	32.8	0.041

Conventional AC: AC Strain vs. AC Thickness

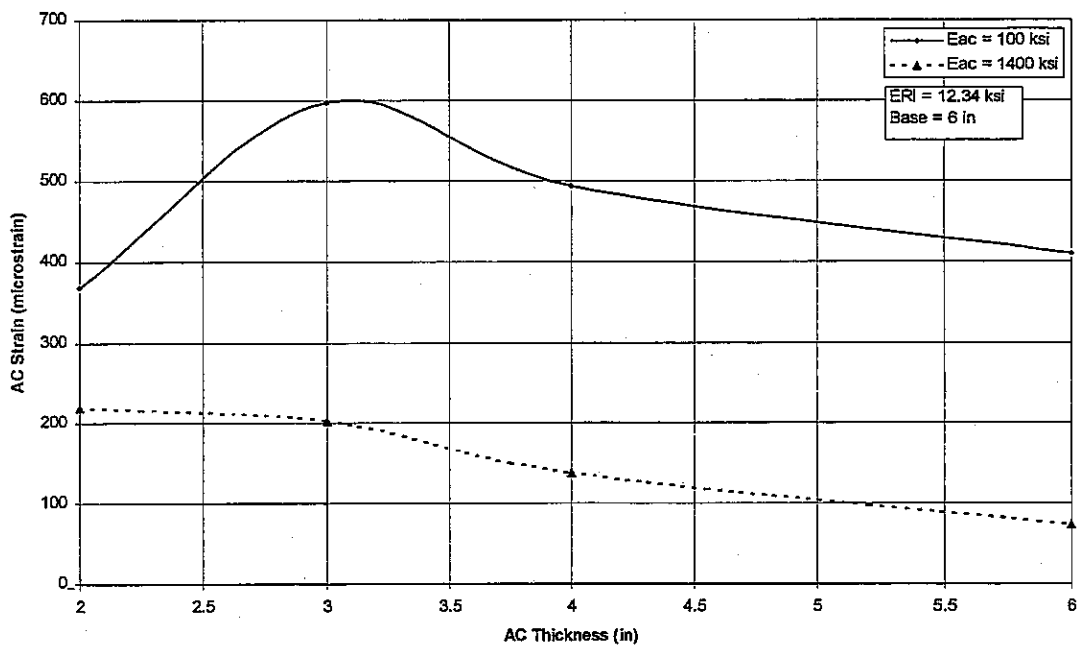


Figure A.6. Illustration of membrane behavior in thin AC layers.

Conventional AC: AC Thickness vs. Surface Deflection

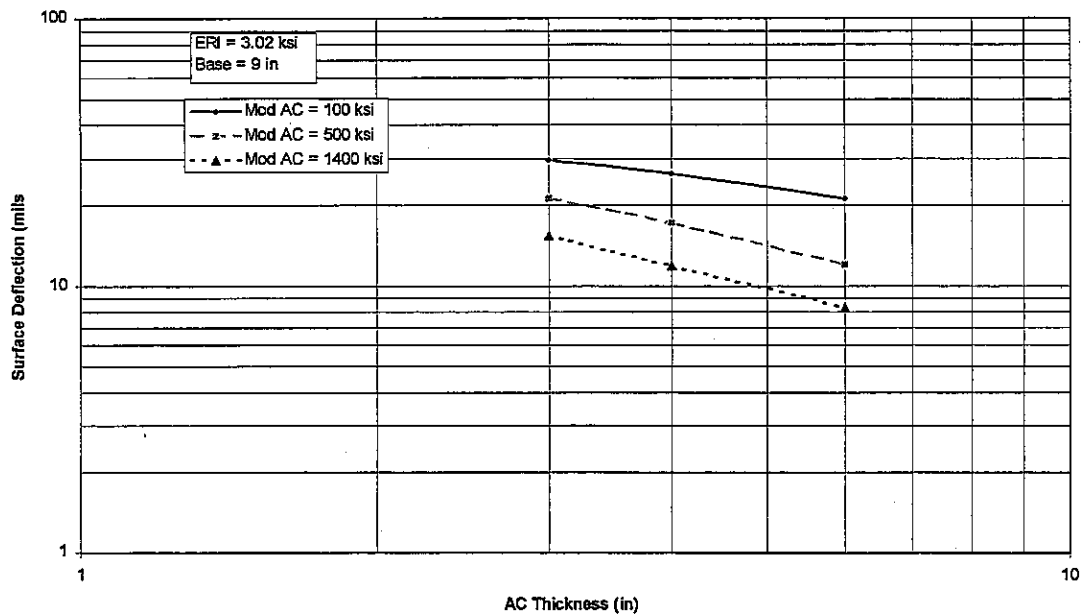


Figure A.7. Relationship between AC thickness and surface deflection (at center of load) for a soft subgrade and a 9 in thick base.

Conventional AC: AC Tensile Strain vs. AC Thickness

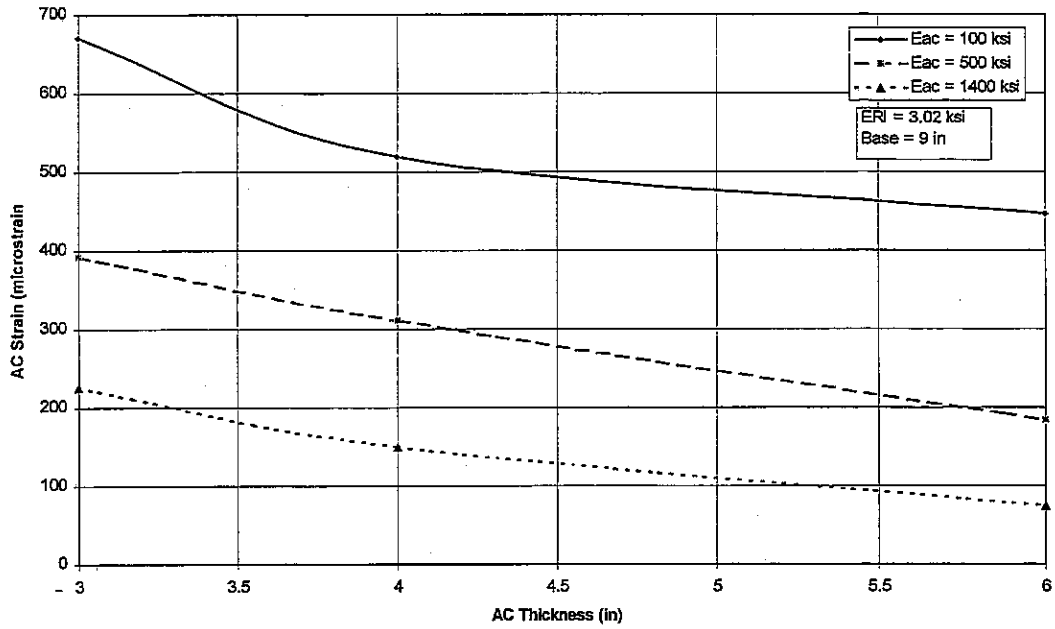


Figure A.8. Relationship between AC strain and AC thickness for soft subgrade and a 9 in base.

Conventional AC: AC Strain vs. Surface Deflection

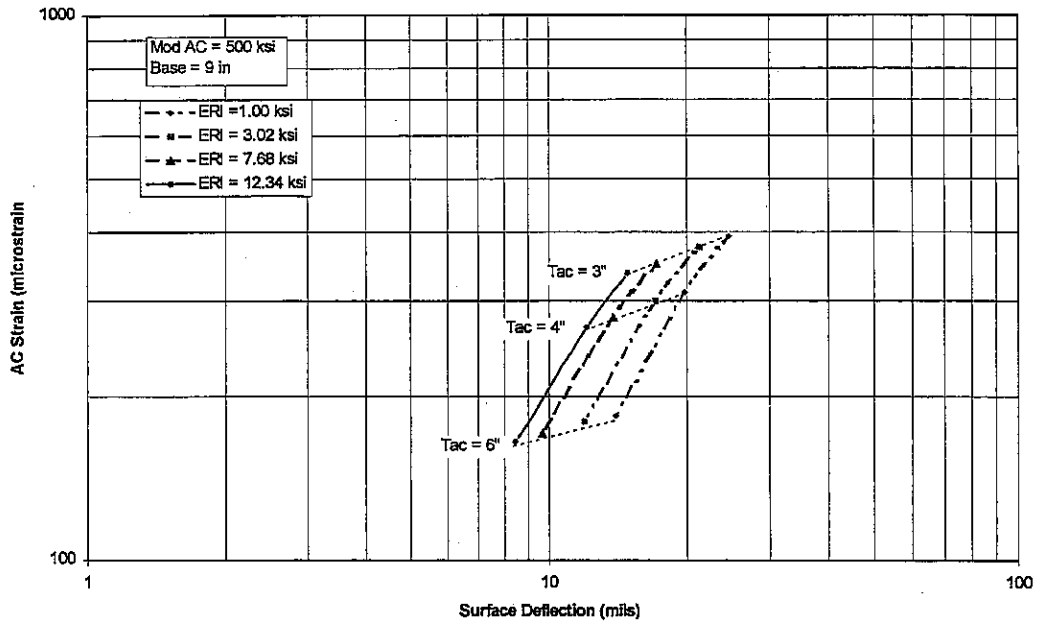


Figure A.9. Relationship between AC strain and surface deflection for AC modulus of 500 ksi and 9 in base.

Conventional AC: AC Strain vs. Surface Deflection

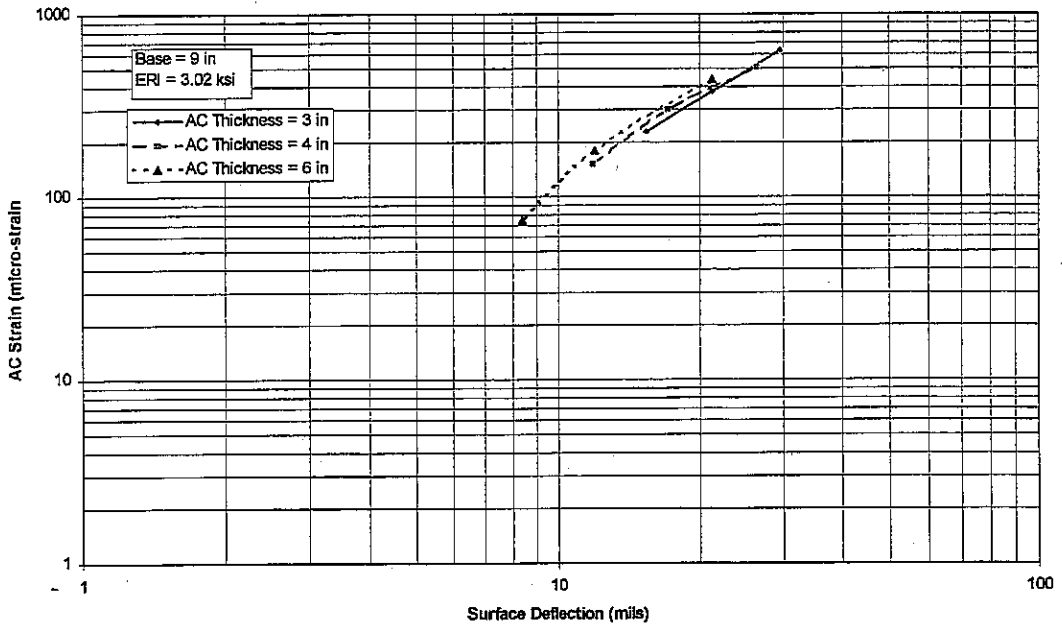


Figure A.10. Relationship between AC strain and surface deflection for a soft subgrade and a 9 in base (E_{AC} varies from 100 ksi to 1400 ksi).

Conventional AC: Stress Ratio vs. Surface Deflection

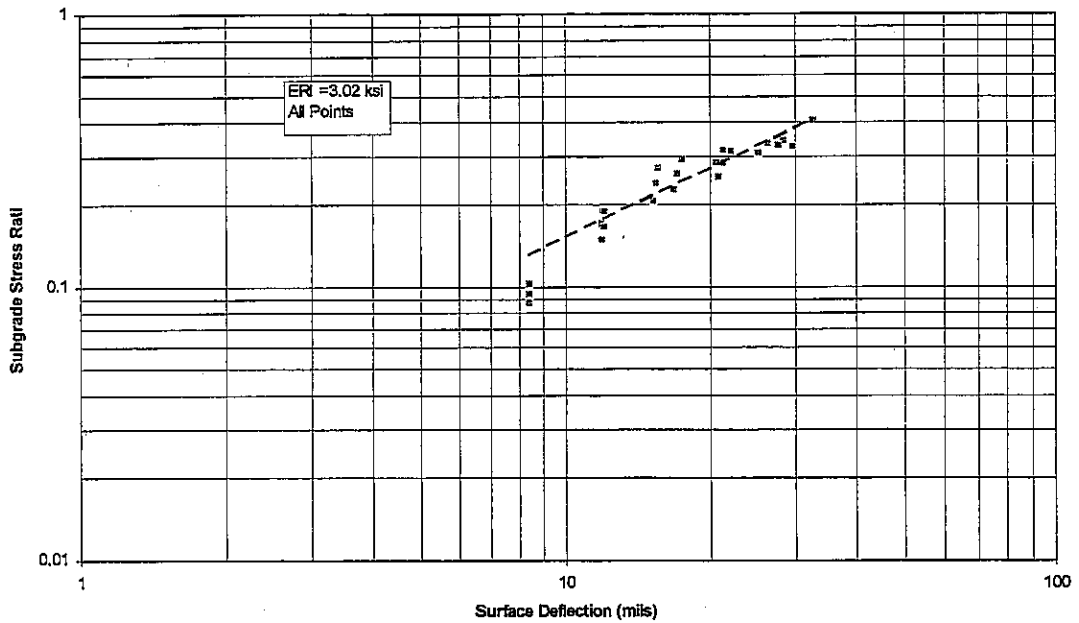


Figure A.11. Variation of subgrade stress ratio as a function of surface deflection for a soft subgrade.

Full-Depth AC: Surface Deflection versus AC Thickness

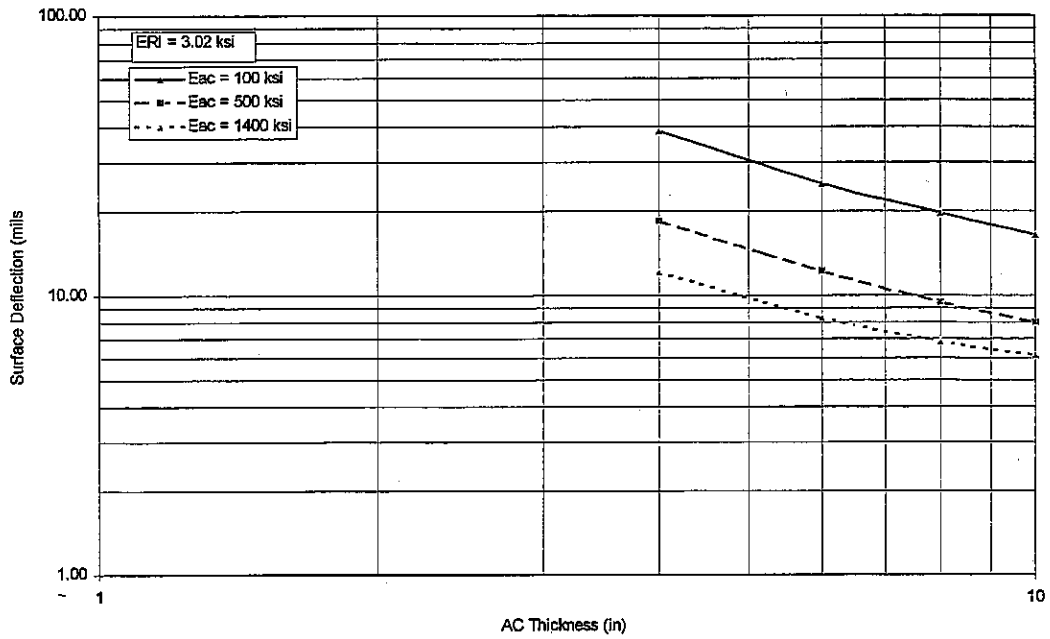


Figure A.12. Relationship between AC thickness and surface deflection for soft subgrade (at center of loading).

Full-Depth AC: Maximum AC Tensile Strain versus Surface Deflection

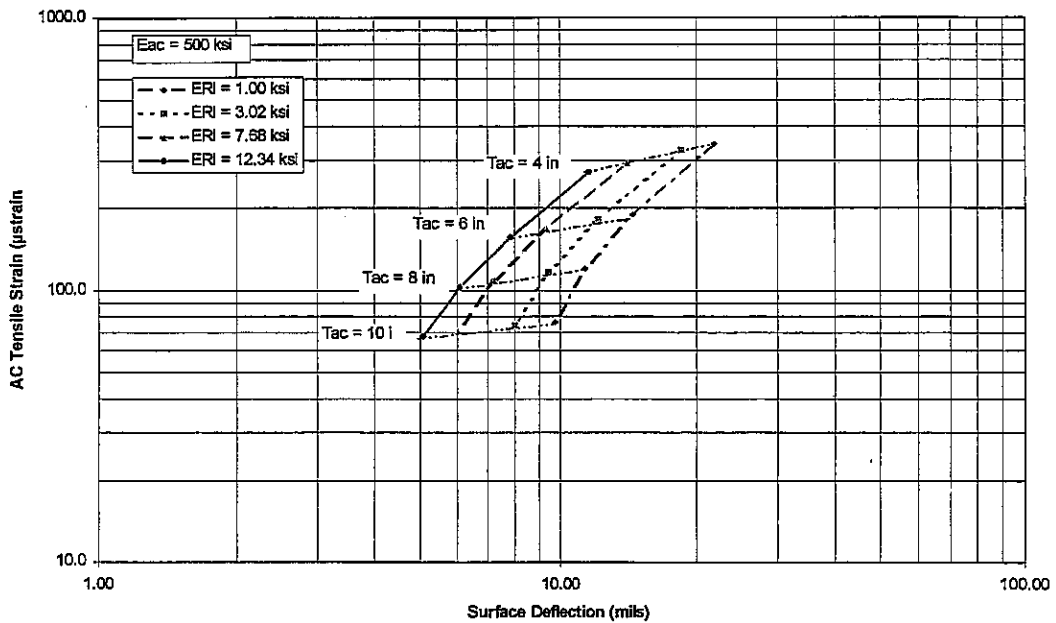


Figure A.13. Relationship between maximum AC tensile strain at the bottom of AC and surface deflection for AC modulus of 500 ksi.

Full Depth AC: Surface Deflection versus Tensile Strain

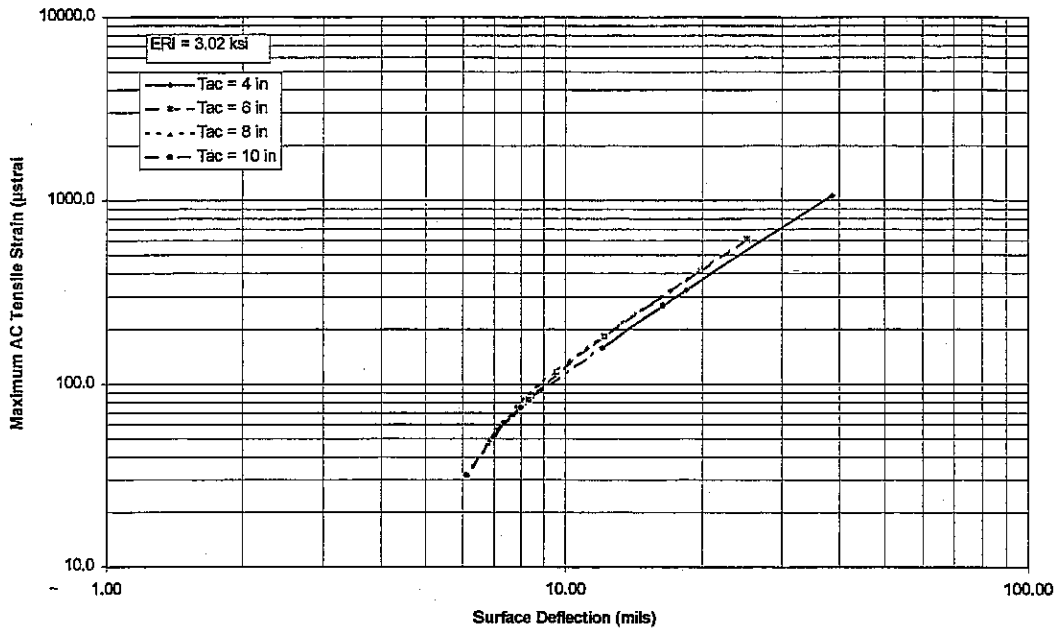


Figure A.14. Relationship between surface deflection and maximum tensile strain at bottom of AC layer for soft subgrade (E_{AC} varies from 100 ksi to 1400 ksi).

Full Depth AC: Stress Ratio versus Surface Deflection

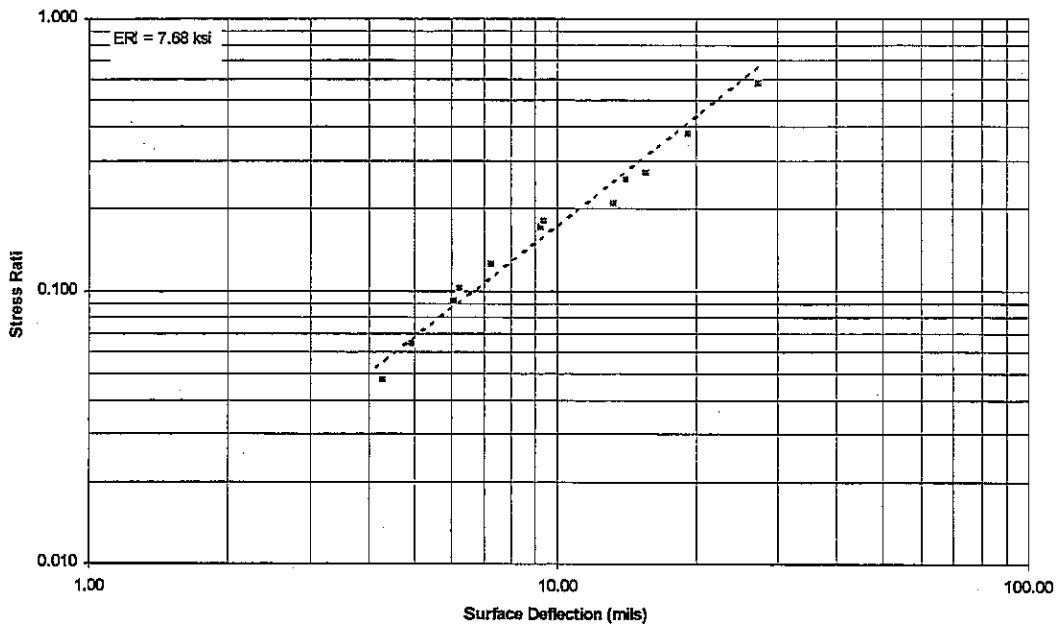


Figure A.15. Variation of subgrade stress ratio as a function of surface deflection for a medium subgrade.

from 100 ksi to 1400 ksi. There is a strong correlation between the surface deflection, the AC thickness, and the AC modulus. As either the AC thickness or AC modulus increases, there is an observed decrease in surface deflection. Figure A.12 for a full depth AC pavement on a soft subgrade shows similar relationships.

Figure A.9 shows the relationship between AC strain and surface deflection in a conventional AC pavement. The AC modulus was set at 500 ksi and a 9-in thick granular base was placed above the subgrade. For a given thickness of AC, there is an increase in AC strain as deflection increases. Both AC strain and surface deflection are reduced with increase AC thickness. Figure A.13 shows the same relationship for full depth AC pavement. Once again, similar trends are observed.

Figure A.10 shows the relationship between AC strain and surface deflection given a 9-in thick base on a soft subgrade. Surface deflection is correlated to AC strain, even over a wide range of AC moduli and thicknesses. As expected, a similar trend is observed for full depth AC as seen in Figure A.14.

Figures A.11 and A.15 show the relationship between the subgrade stress ratio and surface deflection for conventional and full depth AC pavements, respectively. These plots suggest good correlation between the two variables.

As mentioned in Section IV.2.4 in the study, the Systat® statistical analysis program was used to develop pavement response algorithms using the same model forms previously developed for highway conditions [Thompson, 1985] [Gomez-Achecar, 1986]. These algorithms for conventional and FULL-DEPTH pavements are presented in Tables 14 and 15, respectively.



APPENDIX B: FWD TESTING PROCEDURES AND ANALYSIS AT PONTIAC AND MORRIS AIRPORTS

Introduction

Nondestructive deflection testing (NDT) was conducted on two airport projects that were constructed in 1992. One was the new airport at Pontiac, where conventional flexible pavements (3-in P-401 AC, 8-in thick P-209 granular base, 8-in thick lime treated subgrade) were constructed on a runway, taxiway, and apron. The second airport was Morris, where testing was conducted on the new runway and taxiway. The Morris pavements were similar to FULL-DEPTH AC construction (9.5-in P-401/P-201 AC over a 4-in thick P-209 granular base). AC-10 asphalt cement was used in all the AC mixtures. This appendix describes the FWD testing procedures used and the analysis of the collected data.

Testing Procedure

Testing was conducted by the Illinois Department of Transportation (IDOT) with the Dynatest falling weight deflectometer (FWD). The FWD applies an impulse load to the pavement by dropping a weight package onto a 11.81 in (300 mm) diameter loading plate. The magnitude of the load is varied by adjusting the drop height and the weight of the load package. The equipment has a loading range of approximately 4,000 lbs to 27,000 lbs. Four load ranges (approximately 5,500, 7,000, 9,000, and 11,500 lbs) were used in this study.

Load induced deflections are measured through a series of velocity transducers. The recorded pavement deflection is the maximum transducer deflection. In this study, four sensors were used. One was located at the center of the loading plate and the remaining three at 12, 24, and 36 in offsets. The deflection data define the deflection basin.

A temperature point was established in a location representative of the pavement structure. At this point, a hole was drilled to the mid-depth of the pavement and filled with

antifreeze. Temperatures were taken at the pavement surface and at the pavement mid-depth. An FWD test was then conducted. The temperature point was tested again during the course of testing and after testing was completed.

Each 4,000 ft by 75 ft runway was evaluated using the same procedure. Testing was conducted at an approximate offset of 6 ft to each side of the runway centerline in the middle of the paving lane. In the sequence of testing, the first test was conducted to the right of the centerline 100 ft from the runway end. Subsequent tests were then conducted at 200 ft intervals for the entire length of the runway. Testing in the opposite direction was also conducted at 200 ft intervals, but at even stations (i.e. 200 ft, 400 ft, etc.). Thus, test points were staggered at 100 ft intervals for the entire length of the runway.

Testing on the two 35 ft wide taxiways was conducted in a similar manner, although the offset distance from the centerline varied depending on the orientation of the paving lane. Tests were again conducted at 100 ft intervals, staggered from side to side.

At Pontiac, a small apron (150 ft by 250 ft) was also tested. Two north-south testing lanes were chosen and tested at 50 ft intervals. One lane was offset 25 ft from the western edge of the apron and the other 45 ft from the eastern edge of the apron.

The deflection data were normalized to standardized loads of 5,500, 7,000, 9,000, 11,500 lbs. This normalization was conducted assuming a linear load-deflection relationship. Table B.1 and B.2. summarize the normalized deflection data for the Pontiac and Morris airport pavement sections, respectively.

Table B.1. Summary of Pontiac deflection data.

Feature	Load (kips)	D ₀ (mils)		D ₁ (mils)		D ₂ (mils)		D ₃ (mils)	
		Mean	COV	Mean	COV	Mean	COV	Mean	COV
RW	5.5	12.96	22%	6.72	22%	3.35	20%	2.28	21%
	7.0	17.50	22%	9.28	23%	4.66	21%	3.18	21%
	9.0	23.60	22%	12.62	23%	6.37	21%	4.32	22%
	11.5	30.47	24%	16.35	24%	8.21	22%	5.51	22%
TW	5.5	8.54	23%	4.52	18%	2.35	11%	1.65	14%
	7.0	11.17	23%	6.15	19%	3.29	11%	2.32	14%
	9.0	15.07	23%	8.41	19%	4.59	12%	3.23	14%
	11.5	18.98	24%	10.65	19%	5.85	13%	4.09	14%
AP	5.5	13.93	19%	7.08	23%	3.22	25%	2.03	28%
	7.0	18.51	19%	9.69	23%	4.54	25%	2.87	27%
	9.0	25.07	18%	13.25	22%	6.31	25%	3.97	26%
	11.5	32.33	18%	17.18	23%	8.21	25%	5.13	27%

Table B.2. Summary of Morris deflection data.

Feature	Load (kips)	D ₀ (mils)		D ₁ (mils)		D ₂ (mils)		D ₃ (mils)	
		Mean	COV	Mean	COV	Mean	COV	Mean	COV
RW	5.5	5.42	16%	4.24	19%	3.09	23%	2.12	27%
	7.0	7.40	17%	5.88	20%	4.27	23%	2.95	27%
	9.0	9.88	17%	7.87	19%	5.72	22%	3.94	26%
	11.5	12.49	17%	9.94	19%	7.25	22%	4.98	25%
TW	5.5	6.10	21%	4.43	18%	3.06	17%	1.97	18%
	7.0	8.39	22%	6.27	19%	4.31	18%	2.80	19%
	9.0	10.60	19%	8.23	19%	5.74	19%	3.75	20%
	-11.5	14.59	24%	10.97	20%	7.58	18%	4.93	18%

Backcalculation

Temperature

At Pontiac, the pavement surface temperatures increased from 59° F to 71° F during the course of testing, corresponding to a rise in the 1.5 in depth pavement temperature from 65° F to 69° F. At Morris, pavement surface temperature ranged from 74° F to 92° F. The corresponding pavement temperature (at a depth of approximately 4 in) ranged from 72° F to 80° F. The deflection data were not adjusted for temperature.

Backcalculation Algorithms

Backcalculation was accomplished using ILLI-PAVE backcalculation algorithms derived for a normalized 9,000 lb load condition. The following algorithms, developed by the University of Illinois for the use of IDOT-DOH, were used in this study [Thompson, 1989]:

E_{Ri} for thin AC

$$R_i = 25.0 - 5.25D_3 + 0.29D_3^2 \quad \text{Equation B.1}$$

E_{Ri} for FULL-DEPTH AC

$$R_i = 24.7 - 5.41D_3 + 0.31D_3^2 \quad \text{Equation B.2}$$

E_{AC} for FULL-DEPTH AC

$$\begin{aligned} \text{Log}E_{AC} = & 1.846 - 4.902\text{Log}(D_0 - D_1) + \\ & 5.189\text{Log}(D_0 - D_2) - 1.282\text{Log}(D_1 - D_3) \end{aligned} \quad \text{Equation B.3}$$

- Where:
- E_{Ri} is the subgrade breakpoint resilient modulus, ksi.
 - E_{AC} is the resilient modulus of the AC, ksi.
 - D₀ is the deflection at the center of the load plate, mils.
 - D₁, D₂, and D₃ are the deflections at a 12, 24, and 36 in offset, mils.

These algorithms were derived from ILLI-PAVE data bases specifically for backcalculation purposes. The backcalculation of E_{AC} for thin (less than 3-in to 4-in thick) AC layers is not reliable. Thus, E_{AC} values were not calculated for the Pontiac data.

Pontiac

Table B.3 is a summary of the maximum deflection and the backcalculated E_{Ri} results for Pontiac. Normalized (@ 9,000 lbs) maximum deflection profile plots for the runway, taxiway, and apron at Pontiac are shown in Figures B.1, B.2, and B.3. Profile plots of the backcalculated E_{Ri} values for these same features are shown in Figures B.4, B.5, and B.6.

Table B.3. Summary of backcalculation analysis for Pontiac
(for 9,000 lb normalized load).

Feature	Max. Deflection (mils)			ERI (ksi)		
	Mean	Std. Dev.	COV	Mean	Std. Dev.	COV
Runway	23.6	3.24	14%	8.0	2.50	31%
Taxiway	15.1	3.52	23%	10.6	2.27	21%
Apron	23.7	4.00	17%	9.26	2.75	30%

Pontiac: RW Max. Deflection

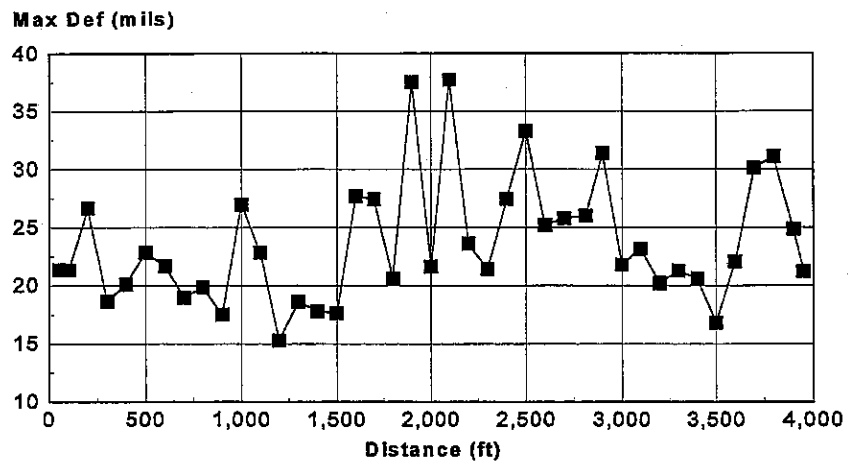


Figure B.1. Pontiac runway maximum deflection profile (@ 9,000 lbs).

Pontiac: TW Max. Deflection

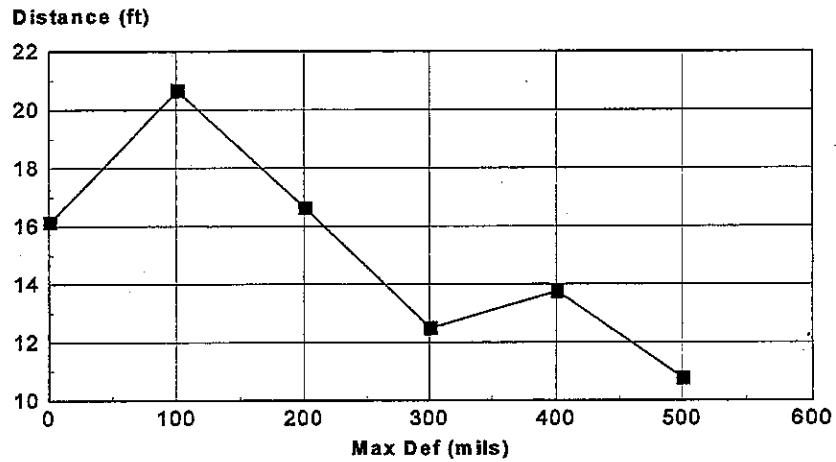


Figure B.2. Pontiac taxiway maximum deflection profile (@ 9,000 lbs).

Pontiac: Apron Maximum Deflections

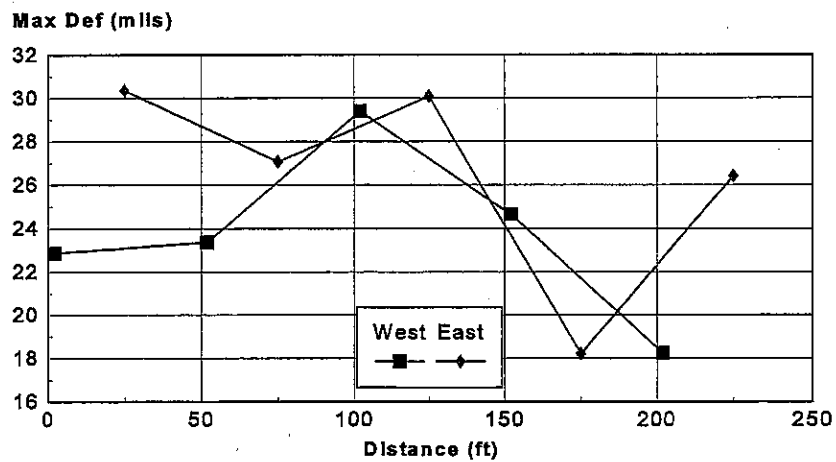


Figure B.3. Pontiac apron maximum deflection profile (@ 9,000 lbs).

Pontiac: RW ERI

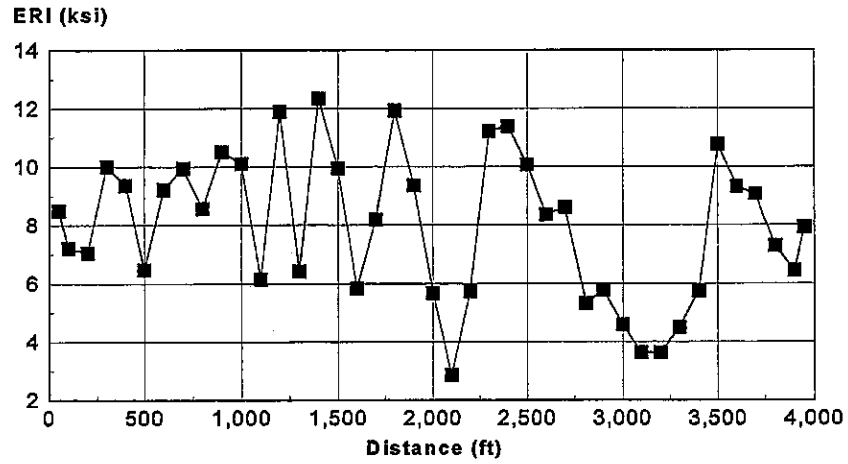


Figure B.4. Pontiac runway E_{Ri} (@ 9,000 lbs).

Pontiac: Taxiway ERI Values

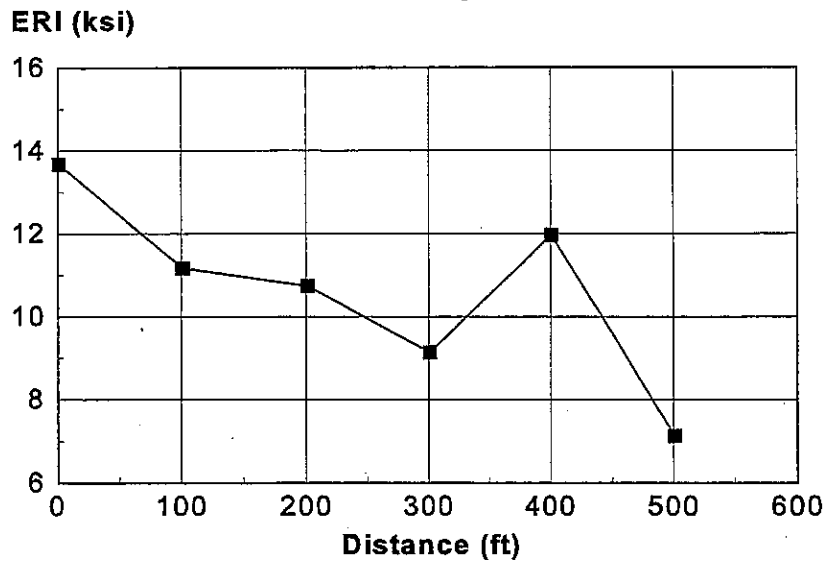


Figure B.5. Pontiac taxiway E_{Ri} (@ 9,000 lbs).

Pontiac: Apron ERI

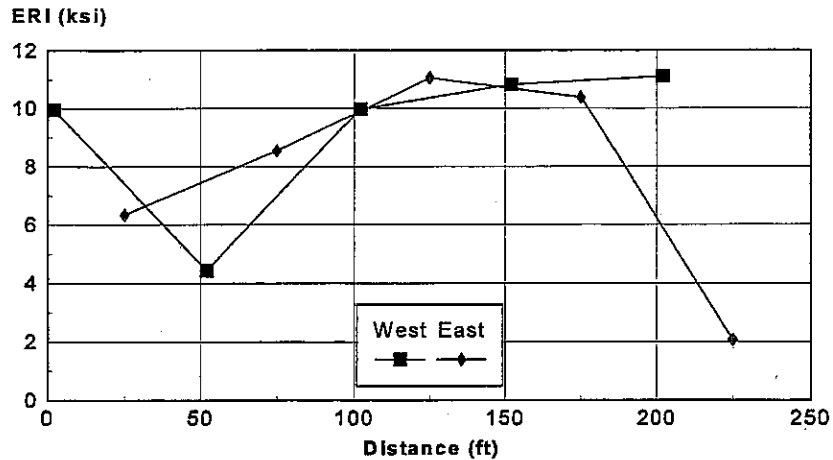


Figure B.6. Pontiac apron E_{Ri} (@ 9,000 lbs).

Morris

Table B.4 provides a summary of the maximum deflection and backcalculated E_{AC} and E_{Ri} values for Morris. Profile plots of the maximum deflection, E_{Ri} , and E_{AC} for the runway and taxiway are provided in Figures B.7 through B.12. There are very noticeable trends observed on the runway, particularly with relation to maximum deflections and backcalculated E_{Ri} values. The site engineer indicated obvious subgrade differences were encountered during construction. There is a significant "soft subgrade" condition at 1,500 ft, where D_0 is very high and E_{Ri} is very low. The backcalculated E_{AC} is fairly consistent along the length of the runway, with the majority of points falling between 300 ksi and 400 ksi.

Table B.4. Summary of backcalculation analysis for Morris (for 9,000 lb normalized load).

Feature	Max. Deflection (mils)			ERI (ksi)			E _{AC} (ksi)		
	Mean	Std. Dev.	COV	Mean	Std. Dev.	COV	Mean	Std. Dev.	COV
Runway	9.9	1.65	17%	8.5	2.59	30%	394	106.0	27%
Taxiway	10.6	2.00	19%	8.9	2.28	26%	314	56.4	18%

Morris: RW Max. Def.

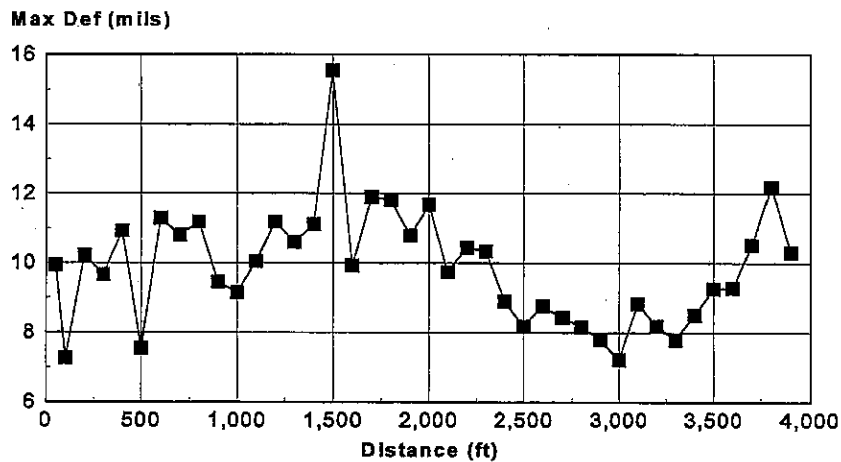


Figure B.7. Morris runway maximum deflection (@ 9,000 lbs).

Morris: TW Max Def

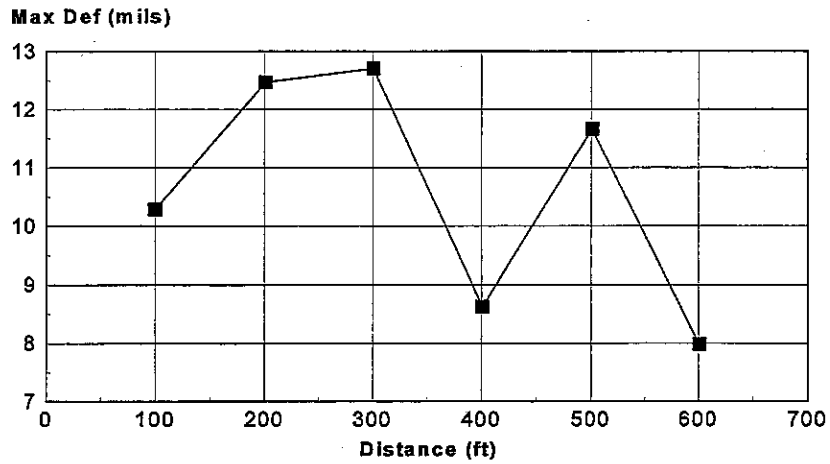


Figure B.8. Morris taxiway maximum deflection (@ 9,000 lbs).

Morris: RW ERI

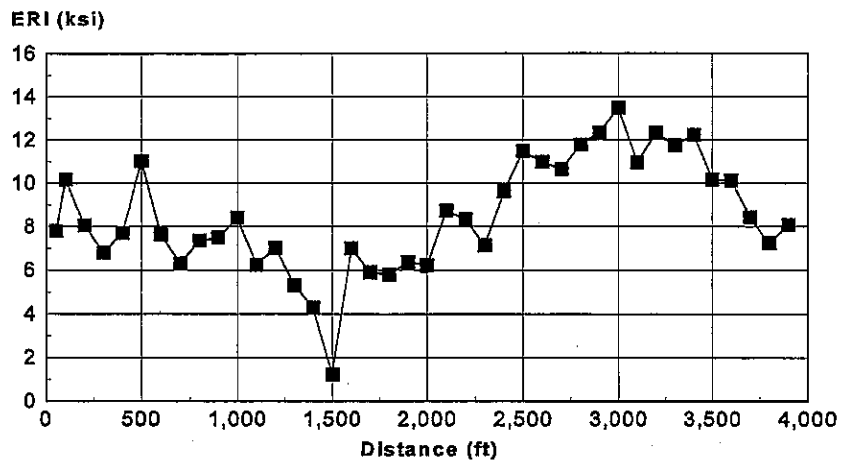


Figure B.9. Morris runway E_{Ri} (@ 9,000 lbs).

Morris: TW ERI

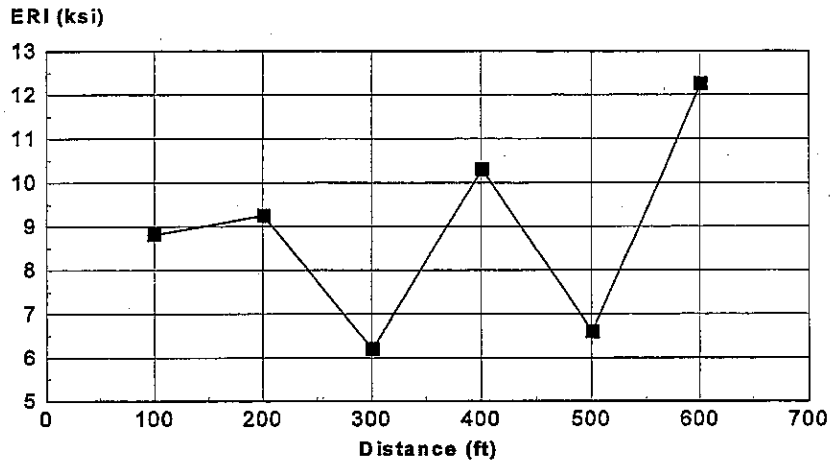


Figure B.10. Morris taxiway E_{Ri} (@9,000 lbs).

Morris: RW AC Modulus

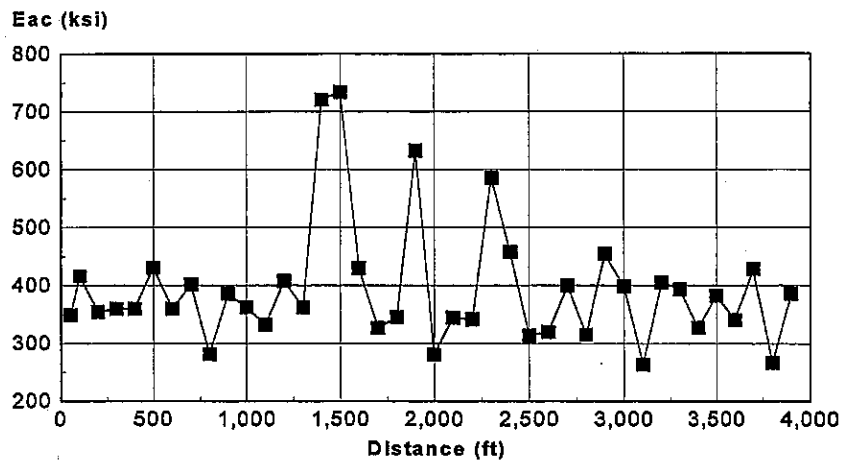


Figure B.11. Morris runway E_{AC} (@ 9,000 lbs).

Morris: TW AC Modulus

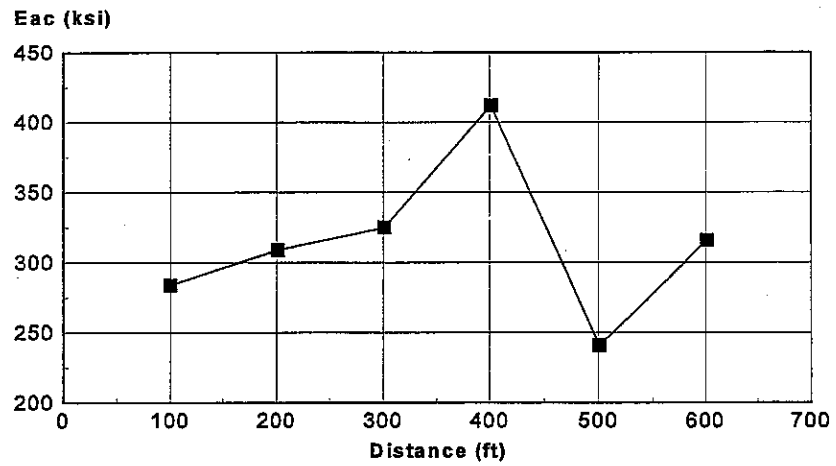


Figure B.12. Morris taxiway E_{AC} (@ 9,000 lbs).



APPENDIX C: AC LABORATORY TESTING PROGRAM

A total of 74 AC core samples (4-in nominal diameter) were obtained from three IDOT-DOA projects constructed in 1992. Thirteen P-401 surface course cores were obtained from Pontiac. From Morris, 34 cores were obtained, many of which were sawed into approximately 2.5 in long specimens. After sawing, 50 specimens were available for testing (3 P-401 surface, 6 composite [containing both P-201 and P-401], and 41 P-201 binder). Twenty seven cores were obtained from Mt. Sterling (11 P-401 surface and 16 P-201 binder). Cores were trimmed to remove embedded base course and/or provide proper sizing for testing.

Bulk specific gravity tests (AASHTO T 166-88) were conducted on all core samples. Sixty five core samples were of sufficient length and quality for AC resilient modulus testing (ASTM 4123). AC Resilient modulus tests were conducted at 70° F and 90° F. The data were used to measure temperature susceptibility as determined by the Slope of the Log AC resilient modulus versus temperature relation. Following modulus testing, the cores were tested for split tensile strength at 72° F (using the ASTM 4123 testing apparatus at a loading rate of 2 in/minute). Tensile strength/resilient modulus relationships were developed. Table C.1 provides a summary of the laboratory results for each core. Blanks in the table indicate that accurate testing could not be conducted due to core damage or inappropriate sample size. Average values are presented in Tables C.2, C.3, and C.4, for Pontiac, Morris, and Mt. Sterling, respectively.

Figures C.1 and C.2 show the distribution of bulk specific gravities for each airport and AC mixture. The binder course at Morris had the highest bulk specific gravities and the Mt. Sterling surface course the lowest.

Figures C.3 through C.6 show the AC resilient modulus (E_{AC}) at 70° F and 90° F for each core tested at Pontiac, Morris, and Mt. Sterling. The E_{AC} values for the Pontiac cores are

Table C.1. Summary of AC laboratory investigation.

Airport	AID	Sample #	Course	Bulk	AC Resilient Modulus			Split
				Spec.	@70 F	@90 F	Slope	Tensile
				Gravity	(psi)	(psi)		Strength (psi)
Pontiac	OC1	10c	Surface	2.315	141195	45879	-0.0244	
Pontiac	OC1	11c	Surface	2.360	221065	54043	-0.0306	113
Pontiac	OC1	12c	Surface	2.360	221950	54240	-0.0306	111
Pontiac	OC1	13c	Surface	2.376	276085	73703	-0.0287	136
Pontiac	OC1	14c	Surface	2.364	186005	58113	-0.0253	127
Pontiac	OC1	15c	Surface	2.338	189570	50205	-0.0289	116
Pontiac	OC1	16c	Surface	2.320	169485	47125	-0.0278	101
Pontiac	OC1	17c	Surface	2.360	124405	35286	-0.0274	86
Pontiac	OC1	19c	Surface	2.303	137140	35398	-0.0294	92
Pontiac	OC1	20c	Surface	2.333	145260	45828	-0.0251	100
Pontiac	OC1	5c	Surface	2.277	153611	40704	-0.0288	
Pontiac	OC1	7c	Surface	2.343				89
Pontiac	OC1	9c	Surface	2.309	141255	51514	-0.0219	99
Morris	C09	1-1	Binder	2.391				183
Morris	C09	1-2	Binder	2.348	779197	226521	-0.0268	155
Morris	C09	1-3	Binder	2.395				171
Morris	C09	1-4	Binder	2.373	743815	220013	-0.0265	165
Morris	C09	2-1	Binder	2.402	650395	197308	-0.0259	178
Morris	C09	2-2A	Binder	2.432	1076816	308514	-0.0271	182
Morris	C09	2-2B	Binder	2.207				171
Morris	C09	2-3	Binder	2.336	649585	168191	-0.0293	115
Morris	C09	2-4	Binder	2.359	682129	149401	-0.0330	156
Morris	C09	3-1	Binder	2.445				180
Morris	C09	3-2	Binder	2.420	847417	246688	-0.0268	182
Morris	C09	3-3A	Binder	2.458	1092023	422802	-0.0206	200
Morris	C09	3-3B	Binder	2.411				180
Morris	C09	3-3C	Binder	2.407	836298	256848	-0.0256	168
Morris	C09	3-4	Binder	2.400				143
Morris	C09	4-1	Binder	2.297	472591	183454	-0.0205	117
Morris	C09	4-2	Binder	2.393	537575	168091	-0.0252	144
Morris	C09	4-3A	Binder	2.373	662372	190022	-0.0271	135
Morris	C09	4-3B	Binder	2.350	711791	208396	-0.0267	142
Morris	C09	4-4	Binder	2.385	645831	175991	-0.0282	135
Morris	C09	4-8	Binder	2.446	813010	213702	-0.0290	170
Morris	C09	5-1	Binder	2.362	410046	151532	-0.0216	140
Morris	C09	5-2	Binder	2.283	336917	101561	-0.0260	75
Morris	C09	5-3	Binder	2.363				132
Morris	C09	5-4	Binder	2.379	796854	192927	-0.0308	144
Morris	C09	6-2A	Binder	2.398	754027	215243	-0.0272	152
Morris	C09	6-2B	Binder	2.414	642959	204126	-0.0249	169
Morris	C09	6-2C	Binder	2.431	511418	169730	-0.0240	147
Morris	C09	6-3	Binder	2.391	556664	177137	-0.0249	147
Morris	C09	6-4	Binder	2.332				131
Morris	C09	7-2A	Binder	2.306	462907	158269	-0.0233	130
Morris	C09	7-2B	Binder	2.397				162
Morris	C09	7-2C	Binder	2.410	791992	241777	-0.0258	165
Morris	C09	7-3	Binder	2.331				112
Morris	C09	8-1	Binder	2.366				143
Morris	C09	8-3	Binder	2.374				126
Morris	C09	8-4	Binder	2.359	568156	193438	-0.0234	125
Morris	C09	8-5	Binder	2.393	731582	242487	-0.0240	132
Morris	C09	S2-2	Binder	2.336				164
Morris	C09	S2-4B	Binder	2.431				166

Table C.1. Summary of AC laboratory investigation.

Airport	AID	Sample #	Course	Bulk Spec. Gravity	AC Resilient Modulus			Split Tensile Strength (psi)
					@70 F (psi)	@90 F (psi)	Slope	
Morris	C09	S2-5B	Binder	2.387	536672	151168	-0.0275	124
Morris	C09	7-4	Composite	2.351	590449	161423	-0.0282	125
Morris	C09	S1-1A	Composite	2.377	603671	182423	-0.0260	140
Morris	C09	S1-2B	Composite	2.355	599757	166882	-0.0278	145
Morris	C09	S2-1	Composite	2.337				133
Morris	C09	S2-4A	Composite	2.353	712643	182337	-0.0296	146
Morris	C09	S2-5A	Composite	2.358	375591	126882	-0.0236	109
Morris	C09	8-2	Surface	2.317	384189	98312	-0.0296	122
Morris	C09	S1-1B	Surface	2.283				119
Morris	C09	S1-2A	Surface	2.357	423638	114508	-0.0284	134
Mt. Sterling	MTS	1-1c	Binder	2.333	359335	55183	-0.0407	143
Mt. Sterling	MTS	1-2c	Binder	2.350	255235	69416	-0.0283	153
Mt. Sterling	MTS	1-3c	Binder	2.372	339445	65920	-0.0356	149
Mt. Sterling	MTS	1-4c	Binder	2.278	288560	49964	-0.0381	113
Mt. Sterling	MTS	1c	Binder	2.312	343935	66896	-0.0356	143
Mt. Sterling	MTS	2-1c	Binder	2.337	247095	51920	-0.0339	139
Mt. Sterling	MTS	2-2c	Binder	2.286				112
Mt. Sterling	MTS	2-3c	Binder	2.360	236275	56474	-0.0311	116
Mt. Sterling	MTS	2-4c	Binder	2.342	385405	75580	-0.0354	133
Mt. Sterling	MTS	3-1c	Binder	2.376	373925	65397	-0.0379	144
Mt. Sterling	MTS	3-2c	Binder	2.354	204625	43682	-0.0335	107
Mt. Sterling	MTS	3-3c	Binder	2.339	353745	59987	-0.0385	156
Mt. Sterling	MTS	3-4c	Binder	2.342	354435	69622	-0.0353	144
Mt. Sterling	MTS	4c	Binder	2.250	245075	54968	-0.0325	123
Mt. Sterling	MTS	5c	Binder	2.274				123
Mt. Sterling	MTS	6c	Binder	2.344	318895	73755	-0.0318	147
Mt. Sterling	MTS	1-1c-s	Surface	2.160	456097	98352	-0.0333	90
Mt. Sterling	MTS	1-2c-s	Surface	2.356				111
Mt. Sterling	MTS	1-3c-s	Surface	2.360				119
Mt. Sterling	MTS	1-6c-s	Surface	2.282	658459	155755	-0.0313	125
Mt. Sterling	MTS	2-1c-s	Surface	2.228	743593	211817	-0.0273	126
Mt. Sterling	MTS	2-2c-s	Surface	2.312	455037	153409	-0.0236	110
Mt. Sterling	MTS	3-1c-s	Surface	2.196				103
Mt. Sterling	MTS	3-3c-s	Surface	2.301	437176	133460	-0.0258	117
Mt. Sterling	MTS	4-1c-s	Surface	2.293				120
Mt. Sterling	MTS	5-1c-s	Surface	2.282				134
Mt. Sterling	MTS	6-1c-s	Surface	2.271				120

Table C.2. Average results for Pontiac core samples.

Laboratory Analysis	Surface Course	
	Mean	COV
Bulk Specific Gravity	2.335	1.25%
AC Resilient Modulus @ 70° F (ksi)	176	25.9%
AC Resilient Modulus @ 90° F (ksi)	49	21.3%
Slope ¹	-0.027	9.82%
Tensile Strength (psi)	106	15.0%

¹ $\text{Log}(E_{AC}) = A + \text{Slope} * \text{Temperature}$

Table C.3. Average results for Morris core samples.

Laboratory Analysis	Surface Course		Composite Course		Binder Course	
	Mean	COV	Mean	COV	Mean	COV
Bulk Specific Gravity	2.319	1.60%	2.355	0.55%	2.377	2.04%
AC Resilient Modulus @ 70° F (ksi)	404	6.91%	576	21.3%	679	26.3%
AC Resilient Modulus @ 90° F (ksi)	106	10.8%	164	13.9%	205	29.4%
Slope ¹	-0.029	2.90%	-0.027	18.6%	-0.026	10.9%
Tensile Strength (psi)	125	6.38%	133	10.7%	150	16.5%

¹ $\text{Log}(E_{AC}) = A + \text{Slope} * \text{Temperature}$

Table C.4. Average results for Mt. Sterling cores.

Laboratory Analysis	Surface Course		Binder Course	
	Mean	COV	Mean	COV
Bulk Specific Gravity	2.277	2.71%	2.328	1.60%
AC Resilient Modulus @ 70° F (ksi)	550	25.7%	308	19.4%
AC Resilient Modulus @ 90° F (ksi)	151	27.4%	61	15.6%
Slope ¹	-0.028	14.12%	-0.035	9.54%
Tensile Strength (psi)	116	10.3%	134	12%

¹ $\text{Log}(E_{AC}) = A + \text{Slope} * \text{Temperature}$

Distribution of Bulk Specific Gravities for Each Airport

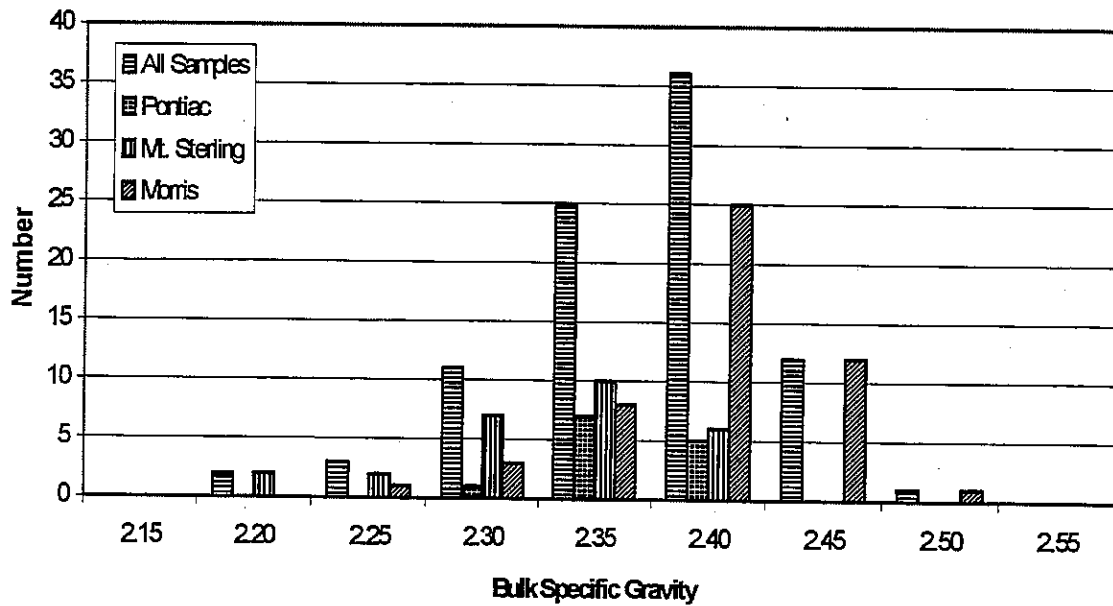


Figure C.1. Distribution of bulk specific gravities for each airport.

Distribution of Specific Gravities According to Airport and Mix Type

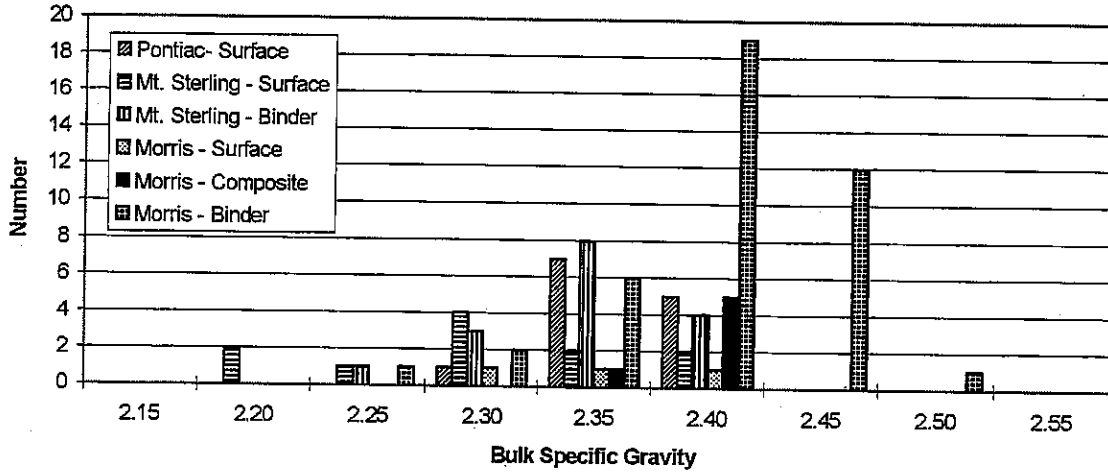


Figure C.2. Distribution of specific gravities for each AC mixture.

Pontiac: AC Resilient Modulus for P-401 Surface Course

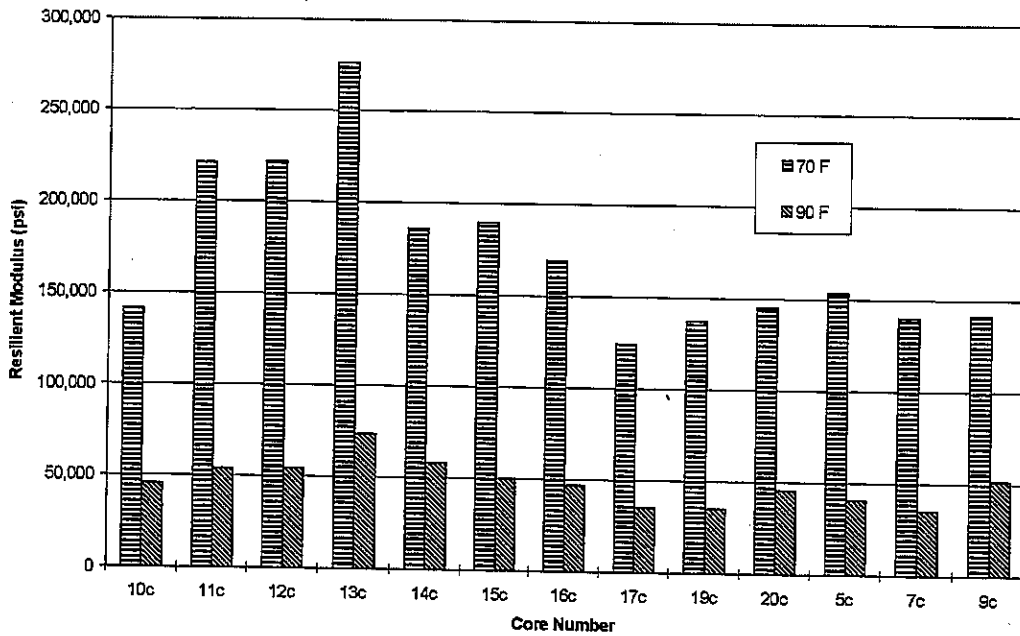


Figure C.3. AC resilient modulus for Pontiac surface course.

Morris: AC Resilient Modulus for Surface and Composite Courses

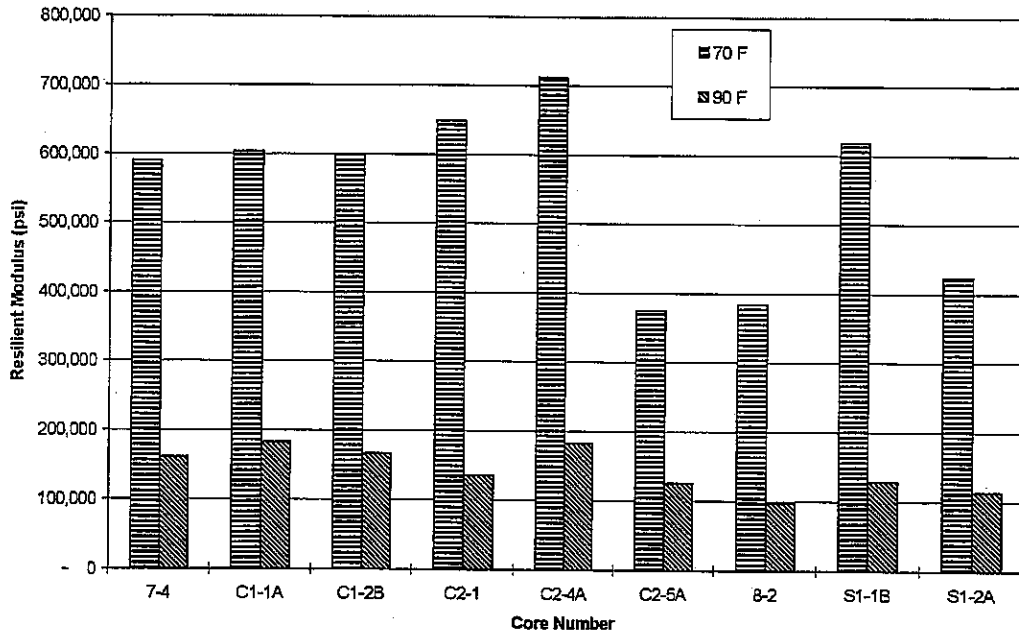


Figure C.4. AC resilient modulus for Morris surface and composite courses.

Morris: AC Resilient Modulus for Binder Course

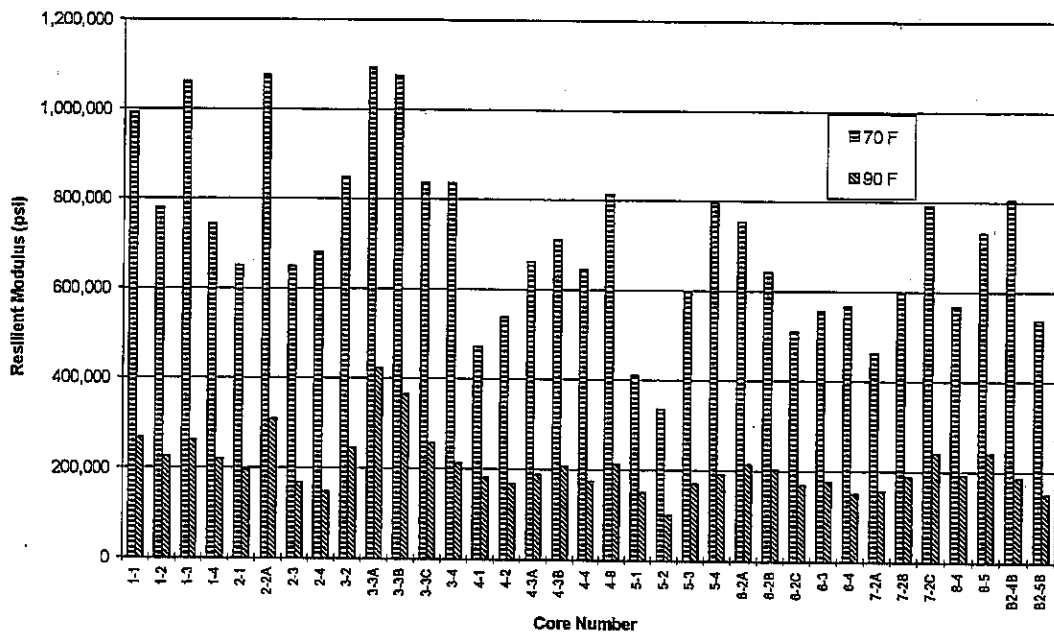


Figure C.5. AC resilient modulus for Morris binder course.

Mount Sterling: AC Resilient Modulus

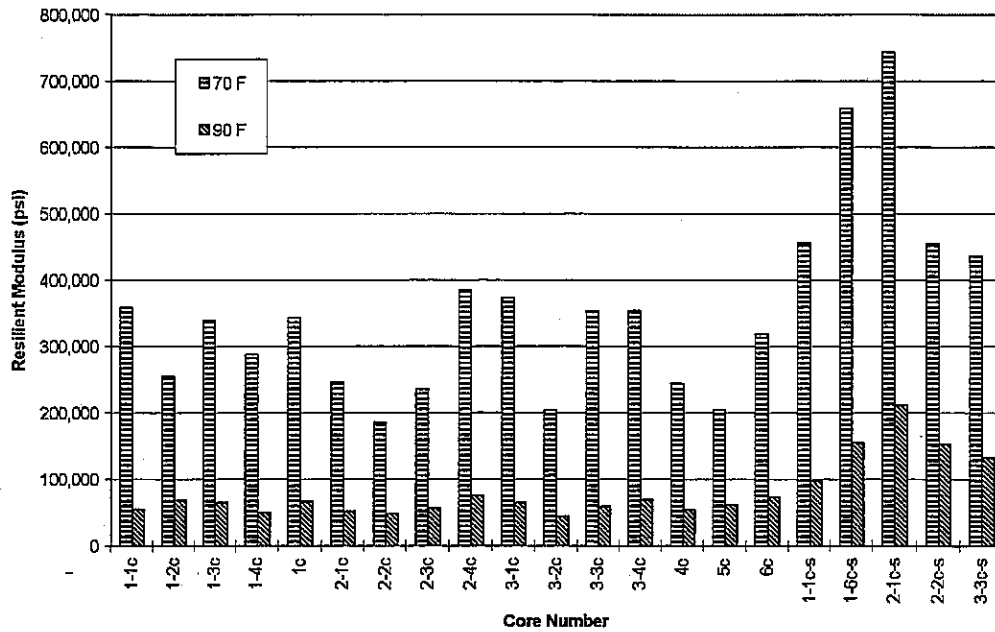


Figure C.6. AC resilient modulus for Mt. Sterling surface and binder courses.

consistently lower than those obtained at the other sites. The E_{AC} at 90° F for the binder layer at Mt. Sterling is relatively low compared to the 70° F data (see Figure C.6). Note that surface cores for Mt. Sterling (to the far right of the bar chart, designated with an "-s") have higher AC moduli than the binder cores.

Figures C.7, C.8, and C.9 show the Log AC resilient modulus versus temperature relationship for the AC mixtures from each airport. The slope of the line ($\text{Log}(E_{AC}) = A + \text{Slope} \cdot \text{Temperature}$) defines the temperature susceptibility of the mixture. The values obtained are typical, except for the binder layer at Mt. Sterling which shows higher than expected temperature susceptibility. This is reflected in the average Slope value of -0.035 shown in Table C.4.

Figures C.10 through C.15 show AC resilient modulus versus split tensile strength (@ 72° F) relationships for the various airports and AC mixtures. The AC resilient modulus

Pontiac: AC Resilient Modulus versus Temperature

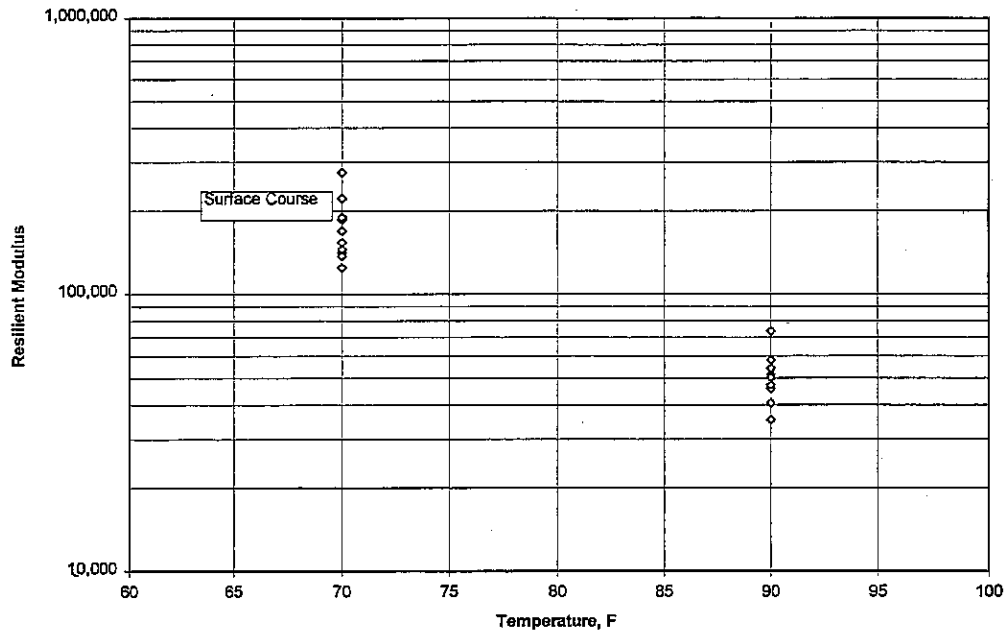


Figure C.7. AC resilient modulus versus temperature for Pontiac cores.

Morris: AC Resilient Modulus versus Temperature

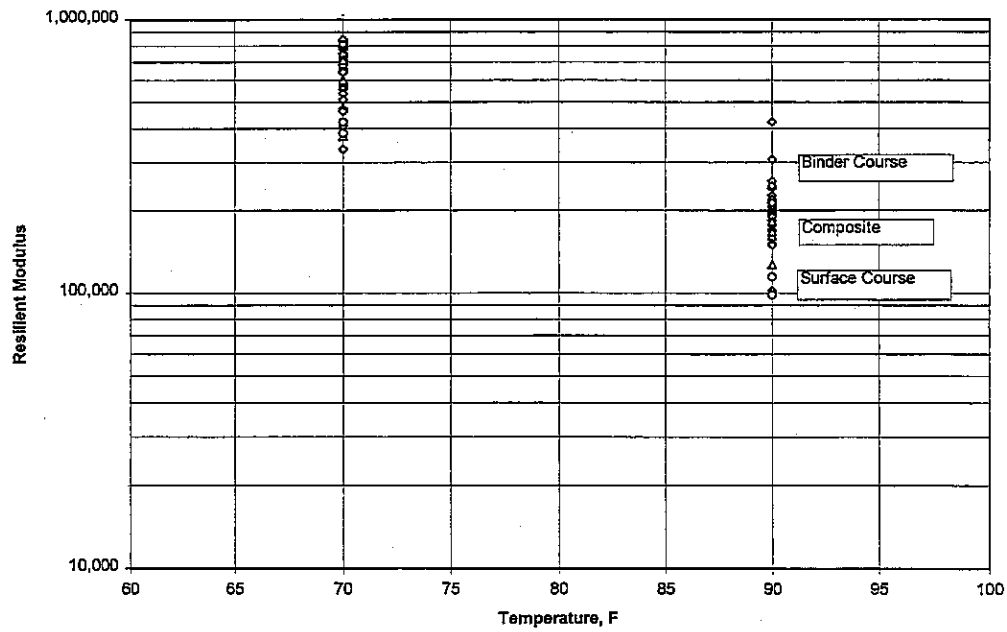


Figure C.8. AC resilient modulus versus temperature for Morris cores.

Mount Sterling: AC Resilient Modulus versus Temperature

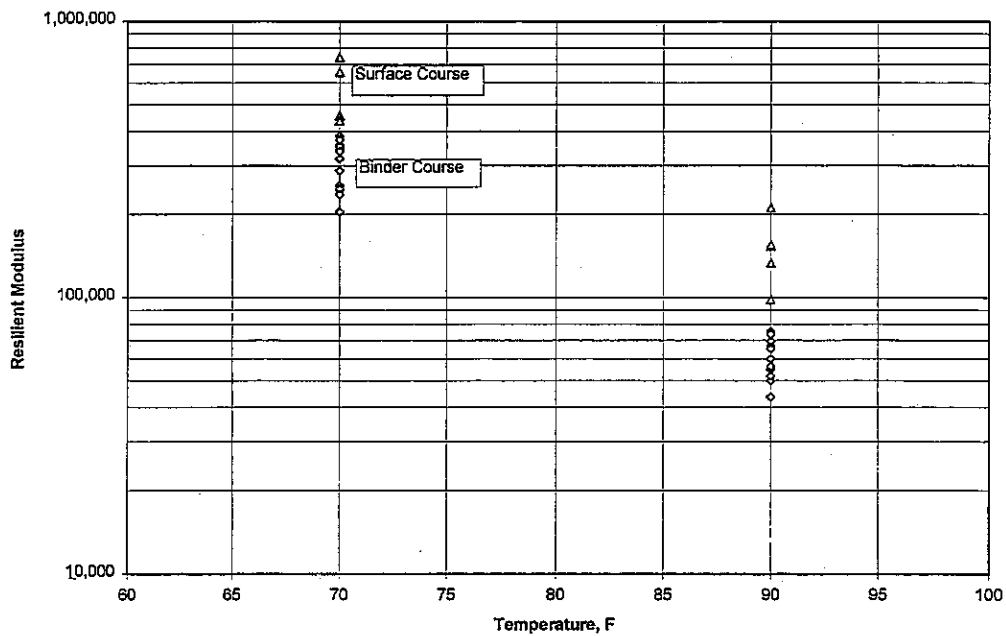


Figure C.9. AC resilient modulus versus temperature for Mt. Sterling cores.

Pontiac: AC Resilient Modulus versus Tensile Strength

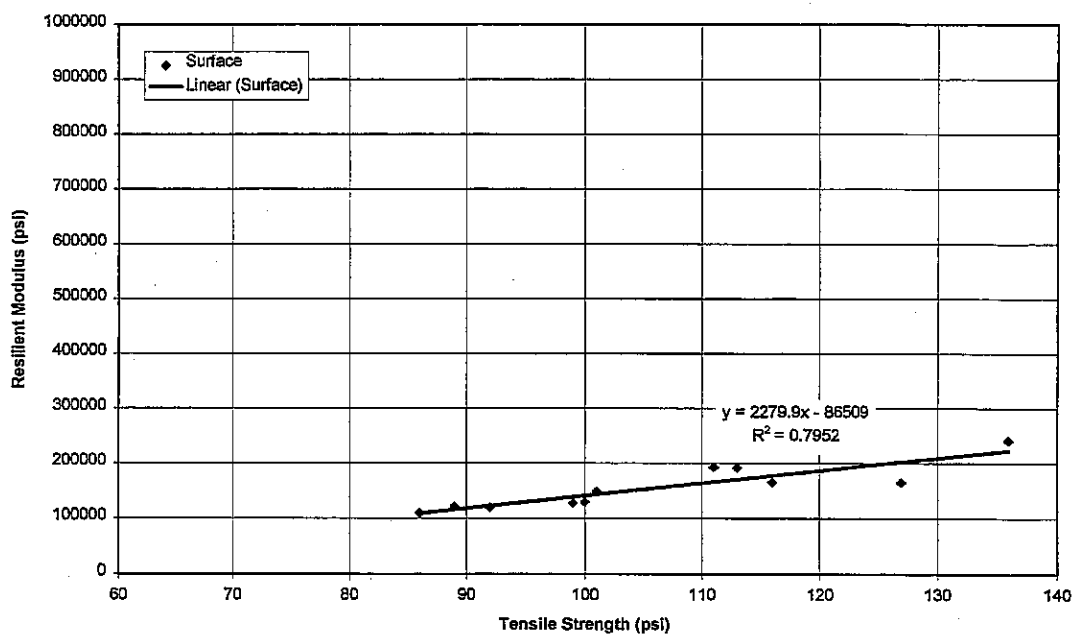


Figure C.10. Pontiac AC resilient modulus versus split tensile strength (@ 72 F).

Morris: AC Resilient Modulus versus Tensile Strength

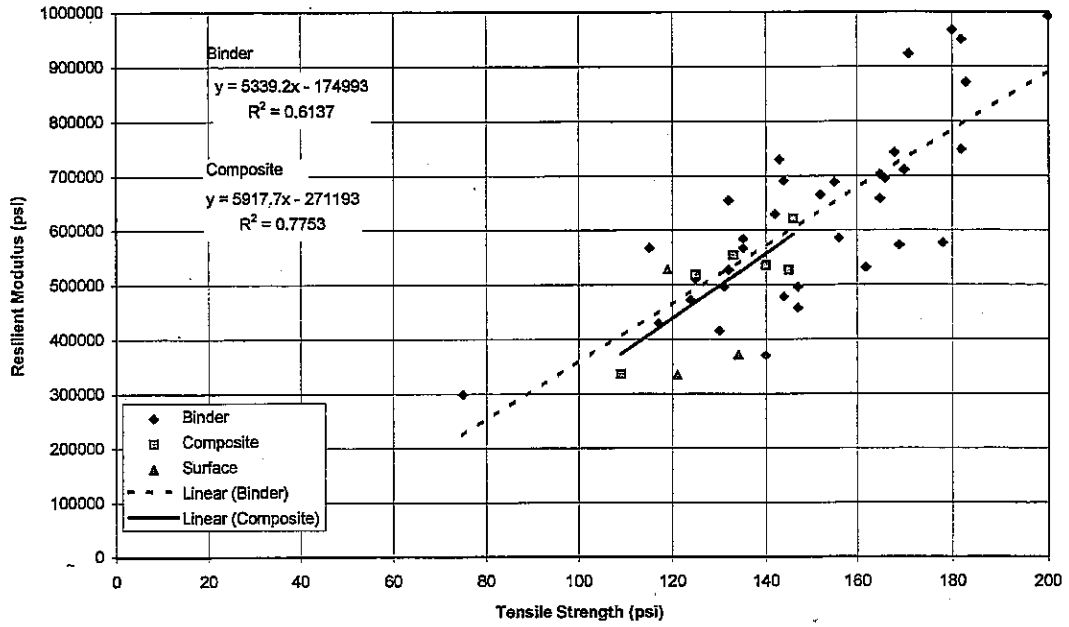


Figure C.11. Morris AC resilient modulus versus split tensile strength (@ 72 F).

Mount Sterling: AC Resilient Modulus versus Tensile Strength

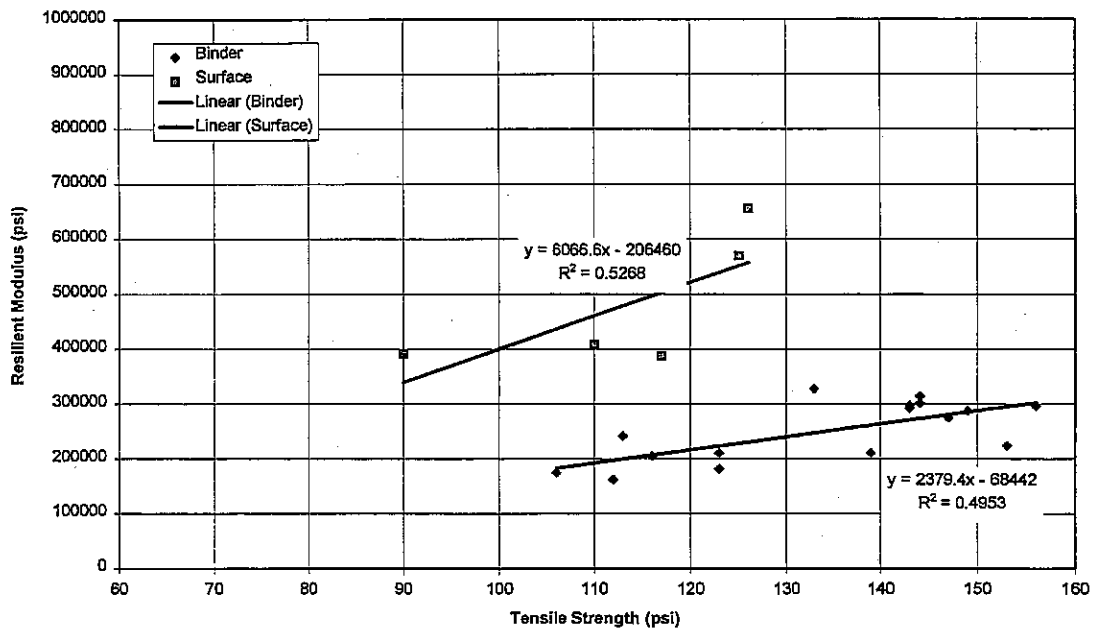


Figure C.12. Mt. Sterling resilient modulus versus split tensile strength (@ 72 F).

Surface:AC Resilient Modulus versus Tensile Strength

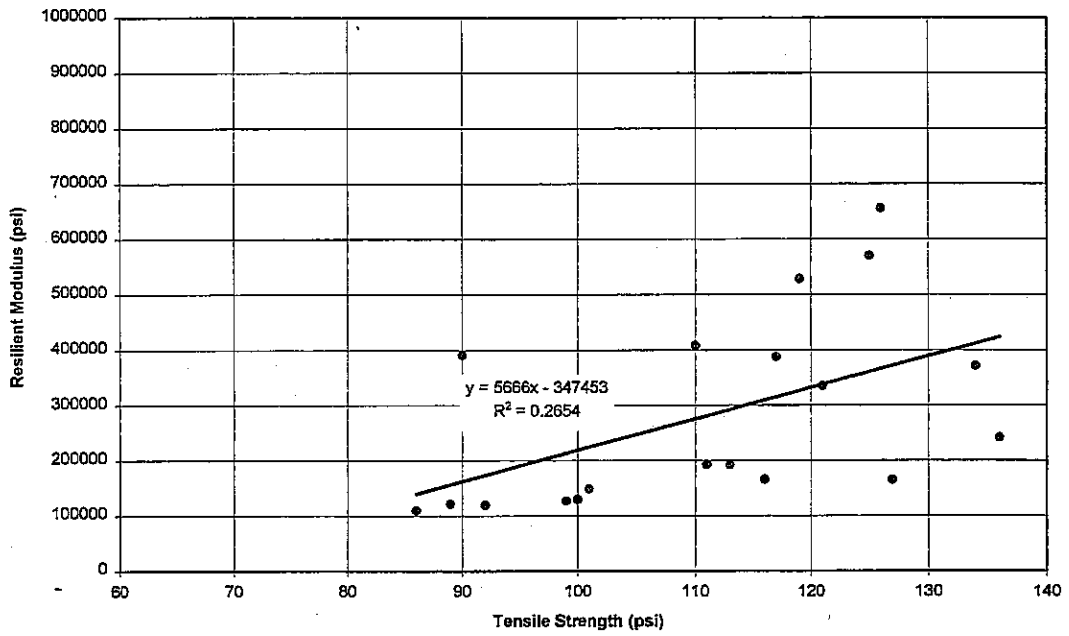


Figure C.13. Surface AC resilient modulus versus split tensile strength (@ 72 F).

Binders: AC Resilient Modulus versus Tensile Strength

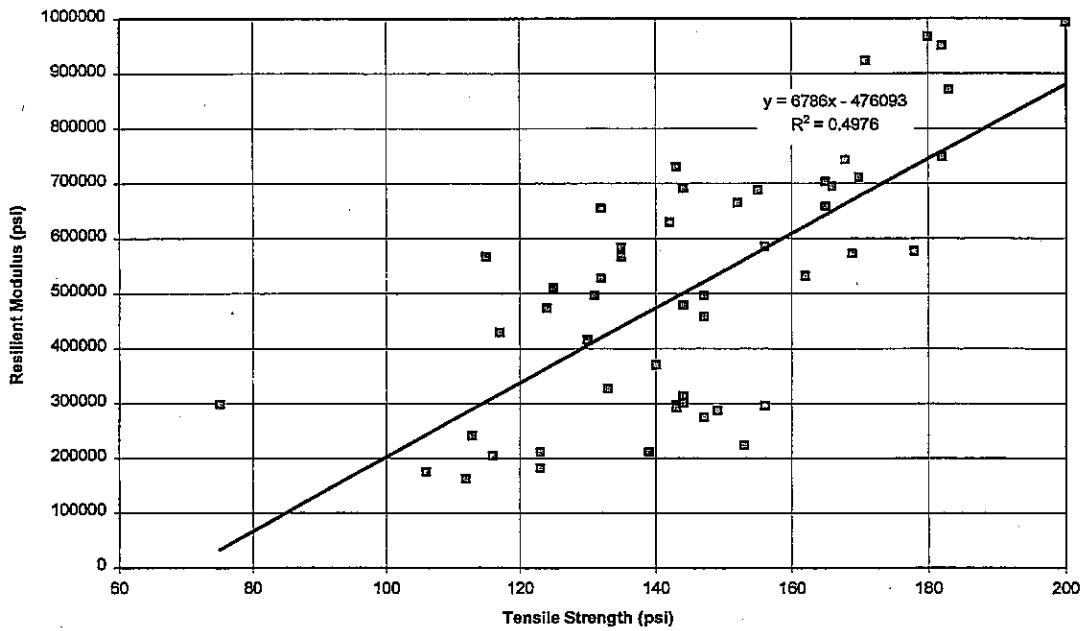


Figure C.14. Binder AC resilient modulus versus split tensile strength (@ 72 F).

AC Resilient Modulus versus Tensile Strength

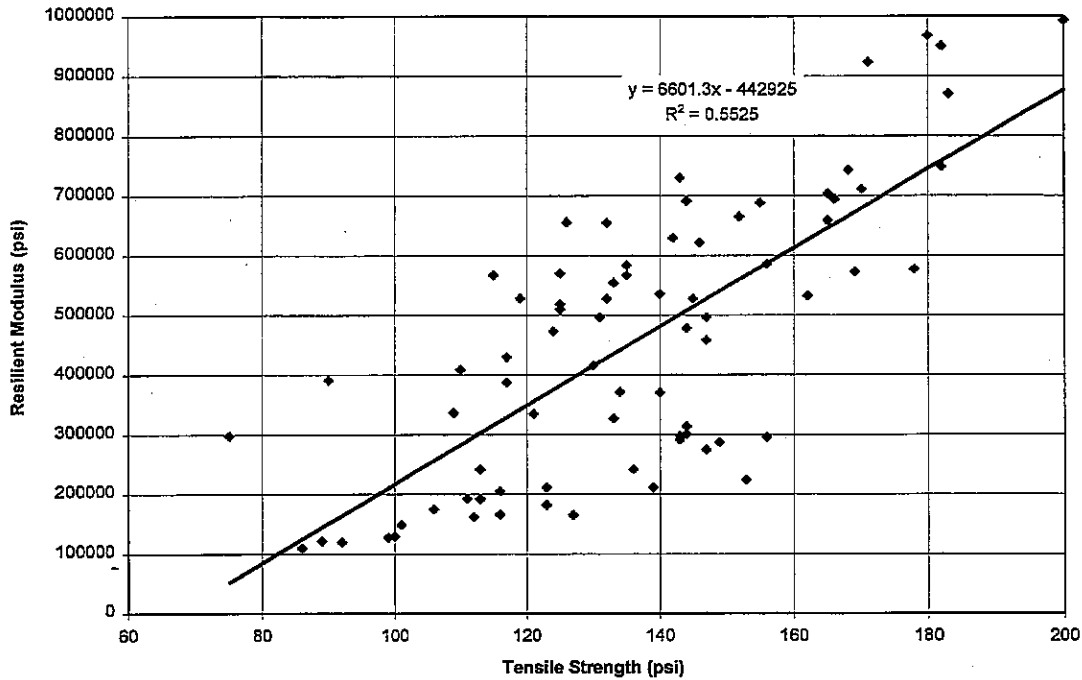


Figure C.15. AC resilient modulus versus split tensile strength (@ 72 F) for all cores.

values are interpolated to 72° F. E_{AC} increases with split tensile strength. The split tensile strengths for all mixes are within the expected range. The coefficients for tensile strength vary considerably among the mixes. These relationships are typically mixture specific, as this analysis indicates.

The P-201/P-401 AC mixtures constructed at Morris and the P-401 surface mixture constructed at Mt. Sterling have modulus characteristics slightly less stiff than IDOT Class I AC-10 mixture. The binder layer at Mt. Sterling shows lower than expected modulus at 70° F and high temperature susceptibility.

The P-401 mixture at Pontiac had lower than expected moduli. An inexplicable creep problem was encountered during testing. Two cores fell apart at 90° F. One core was severely

deformed by the rubber band used to attach the label. This behavior suggests that the mixture is susceptible to permanent deformation under loading at higher temperatures.

APPENDIX D: IDOT-DOA AC MIXTURE PROPERTIES

As part of this study, a preliminary investigation was conducted to identify mix stiffness and fatigue characteristics of typical IDOT-DOA AC mixtures. As only limited laboratory data was available, the approach used was based on the evaluation of mixture specifications. Mix design information obtained from three recently constructed projects (Pontiac, Morris, and Mount Sterling) was also examined.

AC Mixture Stiffness

The first step in estimating AC mixture stiffness is to establish the stiffness characteristics of the asphalt cement binder. IDOT-DOA specifications require that an AC-10 binder be used on all GA airport projects. A recently conducted study at the University of Illinois found that the mean and standard deviation of penetration (at 77° F) for 1019 AC-10 samples used by IDOT in 1991 was 100 pen and 12 pen, respectively.¹ Assuming a typical range in penetrations from 88 pen to 112 pen (mean ± one standard deviation), the asphalt cement absolute viscosities at 70° F was estimated using the following relationship developed by the Asphalt Institute [AI, 1982]:

$$\eta_{70^{\circ}F, 10^6} = 29508.2 \text{pen}_{77^{\circ}F}^{-2.1939} \quad \text{Equation D.1}$$

Where: $\eta_{70^{\circ}F, 10^6}$ is the absolute viscosity at 70° F, poises x 10⁶.
 $\text{Pen}_{77^{\circ}F}$ is the penetration at 77° F.

Equation D.2 shows the relationship developed as part of the University of Illinois study.¹

$$\eta_{70^{\circ}F, 10^6} = 21286.3 \text{pen}_{77^{\circ}F}^{-2.270} \quad \text{Equation D.2}$$

¹ Evaluation of IDOT 1991 Asphalt Cement and Liquid Asphalt Test Report, by John Willis for M.R. Thompson, University of Illinois, 1994.

This relationship was developed from IDOT-DOH data on 2820 AC-5, AC-10, and AC-20 asphalt cement samples ($R^2 = 0.8754$). Table D.1 shows the estimated absolute viscosities for the range in penetrations considered in this analysis.

Table D.1. Summary of asphalt cement stiffness properties.

Penetration @ 77° F (pen)	Absolute Viscosity @ 70° F (poises x 10 ⁶)	
	Asphalt Institute ¹	IDOT ²
88	1.599	0.821
100	1.271	0.648
112	0.942	0.475

¹ Based on Equation D.1.

² Based on Equation D.2.

After establishing reasonable ranges for asphalt cement viscosity, an estimation of AC mixture stiffness was made using the following Asphalt Institute relationship [AI, 1982]:

$$\begin{aligned}
 \text{Log}|E^*| = & 5.553833 + 0.028829 \left(\frac{P_{200}}{f^{0.17033}} \right) - 0.03476(V_v) + 0.070377(\eta_{70^\circ, 10^6}) \\
 & + 0.000005 \left[t_p^{(1.3+0.49825 \log(f))} P_{ac}^{0.5} \right] - 0.00189 \left[t_p^{(1.3+0.49825 \log(f))} \frac{P_{ac}^{0.5}}{f^{1.1}} \right] \\
 & + 0.931757 \left(\frac{1}{f^{0.02774}} \right)
 \end{aligned}
 \tag{Equation D.3}$$

Where: $|E^*|$ is the dynamic modulus (stiffness) of asphalt concrete, psi.

P_{200} is the percent aggregate passing the No. 200 sieve.

f is the frequency, Hz.

V_v is the percent air voids.

P_{ac} is the asphalt content, percent by weight of mix.

t_p is the temperature, ° F.

This relationship shows that a number of mix parameters influence AC mixture stiffness. To investigate these influence, conventional and FULL-DEPTH AC pavements were hypothetically analyzed in Rockford, Springfield, and Cairo. Using the Design Time concept, design AC mixture temperatures were chosen [Thompson, 1986][Thompson, 1988]. The design temperatures shown in Table D.2 were used in this analysis as t_p . From the IDOT-DOA P-401 specification, it was found that P_{200} ranged from 3 to 8 percent, P_{ac} from 5 to 7 percent, and V_v from 2 to 3 percent for the 3/4 in maximum aggregate size gradation [IDOT-DOA, 1994A]. The P-201 specification differed only in the range of P_{ac} , allowing 4.5 to 7 percent. In this analysis, the frequency, f , was established at 10 Hz.

Table D.2. Design AC mixture temperatures for conventional and FULL-DEPTH AC pavements based on the Design Time concept [Thompson, 1986][Thompson, 1988].

Location	Design AC Mixture Temperature(° F)	
	Conventional AC	FULL-DEPTH AC
Rockford	71	77
Springfield	78	80.8
Cairo	84.4	86

A sensitivity analysis was prepared for each location showing the impact of specific parameters on the AC dynamic modulus. Figures D.1 through D.4 show the results of this analysis for Springfield. Similar trends were observed for Rockford and Cairo. Trendlines have been placed on the plots to show average changes in AC dynamic modulus over the parameter range. Note that linear trendlines have been chosen to simply demonstrate net changes in AC dynamic modulus over the range of each parameter. The linear representation is not meant to suggest that the actual change over the range is linear.

Trends observed in Figure D.1. show that the AC dynamic modulus increases as percent material passing the No. 200 sieve increases. The increase in stiffness is approximately 25% over the range specified. It is also observed that the AC material in a conventional pavement is stiffer at the same location, reflecting the lower design temperature.

Springfield: Dynamic Modulus versus Percent Passing #200 Sieve

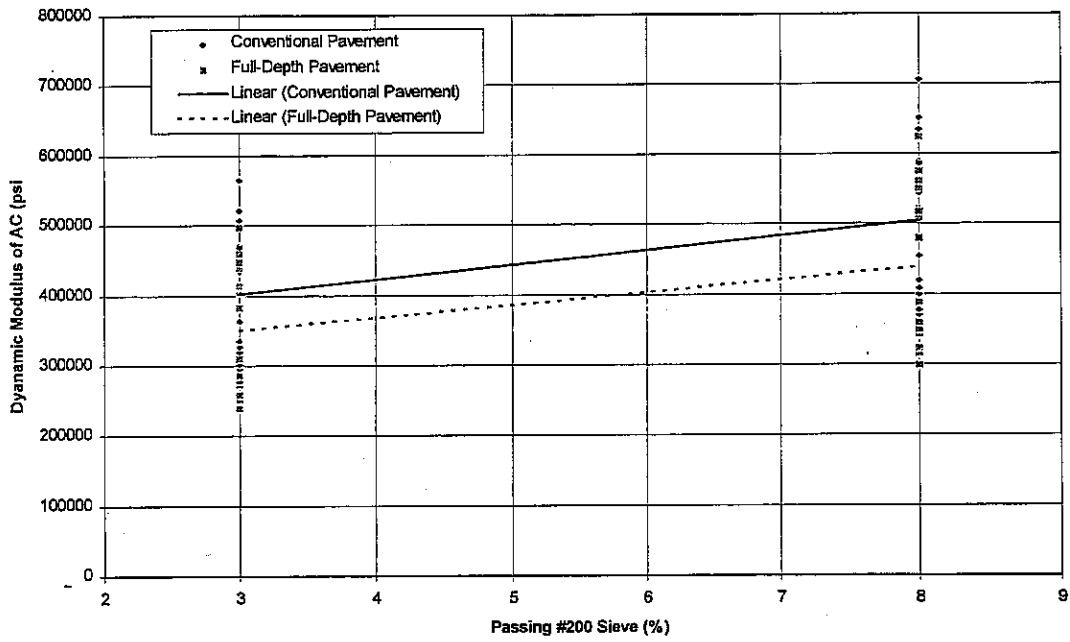


Figure D.1. Relationship between percent aggregate passing No. 200 sieve and the AC dynamic modulus.

Springfield: Dynamic Modulus versus Percent Air Content

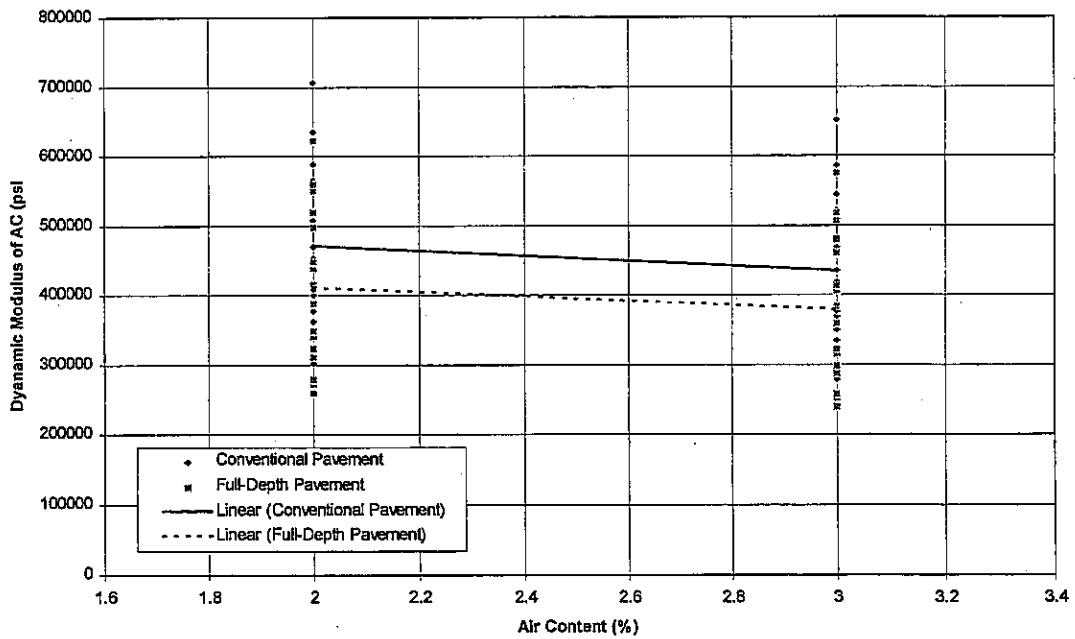


Figure D.2. Relationship between air content and the AC dynamic modulus.

Springfield: Dynamic Modulus versus Percent Asphalt

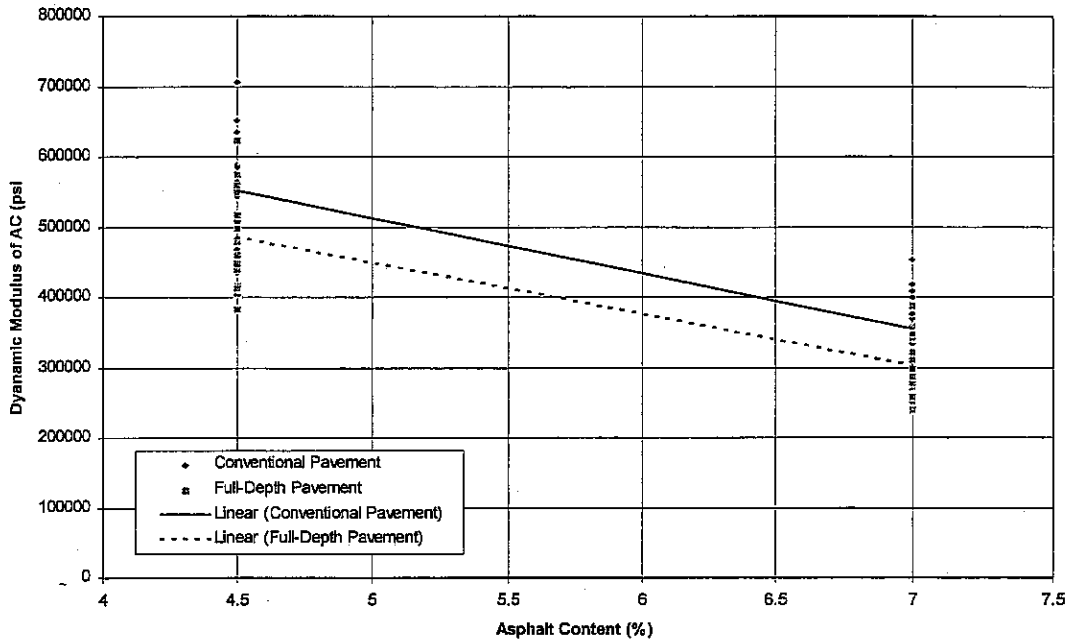


Figure D.3. Relationship between asphalt content and AC dynamic modulus.

Springfield: Dynamic Modulus versus Absolute Viscosity @ 70 F

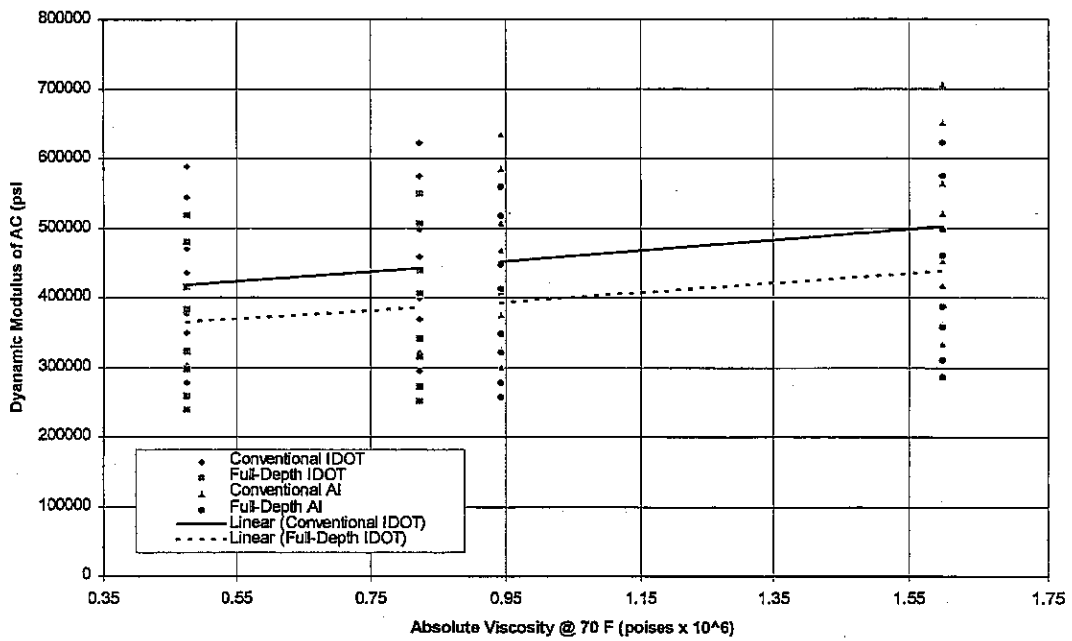


Figure D.4. Relationship between asphalt content and binder absolute viscosity.

In Figure D.2, it is observed that an increase in air content results in a decrease in AC stiffness. This effect, over the range of the specification, is not great, leading to an approximate decrease in AC dynamic modulus of 6%. Figure D.3 shows the effect of asphalt content. Within the range of the specification, asphalt content can strongly effect AC dynamic modulus. As asphalt content increases from 4.5% to 7.0%, the dynamic modulus decreases approximately 36%.

Figure D.4 shows the trends observed over the range of typical absolute viscosities calculated using the AI and IDOT relationships. As can be seen, an increase in binder absolute viscosity leads to an approximate increase in AC stiffness of 20% over the range estimated.

The sensitivity analysis indicates that significant variation in AC mixture stiffness is obtainable within the specified mix limits. An attempt was made to narrow this range by examining actual mix design data obtained from three recent IDOT-DOA projects. Table D.3 shows the relevant mix design parameters obtained for the three projects. Binder viscosity is unknown, so AC stiffnesses were calculated over the entire range of asphalt cement absolute viscosities. Figure D.5 shows a plot of the estimated AC stiffness using a design temperature based on the Design Time concept for each location.

Table D.3. Summary of mix design parameters from three Illinois projects.

Mix Parameter	Morris P-401	Pontiac P-401	Mount Sterling	
			P-201	P-401
P_{200}	5.4%	5.5%	4.9%	5.5%
V_v	2.25%	2.00%	2.00%	2.00%
P_{ac}	6.3%	6.3%	5.5%	6.1%

Estimated Dynamic Moduli for Three Projects

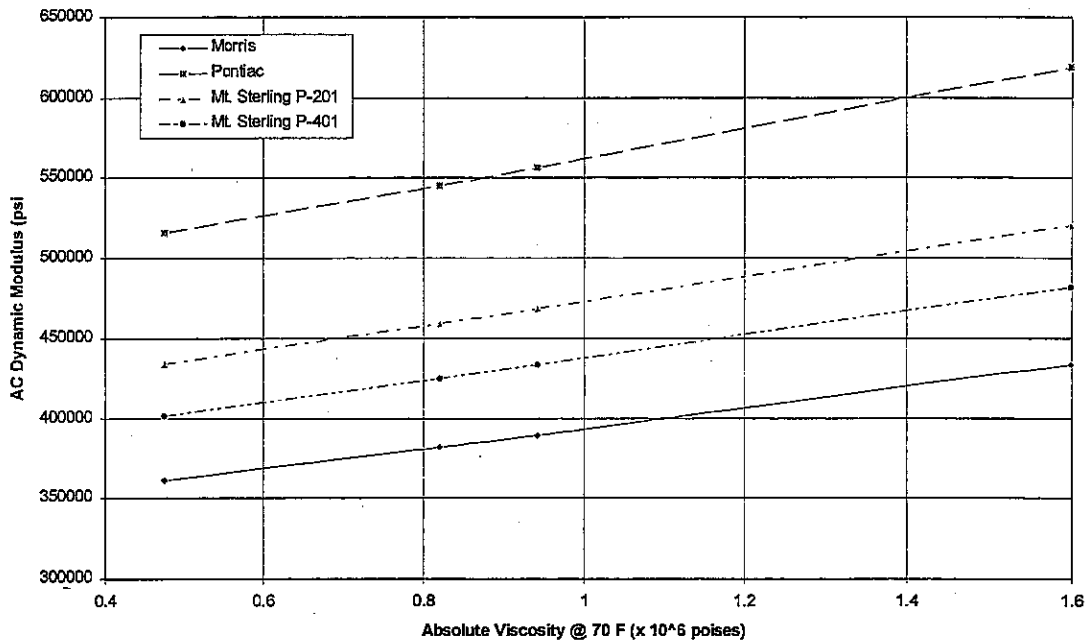


Figure D.5. Estimated dynamic modulus based on mix design parameters and design temperature for three Illinois projects.

Figure D.5 suggests that under local climatic conditions, the mix design a Pontiac would have the stiffest AC material. The P-201 and P-401 at Mount Sterling would be the next stiffest, and the P-401 at Morris would be the least stiff. Calculations were not conducted for the P-201 at Morris because it contained recycled AC pavement.

The previous analysis did not directly compare mix stiffnesses because different design temperatures were used in the calculations. This was addressed by calculating AC stiffnesses for each mix at 70° F and 90° F. This also allowed a direct comparison to be made with the results of the laboratory investigation. Figures D.6 and D.7 show the calculated AC dynamic moduli for each project at 70° F and 90° F, respectively. It is again observed that Pontiac P-401 has the stiffest mix while the Morris P-401 is the least stiff, although the gap between the two has decreased.

Estimated Dynamic Moduli for Three Projects at 70 F

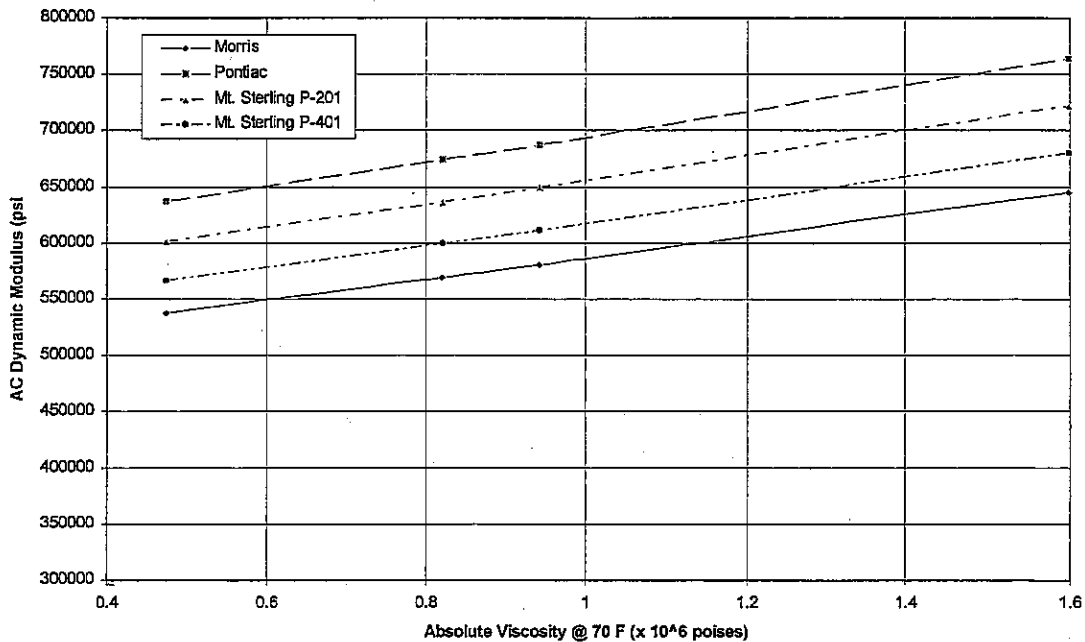


Figure D.6. Estimated dynamic moduli for three Illinois projects at 70° F.

Estimated Dynamic Moduli for Three Projects at 90 F

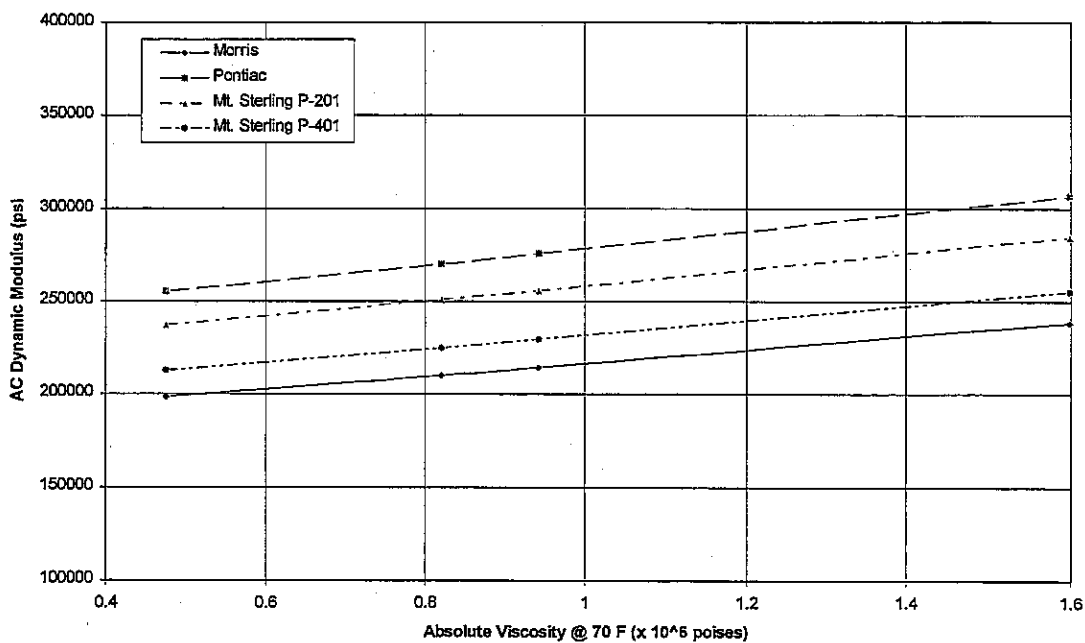


Figure D.7. Estimated dynamic moduli for three Illinois projects at 90° F.

The average laboratory resilient modulus values for the three projects are shown in Table 18 in this report. In comparing these laboratory resilient moduli to those calculated, a rather large discrepancy is noted, particularly for the Pontiac P-401. The estimated range in dynamic modulus at 70° F varies from approximately 640 ksi to 760 ksi, where the average observed in the laboratory was 176 ksi. At 90° F, the laboratory average is 49 ksi, which is substantially lower than the estimated range of approximately 260 ksi to 310 ksi.

The difference in cores obtained at Morris is also great, with an estimated range at 70° F from approximately 540 ksi to 650 ksi compared to a laboratory average of 404 ksi. The laboratory average at 90° F is 106 ksi is substantially lower than the range of 200 ksi to 240 ksi predicted based on mix design properties. The Mount Sterling P-401 surface mix at 70° F was the only laboratory resilient modulus that fell within the estimated range. The laboratory results for the Mount Sterling P-201 have stiffnesses below that estimated from the mix design properties.

The potential reasons for the discrepancies are many and varied. Direct comparison of the laboratory testing procedures (i.e. dynamic versus resilient modulus) is one source of difference that might explain the observation that the laboratory moduli values were overall lower than those predicted from the equations. Additionally, the laboratory testing was conducted on actual cores while the calculations were made from mix properties obtained from the mix design data. Regardless of the cause, the results of this analysis suggest that considerable work is still required to identify the stiffness characteristics of IDOT-DOA GA airport AC mixtures. It is therefore recommended that additional laboratory and analytical investigations be conducted to establish GA mixture stiffness characteristics using known mix parameters.

As a mechanistic based design scheme is considered for GA airport pavements, it will be necessary to establish AC stiffness-temperature relationships similar to those used for IDOT Class I materials [Thompson, 1986][Thompson, 1988]. To consider this in a preliminary fashion, IDOT-DOA P-201 and P-401 specifications were used to select mid-

range values for P_{200} , P_{ac} , and V_v . Mid-range binder absolute viscosities ($\eta_{70 F, 10^6}$) were also selected for an AC-10 using both the AI and IDOT-UI binder stiffness algorithms. The calculated AC stiffness-temperature curves are shown in Figures D.8 and D.9. Also shown in each figure is the IDOT-DOH Class I stiffness-temperature curve for an AC-10 [Thompson, 1986][Thompson, 1988].

In Figure D.8, which shows the relationship based on the AI algorithm, it is observed that the IDOT-DOA mixtures have stiffnesses slightly less than an IDOT Class I mix at a given temperature. Also, the P-401 has an estimated stiffness less than P-201 as a result of the slightly higher mid-range P_{ac} value. The AC stiffness-temperature relationships shown in Figure D.9 are based on IDOT-UI algorithm. It is observed that lower AC stiffness are estimated as a result of the lower calculated binder viscosities. This procedure ultimately may prove to be useful in the development of a mechanistic based design scheme for GA airports. As previously mentioned, additional work is required to better identify IDOT-DOA AC mixture stiffness characteristics.

AC Mixture Fatigue

AC fatigue is commonly linked to maximum tensile strain induced in the AC layer under traffic loading through the use of “transfer functions.” [Thompson, 1990]. Pell documented two general forms of this relationship [Pell, 1987]. The first, which is shown in Equation D.4, relates the number of repetitions to failure solely to the AC strain. The second form, shown in Equation D.5, adds a AC modulus term to the relationship.

$$N = k \left(\frac{1}{\epsilon} \right)^n \quad \text{Equation D.4}$$

$$N = k' \left(\frac{1}{\epsilon} \right)^{n'} \left(\frac{1}{E_{ac}} \right)^{m'} \quad \text{Equation D.5}$$

AC Stiffness - Temperature Relationship for Standard IDOT-DOA AC Mixtures
Using AI Stiffness Relationships

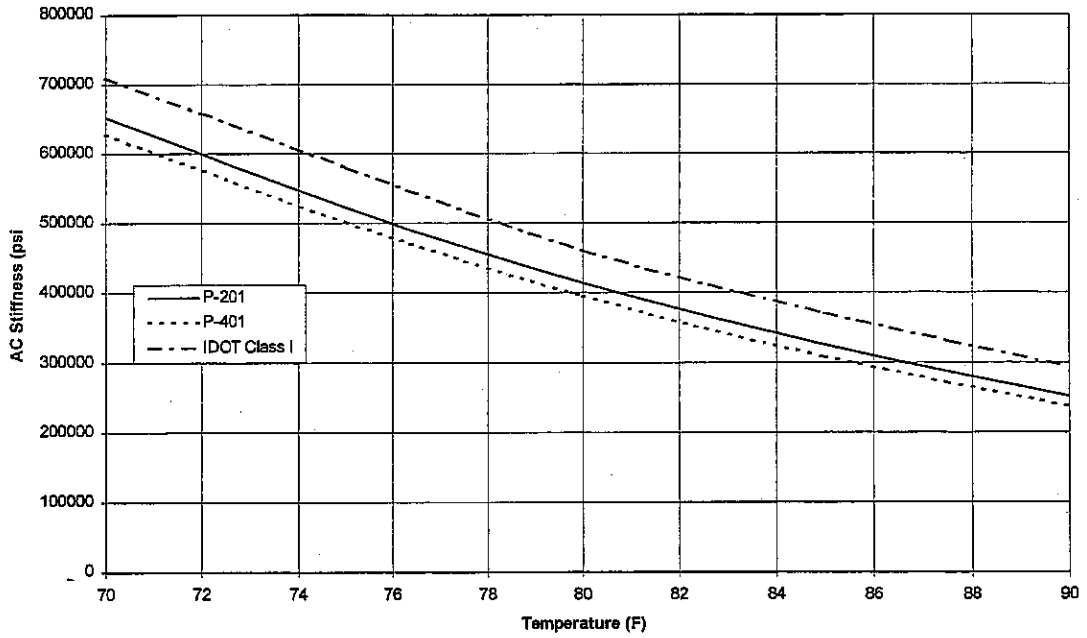


Figure D.8. AC stiffness-temperature relationship for standard IDOT-DOA AC mixtures using the AI algorithm.

AC Stiffness - Temperature Relationship for Standard IDOT-DOA AC Mixtures
Using IDOT Stiffness Relationships

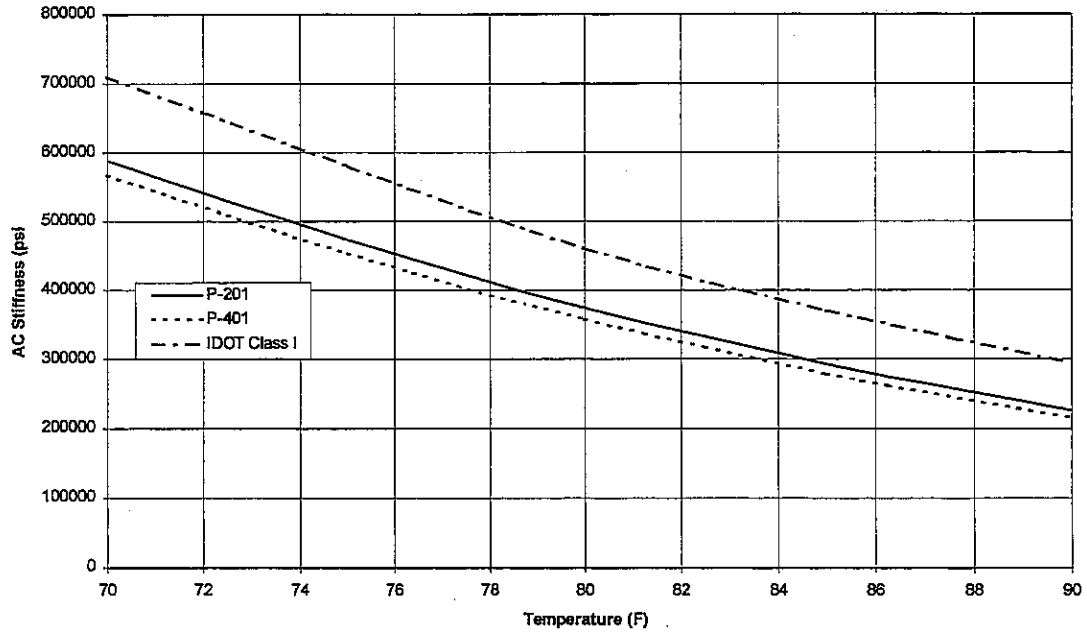


Figure D.9. AC stiffness-temperature relationship for standard IDOT-DOA AC mixtures using the IDOT algorithm.

Where: N is the number of repetitions to failure.
 ϵ is the AC tensile strain.
 E_{ac} is the AC modulus.
 $K, k', n, n',$ and m' are experimentally derived coefficients.

Through consideration of mixture composition factors, split tensile strength characteristics, and field calibration studies, the University of Illinois has developed the following relationship for IDOT Class I AC mixtures [Gomez, 1984][Thompson, 1986]:

$$N = 5 \times 10^{-6} (1 / \epsilon)^{3.0} \quad \text{Equation D.6}$$

Maupin and Freeman analyzed laboratory beam fatigue tests on seven AC materials collected from five different areas in the United States [Maupin, 1976]. They correlated the use of indirect testing methods to AC fatigue characteristics. Their proposed constant strain fatigue curve predication equation follows the same form as shown in Equation D.4, with k and n related to the AC indirect tensile strength at 72°F as follows:

$$n = 0.0374 \sigma_{IT} - 0.744 \quad \text{Equation D.7}$$

$$\text{Log}(k) = 7.92 - 0.122 \sigma_{IT} \quad \text{Equation D.8}$$

Where: σ_{IT} is the indirect tensile strength at 72° F.

Figure D.10 is obtained by plotting the number of repetitions to failure versus the strain in the AC using the Maupin and Freeman relationships for split tensile strengths of 75 psi, 100 psi, 125 psi, and 150 psi. Also plotted is the IDOT Class I relationship. Note that for a given AC strain, the IDOT Class I relationship predicts fewer repetitions to failure than any of the Maupin-Freeman relationships, except the 75 psi mixture at low AC strain levels. This reflects the impact of the field calibration studies.

Asphalt Concrete Fatigue Relationships Based on Maupin and Freeman

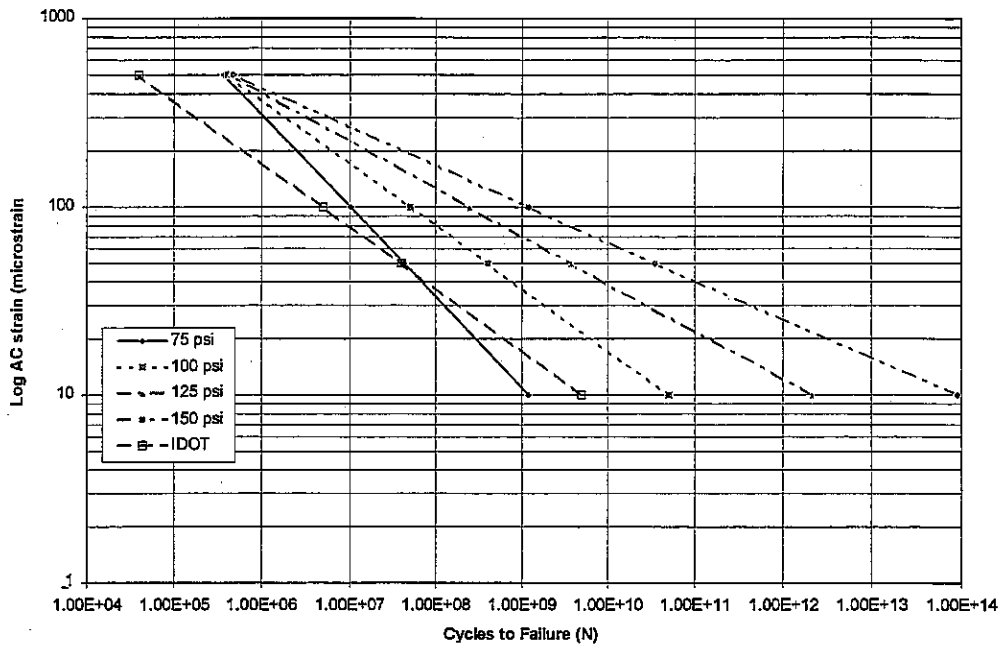


Figure D.10. AC fatigue relationship based on Maupin and Freeman [Maupin, 1976].

The FHWA Cost Allocation Study examined AC fatigue relationships patterned after the 10% fatigue equation developed in NCHRP 1-10B [Rauhut, 1984]. In this study, the initial relationship developed between “k” and “n” for a given reference temperature is shown in Equation D.9:

$$n = 1.35 - 0.252 \text{Log}(k) \quad \text{Equation D.9}$$

In the course of this study, Equation D.9 was modified to reflect the statistical analysis of available fatigue data and the assumptions/approximations of the researchers. The resulting relationship, presented in Equation D.10, is a modified version of Equation D.9.

$$n = 1.75 - 0.252 \text{Log}(k) \quad \text{Equation D.10}$$

Using the coefficient “n” derived from the Maupin-Freeman relationship, the coefficient “k” can be estimated using Equations D.9 and D.10. The resulting AC fatigue

relationships for mix tensile strengths of 75 psi, 100 psi, 125 psi, and 150 psi would appear as shown in Figures D.11 and D.12. Also shown is the IDOT Class I relationship. In Figure D.11, it is observed that the IDOT Class I relationship typically predicts cycles to failure at a higher number of repetitions than the first FHWA equation. Figure D.12 shows that the IDOT Class I relationship predicts slightly fewer cycles to failure than most of the curves generating using the modified FHWA Cost Allocation Study equation.

The mean tensile strengths of the AC materials tested in the course of this project are presented in Table 4.16. The mean split tensile strengths vary from 106 psi to 150 psi. In light of these values and the examination of various fatigue relationships, the use of the IDOT Class I fatigue characteristics is a good starting point for use in examining fatigue of IDOT-DOA P-401 and P-201 AC mixtures.

Summary

As IDOT-DOA moves toward a mechanistic design procedure, P-401 and P-201 AC stiffness and fatigue properties must be characterized. The analysis presented in this appendix is a preliminary step toward identifying a feasible approach to accomplish this task. The variation observed within the specifications and the inconsistencies noted when comparing laboratory results to estimated mixture properties reveals that additional laboratory and analytical work is required. In the interim, the use of the IDOT Class I mixture properties provides a reasonable basis for evaluating expected IDOT-DOA P-401 and P-201 structural behavior.

**Asphalt Concrete Fatigue Relationships Modified Using FHWA Cost Allocation Study
(Based on Equation D.9)**

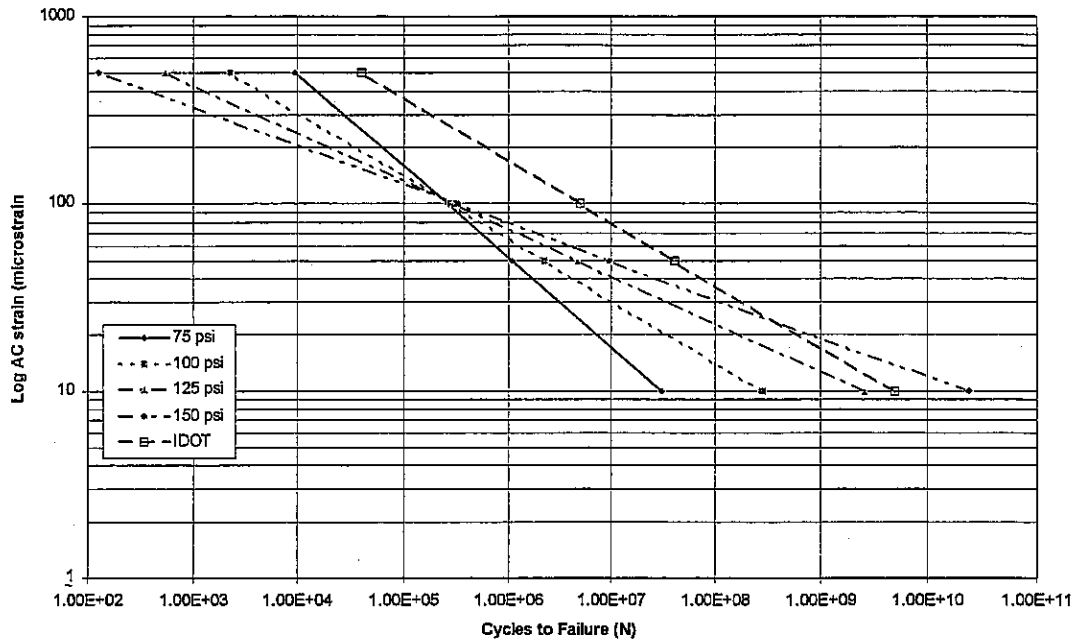


Figure D.11. AC fatigue relationship based on Equation D.9 from the FHWA Cost Allocation Study.

**Asphalt Concrete Fatigue Relationships Modified Using FHWA Cost Allocation Study
(Based on Equation D.10)**

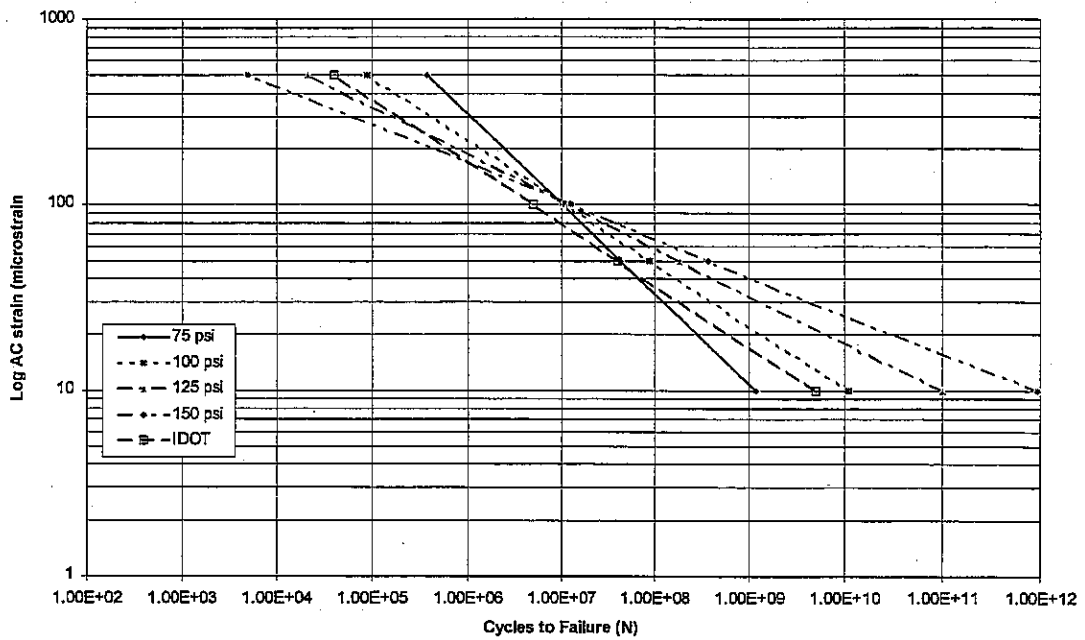


Figure D.12. AC fatigue relationship based on Equation D.10 from the FHWA Cost Allocation Study.



APPENDIX E: SUMMARY OF ILLI-SLAB RESULTS

The ILLI-SLAB two dimensional finite element model was developed at the University of Illinois for the analysis of one and two layer jointed PCC pavement systems [Tabatabaie, 1980]. In its current form, ILLI-SLAB can utilize a variety of slab support characterization models and accommodate a temperature distribution through the slab thickness [Ioannides, 1985].

In this project, the ILLI-SLAB model was used to analyze the structural response of a PCC slab system under Beechcraft King Air B200 loading. The dual wheel system of the King Air B200 was modeled as two 5.0 in by 5.5 in rectangles, spaced 11 in center-to-center. Tire pressure was assumed to be 105 psi. Slab thickness was set at 6 in, corresponding to IDOT-DOA GA practices to-date on all air-side PCC pavements. Three slab sizes (12.5 ft by 12.5 ft, 12.5 ft by 15 ft, and 12.5 ft by 20 ft) were evaluated on support values (modulus of subgrade reaction, k) ranging from 50 to 500 psi/in. Free edge loading for the Beechcraft King Air B200 was placed at mid-slab longitudinal and transverse edge locations. The initial experimental matrix consisted of 108 ILLI-SLAB runs conducted without a temperature gradient. The maximum tensile stress calculated for each configuration is presented in Table E.1. In all cases, the longitudinal joint loading condition was found to be critical. Thus, in the analysis of GA airport pavement loading, the longitudinal joint was selected as the critical loading location.

The climatic effect of slab curling was considered by including a 2.5° F/in temperature gradient (15° F from top to bottom of the slab). As indicated in Table 12 of the report, a temperature gradient of 2.5° F/in is typically exceeded only 10% of the time over the course of a year within the State. A positive temperature gradient (the top of the slab is warmer than the bottom) is most critical as the curl stress is additive to the load stress. A total of 54 ILLI-SLAB runs were conducted with a temperature gradient with the load placed on the longitudinal joint. The calculated maximum tensile stress for each configuration is presented in Table E.1.

The headings in Table E.1 are defined as follows:

Load Orientation	The position of the load relative to the length of the slab.	
Slab Width	The width of the slab.	ft
Slab Length	The length of the slab.	ft
k	Modulus of subgrade reaction.	psi/in
E_{PCC}	PCC modulus of elasticity.	psi
l	Radius of relative stiffness.	in
L/l	Ratio of slab length over the radius of relative stiffness.	
Load σ	Maximum tensile stress generated by applied load (no curl).	psi
Load + Curl σ	Maximum tensile stress generated by applied load and temperature curling.	psi

The results of the ILLI-SLAB analysis were compared to work conducted by Salsilli [Salsilli, 1993] and Lee [Lee, 1993], who independently developed regression model solutions based on ILLI-SLAB. The results of this comparison are plotted in Figures E.1 and E.2 for load induced stresses without and with curling, respectively. For load induced stresses only, both Salsilli's and Lee's model adequately predict the ILLI-SLAB solution for a 6-in thick PCC slab under King Air B200 loading. When the influence of curling stresses are considered, Salsilli's model does not predict as accurately as Lee's model.

This deficiency has been addressed in the current version of ILLI-CON [Barenberg, 1994]. This is evident in Figure E.3, which plots the ILLI-SLAB solution against Lee's and the current regression model incorporated in ILLI-CON. As a result of this comparison, it is believed that either Lee's or the current ILLI-CON regression model can be used to adequately predict combined loading and curling stresses for typical GA airport conditions.

Table E.1. Summary of ILLI-SLAB results.

Load Orientation	Slab Width	Slab Length	k	Epcc	I	L/I	Load σ	Load +Curl σ
Longitudinal	12.5	12.5	50	3000000	32.421	4.6266	403.0	479.4
Longitudinal	12.5	12.5	50	4000000	34.839	4.3055	415.0	501.5
Longitudinal	12.5	12.5	50	5000000	36.837	4.0720	423.6	517.1
Longitudinal	12.5	12.5	100	3000000	27.263	5.5020	370.5	472.9
Longitudinal	12.5	12.5	100	4000000	29.296	5.1202	384.4	504.6
Longitudinal	12.5	12.5	100	5000000	30.976	4.8425	394.8	527.9
Longitudinal	12.5	12.5	200	3000000	22.925	6.5431	336.2	459.1
Longitudinal	12.5	12.5	200	4000000	24.635	6.0889	350.5	500.8
Longitudinal	12.5	12.5	200	5000000	26.048	5.7586	361.5	533.0
Longitudinal	12.5	12.5	300	3000000	20.715	7.2411	316.4	447.6
Longitudinal	12.5	12.5	300	4000000	22.260	6.7385	330.4	495.2
Longitudinal	12.5	12.5	300	5000000	23.537	6.3729	341.4	532.9
Longitudinal	12.5	12.5	400	3000000	19.278	7.7809	302.7	438.1
Longitudinal	12.5	12.5	400	4000000	20.715	7.2411	316.4	489.5
Longitudinal	12.5	12.5	400	5000000	21.904	6.8481	327.3	531.0
Longitudinal	12.5	12.5	500	3000000	18.232	8.2273	292.3	429.9
Longitudinal	12.5	12.5	500	4000000	19.591	7.6566	305.7	484.1
Longitudinal	12.5	12.5	500	5000000	20.715	7.2411	316.4	528.6
Tranverse	12.5	12.5	50	3000000	32.421	4.6266	363.0	
Tranverse	12.5	12.5	50	4000000	34.839	4.3055	375.3	
Tranverse	12.5	12.5	50	5000000	36.837	4.0720	384.0	
Tranverse	12.5	12.5	100	3000000	27.263	5.5020	330.1	
Tranverse	12.5	12.5	100	4000000	29.296	5.1202	344.2	
Tranverse	12.5	12.5	100	5000000	30.976	4.8425	354.8	
Tranverse	12.5	12.5	200	3000000	22.925	6.5431	295.1	
Tranverse	12.5	12.5	200	4000000	24.635	6.0889	309.7	
Tranverse	12.5	12.5	200	5000000	26.048	5.7586	320.9	
Tranverse	12.5	12.5	300	3000000	20.715	7.2411	274.9	
Tranverse	12.5	12.5	300	4000000	22.260	6.7385	289.2	
Tranverse	12.5	12.5	300	5000000	23.537	6.3729	300.4	
Tranverse	12.5	12.5	400	3000000	19.278	7.7809	261.0	
Tranverse	12.5	12.5	400	4000000	20.715	7.2411	274.9	
Tranverse	12.5	12.5	400	5000000	21.904	6.8481	286.0	
Tranverse	12.5	12.5	500	3000000	18.232	8.2273	250.3	
Tranverse	12.5	12.5	500	4000000	19.591	7.6566	264.1	
Tranverse	12.5	12.5	500	5000000	20.715	7.2411	275.0	

Table E.1. Summary of ILLI-SLAB results.

Load Orientation	Slab Width	Slab Length	k	E _{pcc}	I	L/I	Load σ	Load +Curl σ
Longitudinal	12.5	15	50	3000000	32.421	5.5520	405.3	510.1
Longitudinal	12.5	15	50	4000000	34.839	5.1666	419.5	545.2
Longitudinal	12.5	15	50	5000000	36.837	4.8864	430.2	572.1
Longitudinal	12.5	15	100	3000000	27.263	6.6024	370.2	494.6
Longitudinal	12.5	15	100	4000000	29.296	6.1442	384.7	539.6
Longitudinal	12.5	15	100	5000000	30.976	5.8110	396.0	575.8
Longitudinal	12.5	15	200	3000000	22.925	7.8517	335.9	471.2
Longitudinal	12.5	15	200	4000000	24.635	7.3067	350.0	524.8
Longitudinal	12.5	15	200	5000000	26.048	6.9103	361.0	569.8
Longitudinal	12.5	15	300	3000000	20.715	8.6894	316.6	454.5
Longitudinal	12.5	15	300	4000000	22.260	8.0863	330.2	512.5
Longitudinal	12.5	15	300	5000000	23.537	7.6475	341.0	562.3
Longitudinal	12.5	15	400	3000000	19.278	9.3371	303.1	441.8
Longitudinal	12.5	15	400	4000000	20.715	8.6894	316.6	502.4
Longitudinal	12.5	15	400	5000000	21.904	8.2177	327.1	555.3
Longitudinal	12.5	15	500	3000000	18.232	9.8728	292.7	431.4
Longitudinal	12.5	15	500	4000000	19.591	9.1879	306.1	493.8
Longitudinal	12.5	15	500	5000000	20.715	8.6894	316.6	549.0
Tranverse	12.5	15	50	3000000	32.421	5.5520	362.9	
Tranverse	12.5	15	50	4000000	34.839	5.1666	375.1	
Tranverse	12.5	15	50	5000000	36.837	4.8864	383.8	
Tranverse	12.5	15	100	3000000	27.263	6.6024	330.0	
Tranverse	12.5	15	100	4000000	29.296	6.1442	344.1	
Tranverse	12.5	15	100	5000000	30.976	5.8110	354.7	
Tranverse	12.5	15	200	3000000	22.925	7.8517	295.1	
Tranverse	12.5	15	200	4000000	24.635	7.3067	309.6	
Tranverse	12.5	15	200	5000000	26.048	6.9103	320.9	
Tranverse	12.5	15	300	3000000	20.715	8.6894	274.9	
Tranverse	12.5	15	300	4000000	22.260	8.0863	289.2	
Tranverse	12.5	15	300	5000000	23.537	7.6475	300.4	
Tranverse	12.5	15	400	3000000	19.278	9.3371	261.0	
Tranverse	12.5	15	400	4000000	20.715	8.6894	274.9	
Tranverse	12.5	15	400	5000000	21.904	8.2177	286.0	
Tranverse	12.5	15	500	3000000	18.232	9.8728	250.3	
Tranverse	12.5	15	500	4000000	19.591	9.1879	264.1	
Tranverse	12.5	15	500	5000000	20.715	8.6894	274.9	

Table E.1. Summary of ILLI-SLAB results:

Load	Slab	Slab					Load	Load +Curl
Orientation	Width	Length	k	E _{pcc}	I	L/I	σ	σ
Longitudinal	12.5	20	50	3000000	32.421	7.4026	404.8	537.3
Longitudinal	12.5	20	50	4000000	34.839	6.8888	419.5	590.6
Longitudinal	12.5	20	50	5000000	36.837	6.5152	431.0	637.4
Longitudinal	12.5	20	100	3000000	27.263	8.8031	370.3	506.8
Longitudinal	12.5	20	100	4000000	29.296	8.1922	384.5	566.2
Longitudinal	12.5	20	100	5000000	30.976	7.7479	395.6	619.8
Longitudinal	12.5	20	200	3000000	22.925	10.4689	336.7	471.4
Longitudinal	12.5	20	200	4000000	24.635	9.7422	350.6	534.8
Longitudinal	12.5	20	200	5000000	26.048	9.2138	361.4	593.4
Longitudinal	12.5	20	300	3000000	20.715	11.5858	317.3	449.7
Longitudinal	12.5	20	300	4000000	22.260	10.7817	331.0	514.5
Longitudinal	12.5	20	300	5000000	23.537	10.1967	341.8	575.4
Longitudinal	12.5	20	400	3000000	19.278	12.4494	303.6	434.3
Longitudinal	12.5	20	400	4000000	20.715	11.5858	317.3	499.8
Longitudinal	12.5	20	400	5000000	21.904	10.9569	327.9	561.9
Longitudinal	12.5	20	500	3000000	18.232	13.1637	293.2	422.9
Longitudinal	12.5	20	500	4000000	19.591	12.2505	306.7	488.3
Longitudinal	12.5	20	500	5000000	20.715	11.5858	317.3	551.0
Tranverse	12.5	20	50	3000000	32.421	7.4026	362.8	
Tranverse	12.5	20	50	4000000	34.839	6.8888	375.0	
Tranverse	12.5	20	50	5000000	36.837	6.5152	383.6	
Tranverse	12.5	20	100	3000000	27.263	8.8031	330.0	
Tranverse	12.5	20	100	4000000	29.296	8.1922	344.1	
Tranverse	12.5	20	100	5000000	30.976	7.7479	354.6	
Tranverse	12.5	20	200	3000000	22.925	10.4689	295.1	
Tranverse	12.5	20	200	4000000	24.635	9.7422	309.6	
Tranverse	12.5	20	200	5000000	26.048	9.2138	320.9	
Tranverse	12.5	20	300	3000000	20.715	11.5858	274.9	
Tranverse	12.5	20	300	4000000	22.260	10.7817	289.2	
Tranverse	12.5	20	300	5000000	23.537	10.1967	300.4	
Tranverse	12.5	20	400	3000000	19.278	12.4494	261.0	
Tranverse	12.5	20	400	4000000	20.715	11.5858	274.9	
Tranverse	12.5	20	400	5000000	21.904	10.9569	286.0	
Tranverse	12.5	20	500	3000000	18.232	13.1637	250.3	
Tranverse	12.5	20	500	4000000	19.591	12.2505	264.1	
Tranverse	12.5	20	500	5000000	20.715	11.5858	274.9	

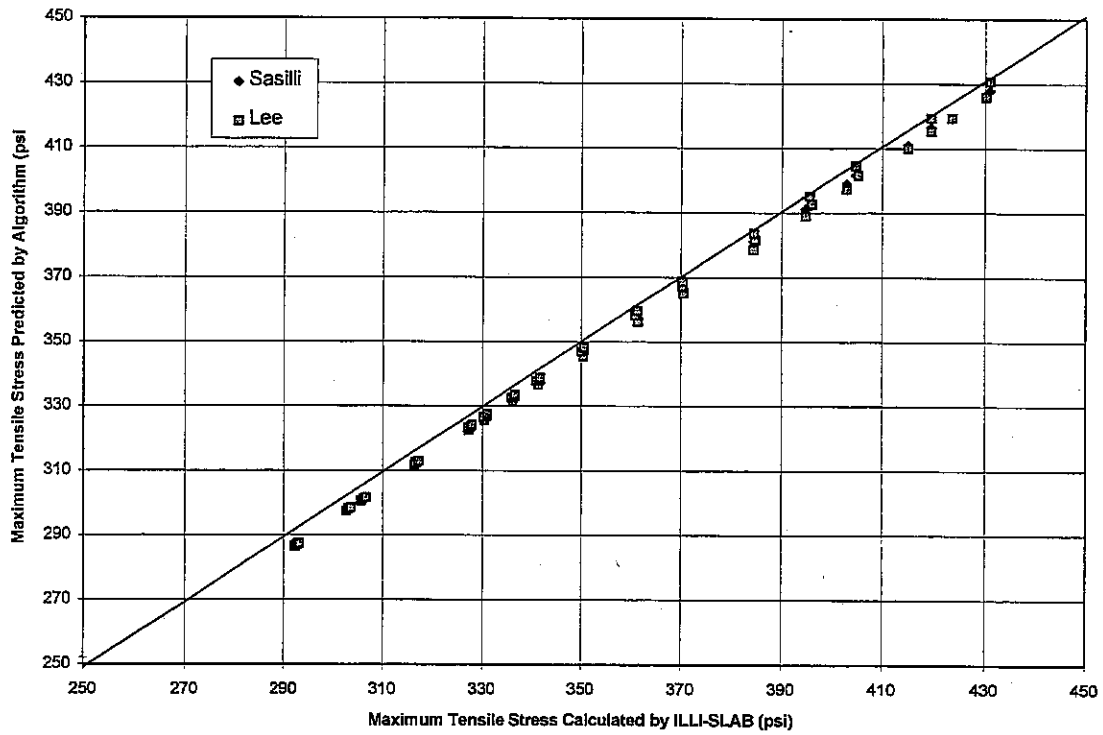


Figure E.1. Comparison of ILLI-SLAB to regression model solutions proposed by Salsilli and Lee for loading stress.

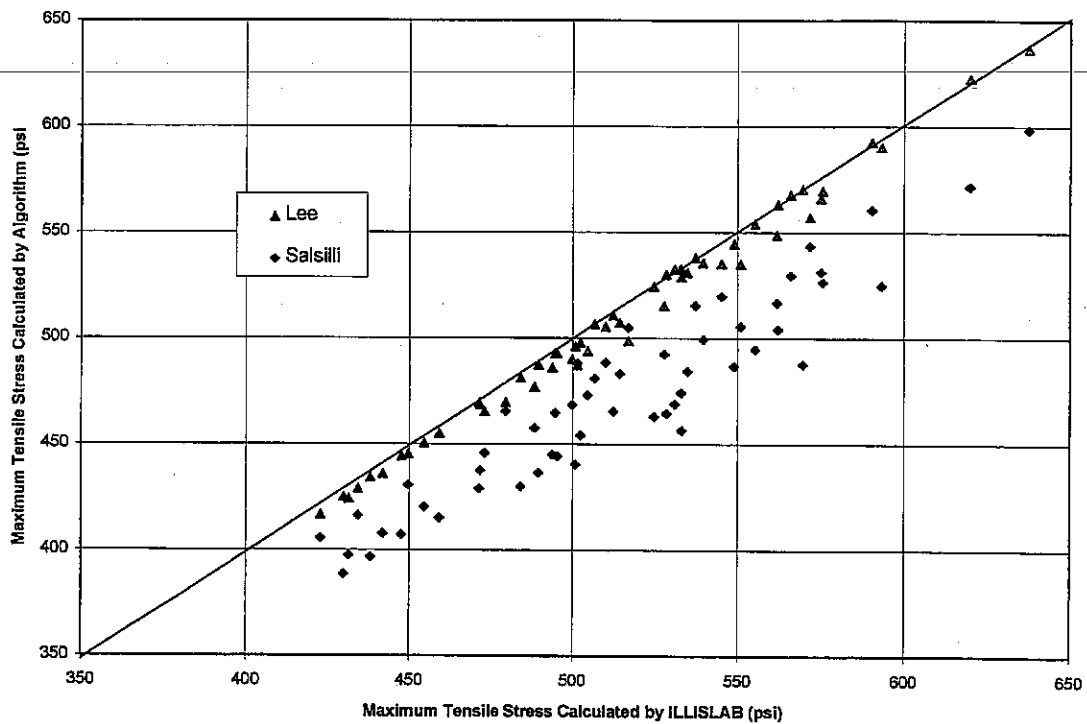


Figure E.2. Comparison of ILLI-SLAB to regression model solutions proposed by Salsilli and Lee for combined maximum loading and curling stress.

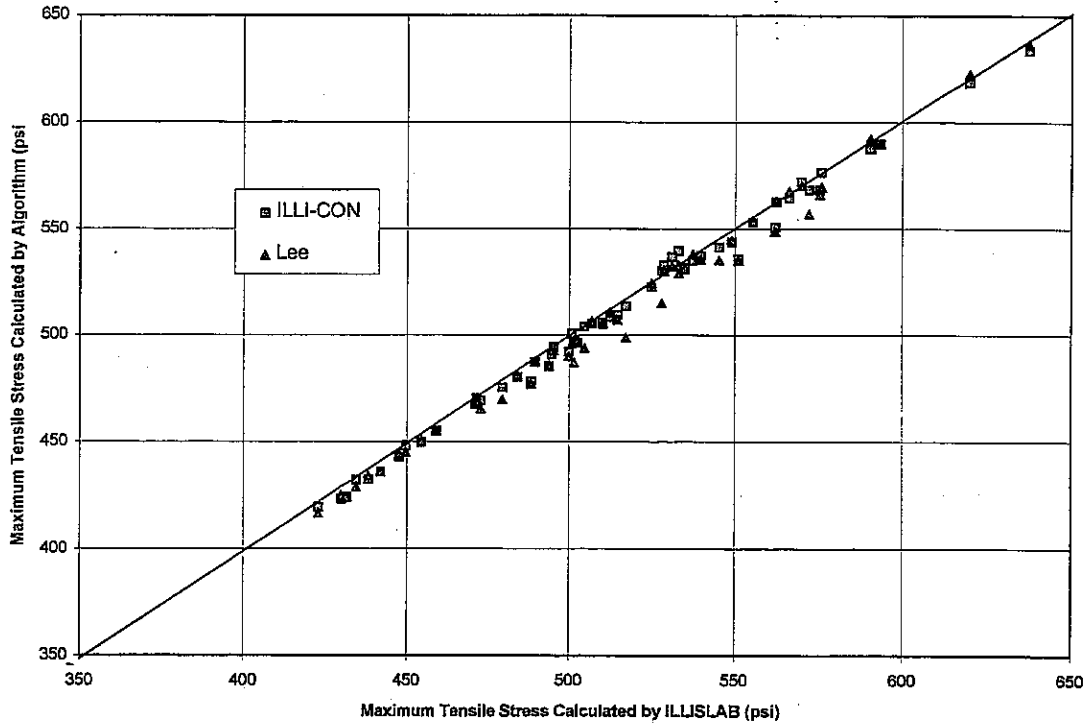


Figure E.3. Comparison of ILLI-SLAB to regression model solutions proposed by ILLI-CON and Lee for combined maximum loading and curling stress.

To analyze anticipated structural performance of PCC pavements under actual field conditions, the free edge stresses were reduced by 25%, reflecting the load transfer efficiency of the joints as recommended by the FAA [FAA, 1978]. It is noted this stress load transfer efficiency translates to a deflection load transfer efficiency of approximately 85%. Figure E.4, E.5, and E.6 show the reduction in critical stress conditions for E_{PCC} of 3,00,000 psi, 4,000,000 psi, and 5,000,000 psi, respectively. Also illustrated is the influence of curling stresses and slab length.

PCC fatigue cracking is commonly related to the stress ratio (SR) defined as the induced tensile stress over PCC modulus of rupture (σ/M_R). Foxworthy developed the following relationship to estimate the PCC modulus of rupture given the E_{PCC} [Foxworthy, 1985]:

Critical Flexural Stresses In PCC Using ILLI-SLAB ($E_{pcc} = 3,000,000$ psi, 25% L-T)

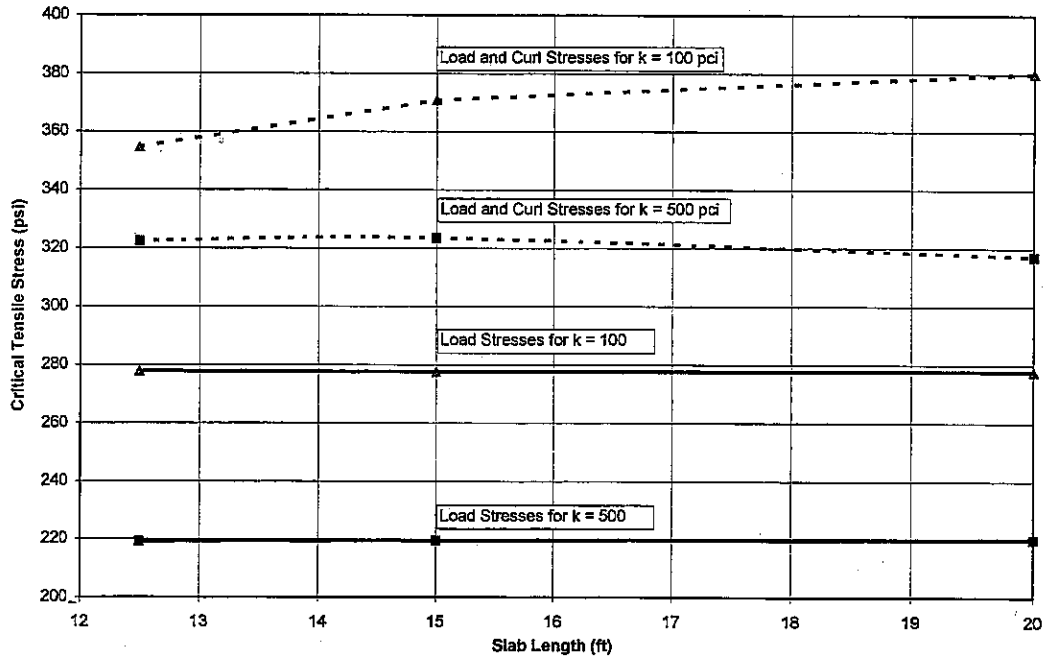


Figure E.4. Calculated critical edge tensile stresses assuming a stress load transfer efficiency of 25% ($E_{PCC} = 3,000,000$ psi).

Critical Flexural Stresses In PCC Based on ILLI-SLAB Analysis ($E_{pcc} = 4,000,000$ psi, 25% L-T)

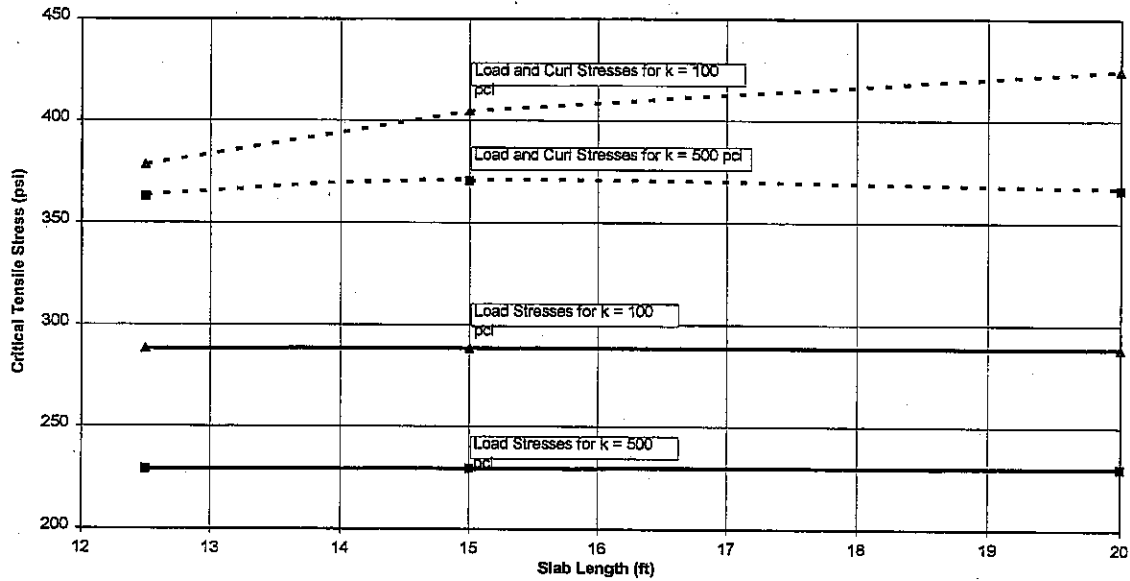


Figure E.5. Calculated critical edge tensile stresses assuming a stress load transfer efficiency of 25% ($E_{PCC} = 4,000,000$ psi).

Calculated Critical Tensile Stresses In PCC Using ILLI-SLAB ($E_{pcc} = 5,000,000$ psi, 25% L-T)

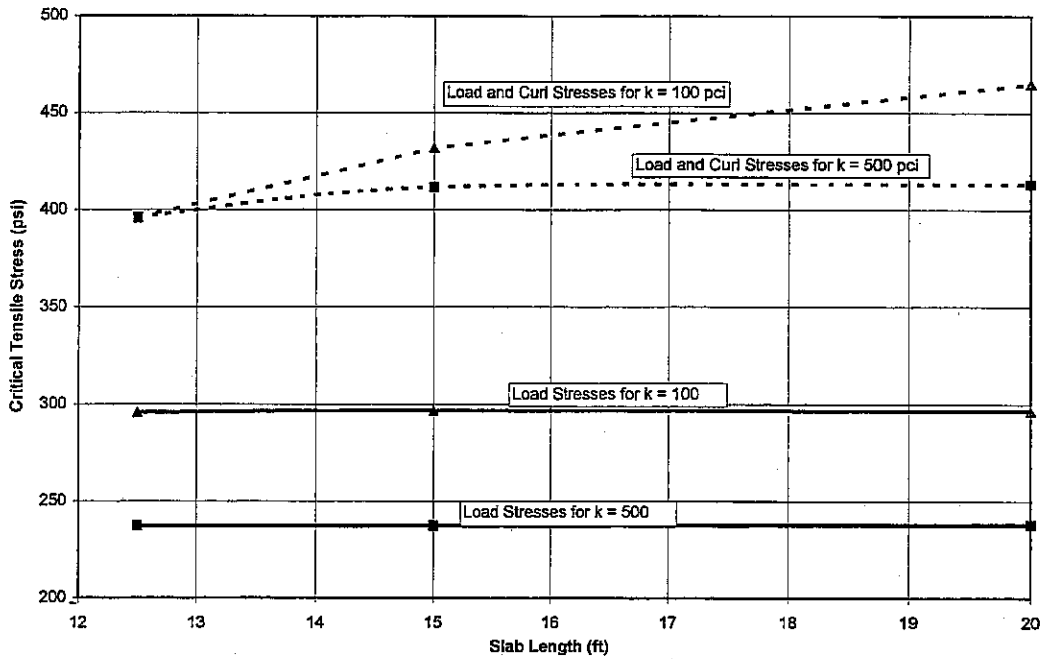


Figure E.6. Calculated critical edge tensile stresses assuming a stress load transfer efficiency of 25% ($E_{PCC} = 5,000,000$ psi).

$$M_R = 43.5 \left(\frac{E_{PCC}}{10^6} \right) + 488.5 \quad \text{Equation E.1}$$

Where: M_R is the PCC modulus of rupture (psi).
 E_{PCC} is the PCC modulus of elasticity (psi).

The equivalent M_R for E_{PCC} of 3, 4, and 5 million psi are 619, 662, and 706 psi, respectively.

A number of PCC fatigue/slab cracking transfer functions are represented in the published literature. Two have been selected for examination in this study. The Zero-Maintenance Design equation (ZM) was derived from a 140 laboratory beam tests collected under three previous studies [Darter, 1977]. The least squares regression curve for a 50% failure probability has the following form [Darter, 1977]:

$$\text{Log } N = 17.61 - 17.61SR$$

Equation E.2

Where: N is equal to the number of stress applications to failure.
 SR is the stress ratio (σ/M_R).

Typically, laboratory testing must be related to field performance to reflect the variability inherent in field conditions (i.e. loading variability, support conditions, construction variability, climatic conditions, etc.). To address these concerns, it is necessary to calibrate laboratory observations to field performance. An example of such a field calibrated mechanistic design model (MD) is presented below [Salsilli, 1993]:

$$\text{Log } N = \left[\frac{-SR^{-5.367} \text{Log}(1-P)}{0.0032} \right]^{0.2276}$$

Equation E.3

Where: N is equal to the number of stress applications to failure.
 SR is the stress ratio (σ/M_R).

P is equal to the failure probability level.

In this analysis, both PCC fatigue transfer functions were used to estimate the allowable coverages to failure. The M_R was set at 619 psi, 662 psi, and 706 psi (for E_{PCC} of 3,000,000 psi, 4,000,000 psi, and 5,000,000 psi, respectively), and the critical tensile stresses were reduced 25% for load transfer. The percent probability of failure was set at 50%. A pass-to-coverage ratio (P/C) of 3.48 was applied per FAA recommendations [FAA, 1978].

Figures E.7, E.8, and E.9 present the estimated allowable passes for a probability of failure of 50% for each fatigue model for the three E_{PCC} values. Both non-curling and curling conditions were considered. For each PCC modulus, the general trends show with increasing modulus of subgrade reaction, there is an increase in estimated allowable passes to failure.

PCC Allowable Passes Using Fatigue Relationships ($E_{pcc} = 3,000,000$ psi)

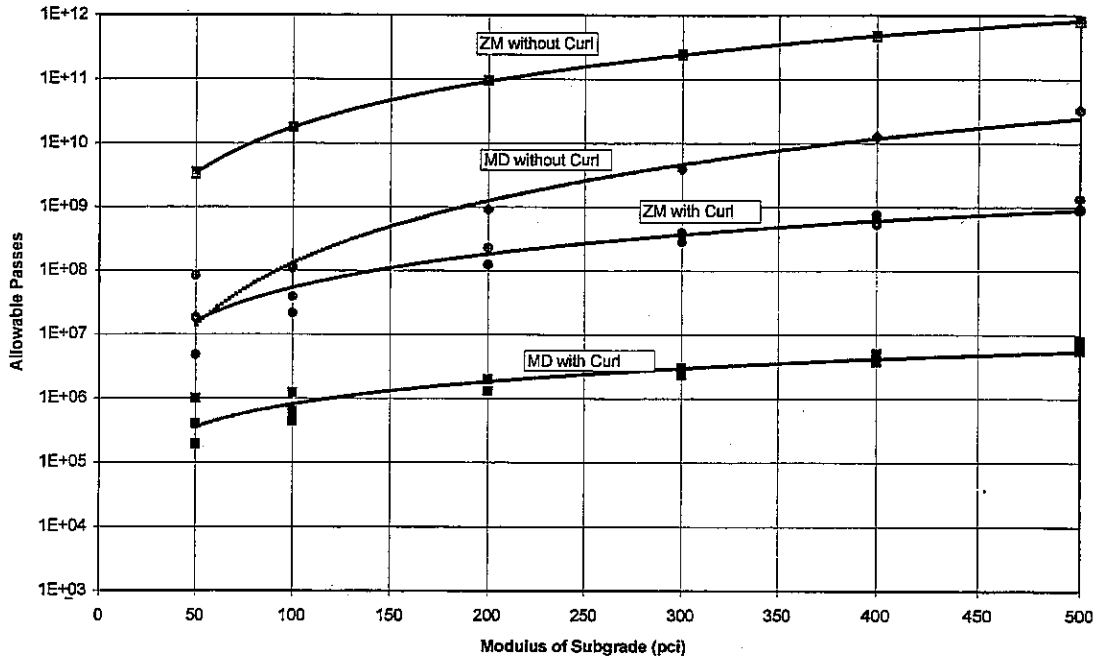


Figure E.7. Estimated allowable passes for $E_{pcc} = 3,000,000$ psi.

PCC Allowable Passes Using Fatigue Relationships ($E_{pcc} = 4,000,000$ psi)

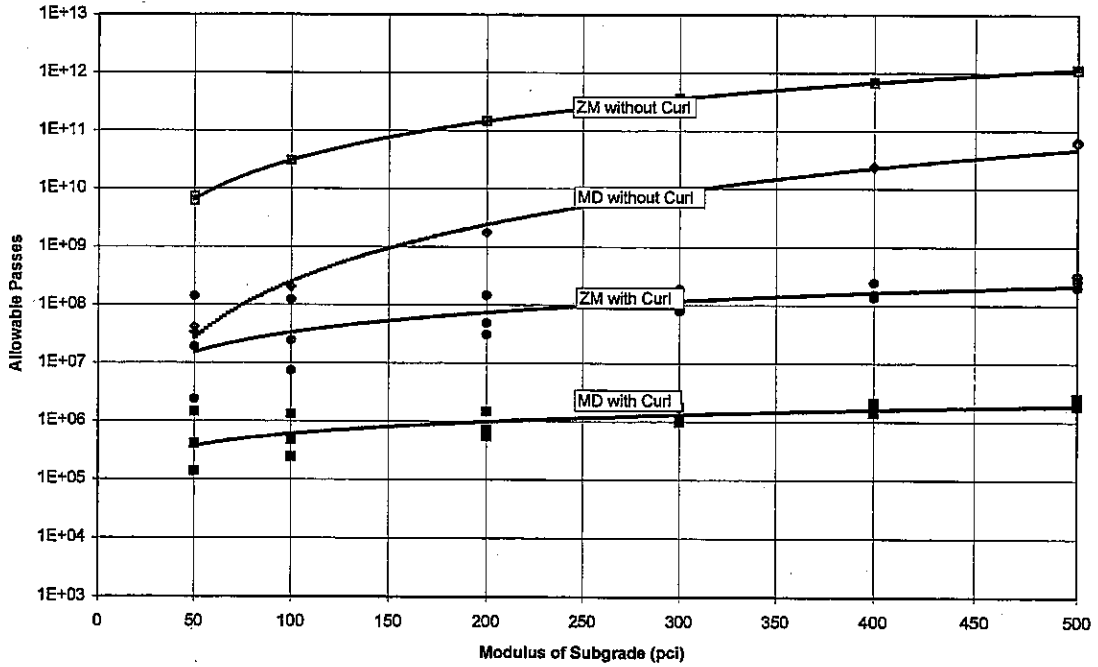


Figure E.8. Estimated allowable passes for $E_{pcc} = 4,000,000$ psi.

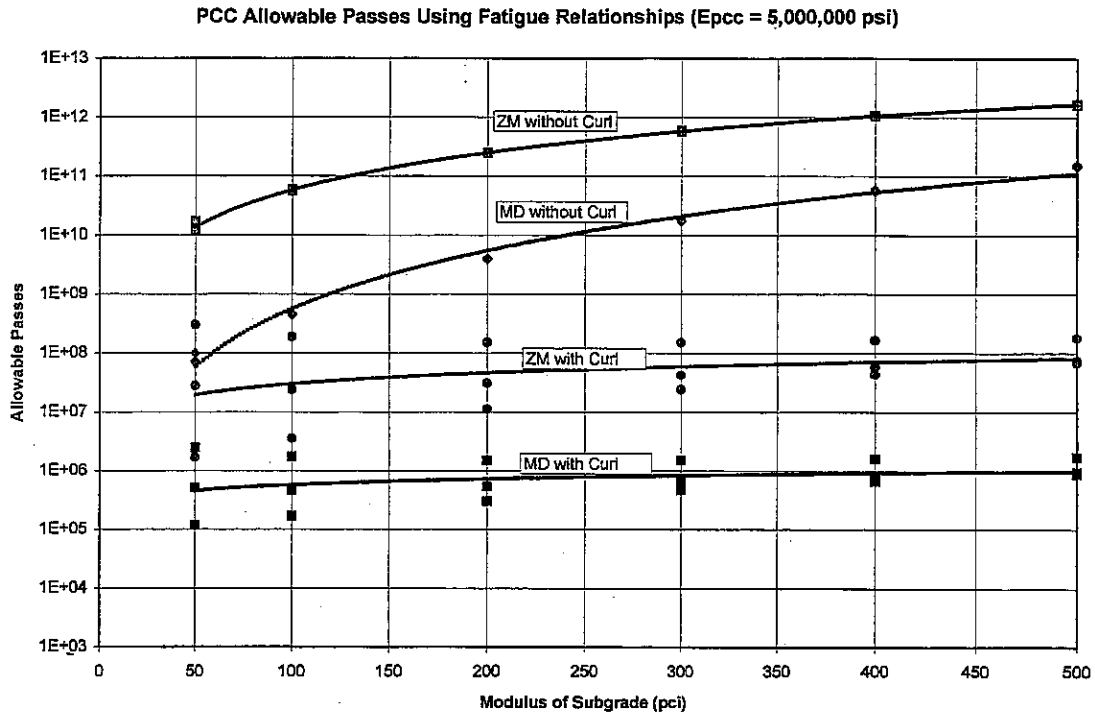


Figure E.9. Estimated allowable passes for $E_{PCC} = 5,000,000$ psi.

This trend is most pronounced when curl is not considered. The Zero- Maintenance (ZM) model predicts higher allowable passes than the Calibrated Mechanistic Design (MD) model under the same conditions.

Both fatigue models predict allowable passes in excess of 10,000,000 if only load related stresses are used in the analysis. When curling stress is combined with loading stress, however, the resulting reduction in passes is several orders of magnitude. With the MD model, the estimated number of allowable passes to failure drops into the hundreds of thousands.

The severe curling condition assumed is quite rare, with the pavement being exposed to such conditions approximately 10% of the time. In typical GA airport applications, King Air B200 loading is infrequent. Under such circumstances, a 6-in thick PCC slab is considered structurally adequate. It is possible under heavier and more frequent traffic

volumes, that the combined effects of load and temperature curl may coincide and lead to structural fatigue failures in 6-in PCC slabs.

The FAA and ACPA allow the use of 5-in thick PCC slabs for aircraft having gross maximum weights of 12,500 lbs or less. The ACPA, in their detailed design procedure, permit the use of 4-in thick PCC for a dual wheeled aircraft weighing 12,500 lbs [ACPA, 1993]. To examine the impact of reduced slab thickness, Lee's closed form solution was used to estimate maximum load and temperature induced tensile stresses. The allowable aircraft passes were calculated using the ZM and MD models using the same procedures and inputs previously described were used. The slab sizes were designed as recommended by ACPA, with 8 ft and 10 ft joint spacing for the 4-in and 5-in thick pavements, respectively.

Results of this analysis are presented graphically in Figures E.10 and E.11 for the ZM and MD models, respectively. In considering loading effects only, both models estimate that the 5-in thick slab could carry over 1,000,000 passes if the modulus of subgrade reaction is greater than 100 pci. Under severe curling conditions, the allowable passes are reduced to just over 100,000. For lightly trafficked GA pavements that service King Air B200 aircraft, a 5-in thickness appears to be structurally adequate. It is emphasized that this conclusion is based on the use of 10 ft joint spacing and does not consider loading applied by service vehicles. Longer joint spacing, heavier and more frequent aircraft volume, and/or the use of heavy service vehicles would be expected to have a negative impact on pavement performance.

Examination of the 4-in thick slab is not as promising. Although the MD fatigue algorithm calculates allowable passes in the tens of thousands, it is likely outside the range for which it was developed. This point is discussed by Salsilli, who states that beyond a stress ratio of 0.8, beam and field data separate due to the plastic behavior of PCC under high stress levels [Salsilli, 1993]. The stress ratio under some loading conditions approaches 92%, a situation that would lead to rapid pavement failure. The Zero Maintenance model, which is based on beam testing, predicts under 100 estimated passes of the King Air B200 aircraft to

Passes to Failure for 4-in and 5-in Thick PCC Slabs Using the Zero-Maintenance Model

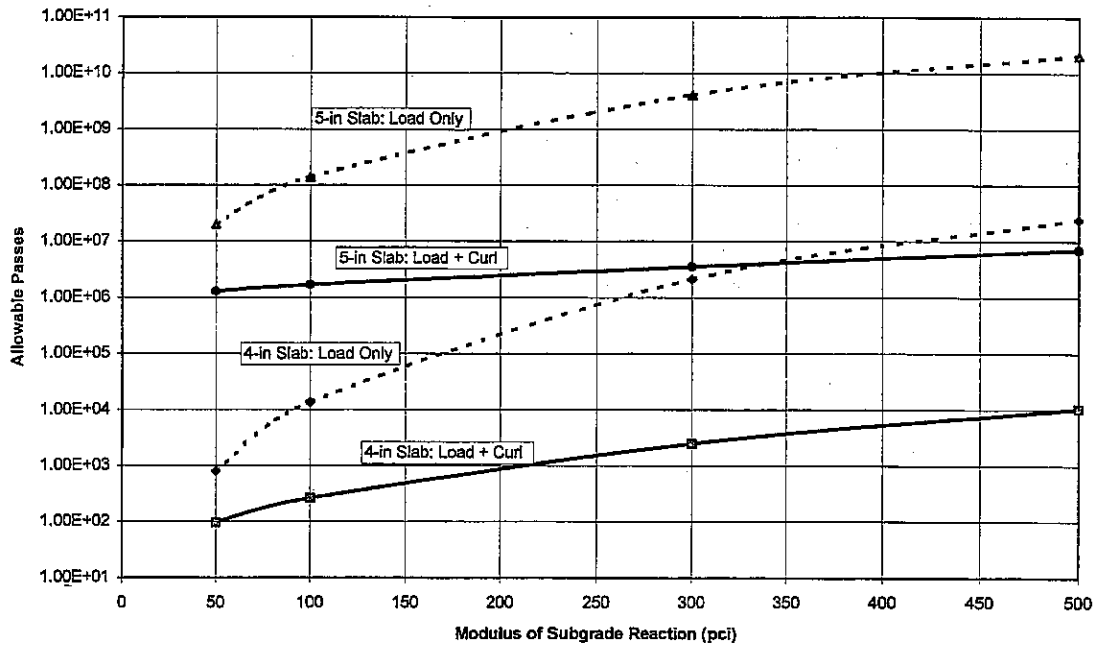


Figure E.10. Estimated allowable passes for 4-in and 5-in thick PCC using the Zero-Maintenance model.

Passes to Failure for 4-in and 5-in Thick PCC Slabs Using the Calibrated Mechanistic Model

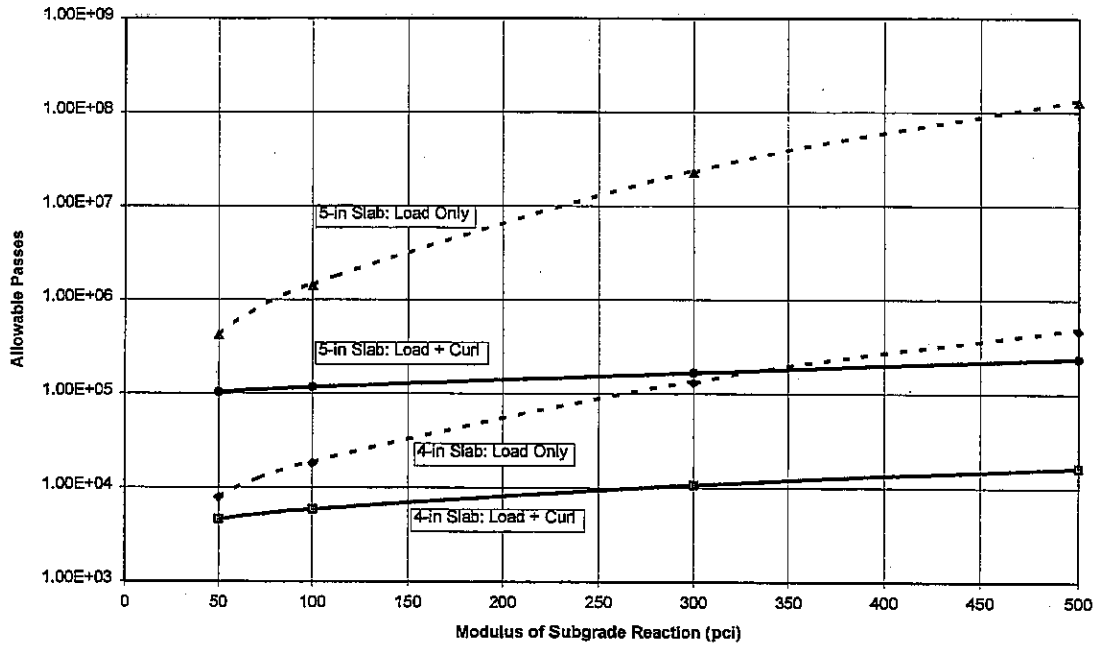
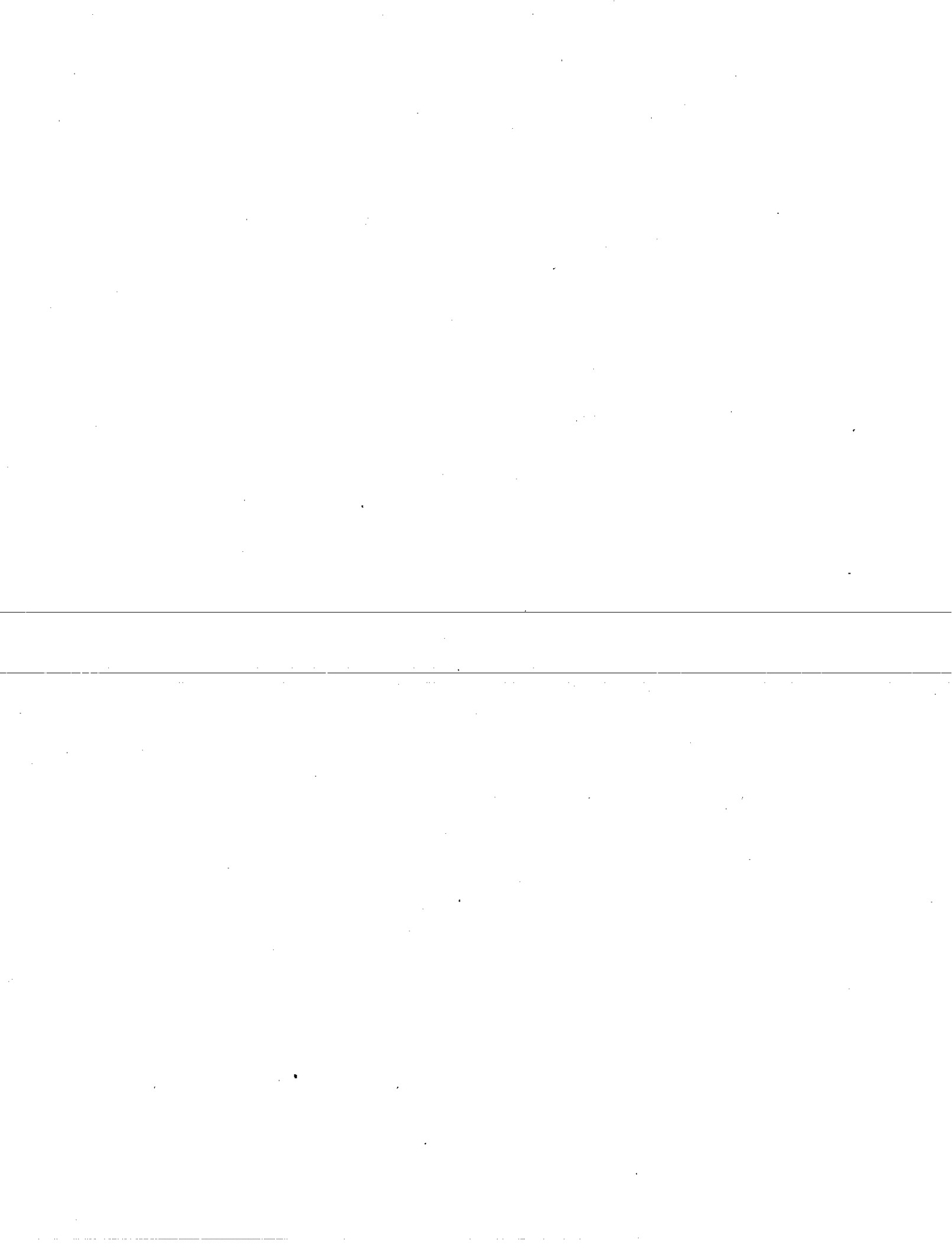


Figure E.11. Estimated allowable passes for 4-in and 5-in thick PCC using the calibrated mechanistic model.

failure (assuming a reliability of 50%) for a modulus of subgrade reaction value of 50 pci. It does not seem likely that a 4-in thick pavement can provide adequate structural performance. This analysis was conducted assuming 8 ft joint spacing and service vehicles were not considered. Longer joint spacing, heavier and/or more frequent aircraft loading, or the use of any service vehicles approaching highway loading conditions would likely lead to early structural failure of a 4-in thick PCC pavement.



APPENDIX F: ACCESS® DATA BASE

This appendix contains two tables. Table F.1 presents section inventory data contained in the ACCESS® data base. The following information is provided:

Airport	Name of Airport.
AID	Three character airport identification number.
Climatic Zone	Climatic Zone in which the airport is located. N for Northern Climatic Zone. C for Central Climatic Zone. S for Southern Climatic Zone.
Section	Pavement section designation. First three characters are AID number. Fourth and fifth characters define feature (e.g. RW, TW, AP). Remaining characters define IDOT-DOA section number.
Code	Pavement Type (e.g. TNAC, TKAC, PCC).
Construction Date	Year that pavement is constructed (all sections are listed as being constructed on June 1).
Thickness Layer 1	Thickness of surface layer, in.
Material Layer 1	FAA material code for surface layer (e.g. P-401 or P-501).
Thickness Layer 2	Thickness of second layer, in.

Material Layer 2 FAA material code for second layer.

Thickness Layer 3 Thickness of third layer, in.

Material Layer 3 FAA material code for third layer.

Thickness Layer 4 Thickness of fourth layer, in.

Material Layer 4 FAA material code for fourth layer.

Slab Length Typical length of PCC slabs, ft

Slab Width Typical width of PCC slabs, ft

The data has been sorted alphabetically according to the airport name, pavement code, and construction date.

Table F.2 provides section PCI values for each inspection date. The PCI at the time of construction was set equal to 100. In addition to the airport name, AID number, section, and code previously defined, the following additional variables are included in this table:

Inspection Date Date of inspection.

Section PCI The section PCI.

NOTE: This appendix only includes section level data. Sample unit and distress data are available in the data base available on diskette.

Table F.1. ACCESS data base section inventory information.

Airport	AID	Climatic Zone	Section	Code	Construction		Material		Thickness		Material		Thickness		Material		Thickness		Slab Length (ft)	Slab Width (ft)	
					Date	Layer 1 (in)	Layer 2 (in)	Layer 3 (in)	Layer 4 (in)	Layer 1 (in)	Layer 2 (in)	Layer 3 (in)	Layer 4 (in)								
Beardstown	K06	C	K06-AP-NN/2	TNAC	6/1/77	2	P-401	4	P-209												
Canton	CTK	C	CTK-RW-09/03	TKAC	6/1/73	2	P-401	6	P-201	6	P-155										
Canton	CTK	C	CTK-TW-A/1-03	TKAC	6/1/73	2	P-401	6	P-201	6	P-155										
Carbondale	MDH	S	MDH-AP-SS/19	PCC	6/1/74	6	P-501	5	P-201										20	12.5	
Carbondale	MDH	S	MDH-AP-SS/20	PCC	6/1/74	7	P-501	5	P-201										20	12.5	
Carmi	CUL	S	CUL-AP-EE/1	PCC	6/1/76	6	P-501												25	20	
Carmi	CUL	S	CUL-TW-B/1	TKAC	6/1/89	1.5	P-401	6.5	P-201	12	P-155										
Casey	1H8	C	1H8-TW-B/2-5	PCC	6/1/81	6	P-501												25	25	
Casey	1H8	C	1H8-TW-C/5	TNAC	6/1/81	2	P-401	8	P-209												
Casey	1H8	C	1H8-TW-B/5	TNAC	6/1/81	8	P-401	8	P-209												
Casey	1H8	C	1H8-TW-B/1-5	TNAC	6/1/81	2	P-401	8	P-209												
Centralla	ENL	S	ENL-AP-WW/06	PCC	6/1/75	6	P-501												12.5	12.5	
Centralla	ENL	S	ENL-AP-WW/09	TKAC	6/1/70	2	P-401	7	P-201												
Centralla	ENL	S	ENL-RW-18/13	TNAC	6/1/86	4	P-401	8	P-209	12	P-155										
Centralla	ENL	S	ENL-TW-A/13	TNAC	6/1/86	4	P-401	8	P-209	12	P-155										
Dekalb	DKB	N	DKB-AP-EE/02	PCC	6/1/89	6	P-501												15	15	
Dekalb	DKB	N	DKB-TW-B/03	TKAC	6/1/83	2	P-401	4	P-201												
Dekalb	DKB	N	DKB-TW-B/4-03	TKAC	6/1/83	2	P-401	4	P-201												
Dekalb	DKB	N	DKB-TW-B/3-03	TKAC	6/1/83	2	P-401	4	P-201												
Dekalb	DKB	N	DKB-TW-B/2-03	TKAC	6/1/83	2	P-401	4	P-201												
Dekalb	DKB	N	DKB-TW-B/1-03	TKAC	6/1/83	2	P-401	4	P-201												
Dekalb	DKB	N	DKB-TW-B/4-04	TKAC	6/1/88	1.5	P-401	4.5	P-201	6	P-209										
Dekalb	DKB	N	DKB-AP-EE/01	TKAC	6/1/88	1.5	P-401	4.5	P-201	12	P-155										
Dekalb	DKB	N	DKB-RW-09/02	TKAC	6/1/80	1.5	P-401	7	P-201												
Dekalb	DKB	N	DKB-TW-D/1-01	TKAC	6/1/91	1.5	P-401	7	P-201	12	P-155										
Dekalb	DKB	N	DKB-TW-D/01	TKAC	6/1/91	1.5	P-401	7	P-201	12	P-155										
Dixon	C73	N	C73-TW-A/09	TKAC	6/1/83	2	P-401	6	P-201												
Dixon	C73	N	C73-RW-08/09	TKAC	6/1/83	2	P-401	6	P-201												
Dixon Sprgs	Y51	S	Y51-RW-15/01	TKAC	6/1/88	1.5	P-401	4.5	P-201												
Dixon Sprgs	Y51	S	Y51-AP-EE/01	TKAC	6/1/88	1.5	P-401	4.5	P-201												
Dixon Sprgs	Y51	S	Y51-TW-A/01	TKAC	6/1/88	1.5	P-401	4.5	P-201												
Dupage	DPA	N	DPA-AP-NE/10	PCC	6/1/77	6	P-501	6	P-208										25	25	
Dupage	DPA	N	DPA-AP-NW/24	PCC	6/1/86	8	P-501	4	P-209										15	12.5	
Dupage	DPA	N	DPA-AP-EE/1	PCC	6/1/88	8	P-501	4	P-209										15	12.5	
Dupage	DPA	N	DPA-RW-1-RV/1	PCC	6/1/92	8	P-501	4	ATPB	8	P-155								15	12.5	
Dupage	DPA	N	DPA-TW-X/4-1	PCC	6/1/92	8	P-501	4	ATPB	8	P-155								15	12.5	
Dupage	DPA	N	DPA-TW-X/1	PCC	6/1/92	8	P-501	4	ATPB	8	P-155								15	12.5	
Dupage	DPA	N	DPA-TW-X/6-1	PCC	6/1/92	8	P-501	4	ATPB	8	P-155								15	12.5	
Dupage	DPA	N	DPA-TW-X/2-1	PCC	6/1/92	8	P-501	4	ATPB	8	P-155								15	12.5	
Dupage	DPA	N	DPA-TW-T/1	TKAC	6/1/82	2	P-401	6	P-201												
Dupage	DPA	N	DPA-TW-T/5-1	TKAC	6/1/84	2	P-401	6	P-201												
Dupage	DPA	N	DPA-TW-T/4-1	TKAC	6/1/84	2	P-401	6	P-201												

Table F. 1. ACCESS data base section inventory information.

Alrport	AID	Climatic Zone	Section	Code	Construction Date	Thickness Layer 1 (in)	Material 1	Thickness Layer 2 (in)	Material 2	Thickness Layer 3 (in)	Material 3	Thickness Layer 4 (in)	Material 4	Slab Length (ft)	Slab Width (ft)
Dupage	DPA	N	DPA-TW-T/3-1	TKAC	6/1/84	2	P-401	6	P-201						
Dupage	DPA	N	DPA-TW-T/2-1	TKAC	6/1/84	2	P-401	6	P-201						
Dupage	DPA	N	DPA-TW-T/1-1	TKAC	6/1/84	2	P-401	6	P-201						
Dupage	DPA	N	DPA-TW-T/2	TKAC	6/1/84	2	P-401	6	P-201						
Dupage	DPA	N	DPA-AP-NW/9	TNAC	6/1/69	4	P-401	6	P-209						
Dupage	DPA	N	DPA-AP-EE/2	TNAC	6/1/87	2	P-401	3	P-201						
Effingham	1H2	S	1H2-RW-11/11	PCC	6/1/83	6	P-501							15	12.5
Effingham	1H2	S	1H2-TW-C/11	PCC	6/1/83	6	P-501							15	12.5
Effingham	1H2	S	1H2-AP-NN/03	PCC	6/1/85	7	P-501	4	P-208					11.25	11.25
Effingham	1H2	S	1H2-RW-01/082	TKAC	6/1/74	2	P-401	6	P-201						
Effingham	1H2	S	1H2-RW-01/091	TKAC	6/1/74	2	P-401	6	P-201						
Effingham	1H2	S	1H2-AP-NN/01	TKAC	6/1/86	6	P-401	4	P-208						
Effingham	1H2	S	1H2-RW-09/08	TNAC	6/1/76	2	P-401	6	P-209						
Fairfield	2H3	S	2H3-TW-A/01	TKAC	6/1/89	1.5	P-401	4.5	P-201	4	P-209	12	P-155		
Fairfield	2H3	S	2H3-TW-A/1-01	TKAC	6/1/89	1.5	P-401	4.5	P-201	4	P-209	12	P-155		
Fairfield	2H3	S	2H3-RW-09/03	TKAC	6/1/89	1.5	P-401	4.5	P-201	4	P-209	12	P-155		
Flora	H84	S	H84-AP-WW/4	TKAC	6/1/79	2	P-401	6	P-201						
Flora	H84	S	H84-RW-3/2	TKAC	6/1/85	1.5	P-401	6.5	P-201						
Flora	H84	S	H84-TW-C/6	TKAC	6/1/85	1.5	P-401	6.5	P-201						
Freeport	FEP	N	FEP-TW-A/04	TKAC	6/1/88	2	P-401	6	P-201	6	P-301				
Freeport	FEP	N	FEP-TW-B/06	TKAC	6/1/83	2	P-401	6	P-201	2	P-154				
Freeport	FEP	N	FEP-TW-C/1-06	TKAC	6/1/83	2	P-401	6	P-201	2	P-154				
Freeport	FEP	N	FEP-TW-C/05	TKAC	6/1/83	2	P-401	6	P-201	2	P-154				
Freeport	FEP	N	FEP-TW-D/01	TNAC	6/1/83	2	P-401	6	P-154						
Freeport	FEP	N	FEP-TW-D/2-01	TNAC	6/1/83	2	P-401	6	P-154						
Freeport	FEP	N	FEP-TW-D/3-01	TNAC	6/1/83	2	P-401	6	P-154						
Freeport	FEP	N	FEP-AP-NN/01	TNAC	6/1/88	1.5	P-401	2	P-201	7	P-209				
Freeport	FEP	N	FEP-RW-06/02	TNAC	6/1/89	4	P-401	12.5	P-209	6	P-155				
Freeport	FEP	N	FEP-TW-D/02	TNAC	6/1/91	4	P-401	7	P-209	6	6" P-208				
Freeport	FEP	N	FEP-TW-D/1-01	TNAC	6/1/91	4	P-401	7	P-209	6	6" P-208				
Freeport	FEP	N	FEP-TW-A/2-01	TNAC	6/1/91	4	P-401	12.5	P-209	6	P-155				
Galesburg	GBG	C	GBG-AP-NN/8	TKAC	6/1/69	2	P-401	6	P-201						
Galesburg	GBG	C	GBG-AP-NN/14	TKAC	6/1/80	2	P-401	7	P-201						
Greenville	GRE	S	GRE-AP-EE/4	TNAC	6/1/76	3	P-401	8	P-209						
Grtr. Kankakee	IKK	N	IKK-RW-04/20	TKAC	6/1/86	8	P-401	6	P-209						
Grtr. Kankakee	IKK	N	IKK-TW-D/23	TKAC	6/1/86	8	P-401	4	P-209	6	P-208				
Grtr. Kankakee	IKK	N	IKK-TW-A/20	TKAC	6/1/86	8	P-401	6	P-209						
Grtr. Kankakee	IKK	N	IKK-RW-16/01	TKAC	6/1/88	2	P-401	4	P-201	4	P-209	6	P-208		
Grtr. Kankakee	IKK	N	IKK-AP-SS/10	TNAC	6/1/78	3	P-401								
Grtr. Kankakee	IKK	N	IKK-TW-A/3-22	TNAC	6/1/86	4	P-401	6	P-209						
Grtr. Kankakee	IKK	N	IKK-TW-D/22	TNAC	6/1/86	4	P-401	6	P-209						
Jacksonville	IUX	C	IUX-AP-SS/9	PCC	6/1/67	6	P-501	6	P-154					20	12.5

Table F.1. ACCESS data base section inventory information.

Airport	AID	Climatic Zone	Section	Code	Construction Date	Thickness Layer 1 (in)	Material 1	Thickness Layer 2 (in)	Material 2	Thickness Layer 3 (in)	Material 3	Thickness Layer 4 (in)	Material 4	Slab Length (ft)	Slab Width (ft)
Mt. Carmel	102	S	102-TW-A/06	TKAC	6/1/84	8	P-401	4	P-208						
Mt. Carmel	102	S	102-RW-12/01	TKAC	6/1/85	4	P-401	6	MIP AC						
Mt. Carmel	102	S	102-TW-A/1-02	TKAC	6/1/85	6	P-401	4	P-208						
Mt. Carmel	102	S	102-TW-B/01	TNAC	6/1/92	4	P-401	6	P-209						
Mt. Carmel	102	S	102-AP-NN/01	TNAC	6/1/92	4	P-401	6	P-209						
Paris	PRG	C	PRG-AP-SS/01	TKAC	6/1/73	2	P-401	6	P-201						
Paris	PRG	C	PRG-TW-A/01	TKAC	6/1/73	2	P-401	6	P-201						
Paris	PRG	C	PRG-RW-09/01	TKAC	6/1/73	2	P-401	6	P-201						
Paris	PRG	C	PRG-TW-B/01	TKAC	6/1/91	1.5	P-401	4.5	P-201	4	P-209				
Pekin	C15	C	C15-AP-EE/07	TNAC	6/1/84	1.5	P-401	3	P-201						
Pekin	C15	C	C15-RW-09/03	TNAC	6/1/88	2	P-401	2	P-201	6	P-209				
Peoria	3MY	C	3MY-AP-EE/5	PCC	6/1/67	6	P-501	6	P-154			15		12.5	
Peoria	3MY	C	3MY-AP-EE/6	TKAC	6/1/73	5.5	P-401	2.5	P-209						
Peoria	3MY	C	3MY-AP-EE/3	TNAC	6/1/67	2	P-401	7	P-209						
Peoria	3MY	C	3MY-AP-EE/8	TNAC	6/1/86	3	P-401	5	P-208						
Peoria	3MY	C	3MY-RW-17/2	TNAC	6/1/88	4	P-401	7	P-209						
Peoria	3MY	C	3MY-TW-A/3-1	TNAC	6/1/92	3	P-401	5	P-208	6	P-154				
Peoria	3MY	C	3MY-TW-A/3	TNAC	6/1/92	4	P-401	7	P-209						
Peru	VYS	N	VYS-AP-EE/02	PCC	6/1/85	6	P-501	4	P-208	12	P-152			15	12.5
Peru	VYS	N	VYS-AP-EE/04	PCC	6/1/80	6	P-501	4	P-209					15	12.5
Peru	VYS	N	VYS-TW-A/01	TKAC	6/1/85	1.5	P-401	6.5	P-201	4	P-208	12	P-155		
Peru	VYS	N	VYS-RW-18/01	TKAC	6/1/85	1.5	P-401	6.5	P-201	4	P-208	12	P-155		
Peru	VYS	N	VYS-AP-EE/05	TKAC	6/1/90	1.5	P-401	6.5	P-201						
Peru	VYS	N	VYS-RW-18/02	TKAC	6/1/92	1.5	P-401	6.5	P-201	4	P-209				
Peru	VYS	N	VYS-AP-EE/01	TNAC	6/1/88	1	P-401	1.75	P-201	8	P-209	12	P-208		
Pickneyville	K16	S	K16-TW-A/02	TKAC	6/1/79	6	P-201								
Pickneyville	K16	S	K16-AP-WW/02	TKAC	6/1/79	6	P-201								
Pickneyville	K16	S	K16-RW-18/01	TKAC	6/1/90	3	P-401	3	P-201	4	P-208				
Pickneyville	K16	S	K16-RW-18/02	TNAC	6/1/78	1.5	P-401	2.5	P-201						
Pickneyville	K16	S	K16-AP-WW/01	TNAC	6/1/78	1.5	P-401	2.5	P-201						
Quincy	UIN	C	UIN-TW-B/1-01	PCC	6/1/46	8.5	P-501	7	P-208					20	12.5
Quincy	UIN	C	UIN-TW-B/01	PCC	6/1/46	8.5	P-501	7	P-208					20	12.5
Quincy	UIN	C	UIN-RW-18/01/1	PCC	6/1/46	8.5	P-501	7	P-208					20	12.5
Quincy	UIN	C	UIN-TW-A/06	PCC	6/1/71	9.5	P-501	9	P-154					20	10
Quincy	UIN	C	UIN-RW-04/06	PCC	6/1/71	9.5	P-501	9	P-154					20	12.5
Rochelle	12C	N	12C-RW-07/03	TKAC	6/1/87	1.5	P-401	6.5	P-201						
Rochelle	12C	N	12C-TW-C/01	TNAC	6/1/91	4	P-401	6	P-209						
Savanna	SFY	N	SFY-AP-WW/01	TNAC	6/1/81	4	P-401								
Savanna	SFY	N	SFY-AP-NN/01	TNAC	6/1/81	4	P-401								
Savanna	SFY	N	SFY-TW-B/01	TNAC	6/1/81	4	P-401								
Shelbyville	2H0	C	2H0-AP-EE/6	TKAC	6/1/79	2	P-401	6	P-201						
Shelbyville	2H0	C	2H0-RW-18/9	TKAC	6/1/84	1.5	P-401	6.5	P-201						

Table F. 1. ACCESS data base section inventory information.

Airport	AID	Climatic Zone	Section	Code	Construction		Thickness		Material		Thickness		Material		Slab Length (ft)	Slab Width (ft)
					Date		Layer 1 (in)		Layer 2 (in)		Layer 3 (in)		Layer 4 (in)			
Shelbyville	2H0	C	2H0-AP-EE/7	TNAC	6/1/80	2 P-401	2 P-201									
Sparta	SAR	S	SAR-TW-B/03	TKAC	6/1/74	2 P-401	7 P-201									
Sparta	SAR	S	SAR-AP-WW/03	TKAC	6/1/74	2 P-401	7 P-201									
Sparta	SAR	S	SAR-RW-18/03	TNAC	6/1/86	4 P-401	8 P-209									
St. Louis DT	CPS	S	CPS-RW-12L/24	PCC	6/1/84	6 P-501	4 P-209					12.5			12.5	
St. Louis DT	CPS	S	CPS-TW-B/1-24	PCC	6/1/84	6 P-501	4 P-209					11			11	8.75
St. Louis DT	CPS	S	CPS-TW-B/2-24	PCC	6/1/84	6 P-501	4 P-209					11			11	8.75
St. Louis DT	CPS	S	CPS-TW-C/10	TKAC	6/1/70	2 P-401	6 P-201									
Sterling	SQI	N	SQI-AP-WW/10	TKAC	6/1/79	2 P-401	6 P-201									
Sterling	SQI	N	SQI-AP-WW/01	TKAC	6/1/86	1.5 P-401	6 MIP AC									
Taylorville	3TV	C	3TV-RW-18/08	TKAC	6/1/86	1.5 P-401	6.5 P-201				4 P-208					
Taylorville	3TV	C	3TV-TW-A/5-02	TKAC	6/1/86	1.5 P-401	6.5 P-201				4 P-208					
Taylorville	3TV	C	3TV-TW-A/4-08	TKAC	6/1/86	1.5 P-401	6.5 P-201				4 P-208					
Taylorville	3TV	C	3TV-TW-A/1-08	TKAC	6/1/86	1.5 P-401	6.5 P-201				4 P-208					
Taylorville	3TV	C	3TV-TW-A/2-08	TKAC	6/1/86	1.5 P-401	6.5 P-201				4 P-208					
Taylorville	3TV	C	3TV-TW-A/3-08	TKAC	6/1/86	1.5 P-401	6.5 P-201				4 P-208					
Taylorville	3TV	C	3TV-AP-EE/04	TNAC	6/1/78	2 P-401	2 P-201				6 P-208					
Taylorville	3TV	C	3TV-AP-EE/07	TNAC	6/1/82	2 P-401	6 P-208									
Vandalia	VLA	S	VLA-TW-D/1-7	TNAC	6/1/75	4 P-401	6 P-209									
Vandalia	VLA	S	VLA-TW-D/7	TNAC	6/1/75	4 P-401	6 P-209									
Vandalia	VLA	S	VLA-TW-B/7	TNAC	6/1/75	4 P-401	6 P-209									
Waukegan	UGN	N	UGN-RW-14/14	PCC	6/1/64	6 P-501	5 P-154								20	12.5
Waukegan	UGN	N	UGN-RW-14/11	PCC	6/1/70	6 P-501	6 P-154								20	12.5
Waukegan	UGN	N	UGN-RW-14/112	PCC	6/1/70	6 P-501	6 P-154								20	12.5
Waukegan	UGN	N	UGN-RW-14/09	PCC	6/1/75	6 P-501	6 P-201								20	12.5
Waukegan	UGN	N	UGN-RW-14/08	PCC	6/1/75	11 P-501	6 P-201								20	12.5
Waukegan	UGN	N	UGN-TW-C/07	TKAC	6/1/82	4 P-401	9 P-201				4 P-208					

Table F.2. Summary of ACCESS data base inspection information.

Airport	AID	Section	Code	Inspection	Section
				Date	PCI
Beardstown	K06	K06-AP-NN/2	TNAC	6/1/77	100
Beardstown	K06	K06-AP-NN/2	TNAC	4/25/83	80
Beardstown	K06	K06-AP-NN/2	TNAC	5/3/85	83
Beardstown	K06	K06-AP-NN/2	TNAC	5/6/88	78
Beardstown	K06	K06-AP-NN/2	TNAC	6/26/90	77
Beardstown	K06	K06-AP-NN/2	TNAC	5/29/92	74
Canton	CTK	CTK-RW-09/03	TKAC	6/1/73	100
Canton	CTK	CTK-TW-A/1-03	TKAC	6/1/73	100
Canton	CTK	CTK-TW-A/1-03	TKAC	8/4/80	80
Canton	CTK	CTK-RW-09/03	TKAC	8/4/80	83
Canton	CTK	CTK-TW-A/1-03	TKAC	4/22/82	74
Canton	CTK	CTK-RW-09/03	TKAC	4/22/82	72
Canton	CTK	CTK-RW-09/03	TKAC	5/16/84	78
Canton	CTK	CTK-TW-A/1-03	TKAC	5/16/84	79
Canton	CTK	CTK-TW-A/1-03	TKAC	5/27/86	78
Canton	CTK	CTK-RW-09/03	TKAC	5/27/86	71
Canton	CTK	CTK-TW-A/1-03	TKAC	5/10/89	72
Canton	CTK	CTK-RW-09/03	TKAC	5/10/89	72
Canton	CTK	CTK-TW-A/1-03	TKAC	5/31/91	75
Canton	CTK	CTK-RW-09/03	TKAC	5/31/91	69
Canton	CTK	CTK-TW-A/1-03	TKAC	8/19/93	44
Canton	CTK	CTK-RW-09/03	TKAC	8/19/93	64
Carbondale	MDH	MDH-AP-SS/20	PCC	6/1/74	100
Carbondale	MDH	MDH-AP-SS/19	PCC	6/1/74	100
Carbondale	MDH	MDH-AP-SS/19	PCC	6/27/80	88
Carbondale	MDH	MDH-AP-SS/20	PCC	6/27/80	81
Carbondale	MDH	MDH-AP-SS/20	PCC	7/22/82	78
Carbondale	MDH	MDH-AP-SS/19	PCC	7/22/82	86
Carbondale	MDH	MDH-AP-SS/20	PCC	6/28/84	78
Carbondale	MDH	MDH-AP-SS/19	PCC	6/28/84	81
Carbondale	MDH	MDH-AP-SS/19	PCC	7/1/86	80
Carbondale	MDH	MDH-AP-SS/20	PCC	7/1/86	74
Carbondale	MDH	MDH-AP-SS/19	PCC	8/14/89	77
Carbondale	MDH	MDH-AP-SS/20	PCC	8/14/89	67
Carbondale	MDH	MDH-AP-SS/19	PCC	6/4/91	71
Carbondale	MDH	MDH-AP-SS/20	PCC	6/4/91	72
Carbondale	MDH	MDH-AP-SS/19	PCC	8/11/93	71
Carbondale	MDH	MDH-AP-SS/20	PCC	8/11/93	68
Carmi	CUL	CUL-AP-EE/1	PCC	6/1/76	100
Carmi	CUL	CUL-AP-EE/1	PCC	5/29/85	44
Carmi	CUL	CUL-AP-EE/1	PCC	6/1/88	56
Carmi	CUL	CUL-AP-EE/1	PCC	8/12/92	48
Carmi	CUL	CUL-TW-B/1	TKAC	6/1/89	100
Carmi	CUL	CUL-TW-B/1	TKAC	8/12/92	100

Table F.2. Summary of ACCESS data base inspection information.

Airport	AID	Section	Code	Inspection	Section
				Date	PCI
Casey	1H8	1H8-TW-B/2-5	PCC	6/1/81	100
Casey	1H8	1H8-TW-B/2-5	PCC	6/15/87	53
Casey	1H8	1H8-TW-B/2-5	PCC	7/2/90	66
Casey	1H8	1H8-TW-B/2-5	PCC	5/5/92	27
Casey	1H8	1H8-TW-B/5	TNAC	6/1/81	100
Casey	1H8	1H8-TW-C/5	TNAC	6/1/81	100
Casey	1H8	1H8-TW-B/1-5	TNAC	6/1/81	100
Casey	1H8	1H8-TW-B/1-5	TNAC	6/15/87	18
Casey	1H8	1H8-TW-C/5	TNAC	6/15/87	37
Casey	1H8	1H8-TW-B/5	TNAC	6/15/87	33
Casey	1H8	1H8-TW-C/5	TNAC	7/2/90	26
Casey	1H8	1H8-TW-B/5	TNAC	7/2/90	62
Casey	1H8	1H8-TW-C/5	TNAC	5/5/92	29
Casey	1H8	1H8-TW-B/5	TNAC	5/5/92	42
Casey	1H8	1H8-TW-B/1-5	TNAC	5/5/92	37
Centralia	ENL	ENL-AP-WW/06	PCC	6/1/75	100
Centralia	ENL	ENL-AP-WW/06	PCC	5/27/81	87
Centralia	ENL	ENL-AP-WW/06	PCC	7/20/82	84
Centralia	ENL	ENL-AP-WW/06	PCC	6/27/84	96
Centralia	ENL	ENL-AP-WW/06	PCC	6/10/86	97
Centralia	ENL	ENL-AP-WW/06	PCC	6/21/89	91
Centralia	ENL	ENL-AP-WW/06	PCC	5/8/91	92
Centralia	ENL	ENL-AP-WW/06	PCC	8/11/93	94
Centralia	ENL	ENL-AP-WW/09	TKAC	6/1/70	100
Centralia	ENL	ENL-AP-WW/09	TKAC	5/27/81	52
Centralia	ENL	ENL-AP-WW/09	TKAC	7/20/82	38
Centralia	ENL	ENL-AP-WW/09	TKAC	6/27/84	46
Centralia	ENL	ENL-AP-WW/09	TKAC	6/10/86	44
Centralia	ENL	ENL-AP-WW/09	TKAC	6/21/89	69
Centralia	ENL	ENL-AP-WW/09	TKAC	5/8/91	33
Centralia	ENL	ENL-AP-WW/09	TKAC	8/11/93	51
Centralia	ENL	ENL-TW-A/13	TNAC	6/1/86	100
Centralia	ENL	ENL-RW-18/13	TNAC	6/1/86	100
Centralia	ENL	ENL-TW-A/13	TNAC	6/21/89	84
Centralia	ENL	ENL-RW-18/13	TNAC	6/21/89	87
Centralia	ENL	ENL-TW-A/13	TNAC	5/8/91	83
Centralia	ENL	ENL-RW-18/13	TNAC	5/8/91	82
Centralia	ENL	ENL-TW-A/13	TNAC	8/11/93	73
Centralia	ENL	ENL-RW-18/13	TNAC	8/11/93	72
Dekalb	DKB	DKB-AP-EE/02	PCC	6/1/89	100
Dekalb	DKB	DKB-AP-EE/02	PCC	8/9/90	100
Dekalb	DKB	DKB-AP-EE/02	PCC	6/12/92	99
Dekalb	DKB	DKB-TW-B/3-03	TKAC	6/1/83	100
Dekalb	DKB	DKB-TW-B/4-03	TKAC	6/1/83	100

Table F.2. Summary of ACCESS data base inspection information.

Airport	AID	Section	Code	Inspection	Section
				Date	PCI
Dekalb	DKB	DKB-TW-B/1-03	TKAC	6/1/83	100
Dekalb	DKB	DKB-TW-B/2-03	TKAC	6/1/83	100
Dekalb	DKB	DKB-TW-B/03	TKAC	6/1/83	100
Dekalb	DKB	DKB-TW-B/03	TKAC	7/18/85	96
Dekalb	DKB	DKB-TW-B/1-03	TKAC	7/18/85	100
Dekalb	DKB	DKB-TW-B/2-03	TKAC	7/18/85	100
Dekalb	DKB	DKB-TW-B/4-03	TKAC	7/18/85	97
Dekalb	DKB	DKB-TW-B/3-03	TKAC	7/18/85	100
Dekalb	DKB	DKB-AP-EE/01	TKAC	6/1/88	100
Dekalb	DKB	DKB-TW-B/4-04	TKAC	6/1/88	100
Dekalb	DKB	DKB-TW-B/03	TKAC	8/1/88	93
Dekalb	DKB	DKB-TW-B/1-03	TKAC	8/1/88	97
Dekalb	DKB	DKB-TW-B/2-03	TKAC	8/1/88	96
Dekalb	DKB	DKB-AP-EE/01	TKAC	8/1/88	100
Dekalb	DKB	DKB-TW-B/3-03	TKAC	8/1/88	99
Dekalb	DKB	DKB-TW-B/4-03	TKAC	8/1/88	94
Dekalb	DKB	DKB-TW-B/4-04	TKAC	8/1/88	100
Dekalb	DKB	DKB-RW-09/02	TKAC	6/1/90	100
Dekalb	DKB	DKB-TW-B/1-03	TKAC	8/9/90	85
Dekalb	DKB	DKB-TW-B/2-03	TKAC	8/9/90	73
Dekalb	DKB	DKB-TW-B/4-04	TKAC	8/9/90	100
Dekalb	DKB	DKB-TW-B/4-03	TKAC	8/9/90	94
Dekalb	DKB	DKB-RW-09/02	TKAC	8/9/90	100
Dekalb	DKB	DKB-TW-B/03	TKAC	8/9/90	79
Dekalb	DKB	DKB-AP-EE/01	TKAC	8/9/90	100
Dekalb	DKB	DKB-TW-B/3-03	TKAC	8/9/90	72
Dekalb	DKB	DKB-TW-D/1-01	TKAC	6/1/91	100
Dekalb	DKB	DKB-TW-D/01	TKAC	6/1/91	100
Dekalb	DKB	DKB-TW-D/01	TKAC	6/12/92	100
Dekalb	DKB	DKB-TW-B/1-03	TKAC	6/12/92	66
Dekalb	DKB	DKB-TW-B/2-03	TKAC	6/12/92	87
Dekalb	DKB	DKB-TW-B/03	TKAC	6/12/92	81
Dekalb	DKB	DKB-AP-EE/01	TKAC	6/12/92	99
Dekalb	DKB	DKB-TW-B/4-04	TKAC	6/12/92	95
Dekalb	DKB	DKB-TW-B/4-03	TKAC	6/12/92	83
Dekalb	DKB	DKB-RW-09/02	TKAC	6/12/92	99
Dekalb	DKB	DKB-TW-D/1-01	TKAC	6/12/92	100
Dekalb	DKB	DKB-TW-B/3-03	TKAC	6/12/92	82
Dixon	C73	C73-RW-08/09	TKAC	6/1/83	100
Dixon	C73	C73-TW-A/09	TKAC	6/1/83	100
Dixon	C73	C73-RW-08/09	TKAC	7/10/84	100
Dixon	C73	C73-TW-A/09	TKAC	7/10/84	100
Dixon	C73	C73-RW-08/09	TKAC	7/14/86	61
Dixon	C73	C73-TW-A/09	TKAC	7/14/86	60

Table F.2. Summary of ACCESS data base inspection information.

Airport	AID	Section	Code	Inspection	Section
				Date	PCI
Dixon	C73	C73-RW-08/09	TKAC	8/1/88	92
Dixon	C73	C73-TW-A/09	TKAC	8/1/88	92
Dixon	C73	C73-TW-A/09	TKAC	7/18/90	59
Dixon	C73	C73-RW-08/09	TKAC	7/18/90	64
Dixon	C73	C73-RW-08/09	TKAC	6/12/92	53
Dixon	C73	C73-TW-A/09	TKAC	6/12/92	40
Dixon Sprgs	Y51	Y51-AP-EE/01	TKAC	6/1/68	100
Dixon Sprgs	Y51	Y51-RW-15/01	TKAC	6/1/68	100
Dixon Sprgs	Y51	Y51-TW-A/01	TKAC	6/1/68	100
Dixon Sprgs	Y51	Y51-AP-EE/01	TKAC	5/30/85	57
Dixon Sprgs	Y51	Y51-RW-15/01	TKAC	5/30/85	46
Dixon Sprgs	Y51	Y51-TW-A/01	TKAC	5/30/85	51
Dixon Sprgs	Y51	Y51-AP-EE/01	TKAC	6/8/87	67
Dixon Sprgs	Y51	Y51-TW-A/01	TKAC	6/8/87	70
Dixon Sprgs	Y51	Y51-RW-15/01	TKAC	6/8/87	63
Dixon Sprgs	Y51	Y51-AP-EE/01	TKAC	8/3/90	75
Dixon Sprgs	Y51	Y51-RW-15/01	TKAC	8/3/90	62
Dixon Sprgs	Y51	Y51-TW-A/01	TKAC	8/3/90	73
Dixon Sprgs	Y51	Y51-TW-A/01	TKAC	8/6/92	80
Dixon Sprgs	Y51	Y51-RW-15/01	TKAC	8/6/92	69
Dixon Sprgs	Y51	Y51-AP-EE/01	TKAC	8/6/92	71
Dupage	DPA	DPA-AP-NE/10	PCC	6/1/77	100
Dupage	DPA	DPA-AP-NE/10	PCC	7/28/82	46
Dupage	DPA	DPA-AP-NE/10	PCC	7/25/84	49
Dupage	DPA	DPA-AP-NW/24	PCC	6/1/86	100
Dupage	DPA	DPA-AP-NE/10	PCC	8/4/86	37
Dupage	DPA	DPA-AP-EE/1	PCC	6/1/88	100
Dupage	DPA	DPA-AP-NE/10	PCC	8/2/88	34
Dupage	DPA	DPA-AP-NW/24	PCC	8/2/88	100
Dupage	DPA	DPA-AP-NW/24	PCC	7/31/91	94
Dupage	DPA	DPA-AP-NE/10	PCC	7/31/91	29
Dupage	DPA	DPA-AP-EE/1	PCC	7/31/91	100
Dupage	DPA	DPA-TW-X/6-1	PCC	6/1/92	100
Dupage	DPA	DPA-RW-1-R/1	PCC	6/1/92	100
Dupage	DPA	DPA-TW-X/2-1	PCC	6/1/92	100
Dupage	DPA	DPA-TW-X/1	PCC	6/1/92	100
Dupage	DPA	DPA-TW-X/4-1	PCC	6/1/92	100
Dupage	DPA	DPA-AP-NE/10	PCC	9/8/93	19
Dupage	DPA	DPA-AP-NW/24	PCC	9/8/93	100
Dupage	DPA	DPA-AP-EE/1	PCC	9/8/93	92
Dupage	DPA	DPA-TW-X/6-1	PCC	9/8/93	100
Dupage	DPA	DPA-TW-X/4-1	PCC	9/8/93	100
Dupage	DPA	DPA-TW-X/1	PCC	9/8/93	100
Dupage	DPA	DPA-TW-X/2-1	PCC	9/8/93	100

Table F.2. Summary of ACCESS data base inspection information.

Airport	AID	Section	Code	Inspection	Section
				Date	PCI
Dupage	DPA	DPA-RW-1-R/1	PCC	9/8/93	100
Dupage	DPA	DPA-TW-T/1	TKAC	6/1/82	100
Dupage	DPA	DPA-TW-T/5-1	TKAC	6/1/84	100
Dupage	DPA	DPA-TW-T/4-1	TKAC	6/1/84	100
Dupage	DPA	DPA-TW-T/3-1	TKAC	6/1/84	100
Dupage	DPA	DPA-TW-T/2-1	TKAC	6/1/84	100
Dupage	DPA	DPA-TW-T/2	TKAC	6/1/84	100
Dupage	DPA	DPA-TW-T/1-1	TKAC	6/1/84	100
Dupage	DPA	DPA-TW-T/1-1	TKAC	7/31/91	59
Dupage	DPA	DPA-TW-T/2-1	TKAC	7/31/91	86
Dupage	DPA	DPA-TW-T/4-1	TKAC	7/31/91	87
Dupage	DPA	DPA-TW-T/2	TKAC	7/31/91	76
Dupage	DPA	DPA-TW-T/5-1	TKAC	7/31/91	92
Dupage	DPA	DPA-TW-T/3-1	TKAC	7/31/91	78
Dupage	DPA	DPA-TW-T/1	TKAC	7/31/91	76
Dupage	DPA	DPA-TW-T/2-1	TKAC	9/8/93	67
Dupage	DPA	DPA-TW-T/1-1	TKAC	9/8/93	82
Dupage	DPA	DPA-TW-T/3-1	TKAC	9/8/93	89
Dupage	DPA	DPA-TW-T/5-1	TKAC	9/8/93	84
Dupage	DPA	DPA-TW-T/4-1	TKAC	9/8/93	81
Dupage	DPA	DPA-TW-T/1	TKAC	9/8/93	75
Dupage	DPA	DPA-TW-T/2	TKAC	9/8/93	77
Dupage	DPA	DPA-AP-NW/9	TNAC	6/1/69	100
Dupage	DPA	DPA-AP-NW/9	TNAC	8/14/80	30
Dupage	DPA	DPA-AP-NW/9	TNAC	7/28/82	53
Dupage	DPA	DPA-AP-NW/9	TNAC	7/25/84	6
Dupage	DPA	DPA-AP-NW/9	TNAC	8/4/86	10
Dupage	DPA	DPA-AP-EE/2	TNAC	6/1/87	100
Dupage	DPA	DPA-AP-NW/9	TNAC	8/2/88	0
Dupage	DPA	DPA-AP-NW/9	TNAC	7/31/91	0
Dupage	DPA	DPA-AP-EE/2	TNAC	7/31/91	100
Dupage	DPA	DPA-AP-EE/2	TNAC	9/8/93	91
Dupage	DPA	DPA-AP-NW/9	TNAC	9/8/93	20
Effingham	1H2	1H2-TW-C/11	PCC	6/1/83	100
Effingham	1H2	1H2-RW-11/11	PCC	6/1/83	100
Effingham	1H2	1H2-AP-NN/03	PCC	6/1/85	100
Effingham	1H2	1H2-RW-11/11	PCC	10/2/85	92
Effingham	1H2	1H2-TW-C/11	PCC	10/2/85	95
Effingham	1H2	1H2-TW-C/11	PCC	5/19/87	94
Effingham	1H2	1H2-RW-11/11	PCC	5/19/87	88
Effingham	1H2	1H2-TW-C/11	PCC	7/2/90	96
Effingham	1H2	1H2-RW-11/11	PCC	7/2/90	81
Effingham	1H2	1H2-AP-NN/03	PCC	7/2/90	100
Effingham	1H2	1H2-AP-NN/03	PCC	6/24/92	100

Table F.2. Summary of ACCESS data base inspection information.

Airport	AID	Section	Code	Inspection	Section
				Date	PCI
Effingham	1H2	1H2-RW-11/11	PCC	6/24/92	95
Effingham	1H2	1H2-TW-C/11	PCC	6/24/92	86
Effingham	1H2	1H2-RW-01/091	TKAC	6/1/74	100
Effingham	1H2	1H2-RW-01/092	TKAC	6/1/74	100
Effingham	1H2	1H2-RW-01/091	TKAC	6/11/81	81
Effingham	1H2	1H2-RW-01/091	TKAC	5/17/83	73
Effingham	1H2	1H2-RW-01/092	TKAC	5/17/83	74
Effingham	1H2	1H2-RW-01/091	TKAC	10/2/85	53
Effingham	1H2	1H2-RW-01/092	TKAC	10/2/85	57
Effingham	1H2	1H2-AP-NN/01	TKAC	6/1/86	100
Effingham	1H2	1H2-RW-01/092	TKAC	5/19/87	74
Effingham	1H2	1H2-RW-01/091	TKAC	5/19/87	71
Effingham	1H2	1H2-AP-NN/01	TKAC	7/2/90	97
Effingham	1H2	1H2-AP-NN/01	TKAC	6/24/92	90
Effingham	1H2	1H2-RW-09/08	TNAC	6/1/76	100
Effingham	1H2	1H2-RW-09/08	TNAC	6/11/81	93
Effingham	1H2	1H2-RW-09/08	TNAC	5/17/83	69
Fairfield	2H3	2H3-TW-A/1-01	TKAC	6/1/89	100
Fairfield	2H3	2H3-TW-A/01	TKAC	6/1/89	100
Fairfield	2H3	2H3-TW-A/1-01	TKAC	5/14/91	100
Fairfield	2H3	2H3-TW-A/01	TKAC	5/14/91	100
Fairfield	2H3	2H3-RW-09/03	TKAC	6/1/91	100
Flora	H84	H84-AP-WW/4	TKAC	6/1/79	100
Flora	H84	H84-AP-WW/4	TKAC	6/11/81	86
Flora	H84	H84-AP-WW/4	TKAC	7/20/82	95
Flora	H84	H84-AP-WW/4	TKAC	6/27/84	92
Flora	H84	H84-TW-C/6	TKAC	6/1/85	100
Flora	H84	H84-RW-3/2	TKAC	6/1/85	100
Flora	H84	H84-TW-C/6	TKAC	6/9/86	100
Flora	H84	H84-RW-3/2	TKAC	6/9/86	100
Flora	H84	H84-AP-WW/4	TKAC	6/9/86	79
Flora	H84	H84-RW-3/2	TKAC	4/26/89	93
Flora	H84	H84-AP-WW/4	TKAC	4/26/89	82
Flora	H84	H84-TW-C/6	TKAC	4/26/89	93
Flora	H84	H84-AP-WW/4	TKAC	5/8/91	82
Flora	H84	H84-TW-C/6	TKAC	5/8/91	93
Flora	H84	H84-RW-3/2	TKAC	5/8/91	85
Flora	H84	H84-AP-WW/4	TKAC	5/19/93	87
Flora	H84	H84-RW-3/2	TKAC	5/19/93	83
Flora	H84	H84-TW-C/6	TKAC	5/19/93	85
Freeport	FEP	FEP-TW-A/04	TKAC	6/1/68	100
Freeport	FEP	FEP-TW-A/04	TKAC	7/22/81	76
Freeport	FEP	FEP-TW-C/06	TKAC	6/1/83	100
Freeport	FEP	FEP-TW-B/06	TKAC	6/1/83	100

Table F.2. Summary of ACCESS data base inspection information.

Airport	AID	Section	Code	Inspection	Section
				Date	PCI
Freeport	FEP	FEP-TW-C/1-06	TKAC	6/1/83	100
Freeport	FEP	FEP-TW-B/06	TKAC	7/14/83	100
Freeport	FEP	FEP-TW-A/04	TKAC	7/14/83	60
Freeport	FEP	FEP-TW-C/1-06	TKAC	7/16/85	100
Freeport	FEP	FEP-TW-C/06	TKAC	7/16/85	100
Freeport	FEP	FEP-TW-A/04	TKAC	7/16/85	57
Freeport	FEP	FEP-TW-B/06	TKAC	7/16/85	100
Freeport	FEP	FEP-TW-C/06	TKAC	8/6/87	88
Freeport	FEP	FEP-TW-C/1-06	TKAC	8/6/87	86
Freeport	FEP	FEP-TW-A/04	TKAC	8/6/87	50
Freeport	FEP	FEP-TW-B/06	TKAC	8/6/87	88
Freeport	FEP	FEP-TW-C/1-06	TKAC	6/6/89	86
Freeport	FEP	FEP-TW-C/06	TKAC	6/6/89	88
Freeport	FEP	FEP-TW-A/04	TKAC	6/6/89	59
Freeport	FEP	FEP-TW-B/06	TKAC	6/6/89	77
Freeport	FEP	FEP-TW-C/06	TKAC	5/8/91	73
Freeport	FEP	FEP-TW-C/1-06	TKAC	5/8/91	89
Freeport	FEP	FEP-TW-B/06	TKAC	5/8/91	74
Freeport	FEP	FEP-TW-A/04	TKAC	5/8/91	55
Freeport	FEP	FEP-TW-A/04	TKAC	7/30/93	65
Freeport	FEP	FEP-TW-D/01	TNAC	6/1/83	100
Freeport	FEP	FEP-TW-D/2-01	TNAC	6/1/83	100
Freeport	FEP	FEP-TW-D/3-01	TNAC	6/1/83	100
Freeport	FEP	FEP-AP-NN/01	TNAC	6/1/88	100
Freeport	FEP	FEP-RW-06/02	TNAC	6/1/89	100
Freeport	FEP	FEP-AP-NN/01	TNAC	6/6/89	93
Freeport	FEP	FEP-RW-06/02	TNAC	5/8/91	96
Freeport	FEP	FEP-AP-NN/01	TNAC	5/8/91	79
Freeport	FEP	FEP-TW-D/1-01	TNAC	6/1/91	100
Freeport	FEP	FEP-TW-D/02	TNAC	6/1/91	100
Freeport	FEP	FEP-TW-A/2-01	TNAC	6/1/91	100
Freeport	FEP	FEP-TW-D/01	TNAC	5/1/93	91
Freeport	FEP	FEP-TW-D/1-01	TNAC	5/1/93	89
Freeport	FEP	FEP-TW-D/02	TNAC	5/1/93	92
Freeport	FEP	FEP-TW-D/3-01	TNAC	5/1/93	66
Freeport	FEP	FEP-TW-D/2-01	TNAC	5/1/93	79
Freeport	FEP	FEP-TW-A/2-01	TNAC	5/1/93	97
Freeport	FEP	FEP-RW-06/02	TNAC	7/30/93	85
Freeport	FEP	FEP-AP-NN/01	TNAC	7/30/93	82
Galesburg	GBG	GBG-AP-NN/8	TKAC	6/1/69	100
Galesburg	GBG	GBG-AP-NN/14	TKAC	6/1/80	100
Galesburg	GBG	GBG-AP-NN/14	TKAC	7/23/81	89
Galesburg	GBG	GBG-AP-NN/8	TKAC	7/23/81	60
Galesburg	GBG	GBG-AP-NN/8	TKAC	7/12/83	68

Table F.2. Summary of ACCESS data base inspection information.

Airport	AID	Section	Code	Inspection	Section
				Date	PCI
Galesburg	GBG	GBG-AP-NN/14	TKAC	7/12/83	94
Galesburg	GBG	GBG-AP-NN/8	TKAC	7/16/85	83
Galesburg	GBG	GBG-AP-NN/14	TKAC	7/16/85	81
Galesburg	GBG	GBG-AP-NN/14	TKAC	8/5/87	75
Galesburg	GBG	GBG-AP-NN/8	TKAC	8/5/87	84
Galesburg	GBG	GBG-AP-NN/8	TKAC	5/10/89	82
Galesburg	GBG	GBG-AP-NN/14	TKAC	5/10/89	73
Galesburg	GBG	GBG-AP-NN/14	TKAC	8/15/91	76
Galesburg	GBG	GBG-AP-NN/14	TKAC	8/19/93	58
Greenville	GRE	GRE-AP-EE/4	TNAC	6/1/76	100
Greenville	GRE	GRE-AP-EE/4	TNAC	5/28/81	86
Greenville	GRE	GRE-AP-EE/4	TNAC	4/25/83	80
Greenville	GRE	GRE-AP-EE/4	TNAC	8/30/85	76
Greenville	GRE	GRE-AP-EE/4	TNAC	5/13/87	73
Greenville	GRE	GRE-AP-EE/4	TNAC	6/12/90	59
Greenville	GRE	GRE-AP-EE/4	TNAC	6/24/92	58
Grtr. Kankakee	IKK	IKK-RW-04/20	TKAC	6/1/86	100
Grtr. Kankakee	IKK	IKK-TW-A/20	TKAC	6/1/86	100
Grtr. Kankakee	IKK	IKK-TW-D/23	TKAC	6/1/86	100
Grtr. Kankakee	IKK	IKK-RW-16/01	TKAC	6/1/88	100
Grtr. Kankakee	IKK	IKK-TW-A/20	TKAC	8/3/88	100
Grtr. Kankakee	IKK	IKK-TW-D/23	TKAC	8/3/88	100
Grtr. Kankakee	IKK	IKK-RW-04/20	TKAC	8/3/88	100
Grtr. Kankakee	IKK	IKK-RW-16/01	TKAC	6/6/91	100
Grtr. Kankakee	IKK	IKK-RW-04/20	TKAC	6/6/91	81
Grtr. Kankakee	IKK	IKK-TW-A/20	TKAC	6/6/91	84
Grtr. Kankakee	IKK	IKK-TW-D/23	TKAC	6/6/91	93
Grtr. Kankakee	IKK	IKK-RW-16/01	TKAC	7/15/93	89
Grtr. Kankakee	IKK	IKK-TW-A/20	TKAC	7/15/93	83
Grtr. Kankakee	IKK	IKK-TW-D/23	TKAC	7/15/93	92
Grtr. Kankakee	IKK	IKK-RW-04/20	TKAC	7/15/93	77
Grtr. Kankakee	IKK	IKK-AP-SS/10	TNAC	6/1/78	100
Grtr. Kankakee	IKK	IKK-AP-SS/10	TNAC	7/30/80	93
Grtr. Kankakee	IKK	IKK-AP-SS/10	TNAC	7/8/82	90
Grtr. Kankakee	IKK	IKK-AP-SS/10	TNAC	7/24/84	85
Grtr. Kankakee	IKK	IKK-TW-D/22	TNAC	6/1/86	100
Grtr. Kankakee	IKK	IKK-TW-A/3-22	TNAC	6/1/86	100
Grtr. Kankakee	IKK	IKK-AP-SS/10	TNAC	7/15/86	79
Grtr. Kankakee	IKK	IKK-TW-D/22	TNAC	8/3/88	100
Grtr. Kankakee	IKK	IKK-AP-SS/10	TNAC	8/3/88	75
Grtr. Kankakee	IKK	IKK-TW-A/3-22	TNAC	8/3/88	100
Grtr. Kankakee	IKK	IKK-TW-D/22	TNAC	6/6/91	91
Grtr. Kankakee	IKK	IKK-TW-A/3-22	TNAC	6/6/91	81
Grtr. Kankakee	IKK	IKK-AP-SS/10	TNAC	6/6/91	53

Table F.2. Summary of ACCESS data base inspection information.

Airport	AID	Section	Code	Inspection	Section
				Date	PCI
Grtr. Kankakee	IKK	IKK-TW-A/3-22	TNAC	7/15/93	77
Grtr. Kankakee	IKK	IKK-TW-D/22	TNAC	7/15/93	88
Jacksonville	IJX	IJX-AP-SS/9	PCC	6/1/67	100
Jacksonville	IJX	IJX-AP-SS/9	PCC	5/20/81	78
Jacksonville	IJX	IJX-AP-SS/9	PCC	4/25/83	90
Jacksonville	IJX	IJX-AP-SS/9	PCC	5/3/85	83
Jacksonville	IJX	IJX-AP-SS/9	PCC	5/6/88	76
Jacksonville	IJX	IJX-AP-SS/9	PCC	6/26/90	84
Jacksonville	IJX	IJX-AP-SS/9	PCC	9/3/92	78
Jacksonville	IJX	IJX-TW-B/8	TNAC	6/1/67	100
Jacksonville	IJX	IJX-TW-B/8	TNAC	5/20/81	75
Jacksonville	IJX	IJX-TW-B/8	TNAC	4/25/83	55
Jacksonville	IJX	IJX-TW-B/8	TNAC	5/3/85	49
Jacksonville	IJX	IJX-TW-B/8	TNAC	5/6/88	37
Jacksonville	IJX	IJX-TW-B/8	TNAC	6/26/90	37
Joliet PD	JOT	JOT-AP-NW/4	PCC	6/1/91	100
Joliet PD	JOT	JOT-AP-NW/4	PCC	8/3/93	100
Joliet PD	JOT	JOT-TW-C/2	TKAC	6/1/84	100
Joliet PD	JOT	JOT-TW-C/2-2	TKAC	6/1/84	100
Joliet PD	JOT	JOT-TW-C-1/2-2	TKAC	6/1/84	100
Joliet PD	JOT	JOT-AP-NW/2	TKAC	6/1/84	100
Joliet PD	JOT	JOT-TW-D/2-6	TKAC	6/1/85	100
Joliet PD	JOT	JOT-TW-C/5	TKAC	6/1/85	100
Joliet PD	JOT	JOT-TW-D/6	TKAC	6/1/85	100
Joliet PD	JOT	JOT-TW-D/1-6	TKAC	6/1/85	100
Joliet PD	JOT	JOT-TW-D/3-6	TKAC	6/1/85	100
Joliet PD	JOT	JOT-AP-NW/2	TKAC	7/16/86	100
Joliet PD	JOT	JOT-TW-D/3-6	TKAC	7/16/86	100
Joliet PD	JOT	JOT-TW-C/2-2	TKAC	7/16/86	100
Joliet PD	JOT	JOT-TW-D/2-6	TKAC	7/16/86	100
Joliet PD	JOT	JOT-TW-D/1-6	TKAC	7/16/86	100
Joliet PD	JOT	JOT-TW-D/6	TKAC	7/16/86	100
Joliet PD	JOT	JOT-TW-C-1/2-2	TKAC	7/16/86	100
Joliet PD	JOT	JOT-TW-C/2	TKAC	7/16/86	100
Joliet PD	JOT	JOT-TW-C/5	TKAC	7/16/86	100
Joliet PD	JOT	JOT-TW-D/2-6	TKAC	6/30/89	79
Joliet PD	JOT	JOT-TW-D/6	TKAC	6/30/89	89
Joliet PD	JOT	JOT-AP-NW/2	TKAC	6/30/89	79
Joliet PD	JOT	JOT-TW-C/2	TKAC	6/30/89	92
Joliet PD	JOT	JOT-TW-D/3-6	TKAC	6/30/89	85
Joliet PD	JOT	JOT-TW-C/5	TKAC	6/30/89	93
Joliet PD	JOT	JOT-TW-C-1/2-2	TKAC	6/30/89	95
Joliet PD	JOT	JOT-TW-C/2-2	TKAC	6/30/89	97
Joliet PD	JOT	JOT-TW-D/1-6	TKAC	6/30/89	86

Table F.2. Summary of ACCESS data base inspection information.

Airport	AID	Section	Code	Inspection	Section
				Date	PCI
Joliet PD	JOT	JOT-TW-D/1-1	TKAC	6/1/90	100
Joliet PD	JOT	JOT-TW-D/2-1	TKAC	6/1/90	100
Joliet PD	JOT	JOT-AP-NW/2	TKAC	8/13/91	75
Joliet PD	JOT	JOT-TW-C/2-2	TKAC	8/13/91	90
Joliet PD	JOT	JOT-TW-C/5	TKAC	8/13/91	82
Joliet PD	JOT	JOT-TW-C/2	TKAC	8/13/91	87
Joliet PD	JOT	JOT-TW-D/3-6	TKAC	8/13/91	77
Joliet PD	JOT	JOT-TW-C-1/2-2	TKAC	8/13/91	84
Joliet PD	JOT	JOT-TW-D/2-6	TKAC	8/13/91	78
Joliet PD	JOT	JOT-TW-D/1-6	TKAC	8/13/91	83
Joliet PD	JOT	JOT-TW-D/6	TKAC	8/13/91	71
Joliet PD	JOT	JOT-TW-D/2-1	TKAC	8/13/91	100
Joliet PD	JOT	JOT-TW-D/1-1	TKAC	8/13/91	100
Joliet PD	JOT	JOT-TW-D/1-1	TKAC	8/3/93	100
Joliet PD	JOT	JOT-TW-D/3-6	TKAC	8/3/93	64
Joliet PD	JOT	JOT-TW-D/2-1	TKAC	8/3/93	100
Joliet PD	JOT	JOT-TW-C-1/2-2	TKAC	8/3/93	86
Joliet PD	JOT	JOT-TW-D/1-6	TKAC	8/3/93	78
Joliet PD	JOT	JOT-TW-D/6	TKAC	8/3/93	78
Joliet PD	JOT	JOT-TW-D/2-6	TKAC	8/3/93	81
Joliet PD	JOT	JOT-TW-C/2	TKAC	8/3/93	88
Joliet PD	JOT	JOT-TW-C/5	TKAC	8/3/93	79
Joliet PD	JOT	JOT-TW-C/2-2	TKAC	8/3/93	88
Joliet PD	JOT	JOT-AP-NW/2	TKAC	8/3/93	75
Joliet PD	JOT	JOT-TW-B/1-1	TNAC	6/1/82	100
Joliet PD	JOT	JOT-TW-B/3-1	TNAC	6/1/82	100
Joliet PD	JOT	JOT-TW-B/2-1	TNAC	6/1/82	100
Joliet PD	JOT	JOT-TW-B/1	TNAC	6/1/82	100
Joliet PD	JOT	JOT-TW-B/1	TNAC	7/12/84	100
Joliet PD	JOT	JOT-TW-B/1-1	TNAC	7/12/84	100
Joliet PD	JOT	JOT-TW-B/3-1	TNAC	7/12/84	100
Joliet PD	JOT	JOT-TW-B/2-1	TNAC	7/12/84	100
Joliet PD	JOT	JOT-TW-B/1-1	TNAC	7/16/86	100
Joliet PD	JOT	JOT-TW-B/3-1	TNAC	7/16/86	100
Joliet PD	JOT	JOT-TW-B/1	TNAC	7/16/86	100
Joliet PD	JOT	JOT-TW-B/2-1	TNAC	7/16/86	100
Joliet PD	JOT	JOT-TW-B/1	TNAC	6/30/89	81
Joliet PD	JOT	JOT-TW-B/1-1	TNAC	6/30/89	79
Joliet PD	JOT	JOT-TW-B/2-1	TNAC	6/30/89	78
Joliet PD	JOT	JOT-TW-B/3-1	TNAC	6/30/89	81
Joliet PD	JOT	JOT-TW-B/1-1	TNAC	8/13/91	71
Joliet PD	JOT	JOT-TW-B/1	TNAC	8/13/91	71
Joliet PD	JOT	JOT-TW-B/2-1	TNAC	8/13/91	55
Joliet PD	JOT	JOT-TW-B/3-1	TNAC	8/13/91	66

Table F.2. Summary of ACCESS data base inspection information.

Airport	AID	Section	Code	Inspection	Section
				Date	PCI
Kewanee	C07	C07-AP-SE/04	TKAC	6/1/79	100
Kewanee	C07	C07-AP-SE/04	TKAC	7/14/81	98
Kewanee	C07	C07-AP-SE/06	TKAC	6/1/83	100
Kewanee	C07	C07-TW-A/05	TKAC	6/1/83	100
Kewanee	C07	C07-AP-SE/04	TKAC	7/12/83	97
Kewanee	C07	C07-AP-SE/04	TKAC	7/17/85	93
Kewanee	C07	C07-AP-SE/06	TKAC	7/17/85	100
Kewanee	C07	C07-TW-A/05	TKAC	7/17/85	100
Kewanee	C07	C07-AP-SE/04	TKAC	6/17/88	81
Kewanee	C07	C07-AP-SE/06	TKAC	6/17/88	83
Kewanee	C07	C07-TW-A/05	TKAC	6/17/88	93
Kewanee	C07	C07-RW-09/01	TKAC	6/1/89	100
Kewanee	C07	C07-AP-SE/06	TKAC	7/17/90	86
Kewanee	C07	C07-AP-SE/04	TKAC	7/17/90	68
Kewanee	C07	C07-RW-09/01	TKAC	7/17/90	98
Kewanee	C07	C07-TW-A/05	TKAC	7/17/90	89
Kewanee	C07	C07-AP-SE/04	TKAC	5/19/92	68
Kewanee	C07	C07-AP-SE/06	TKAC	5/19/92	75
Kewanee	C07	C07-RW-09/01	TKAC	5/19/92	100
Kewanee	C07	C07-TW-A/05	TKAC	5/19/92	84
Lacon	C75	C75-RW-13/01	TKAC	6/1/87	100
Lacon	C75	C75-TW-C/01	TKAC	6/1/87	100
Lacon	C75	C75-RW-13/01	TKAC	6/6/89	99
Lacon	C75	C75-TW-C/01	TKAC	6/6/89	100
Lacon	C75	C75-AP-VVV/03	TKAC	6/1/90	100
Lacon	C75	C75-AP-VVV/03	TKAC	6/26/91	96
Lacon	C75	C75-RW-13/01	TKAC	6/26/91	90
Lacon	C75	C75-TW-C/01	TKAC	6/26/91	90
Lansing	3HA	3HA-AP-NN/01	PCC	6/1/87	100
Lansing	3HA	3HA-AP-NN/03	PCC	6/1/90	100
Lansing	3HA	3HA-AP-NN/01	PCC	8/3/90	100
Lansing	3HA	3HA-AP-NN/03	PCC	8/3/90	100
Lansing	3HA	3HA-AP-NN/04	PCC	6/1/91	100
Lansing	3HA	3HA-AP-NN/01	PCC	7/24/92	94
Lansing	3HA	3HA-AP-NN/04	PCC	7/24/92	100
Lansing	3HA	3HA-AP-NN/03	PCC	7/24/92	98
Lansing	3HA	3HA-RW-09/02	TNAC	6/1/88	100
Lansing	3HA	3HA-TW-B/2-01	TNAC	6/1/90	100
Lansing	3HA	3HA-TW-B/1-01	TNAC	6/1/90	100
Lansing	3HA	3HA-AP-VVV/02	TNAC	6/1/90	100
Lansing	3HA	3HA-TW-A/01	TNAC	6/1/90	100
Lansing	3HA	3HA-TW-B/3-01	TNAC	6/1/90	100
Lansing	3HA	3HA-TW-B/01	TNAC	6/1/90	100
Lansing	3HA	3HA-RW-09/02	TNAC	8/3/90	100

Table F.2. Summary of ACCESS data base inspection information.

Airport	AID	Section	Code	Inspection	Section
				Date	PCI
Lansing	3HA	3HA-AP-WW/02	TNAC	8/3/90	100
Lansing	3HA	3HA-TW-B/2-01	TNAC	7/24/92	100
Lansing	3HA	3HA-RW-09/02	TNAC	7/24/92	85
Lansing	3HA	3HA-TW-A/01	TNAC	7/24/92	100
Lansing	3HA	3HA-TW-B/01	TNAC	7/24/92	100
Lansing	3HA	3HA-TW-B/1-01	TNAC	7/24/92	100
Lansing	3HA	3HA-AP-WW/02	TNAC	7/24/92	94
Lansing	3HA	3HA-TW-B/3-01	TNAC	7/24/92	100
Litchfield	3LF	3LF-AP-EE/1	PCC	6/1/84	100
Litchfield	3LF	3LF-AP-EE/1	PCC	7/10/85	100
Litchfield	3LF	3LF-AP-EE/1	PCC	5/13/87	99
Litchfield	3LF	3LF-AP-EE/1	PCC	6/12/90	95
Litchfield	3LF	3LF-AP-EE/1	PCC	8/20/92	91
Litchfield	3LF	3LF-AP-EE/7	TKAC	6/1/73	100
Litchfield	3LF	3LF-AP-EE/7	TKAC	7/10/85	81
Litchfield	3LF	3LF-AP-EE/7	TKAC	5/13/87	79
Litchfield	3LF	3LF-AP-EE/7	TKAC	6/12/90	82
Litchfield	3LF	3LF-AP-EE/7	TKAC	8/20/92	57
MaComb	MQB	MQB-RW-08/03	TKAC	6/1/88	100
MaComb	MQB	MQB-RW-08/03	TKAC	6/4/91	100
MaComb	MQB	MQB-RW-08/03	TKAC	8/19/93	97
Marion	MWA	MWA-TW-D/1-1	PCC	6/1/88	100
Marion	MWA	MWA-TW-D/1	PCC	6/1/88	100
Marion	MWA	MWA-RW-11/3	PCC	6/1/88	100
Marion	MWA	MWA-RW-11/3	PCC	6/18/91	100
Marion	MWA	MWA-TW-D/1	PCC	6/18/91	100
Marion	MWA	MWA-TW-D/1-1	PCC	6/18/91	100
Marion	MWA	MWA-RW-11/3	PCC	6/18/93	98
Marion	MWA	MWA-TW-D/1	PCC	6/18/93	99
Marion	MWA	MWA-TW-D/1-1	PCC	6/18/93	100
Metropolis	M30	M30-RW-18/04	TKAC	6/1/85	100
Metropolis	M30	M30-RW-18/04	TKAC	6/2/88	96
Metropolis	M30	M30-RW-18/04	TKAC	8/3/90	81
Metropolis	M30	M30-RW-18/05	TKAC	6/1/92	100
Metropolis	M30	M30-RW-18/04	TKAC	8/6/92	83
Metropolis	M30	M30-RW-18/05	TKAC	8/6/92	100
Mt. Carmel	I02	I02-TW-A/06	TKAC	6/1/84	100
Mt. Carmel	I02	I02-TW-A/06	TKAC	5/29/85	100
Mt. Carmel	I02	I02-TW-A/1-02	TKAC	5/29/85	100
Mt. Carmel	I02	I02-TW-A/1-02	TKAC	6/1/85	100
Mt. Carmel	I02	I02-RW-12/01	TKAC	6/1/85	100
Mt. Carmel	I02	I02-TW-A/06	TKAC	6/8/87	96
Mt. Carmel	I02	I02-TW-A/1-02	TKAC	6/8/87	100
Mt. Carmel	I02	I02-RW-12/01	TKAC	6/8/87	100

Table F.2. Summary of ACCESS data base inspection information.

Airport	AID	Section	Code	Inspection	Section
				Date	PCI
Mt. Carmel	I02	I02-TW-A/1-02	TKAC	7/20/90	93
Mt. Carmel	I02	I02-TW-A/06	TKAC	7/20/90	87
Mt. Carmel	I02	I02-RW-12/01	TKAC	7/20/90	80
Mt. Carmel	I02	I02-TW-A/1-02	TKAC	8/20/92	93
Mt. Carmel	I02	I02-RW-12/01	TKAC	8/20/92	77
Mt. Carmel	I02	I02-TW-A/06	TKAC	8/20/92	85
Mt. Carmel	I02	I02-AP-NN/01	TNAC	6/1/92	100
Mt. Carmel	I02	I02-TW-B/01	TNAC	6/1/92	100
Mt. Carmel	I02	I02-AP-NN/01	TNAC	8/20/92	100
Mt. Carmel	I02	I02-TW-B/01	TNAC	8/20/92	100
Paris	PRG	PRG-AP-SS/01	TKAC	6/1/73	100
Paris	PRG	PRG-RW-09/01	TKAC	6/1/73	100
Paris	PRG	PRG-TW-A/01	TKAC	6/1/73	100
Paris	PRG	PRG-RW-09/01	TKAC	6/1/81	88
Paris	PRG	PRG-TW-A/01	TKAC	6/1/81	78
Paris	PRG	PRG-AP-SS/01	TKAC	6/1/81	93
Paris	PRG	PRG-RW-09/01	TKAC	6/7/83	83
Paris	PRG	PRG-TW-A/01	TKAC	6/7/83	79
Paris	PRG	PRG-AP-SS/01	TKAC	6/7/83	83
Paris	PRG	PRG-AP-SS/01	TKAC	5/28/85	82
Paris	PRG	PRG-TW-A/01	TKAC	5/28/85	81
Paris	PRG	PRG-RW-09/01	TKAC	5/28/85	77
Paris	PRG	PRG-TW-A/01	TKAC	6/15/87	79
Paris	PRG	PRG-AP-SS/01	TKAC	6/15/87	81
Paris	PRG	PRG-RW-09/01	TKAC	6/15/87	74
Paris	PRG	PRG-TW-A/01	TKAC	7/2/90	86
Paris	PRG	PRG-RW-09/01	TKAC	7/2/90	82
Paris	PRG	PRG-AP-SS/01	TKAC	7/2/90	77
Paris	PRG	PRG-TW-B/01	TKAC	6/1/91	100
Paris	PRG	PRG-TW-A/01	TKAC	5/5/92	82
Paris	PRG	PRG-AP-SS/01	TKAC	5/5/92	66
Paris	PRG	PRG-TW-B/01	TKAC	5/5/92	97
Paris	PRG	PRG-RW-09/01	TKAC	5/5/92	79
Pekin	C15	C15-AP-EE/07	TNAC	6/1/84	100
Pekin	C15	C15-AP-EE/07	TNAC	5/7/86	100
Pekin	C15	C15-RW-09/03	TNAC	6/1/88	100
Pekin	C15	C15-AP-EE/07	TNAC	8/24/88	79
Pekin	C15	C15-RW-09/03	TNAC	8/15/91	100
Pekin	C15	C15-AP-EE/07	TNAC	8/15/91	79
Pekin	C15	C15-AP-EE/07	TNAC	6/11/93	64
Pekin	C15	C15-RW-09/03	TNAC	6/11/93	82
Peoria	3MY	3MY-AP-EE/5	PCC	6/1/67	100
Peoria	3MY	3MY-AP-EE/5	PCC	8/5/80	77
Peoria	3MY	3MY-AP-EE/5	PCC	4/14/82	76

Table F.2. Summary of ACCESS data base inspection information.

Airport	AID	Section	Code	Inspection Date	Section PCI
Peoria	3MY	3MY-AP-EE/5	PCC	5/9/84	77
Peoria	3MY	3MY-AP-EE/5	PCC	5/7/86	78
Peoria	3MY	3MY-AP-EE/5	PCC	7/31/89	81
Peoria	3MY	3MY-AP-EE/5	PCC	5/31/91	82
Peoria	3MY	3MY-AP-EE/5	PCC	6/11/93	70
Peoria	3MY	3MY-AP-EE/6	TKAC	6/1/73	100
Peoria	3MY	3MY-AP-EE/6	TKAC	8/5/80	79
Peoria	3MY	3MY-AP-EE/6	TKAC	4/14/82	69
Peoria	3MY	3MY-AP-EE/6	TKAC	5/9/84	71
Peoria	3MY	3MY-AP-EE/6	TKAC	5/7/86	76
Peoria	3MY	3MY-AP-EE/6	TKAC	7/31/89	77
Peoria	3MY	3MY-AP-EE/6	TKAC	5/31/91	75
Peoria	3MY	3MY-AP-EE/6	TKAC	6/11/93	82
Peoria	3MY	3MY-AP-EE/3	TNAC	6/1/67	100
Peoria	3MY	3MY-AP-EE/3	TNAC	8/5/80	79
Peoria	3MY	3MY-AP-EE/3	TNAC	4/14/82	48
Peoria	3MY	3MY-AP-EE/3	TNAC	5/9/84	43
Peoria	3MY	3MY-AP-EE/8	TNAC	6/1/86	100
Peoria	3MY	3MY-RW-17/2	TNAC	6/1/88	100
Peoria	3MY	3MY-AP-EE/3	TNAC	7/31/89	46
Peoria	3MY	3MY-AP-EE/8	TNAC	7/31/89	91
Peoria	3MY	3MY-RW-17/2	TNAC	5/31/91	92
Peoria	3MY	3MY-AP-EE/8	TNAC	5/31/91	93
Peoria	3MY	3MY-AP-EE/3	TNAC	5/31/91	61
Peoria	3MY	3MY-TW-A/3-1	TNAC	6/1/92	100
Peoria	3MY	3MY-TW-A/3	TNAC	6/1/92	100
Peoria	3MY	3MY-AP-EE/8	TNAC	6/11/93	87
Peoria	3MY	3MY-TW-A/3-1	TNAC	6/11/93	100
Peoria	3MY	3MY-TW-A/3	TNAC	6/11/93	100
Peoria	3MY	3MY-RW-17/2	TNAC	6/11/93	100
Peoria	3MY	3MY-AP-EE/3	TNAC	6/11/93	53
Peru	VYS	VYS-AP-EE/02	PCC	6/1/85	100
Peru	VYS	VYS-AP-EE/02	PCC	6/13/88	94
Peru	VYS	VYS-AP-EE/04	PCC	6/1/90	100
Peru	VYS	VYS-AP-EE/04	PCC	7/18/90	100
Peru	VYS	VYS-AP-EE/02	PCC	7/18/90	84
Peru	VYS	VYS-AP-EE/04	PCC	6/1/92	99
Peru	VYS	VYS-AP-EE/02	PCC	6/1/92	81
Peru	VYS	VYS-RW-18/01	TKAC	6/1/85	100
Peru	VYS	VYS-TW-A/01	TKAC	6/1/85	100
Peru	VYS	VYS-RW-18/01	TKAC	6/13/88	92
Peru	VYS	VYS-TW-A/01	TKAC	6/13/88	94
Peru	VYS	VYS-AP-EE/05	TKAC	6/1/90	100
Peru	VYS	VYS-RW-18/01	TKAC	7/18/90	83

Table F.2. Summary of ACCESS data base inspection information.

Airport	AID	Section	Code	Inspection	Section
				Date	PCI
Peru	VYS	VYS-TW-A/01	TKAC	7/18/90	93
Peru	VYS	VYS-TW-A/01	TKAC	6/1/92	82
Peru	VYS	VYS-RW-18/01	TKAC	6/1/92	74
Peru	VYS	VYS-RW-18/02	TKAC	6/1/92	100
Peru	VYS	VYS-AP-EE/01	TNAC	6/1/88	100
Peru	VYS	VYS-AP-EE/01	TNAC	6/13/88	100
Peru	VYS	VYS-AP-EE/01	TNAC	7/18/90	94
Peru	VYS	VYS-AP-EE/01	TNAC	6/1/92	82
Pickneyville	K16	K16-AP-WW/02	TKAC	6/1/79	100
Pickneyville	K16	K16-TW-A/02	TKAC	6/1/79	100
Pickneyville	K16	K16-AP-WW/02	TKAC	5/28/81	89
Pickneyville	K16	K16-TW-A/02	TKAC	5/28/81	91
Pickneyville	K16	K16-TW-A/02	TKAC	7/21/82	78
Pickneyville	K16	K16-AP-WW/02	TKAC	7/21/82	83
Pickneyville	K16	K16-AP-WW/02	TKAC	6/27/84	89
Pickneyville	K16	K16-TW-A/02	TKAC	6/27/84	88
Pickneyville	K16	K16-AP-WW/02	TKAC	7/1/86	80
Pickneyville	K16	K16-TW-A/02	TKAC	7/1/86	72
Pickneyville	K16	K16-AP-WW/02	TKAC	8/14/89	81
Pickneyville	K16	K16-TW-A/02	TKAC	8/14/89	60
Pickneyville	K16	K16-RW-18/01	TKAC	6/1/90	100
Pickneyville	K16	K16-RW-18/01	TKAC	6/4/91	100
Pickneyville	K16	K16-AP-WW/02	TKAC	6/4/91	78
Pickneyville	K16	K16-RW-18/01	TKAC	5/26/93	100
Pickneyville	K16	K16-TW-A/02	TKAC	5/26/93	79
Pickneyville	K16	K16-AP-WW/02	TKAC	5/26/93	79
Pickneyville	K16	K16-AP-WW/01	TNAC	6/1/78	100
Pickneyville	K16	K16-RW-18/02	TNAC	6/1/78	100
Pickneyville	K16	K16-RW-18/02	TNAC	5/28/81	95
Pickneyville	K16	K16-AP-WW/01	TNAC	5/28/81	79
Pickneyville	K16	K16-AP-WW/01	TNAC	7/21/82	72
Pickneyville	K16	K16-RW-18/02	TNAC	7/21/82	93
Pickneyville	K16	K16-AP-WW/01	TNAC	6/27/84	68
Pickneyville	K16	K16-RW-18/02	TNAC	6/27/84	87
Pickneyville	K16	K16-AP-WW/01	TNAC	7/1/86	56
Pickneyville	K16	K16-RW-18/02	TNAC	7/1/86	82
Pickneyville	K16	K16-RW-18/02	TNAC	8/14/89	85
Pickneyville	K16	K16-AP-WW/01	TNAC	8/14/89	61
Pickneyville	K16	K16-AP-WW/01	TNAC	6/4/91	71
Pickneyville	K16	K16-RW-18/02	TNAC	6/4/91	68
Pickneyville	K16	K16-RW-18/02	TNAC	5/26/93	77
Pickneyville	K16	K16-AP-WW/01	TNAC	5/26/93	88
Quincy	UIN	UIN-RW-18/011	PCC	6/1/46	100
Quincy	UIN	UIN-TW-B/01	PCC	6/1/46	100

Table F.2. Summary of ACCESS data base inspection information.

Airport	AID	Section	Code	Inspection Date	Section PCI
Quincy	UIN	UIN-TW-B/1-01	PCC	6/1/46	100
Quincy	UIN	UIN-TW-A/06	PCC	6/1/71	100
Quincy	UIN	UIN-RW-04/06	PCC	6/1/71	100
Quincy	UIN	UIN-TW-B/01	PCC	7/9/80	86
Quincy	UIN	UIN-TW-B/1-01	PCC	7/9/80	91
Quincy	UIN	UIN-RW-04/06	PCC	7/9/80	97
Quincy	UIN	UIN-TW-A/06	PCC	7/9/80	93
Quincy	UIN	UIN-RW-18/011	PCC	7/9/80	87
Quincy	UIN	UIN-RW-04/06	PCC	6/1/82	89
Quincy	UIN	UIN-RW-18/011	PCC	6/1/82	89
Quincy	UIN	UIN-TW-B/1-01	PCC	6/1/82	95
Quincy	UIN	UIN-TW-B/01	PCC	6/1/82	89
Quincy	UIN	UIN-TW-A/06	PCC	6/1/82	100
Quincy	UIN	UIN-TW-B/1-01	PCC	8/14/84	96
Quincy	UIN	UIN-RW-04/06	PCC	8/14/84	96
Quincy	UIN	UIN-TW-B/01	PCC	8/14/84	92
Quincy	UIN	UIN-TW-A/06	PCC	8/14/84	98
Quincy	UIN	UIN-RW-18/011	PCC	8/14/84	92
Quincy	UIN	UIN-TW-A/06	PCC	7/25/86	83
Quincy	UIN	UIN-TW-B/1-01	PCC	7/25/86	96
Quincy	UIN	UIN-RW-18/011	PCC	7/25/86	92
Quincy	UIN	UIN-RW-04/06	PCC	7/25/86	92
Quincy	UIN	UIN-TW-B/01	PCC	7/25/86	92
Quincy	UIN	UIN-RW-18/011	PCC	5/2/89	83
Quincy	UIN	UIN-TW-B/1-01	PCC	5/2/89	91
Quincy	UIN	UIN-RW-04/06	PCC	5/2/89	96
Quincy	UIN	UIN-TW-A/06	PCC	5/2/89	94
Quincy	UIN	UIN-TW-B/01	PCC	5/2/89	84
Quincy	UIN	UIN-TW-B/1-01	PCC	5/24/91	87
Quincy	UIN	UIN-RW-04/06	PCC	5/24/91	95
Quincy	UIN	UIN-RW-18/011	PCC	5/24/91	81
Quincy	UIN	UIN-TW-B/01	PCC	5/24/91	86
Quincy	UIN	UIN-TW-A/06	PCC	5/24/91	93
Quincy	UIN	UIN-TW-A/06	PCC	5/21/93	98
Quincy	UIN	UIN-RW-04/06	PCC	5/21/93	91
Quincy	UIN	UIN-TW-B/1-01	PCC	5/21/93	92
Quincy	UIN	UIN-RW-18/011	PCC	5/21/93	82
Rochelle	12C	12C-RW-07/03	TKAC	6/1/87	100
Rochelle	12C	12C-RW-07/03	TKAC	8/9/90	81
Rochelle	12C	12C-RW-07/03	TKAC	6/4/92	83
Rochelle	12C	12C-TW-C/01	TNAC	6/1/91	100
Rochelle	12C	12C-TW-C/01	TNAC	6/4/92	100
Savanna	SFY	SFY-AP-NW/01	TNAC	6/1/81	100
Savanna	SFY	SFY-AP-WW/01	TNAC	6/1/81	100

Table F.2. Summary of ACCESS data base inspection-information.

Airport	AID	Section	Code	Inspection	Section
				Date	PCI
Savanna	SFY	SFY-TW-B/01	TNAC	6/1/81	100
Savanna	SFY	SFY-AP-NW/01	TNAC	7/14/83	99
Savanna	SFY	SFY-AP-WW/01	TNAC	7/16/85	100
Savanna	SFY	SFY-TW-B/01	TNAC	7/16/85	100
Savanna	SFY	SFY-AP-NW/01	TNAC	7/16/85	82
Savanna	SFY	SFY-AP-NW/01	TNAC	6/17/88	85
Savanna	SFY	SFY-AP-WW/01	TNAC	6/17/88	98
Savanna	SFY	SFY-TW-B/01	TNAC	6/17/88	90
Savanna	SFY	SFY-AP-NW/01	TNAC	6/28/91	80
Savanna	SFY	SFY-AP-WW/01	TNAC	6/28/91	95
Savanna	SFY	SFY-TW-B/01	TNAC	6/28/91	91
Savanna	SFY	SFY-AP-NW/01	TNAC	7/30/93	83
Savanna	SFY	SFY-TW-B/01	TNAC	7/30/93	87
Savanna	SFY	SFY-AP-WW/01	TNAC	7/30/93	94
Shelbyville	2H0	2H0-AP-EE/6	TKAC	6/1/79	100
Shelbyville	2H0	2H0-AP-EE/6	TKAC	7/17/80	98
Shelbyville	2H0	2H0-AP-EE/6	TKAC	4/13/82	91
Shelbyville	2H0	2H0-AP-EE/6	TKAC	5/9/84	85
Shelbyville	2H0	2H0-RW-18/9	TKAC	6/1/84	100
Shelbyville	2H0	2H0-RW-18/9	TKAC	5/7/86	100
Shelbyville	2H0	2H0-AP-EE/6	TKAC	5/7/86	79
Shelbyville	2H0	2H0-AP-EE/6	TKAC	6/1/88	68
Shelbyville	2H0	2H0-RW-18/9	TKAC	6/1/88	91
Shelbyville	2H0	2H0-RW-18/9	TKAC	4/22/91	88
Shelbyville	2H0	2H0-AP-EE/6	TKAC	4/22/91	73
Shelbyville	2H0	2H0-AP-EE/7	TNAC	6/1/80	100
Shelbyville	2H0	2H0-AP-EE/7	TNAC	4/13/82	100
Shelbyville	2H0	2H0-AP-EE/7	TNAC	5/9/84	57
Shelbyville	2H0	2H0-AP-EE/7	TNAC	5/7/86	81
Shelbyville	2H0	2H0-AP-EE/7	TNAC	6/1/88	91
Shelbyville	2H0	2H0-AP-EE/7	TNAC	4/22/91	89
Shelbyville	2H0	2H0-AP-EE/7	TNAC	6/1/93	78
Sparta	SAR	SAR-TW-B/03	TKAC	6/1/74	100
Sparta	SAR	SAR-AP-WW/03	TKAC	6/1/74	100
Sparta	SAR	SAR-TW-B/03	TKAC	6/24/81	91
Sparta	SAR	SAR-AP-WW/03	TKAC	6/24/81	92
Sparta	SAR	SAR-TW-B/03	TKAC	6/14/83	52
Sparta	SAR	SAR-AP-WW/03	TKAC	6/14/83	64
Sparta	SAR	SAR-TW-B/03	TKAC	5/30/85	95
Sparta	SAR	SAR-AP-WW/03	TKAC	5/30/85	99
Sparta	SAR	SAR-AP-WW/03	TKAC	6/9/87	98
Sparta	SAR	SAR-TW-B/03	TKAC	6/9/87	90
Sparta	SAR	SAR-AP-WW/03	TKAC	8/21/90	82
Sparta	SAR	SAR-TW-B/03	TKAC	8/21/90	55

Table F.2. Summary of ACCESS data base inspection information.

Airport	AID	Section	Code	Inspection	Section
				Date	PCI
Sparta	SAR	SAR-TW-B/03	TKAC	7/17/92	76
Sparta	SAR	SAR-AP-WW/03	TKAC	7/17/92	76
Sparta	SAR	SAR-RW-18/03	TNAC	6/1/86	100
Sparta	SAR	SAR-RW-18/03	TNAC	6/9/87	100
Sparta	SAR	SAR-RW-18/03	TNAC	8/21/90	100
Sparta	SAR	SAR-RW-18/03	TNAC	7/17/92	99
St. Louis DT	CPS	CPS-TW-B/2-24	PCC	6/1/84	100
St. Louis DT	CPS	CPS-RW-12L/24	PCC	6/1/84	100
St. Louis DT	CPS	CPS-TW-B/1-24	PCC	6/1/84	100
St. Louis DT	CPS	CPS-TW-B/2-24	PCC	9/30/87	100
St. Louis DT	CPS	CPS-TW-B/1-24	PCC	9/30/87	100
St. Louis DT	CPS	CPS-RW-12L/24	PCC	9/30/87	99
St. Louis DT	CPS	CPS-TW-B/2-24	PCC	7/25/90	100
St. Louis DT	CPS	CPS-TW-B/1-24	PCC	7/25/90	100
St. Louis DT	CPS	CPS-RW-12L/24	PCC	7/25/90	97
St. Louis DT	CPS	CPS-TW-B/1-24	PCC	9/3/92	97
St. Louis DT	CPS	CPS-RW-12L/24	PCC	9/3/92	95
St. Louis DT	CPS	CPS-TW-B/2-24	PCC	9/3/92	96
St. Louis DT	CPS	CPS-TW-C/10	TKAC	6/1/70	100
St. Louis DT	CPS	CPS-TW-C/10	TKAC	7/8/81	87
St. Louis DT	CPS	CPS-TW-C/10	TKAC	4/29/83	64
St. Louis DT	CPS	CPS-TW-C/10	TKAC	8/30/85	56
St. Louis DT	CPS	CPS-TW-C/10	TKAC	9/30/87	79
St. Louis DT	CPS	CPS-TW-C/10	TKAC	7/25/90	85
St. Louis DT	CPS	CPS-TW-C/10	TKAC	9/3/92	70
Sterling	SQI	SQI-AP-WW/10	TKAC	6/1/79	100
Sterling	SQI	SQI-AP-WW/10	TKAC	8/7/80	99
Sterling	SQI	SQI-AP-WW/10	TKAC	7/26/82	97
Sterling	SQI	SQI-AP-WW/10	TKAC	7/10/84	86
Sterling	SQI	SQI-AP-WW/01	TKAC	6/1/86	100
Sterling	SQI	SQI-AP-WW/10	TKAC	7/14/86	83
Sterling	SQI	SQI-AP-WW/10	TKAC	6/30/89	69
Sterling	SQI	SQI-AP-WW/01	TKAC	6/30/89	100
Sterling	SQI	SQI-AP-WW/01	TKAC	6/28/91	77
Sterling	SQI	SQI-AP-WW/10	TKAC	6/28/91	77
Sterling	SQI	SQI-AP-WW/10	TKAC	7/30/93	77
Sterling	SQI	SQI-AP-WW/01	TKAC	7/30/93	83
Taylorville	3TV	3TV-TW-A/2-08	TKAC	6/1/86	100
Taylorville	3TV	3TV-TW-A/5-02	TKAC	6/1/86	100
Taylorville	3TV	3TV-TW-A/4-08	TKAC	6/1/86	100
Taylorville	3TV	3TV-TW-A/1-08	TKAC	6/1/86	100
Taylorville	3TV	3TV-RW-18/08	TKAC	6/1/86	100
Taylorville	3TV	3TV-TW-A/3-08	TKAC	6/1/86	100
Taylorville	3TV	3TV-RW-18/08	TKAC	5/13/87	100

Table F.2. Summary of ACCESS data base inspection information.

Airport	AID	Section	Code	Inspection	Section
				Date	PCI
Taylorville	3TV	3TV-TW-A/1-08	TKAC	5/13/87	100
Taylorville	3TV	3TV-TW-A/2-08	TKAC	5/13/87	100
Taylorville	3TV	3TV-TW-A/3-08	TKAC	5/13/87	100
Taylorville	3TV	3TV-TW-A/4-08	TKAC	5/13/87	100
Taylorville	3TV	3TV-TW-A/5-02	TKAC	5/13/87	100
Taylorville	3TV	3TV-RW-18/08	TKAC	4/19/89	89
Taylorville	3TV	3TV-TW-A/1-08	TKAC	4/19/89	90
Taylorville	3TV	3TV-TW-A/3-08	TKAC	4/19/89	90
Taylorville	3TV	3TV-TW-A/4-08	TKAC	4/19/89	98
Taylorville	3TV	3TV-TW-A/5-02	TKAC	4/19/89	89
Taylorville	3TV	3TV-TW-A/2-08	TKAC	4/19/89	91
Taylorville	3TV	3TV-RW-18/08	TKAC	4/22/91	83
Taylorville	3TV	3TV-TW-A/5-02	TKAC	4/22/91	88
Taylorville	3TV	3TV-TW-A/4-08	TKAC	4/22/91	91
Taylorville	3TV	3TV-TW-A/3-08	TKAC	4/22/91	91
Taylorville	3TV	3TV-TW-A/2-08	TKAC	4/22/91	91
Taylorville	3TV	3TV-TW-A/1-08	TKAC	4/22/91	88
Taylorville	3TV	3TV-TW-A/4-08	TKAC	6/1/93	85
Taylorville	3TV	3TV-TW-A/3-08	TKAC	6/1/93	85
Taylorville	3TV	3TV-TW-A/2-08	TKAC	6/1/93	87
Taylorville	3TV	3TV-TW-A/1-08	TKAC	6/1/93	91
Taylorville	3TV	3TV-RW-18/08	TKAC	6/1/93	81
Taylorville	3TV	3TV-AP-EE/04	TNAC	6/1/78	100
Taylorville	3TV	3TV-AP-EE/04	TNAC	3/30/81	99
Taylorville	3TV	3TV-AP-EE/07	TNAC	6/1/82	100
Taylorville	3TV	3TV-AP-EE/07	TNAC	5/17/83	100
Taylorville	3TV	3TV-AP-EE/07	TNAC	7/10/85	90
Taylorville	3TV	3TV-AP-EE/04	TNAC	7/10/85	74
Taylorville	3TV	3TV-AP-EE/07	TNAC	5/13/87	82
Taylorville	3TV	3TV-AP-EE/04	TNAC	5/13/87	81
Taylorville	3TV	3TV-AP-EE/07	TNAC	4/19/89	68
Taylorville	3TV	3TV-AP-EE/04	TNAC	4/19/89	70
Taylorville	3TV	3TV-AP-EE/04	TNAC	4/22/91	83
Taylorville	3TV	3TV-AP-EE/07	TNAC	4/22/91	85
Taylorville	3TV	3TV-AP-EE/07	TNAC	6/1/93	77
Vandalia	VLA	VLA-TW-B/7	TNAC	6/1/75	100
Vandalia	VLA	VLA-TW-D/1-7	TNAC	6/1/75	100
Vandalia	VLA	VLA-TW-D/7	TNAC	6/1/75	100
Vandalia	VLA	VLA-TW-B/7	TNAC	5/26/81	86
Vandalia	VLA	VLA-TW-B/7	TNAC	7/13/82	87
Vandalia	VLA	VLA-TW-D/1-7	TNAC	5/9/84	76
Vandalia	VLA	VLA-TW-D/7	TNAC	5/9/84	85
Vandalia	VLA	VLA-TW-B/7	TNAC	5/9/84	86
Vandalia	VLA	VLA-TW-B/7	TNAC	5/7/86	80

Table F.2. Summary of ACCESS data base inspection information.

Airport	AID	Section	Code	Inspection	Section
				Date	PCI
Vandalia	VLA	VLA-TW-D/7	TNAC	5/7/86	69
Vandalia	VLA	VLA-TW-D/1-7	TNAC	5/7/86	74
Vandalia	VLA	VLA-TW-D/7	TNAC	6/21/89	86
Vandalia	VLA	VLA-TW-D/1-7	TNAC	6/21/89	86
Vandalia	VLA	VLA-TW-B/7	TNAC	6/21/89	86
Vandalia	VLA	VLA-TW-D/7	TNAC	8/26/91	68
Vandalia	VLA	VLA-TW-B/7	TNAC	8/26/91	74
Vandalia	VLA	VLA-TW-D/1-7	TNAC	8/26/91	68
Vandalia	VLA	VLA-TW-D/1-7	TNAC	6/15/93	77
Vandalia	VLA	VLA-TW-B/7	TNAC	6/15/93	75
Vandalia	VLA	VLA-TW-D/7	TNAC	6/15/93	78
Waukegan	UGN	UGN-RW-14/14	PCC	6/1/64	100
Waukegan	UGN	UGN-RW-14/111	PCC	6/1/70	100
Waukegan	UGN	UGN-RW-14/112	PCC	6/1/70	100
Waukegan	UGN	UGN-RW-14/08	PCC	6/1/75	100
Waukegan	UGN	UGN-RW-14/09	PCC	6/1/75	100
Waukegan	UGN	UGN-RW-14/08	PCC	8/6/81	77
Waukegan	UGN	UGN-RW-14/112	PCC	8/6/81	48
Waukegan	UGN	UGN-RW-14/09	PCC	8/6/81	67
Waukegan	UGN	UGN-RW-14/14	PCC	8/6/81	59
Waukegan	UGN	UGN-RW-14/111	PCC	8/6/81	63
Waukegan	UGN	UGN-RW-14/09	PCC	8/3/83	72
Waukegan	UGN	UGN-RW-14/111	PCC	8/3/83	69
Waukegan	UGN	UGN-RW-14/112	PCC	8/3/83	57
Waukegan	UGN	UGN-RW-14/14	PCC	8/3/83	62
Waukegan	UGN	UGN-RW-14/08	PCC	8/3/83	90
Waukegan	UGN	UGN-RW-14/09	PCC	6/27/85	70
Waukegan	UGN	UGN-RW-14/111	PCC	6/27/85	62
Waukegan	UGN	UGN-RW-14/112	PCC	6/27/85	64
Waukegan	UGN	UGN-RW-14/14	PCC	6/27/85	65
Waukegan	UGN	UGN-RW-14/08	PCC	6/27/85	93
Waukegan	UGN	UGN-RW-14/14	PCC	6/17/87	75
Waukegan	UGN	UGN-RW-14/08	PCC	6/17/87	94
Waukegan	UGN	UGN-RW-14/09	PCC	6/17/87	82
Waukegan	UGN	UGN-RW-14/111	PCC	6/17/87	77
Waukegan	UGN	UGN-RW-14/112	PCC	6/17/87	75
Waukegan	UGN	UGN-RW-14/09	PCC	8/8/89	72
Waukegan	UGN	UGN-RW-14/111	PCC	8/8/89	65
Waukegan	UGN	UGN-RW-14/112	PCC	8/8/89	73
Waukegan	UGN	UGN-RW-14/14	PCC	8/8/89	54
Waukegan	UGN	UGN-RW-14/08	PCC	8/8/89	79
Waukegan	UGN	UGN-RW-14/111	PCC	7/24/91	63
Waukegan	UGN	UGN-RW-14/09	PCC	7/24/91	51
Waukegan	UGN	UGN-RW-14/14	PCC	7/24/91	55

Table F.2. Summary of ACCESS data base inspection information.

Airport	AID	Section	Code	Inspection	Section
				Date	PCI
Waukegan	UGN	UGN-RW-14/112	PCC	7/24/91	58
Waukegan	UGN	UGN-RW-14/08	PCC	7/24/91	77
Waukegan	UGN	UGN-RW-14/112	PCC	7/20/93	61
Waukegan	UGN	UGN-RW-14/08	PCC	7/20/93	78
Waukegan	UGN	UGN-RW-14/14	PCC	7/20/93	61
Waukegan	UGN	UGN-RW-14/111	PCC	7/20/93	74
Waukegan	UGN	UGN-RW-14/09	PCC	7/20/93	68
Waukegan	UGN	UGN-TW-C/07	TKAC	6/1/82	100
Waukegan	UGN	UGN-TW-C/07	TKAC	8/3/83	100
Waukegan	UGN	UGN-TW-C/07	TKAC	6/27/85	99
Waukegan	UGN	UGN-TW-C/07	TKAC	6/17/87	94
Waukegan	UGN	UGN-TW-C/07	TKAC	8/8/89	92
Waukegan	UGN	UGN-TW-C/07	TKAC	7/24/91	83

SUPPLEMENTAL REPORT
Project 1A-A1, FY 92

AGING PHENOMENON IN
ASPHALT CONCRETE
PAVEMENTS -
A LITERATURE REVIEW

Prepared by
Claribel Alvarez and Marshall R. Thompson
Department of Civil Engineering
University of Illinois at Urbana-Champaign

December 1994

Illinois Transportation Research Center
Illinois Department of Transportation

ILLINOIS TRANSPORTATION RESEARCH CENTER

This research project was sponsored by the State of Illinois, acting by and through its Department of Transportation, according to the terms of the Memorandum of Understanding established with the Illinois Transportation Research Center. The Illinois Transportation Research Center is a joint Public-Private-University cooperative transportation research unit underwritten by the Illinois Department of Transportation. The purpose of the Center is the conduct of research in all modes of transportation to provide the knowledge and technology base to improve the capacity to meet the present and future mobility needs of individuals, industry and commerce of the State of Illinois.

Research reports are published throughout the year as research projects are completed. The contents of these reports reflect the views of the authors who are responsible for the facts and the accuracy of the data presented herein. The contents do not necessarily reflect the official views or policies of the Illinois Transportation Research Center or the Illinois Department of Transportation. This report does not constitute a standard, specification, or regulation.

Neither the United States Government nor the State of Illinois endorses products or manufacturers. Trade or manufacturers' names appear in the reports solely because they are considered essential to the object of the reports.

Illinois Transportation Research Center Members

Bradley University
DePaul University
Eastern Illinois University
Illinois Department of Transportation
Illinois Institute of Technology
Lewis University
Northern Illinois University
Northwestern University
Southern Illinois University at Carbondale
Southern Illinois University at Edwardsville
University of Illinois at Chicago
University of Illinois at Urbana-Champaign
Western Illinois University

Reports may be obtained by writing to the administrative offices of the Illinois Transportation Research Center at 200 University Park, Edwardsville, IL 62026-1806 [telephone (618) 692-2972], or you may contact the Engineer of Physical Research, Illinois Department of Transportation, at (217) 782-6732.

Technical Report Documentation Page

1. Report No. IA-A1, FY 92 - SR		2. Government Accession No.		3. Recipient's Catalog No.	
4. Title and Subtitle AGING PHENOMENON IN ASPHALT CONCRETE PAVEMENTS - A LITERATURE REVIEW				5. Report Date December, 1994	
				6. Performing Organization Code	
7. Author(s) C. Alvarez - M. Thompson				8. Performing Organization Report No.	
9. Performing Organization Name and Address Department of Civil Engineering University of Illinois at Urbana-Champaign				10. Work Unit (TRAIS)	
				11. Contract or Grant No.	
12. Sponsoring Agency Name and Address Illinois Transportation Research Center Illinois Department of Transportation 200 University Park Edwardsville, IL 62026-1806				13. Type of Report and Period Covered Supplemental Report	
				14. Sponsoring Agency Code	
15. Supplementary Notes This report is a supplement to Report IA-A1, FY 92 - "Concepts and Practices for considering GA Airport Pavement Performance and Longevity" - December 1994, by T. VanDam, M. Thompson, E. Barenberg and B. Dempsey.					
16. Abstract <p>The properties of the asphalt cement binder in asphalt concrete (AC) significantly affect flexible pavement performance. These properties change as a function of service time. The GA airport performance and longevity part of this study confirmed the significant contribution of "asphalt aging" to the loss of flexible pavement serviceability. A comprehensive literature review was conducted to consider the various factors that influence "asphalt aging" and techniques for alleviating the problem.</p> <p>Two major effects dominate asphalt cement aging: (a) loss of volatile components and oxidation in the construction phase - primarily during mixing - (short-term aging), and (b) progressive oxidation of the in place mixture in the field (long-term aging).</p> <p>Many efforts have been directed to better understand the aging phenomenon and the laboratory simulation of field asphalt cement aging. Laboratory aging studies have primarily been conducted with asphalt cement, ignoring the effect of the aggregate on the AC aging phenomenon.</p> <p>Some significant observations are:</p> <ul style="list-style-type: none"> • Aggregate type may have a significant effect on AC aging. • The oxidation products that form during aging do not necessarily relate to a viscosity increase. • Asphalt film thickness and air voids level play an important role in the AC aging phenomenon. Very thin asphalt film thickness contributes to more rapid age hardening. Higher air voids produce a higher AC modular ratio (aged modulus/original modulus). • Laboratory simulation tests should relate to field aging. The maximum laboratory testing temperature that should be used is 110°C (230°F) for the asphalt binder and 85°C (185°F) for AC specimens. • Lime addition to asphalt-aggregate mixtures has a beneficial effect. It reduces age hardening. 					
17. Key Words Airport Pavements Paving Materials Asphalt Asphalt Aging			18. Distribution Statement No restrictions. This document is available to the public through the National Technical Information Service, Springfield, Virginia 22161		
19. Security Classif. (of this report) Unclassified		20. Security Classif. (of this page) Unclassified		21. No. of Pages 41	22. Price

TABLE OF CONTENTS

	<u>Page</u>
EXECUTIVE SUMMARY	ii
1. Introduction	1
2. Laboratory Aging and Evaluation Methods	2
2.1 Binder Aging	2
2.2 Asphalt Concrete Aging	3
3. Summary of Research Findings	3
3.1 Oxidation and Hardening	4
3.2 Test Temperature	5
3.3 Air voids and Film thickness	6
3.4 Molecular Size Distribution	7
3.5 Solvent Aging	7
3.6 Lime Effect on Aging	7
4. Summary	8
REFERENCES	9
ABSTRACTS OF SELECTED REFERENCES	11
APPENDIX A - SHRP Extraction and Recovery Method	33

EXECUTIVE SUMMARY

The properties of the asphalt cement binder in asphalt concrete (AC) significantly affect flexible pavement performance. These properties change as a function of service time. Quantitative information about the properties and characteristics of the aged asphalt is essential to the successful prediction of AC field performance. The GA airport performance and longevity part of this study confirmed the significant contribution of "asphalt aging" to the loss of flexible pavement serviceability.

Two major effects dominate asphalt cement aging: (a) loss of volatile components and oxidation in the construction phase - primarily during mixing- (short-term aging), and (b) progressive oxidation of the in place mixture in the field (long-term aging). Other factors, like thixotropy, may also contribute to aging.

Many efforts have been directed to better understand the aging phenomenon and the laboratory simulation of field asphalt cement aging. Laboratory aging studies have primarily been conducted with asphalt cement, ignoring the effect of the aggregate on the AC aging phenomenon. The temperatures used in past studies appear to be too high to reproduce field aging conditions/mechanisms.

Some significant observations are:

- Aggregate type may have a significant effect on AC aging.
- The oxidation products that form during aging do not necessarily relate to a viscosity increase.
- Asphalt film thickness and air voids level play an important role in the AC aging phenomenon. Very thin asphalt film thickness contributes to more rapid age hardening. Higher air voids produce a higher AC modular ratio (aged modulus/ original modulus).
- Laboratory simulation tests should relate to field aging. The maximum laboratory testing temperature that should be used is 110°C for the asphalt binder and 85°C (185°F) for AC specimens.
- Extracting and recovering asphalts from aged mixtures should be accomplished using the SHRP method. ASTM methods produce greater solvent aging of the asphalt and do not recover the asphalt from the aggregate as effectively as the SHRP method (See Appendix A).
- Lime addition to asphalt-aggregate mixtures has a beneficial effect. It reduces age hardening.

1. Introduction

The properties of the asphalt cement binder in asphalt concrete (AC) significantly affect flexible pavement performance. These properties change as a function of service time in the pavement. Quantitative information about the properties and characteristics of the aged asphalt is essential to the successful prediction of AC field performance.

Two major effects dominate asphalt cement aging: (a) loss of volatile components and oxidation in the construction phase - primarily during mixing- (short-term aging), and (b) progressive oxidation of the in place mixture in the field (long-term aging). Other factors may contribute to aging. Thixotropy (a progressive hardening due to the formation of "structure" within the asphalt cement) is likely to occur over an extended period of time.

Asphalt aging contributes to hardening (stiffening) of the AC, which obviously alters the AC performance potential. This may be beneficial. Increased AC stiffness effects improved AC layer load distribution properties and increased permanent deformation resistance. However, if the "aged AC" becomes too stiff, other distresses (e.g. fatigue cracking, low-temperature cracking, brittleness/block cracking, increased moisture sensitivity) may develop.

Many efforts have been directed to better understand the aging phenomenon and the laboratory simulation of field asphalt cement aging. Laboratory aging studies have primarily been performed with asphalt cement, ignoring the effect of the aggregate on the AC aging phenomenon. The temperatures used in past studies appear to be too high to reproduce field aging

conditions/mechanisms.

2. Laboratory Aging and Evaluation Methods

Tests have been developed to simulate short-term and long-term aging of the asphalt. These tests are generally conducted on the asphalt binder.

2.1 Binder Aging

The asphalt hardens during short-term aging in the hot-mix plant and during AC laydown operations. This hardening is mainly caused by the loss of volatile components. The tests commonly used to simulate this phase are the Thin Film Oven Test (TFOT) (ASTM D-1754) and Rolling Thin Film Oven Test (RTFOT) (ASTM D-2872). Research has shown that these tests fairly well simulate the short-term aging of the asphalt (Jones and Youtcheff, 1992).

The TFOT and RTFOT are recommended by the Asphalt Aging Working Group of the Strategic Highway Research Program (SHRP).

Long-term aging occurs at ambient temperature in the road. It is mainly caused by progressive oxidation and the formation of structures by the asphalt molecules. Researchers have tried to reproduce long-term aging. The most widely used methods are: extended oven heating, Pressure Aging Vessels (PAV), and ultraviolet and infrared exposures. SHRP has recommended PAV conditions of 1) 300 psi air pressure, 2) temperature of 100°C, and 3) aging time of 20 hours (Jones and Youtcheff, 1992).

The properties of the aged asphalt binder have been evaluated using various methods (e.g. viscosity, penetration, ductility, oxidation products, asphaltene content, Ring and Ball Softening Point, Roestler-Sternberg analysis, chromatographic

separation).

2.2 Asphalt Concrete Aging

The ultimate goal is to successfully predict AC field performance. Thus it is equally important to investigate the aggregate role in the asphalt aging phenomenon.

Several procedures have been used to simulate AC aging. For short-term aging, oven exposure of uncompacted AC is frequently used. Commonly used for long-term aging methods for AC specimens are extended oven heating, pressure oxidation, and ultraviolet/infrared treatment.

Numerous methods are used to evaluate the aged AC. The most frequently used are resilient modulus, indirect tensile strength, and dynamic modulus. Tests also may be conducted on the recovered asphalt to quantify the changes in properties of the aged asphalt cement.

3. Summary of Research Findings

Over the years, most of the research has been conducted on the asphalt and the results related to the AC aging characteristics. Many studies investigated the suitability of this practice. More recently Sosnovske et al. (1993) found little relationship between the effect of laboratory aging on the asphalt cement and AC aging. There was a significant difference between the ranking of asphalts aged alone, and the same asphalts aged in an AC mixture. The rankings were based on aging susceptibility (viscosity ratios for the asphalts and modular ratios for the AC). Asphalts ranked as "good" when aged alone were ranked as "bad" when aged in the AC. It was concluded that the aging of the asphalt is not an adequate indicator of mixture

aging potential.

3.1 Oxidation and Hardening

In many past studies, aged asphalts have been characterized by infrared analyses. The growth in the carbonyl band (from 1800 cm^{-1} - 1600 cm^{-1} approx.) has been used as a measure of oxidation. Scientists have tried with little success to correlate the oxidation products formed during the laboratory long-term aging to the increase in asphalt viscosity. The sensitivity of asphalt viscosity to the oxidation products varies with asphalt source. An asphalt may oxidize relatively rapidly but not harden a great deal, or it may harden considerably while oxidizing at a slower rate (Lau et al., 1992; Petersen et al., 1993).

The SHRP asphalt model explains this previously anomalous behavior. In this model the asphalt includes two functional families of molecules: polar and non-polar. The polar molecules interact to form associations through weak bonds. These bonds break as the temperature increases causing the asphalt to behave as a Newtonian fluid at elevated temperatures.

A molecular fraction that has been isolated through Ion Exchange Chromatography explains the lack of correlation between oxidation products and viscosity increases and the tendency of the polar material in the asphalt to associate. These molecules, termed amphoteric, have the distinctive characteristic of possessing both an acid and a basic group in the asphalt molecule, but not at the same site. When a non-polar site in an amphoteric molecule oxidizes, it can act as a polar molecule and form associations. An amphoteric molecule can associate as many

times as polar sites are available. In an asphalt with low amounts of amphoteric, most of the molecules will have only one oxidizable site. Thus, the asphalt cannot form many associations and effect a viscosity increase.

The oxidation of asphalt is independent of aggregate type. That is, the oxidative products measured in the asphalt (usually carbonyl and sulfoxide) do not vary when the same asphalt is aged on different aggregates (Jones, 1992).

However AC aging (as measured by changes in resilient modulus, dynamic modulus, or viscosity measurements of the recovered asphalt) is significantly affected by aggregate type. Clearly the most important contributor to AC aging is the asphalt cement, but the aggregate type also influences the phenomenon. Asphalt-aggregate mixture aging patterns produced with the same asphalt may be very different depending on the aggregate. The observed aging phenomenon appears to be related to the adhesion of the asphalt and the aggregate. The greater the adhesion, the greater the mitigation of aging (Sosnovske et al., 1992; AbWahab et al., 1992).

3.2 Test Temperature

Testing temperature is one of the most important factors in laboratory long-term aging. The temperatures traditionally used are too high to relate oven aging to road aging. At higher temperatures, light constituents of asphalt evaporate, producing unrealistic changes in the chemistry of the oxidation reactions when compared with field-aged asphalts. In addition, the high molecular constituents are believed to dehydrogenate, and a large percentage of oxygen consumed is discharged in the form of water

vapor and other gases, which does not occur at normal service temperatures.

Asphalt aging mechanisms are the same in the laboratory and the field up to temperatures approaching 100°C-115°C (212°F-239°F) (Jones, 1992; Vershasselt et al., 1993). It is necessary to use laboratory temperatures that effect aging mechanisms similar to the ones observed in the field in order to make realistic predictions of the mixture performance. SHRP recommends a maximum temperature for asphalt accelerated aging of 110°C (Jones and Youtcheff, 1992). Bell et al.(1994-2) indicated compacted AC specimens may suffer "structural damage" if exposed to temperatures greater than 85°C (185°F).

3.3 Air Voids and Film Thickness

High air voids in the AC shorten road life. Air voids is one of the most important factors affecting the rate of hardening of an asphalt pavement. The Martin et al. study (1989) showed that oxidation (as reflected in the growth of the carbonyl peak) increases as air voids increases. Research suggests that higher air voids produce higher modular ratios (modulus after aging/original modulus) in the aged AC (C.A. Bell et al., 1991).

Another factor that has been studied is the effect of film thickness on aging of the asphalt. Very thin film thickness presents durability problems. Recently, Button et al. (1993) found a relationship between the asphalt cement film thickness and age hardening. The relationship is asphalt dependent. In general, the thinner films were associated with lower recovered asphalt penetration values.

3.4 Molecular Size Distribution

Asphalt cements subjected to artificial (laboratory) aging, experience composition changes. High Pressure Gel Permeation Chromatography (GPC) has been used to quantify these changes. In general, there is a significant change in the Large Molecular Size fraction due to aging (Kim et al., 1991). Statistical analyses have correlated viscosity increase with the amount of large molecular size molecules, and penetration with medium-sized molecules.

3.5 Solvent Aging

After asphalt mixture aging, the extracted asphalt may be evaluated to study changes in various properties and composition. ASTM D-2172 methods are widely used but they are not very reliable. Asphalts harden during solvent extraction. Cold extraction reduces solvent aging. The new SHRP method (See Appendix A) for recovering and extracting asphalt limits solvent aging and it also extracts more of the strongly adsorbed material from the aggregate (Burr et al., 1993).

3.6 Lime Effect on Aging

Hydrated lime is extensively used as an anti-stripping agent. It has been reported that adding hydrated lime to AC decreased the rate of hardening of the asphalt, thereby prolonging service life. Research has demonstrated (Plancher et al., 1977; Edler et al. 1985) that lime addition to the asphalts greatly reduces the asphalt hardening as measured by viscosity index. Lime treatment reduces the oxidation levels (growth in carbonyl area) measured using the infrared spectra. Another finding of the Edler et al. study is that lime addition reduces the formation of High Molecular

Weight components, which have a direct effect on the viscosity increase of the asphalt cement. Plancher et al. (1977) reported a significant decrease (around 50%) of the modulus aging indices of all samples prepared with lime-treated asphalts compared to their untreated counterparts. Results of a recent study, in which AC was prepared with a lime-treated asphalt, suggest that lime may reduce the variability in aging patterns of an asphalt aged with different types of aggregates (Bell et al. 1994-1).

4. Summary

- Aggregate type may have a significant effect on AC aging.
- The oxidation products that form during aging do not necessarily relate to a viscosity increase.
- Asphalt film thickness and air voids level play an important role in the AC aging phenomenon. Very thin asphalt film thickness contributes to more rapid age hardening. Higher air voids produce a higher AC modular ratio (aged modulus/original modulus).
- Laboratory simulation tests should relate to field aging. The maximum laboratory testing temperature that should be used is 110°C for the asphalt binder (SHRP, 1992) and 85°C (185°F) for AC specimens.
- Extracting and recovering asphalts from aged mixtures should be accomplished using the SHRP method. ASTM methods produce greater solvent aging of the asphalt and do not recover the asphalt from the aggregate as effectively as the SHRP method (See Appendix A).
- Lime addition to asphalt-aggregate mixtures has a beneficial effect. It reduces age hardening.

REFERENCES

Y. AbWahab, D. Sosnovske, C. A. Bell and P. Ryrus. Evaluation of Asphalt-Aggregate Mixture by Dynamic Mechanical Analysis. *Transportation Research Record* 1386, TRB, Washington DC, 1993, pp. 22-30.

C.A. Bell, Y. AbWahab, and M.E. Cristi. Investigation of Laboratory Aging Procedures for Asphalt-Aggregate Mixture. *Transportation Research Record* 1323, TRB, Washington DC, 1991, pp. 32-42

C.A. Bell, D. Sosnovske, and Julie E. Kliever. Relating Asphalt and Aggregate Properties and Their Laboratory Aging to Field Performance of Asphalt Mixtures. Transportation Research Board, Preprint Paper No.94-0873, Washington DC, 1994-1.

C.A. Bell, M.J. Fellin, and A. Wieder. Field Validation of Laboratory Aging Procedures for Asphalt and Aggregate Mixtures. Preprint Paper, *Association of Asphalt Paving Technologists*, St. Louis, Missouri, March 21-23, 1994-2.

C.A. Bell. Summary Report on Aging of Asphalt-Aggregate Systems (SR-OSU- A-003A-89-2). Strategic Highway Research Program (SHRP), National Research Council, Washington, D.C., 1989

S.W. Bishara, R.L. McReynolds, and E.R. Lewis. Interrelationship Between Performance Related Properties of Asphalt Cement and Their Correlation with Molecular Size Distribution. *Transportation Research Record* 1323, TRB, Washington, D.C , 1991, pp. 1-9.

B.L. Burr, R.R. Davison, H.B. Jemison, C.J. Glover, and J.A. Bullin. Asphalt Hardening in Extraction Solvents. *Transportation Research Record* 1323, TRB, Washington, D.C., 1991, pp. 70-76.

B.L. Burr, C.J. Glover, R.R. Davison and J.A. Bullin. New Apparatus and Procedure for the Extraction and Recovery of Asphalt Binder from Mixtures. *Transportation Research Record* 1391, TRB, Washington, D.C., 1993, pp. 20-29.

Joe W. Button, Manoj Jawle, Vidyasagar Jagadam, and Dallas N. Little. Evaluation and Development of a Pressure Aging Vessel for Asphalt Cement. *Transportation Research Record* 1391, TRB, Washington, D.C., 1993, pp. 11-19.

A.C. Edler, M.M. Hatting, V.P. Servas, and C.P. Marais. Use of Aging Tests to Determine the Efficacy of Hydrated lime Addition to Asphalt in Retarding its Oxidative Hardening. Proceedings, Association of Asphalt Paving Technologists, Vol. 54, 1985, pp. 118-139.

David R. Jones. An Asphalt Primer: Understanding How the Origin and Composition of Paving-Grade Asphalt Cements Affect Their Performance. SHRP Asphalt Research Program, Technical Memorandum #4, 1992.

David R. Jones and Jack S. Youtcheff. Binder and Mixture Aging in Asphaltic Pavements: A Specification. SHRP Asphalt Research Program, Technical Research Memorandum #5, 1992.

Kwang W. Kim and James L. Burati Jr. Use of GPC Chromatograms to Characterize Aged Asphalt Cements. *Journal of Materials in Civil Engineering*, ASCE, Vol. 5, No. 1, February 1993, pp. 41-52.

C.K. Lau, K. M. Lunsford, C. J. Glover, R.R. Davison, and J.A. Bullin. Reaction Rates and Hardening Susceptibilities as Determined from Pressure Oxygen Vessel Aging of, Asphalts. *Transportation Research Record* 1342, TRB, Washington DC, 1992, pp. 50-57.

K.L. Martin, R.R. Davison, C.J. Glover and J.A. Bullin. Asphalt Aging in Texas Roads and Tests Sections. *Transportation Research Record* 1269, TRB, Washington, D.C., 1989, pp. 9-19.

J.C. Petersen, Jan F. Branthaver, Raymond E. Robertson, P. Michael Hansberger, John J. Duvall, and E. Keith Ensley. Effects of Physicochemical Factors on Asphalt Oxidation Kinetics. *Transportation Research Record* 1391, TRB, Washington DC, 1993, pp. 1-10.

H. Plancher, E.L. Green, and J.C. Petersen. Paving Asphalts: Reduction of Oxidative Hardening of Asphalts by Treatment with Hydrated Lime - A Mechanistic Study. Interim Report, Federal Highway Administration, Washington, D.C., April 1977.

Jih-Min Shiau, Mang Tia, Byron E. Ruth, and Gale G. Page. Evaluation of Aging Characteristics of Asphalts by Using TFOT and RTFOT at Different Temperature Levels. *Transportation Research Record* 1342, TRB, Washington, D.C., 1992, pp. 58-66.

D.A. Sosnovske, Y. AbWahab., and C.A. Bell. Role of Asphalt And Aggregate in the Aging of Bituminous Mixtures. *Transportation Research Record* 1386, TRB, Washington, D.C., 1993, pp. 10-21.

A.F. Verhasselt and F.S. Choquet. Comparing Field and Laboratory Aging of Bitumens on a Kinetic Basis. *Transportation Research Record* 1391, TRB, Washington, D.C., 1993, pp. 30-38.

ABSTRACTS OF SELECTED REFERENCES

Evaluation of Asphalt-Aggregate Mixture by Dynamic Mechanical Analysis.

Y. AbWahab, D. Sosnovske, C.A. Bell, and P. Ryrus.

Transportation Research Record 1386, TRB, Washington, D.C., 1993, pp. 22-30

Dynamical Mechanical Analysis (DMA) and other methods of rheological testing have been used to characterize the time and temperature dependent responses of viscoelastic materials. This method uses the time-temperature superposition method.

Five different aging-treatments were considered for the experiment: no aging, STOA (Short-term Oven Aging) for 4 hr at 135°C (275°F), LTOA (Long-term Oven Aging) for 5 days at 85°C (185°F), LTOA for 2 days at 100°C (212°F), LPO (Low Pressure Oxidation) for 5 days at 60°C (140°F) and LPO for 5 days at 85°C (185°F). DMA was performed using a repeated sinusoidal waveform load. The load was applied at 11 different frequencies from 15 to 0.01 Hz., and at three different temperatures 0°C, 25°C, and 40°C (32°F, 77°F and 104°F).

It was observed that the Asphalt Concrete modulus decreases monotonically as the frequency is reduced, also it was noted that at an intermediate temperature or frequency, the asphalt-aggregate mixture is more viscous than at high or low frequencies where either the asphalt or aggregate dominates the elastic response. The results showed that the short-term-aged specimens are consistently stiffer than the unaged specimens for all asphalt-aggregate combinations. The long-term-aged specimens are consistently more stiffer than the short-term aged and unaged specimens for certain asphalt-aggregate combinations.

Master curves of complex modulus versus frequency for asphalt mixtures were constructed, they show that the complex modulus at high frequencies approaches a limiting value of 5,000 Ksi. after long-term aging treatments.

DMA results suggest that Low-Pressure Oxidation (LPO) for 5 days at 85°C is the most severe treatment among the evaluated long-term aging treatments. DMA rankings of the evaluated asphalt-aggregate combinations based on complex modulus at 1 Hz. are similar to the diametral resilient modulus rankings for the same mixtures.

Investigation of Laboratory Aging Procedures for Asphalt-Aggregate Mixture.

C.A. Bell, Y. AbWahab, and M.E. Cristi.

Transportation Research Record 1323, TRB, Washington, D.C., 1991, pp. 32-42

A preliminary program to evaluate the most promising aging methods to simulate short- and long-term aging effects is presented. The program involves two groups of aging procedures; for the short-term, forced draft oven aging and extended mixing methods were used; for the long-term aging, pressure oxidation and triaxial cell aging were evaluated. To quantify the effect of the aging methods, tests were performed on the Asphalt Concrete(AC) and the asphalts. For the AC, Resilient modulus, Dynamic modulus, and Tensile tests were used; and for the asphalts rheology tests.

For the short-term aging methods both the oven aging and the extended mixing resulted in an increase of modulus ratio. The oven aging is advantageous because several trays can be aged at the same time. Extended mixing requires oven modification. Long term oven aging can cause a very large increase in resilient modulus (50% higher than the moduli of cores recovered from the field).

The results from the pressure oxidation test program for either oxygen or air showed a decrease in modulus. A trend contrary to that anticipated and was attributed to disruption of the sample when the gas pressure was relieved. The triaxial cell aging approach is an alternate method of oxygen enrichment to the pressure oxidation technique. It involves conditioning a sample while it is positioned in a triaxial test cell. Oxygen or air is passed through the sample and the resilient modulus determined at any time during the conditioning process. A flow rate of 4 ft³/hr. was used, which required a pressure of about 50 psi. This method requires further investigation.

Relating Asphalt and Aggregate Properties and their Laboratory Aging to Field Performance of Asphalt Mixtures.

C.A.Bell, D. Sosnovske, and Julie E. Kliewer.

Preprint Paper no. 94-0873, TRB, Washington, D.C., 1994.

Eight different asphalt types and four different aggregates were used to prepare Asphalt Concrete (AC) mixture samples. The materials used for this testing program were selected from those stored at the SHRP Material Reference Library (MRL) in Austin, Texas. The aggregates used represent a broad range of aggregate characteristics, from high absorption crushed limestone to a river run gravel. The asphalts used also cover a broad range of asphalt grades. All specimens were short-term aged for 4 hours at a temperature of 135°C (275°F) before compaction. Four different long-term aging procedures were examined: low pressure oxidation (LPO) at 60°C and 85°C (140°F and 185°F), long-term oven aging (LTOA) at 85°C (185°F), all for five days, and LTOA at 100°C (212°F) for 2 days. The aging characteristics of the samples were evaluated by their resilient modulus as determined using the diametral (indirect tension) (ASTM D-4123) and triaxial compression modes of testing. The modulus data was adjusted for air voids level. It was found that, on the average, the modulus decreased 15 Ksi. for each 1 percent increase in air voids.

The AC were ranked based in their modulus ratio (before and after aging) by aggregate type. The field validation program consisted in taking cores from different projects (new, young and old projects) to compare the performance of laboratory aged AC with that of field projects. A statistical analysis of the moduli of field cores and laboratory specimens was done to determine which of the laboratory treatments most closely matched the field aging for each site. The sites were grouped according to climatic regions.

The study also compared the ranking obtained for the asphalts based on AC aging to the ranking observed by aging the asphalt alone. There is little similarity between the two rankings for both short-term and long-term aging. This suggests that the aging of the AC is influenced by both the asphalt and the aggregate. Aging of the asphalt alone and subsequent testing does not appear to be an adequate means of predicting AC performance, with respect to aging, because of the apparent mitigating effect aggregate has on aging.

Based on the study of new and young field sites, 4 hours of oven aging at 135°C appears to be representative of the short-term aging which occurs in the

field during mixing and placement. Two days of long-term oven aging at 85°C is representative of field aging of about 15 years in a Wet-No Freeze zone and about 7 years in a Dry-Freeze zone.

**Field Validation of Laboratory Aging Procedures for Asphalt Aggregate
Mixtures.**

C.A. Bell, M.J. Fellin and A.Wieder.

For Presentation and Publication (Preprint), Association of Asphalt Paving Technologists, St. Louis, Missouri. March 21-23, 1994.

Accelerated Laboratory Testing (ALT) procedures have been developed at Oregon State University (OSU), in an attempt to simulate short- and long-term field aging. These ALT's enable asphalt technologists to incorporate evaluation of mixture aging into asphalt mixture analysis procedures. This paper is a summary of the validation of two ALT's developed at OSU, Short-Term Oven Aging (STOA) at 135°C and Long-Term Oven Aging (LTOA) at 85°C or 100°C, to simulate short- and long-term aging, respectively.

During the selection process of the sites to study, the climatic region where the pavement is located was a factor considered. At least two sites of all climatic regions were included in the study.

Based on the results, 4 hours of oven aging at 135°C appears representative of the short term aging which occurs in the field during mixing and placement. This is also sufficient for field aging of young projects less than two years old.

Two days of long term oven aging at 85°C is representative of pavement up to five years old depending on the climate. Also results suggest that four days of oven aging at 85°C appears to be representative of field aging of about 15 years in a Wet-No Freeze zone and about 7 years in a Dry-Freeze zone. No guidelines were developed for Wet-Freeze or Dry-No Freeze zones, because no projects of sufficient age could be located.

Oven Aging at 100°C for 1, 2 and 4 days cause similar changes in modulus to 85°C aging for 2, 4, and 8 days, but damages the samples in the process. Oven aging at 85°C is considered to be more reliable.

Interrelationship Between Performance-Related Properties of Asphalt Cement and their Correlation with Molecular Size Distribution.

S.W. Bishara, R.L. McReynolds, and E.R. Lewis.

Transportation Research Record 1323, TRB, Washington, D.C., 1991, pp. 1-9

Molecular Size Distribution (MSD), Corbett analysis, and colloidal instability were determined to investigate relationships between several asphalt physicochemical parameters. Twenty (20) virgin asphalts covering a wide viscosity range were studied. The samples were supplied over a seven years period by 14 refineries. Two of the asphalt samples (Shamrock asphalts) have unique characteristics as opposed to the other 18.

A 16-hr. TFOT (Thin Film Oven Test) (ASTM D-1754) causes penetration and Medium Molecular Size components to decrease, but Absolute viscosity, Kinematic viscosity, Viscosity-Temperature Susceptibility (VTS), Penetration-Viscosity Number (PVN) and Large Molecular Size components to increase. Field aging (up to 7 years) caused similar changes but of less drastic magnitude.

A weak correlation was found between MSD and viscosity ratio (after and before TFOT) at 60°C. This may be attributable to shortcomings of the TFOT method. MSD correlates strongly with PVN at 135°C, viscosity at 135°C, VTS, colloidal instability and asphaltene content, but less strongly with viscosity ratio at 60°C. The colloidal instability index correlates fairly well with MSD.

For all correlations, directions of associations points out that high PVN at 135°C and low VTS (low temperature susceptibility), low viscosity ratio (high resistance to aging), high colloidal stability, and low asphaltene content are all favored by high LMS (Large Molecular Size) and low MMS (Medium Molecular Size) proportions. SMS (Small Molecular Size) has a weak correlation with most of the variables investigated and constitutes less than 10% of all asphalt investigated. Direction of association favors low SMS fraction. Virgin asphalts with high LMS/MMS ratio (>0.75) are characterize by low temperature susceptibility and high resistance to aging.

Since asphalts with these properties are expected to exhibit good field performance it is recommended that HPGPC (High-Performance gel permeation Chromatography) be used to determine the MSD of a given asphalt. However, further work to tie the optimum MSD to actual field performance is needed.

Asphalt Hardening in Extraction Solvents.

B.L. Burr, R.R. Davison, H.B. Jemison, C.J. Glover, and J.A. Bullin

Transportation Research Record 1323, TRB, Washington, D.C., 1991, pp. 70-76

To study the changes that occur in asphalt as it ages during the hot-mix operation or on the road, asphalts must be extracted from the associated aggregate. An early study reported, a coefficient of variation (COV) of 25% on recovered viscosities. The errors appear likely to be in: 1. The solvent has some hardening effect on the asphalt that increases with temperature and time of exposure. 2. Solvent is often not completely removed from asphalt during recovery, resulting in viscosities lower than the true value. 3. Asphalt is not completely removed from the aggregate.

It is known that asphalts do harden upon exposure to solvents. However, little is known about the causes or extent of solvent aging. A number of asphalts and a variety of solvents were used to quantify the solvent hardening with respect to time of exposure, temperature, and concentration of dissolved asphalt.

GPC chromatograms were used to study the aging effects (increase in Large molecular size components) of the asphalt. The results obtained were erratic, but it was clear that for all solvents increasing temperature increased aging. Some rapid hardening apparently occurs at the beginning or during recovery, thought with many asphalts and perhaps all tank asphalts, part of this is loss of volatile components during recovery. Results suggest all solvents appear about equal in hardening, except CCl_4 , which causes much greater hardening. Also light seems to accelerate hardening both with and without oxygen.

Solvent hardening appears to occur to roughly the same degree in most solvents, so it is not a reaction between asphalt and solvent. It occurs with the asphalts investigated and is much more asphalt -than solvent- dependent. The solvent aging can be minimized by using cold extraction and completing asphalt recovery from the resulting solutions as rapidly as possible.

The mechanism of solvent aging is still unclear; like oxidative aging, it involves changes that increase the fraction of Large molecular size material, but the mechanism must be quite different, as it occurs in the absence of oxygen. The infrared spectra indicates chemical changes occur, but unlike oxidative hardening, the species formed vary from asphalt to asphalt and do not seem to be related necessarily to the hardening process.

**New Apparatus and Procedure for the Extraction and Recovery of Asphalt Binder
from Mixtures.**

B.L. Burr, C.J. Glover, R.R. Davison, and J.A. Bullin

Transportation Research Record 1391, TRB, Washington, D.C., 1993, pp. 20-29

To properly measure the chemical and physical properties of the asphalt in the hot mix plant or pavement samples, an accurate extraction and recovery procedures are required. Studies done have determined that the coefficient of variation for extracted asphalt viscosities have ranged from 25 to 42 %, using the ASTM D-2172 methods. The probable areas of problems causing the variation are three: 1. The solvent has some hardening effect on the asphalt that increases with temperature and time of exposure. 2. Solvent is often not completely removed from asphalt during recovery, resulting in viscosities lower than the true value. 3. Asphalt is not completely removed from the aggregate.

The SHRP method is an integrated asphalt extraction and recovery procedure (See Appendix A). It improves on previous methods by accomplishing complete solvent removal, limiting solvent aging, and extracting more of the strongly adsorbed material from the aggregate. Reproducibility tests indicate that the method is precise to about 7% for one standard deviation for a single operator.

Tests for solvent aging in the recovery method shows that little hardening occurs during recovery for the SHRP method. ASTM methods A and B, modified using toluene and toluene/15 percent EtOH as solvents, were also tested for comparison. The modified method A left about 5% of the total asphalt on the aggregate after extraction on some samples, whereas the SHRP method removed all but the last one percent.

Comparison of viscosities of asphalts extracted using different methods showed that viscosities varied directly with solvent strength, contacting efficiency and volume of solvent used in the extraction.

Evaluation and Development of a Pressure Aging Vessel for Asphalt Cement.

Joe W. Button, Manoj Jawle, Vidyasagar Jagadam, and Dallas N. Little.

Transportation Research Record 1391, TRB, Washington, D.C., 1993, pp. 11-19

This study evaluates a Pressure Aging Vessel (PAV) for asphalt cement, with the specific objectives of examining the safety of the procedure and the effects of aging temperature, film thickness on aging, vertical location within the PAV, and proximity of aging asphalt to other asphalts.

Four SHRP core asphalts were used in the study. The safety investigation phase of the study concluded with the decision of using dry air instead of pure oxygen in the PAV. The replacement of oxygen with air made very little difference in the extent of oxidation of asphalts, and is a lot safer.

It was found that the relative degree of hardening of asphalts varies at different PAV aging temperatures; that is, two asphalts may age similarly at one temperature, but age differently at another temperature. This fact is significant, because the relative results of an aging test will be dependent on the temperature at which the temperature is conducted.

An almost linear relationship was found between asphalt film thickness and age hardening, for the range of film thickness tested at different temperatures. This relationship is mostly asphalt dependent. A decrease in film thickness results in an increase in hardening.

Results suggest that differential aging did not occurred with respect to the vertical position in the PAV. Also it was found, that for the asphalts tested and the conditions used, aging asphalts simultaneously in the PAV has no effect in the extent of hardening.

Use of Aging Tests to Determine the Efficacy of Hydrated Lime Addition to Asphalt in Retarding its Oxidative Hardening.

A.C. Edler, M.M. Hatting, V.P. Servas, and C.P. Marais.

Proceedings, Association of Asphalt Paving Technologists, Vol. 54,
1985, pp. 118-139

In the laboratory study, 60/70 and 80/100 penetration grade asphalts were used to determine the effect of lime treatment on asphalt hardening after aging. The asphalts were modified with 6 and 12 percent of hydrated road lime. After aging they were tested to determine the oxidative hardening by viscosity measurements, infra-red spectra and quantitative measurement of the High Molecular Weight Constituents (HMWC) of the samples.

Results demonstrated that lime addition greatly reduces the asphalt hardening as measured by viscosity index. The addition of 12% of hydrated lime retarded the age hardening to a greater extent than the addition of 6% of hydrated lime.

All the asphalts exhibited an increase in oxidation levels on aging. Results showed that the addition of lime reduced the oxidation levels, as measured by infra-red spectra; the addition of 12% lime being more beneficial than the addition of 6% lime.

The formation of HMWC due to laboratory aging tests is reduced by the addition of hydrated lime. However, owing to the detrimental effect of lime particles on viscosity, the overall effect on the reduction of age-hardening as measured by aging indexes after laboratory long-term aging tests is similar for the two hydrated lime contents.

Binder and Mixture Aging in Asphaltic Pavements: A Specification.

David R. Jones and Jack S. Youtcheff.

SHRP Asphalt Research Program Technical Memorandum # 5, 1992

It is generally accepted that asphalt aging is not a pavement distress, but is rather a conditioning step that can lead to pavement distress through the Asphalt Concrete (AC) embrittlement. The Strategic Highway Research Program (SHRP) formed the Aging Working Group to try to answer the complex questions of pavement aging.

The aging of bituminous binders is a complex process, involving several reactions which occur simultaneously. As oxidation of heteroatoms or oxidizable carbons takes place, volatile material is also lost at a rate that depends on both the asphalt temperature and service environment.

The Aging Working Group found no direct correlation between aging behavior and carbonyl or sulfoxide levels, also studies have shown that both functional groups may be unstable at the high temperatures used in some accelerated aging tests.

It was the finding of the Group that the oxidative mechanism were the same in the laboratory and the field up to temperatures approaching 115°C(239°F). Based on these studies the maximum temperature at which accelerated aging of binders should be carried out is 110°C(230°F). The overall conclusion of the researchers is that the aggregate plays a minor role in the aging of asphaltic pavements, and that there is no aggregate induced catalytic oxidation of the asphalt.

It was determined that for AC mixtures, a short-term oven aging test would accurately duplicate the aging occurring to the binder during mixing and laydown. The test involves four (4) hours aging of the loose mix in a forced draft oven at 135°C(275°F).

The Group also states that samples of binder show different physical properties depending on their thermal history. The slow annealing of asphalts will allow the molecules to orientate into a preferred status, resulting in a viscosity increase after annealing. Annealing can nearly double the viscosity of the sample. The Aging Working Group concluded that the limited affect of aggregates on binder aging suggests that binder aging can be used to predict pavement properties.¹

¹ This report was finished in 1992, more recent studies have shown that the aggregates do have a significant effect in the asphalt aging, thus asphalt aging alone is not an adequate indicator of how the AC will age in the field.

Use of GPC Chromatograms to Characterize Aged Asphalt Cements.

By Kwang W. Kim and James L. Burati Jr.

Journal of Materials in Civil Engineering, ASCE, Vol. 5, No. 1, February
1993, pp. 41-52.

Asphalt Cements of three different grades and three different sources were subjected to artificial aging using the TFOT (Thin Film Oven Test) (ASTM D-1754) at three different duration. The change in some of their physical properties were measured (Absolute viscosity, Kinematic viscosity and Penetration), also the change in their MSD (Molecular Size Distribution) was monitored.

The GPC Chromatograms were compared to characterize the MSD of the different asphalt/grade/aging condition combinations. The different fractions of the GPC curve (Large Molecular Size (LMS), Medium Molecular Size (MMS), and Small Molecular Size (SMS)) were correlated to the physical properties measured. It was found that in general there is a significant change in LMS area due to aging. Also LMS area increased more for lower viscosity asphalt cement than for higher viscosity ones.

Statistical analysis showed that the absolute viscosity and the kinematic viscosity were related to large-size molecules and some of the small-size molecules, and penetration was related to medium-size molecules. The study demonstrated the applicability of using GPC analysis to characterize asphalt cements, predict their physical properties, and identify the aging of the asphalt cement.

Reaction Rates and Hardening Susceptibilities as Determined from Pressure Oxygen Vessel Aging of Asphalts.

C.K. Lau, K.M. Lunsford, C.J. Glover, R.R. Davison, and J.A. Bullin.

Transportation Research Record 1342, TRB, Washington, D.C., 1992, pp. 50-57

Attempts have been made to simulate road aging with laboratory tests. Aging occurs in two modes: first there is the very rapid aging that occurs in the hot-mix plant at high temperatures on the aggregate surface. This is followed by a much slower, low-temperature aging in the road.

The TFOT (Thin Film Oven Test) (ASTM D-1754) and RTFOT (Rolling Thin Film Oven Test) (ASTM D-2872) have been used to simulate the long term aging that occurs in the pavement. The results do not appear to correlate to road aging. One likely reason is that the tests are still conducted much above field temperatures, so that the aging rates and mechanisms are not relevant to field aging. In order to simulate road aging, the mechanism of aging in the binder must be the same of the one that occurs in the pavement.

Five asphalts (AC-20) were aged using the Pressure Oxygen Vessel (POV) at 300 psi oxygen pressure at temperatures of 60°C, 71.1°C and 82.2°C. The samples were removed periodically for viscosity measurements and infrared analysis.

It was found that the degree of oxidation, as measured by the increase in carbonyl peak area relative to the unaged neat asphalt, increases linearly with oxidation time at a given temperature over a range from 60°C to 82.2°C. This suggests that the aging mechanism for this range is the same. Also the degree of hardening due to oxidation increases linearly with time and, hence, is linearly related to the carbonyl peak area. The hardening susceptibility is a key measure of the effect of oxidative aging on a physical property.

It was observed that different asphalts exhibit different reaction rates at the same temperature. Results showed that AAG-1 asphalts when oxidized to the same extent as the other asphalts didn't present the same increase in viscosity. Thus one asphalt may age faster than another at one temperature, whereas it may age slower at a different temperature. Asphalt aged in contact with two different aggregates suggest that the reaction mechanisms are not significantly changed by the aggregate up to 107°C. There is not a significant difference between POV aging of neat asphalt and core aging of asphalt concrete pavements at temperatures below 93.3°C.

Asphalt Aging in Texas Roads and Tests Sections.

K.L. Martin, R.R. Davison, C.J. Glover, and J.A. Bullin.

Transportation Research Record 1269, TRB, Washington, D.C., 1989, pp. 9-19

In 1982-1983, test sections were laid at three Texas locations using five asphalt sources and two grades (AC-10 and AC-20). The roads were cored 1984, 1985 and 1987. Viscosities, penetrations, voids, gel permeation chromatography (GPC), and infrared analysis were run. The data obtained from the cores, showed a surprisingly high void level in two of the test sections locations, which led to rapid aging and early demise of the test sections.

High void levels relate to shortened road life. As has been identify in previous studies, the void level is considered as one of the most important factors affecting the rate of hardening of an asphalt pavement.

It was found that oxidation, as reflected in the growth of the carbonyl peak, increases rapidly with voids. Also, the data collected showed that the sections constructed with the lower viscosity grade were oxidizing less rapidly.

All the data and the results of tests tend to indicate that carbonyl peak height is a good measure of road aging for any particular asphalt with respect to both viscosity and penetration, and can probably be used as an effective parameter in laboratory aging tests. However carbonyl peak height, cannot be related to road age in years, because the percentage of voids, and probably other factors also exert a significant influence on aging.

The use of GPC to measure asphalt aging is also very useful, but GPC results are more difficult to correlate. Each asphalt yields a chromatogram with a distinctive shape that is dependent on the procedures used.

Effects of Physicochemical Factors on Asphalt Oxidation Kinetics.

J.C. Petersen, J.F. Branthaver, R.E. Robertson, P.M. Harnsberger, J.J. Duvall, and E.K. Ensley.

Transportation Research Record 1391, TRB, Washington, D.C., 1993, pp. 1-10

The oxidative hardening of asphalt contributes significantly to the embrittlement of asphalt pavements. This hardening is attributed primarily to the formation of polar, oxygen-containing chemical functionality that increases interactions among asphalt molecules. The sensitivity of an asphalt to the oxidation products varies with asphalt source.

A model for asphalt oxidation has been proposed suggesting that physicochemical factors dominate the kinetics of oxidative age hardening of most asphalts. This model proposes that potentially reactive polar asphalt molecules associate to form microstructure. These molecular associations immobilizes the inherently reactive components thus reducing their ability to react with atmospheric oxygen.

Molecular association of polar asphalts components plays a major role in determining aging characteristics, and because it is known that molecular association is reversible and highly temperature susceptible; studying the kinetics of aging as a function of temperature is needed.

Two laboratory aging tests were selected for the study of age-hardening kinetics. For the low temperature range, Pressure Oxygen Vessel (POV) was used, and to evaluate aging at higher temperatures, the Thin Film Accelerated Aging Test (TFAAT) was used.

Results indicate that two asphalts can be ranked as having similar age-hardening characteristics at one temperature, but at higher (other) temperature this may not be the true; this depends on the degree of dispersion or association of the asphalt's polar molecules.

The age hardening kinetics at pavement temperature of all but the most highly dispersed asphalts are dominated by the immobilization of polar, reactive asphalt molecules through microstructure formation. The sensitivity of an asphalt to viscosity increase on oxidation is strongly influenced by its component compatibility (asphaltene and maltene). The more highly structured an asphalt cement, the more sensitive it is to viscosity increase with increasing temperature of oxidation. The hydrocarbon oxidation chemistry

is similar for both ambient and pressure vessel aging of asphalts, and it also similar throughout the temperature range of 60°C to 130°C.

Paving Asphalts: Reduction of Oxidative Hardening of Asphalts by Treatment with Hydrated Lime -A Mechanistic Study.

H. Plancher, E.L. Green, and J.C. Petersen

Interim Report. Federal Highway Administration. Washington, D.C., April 1977.

Four asphalts and four aggregates supplied by the Material Division, Office of Research and Development, Federal Highway Administration, were used in the study. Samples (AC (Asphalt Concrete) and asphalt alone) were prepared with and without lime treatment.

The use of lime treatment has a beneficial effects in reducing the oxidative hardening of asphalts; this was demonstrated by the significant decrease of the viscosity and aging indexes of the lime treated samples. The decrease was around 50%. Modulus aging indexes of all the samples prepared with lime treated asphalts were lower than those prepared from untreated asphalts. The decrease ranged from 6 to 29 percent.

Results showed that the aggregate type had an effect on Resilient modulus (M_R). M_R values of samples prepared from limestone aggregates presented larger modulus than the ones prepared from granite. These differences are believed to result primarily from differences in the physical properties of the aggregates; i.e., the softer aggregates are crushed or abraded during compaction.

A comparison of the data on untreated and lime-treated asphalts shows that the lime-treated asphalts contain smaller amounts of the determined oxidation products than the untreated asphalts. Lime treatment reduced the amount of carbonyl type oxidation products formed in asphalt, this reduction was relatively small when compared with the reduction in hardening as measured by the aging indexes.

Analysis of the asphalt cement before and after lime treatment, showed that the lime removes polar molecules that are capable of exhibiting strong molecular interaction forces; these components probably play an important role in asphalt hardening.

In all cases, lime treatment reduced the viscosity of the asphalts, demonstrating that the polar material removed by the lime are viscosity-building components.

**Evaluation of Aging Characteristics of Asphalts by Using TFOT and RTFOT at
different Temperature levels.**

Jih-Min Shiau, Mang Tia, Byron E. Ruth, and Gale C. Page.

Transportation Research Record 1342, TRB, Washington, D.C., 1992, pp. 58-66

Thin Film Oven Test (TFOT) and Rolling Thin Film Oven Test (RTFOT) were used to investigate the aging characteristic of 20 asphalts at three different temperature 285°F, 325°F and 365°F (140°C, 163°C and 185°C). Penetration, Absolute viscosity, Infrared absorption spectrophy and Schweyer rheometer were used to evaluate the characteristics of the asphalts before and after the TFOT and RTFOT.

On the basis of percent penetration retained and absolute viscosity ratio, the RTFOT is a more severe aging process than the TFOT for oven temperatures of 285°F and 325°F. However, the two processes are not significantly different at an oven temperature of 365°F.

The carbonyl ratio, a ratio of infrared absorbance at 1700 cm^{-1} and 1600 cm^{-1} was used to quantify the level of oxidation in the binders. Based on the carbonyl ratio, the effects of TFOT and RTFOT are not significantly different from each other at oven temperatures of 285°F and 325°F. However, at 365°F, the TFOT is more severe from the standpoint of carbonyl ratio.

On the basis of constant power viscosity, the effects of TFOT and RTFOT are not significantly different from each other at any of the three temperatures.

It was found that higher oven temperatures result in increased differentials in properties (i. e., the change in viscosity between 325°F and 365°F is greater than that between 285°F and 325°F. Also results showed that the constant power viscosity-temperature relationship of asphalt is shifted parallel to the original relationship after the aging process. The relationship shifts more for higher oven temperature than for lower oven temperature.

Role of Asphalt and Aggregate in the Aging of Bituminous Mixtures

D.A. Sosnovske, Y. AbWahab, and C.A. Bell

Transportation Research Record 1386, TRB, Washington, D.C., 1993, pp. 10-21

Eight different asphalt types and four different aggregates were used in the experiment. Mixture samples were prepared using each asphalt with each of the four aggregates. The samples were subjected to four different aging methods: no aging, short-term aging, long-term oven aging, and low pressure oxidation (LPO).

The aging characteristics of the samples were evaluated by the resilient modulus as determined using the diametral (indirect tension) (ASTM D-4123) and triaxial compression modes of testing.

The modulus ratio (before and after aging) for short-term and long-term aging were used to rank the asphalts with each aggregate. Data from another study, in which the asphalt cement alone was aged and ranked, was used for comparison purposes. The asphalts were ranked based on aging ratio (ratio of the aged viscosity at 60°C (140°F) and the original viscosity at 60°C).

The comparisons showed significant differences in ranking between mixtures and asphalts for both Short-term aging and Long-term aging. This suggests that the aging susceptibility of the mixture is not only dependent on the asphalt but also on the aggregate present in the mixture. The aging phenomenon appears to be related to the adhesion of the asphalt and aggregate.

The differences obtained in the rankings also indicates the need for testing to evaluate the mixture's aging susceptibility. Aging the asphalt alone is not an indicator of how a mixture will age. It was observed that the aging of certain asphalts is strongly mitigated by some aggregates but not by others. Also it appears that the short-term aging procedure does not enable prediction of long-term aging. The LPO long-term aging procedure causes the most aging and less variability in the rankings of aging susceptibility relative to short-term aging rankings.

Comparing Field and Laboratory Aging of Bitumens on a Kinetic Basis.

A.F. Verhasselt and F.S. Choquet.

Transportation Research Record 1391, TRB, Washington, D.C., 1993, pp. 30-38

Asphalt cements in pavements are subjected to two types of aging during its life: rapid aging in construction and slow aging in service. To study the aging in the laboratory of bitumens in a kinetic basis, it is necessary to evaluate the activation energy of oxidation reactions from developments in certain characteristics such as asphaltene content, R&B and Penetration.

Taking classical kinetic theory and the concept of extent of reaction, a , as a basis and using the one-dimensional diffusion model for solid-state reactions, it is possible to clarify the process of bitumen aging in time. By randomly selecting a reaction indicator S , the general equation after mathematical transformation can be written as follows:

$$S_t = S_0 + K^{1/2} * t^{1/2}$$

where

S_t = value of indicator at time t ,

S_0 = value of indicator at time $t=0$ and

K = reaction or rate constant (at test temperature).

Using this equation, it is possible to determine the overall reaction constant, K , from experimental data as far as the test have been conducted at temperatures no higher than 100°C (212°F). After this temperature the reaction mechanism is different from that which occurs on site.

On site, a pavement is subjected to variations in temperature according to the surrounding climatic conditions. Equal time of exposure to various temperatures will contribute in different ways to the aging of the binder. Because of the variations in field temperature, the total in-service aging of a binder, will be the sum of a series of partial aging processes, the contribution of which depends on the time of exposure to a given temperature.

One of the important factors in the kinetic approach to aging is temperature. Accelerated laboratory tests make it possible to determine the overall reaction constant, K , for various indicators at several exposure temperatures. To transfer this approach from laboratory results to in-service road conditions, the concept of kinetic mean temperature must be used. This temperature can be evaluated: 1. From the activation energy of the reactions

evaluated and 2. From statistical data on the distribution of temperatures at the surface of road structures.

When overall reaction constant calculated from the results obtained on sites in regions with different climates are compared with those extrapolated from the results of accelerated laboratory aging tests and from relevant presumed kinetic mean temperatures, the proposed kinetic approach is found to be valid for assessing the aging of bituminous binders in service.

APPENDIX A

SHRP Extraction and Recovery Method

The SHRP extraction and recovery apparatus is presented in Figure 1.

The extractor drum has a filter arrangement consisting of a 10-mesh steel screen followed by about 2.54 cm (1 in.) of glass wool packing, an 8-mm polypropylene monofilament filter(Filter-All, Inc. #13118, from Mongolia, Texas), and another 10-mesh steel screen for filter support. The drum is also fitted with four baffles to improve mixing. The fine filter is composed of two 33-cm(13 in.) aluminum discs containing about 1.27 cm(1/2 in.) of liquid space followed by a 1-to 2-mm polypropylene monofilament filter(Filter-All, Inc. #13107) and a 10-mesh screen filter support. To begin an extraction, 1 Kg of pavement sample and 600 mL of toluene (or TCE) are charged to the extractor drum. The drum is attached to the 30 rpm, 49.7W (1/15 h) shaded pole gear motor and turned for 5 min. Next, the drum is connected above the first filtrate flask, about 39.9 kPa vacuum is applied (61.3 kPa pressure, absolute), and the extract is filtered. This filtrate is further put through the fine filter to remove as many small particles as possible. Unfortunately the coarse filter by itself passes too many fines to the recovery step, and a 1- to 2mm filter plugs when it is used as the drum filter.

The filtrate from the fine filter is transferred to the rotary evaporator's 100 mL recovery flask, which contains several 3-mm glass boiling heads. The rotary evaporator is a Buchii RE-111, and a common kitchen fryer is used as an oil bath. The bath temperature is held at 100°C and pressure is lowered into the oil bath and the solvent is distilled until the condensate rate is down to about one

drop every 15 seconds when the flask is raised from the oil bath. The condensate flask is emptied into a container where the solvent is used for subsequent washes.

The oil bath temperature and recovery pressure were chosen to obtain a relatively low distillation temperature without overwhelming the condenser. Having the boiling temperature low limits the rate of solvent aging during the recovery step. The relative low bath temperature helps reduce unstable boiling in the recovery flask.

While the solvent is distilling, the extractor drum is charged with 400-mL solvent and turned for 15 min. The mixing, filtering and distilling sequence is repeated for this second wash. The third wash follows similarly, except that the mixing time is 30 min. After distilling the third wash, the recovery flask is removed and set aside. This flask contains about 90% of the asphalt in the sample, and removing it from the recovery conditions helps prevent solvent aging. Another recovery flask is attached to the rotary evaporator for the remaining washes. For the fourth and subsequent washes, toluene (or TCE) with 15 percent ethanol is used. The mix times are 30 min. each. When the extract flowing through the transfer tube attains a light brown color, the extraction is completed. This usually takes a total of seven washes, or about 3000 mL of solvent contacting the sample.

Before the final recovery, the asphalt in both flasks is mixed into solution and poured into two 250 mL centrifuge jars. The last remaining aggregate fines are centrifuged for 25 min. at 3600 rpm. After centrifuging, the solution is decanted into a 1000-mL recovery flask with boiling heads.

For the final recovery, the bath is heated to 171°C. The recovery flask is attached to the rotary evaporator, pressure is set at 8.0 kPa absolute, the flask is lowered into the bath, and solvent is distilled. When the condensate rate falls to less than one drop every 30 sec, a nitrogen (N₂) purge tube is inserted through the condenser and down to the asphalt surface. The N₂ is bubbled at 1000 mL/min through the asphalt for 30min. to complete the extraction and recovery.

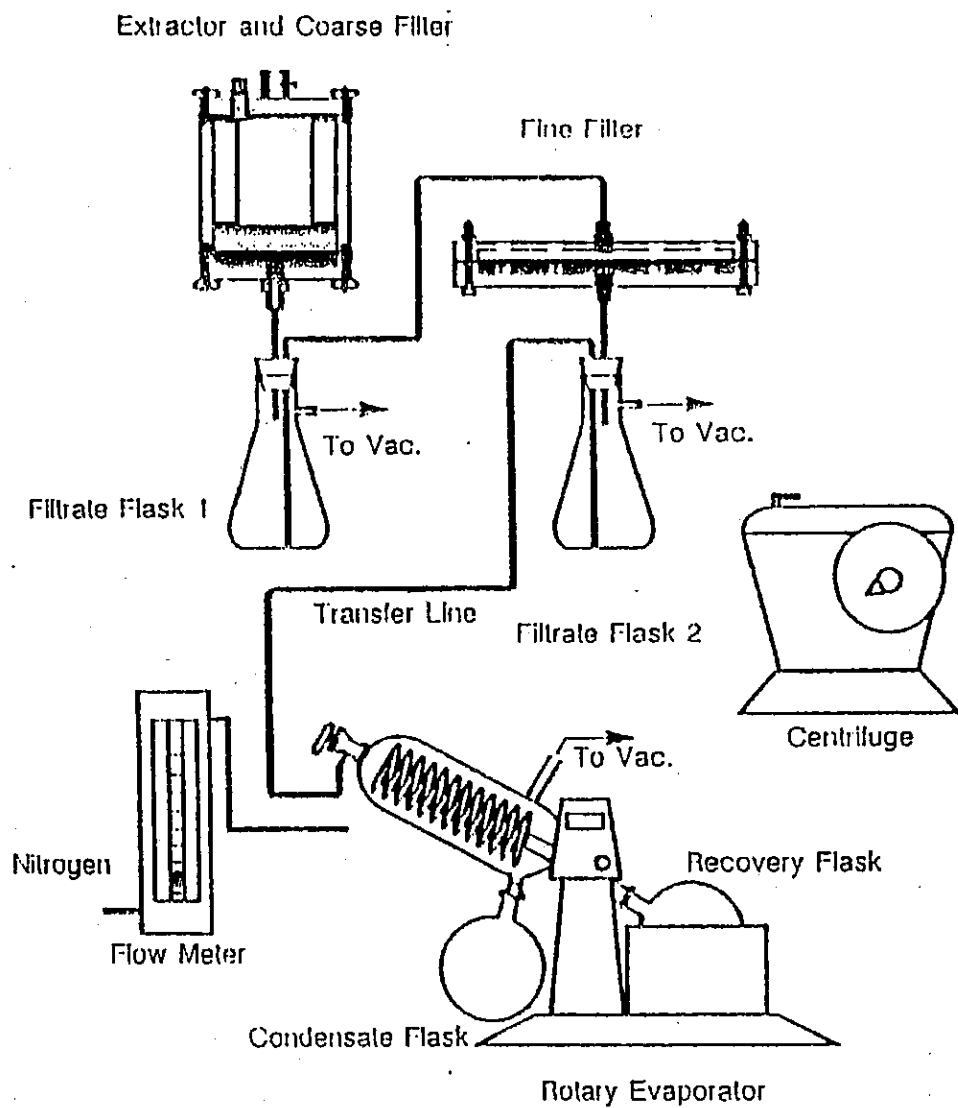


Figure 1. Schematic representation of SHRP extraction and recovery apparatus.